IOSTC

FIRST INTERNATIONAL

OIL SANDS

TAILINGS CONFERENCE

Edmonton, Alberta
Canada

December 2008

Forward

Management of Oil Sands Tailings is beset with technical challenges and is an area of increasing public interest. The large volume of mature fine tailings (MFT) requiring safe containment and the vigilant management of capping waters represent the most visible of these challenges. The vast quantities of tailings sand produced during bitumen extraction have been extensively used to construct the safe containment dykes that contain the MFT and capping water. Over the last 10 years this sand has also been used to assist with disposal of MFT in the form of consolidated/composite tailings (CT). Considerable technical work has been carried out over the last 40 years but much of it is not easily accessible to the public so these extensive efforts which resulted in major advancements are not properly acknowledged. Much of these scientific and engineering advancements are published in diverse specialized conferences and journals making it a challenge to compile the important literature. The Fine Tailing Fundamentals Consortium in 1995 synthesized many of these studies in the **Advances in Oil Sands Tailings Research** known as the "***Silver Bullet***". This conference is the first meeting to focus on compiling the advances since 1995.

The aim of the **International Conference on Oil Sands Tailings 2008** is to provide an exchange of information between people responsible for managing the oil sands tailings, researchers and providers of tailings management services who have experience with this industry. The presentations and conference proceedings will provide an update to the advances since 1995 and will highlight the extensive research underway at present.

I want to personally thank the Oil Sands Tailings Research Facility (OSTRF) and the Canadian Oil Sands Network for Research and Development (CONRAD) for their encouragement and support for the conference. The conference would not have been possible without the dedication of Nicholas Beier and Sally Petaske who carried the torch thrown to them.

The success of this conference is only possible due to the breadth of the presentations and the quality of the manuscripts contained in the Proceedings. I want to thank all our professional colleagues who willingly took the time and expended the effort to share their experiences and insight with us. To all the authors, thank you for contributing your technical knowledge and for your efforts in submitting your manuscripts, especially in these extremely busy days when time is our most precious commodity.

The Proceedings contain information representing hundreds of years of collective experience. I hope you find insight and answers that will assist you in a better understanding of oil sands tailings.

David C. Sego

Chair, Organizing Committee

Thank you to the following sponsors for their support in making the 1st International Oil Sands Tailings Conference a success:

CONRAD

UNIVERSITY OF ALBERTA
QUAECUMQUE VERA

OSTRF
Oil Sands Tailings Research Facility

SUNCOR ENERGY

Champion Technologies™

CONETEC

ALFA LAVAL
Alfa Laval Inc.

TOTAL

FLSmidth MINERALS

Golder Associates

GEA
GEA Westfalia Separator Canada, Inc.

TABLE OF CONTENTS

Session 3 New Tailings Concepts

SESSION 4 – WATER AND HEAT CONSIDERATIONS

SESSION 5 - TAILINGS AND LANDSCAPE ENGINEERING

Keynote

Presentations

NON SEGREGATING TAILINGS AT THE HORIZON OIL SANDS PROJECT

Andy Chu[1], Theo Paradis[1], Vince Wallwork[1], James Hurdal[2]
1. Canadian Natural, Fort McMurray, Alberta, Canada
2. Wigwam Technical Services Limited, Calgary, Alberta, Canada

ABSTRACT

Canadian Natural has invested in Alberta's Oil Sands industry with the Horizon Oil Sands Project. During the development of this project, targets for the Extraction area have included high recovery of bitumen, improved energy and water use efficiency as well as reduced waste volumes. The Extraction process developed involves gravity separation cells, flotation units, cyclones and thickeners. The waste streams from this process are managed as non segregating tailings (NST) and deposited in the tailings facility.

The developed configuration of the Extraction process has advantages including increased bitumen recovery through the utilization of cyclones and flotation units combined with stabilization of these units through process design. Energy consumption is optimized and green house gas emissions are reduced (per barrel of oil produced) by reusing warm water from thickeners. Tailings storage requirements and water use are minimized with the production of NST.

INTRODUCTION

Canadian Natural Resources Limited has purchased extensive oil sand leases in the regional Municipality of Wood Buffalo, northwest of Fort McMurray, Alberta, Canada.

The Horizon Project is located about 75 km northwest of Fort McMurray, near Fort McKay. Figure 1 shows the location of the project site in relation to other leases in the area, and its overall location within Alberta.

The overall objective of the Horizon Oil Sands Project is the phased development of the oil sands resource, continuing without decline for over 50 years. Canadian Natural intends to develop the available bitumen reserves by installing facilities to mine the oil sand, extract the bitumen, and then upgrade the bitumen to generate synthetic crude oil to be sold as a product.

The first stage, Phase 1, is scheduled for start-up in 2008 with a production target of 110 kbbl/cd of synthetic crude oil.

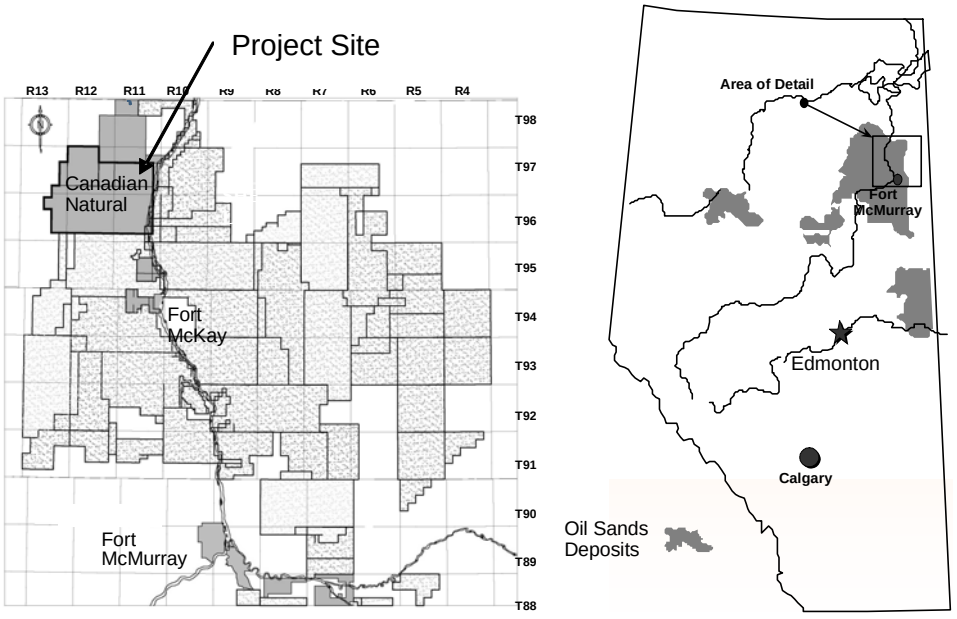

Figure 1: Horizon Project Site

The Horizon Project includes the following major components:

- surface mining operations using shovels and trucks to deliver oil sand to the bitumen production area
- extraction of bitumen from solids, tailings processes and froth treatment
- upgrading of bitumen by coking and hydro-processing to a range of marketable petroleum fractions that will constitute the synthetic crude oil
- utilities and offsite facilities necessary for the bitumen separation and upgrading operations
- and infrastructure to support operations of the entire project

The overall alignment of the major processing steps and plant areas is shown in Figure 2.

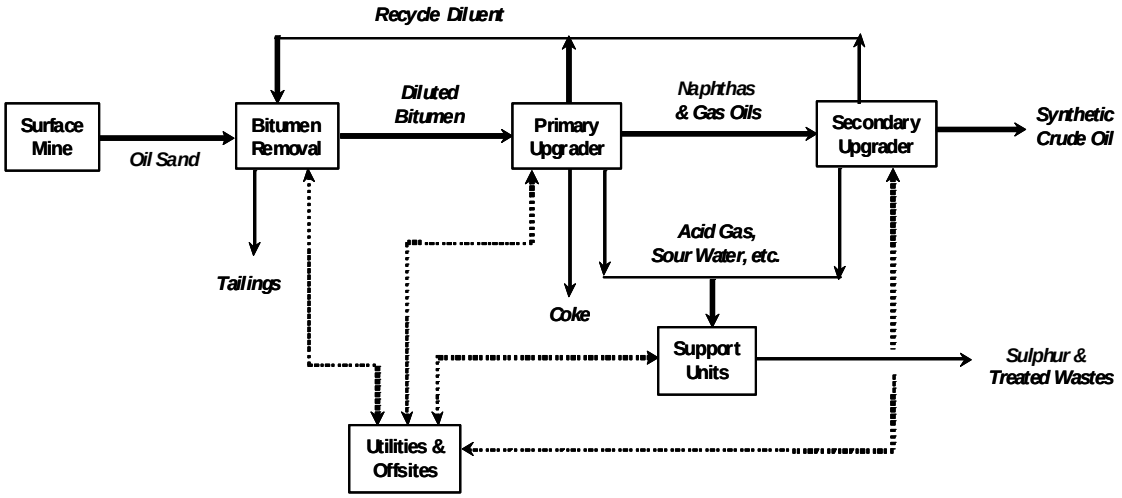

Figure 2: Major Processing Steps and Plant Areas

EXTRACTION PROCESS DESCRIPTION

The hydrotransport pipeline corridor contains a series of large diameter pipelines used for oil sands slurry transportation and conditioning. The slurry originates from ore preparation plants (OPP) as a mixture of minus 100 mm (4") oil sands lumps and hot water. The slurry specifics are highly dependent on the ore body being mined. The hydrotransport pipelines deliver the slurry to the extraction plant at a temperature greater than 50^{o}C.

At the extraction plant (Figure 3) the feed from the oil sand slurry pipelines are distributed among the primary separation cells (PSC). The recovered bitumen froth from the PSC flows by gravity to the deaerator and then it is pumped to the froth treatment plant.

The PSC underflow streams are pumped to two stages of cyclones. The second stage cyclone overflow combines with the PSC middlings as flotation feed. The recovered flotation froth is recycled to the PSC and the flotation tailings feed the thickeners. The thickener overflow is used mainly as dilution water for the cyclones and PSC feed.

The cyclone underflow streams are mixed with thickener underflow and carbon dioxide to form NST that are pumped to the tailings pond (Figure 4).

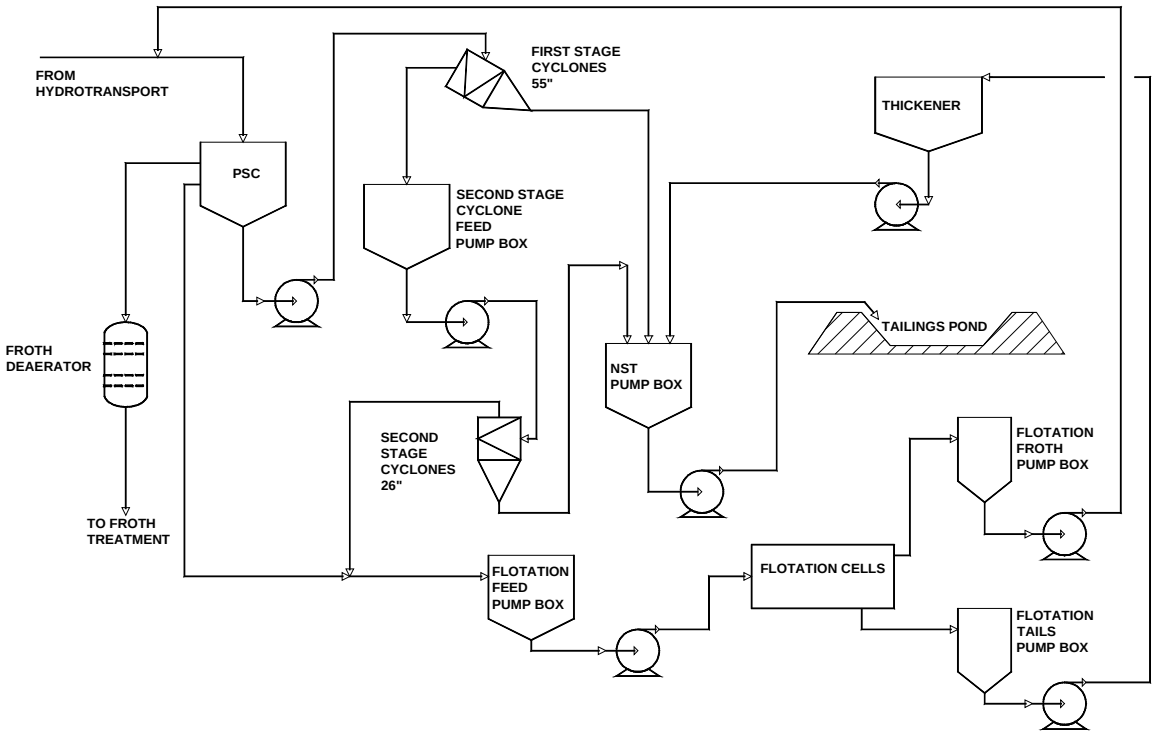

Figure 3: Extraction Diagram (single train represented)

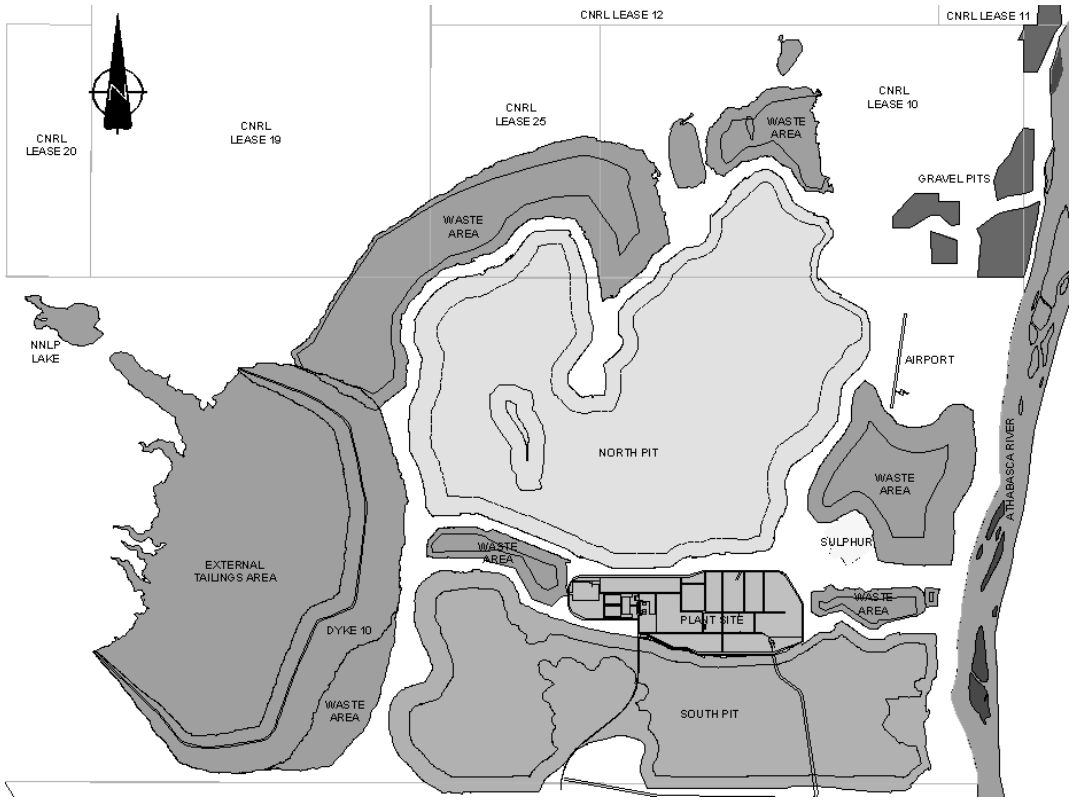

Figure 4: Plant Site

NON SEGREGATING TAILINGS

If the tailings generated in the oil sand extraction process (flotation tailings and PSC tailings) are dumped directly to the tailings pond they will segregate. The coarse material will settle however the fine solids will remain in suspension. Segregating tailings:

- tie up large volumes of the process water hence increasing fresh water requirements
- increase the required capacity of the tailings pond, resulting in increased costs and increased environmental footprint
- increase the time required for pond reclamation

Non segregating tailings are produced by thickening the tailings streams prior to mixing and modifying the pH of the mixture.

The fine flotation tailings are thickened in gravity thickeners using polymer flocculants to collect the fine particles, increase the settling rate and release the warm process water. The warm water is captured for reuse in extraction processes.

The coarser PSC underflow tailings are thickened with hydrocyclones. The PSC underflow contains significant amounts of fine solids, warm process water and bitumen. The hydrocyclones use centrifugal forces (inertia) to increase the settling rates and classify the PSC underflow. The cyclones separate the fine solids, bitumen and warm water from the coarse sand particles. The fine solids, bitumen and water are recovered and sent to the flotation cells for bitumen recovery. The thickened coarse solids from the cyclones are blended with the thickened fine solids from the thickeners and pumped to the tailings pond.

Carbon dioxide is added to the NST pipeline. For Horizon the addition rate is between 250 to 1000 ppm. The carbon dioxide:

- is converted to carbonic acid and lowers the pH of the NST
- increases the stability of the NST by increasing the viscosity
- improves the clarity of the released water
- accelerates settling and water release in the pond

The tailings pH is buffered back to normal soon after the tailings are deposited.

The production of non segregating tailings requires that a recipe be followed. In order to make NST the thickened tailings blend must have the right combination solids, fines and water. Also, the right water chemistry is important.

Certain types of oil sands ore produce tailings that adhere to the NST recipe better than others. A ternary plot (Figure 5) is used to determine whether or not a specific tailings blend will be non-segregating. The fines concentration (on the right axis) is estimated as fines over fines plus water.

In order to be non segregating, the tailings mixture composition must fall within the boundaries of the ternary diagram.

The envelope for the Horizon tailing compositions is plotted on Figure 5. The tailings from most of the ore types are suitable for NST production. The ore types that fall outside the NST boundary area only form a small percentage of the overall feed and will have to be blended with other ores to produce NST tailings. The benefits of NST production are:

- reduced tailings pond capacity
  - lower costs
  - smaller environmental footprint
- reuse of warm process water
  - less natural gas used to heat water, reducing greenhouse gas emissions
  - less fresh water pumped from the river
- bitumen is recovered by the processes used to thicken the tailings
- accelerated pond site reclamation

The process unit operations that directly impact NST production are the cyclone circuit and the thickeners. The balance of this paper will focus on the design, benefits and limitations of these two circuits.

Figure 5: Ternary Diagram

HYDROCYCLONES

There are many different types of hydrocyclones: classifying, water only, thickening, de-sanding, dense media, etc. Selection of the proper cyclone type and configuration is application dependent. Classifying cyclones are best suited to processing the PSC underflow for NST production. Similar to thickeners, cyclones rely on the settling rate of solids for separation. However, in a cyclone the feed is spun at high velocity. The apparent mass and mass differences of the particles are amplified, allowing the separation to take place in a few seconds (Figure 6).

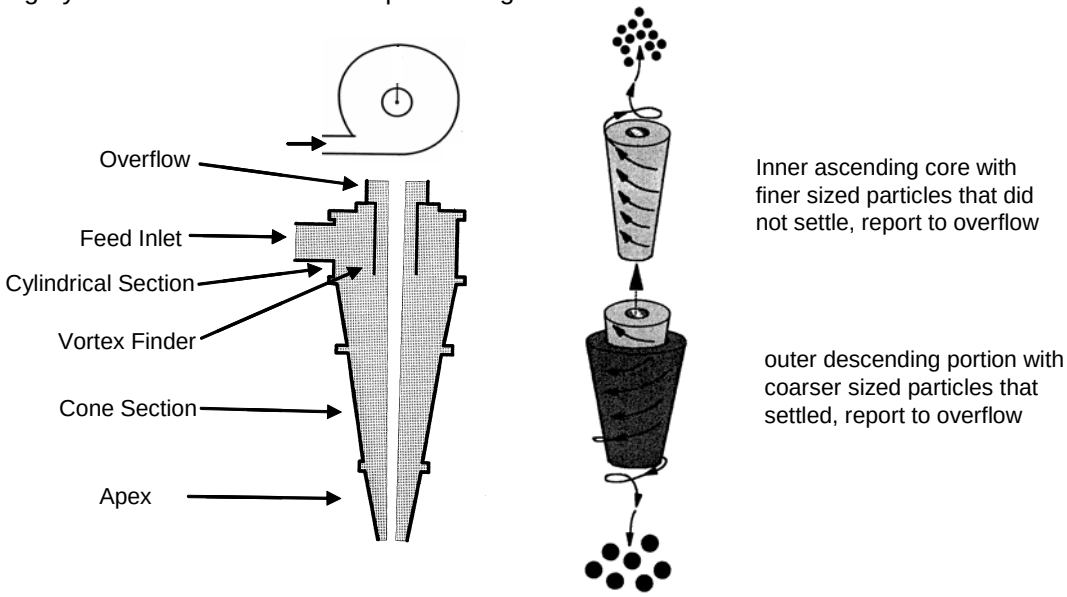

Figure 6: Classifying Cyclone

Hydrocyclones are very simple and reliable pieces of equipment with no moving parts. The feed is introduced tangentially into the top of the cyclone.

An air core forms inside the cyclone extending from the apex to the vortex finder. There are two vertical flow streams within the cyclone. The inner stream ascends toward the vortex finder, while the outer stream descends toward the apex.

As the feed enters the cyclone the linear velocity at the inlet is converted into circular velocity in the cyclone body and the wall of the cyclone generates centrifugal forces. The particles in the feed settle very rapidly.

The larger and/or higher density particles settle faster and end up in the outer descending stream. As these particles travel down the cone of the cyclone they are subjected to greater centrifugal force as the cone diameter decreases.

Finer and/or less dense solids will occupy the ascending stream and report to the cyclone overflow.

Cyclone performance is typically characterised by the cut point (d_{50}) and the efficiency of the separation (EPM). For a classifying cyclone the d_{50} is defined as the particle size that has a 50% probability of reporting to either the underflow or the overflow, neglecting the non-selective recovery due to the water split. The EPM is a measure of how much material is misplaced. The misplaced material is the $+d_{50}$ sized material reporting to overflow and the $-d_{50}$ sized material reporting to the underflow. A steeper portion of the curve between d_{25} and d_{75} corresponds to a better EPM.

The actual recovery curve includes the non selective recovery resulting from the water split. The very fine material is more influenced by its surface area than by its mass and tends to follow the water. The reduced recovery curve excludes the impact of the water split. Figure 7 shows the partition (recovery) curves for the Horizon NST cyclone simulations. Cyclone performance is impacted by both the cyclone configuration and the feed characteristics.

The cyclone parameters, including: diameter, inlet area, cone angle, vortex finder diameter and apex diameter, affect the cyclone performance. The cyclone diameter, inlet area and cone angle are all set at the time the cyclone is designed and are not easy to change. The vortex finder and apex diameters can be changed after start up, in order to manipulate cyclone performance.

The feed characteristics that influence cyclone performance are the weight percent solids, solid particle density, fluid viscosity and the feed pressure. The solid particle density and the fluid viscosities are inherent characteristics of the slurry. The feed pressure and feed weight percent solids can be manipulated by the plant operator. Manipulating the feed weight percent solids is a very effective way to manipulate cyclone performance. In contrast, manipulating the cyclone feed pressure within normal ranges has very little impact on cyclone performance.

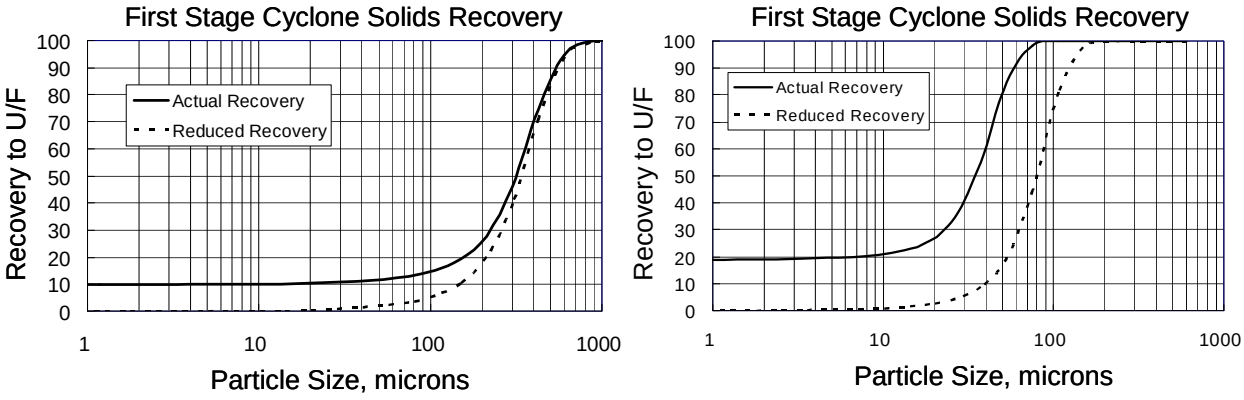

Figure 7: Partition Curves (average grade ore)

Table 1: Influence of Feed Weight Percent Solids and Feed Pressure on Cyclone Performance

Run	First Stage Cyclone						Second Stage Cyclone						
	Number of Cyclones	Feed Pressure (psi)	Feed Solids (wt%)	Overflow Solids (wt%)	Underflow Solids (wt%)	Cyclone d_{50} (microns)	Number of Cyclones	Feed Pressure (psi)	Feed Solids (wt%)	Overflow Solids (wt%)	Underflow Solids (wt%)	Overflow SFR	Cyclone d_{50} (microns)
1	2	17.0	55	51.0	74.0	263	10	15.7	45	18	72	0.42	56
2	2	13.5	59	57.0	72.0	337	11	14.2	45	18	72	0.46	58
3	2	10.0	65	64.0	72.0	513	11	15.7	45	17	72	0.43	56
4	2	13.5	59	57	72	337	10	17.1	45	17	74	0.39	55
5							12	11.9	45	18	69	0.54	61
6							11	19.6	40	13	72	0.24	47
7							11	10.4	50	26	71	0.92	73

Note that the data in this table is derived from cyclone simulations.

Increasing the feed weight percent solids reduces the settling rate, hence increasing the cyclone cut point. Increasing the feed pressure increases the settling rate, hence decreasing the cyclone cut point.

Table 1 contains simulation data for the Horizon plant NST cyclones. The impact of feed weight percent solids and feed pressure on cyclone performance is demonstrated in runs 1, 2, 3, 6 and 7.

For runs 1, 2 and 3 the feed weight percent solids to the first stage cyclones was varied from 55 to 65 weight percent solids. The same number of cyclones was used, so the feed pressure dropped as the feed weight percent solids was increased. Comparing runs 1 and 3, the feed weight percent solids increase of 18%, coupled with a feed pressure drop of 41%, increased the cut point by 95%. Dilution water was added to the second stage cyclones to maintain 45 weight percent feed solids. The performance of the first stage cyclones did not significantly impact the performance of the second stage cyclones.

Runs 4 through 7 all used the same first stage cyclone simulation. In runs 6 and 7 the feed weight percent solids to the second stage cyclones was increased by 25 % resulting in a feed pressure decrease of 47%. The cut point of the cyclones increased by 55%.

For runs 4 and 5 the feed weight percent solids were held constant and the pressure was dropped by bringing two more cyclones on line. The feed pressure decreased by 30% resulting in an 11% increase in cyclone cut point. The impact of feed pressure on cyclone performance is relatively small compared to the impact of feed weight percent solids.

Understanding the relationships between the cyclone geometry and the cyclone performance allows the designer to select the right cyclone for the application. Understanding the impact of changes in feed parameters on cyclone performance allows the process designer and the plant operator to optimize plant performance.

In the case of NST cyclones, the cyclone circuit should be designed to process the PSC underflow to produce 72 weight percent underflow solids, minimize sand bypass to the cyclone overflow and handle the top size material without plugging. It is possible for a cyclone to achieve all three objectives, as long as the feed rate is stable and the top size solids do not dictate the apex diameter.

One process design option is to directly feed the cyclone circuit with the PSC underflow stream. The cyclone underflow reports to the NST pump box while the cyclone overflow reports to the flotation feed pump box. However, the large static head in the PSC coupled with the short pipe run to the cyclones, results in a very flat system curve for the PSC underflow pumps. The PSC underflow pumps constantly hunt for a stable operating point. Changes in PSC underflow density or other changes in head result in large fluctuations in flow rate.

The bulk of the bitumen recovery occurs in the PSC, so priority is typically given to the operation of the PSC. One of the primary levers used in optimizing PSC performance is the rate of underflow withdrawal.

The net result is that the feed to the cyclones may vary significantly. Unstable feed rates to the cyclones impact cyclone performance. Oversize material may be misplaced to the cyclone overflow and undersize material (water, fines and bitumen) may be misplaced to the cyclone underflow. The number of cyclones operating is typically varied to compensate for the variations in the feed. Changing the number of cyclones running changes the head on the system and causes more PSC underflow pump flow instability.

The extraction and NST process circuits for Horizon have been designed to address the control issue between the PSC underflow pumps and the cyclones. That is accomplished by using a two stage classifying cyclone circuit.

The first stage cyclones (55") are directly coupled to the PSC underflow pumps. The first stage cyclone underflow reports to the NST tank, while the overflow reports to the second stage cyclone feed pump box. The second stage cyclone underflow reports to the NST pump box while the overflow reports to the flotation feed pump box.

The first stage cyclones have only one design objective and that is to produce a 72 weight percent underflow solids under all operating feed conditions. The 13" apexes are large enough to handle the 100mm top size material. The quality of the overflow does not mater because the overflow is reprocessed by the second stage cyclones.

The second stage cyclone feed pump box decouples the second stage cyclones from the first stage cyclones and the PSC. The pump box is equipped with water make up for level control.

Using variable speed pumps, the second stage cyclones are fed at a constant feed pressure, while the feed weight percent solids are permitted to vary within a range. If the feed weight percent solids get too high, dilution water is added to the pump box and another cyclone will be brought on line. Rather than seeing a constantly shifting feed, the cyclones see steady state operation with step changes in the feed. The second stage cyclones are configured to produce 72 weight percent underflow solids and minimize bypassing of sand to the overflow.

Table 1 shows data for the 55" and 26" cyclone simulations on average grade ore. The partition curves for average grade ore and normal feed conditions are shown in Figure 7.

The cut point for the first stage cyclone is 300 micron. The actual recovery curve converges with the reduced recovery curve on the coarse side, because the first stage cyclone is configured for high weight percent underflow solids with very little bypass.

Simulations at the different expected feed conditions result in a cut point range of 250 to 600 micron, creating no top size issues for the second stage cyclones.

The performance of the second stage cyclones was simulated for the expected range of feed conditions and feed types. The cyclone performance is acceptable for all cases. Dilution water is used to manipulate the cut point of the second stage cyclones. Bitumen and water recoveries for the second stage cyclones are expected to be in the range of 70%.

THICKENERS

Within the mineral process industry, thickeners are a well understood piece of mechanical equipment. There are different kinds of thickeners:

- conventional
- high rate
- lamella
- tray

The different kinds of thickener all work on the common principle of allowing the suspended solids to settle in a laminar environment, where the rise rate of the liquid is lower than the settling rate of the particles.

The characteristics of the feed determine which type of thickener is best for the application. For oil sand tailings the solids initially settle freely; but, the settling rate quickly decreases as the solids concentration increases and the solids bed compresses. Conventional thickeners can work well for this application (Figure 8).

A conventional thickener is a large tank with a sloped bottom and an overflow weir on the top. The slurry feed is introduced to thickener through a feed well located at the center of the thickener. The solids settle to the bottom of the thickener while the liquid rises to the top. A rotating rake is

used to move settled solids toward the center of the tank, where an underflow pump is used to extract the settled solids. The liquid rises to the top of the thickener where it overflows into radial collection launders.

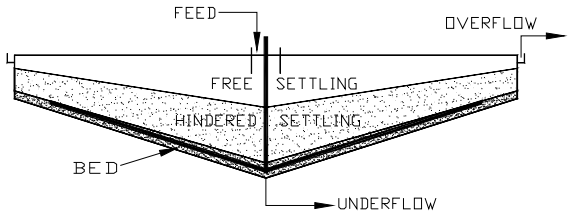

Figure 8: Conventional Thickener

Polymers are added to the thickener feed to bind the fine solids together. The polymers increases the settling rate of the solids and improve water clarify.

The design of the thickener depends on the quantity and nature of the feed. The important parameters are:

- settling rate
  - density of solid particles
  - solids size distribution
  - weight percent solids in slurry
  - water chemistry
- thickened solids rheology

The settling rate determines the size of thickener (thickener area) required for the process. The higher the settling rate, the smaller the required thickener area. High density solids settle faster than low density solids of the same size. Large particles settle faster than small particles of the same density. If the feed weight percent solids are too high, then the settling rate is reduced due to hindered settling. Water chemistry can affect interparticle forces which may impact settling rate.

The thickened solids rheology is very important. The yield stress of the settled solids impacts the rake and pump designs. The thickener must be designed such that the thickened solids can be moved by the rakes to the center and discharged to the underflow pump. The pump must also be designed to handle the solids. A yield stress of 150 Pa is the upper limit for pumping with a centrifugal pump.

Thickener design starts with the acquisition of representative samples of thickener feed. Acquiring representative samples is, by far, the most important step in the design process. If the samples are representative of the ore to be processed, then the thickener will work as expected.

Within an operating plant, pilot testing with a small thickener is preferable. Pilot plants allow data collection on a large variety of feed blends and process conditions. However, pilot testing requires that the plant providing the feed stream run at steady state for several thickener residence times. Bench tests can also be used to accurately determine thickener design. Testing will ultimately determine the thickener design loading rate, polymer selection, polymer dosing strategy and the thickened solids rheology.

The thickener designer uses the test data to design the thickener. In order to accommodate the thickener feed characteristics, the designer manipulates the following thickener design parameters:

- diameter
- sidewall height
- feed well design
- rake design
- rake torque
- rake lift
- bottom slope
- froth removal system
- underflow pump
- polymer addition points

The testing on the Horizon ore types resulted in the thickener design summarized in Table 2.

Based on the design loading rate of 14–15 tpd/m^2, 70 meter diameter thickeners have been selected. The testing determined that a 5 hour minimum retention time is required, in order to achieve the underflow weight percent solid targets for all feed types. The thickener has been designed with a 14 degree cone angle and high torque rakes to ensure that the settled solids can be moved to the underflow pump. A rake lift mechanism has been added as an additional precaution. At higher underflow weight percent solids the thickened tailings may reach the upper pumping limit of 150 Pa, so the underflow weight percent solids must be closely monitored. The underflow pump is expected to shear thin the thickened tailings.

Higher side walls and staged polymer addition are used to improve overflow water clarity.

Table 2: Summary of Thickener Sizing Data

Design Tonnage (total mineral), mtph	2,319
Feed to Thickener, wt % solids	28.2
Feed Solids for Flocculation, wt % solids	10 -15
Pre-Conditioning Flocculant Type	Polymer, 3 point stage addition
Pre-Conditioning Flocculant Dose, g/t	40
Feed well Flocculant Dose, g/t	25 – 40
Predicted Underflow, wt % solids	46 – 60
Retention Time, hr	5 (minimum)
150 Pa Solids Concentration, wt % solids	56 - 67
Design Loading, tpd/m^2	14 – 15
Design Unit Area, m^2/tpd	0.07
Cone Angle, degrees	14
Side Wall, m	6

Note: This thickener design is unique to the Horizon ore characteristics and process configuration.

CONCLUSIONS

Producing NST requires adherence to a recipe. The site specific nature of the ore has a large impact on the design of the unit operations that are used to make the components for the NST recipe.

Representative samples of the tailings streams must be acquired in order to design the process equipment. The cyclones and thickeners must be sized and configured for the feed characteristics and process conditions. The process must be designed to accommodate upstream and downstream processes while giving operations the levers it needs to make the process work.

The two stage cyclone configuration used in the Horizon flow sheet, addresses the control issues between the PSC and the cyclone circuit, facilitating the production of NST.

The thickener design for the Horizons plant was based on the testing of hundreds of samples. The design takes into account the critical characteristics of oil sand fine tailings. The increased sidewall height will improve overflow clarity as will the staged addition of polymers to the feed. The fourteen degree cone angle, coupled with the high torque rake mechanism and the rake lift, will ensue that the thickener can produce the required underflow weight percent solids.

During the design of the Horizon plant, every effort has been made to ensure that the Operations Team has the process equipment in place to make on spec Non Segregating Tailings.

ACKNOWLEDGEMENTS

Our understanding of the processes required to make NST has been made possible by:

- the cooperation of the Oil Sand Operators. Learning and understanding of the tailings processes has been advanced by sharing lessons learned, research and process data.
- the many hours spent by Researchers, Vendors, Contractors and Owners, testing the processes and analysing the data.

The carbon dioxide test work was executed for Canadian Natural Resources by CETC-DEVON.

Figures 6, Figure 7 and the cyclone simulations were provided by FLSmidth Krebs.

CONSIDERATIONS IN OILSANDS TAILINGS CONTAINMENT

Ed McRoberts
Amec Earth & Environmental, Edmonton, Alberta

ABSTRACT

Forty years into the operations of open-pit oil sands mines, oil sand tailings have evolved to encompass a wide range of possibilities deriving from the wet extraction process. This paper focuses on the safe geotechnical containment of these tailings. Subjects not considered here are environmental issues including foundation seepage, the impact of seepage on reclamation covers, and the closure landscape.

OIL SANDS TAILINGS

Tailings can be broadly defined as the materials remaining after all economically and technically recoverable bitumen or energy has been removed from the ore during processing. Water is added to the ore to float-off bitumen as a froth, and a variety of chemical additions are used for process aids. Tailings encompass many different combinations of sand, fines, and sand-fines mixtures and process affected water. In addition inherited physico-chemical effects from process aids, unrecovered bitumen - especially coating on clay sized particles, and rejected asphaltenes, all affect fine tailings properties and complicate the geotechnical understanding of these materials. Upgrading the raw bitumen into a synthetic crude produces additional tailings streams. Coke, a byproduct primarily of napthenic processes has considerable energy value, must be stored in a recoverable manner and strictly speaking is not tailings, as it has economic value. Nevertheless coke can also be part of the tailings landscape.

THE PLANNING IMPERATIVES

Fine Tuning the Business Plan

The exigencies of the business plan reflecting for example optimization of dyke placement schedules, changes in pit sizes and bitumen production driven by major swings in oil prices, and demands for storage resulting from unforeseen tailings performance are external pressures bearing on the geotechnical designer. This is often reflected in requirements to modify or change a dam's design section (even before construction has begun) and to raise dams under construction to higher elevations. Given the cost of dealing with tailings, the geotechnical engineer faces on-going challenges to defend the design bases. Experience indicates that these issues are the rule not the exception.

Nevertheless, over the years these pressures have led to many cost savings and innovations, as mining methods and equipment types have changed, and as new tailings technologies are developed.

Variability in Extraction Processes

Extraction processes, reflecting variability in ore type, fines contents and process-ability, combined with start-ups and shut-downs requiring flushing of lines, result in a highly variable end-of-pipe whole tailings stream. The original method of dealing with wet segregating tailings with compacted cells and beaches offers a highly robust method of dealing with these unavoidable variations.

When a new technology is introduced "downstream" of extraction, variability inherent in requirement for continuous bitumen production militates against consistent tailings production. The geotechnical engineer must be cautioned against designing for the expected nominal operating condition (as found in a typical extraction process flow diagram) especially for non-segregating streams, or for that matter most of the development strategies currently under consideration without clear operational commitments on factors outside of the geotechnical engineers control. Designs must accommodate upsets, and current experience suggests variability will the rule for any step-out technology on-line with extraction.

External Versus Inpit Containment

In a typical operating mine, tailings can be found both externally or inpit. In new currently licensed greenfield operations an external tailings pond is necessary in order to store tailings until inpit space is available. External tailings ponds tend to be ring structures as topographical variations in the region rule out the classical dam in a valley. As such most external tailings ponds do not have significant abutment design considerations. For closure, external tailings ponds must be converted to a terrestrial landscape. In the future one might speculate that regulatory authorities will stipulate that the empty pits or "End Pit Lakes" currently contemplated by all lease operators, will need to be used for either tailings or overburden deposition by adjacent lease holders in order to minimize incremental effects and reduce the need for fresh water to be forever sequestered in deep pits.

External dykes are usually raised with overburden starter dykes in low areas and then with a switch-over to tailings construction to final height. Depending on the overall tailings plan, and the amount of overburden and/or intraburden available, at least one main external dyke has been designed as an all overburden structure.

Foundation conditions for external dykes will depend on lease conditions and have ranged from competent tills and McMurray Km formation, to thin overburden over weak Km, to weak Clearwater Kc, to deep Pleistocene sands, to near surface lightly overconsolidated Holocene to Pleistocene age clays. Inpit dams typically have reasonable foundations, but locally weak sheared basal pond muds, and Paleo-clays at the limestone contact can be present, as can loose dumped over and intraburdens.

Inpit dykes are used to form containment cells within the mine pit. As such there are two abutments with either both against the pit wall or in some cases with one or more abutments against an existing dyke. Multiple dykes with a common inpit abutment raise design complications if internal filter drains are required. In some mine plans it can be necessary to start construction of the inpit dam footprint but still continue mining within the future pond and therefore allow for a major haul road through the dam axis. In one case at Suncor the long inpit East/West Dam was built to full height at one end, when the mine excavation had not been completed at the other.

Clarification Ponds, Water Storage & Pond Management

A planning factor that must also be considered is the necessity for large ponds to allow for clarification of recycle water, and for storage of non-releasable water. All precipitation that contacts oil sands, dyke drainage waters, run-off from waste dumps and so forth cannot be released. Such waters are stored in tailings ponds increasing water on inventory. Ground water from surface and basal aquifers also can be stored in ponds. These waters with their accompanying ionic content can also strongly impact both settlement and consolidation characteristics of clay sized tailings.

The requirement for clarification of fine clays to meet process recycle water requirements of low clay content leads to significant pond areas. In some cases multi-use of pond space and especially with clarification requirements means that water is generally impounded against the upstream face of the retention dam. This can be readily accommodated with for example an upstream method and subaerial beaches [BAW] but introduces design and construction complications for overburden structures.

While some tailings such as CT / NST could be contained by simpler overburden retention structures, the requirements for a water cap or MFT cap drives designs to requiring provisions for internal drainage control. In addition, uniform production of a non-segregating tailings stream, such as CT, in conjunction with a CT-Pond with substantial subaerial CT beaches offers the possibility of design savings in tailings retention structures. This involves a trade-off between geotechnical design and construction factors versus operational control of pond waters and effective commitment to CT production.

Tailings Types and Materials

Other papers in this conference address the types of tailings "past, present and future". Unless there is a break-through in a non-water based or dry extraction process - currently below today's event horizon - the geotechnical

engineer will be dealing with sands, fines, and water.

One starting point in any retention design is whether or not the tailings stream from extraction is intended to be "segregating" or "non-segregating" on deposition. In a conventional extraction scheme whole tailings is pumped at relatively low solids contents and the tailings stream separates on deposition into mostly sand and some trapped fines, with the remainder of the fines and some sand collecting in a pond as sludge or MFT. In more complex schemes involving in-plant cyclones the tailings is hydraulically segregated and varying schemes are considered for the separate disposal of these streams, with the fines being thickened to a solids content approximating or somewhat exceeding what MFT will get to in a pond after several years of self-thickening. Alternative strategies combine cyclone underflow (at higher solids contents) with either thickener underflow or MFT from a pond. This mixture when combined with coagulants resulting in a non-segregating deposit. Such re-combined sand-fines streams are referred to as CT or NST by various proponents.

Suncor (then G.C.O.S) pioneered the first tailings containment facility at Tar Island Pond, using the upstream approach. Initially in the early stages of project development the creation of MFT was a surprise. That, and the fact that achieved beach slopes were much flatter than bench scale flume testing resulting in a structure originally conceived to be built out of overburden to a height of 12 m finally topping out at around 98 m. The geotechnical history of this structure can be found in Hardy (1974) Mittal and Hardy (1977), Chan et al. (1983) and McRoberts et.al. (1995).

The upstream method has proved to be robust and economical. The major drawback is that unacceptable amounts of MFT have been generated. Currently Tar Island Pond is being infilled with tailings sands prior to reclamation to develop a plateau. For some upstream ponds the plan is to remove the MFT leaving a vast bowl formed from tailings sand that must eventually include building-in an outlet for run-off. These plans will no doubt provide a new range of geotechnical challenges once they reach the implementation phase.

The primary focus for controlling both the current MFT volumes and future production is by CT. Alternatives to CT focusing on stand-alone MFT treatment technologies are currently considered to be more expensive than CT production. In the future it may be found that the total cost of CT production, including environmental factors, may rise and the costs of alternative technologies may decrease. In addition application of alternative MFT management approaches is on way of addressing the so-called legacy volumes. Therefore, new challenges can be expected in the retention of these types of tailings.

Overburden Construction

Overburden obtained by pre-stripping the opening mine cut is a potential source of material for starter dam construction as this material must in any event be moved to access the ore body. In addition CT dominated tailings plans requiring sand to sequester MFT and to cap the CT means that inpit dams require considerable select overburden for zoned fills. There is considerable pressure on the geotechnical engineer to use all fills coming from these operations, including construction of inpit dykes. However, overburden quality varies from mine to mine, and a lack of understanding of local conditions generally has lead to over-optimistic assumptions on borrow availability. This in turn drives tailings storage demand to requiring tailings sand for dyke construction, directly impacting sand available for other uses such as CT production.

An overburden starter dam usually provides several functions. Initially, the first external dam more than likely has to retain a significant volume of water. As governed by licensing approvals, water can only be obtained during high flow periods from the Athabasca River, and main tributaries, therefore a substantial inventory must be carried prior to start-up of extraction for a new mine. As tailings are placed behind the overburden dam some time must elapse before tailings beaches can be raised above water [BAW]. Until this time and resulting elevation water is impounded directly against the overburden structure. Therefore internal erosion or piping of an overburden dyke is a design concern, requiring a chimney drain. In addition BAW sands are needed in order for compacted cells to stepout over tailings in the upstream direction. Beaches placed below water [BBW] are relatively loose and subject to liquefaction.

Consequently, the overall tailings dam section will contain loose liquefiable sands within the design section. The second function of the overburden dam is to provide sufficient width and strength, in conjunction with the compacted cell sand to retain potentially liquefied BBW. Finally, the overburden must be internally self-supporting. For sites with weak Kc clays for example, this means that the overall slope angle may be relatively flat [say 12H:1V to 20H:1V] and therefore relatively poor overburden can be tolerated in some parts of the starter dam.

Overburden required within a tailings retention dam must therefore meet geotechnical specifications in terms of mobilized strength. The types of overburden vary from lease to lease depending on the Quaternary geology and the presence or absence of Kc formation over the ore body. Once a mine is developed beyond the opening cuts then intraburden within ore body also becomes available. A wide range of wet to dry fills is therefore possible. Generally footprints for tailings retention are always constrained by setbacks from natural features, mine pits, and other facilities. The geotechnical designer is asked to construct dam slopes as steep as possible with the most immediately to hand overburden. Where overburden fills are wet relative to optimum water contents and foundations conditions are poor some amount of wet fills can be tolerated. On the other hand a site with good foundations but wet fills and limited tailings space requires steep slopes which may mean that much wet fill must be rejected and wasted to dumps. This in turn puts additional pressure on dumps, and competing demand for plating to raise the dumps.

The last 40 years has seen the development of bigger mine trucks with both positive and negative geotechnical implications for overburden construction. Excavating many of the dry fills such as Kc and clay rich Km intraburden by large shovels with cuts 10m high or more results in a fill with many high strength blocks of cobble to boulder size. While some of this blocky fill is broken down by the D-10 Type Dozers used to spread fill, trafficking by loaded heavy haul trucks is necessary to meet compaction specifications and ensure a tight structure-less low permeability fill. This cannot be readily accomplished by smaller mine trucks. On the other hand fills wet of optimum water content are highly sensitive to pore pressure generation and heavy hauler loading can quickly result in rutting and trafficability problems. Experience indicates that construction guidelines developed for conventional earthworks can be misleading in marginal fill types using heavy haulers, and when combined with optimistic interpretations of borrow quality can lead to considerable start-up difficulties.

Winter Construction

The winters in Fort McMurray are long and cold, and the summers are often wet. Limiting construction to the traditional summer months was an early premise for construction of overburden dams in Fort McMurray, reflecting conventional practice. However, this is a severe limitation, as equipment would be left idle for at least the 4 core coldest months, with substantial economic implications.

The use of cold weather winter fill was pioneered at Suncor, see McRoberts et al. (1983) and has been used extensively since that time at Suncor, and then at Syncrude, see also Cameron and Fong (2001) and has become the norm. This approach began at Suncor following from the observations that shells of winter constructed waste dumps had more favorable geotechnical properties that summer fills built in the wet summer weather. The development of heavy haul trucks has favored this application as insitu ground temperatures can be retained within the large volume of fill being transported, and the fill can be quickly compacted by the haul trucks once it is spread by dozer.

Winter construction also affects cell sand placement, especially due to fog generated by sluicing operations in the cells. While it is possible to run all weather operations sand capture rates in cells suffers.

CT & Thickened Tailings

Non-segregating hydraulically tailings such as CT, NST, or similar thickened products are too wet to be self-supporting. Such tailings cannot form any significant beach slope given the mechanisms of movement within the deposit slope as it is formed. Such tailings require full support in the initial deposition cycle, although such tailings will eventually consolidate, develop a crust, and support reclamation covers.

Retention for such tailings requires a Centreline or Downstream Method as stepping out over CT

deposits does not appear practical. Given the current geotechnical data base for such tailings, and the times required for consolidation it is unlikely that an Upstream Method can be contemplated for any significant stepouts over anything but the highest SFR CT. However depending on staging of construction it is possible to raise the upstream dam slope steeper than the downstream relying on the fluid weight of the non-segregated deposits to support the upstream slope

The geotechnical basis for CT is non-segregation, and consideration must also be given to end-of-pipe effects, mixing, and the effects of shearing on disrupting the segregation boundary. One way to control energy effects is by on-pond operations with sub-CT tremie deposition. However this requires a pond and therefore relatively costly dams to support a water cap.

Stacked Tailings Dry Tailings

Recently, a renewed interest in the oilsands surrounding so-called stacked tailings has been resurrected in combination with stand-alone technology for dealing with fines. So called "dry" tailings are generally loose on deposition and cannot be reliably considered self-supporting unless compacted. The industry chooses to refer to tailings products such as filter tailings, or cyclo-stacker sands as dry, which is reasonable as compared to the same hydraulically deposited sand. However, such sands still contain significant water content, potentially well above the optimum. This indicates problems with both trafficability and self supporting capability.

The potential for liquefaction of loose tailings sands in the design of oil sands retention structures was first identified by Hardy (1967) who stated:

> *…"my opposition to your application was very emphatic that a major problem existed with the stability of sand tailings if they were discharged from a stacker, or alternatively by hydraulic procedures. Technically my position has always been that the instability of sand resulted from the low density assumed by the sand when stacked or deposited hydraulically. There never has been any question but that it was possible to produce a stable sand from the tailings if they could be sufficiently densified by compaction. The difficulty has always been to devise an economic procedure … and compaction achieved" [underlining added].*

In these early days potential consideration was being given to disposing of "dry" sand using the German conveyor belt / stacker dumper technology. Experience highly relevant to this potential failure mode can be found in the stacker or spreader dumped overburden sands in the German brown-coal strip mines, see McRoberts et al (1984). Significant perimeter pit dewatering is required to excavate these sands but in addition it is continued until well after the backfilled slopes are dumped with the express purpose of controlling liquefaction failures. McRoberts et al (1986) reported on the state of lean oil sands fill placed by a simulated stacker-dumper and reported a sensitivity to liquefaction. More recently Tiedemann and Nestler (1998) report on the method for stabilizing sand dumps formed by stackers which are prone to liquefaction. They note that in the former East Germany that some 450 dump slopes of stacked sand are thought to be unstable due to liquefaction concerns. Recent oil sands trials with cyclo-stacked sand have also confirmed looser densities.

This is not to say that sand stacking cannot be adopted for safe retention of sand tailings, but that the potential for liquefaction must addressed during design.

Environmental Factors

The effective and economic resolution of environmental factors requires consideration by the geotechnical engineer in design and construction. These issues are beyond the scope of this paper. Considerations such as control of environmental impacts of foundation seepage, the impact of seepage on reclamation covers require multi-discipline inputs. The long term integrity of the closure landscape and resolutions of the dichotomy between the theoretical concept of "maintenance-free" versus the inevitable realities of custodial care must also be addressed.

DEVELOPING THE DESIGN CROSS SECTION

The development of a safe design cross-section is the focus of geotechnical effort in tailings retention design. The importance of fitting the design to the dictates of tailings management, mine operations, and available fill types cannot be overstressed.

The 3 basic methods for tailings dam construction are: Upstream [modified], Centerline an Downstream. These methods have all been used or considered in oilsands retention structures at one time or another. Some of the drivers in arriving at a suitable design are discussed as follows.

Fill Types

The first issue for the designer is matching the requirements of the tailings plan and available materials both overburden and tailings sands. Leases with high fines contents in the ore body, and a tailings plan that seeks to achieve a high utilization of CT / NST, are ironically short of sand. A lease with dense relatively dry materials, either Quaternary deposits, Cretaceous clay shales, and reject McMurray formation can supply reasonable overburden for dam construction. For leases with a high proportion of wetter deposits the conflicting demands for plating of waste dump construction puts additional pressure on higher quality fills required for dam construction. This problems ripples through the design for external tailings, into the inpit structures, and in fact essentially controls the mine plan. Having then addressed materials availability, the designer must address how to combine the different material in a safe structure.

Foundation Stability

Weak foundations such as pre-sheared Kc clays, near surface Km clay rich facies, and thick deposits of Quaternary clays control the overall downstream slope for external tailings dams. Inpit dams can also require flatter slopes to manage weak basal clays or pond muds within the Km, and Paleo-clays at the limestone contact.

Leases with Kc clay-shales deposits have significant slope stability challenges for external tailings structures and/or ring dykes surrounding the mine pit perimeter. These shales are generally found to be pre-sheared and exhibit low strength near the residual angle. In addition, these clays can exhibit a range of pore pressure induced by construction. Adopting conservative strength and pore pressure parameters and a minimum acceptable FoS of 1.3 in accordance with Canadian Dam Association standards can readily lead to slopes as flat as 17-20H:1V, especially if the Quaternary cover in the passive toe area is relatively thin.

Several strategies have evolved to deal with the design uncertainties introduced by designing on stability and FoS, but monitoring on deformations. To elaborate on this, the current state-of-art is lacking a well developed, coupled analysis between deformations and stability for construction over clay-shales. How much deformation is excessive involves a considerable degree of judgment and prudence, given the consequences of failure. However, one strategy which can at least reduce initial capital expenditures is to start with relatively steeper slope as for example indicated by case records. The structure is monitored and in the event of movements pre-planned contingency measures are executed. This approach requires that toe areas reserved for stabilization berms are clearly identified. The other option available is stepping out over upstream beaches into pond and this option has been used. This however reduces available tailings volumes.

Internal Erosion and Piping in Overburden Fills

Internal erosion or piping is a major cause of failures of dams - reported worldwide - that have not provided sufficient defensive measures against this mechanism. Homogenous earth fills are highly sensitive to internal erosion focused in defects that can grow or tunnel leading to rapid loss of contents. One source of internal erosion is flow along defects or cracks that exist or are induced in the dam. The potential source of defects are many ranging from construction defects at lift contacts, cracking induced by differential settlement, or by hydraulic fracture. These mechanisms can negatively interact and can be primarily thought of as flow from the pond down-gradient to the exit point. This design concern also exists at the relatively steep abutments with pit walls. The other form of internal erosion that can develop in sand is “roofing”. When sand erodes under a cohesive

"roof" back-sapping of an erosion tunnel from an exit point up-gradient to the pond is possible.

Internal erosion develops rapidly and it is not safe or practical to contemplate an observational approach. Therefore defensive measures in-depth are required. The first line of defense for overburden structures is to specify a wide core of well compacted, low permeability fill. In most cases the second line of defense is a chimney filter-drain.

For low permeability overburden structures the time to develop a steady-state seepage regime is likely in the order of many decades or longer. The real threat is flow in defects. Cracks can develop with any configuration short-circuiting the presumptive transient and steady state flow paths to drainage boundaries. The primary control system is a chimney filter-drain that intercepts all possible defect dominated flow paths, and an offtake system that ensures the chimney can drain. The chimney basically must function as a "crack-stopper" in the sense that the filter component stops eroded fines at the overburden to filter contact.

Oil sands practice is usually to require a chimney up to the same elevation against which fluids [water or MFT] is impounded. MFT is considered as at least if not a more significant threat compared to water. In the case of tailings sands over overburden section, once well developed BAW zones are developed the chimney is no longer needed. The second line of defense has become the subaerial BAW zone. This sand is considered to be available to plug cracks, and in any event limits the flow from the pond to the putative crack. In this design configuration MFT and bitumen in the pond also seals the tailings sands at the pond contact.

An alternative second line of defense has been developed for inpit dams on the Syncrude lease by over-weighting and rigorous fill specifications. Rigorous construction specifications (including elimination of any freezing in the fill) coupled with an over-build, weighting the possible flow paths. This weighting reduces widening of existing defects and of hydraulic fracturing inducing new cracks or defects. The techniques to be considered were presented by Barlow et al. (1998) and further described by Cameron et al. (2008). Cameron and Fong (2001) provide an example of the performance of the Highway Berm built according to these concepts. For those geotechnical engineers contemplating such a design approach it is necessary to have a sound operational control on fill placement and continuous geotechnical monitoring, with the ability to stop construction and address deficiencies. The stringent specifications required for this method are addressed by Cameron et al (2001).

Liquefaction

Working in the 1960's Dean RM Hardy recognized the potential for liquefaction of the downstream section of Tar Island Dyke, and consulted with Professor Arthur Casagrande to develop a cross section of sufficient compacted cell width to contain beached tailings sands if it liquefied. This basically introduced the precautionary principle, still followed today in hydraulic fill construction in the oilsands, that liquefaction should be assumed however potentially unlikely the triggering event might be.

There have been several liquefaction events in oil sands tailings ponds in the early days of lease development. These failures occurred on the upstream or pond side, when either BAW or compacted cell sands are rapidly placed over loose BBW. Some of these failures are discussed by Mittal and Hardy (1977) and in more detail by Plewes et al. (1989) who provide operational guidance in dealing with this type of failure.

Full scale oil sands field experience with stacked tailings types is not available. Some test trials have indicated that cyclo-stacker sand is relatively loose. Such sands if they become saturated could be vulnerable to static liquefaction. One mode for saturation is downwards seepage of water from the moist and loose tailings creating saturated conditions at the base of a dump.

On going research over the last 20 years indicates the ability of loose sand to self-densify with increasing effective stress, see McRoberts (2005). This is an important factor that can be considered in design. If sands do not meet certain minimum levels of densification, they are considered vulnerable to liquefaction and must be assigned a liquefied shear strength. Assigning an appropriate strength to liquefied sand has been the topic of considerable debate in geotechnical practice, and is still not fully resolved. Given that the onset of this condition

cannot be practically managed by the observational method, then prudence is required in setting liquefied design strengths.

The seismic risk levels are low in McMurray reflecting the tectonically quiescent nature of the interior craton. Structures designed to accommodate the possibility of static liquefaction and which meet standards for static stability will always prove to be able to withstand realistic seismic loadings.

Internal Drainage of Sand Sections

The provision of internal drainage has been a central feature of slopes constructed from cell sand. The main failure mechanism for uncontrolled seepage on sand slopes is spring sapping leading to gully formation. Oil sands tailings are highly erodible and once gully formation begins the focusing of subsurface flow into a gully from both seepage and runoff results in rapid progression of a gully. Other surface disruption mechanisms include heaving due to pressure build-up under frost penetration layers and lower permeability reclamation covers. In order to provide local surface stability against these mechanisms, internal drainpipes are required to keep the phreatic surface well contained within the slope, and where they have been deployed good performance has been achieved.

All tailings types, including sand, are also potentially vulnerable to internal erosion considering the mechanisms first described by Bligh in the 1890's and summarized by recently by Schmertmann (2000). There has been no evidence of such a mechanism developing in oil sands tailings slopes with no 'roofing'; that is, where the sands above the phreatic surface are able to collapse into the pipe. However designs which contemplate overburden over sand on a downstream seepage face could readily permit a roofing mechanism to develop, and should be avoided.

Control of these mechanisms can obtained by internal drains installed to maintain the phreatic surface well within the sand slope, and where flow is directed to appropriately designed drains. For the filtering component of the drain design is to vital to ensure that sand loss into the drainpipe does not occur. This controls the potential for the internal erosion mechanism. The first drainpipes installed in Tar Island Dyke consisted of perforated galvanized metal pipe with a coke surround. The coarse coke produced at Suncor was selected as an economic alternative to gravel, and meet the filter rules for tailings sand. Syncrude's Mildred Lake Tailings Dam was not able to use coke as Syncrude coke is much finer grained. Instead perforated pipes with a zoned filter were adopted. Practice at Suncor then evolved to use HDPE pipes and a filter fabric and common practice is to now use the pipe/fabric system, sometimes with a backup granular surround.

Seepage analysis in support of drainage designs is common practice. In most cases however flow is dominated by downwards seepage during cell placement, and not flow from the pond. It is also of interest to comment that for most sand structures the main flow out of the dyke is not from the pond. In fact the presence of MFT and floating bitumen creates seals against the beach limiting the flux out off the pond and into the system. Generally it will be found that after cell construction ceases the flow to the drainage systems is due to the storativity of the cells and beach, infiltration of fresh water, and some flux through the developing pond bottom seals.

Foundation Seepage

Many of the current dams are founded on low permeability units and in general foundation seepage has not been a major geotechnical issue. One exception being the local presence of local sand channels incised into the lower permeability till, clay-shale and insitu oil sand. As new leases with thick granular deposits including buried Pleistocene channels are encountered more attention is being paid to geotechnical aspects of foundation seepage, along with the associated environmental aspects, see for example Stephens et al (2006).

Abutment Issues

Abutments designs are primarily an issue for inpit dykes. Abutments can either be the pit wall or in some cases a previously constructed dyke where a T-Alignment must be used based on the mine plan.

One interesting aspect of the oilsands is the effect of insitu stress release. Insitu Ko stresses are considered to exceed unity and possibly significantly higher. Stress release consequent on mining can cause both shear band

propagation along weak facies, and gas exsolution. These mechanisms can result in exfoliation type cracking behind the oilsands face creating jointing that offers potential leakage paths from the pond to the downstream.

With the advent of shovel mining the typical pit slope consists of a stair-step series of fall-down shovel slopes, and mine benches. In highly gassy ores, the oil sands slopes can flow or creep likely increasing the mass permeability of the slope thus effected. One measure that is taken in design is to flatten the abutment slope, creating a notch within which the low permeability element of the dam core can be inserted. This requires advance planning to ensure that the necessary setbacks are available.

Typically fill compaction is provided by heavy haul trucks. Given the size of these trucks, special provisions are required so that the truck wheels can compact right up to a prepared mine face. This typically requires that the fill dozer places a small ramp up the slope and backs up the ramp, into the slope.

Risk Management

The failure of any one of the major tailings dams in the Fort McMurray area is not ponderable. At the same time there is continued pressure to innovate and to deal with uncertainty in a risk adverse manner. One method of allowing design to evolve is the observational method.

The observational method provides a powerful method for dealing with geotechnical uncertainty of key parameters. The method allows the design to be based on reasonable parameters, to monitor, and to execute pre-planned contingency measures if performance is outside of tolerable limits. The method also explicitly requires that the monitoring and execution plan can be implemented within the constraints of the mine and tailings plans. That is if the contingency plan, cannot be practically executed due to timing, lack of resources or alternative tailings storage the method cannot be adopted. It is also stressed that the designer must clearly communicate the need for a comprehensive monitoring plan, and timely observations and interpretation of key performance indicators. Handford et al (1982) followed by Nicol (1994) provide an early example of the use of the method for foundation stability concerns at Syncrude. McRoberts et al (1995) report on the application of the method for Tar Island Dyke on the Suncor Lease.

The observational method is not suitable for considerations of internal erosion / piping within overburden structures, and for some issues around the control of static liquefaction.

CLOSURE

The opinions expressed herein are those of the author and do not necessarily reflect those of Amec, or of his many colleagues. Thanks are due to Bill Chin, Gord Pollock, and Angela Küpper who commented on a draft.

REFERENCES

Barlow P, McRoberts, E.C., Lach P., and Cameron B. 1998. Mature Fine Tails Hydraulic Fracturing Study. 51st Canadian Geotechnical Conference Edmonton

Chan W.K., McRoberts, E.C., with J. Martschuk and W. K Performance Review of Tar Island Dyke. Seventh Pan American Conference SMFE Vancouver, 1983.

Cameron R. and Fong. V. 2001 Performance of a quasi-homogenous earthfill dam retaining 35 m of tailings fluid with no filters or clay core: Syncrude's Highway Berm. 54th Canadian Geotechnical Conference

Cameron R., Mimura W., Fong V., and Lussier L. 2001 Detailed construction procedures and considerations in Syncrudes's quasi-homogeneous earth fill dams. 54th Canadian Geotechnical Conference

Cameron R., Madden B. and Danku M. 2008 Hydraulic fracture considerations in oil sand overburden dams. GeoEdmonton 2008. 61st Canadian Geotechnical Conference

Handford G, Buckles, J., Ellis H and Khan F. 1982 The use of the observational approach in the design and construction of the Syncrude tailings dyke. Seminar "Geotechnical Aspects of Mine Design and Containment" April 1982 University of Calgary.

Hardy R.M. 1967 Report to C.H.Thayer President GCOS 9 November 1967.

Hardy R.M. 1974 Tailings Dams EIC Western Regional Tar Sands Conference Edmonton Alberta

McRoberts, E.C., Kupper A. and Small A. 1995. Foundation Considerations for Tar Island Dyke. 9th Annual Symposium Vancouver Geotechnical Society "Construction on Soft Soils and Peat"

McRoberts, E.C., J. Marschuk and W. K. Chan. 1986 Geotechnical Considerations of Stacker Dumped Spoil at Suncor. International Symposium on Continuous Surface Mining, Edmonton, Alberta, Sept. 29 to Oct. 1, 1986. Bi-Tech Publishers Ltd.

McRoberts, E.C., T. S. Goloskinski and W. F. Gilmore. Assessment of European Bucket Wheel Excavator Technology. *CIM Bulletin* Vol. 77, No. 867, 1984.

McRoberts, E.C., with J. Martschuk and W. K. Chan. Winter Fill Construction and Performance at the Suncor Tar Sands Mine. VII Pan American Conference SMFE Vancouver, 1983.

Mittal H.K. and Hardy R.M. 1977 Getoechnical aspects of a Tar Sands tailings Dyke. Proc Conf Getoechnical Practice for Disposal of silid waste Management ASCE Ann Arbor Mich June 13-15 1977

Nicol D 1994 The Syncrude Mildred Lake Tailings Dyke Redesign. ICOLD 18th Commission Internationale des Grands Barrage. [Q70 R12] Durban.

Plewes H.H., McRoberts, E.C. with, H. D. O'Neill and W. K. Chan. 1989. Liquefaction Considerations for Suncor Tailings Ponds. Second Alberta Dam Safety Seminar, Sept. 1989.

Morgenstern N, McRoberts E.C. and A. E. Fair. 1988. Geotechnical Engineering Beyond Soil Mechanics - A Case Study, *Canadian Geotechnical Journal* Vol. 25 No. 4.

Stephens B,, Langton C, and Bowron M, 2006 Design of Tailings Dams on Large Pleistocene Channel Deposits a Case Study – Suncor's South tailings Pond. CDA Conference Quebec City September 30 – October 5 2006.

Tiedemann J and Nestler P. 1998 "A new procedure for the stabilization of soils prone to liquefaction". 8th International IAEG Congress Balkema Rotterdam.

THE CHEMISTRY OF OIL SANDS TAILINGS: PRODUCTION TO TREATMENT

R.J. Mikula, O.Omotoso, K.L. Kasperski
Natural Resources Canada, CANMET Energy Technology Centre–Devon, Devon, Alberta

ABSTRACT

Water availability and water quality are critical to surface mined oil sands operations. The zero discharge water policy that the surface mined oil sands plants work under not only limits tailings treatment options, but also implies a future requirement for water treatment. In general, water chemistries that result in favourable tailings properties are thought to be detrimental to the extraction process. This paper discusses the water chemistry impacts of various tailings treatment options that lead to changes in the release water quality, and to increases in the recycle water volumes. Increasing the recycle water volume means less dilution or make up water from the river, ultimately increasing the total ionic strength in the recycle water to extraction. The advantages and disadvantages of various consolidated, composite, non-segregating, and other dry stackable tailings treatment processes are outlined. Some myths about both the short and the long term behaviour of these deposits are discussed from a chemistry point of view, along with an example of the use of mature fine tailings (MFT) to control water chemistry in the extraction process water. This paper also provides an overview of several concepts and mis-conceptions about the role of water chemistry in determining tailings behaviour, and perhaps more interesting, the role of clays and tailings management in determining recycle water chemistry. Examples are largely drawn from the last 15 years experience in consolidated tailings (also known as composite tailings or non-segregating tailings).

INTRODUCTION

Tailings management in surface mined oil sands is a very complex endeavor [(1)]. In order to appreciate the impact of various tailings management options in terms of water chemistry, and vice versa, it is useful to apply several simplifying assumptions. In this discussion, the tailings management options and their impact on recycle water chemistry are simplified, and where possible, the shortcomings of these simplifications is noted. It is possible to be much more rigorous when discussing the impact of water chemistry on tailings behaviour because this is more amenable to laboratory testing.

In general, there are three oil sands tailings streams. These are the coarse tailings from the primary bitumen separation step, the fine tailings from the secondary and/or tertiary bitumen recovery step, and the froth treatment tailings. Solvent addition to the bitumen froth in the froth treatment process reduces the viscosity and allows for the removal of the froth minerals and water. The resulting froth treatment tailings are particularly important because of the environmental impact of the residual solvent or diluent. In terms of their contribution to the total tailings volume, however, they represent a relatively minor stream[(2,3)].

Surface mined oil sands convention defines sand as the mineral fraction greater than 44 μm and the fines as the mineral fraction less than 44 μm. The coarse tailings are predominantly made up of the sand fraction, and the fine tailings are predominantly made up of fines. It has been demonstrated that it is the clay fraction, both as a size and in the mineral form that defines the tailings properties, and in particular the tailings volume and water holding capacity. For comparison purposes, however, it can be a useful shortcut to discuss the fines fraction, with the underlying assumption that the clay to fines ratio is 0.5. Water chemistry is important in determining the charge associated with a clay particle and its subsequent settling and consolidation behaviour. The charge exchange properties of the clays in turn can affect the water chemistry. The present discussion will present a series of common examples where process water chemistry has affected the clay properties, and less common examples where clay properties have affected process water chemistry[(4-7)].

RESULTS AND DISCUSSION

Cation Exchange

The cation exchange capacity (CEC) of clays is a function of the type of clay, and it is well known that a variety of clay minerals have been observed in oil sands. Regardless of the clay type, there is a simple relationship between the divalent and monovalent ions in solution and those located at the cation exchange sites on a clay particle.

$$ClayNa_2 + Ca^{2+} \leftrightarrow ClayCa + 2Na^{+}$$

This equation, more rigorously would include magnesium and potassium, but for the purposes of this discussion, the most dominant ions will be considered. An equilibrium between calcium on the clay and calcium in the water is established according to the following:

$$K_{eq} = ClayCa \bullet \left[Na^{+}\right]^2 \Big/ ClayNa_2 \bullet \left[Ca^{2+}\right]$$

Solution of this equation is an iterative process, and leads to the relationship shown in Figure 1. Figure 1 plots the molar fraction of calcium on the clays to calcium in the water.

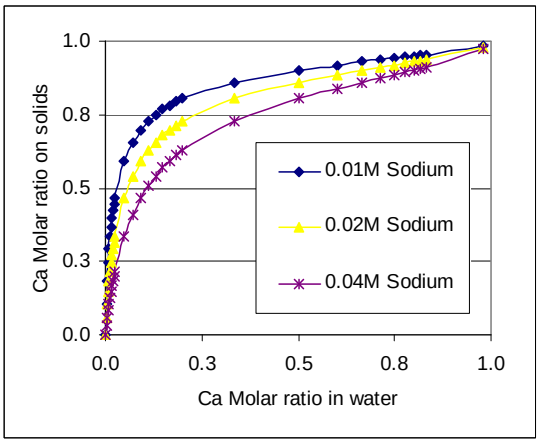

Figure 1. The molar ratio of calcium on clays versus calcium in the water phase for a variety of sodium concentrations.

It can be seen that the divalent calcium ion concentrates on the clays relative to the aqueous phase. Affinity for the cation exchange sites on the clays is dominated by the relative charge on the cation, but it is also affected by ion size and hydration energy, and this leads to slight differences between calcium and magnesium, and sodium and potassium.

Cation exchange and the affinity of calcium for the clay surface play an important role in almost all tailings treatment strategies. At high levels, calcium can inhibit the bitumen flotation process, so controlling calcium levels in the recycle water is an important part of any tailings treatment strategy. Implementation of the consolidated tailings process by Suncor in 1994 by using gypsum as a process aid meant that calcium control involved both optimization of gypsum dosage to obtain the required tailings properties, and at the same time minimizing calcium and total dissolved salts in the resulting recycle water. An interesting aspect of the calcium control was the role of cation exchange in maintaining low calcium levels in the recycle water.

Non-Caustic or Low pH Extraction

The development of the OSLO process as an alternative to the traditional Clark hot water process promised to improve tailings properties. This would occur by avoiding the dispersive water chemistry associated with elevated bicarbonate levels in the Clark process recycle water.

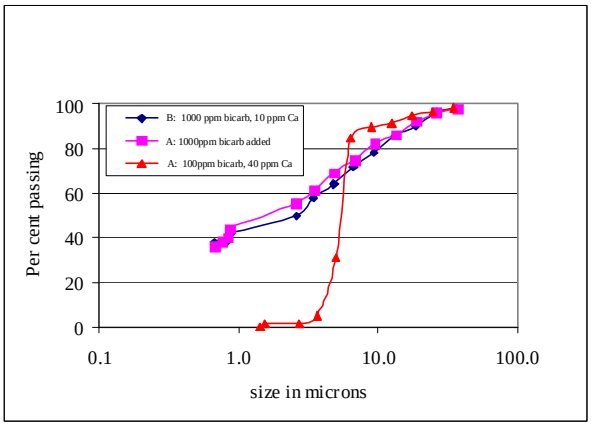

Figure 2. Apparent particle size for identical ores extracted with river water (40ppm Ca) and with Clark process recycle water (1000ppm bicarbonate).

Figure 2 summarizes the purported advantages of a low pH or non-caustic extraction process. In the absence of an elevated pH in the extraction process, bicarbonate ion concentrations are low, and the clays effectively behave as though they are larger than 10 microns in size. Since the ore is a major source of bicarbonate ion in most oil sands leases, long term recycle can elevate the bicarbonate ion concentration even without the NaOH additive sometimes associated with the Clark hot water process. The non-caustic OSLO process still disperses the clays, it is just that in the absence of a dispersive water chemistry, the clays behave as if they have an effectively larger particle size. This can be seen in Figure 3 where the same clay suspensions are tested for their degree of flocculation or elastic modulus. The OSLO tailings show a measurable G' or elastic modulus at a much lower solids content than the same tailings from the Clark extraction process. This would not happen if the clays were simply still present as undispersed 5 to 10µ tactoids. Figure 2 shows that when the water chemistry is changed after the fact, the OSLO tailings exhibit exactly the same particle size distribution as the Clark tailings. This shows that both extraction processes produce the same tailings streams.

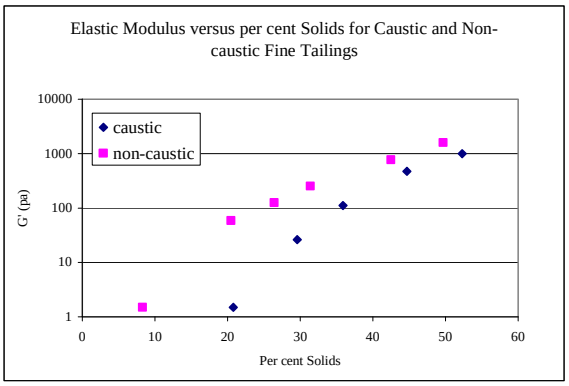

Figure 3. The G' or elastic modulus of the dispersed (caustic) and undispersed (non-caustic) tailings from Figure 2. This illustrates that the undispersed tailings are interacting more strongly, and that their behaviour as apparently larger particles is a function of the water chemistry.

A positive tailings consequence of the OSLO extraction water chemistry is a significantly compressed transition zone in the tailings pond. Even though the final settled volume of the two process chemistries results (over long periods of time) in the same mature fine tailings storage volumes, the OSLO tailings settle much faster. This will mean that the volume of material in the transition zone between 1% and 30% solids will be considerably smaller. This volume can represent a significant proportion of the available recycle water capacity.

The Consolidated Tailings Process

The basis of the consolidated (or composite) tailings (CT) process is the creation of a mixture of clays, silt, and sand that is pumpable and that will rapidly consolidate to more than 80 wt% solids to create a trafficable deposit. The source of the sand is typically a cycloned sand tailings at about 70 wt% solids, and the clays and silt can come from mature fine tailings consolidated in a recycle water pond, or from a thickener underflow (typically about 30% solids). The clays and silt usually need a chemical amendment in order to have a viscosity and yield point that can support the loading due to the sand. The ability of the clays and silt to support the sand is critical to the creation of a suitable non-segregating (NST) or CT process.

A chemical amendment such as gypsum is used to adjust the viscosity and yield point of the fluid tailings (clays and silt), so that the sand can be supported and provide some consolidation force to the mixture. A typical CT or NST mixture or recipe would be 60% solids, with a sand to fines ratio of about 4 to 1, a clay to water ratio of 0.1 or greater, and 600 to 1000 ppm gypsum (on a weight gypsum to weight slurry basis). It is clear that it is the fluid tailings properties, or clay content that determines CT performance. A viscosity of about 200 mPa·s and a yield point of about 4 Pa·s in the fluid phase will generally be adequate for the creation of a non-segregating mixture. Although it may be potentially attractive to measure fluid phase rheological properties from a process control perspective, there are so many interferences with this measurement that it is generally more practical to simply measure the segregation behaviour directly for a variety of mixtures. Figure 4

shows a series of experiments where the clay content has been varied for a 4.5 to 1 sand to fines CT with 900ppm gypsum addition. The content has been varied for a 4.5 to 1 sand to fines CT with 900ppm gypsum addition. The series of lines represents various degrees of segregation or fines capture. The lowest line represents 100% fines capture, and the highest, >95% fines capture. Note that these are all experimentally determined segregation boundaries for each of the 6 different clay contents. The curved line represents the line of constant clay to water ratio, at 0.1. In the absence of any additives, the clay to water ratio determines the rheological properties of the fluid phase, and therefore the segregation behaviour. In this series of experiments, the segregation behaviour does not follow the line of constant C:W. This can be understood in terms of the 900 ppm gypsum addition, which is on a slurry weight basis. As the total clay content decreases, the amount of gypsum per unit clay increases, a factor which increases the viscosity and yield point of the fluid phase. As a result, the measured segregation boundary does not follow the constant C:W ratio because the gypsum dosage per clay is not constant along that line.

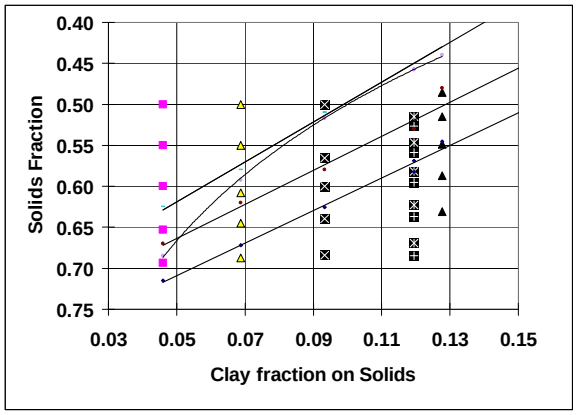

Figure 4. Segregation boundary lines for a series of 30 experiments. The curved line represents a constant C:W of 0.1.

Adding more gypsum than is necessary to maintain the non-segregating nature of the CT mixture will unnecessarily impact the total ionic strength of the CT release water, possibly making it difficult to re-introduce it into the recycle stream. CT or NST production on a commercial scale involves the combination of a sand stream, a clay and silt stream, and the appropriate additive. Ideally, the properties of the mineral slurries would be fixed, and one would only need to determine a gypsum dosage with the appropriate safety factor to maintain the non-segregating and rapid settling or water release properties of the CT mixture.

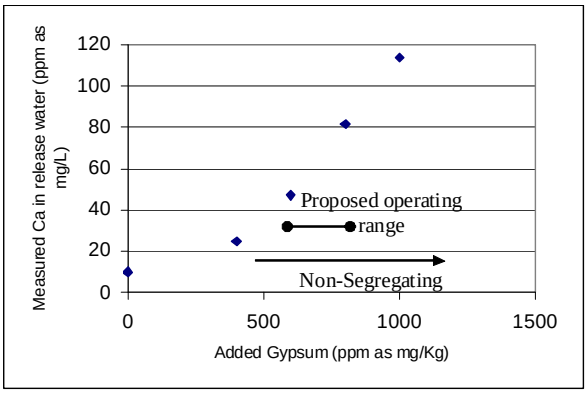

Figure 5. Operating window for the CT process using gypsum.

Since the sand slurries available for CT production are generally about 70% solids, for a C:W ratio in the CT mixture to be maintained, a mature fine tailings or thickened tailings with a C:W of >0.2 is required. For a 60% solids CT mixture, the gypsum addition rate and the resulting release water chemistry are shown in Figure 5. Figure 5 represents an operating window for the CT process that incorporates enough gypsum to ensure a non-segregating behaviour, and at the same time, keeps the calcium level in the release water at manageable levels.

There are many additive options that can achieve the required strength change in the mature, or fluid fine tailings so that it can support the sand fraction. Suncor has implemented this process using gypsum as the additive to manipulate the fluid fine tailings strength [8]. Other process aid options include carbon dioxide, lime, acid and lime, and polymers[9-11]. Tailings management options known as composite tailings, or non-segregating tailings are simply alternative names for the same basic process, with perhaps some modification to the sand to fines ratio, solids content, or chemical additive used. The impact on the recycle water chemistry will be a function of the choice of additives. On the other hand, as discussed in the previous

section, choice of extraction process can also determine the performance of the CT or NST process. With a recognition that control of the total ionic strength in the recycle water to extraction is important, it might be more efficient to modify tailings properties after the extraction process.

Modification of the tailings properties to enable NST or CT production and at the same time, minimizing impact on the recycle water chemistry, has led to the investigation of a wide variety of alternatives. The use of non-caustic tailings is one approach, since the stronger interaction of the clays in the OSLO (or other non-dispersive extraction processes) should mean it will be possible to create a non-segregating or CT mixture will less additive.

Figure 6 shows that with no chemical additive, the segregation boundary for fine tailings from a non-dispersive process is at a clay to water ratio of 0.13 compared to C:W of 0.17 for the Clark process tailings. With 900ppm gypsum in a CT mixture, the segregation boundary is at C:W = 0.08 compared to 0.1 for the Clark process CT discussed in earlier. The addition of polymer also has a significant impact on the observed segregation boundary, but without impacting the release water chemistry.

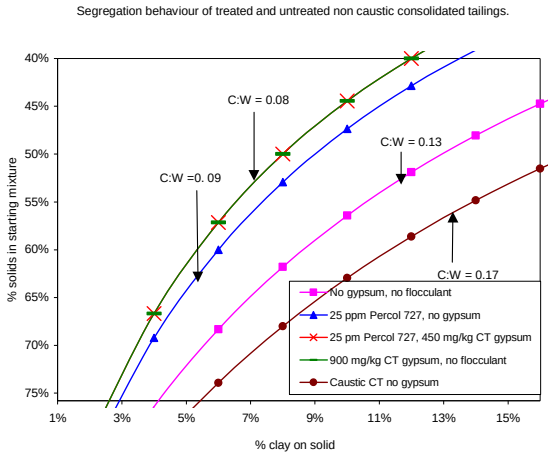

Figure 6: The segregation boundary for a variety of alternative tailings water chemistries and CT additives.

Although polymer addition can have significant positive impacts on the segregation boundary in the sense that a lower clay to water ratio can still create a non-segregating mixture, they often inhibit the consolidation rate or the rate at which water is released from the CT or NST mixture.

Of all the choices, the carbon dioxide process proposed for commercialization by Canadian Natural Resources will have the most beneficial impact on recycle water chemistry. Because of the years of operational experience, however, the gypsum process for CT used by Suncor[8], has the most interesting examples of the linkage between water chemistry and tailings behaviour.

Tailings Clays and the Impact on Water Chemistry

Tailings management practice, and in particular the drive towards dry stackable tailings, will have a variety of impact on recycle water chemistry. From a mine management perspective, and in particular the tailings volume control, there will be no benefit to a tailings treatment process that separates water from solids, leaving a water chemistry that is unsuitable for use in the extraction process.

The relatively intractable nature of the fluid fine tailings in surface mined oil sands means that some tailings water chemistry modification will be required. This will have an obvious effect on recycle water quality and the implications of these can be relatively straightforward to predict. Less obvious might be the consequences of dry stackable tailings technology on the water quality and quantity due to the reduced requirement for make up water. The following sections discuss some interesting examples of the role of clays in determining recycle water chemistry, in controlling recycle water chemistry, and implications of dry stackable tailings on recycle water chemistry.

Clay control of calcium in the extraction process

The cation exchange on the clays discussed earlier has a significant impact on recycle water chemistry. Figure 7 shows the relationship between total divalent ions in the recycle water from a series of bench scale extraction tests with a variety of ores. The extraction water was river water with approximately 40ppm calcium and 12 pm

magnesium (1.5mMoles of total divalent ions). The higher the clay content in the ore, the greater is the ability (via cation exchange) for the clays to take calcium and magnesium out of the extraction recycle water.

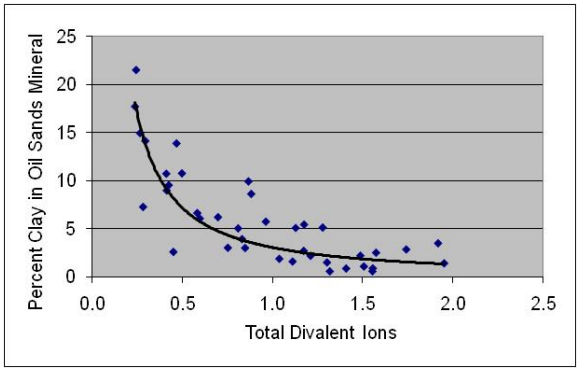

Figure 7. The relationship between divalent ions in the tailings recycle water and clay content in the ore. Total divalent ions is in mMole.

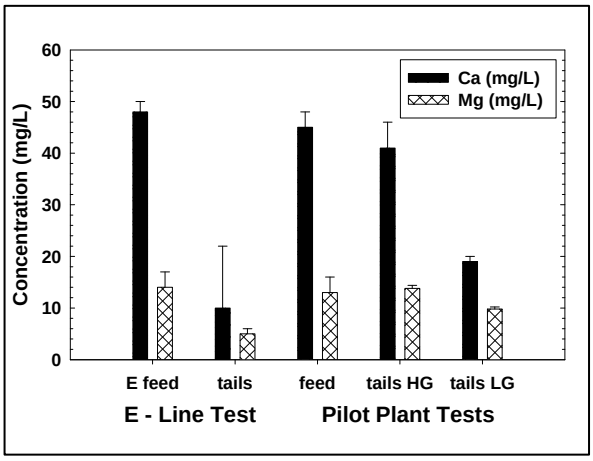

Figure 8. Calcium and magnesium reduction during pilot and commercial scale evaluations of the non-caustic extraction process.

Figure 8 shows similar reductions in calcium and magnesium in the process waters during pilot and commercial scale evaluations of the OSLO non-caustic extraction process. Evaluation of calcium uptake from these types of studies, along with tests of oil sands clays showed that calcium uptake was 0.0006 gm of calcium per gram of clay present. This simple relationship allows for calculation of the impact of clay cation exchange across a wide variety of process conditions and sample types. This simple shortcut works because on average the cation exchange capacity (CEC) for oil sands clays is about 16meq per 100g. In addition, the process water chemistry is elevated in sodium relative to calcium, meaning that for a wide variety of process water chemistries, the relevant area of the cation exchange curve shown in Figure 1 is in the bottom left corner, where the calcium on clay to calcium in the water is similar for the wide range of sodium concentrations plotted. When details of the water chemistry and charge or cation exchange capacity are known, it is a straightforward calculation to determine the final water chemistry, and therefore the clay behaviour, either in the CT process or in the recycle water pond.

The use of clay to control calcium in the CT process

When calcium is added to water with high levels of bicarbonate, as in the gypsum CT process, there is a potential for calcium to be removed from the water phase by precipitation as calcite. The cation exchange reactions occur very quickly relative to the precipitation reactions. At pH less than about 8.5, the bicarbonate ion dominates the water chemistry, leaving relatively little carbonate, resulting in a slow rate of calcite precipitation.

Figure 9 shows that calcite precipitation occurs over days, while the calcium changes due to cation exchange shown in Figures 7 and 8 occur almost immediately. With knowledge of the clay properties (cation exchange capacity most importantly), the water chemistry can be predicted, and with the water chemistry, the clay settling and rheological properties can be estimated as well. In terms of the gypsum CT process water chemistry, this slow precipitation of calcite will result in a shift in the calcium on the clay surface to the now depleted water phase. Over long periods of time, this will mean that the net effect on water chemistry will be negligible as the calcium and sodium concentrations tend to the original. In the time frame required for this to happen, however, the CT mix will have consolidated to more than 80% solids, a point where the water chemistry is less important in defining the rheological properties. This is seen in Figure 3 where the

elastic modulus is less sensitive to water chemistry as the solids fraction increases.

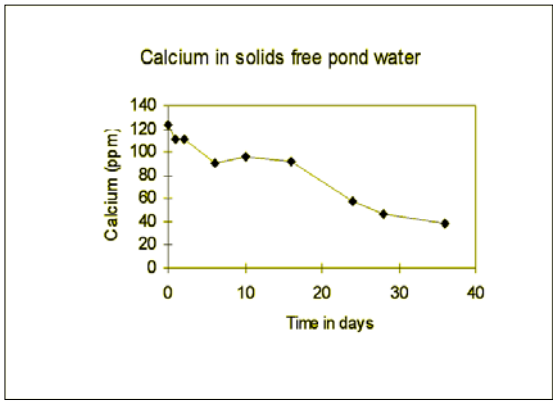

Figure 9. The relatively slow change in calcium concentration due to calcite precipitation in an oil sands process water.

Commercial implementation of the consolidated tailings process by Suncor in the mid 90's used gypsum as the process aid to manipulate the fluid fine tailings properties. Figure 5 shows the desirable operating range in terms of the gypsum addition. When properly controlled, the release water calcium would not exceed 80ppm, and would normally be approximately 50ppm. This release water is combined with the inventory of water in the recycle pond and should result in a net calcium concentration of less than 20ppm in the extraction process.

For a variety of reasons, the gypsum dosage slowly moved out of range to a point where the CT release water calcium exceeded 160ppm. Figure 10 shows that in spite of this significant increase in the resulting recycle divalent ions (in excess of 80ppm calcium equivalent), there was no significant impact on the bitumen recovery in the extraction process. There was, however, a significant increase in heat exchanger scaling that required control of calcium to the originally targeted levels.

An elegant method was used to control calcium with the fine tailings from the extraction process. With knowledge of the cation exchange properties of the clay in the ore, and the reaction kinetics of calcite precipitation, it was determined that calcium could be controlled if the CT release water would first be combined with fine tailings from the extraction process.

A combination of cation exchange and calcite precipitation due to this mixing would much more rapidly decrease calcium concentration in the extraction process water. Figures 11 and 12 show the predicted actual calcium concentrations for both the recycle water and the release water (as the gypsum dosage to CT returned to normal).

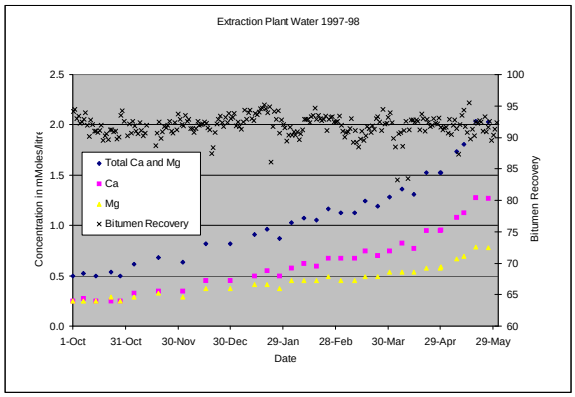

Figure 10. The relationship over several months between extraction process water calcium content and bitumen recovery.

In hindsight, the correspondence between the predicted and measured calcium does not appear so spectacular. At the time, however, the model predictions were based on the clay fundamental properties. In the case of the recycle water chemistry, the model accurately predicted the rise in calcium concentration as the CT process gypsum dosage was increasing.

Once the CT gypsum dosage was brought under control, the prediction for the decrease in the release water calcium in the release water was also very good. The actual modeling also considered magnesium, potassium and sodium, but these are not shown in order to maintain clarity.

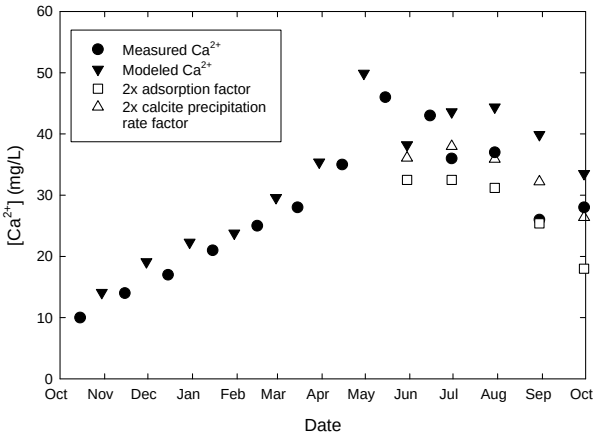

Figure 11. Actual and predicted calcium concentration as the CT process gypsum dosage increased. .

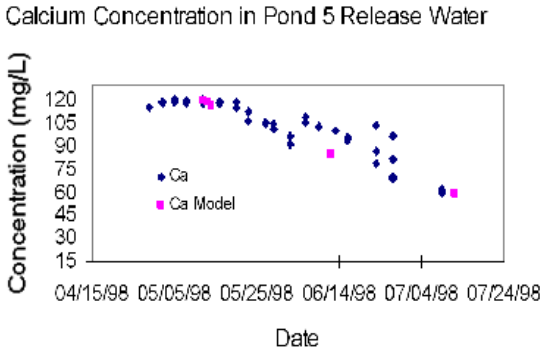

Figure 12. Predicted compared to modeled calcium concentration in the CT release water.

Recycle Water Chemistry Implications of Various Tailings Management Options

The previous discussion focused on the interesting interactions between clay type and water chemistry that can be important in controlling oil sands tailings properties. A more mundane, but in the end a far more important effect simply is the reduction in dilution water that will results from more aggressive tailings treatments.

The oil sands extraction process requires an elevated temperature, mechanical energy, and the appropriate water chemistry in order to achieve the high recoveries mandated by the current regulations. Although there is some debate as to the level of dissolved salts or total divalent ions that might impact the extraction process, there is no debate that at some point an increase in either or both will reduce recovery of bitumen. With the current policy of zero discharge of water to the environment, the extraction recycle water chemistry will inevitably increase to equal the dissolved ions in the connate water from the ore, diluted by the make up water. When one adds the impact of process aids, the total dissolved ions, and therefore the likelihood of an impact on extraction goes up proportionally [12-16].

For many ions, there can be cation exchange or other chemical and biological processes occurring which can alter the water chemistry. These processes are further complicated by separation of various water streams in the complex water and tailings management in a typical oil sands mining, extraction, and upgrading operation. If one looks at the operation as a whole, however, one can still quickly assess the broad water chemistry aspects of any of the dry stackable tailings options.

Table 1 shows the relative reduction in make up water required for a series of tailings management options that are being evaluated. Note that these are a function of the fines (with an assumption about the clay) content in the ore. The last column shows the relative increase in Cl content for a given tailings treatment option. In general, the creation of a dry stackable tailings would result in a reduction in the water lost to produce a barrel of bitumen from about four to about two. For an oil sands with 10% bitumen and 5% connate water, decreasing the amount of make up water required will increase the ionic strength by the same proportion. Any increase in ionic strength would be further magnified for operations which use process aids that alter the water chemistry. It is unlikely that ionic strength or divalent ions will be controlled without some form of water treatment. A move toward water treatment and discharge to the environment prior to the final reclamation might have to be considered in order to implement dry stackable tailings technologies.

SUMMARY

Although it is possible to characterize oil sands tailings clays in considerable detail, it is often not necessary when predicting the behaviour of fluid fine tailings. This is due to several factors. First, in spite of some wide variations observed in the clay content and clay properties over the Athabasca formation, or even over a given lease, these unusual clay types do not represent significant proportions of the total clay content. Second, there is usually some attempt at blending ores of widely different fines or clay content. This blending or averaging of properties is even more pronounced when dealing with MFT from a pond. In cases when clay type (properties) and content are important, it is possible to obtain the data required, either by sophisticated x-ray quantification techniques, or by using simpler methods that are known to correlate with the more detailed analyses. An example of the requirement for a more detailed clay characterization might be mud line or transition zone volume prediction where week to week clay properties can be significant.

As illustrated in the previous discussion, our fundamental understanding of clays and water chemistry in the various oil sands process streams is reasonably complete. It allows us to accurately predict the properties of important clay suspensions, and to understand not only the role of water chemistry in determining clay behaviour, but also the role of clays in determining water chemistry.

In the final analysis, in order to move away from wet landscape reclamation toward dry stackable tailings, there will be water chemistry implications that may require water treatment to control process water chemistry.

ACKNOWLEDGEMENT

The authors would like to thank PERD, the panel for energy research and development for financial support, and Suncor for permission to discuss the CT process water chemistry.

REFERENCES

Alberta Chamber of Resources. Oil Sands Technology Roadmap: Unlocking the Potential. Alberta Chamber of Resources, Edmonton, Alberta, 2004.

Kasperski, K.L., A review of properties and treatment of oil sands tailings. AOSTRA J. Res. 8, 11-53, 1992.

Fine Tailings Fundamentals Consortium, Advances in oil sands tailings research; Vol. 2 -12 and Vol. 3-52, edited by the Fine Tails Fundamentals Consortium, 1995.

Kasperski, K.L. and Mikula, R.J., Modeling the effect of gypsum addition on Suncor plant water chemistry: interim report. WRC 95-13 (CF) Natural Resources Canada, Devon, Alberta, 1995.

Mikula, R.J., Kasperski, K.L., Burns, R. and MacKinnon, M.D., The nature and fate of oil sands fine tailings in "Suspensions, Fundamentals and Applications in the Petroleum Industry", Schramm, L.L. (ed.), pp. 677-723, American Chemical Society, Washington D.C., 1989.

Mikula, R. J., Munoz, V., Kasperski, K. L., Omotoso, O., and Sheeran, D., Commercial implementation of a dry landscape oil sands tailings reclamation option: consolidated tailings, in "Proceedings 7th UNITAR Conference No. 1998.096", UNITAR, Beijing, China, 907-921, 1998.

Mikula, R. J., Kasperski, K. L., and Burns, R., Consolidated tailings release water chemistry, in "Proceedings, Tailings and Mine Waste 1996", Fort Collins (Colorado State University), Colorado, 1996.

Mikula, R. J. and Zrobok, R., Oil sands tailings reclamation via manipulation of clay behaviour: the role of rheology, in "1999 Meeting of the Engineering Foundation", Hawaii, USA, 1999.

Mikula, R.J., Zrobok, R. and Omotoso, O. (2004). The potential for CO_2 sequestration in oil sands processing streams. Journal of Canadian Petroleum Technology 43(8) 48-52.

Omotoso, O. and Mikula, R. J. Alternative consolidated tailings chemicals. CWRC 99-23 (CF) CANMET Natural Resources Canada, Devon, Alberta , 1999.

Chalaturnyk, R. J., Scott, J. D. and Ozum, B (2002). Management of oil sands tailings. Petroleum Science and Technology, 20 (9-10) 1025-1046.

P.S. Wells, P.S., and Riley, D.A., "MFT Drying — Case Study in the Use of Rheological Modification and Dewatering of Fine Tailings Through Thin Lift Deposition in the Oil Sands of Alberta". Tenth International Seminar on Paste and Thickened Tailings, Perth, Australia, Mar 2007.

Mikula, R.J., Munoz, V.A. and Kasperski, K.L., Comparison of tailings behaviour for several bitumen extraction methods. WRC 96-19 (CF) CANMET Natural Resources Canada, Devon, Alberta , 1996.

Kasperski, K.L. and Mikula, R.J., Tailings release water chemistry and toxicity: comparison of tailings treatments. WRC 95-11 (CF) Natural Resources Canada, Devon, Alberta, 1995.

Mikula, R.J. and Kasperski, K.L., Nonsegregating tailings release water chemistry. WRC 95-23 (CF) Natural Resources Canada, Devon, Alberta, 1995.

Kasperski, K.L. and Mikula, R.J., Modeling the effect of gypsum addition on Suncor plant water chemistry: interim report. WRC 95-13 (CF) Natural Resources Canada, Devon, Alberta, 1995.

Table 2. Comparison of various tailings treatment options with initial conditions 35% mineral MFT, 80% mineral coarse tailings, 80% mineral CT, 80% mineral dried MFT, and 90% mineral filtered coarse tailings.

		Treatment results		
Tailings Treatment	Ore Type	Volume water lost per volume bitumen produced	% saved water	relative chloride ion concentration
No Treatment	15% Fines	4.5		1.0
No Treatment	10% Fines	3.7		1.0
No Treatment	5% Fines	2.9		1.0
CT	15% Fines	3.1	40%	1.5
CT	10% Fines	2.9	32%	1.3
CT	5% Fines	2.7	20%	1.1
Sand Filtration	15% Fines	4.1	21%	1.1
Sand Filtration	10% Fines	3.1	26%	1.2
Sand Filtration	5% Fines	2.2	35%	1.3
Both	15% Fines	3.0	40%	1.5
Both	10% Fines	2.5	42%	1.5
Both	5% Fines	1.9	45%	1.6
MFT dewatering	15% Fines	2.1	54%	2.2
MFT dewatering	10% Fines	2.0	45%	1.8
MFT dewatering	5% Fines	2.0	30%	1.4

Session 1

Tailings Containment

CSM CUTTER SOIL MIXING AND TRENCH CUTTING - TECHNIQUES FOR THE CONSTRUCTION OF CUT-OFF WALLS

Wolfgang G. Brunner, Stefan Schwank, Renato Fiorotto, BAUER Maschinen GMBH, Germany
Holger Itzeck, BAUER Equipment of Canada Ltd.

ABSTRACT

The new Cutter Soil Mixing or CSM technique can largely replace the more conventional single or multiple auger methods of soil mixing or jet grouting. This system allows much deeper walls to be installed and enables hard soil layers to be penetrated as well.
The CSM technique differs from the traditional deep mixing method in so far as it makes use of two sets of cutting wheels, as used on a trench cutter, that rotate around a horizontal axis to produce rectangular panels of treated soil rather than one or more vertical rotating shafts that produce circular columns of treated soil. Two cutter gearboxes are mounted on a special V-shaped link frame that is in turn connected to a robust kelly bar. The kelly bar is linked to the mast of a base machine by two guide frames that steer, provide crowd and extraction forces and, if necessary, rotate the cutter assembly. As the cutter wheels rotate and penetrate into the ground, they break up and loosen the soil. In order to achieve deep walls the CSM tool can be operated suspended from the rope of the base machine.

Case histories of cut off walls illustrate the use of CSM in Leuna, Germany, for partially enclosing an area of contaminated soil to prevent the contamination spreading, a recently executed CSM cut-off wall for waterproofing dams constructed at the MOSE flood control project in Venice, Italy and a cut-off wall constructed with trench cutter, hydraulic grabs and heavy chisels in Diavik, Canada.

CUTTER SOIL MIXING CSM

In the year 2003 Bauer developed the CSM method by exploiting its experience in the manufacture and use of the trench cutter systems to excavate diaphragm walls panels. The CSM method differs from the traditional DMM method in so far as it makes use of two sets of cutting wheels that rotate around a horizontal axis to produce rectangular panels of treated soil rather than one or more vertical rotating shafts that produce circular columns of treated soil. Two cutter gear boxes are connected to a special mounting that is in turn connected to a robust kelly bar. The kelly bar is connected to the mast of a drill rig by two guide sledges that steer and provide crowd and extraction forces and, if necessary, rotation to the cutting tool assembly (Figure 1). As the cutting wheels rotate and penetrate into the ground they break up and loosen the soil. During this phase a fluidifying agent or the binder itself is injected into the area between the two cutting wheels. In the extraction phase the cutting wheels rotate in a mixing mode and blend the binder and soil to form a rectangular panel of treated material in a cut-off wall.

The CSM tool as rope suspended version is used when greater depth has to be achieved (Figure 2).

The parameters of the machines we have designed and built to-date are:

Length of panel	2200, 2400 & 2800 mm
Width of panel	500 mm to 1200 mm
Torque output	30 kNm, 50 kNm, 80 kNm
Weight of cutter unit	3700 kg, 5100 kg, 7400 kg

Maximum depth capability with single tube Kelly 35 m
Maximum depth capability with cable suspension 70 m

Figure 1. CSM head mounted to Kelly bar

When additional strength or resistance to bending moments is required, the CSM wall can be reinforced efficiently with steel 'H' sections.

There is a much lower risk of leakage through the CSM panel (Figure 3).

There are a number of other advantages that the CSM method and machinery offers when compared to the traditional rotating augers or paddles, notably: the only moving parts in the CSM method are the cutting wheels, as a result we can mount instruments inside the cutter gearbox support frame that give real time information throughout the treatment depth, information such as verticality, deviations, excess pressure build-up in the surrounding soil etc.

In addition, by varying the relative speeds of the two cutting wheels the operator can correct any deviation that may occur. Further as the kelly bar does not rotate there is no energy expenditure like in the traditional DMM methods where a certain amount of energy is lost to overcome friction between the long shafts of the augers and the soil/cement mix.

Figure 2. Wire rope-suspended CSM unit

The CSM constitutes a new item in the Soil Mixing Methods, it offers numerous advantages over the more conventional methods of mixing soils using standard rotary tools. Meanwhile many projects using the CSM-System were carried out successfully in Germany, Netherlands, Belgium, Italy, USA, Canada, Australia and New Zealand. The technique offers a great diversity of possible applications, such as cut-off walls, structural retaining walls, foundation elements and numerous others. The capacity to reach great depths offers an enormous potential for the construction of deep cut-off walls for dams or the encapsulation of contaminated sites.

Figure 3. Top of excavated CSM wall

CSM CUTTER SOIL MIXING PROJECT EXAMPLES

Cut-off Wall MOSE Flood Control Project Venice, Italy

In a highly sensitive environment like the Venice Lagoon the new CSM method has proven highly effective in producing an important cut off wall and respecting the stringent environmental constraints.

During the last century, "high waters" have invaded the built up areas in the Venice lagoon with increasing frequency and intensity. The worsening of this phenomenon is due to the difference in the height of the land with respect to the sea which, between the beginning of the 20th century and today is of more than - 23 cm as a result of the rise of the level of the sea and subsidence of the land.

As well as causing considerable inconvenience to the population and businesses, high waters lead to the slow but relentless degradation of the environment and of the artistic and architectural heritage of Venice. There is also a very high risk of a catastrophic event such as the 4 November 1966 flood where built up areas in the lagoon were completely submerged by up to a metre of water.

At the beginning of the 1970s, following these dramatic floods, work began by the authorities to draw up a complex and "extraordinary" body of legislation and financial provisions to safeguard Venice.

In 1984, after many discussions and fiery controversies work began on a General Feasibility Plan covering all the measures necessary to preserve the hydro-geological balance of the lagoon and to mitigate high waters in the historic city and town centres. Finally in 1989 a conceptual design was completed for an integrated system of various types of measures that would provide complete protection for all built-up areas in the lagoon from high waters of all levels. This included mobile barriers, that is, rows of gates to be installed at the three lagoon inlets that are able to isolate the lagoon from the sea during high tides above an established level; a series of complementary structures such as breakwaters outside the inlets designed to attenuate the levels of the most frequent tides and the raising of quaysides and paving in the lowest lying urban areas.

Between 1989 and 2001 the preliminary conceptual design was gradually developed and updated and a number of alternative solutions were modelled, tested and optimized. In 2003 the MOSE project to save Venice was given the go-ahead to start. The expected duration of construction is 8 years (Figure 4).

The mobile barriers are the heart of the defence system and consist of a total of 79 gates, each 5 m thick, 20 m wide and 30 m long, placed in the inlet channels, they are designed to withstand a difference in level of up to 2 metres between the sea and the lagoon. When at rest the gates are full of water and lie in caissons in the sea bed. When a high tide (above +110 cm) is forecast compressed air is introduced into the gates, expelling the water, they swing upwards until they emerge above the water level and block the tidal flow entering the lagoon. The mobile barriers remain in position for the duration of the high water only. When the tide drops and the sea and lagoon return to the same level the gates are filled with water again and they return to their caissons.

To allow port activities to continue and pleasure craft, emergency vessels and fishing boats to shelter and pass through when the barriers are in operation, a lock will be constructed at the Malamocco inlet for the larger ships. Small craft harbours and locks will also be constructed at the Lido and Chioggia inlets (Figure 5).

One of the small craft harbours at the Lido inlet will serve initially as a construction pit for the precast caissons that will form the foundations for the gates. In order for the pit to be dewatered an impermeable cut-off needs to be installed to circumscribe the dock and to extend to a depth of 28 m where it will socket into a relatively impermeable clayey layer (Figure 6).

A number of solutions to produce the cut-off wall were evaluated by the contractor, amongst these were sheet piles, diaphragm walls, plastic diaphragm walls, secant piles and CSM. The CSM alternative proved to be the optimum solution.

Figure 4. Venice Lagoon

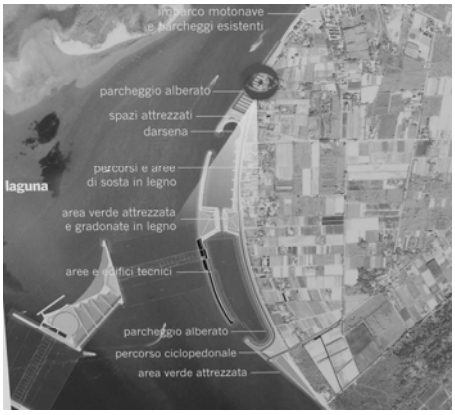

Figure 5. Malamocco Ship Lock

The specifications required the cut-off wall to have two main characteristics: a permeability better than 10^{-6} cm/sec and a strength better than 500 kPa.

The first step in the operation was to take a number of representative samples of soil from the site to a laboratory where they were

mixed with different quantities of water + cement and with plastic binders. The cement used was a pozzolanic cement and all samples were prepared with potable water but left to hydrate under a head of water sampled from the lagoon. Quantities and proportions were chosen to represent cement contents in the final soil/binder mix of 200, 250 and 300 kg/m^3 of soil.

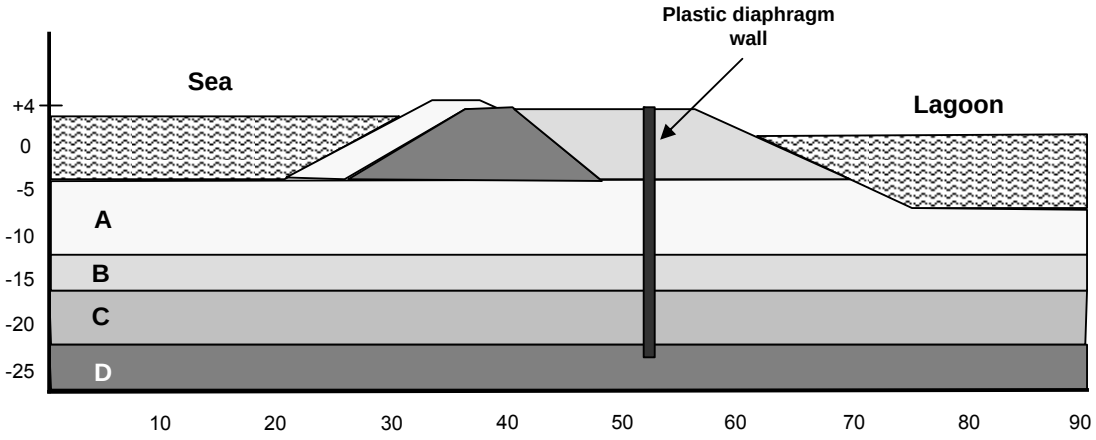

Figure 6. Cross Section through Cut-off Wall

The typical ground formation at the site is summarized in Table 1:

Layer	Level	Material Description	Soil parameters
	+3 m to -8 m	Sand Fill	γ = 18 kN/m^3; Φ = 32°; C_u = 0
A	-8 m to -12 m	Fine silty sand	γ = 19 kN/m^3; Φ = 40°; C_u = 0
B	-12 m to -18 m	Clayey silt and Silty clay	γ = 19.5 kN/m^3; C_u = 50 kPa
C	-18 m to -23 m	Fine sand with some silt	γ = 19 kN/m^3; Φ = 40°; C_u = 0
D	-23 m to -36 m	Clayey silt	γ = 18 kN/m^3; C_u = 75 kPa

Figure 7. CSM Machine mounted on BG2

Permeability and compressive strength tests were carried out at 11 and 28 days, these gave good results with compressive strengths well over the 500 kPa limit. Average permeabilites at 28 days were of the order of 4.03 x 10^{-7} cm/sec.

Given the depth of the wall we chose to use the cable suspended CSM machine mounted to a Bauer BG 28 base carrier and, using parameters derived from the results of the laboratory tests on different soil/binder mixes, a number of CSM test panels were mixed on site to optimize the construction method and parameters (Figure 7).

A series of panels were mixed with the CSM machine to depths of 30 m using different binder mix ratios and quantities and giving primary panels different hydrating times before intersecting them with secondary panels. In addition the following alternative construction methods were tested:

The One Phase method – Primary and secondary panels and a series of fresh-in-fresh panels were mixed using a plastic mix on both the down and up strokes. In this case the intersection between the adjacent primary panels and the secondary is 700 mm (Figure 8).

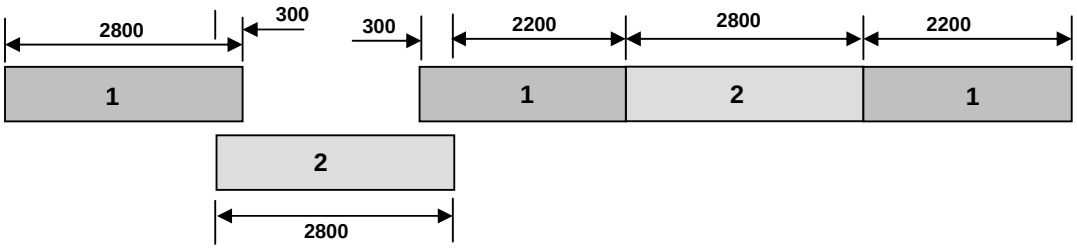

Figure 8. One Phase Method

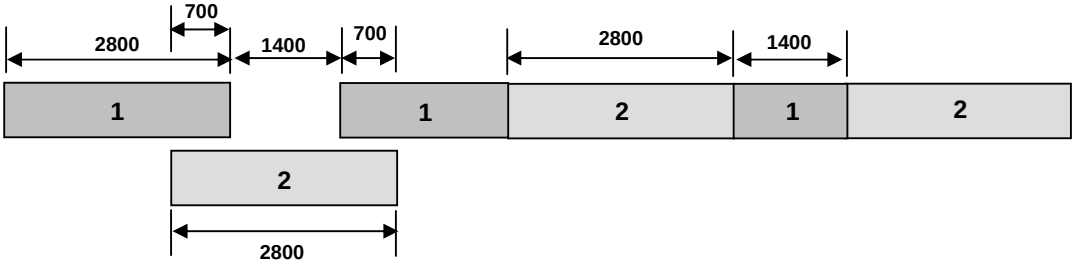

Figure 9. Two Phase method

The Two phase method – Primary and secondary panels were mixed using a pure bentonite mix on the down stroke and a water + cement binder, with a w/c ratio of 0,8 on the up-stroke. In this case the intersection between the adjacent primary panels and the secondary is 300 mm (Figure 9).

During this work, spoil from the panels was collected in a pit and its volume was carefully measured as the specifications required this to be minimized. The one phase system produced the lesser amount of spoil – 40% of the total panel volume compared to 47% for the two phase system.; samples of spoil were also taken when the CSM machine was at various depths and these were compared to samples of the soil/binder mix taken with a sampling tool at the same depth after the panel was completed.

Upon analysis of the test results, values of permeability and strength were very similar for the two methods of execution but even though the one phase method produced less spoil the two phase system was chosen for the project. This choice was based upon the condition that when carrying out CSM it is important that at the end of the down stroke the soil/binder mix above the CSM be fluid enough to facilitate extraction of the machine. On some areas of this site however the salt content in the soil is such that when work was carried out using the one phase method, it causes the soil/cement mix to lose fluidity very rapidly and thereby to make extraction of the machine difficult. In the two phase method however the soil/bentonite mix above the machine remains very fluid and the extraction process becomes easy thereby increasing productivity and causing the soil/binder mix below the machine to be well blended and very homogenic.

Figures 10 and 11. Data Computer

Verticality of the panels was another important parameter on this site as it is fundamental that

the wall be impermeable throughout its length and depth. In order to reduce the risk of panels not overlapping, we chose a safe overlap length of 300 mm on this project. Deviation readings from the machine's computer however indicate that the maximum deviations recorded to-date are less than 0.3%, ie. 84 mm on the "X" axis and less than 0.2%, ie. 50 mm on the "Y" axis (Figure 10, 11).

The amount of spoil that is produced was of concern at the beginning of the project, but a solution was found that makes good use of the spoil material: it is being used to build the sub-base and base for a cycle track that is to be built around the basin and that forms part of the services to be provided in the area.

Given that the work is being carried out using the two phase method the contractor carries out a series of primary panels for 3 days and then returns to carry out the secondary, closure panels. This work programme optimises productivity as after three days the machine is able to intersect the primary panels with some ease. Average daily productivity is 3 panels or 235 m^2. On peak production days they are able to mix 4 panels or 310 m^2 (Figure 12).

Figure 12. Malamocco Ship Lock

Cut-off Wall, Flow Path Protection Project Leuna, Germany

The town of Leuna is situated approximately 25 km south of the City of Halle (Saale) in the State of Saxony-Anhalt. Leuna was and still is one of the most important synthetic chemical industry sites in Germany. In 1916 Leuna began its chemical industrial development and became Germany's largest synthetic oil factory and producer of fuel from liquefied coal during World War II. As the Leuna plant played such a key role in the German war economy, the plant was the target of numerous air attacks in which around 80% of the Old Refinery was destroyed. During the 1950s fuel production was switched completely to the processing of mineral oils Figure 13).

Figure 13. The Old Refinery Leuna

After its closure in 1995/96, the Old Refinery was demolished completely. Left behind were large quantities of contaminants that had seeped into the subsoil and groundwater as a result of the effects of the war, accidents, leakages and spillages during processing and handling. It is estimated that fuel in excess of 10 million litres seeped into the ground, contaminating approximately 1,8 million tonnes of soil with fuel at the site of the Old Refinery in the form of petroleum hydrocarbons, together with other problematic compounds such as the fuel additive MTBE (methyl-tertiary-butyl-ether) manufactured on the site as an anti-knock agent. Over a period of some 80 years, the Leuna chemical complex had developed into a mega-contaminated site and was having a significant impact on the area's ecological and human environment by discharging approximately 1,400 kg of MTBE and 800 kg of benzene annually in the direction of the River Saale. By 2004, the flow of contaminated groundwater in the form of an extensive "contamination plume" had reached a length of several hundred metres and was threatening the town's Water Works some 2000 m east of the Old Refinery.

In view of the extend of the contamination and the imminent thread this caused to the local community, the commercial, technical, social and political stakeholders of the site finally agreed to act within the framework of the "Ecological Mega-Project Leuna". Between 2004 and 2005, after approval of the overall remediation strategy, both the concept and engineering design was completed and construction works could finally begin.

As it had been acknowledged by all stakeholders that the site could not be "cleaned up" in the short term and a complete removal of the soil and groundwater contamination was practically impossible, the remediation strategy focused on the containment of this legacy of industrial pollution. Central to the containment strategy

was the construction of an impermeable cut-off wall at the southern flank of the contaminant source zone that would protect the downstream groundwater flowpath from further contamination. The contract for the design and supervision of the construction of the scheme was awarded to the "ARGE Abstromsicherung", a joint venture between GUT Gesellschaft für Umwelt-technologie mbH and GuD Consult GmbH.

First, the areas to be remediated were divided into an inner and an outer zone. Appropriate technical measures had to ensure that none of the contaminants in the inner zone would be able to migrate into the outer zone. The core element of the Southern Downstream Flowpath Protection Scheme was the construction of an impermeable subterranean barrier in the shape of a single-phase cut-off wall that would prevent the outward flow of groundwater and thus the continued migration of contaminants. The contract for the construction of the cut-off wall was awarded to BAUER of Schrobenhausen. The successful bid was based on the proposal to employ the Cutter-Soil-Mixing (CSM) technique developed by Bauer Maschinen.

Based on a geological and hydrogeological subsoil investigation, the effectiveness of the cut-off wall was designed for the contaminant-rich water bearing formations in the Quaternary deposits and the upper aquifers in the Tertiary formations, in order to prevent contaminant transport via hydraulic windows between the Quaternary and the Tertiary (Figure 14).

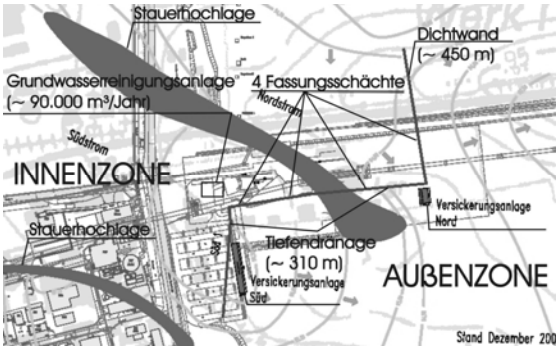

Figure 14. Basic design concept of the Southern Downstream Flowpath Protection Scheme with Groundwater isohypses

To prevent groundwater from banking up in front of the cut-off wall, the contaminated groundwater is collected in a deep collector drain system upstream of the cut-off wall, from where it is pumped to a groundwater treatment plant and cleaned by a multi-stage system of chemical and physical remediation processes. The treated groundwater is then discharged via a pipeline into infiltration basins located downstream of the cut-off wall, from where it is reintroduced into the downstream groundwater flowpath through infiltration or recharge wells, ensuring a balanced groundwater regime.

The volume of water being treated annually currently amounts to 90,000 m³. After an initial pilot operation, the plant went into permanent operation on schedule during the autumn of 2006. In line with the current state of technology, the Southern Downstream Flowpath Protection Scheme is expected to be in operation over a period of some 15 years (Figure 15).

Figure 15. Excavated top of Cut-off Wall

Cut-off Wall Diavik Diamond Mine, Canada

DIAVIK Project Summary Kimberlite A154

The Diavik project site is on a large island in Lac de Gras, located about 35 km southwest of the Ekati mine, and 300 kilometers northeast of Yellowknife, the capital of the Northwest Territories. The kimberlite pipes lie within Lac de Gras, fairly close to shore, in water of 15 to 30 meters depth. All of the kimberlite pipes are planned to be mined initially using open pit techniques. In order to enable this, encircling dikes are built that are subsequently made water-tight by installation of a plastic concrete cut-off wall. Connection to the bedrock surface is accomplished by jet grouting the contact zone and fractures in the upper granite bedrock are sealed by pressure grouting. When the dike is built, and the water seepage cut-off components are completed, the pool is pumped out.

Due to the northern location of the construction site, being only 200 km south of the Arctic Circle, the construction season for dike building, and

especially for excavation of the cut-off walls, is limited to the period from the middle of May to the middle of October each year. The construction site is only accessible by road for a period of about 10 weeks, beginning in February, when an annual ice road is constructed from Yellowknife. Thorough planning and attention to logistics are essential for the entire summer construction effort. Any parts or materials that are overlooked when the winter road is closed, must be flown to site from either Yellowknife or Edmonton, Alberta. The dike construction scope can be summarized as follows:

Length of the dike centreline: 3,809 m
Volume of dike materials 3,000,000 cbm
Vibro-densification: 290,000 cbm
Diaphragm wall: 33,000 squm
Jet grout wall: 18,000 squm
Dewatering: 10,300,000 cbm
Seepage rate: 800 liters/min total average

Technical Project Considerations

Dike Construction

No natural, suitable materials were available on the island, so all the dike construction materials had to be produced from quarried rock. A granite quarry was established that fed up to 28,000 tons per day of blasted rock to a mobile crushing and screening plant. Primary and secondary crushers, a wash plant and multiple screen decks were used to produce the necessary gradations of crushed rock.

Dike Core Compaction

The central core of the dike was compacted by vibro-densification, using BAUER TR75 deep vibrators, carried by a BS 6100 track-mounted crane with integrated hydraulics (Figure 16, 17).
An area extending 5 meters on either side of the panel wall centreline was densified, from the surface down to the contact between the A1 material and the natural lakebed. The maximum depth of vibro-densification was 27 meters.

With this deep compaction, the internal deformation resistance of the dike is increased, settlement potential is decreased, and a dense core material is created that will support construction of the cut-off wall. Becker hammer testing, that was conducted before and after vibro-densification of the zone A1 material, established that a very good compaction effect was achieved. Blow counts of about 5 were recorded in the A1 before compaction, while typical values of 20 or more were recorded afterwards. In total, about 290,000 cubic meters of A1 material were compacted.

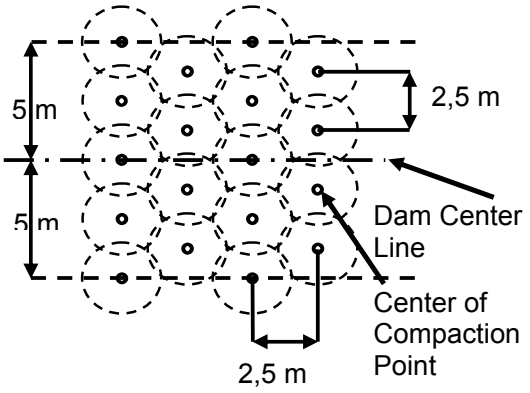

Figure 16 Dike core compaction layout

Figure 17. Compaction with TR75 deep Vibrators

Diaphragm Wall Construction

Excavation Conditions and Equipment

Excavation for the diaphragm wall construction encountered 5 different ground conditions:

1. A1 crushed rock
2. Till
3. Frozen till
4. Boulders
5. Weathered granite

- A1 Crushed rock.

Due to the careful quality control of gradation during crushing and screening, and the vibro-densification after placement, this material was very stable during excavation.

- Till

Glacial deposits at the site were typically very heterogeneous. Especially in shallow water near shorelines, boulder fields up to 3 meters thick

were often encountered. In other areas, sandy zones were found, of varying consistency.

- Frozen Till

The project site lies within the continuous permafrost zone of Canada, and permanently frozen ground occurs on all islands within Lac de Gras, near shorelines where the water depth is less than 2 meters, and on the mainland. The ground surface only thaws to a maximum depth of 3 meters in the summer. The composition of this material is the same as unfrozen till, except that some ice also exists in the material. Boulders that are a frozen part of this till are very difficult to break using heavy chisels, because they are frozen elastically in the ice/soil matrix. The cutter was equipped with roller bits wheels, which worked satisfactorily from the outset. Boulders embedded in the till could be cut quickly enough to allow the cutter to reach the desired trench depth.

- Boulders

Typical boulders consisted of hard granite, with an unconfined compression strength averaging 115 MPa. Boulders measuring up to 1 meter on a side were excavated with the hydraulic grabs, while larger boulders were cut by the trench cutter BC 40.

- Weathered bedrock

The diaphragm wall had to be connected to bedrock, to ensure the performance of the cutoff. Weathered bedrock was reliably cut using the cutter with hard rock roller bits.

The following equipment was selected:

- 1 BC 40 Trench Cutter, 800 x 3200 mm, with hard rock roller bits.
- 3 GB 60 hydraulic panel excavation grabs with 800 x 3200 mm buckets.
- 1 GB 60 chassis equipped for chisel handling, with round and box chisels.
- 2 BE 500 desanding units, with all necessary equipment for bentonite slurry formulation and processing.

Diaphragm Wall Construction

A total of 32,700 square meters of 80 cm thick diaphragm wall were built for the dike cut-off, using a two-phase procedure. Diaphragm wall support during the excavation was provided by means of a bentonite slurry, which was subsequently displaced by tremieing a plastic concrete mixture into the trench (Figure 18).

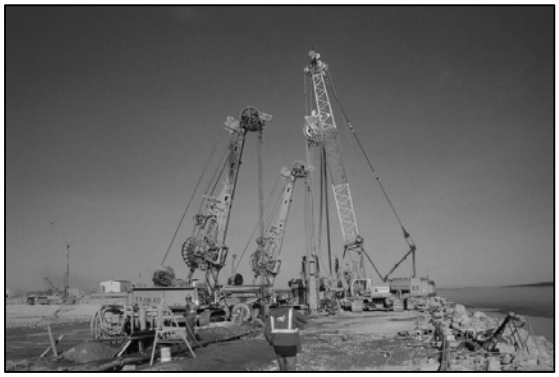

Figure 19. Cutter and Grab used in Panel Wall Construction

When design of the plastic concrete mix was being determined, the following factors had to be taken into consideration:

- Only crushed aggregates are available on site.
- There is only a limited supply of natural sand in the local area.
- Cement and bentonite must be transported over long distances to the construction site, making those materials very expensive.
- The water supply is from Lac de Gras, where the temperature was +3º C, thus requiring heating of the water before use.
- Concrete installation by the use of tremie pipes.
- Plastic concrete delivery trucks would occasionally be exposed to temperatures down to –20º C.
- Typical curing conditions in-situ, will be at a temperature of only +3º C.
- In permafrost areas, curing concrete will be exposed to ground temperatures of –10º C.
- The plastic concrete must withstand deformation of the dike during dewatering of the pool.
- The plastic concrete must withstand shock created by production blasting in the mine.
- Long term behavior.
- Freeze / thaw behavior in the upper permafrost zone.

The plastic concrete mix design that was used, produced a 28 day compressive strength of 2 MPa and consisted of the following proportion of components:

1.	cement	158 kg
2.	bentonite	40 kg
3.	water	412 kg
4.	fine aggregate, 0-8 mm	668 kg
5.	coarse aggregate, 8-16 mm	668 kg

Jet Grout Injection

Equipment

Since the jet grout installation could not be done until the plastic concrete had cured sufficiently, and since the jet grouting was the last step in the construction of the cut-off system, this activity was always on the critical path of the construction schedule.

Based on the requirements, Mischanlagen-technik (MAT), a sister company of Bauer Maschinen GmbH, developed and optimized the following for use on the project:

- Big Bag task stations with heated horizontal silos.
- Water heating station that used water from the lake and heated it 6 degrees C.
- Fully automatic mixing station for both 2 and 3 phase jet grout injection.
- High pressure jet grout injection pump built into a heated container.
- UBW 09, a compact drill rig with drill rod magazine, that could handle rods 4 meters long and 152 mm in diameter.
- BG 22, a jet grout injection unit, with a lattice mast capable of working in arctic conditions at depths up to 27 meters.

Jet Grouting at the Dike

A row of jet grout test columns was constructed to determine the diameter created in typical A1 crushed rock, as well as in frozen till. It was demonstrated that columns greater than 2 meters in diameter were produced in the A1 material, and 0.8 meters diameter in frozen till. Consequently the column spacing to create a continuous cut-off was chosen to be 0.75 meters in unfrozen till and A1 material and 0.6 meters in frozen till.

The following jet grout injection parameters were selected:

1. System: two phase, with compressed air and high pressure grout.
2. Column spacing: 0.6 / 0.75 m on the cut-off wall centerline.
3. Nozzle diameter: 4 mm.
4. grout pressure: 400 bar.
5. Jet grout mix:
    a. 464 kg of cement
    b. 30 kg of bentonite
    c. 1000 kg of water.

The original design for the diaphragm wall required that it be installed down to the top of bedrock. Jet grouting was planned to begin 1.5 meters into the bedrock, and extend upward 0.5 meters into the previously-constructed diaphragm wall. With that design, weathering of the upper bedrock, as well as imperfections at the bottom of the plastic concrete wall would be addressed, and the diaphragm wall together with the jet grouting would provide a continuous cut-off.

A critical requirement, especially when drilling jet grout holes through till, was to achieve the required verticality tolerance of 0.5% in all directions, thus ensuring adequate overlap of adjacent single columns. Also, it was vital to complete the 152 mm diameter jet grout drilling through the recently-completed panel wall sections, without breaking through either side of the panels. The UBW 09 drill rig with rod magazine achieved this drilling accuracy satisfactorily. Each completed borehole was surveyed for deviation, and it was confirmed that about 98% of all holes met the required specification (Figure 19).

The BG 22 jet grout injection unit with lattice mast extension allowed the production of jet grout columns up to 27 meters high, without disconnecting the drill rods. In very deep locations, the drill rods string was extended to 33 meters maximum.

Figure 19 UBW 09 drilling jet-grouting Holes

Quality Control and Production Data Recording

All production and equipment operating readings (about 20 parameters per rig) were recorded each second, and temporarily stored

electronically at each rig. At the end of each working shift, the accumulated data were transmitted by radio to the site office, reviewed and archived. The analyzed results were delivered to the customer every day, both electronically and in paper form (Figure 21). The individual data records were combined electronically in an “as-Built Drawing”, which graphically represented the overlap of the diaphragm wall elements and the jet grout columns. The connection to bedrock was also shown, and the overall drawing documents considerably eased the analysis and quality control efforts required.

CONCLUSIONS

CSM is an extremely competitive and useful Soil Mixing method. In both CSM projects MOSE and Leuna, where site constraints and ground conditions were particularly difficult, the method proved to be technically superior and more cost effective than other common methods.

The combined system of trench cutter, hydraulic grabs and chisels proved to be the proper solution for a cut-off wall in difficult soil and climate conditions as Diavik. The high quality of the cut-off wall system resulted in a seepage rate of only 800 liters per minute for the entire dike. In the meantime the A418 kimberlite pipe was developed in the same way.

SEEPAGE MONITORING AND CONTROL IN TAILING DAMS

Elehinle Emmanuel Olatunbosun
Gilmor Engineering Limited, Abuja, Nigeria

ABSTRACT

Seepage flow through Tailings stored in a Surface Impoundment is a possible occurrence and its control is a very important water management requirement in the construction, operational and post operational stages of any Tailing Dam. This paper covers the building of Tailing Dams, Seepage detection using temperature measurements (Sam Johannsson and Pontus Sjodahl, 2004), Seepage control through Barrier System method (in which Liners are used to prevent or resist seepage flow) and Collection System method (in which pathways are made for seepages to accumulate and flow into a secondary storage embankment) and the conclusion is based on how effective these methods would be in the prevention of ground water contamination.

INTRODUCTION

Tailings are waste products which has no financial gain to a mineral operator at that particular point in time during mining and mineral processing activities. They are usually generated in the course of separating the valuable substance otherwise known as the concentrate from the gangue. For example, during the process of separating bitumen from tar sands, a great amount of water is mixed with the sand and once the oil has been removed, the leftover is the mixture of water, sand, clay and residual bitumen which make up what is known as “oil sand tailings”. The challenges associated with a sustainable disposal, management and storage of these tailings are ever increasing. Usually, the tailings are pumped in a slurry form to sedimentation ponds which are surrounded by natural heights or Dams. Pumping them in slurry form means their water content is high; hence a major issue is the control of water, the water content of the tailings and the possible seepage of this water from the dam.

Looking at the theme of this conference, “oil sand tailings” are the key words. And when we are talking about “Tailings”, we are talking about our environment and our environment means our planet and our planet means our lives. Proper tailing management therefore, is highly imperative for the preservation of our world and of our lives.

The effects of tailings has been a matter of concern from ages to renowned miners like Georgius Agricola who specified in his write up; *De Re Metallica* in 1556 as thus;

“….when the ores are washed, the water which has been used poisons the brooks and streams and either destroys the fishes or drives them away….thus, it is clear to all that there is greater detriment from mining than the value of the metals (materials) which mining produces…”

Going by today statistical findings, tailings are by volume, probably the most handled products in the world. About 25-30 MT per year are been handled only in Sweden (Annika Benckert et.al). I wonder what the figure will be if other countries are to be assessed. Many Canadians today know that one of the world largest dams is in Canada but few are aware that it is built to hold tailings from just only one of the oil sand operations. These tailings contain materials such as asphaltenes, sulphur and heavy metals which if not properly attended to can, through seepage contaminate the groundwater and river systems.

The failure of the Stava tailing dam in 1985 as described by Berti et al (1988) was attributed to seepage caused by the blockage of the culvert at the toe of the dam. The failure caused the death of 269 people. The water and the river systems around Stava and Tesero Villages were also contaminated.

Seepage is generally a major environmental issue in tailing dam construction and its influence on stability must be highly acknowledged. However, its control can reduce the environmental impacts of tailings and even the threats to the stability of the dam.

CONSTRUCTION OF TAILING DAMS

People in general are more familiar with conventional water dams but tailing dams on the other hand are constructions hardly known to many people than “experts and professionals” in the field.

A tailing dam is a retaining structure for the storage of both tailings and mine water. There are principally two types, the water retention dam and the raised embankment dams (Steven G.Vick 1990).

The water retention dam is usually constructed to its full height before usage while raised embankment dams are built higher in the course of their usage and are further classified into upstream, Downstream and Centreline based on the methods of their construction. The water retention tailing dam is not quite too common because it is very similar to the conventional water dam and its long term performance may be difficult to guarantee.

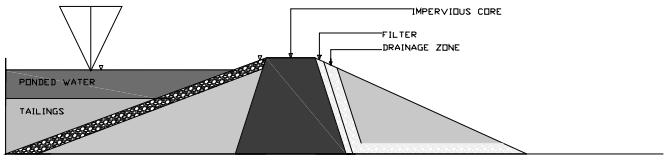

Figure 1. Water retention Dam

The Upstream method is the most popular design for tailing dams and it requires little amount of fill materials. Therefore, the coarse fractions of the tailings are usually used. This method is usually started with a pervious (water allowing) starter dyke. The tailings are discharged from top of the dam crest and this creates a bench for the foundation. The dam crest moves progressively upstream as the impoundment is raised. This method of design (Figure 2) is the most common to fail and it is the most prone to seepage because of its pervious starter dyke. This method has a low construction cost.

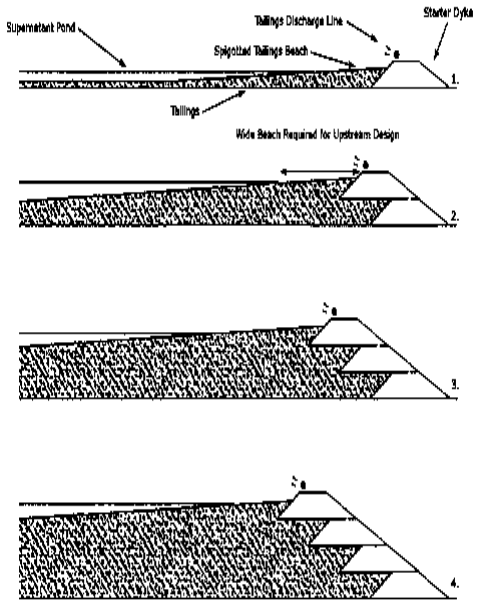

Figure 2. Upstream method

-**The Downstream method** requires large amount of fill materials. It is usually started with an impervious (water sealed) starter dyke. The tailings are first deposited behind the dyke and the dam crest moves downstream as the impoundment is raised. The volume of materials needed is directly proportional to the raise of the dam. This method is not as sensitive as the upstream type because it is built on solid ground instead of deposited tailings. But it has higher cost.

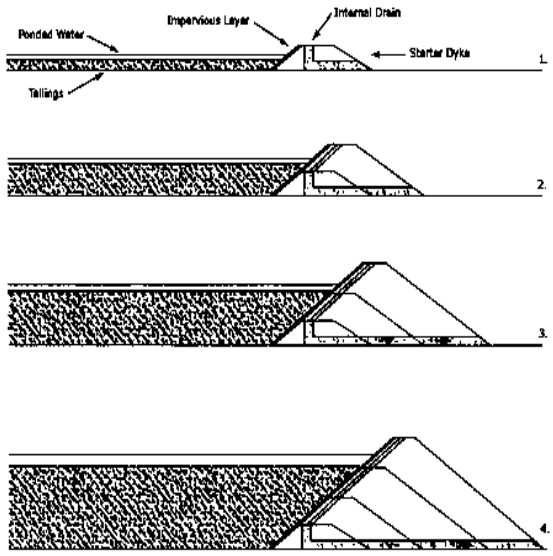

Figure 3. Downstream method

-The Centreline method combines the features of both the upstream and the downstream methods. For each raise, materials are placed on both the deposited tailings and the existing embankment. Like the upstream method, the tailing is discharged through spigot from the dam crest. The dam crest moves progressively vertically and does not go toward upstream or downstream directions.

All the phases of a tailing dam and their objectives must be put into consideration in order to construct a safe dam and the objectives must be review from time to time as conditions change with time.

The right knowledge of other phenomena like seepage is also essential in the management and operation of any tailing dam.

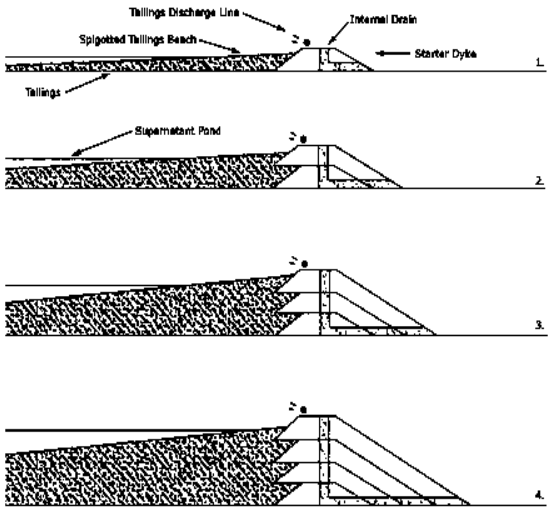

Figure 4. Centreline method

SEEPAGE IN TAILING DAMS

Seepage is the continuous movement of water (contaminated or uncontaminated) through and around a dam or an impoundment. It usually occurs from the upstream face of the dam towards the downstream face as water seeks paths of least resistance through the dam and its foundation.

The primary factors affecting the volume of seepage present in a (dam) system are; the depth to the ground water table and the infiltration capacities of the unsaturated zone and tailings. When seepage velocity is great enough, it reduces the effective stress within the soil and exerts a frictional drag on the particles to cause erosion of the soil known as “piping”. Piping can lead to the failure of the structure and to a sinkhole formation. (Jones, J.A.A, 1976)

Regular monitoring is essential to detect Seepage in dams and this can be done

- Through the faculty of vision as outflow can be seen.
- Through auditory sense as seepage outflow can be heard.
- Through the sense of smell as vegetation around the wet areas smell differently (but this may not apply to oil sands tailing dams because there is basically no vegetation around the operations areas).
- Through the assessment of flow lines in flow nets
- Through temperature measurement

The latter is gaining popularity and therefore will be discussed in this paper. However, the combination of all the above factors can bring about a clear and subjective detection of seepage.

Seepage monitoring and detection using temperature measurement

There are many physical parameters to which many naturally and technically oriented processes are connected to. Detailed knowledge of the variations of these physical parameters, either temporal or spatial is the basis for risk management, process optimization and fault detection in most engineering works. In many cases, these parameters can not be measured directly but they are connected to a long term or short term variations of the temperature field.

Temperature therefore is a key parameter in many engineering monitoring tasks such as the detection and localization of leakages in pipelines, water construction and dams, groundwater contamination and early fire detection.

The use of Temperature measurement for seepage detection in dams is gaining acceptance and popularity worldwide and has been used successfully in Sweden and Germany.

This method has been in use as far back as the late 1950’s (Kappelmayer, 1957). To look into this method critically, one may need to know the general temperature process or condition in an embankment.

The general thermal condition in any embankment dam is a function of the temperature in the air and the temperature in the upstream reservoir. These two temperatures create seasonal temperature variation within the dam as a result of heat conduction and **advection** (transport mechanisms of a substance or a conserved property with a moving fluid). The magnitude of this temperature variation can be measured in the dam and correlated to the seepage flow through the dams. This approach was described by Johannson 1991.

Low seepage flows will not affect the thermal condition in the dam and temperature will remain constant but as seepage increases, the temperature in the dam will begin to vary seasonally and the amplitude of the variation is dependent on the seepage flow, seasonal variation at the inflow boundary and the distance from the boundary of the measuring point or in open drainage ditches running to the dam.

To measure temperature and to note the temperature variations, many works by HydroResearch of Sweden and Sensornet of United Kingdom have brought about a simplified sensing system with which temperature measurement can be performed over long distance. This distributed sensing system takes advantage of the

fact that scattering properties of laser light traveling down a fiber vary with temperature and strain along its length. With the optical fiber as sensor, real time reading of temperature can be done even for a distance of up to 30 km. During the measurement, it would be noted that the temperature of the groundwater seepages through the dam would be different from the temperature of the non influenced soil or the open drainage system. Therefore, temperature anomalies are found at locations of seepage paths and the temperature acts as tracer to detect seepage sections.

Working on the data of these temperature anomalies and variations, seepage can be detected but the interpretation of the data is usually complex. However, a software package known as DamTemp has been developed by Hydroresearch and Sensornet to simplify the interpretations and the software can also give an improved understanding of the Thermal Processes in dams.

According to S. Johannsson and P. Sjodahl (2004), temperature measurement sensors have been installed in the following dam sites in Sweden;

Lovon (1998)	Seepage
Sadva (1999)	Movements
Aitik (2000)	Seepage & Movement
Ajaure (2001)	Movements
Vargfors (2001)	Seepage
Hylte Dam (2002)	Seepage
Suorva West (2003)	Seepage
Suorva East (2004)	Movements
Bastusel Dams (2004)	Seepage
Gallejaure Dams (2004)	Seepage

Although most of these dams are conventional Water dams but the Ideal here is that the same method can be applied to tailing Dams and as shown the method is mostly used for Seepage detection.

Seepage Control

Seepage can be controlled in two basic ways by using either the Barrier system Method or the Collection system Method. These two methods actually imply that the seepage can be kept within the dam or captured after it leaves the dam.

The Barrier systems method resists the flow of seepage in the impoundment. This method consists of liners and embankment barriers to prevent seepage passing through the tailing dam. The embankment barriers are usually installed beneath the entire impoundment and are most suitable for downstream and Centreline dams other than upstream dams which generally rely on a pervious foundation. There are several of these barriers and include;

- **Grout curtains** which make use of cement, silicate materials or acrylic resins and limited to sites with coarse grain material. They are thin, vertical, grout walls installed in the ground. They are constructed by pressure-injecting grout directly into the soil at closely spaced intervals. The spacing is selected so that each “pillar” of grout intersects the next to form a continuous wall or curtain.

- **Cut off trenches** which are usually 5 t0 20 ft in depth. Dewatering may be necessary during installation of a cut off trench.

- **Slurry walls** are installed by excavating a trench to a zone of low permeability material and filling the trench with soil/bentonite slurry which is then allowed to set to a consistency of clay which forms a filter cake that serves as a barrier.

The use of the Barrier system liners started about two decades ago but because of its high cost most tailings dams in use today do not contain a lining system. The liners are made of synthetic materials but constructed liners can be made from local clays or other available materials like slime, which can be used as low permeability barriers. Clay can be an inexpensive option for liners but it can also be used in combination with synthetic material liners.

In the collection system method, pathways are made for the seepage to flow out into a secondary entrapment. There are two ways by which this can be done;

The use of Ditches: This is usually the most common and the cheapest of the collection system methods. A collection ditch (Figure 5) is usually dung around the toe of the tailing dam wall allowing the seepage to flow through the pervious layer underneath of the impoundment into the ditch (Vick, 1990). The seepage collected in the ditch is eventually pumped back into the dam with the aid of a submersible pump which steadily removes the seepage, and thus allowing more to import through the pervious layer into the ditch**.**

Figure 5 Collection ditch **Figure 6 Collection well**

The use of well: This is the same as a dewatering system from a mine. The collection wells (Figure 6) are installed at the toe of the tailing dam. This type of collection system is very expensive to install and manage because each of the well has to be pumped dry. Hence the ditch is preferred to the well but collection well method can be used as a remedial measure for a dam with drainage problems or with a risk of liquefactions.

CONCLUSION

There is a variety of environmental effects that is associated with seepage from tailing dams. Two of these effects are the possible failure of the dam and the alteration of the subsurface hydrological settings. The present methods of controlling seepage cannot give a satisfactory percentage in its efficiency. To get a zero discharge of seepage from a tailings Dam is an elusive goal even with a complex liner systems. Proper monitoring and control of Seepage is therefore a case for research to stake holders in the mining industry so that a step forward can be ensured in ascertaining the safety of our environment.

ACKNOWLEDGEMENTS

Special thanks to Dr. Sam Johansson of Hydroresearch AB in Sweden for the permission to use some of his works.

REFERENCES

St. GroBwig, A. Graupner, E. Hurtig, K. Kuhn, A. Trostel (2001) Distributed Fibre Optical Temperature Sensing Technique- A Variable Tool for Monitoring Tasks.

Ake Nilsson (2001) Safe Dam Constructions

Sam Johansson, Pontus Sjodahl (2003) Downstream Seepage Detection using Temperature Measurement and Visual Inspection – Monitoring Experiences from Rosvatn Field Test Dam and Large Embankment Dams in Sweden.

Kappelmeyer, O. (1957) The use of Near surface Temperature Measurements for Discovering Anomalies due to causes at Depths. Geophysical prospecting.

Sam Johansson, Mahmoud Farhadiroushan , (2000) Seepage and Strain Monitoring in Embankment Dams Using Distributed Sensing In Optical Fibres – Theoretical Background and Experiences from Some Installations in Sweden.

J. EnGels & D. Dixion-Hardy, Tailing Info

Agricola G. (1556) De Re Metallica, (Translated by H.C Hoover and L.H. Hoover)

Jones, J. A. A. (1976). "Soil piping and stream channel initiation".

Session 2

Chemical Interactions

IMPACT OF ION EXCHANGE PROPERTIES ON THE SEDIMENTATION PROPERTIES OIL SANDS MATURE FINE TAILINGS, AND SYNTHETIC CLAY SLURRIES.

Robert Donahue, Dave Sego, Ben Burke, Alix Krahn, Jasmine Kung, Nafisul Islam
University of Alberta, Edmonton, Alberta, Canada

ABSTRACT

The cation exchange properties of oil sands tailings materials and the impact of these properties on the sedimentation behavior of clay-sand slurries are presented. The oil sands inter-ore clay deposits are primarily responsible for the formation of mature fines tailings (MFT) that are problematic in tailings reclamation. Cation exchange in the tailings clay and fines fraction was characterized and the influence of changes in cationic species distribution on exchange sites on sedimentation behaviour was investigated. Cation exchange capacity (CEC) and exchangeable cations (EC) were measured on the clay and fine fractions using ion chromatography (IC). Standpipe sedimentation tests were used to characterize the sedimentation behaviour of the clay-sand slurries. Reagent-grade kaolinite and bentonite were used as control materials for the exchange and sedimentation tests. Exchangeable cations were found to be between 42 and 76 % of the cation exchange capacity which suggests that ammonium acetate extraction may not be able to desorb all that cations present on the clay surfaces. The exchangeable cations in MFT samples were dominated by Na (20 to 40%) and Calcium (10 to 30%). The treatment of clay minerals with NaOH resulted in the complete desorption of exchangeable Mg and the adsorption of sodium. Clay sand slurry Sedimentation tests at constant solids and fines content indicates that the addition of 10% bentonite converted the slurry to a non-segregating mixtures. The change in sedimentation behaviour was the results of cation exchange of Ca and Mg from the bentonite to the kaolinite clay minerals due to a reduction in solution ionic strength. The sedimentation behaviour of kaolinite sand slurries could be changed to non-segregating by increasing the exchangeable Ca to 50% of the total CEC. Increases in exchangeable calcium beyond 50% did not improve sedimentation behaviour.

INTRODUCTION

The study presented is a series of laboratory experimental programs designed to investigate ion exchange processes to support oils sands tailings performance enhancement technologies. The Energy Resources Conservation Board draft directive (ERCB 2008) makes it clear to the oil sands industry that substantial improvements in tailings management must be accomplished by 2011. The most substantial directives are an overall reduction in fluid fine tailings volumes, and that combined tailings (CT) be deposited in a manner that minimizes segregation. Oil sand extraction and tailings management is a continuum of geochemical interactions. Chemical reactions in the bitumen extraction process influences tailings behaviour, and tailings processing impacts bitumen extraction due to the use of recycled water. Water is the Achilles heel of tailings management in oil sands development. Water trapped in the tailings mass requires ever-increasing storage capacity and inhibits future resource development. Reclamation of water from the tailings in an efficient and timely matter is critical to future oil sands developments. Improvement in tailings sedimentation and consolidation properties would allow producers to meet ERCB performance criteria for CT tailings, which would improve both the public perception of the oil sands industry and reduce the environmental footprint of oil sands resource developments.

To date, most of the research on oil sands tailings, CT, fluid fine tailings, and MFT behaviour has been conducted empirically, without water chemistry. The original CT work by Caughill (1993) investigated lime and sulphuric acid amendments to produce non-segregating tailings mixtures. Clay mineralogy and water chemistry were not evaluated or used for interpretation, and amendment dosages were calculated based on whole tailings volumes. Subsequent work by (TANG, 1997), indicated that there was a strong relationship between bitumen content and tailings water chemistry on the tailings settlement and consolidation behaviour. The research provided

insight into the segregation behaviour but, without accompanying pore fluid chemistry, the researcher was unable to characterize the fundamental geochemical interactions between the clay minerals and water.

Similar work conducted by Boratynec (2003) and OZUM et al., 2004 has shown empirically that manipulation of calcium concentrations by lime addition and pH by CO_2 concentrations can raise the segregation boundary to a lower solids content and improve recycled water quality. Ozum (2004) included detailed water analysis and indicated that divalent cation concentrations could be suppressed in recycled water using CO_2. Sedimentation and geochemistry experiments by Islam (2008) demonstrated that, while segregation behaviour for clay-sand slurries is known to be a function of solids and fines (clay mineral) content (Caughill 1993, Boratynec 2003 and OZUM et al., 2004), it is also a function of the distribution of monovalent and divalent cations on the clay mineral surfaces. At a constant solids content and fines content, a clay-sand slurry can be changed from a segregating to a non-segregating mixture by changing the distribution Ca^{2+} and Na^{+} ions adsorbed to the clay mineral surface. The chemistry of the water in contact with the tailings solids will control the distribution of cations on the clay surfaces and its subsequent sedimentation and consolidation behaviour.

The methodology for the study was to characterize the geochemical interaction of the clay-water system and its impact on tailings geotechnical behaviour. The surface properties of interest are exchangeable cations (EC), cation exchange capacity (CEC) and selectivity coefficients (Kd). Exchangeable cations are the distribution of species present on the clay mineral surface while cation exchange capacity is a measure of the absolute charge capacity of the clay surface.

Clay surface properties and exchange reactions are of little direct interest to oil sands developers who are primarily focused on bitumen extraction, tailings management and complying with ERCB oils sands tailings performance criteria. The geotechnical performance, sedimentation and consolidation processes of oils sands whole tailings and CT has been the primary focus of tailings research to date. This study is designed to link geochemical ion exchange reactions to changes in geotechnical behaviour. Water release tests (WRT), i.e. standpipe sedimentation tests, have been used successfully to predict segregation behaviour (Caughhill 1993 and Ozum 2004) in both whole tailings and CT. A series of water release tests were conducted to determine how changes in the distribution of cations on the clay surface affect the sedimentation behaviour of various clay sand slurries.

EXPERIMENTAL MATERIALS AND METHODS

Test Materials

- MFT N: mature fine tailings from a Suncor sample marked, “MFT Jan16/07
- MFT S: mature fine tailings from a Syncrude sample marked, “Syncrude MFT (March 5/08)
- Kaolin: reagent grade, produced by ACRÕS ORGANICS to serve as a control
- Bentonite: reagent grade, produced by ACRÕS ORGANICS to serve as a control

Cation Exchange Capacity

Cation exchange capacity (CEC) is used as a measure of soil fertility, nutrient retention capacity, and the capacity to protect groundwater from cation contamination. It is a bulk measurement of all the available negatively charged surfaces on a soil particle. Several methods for the determination of cation exchange capacity exist: extractions using ammonium acetate, silver thiourea, barium chloride or lithium chloride have all been used, with varying degrees of accuracy. EPA Method 9081, the most widely accepted method, is a three stage process. Firstly, a small sample of soil (~4g) was washed with an excess of sodium, in the form of 1N sodium acetate, which replaced the majority of other cations on the exchange sites. The sample was then shaken via Wrist Action mechanical shaker for 5 minutes. Once mixed, the sample was centrifuged at 4150 rpm for 15 minutes. Separated water was decanted and the process was repeated a total of 4 times. Secondly, the sample was washed with isopropanol to remove any pore fluid that may contain exchanged ions. The sample was again shaken and centrifuged as above, a total of 3 times. Thirdly, the sample was mixed with an ammonium acetate solution; the ammonium ion replaces the sodium ion on the exchange surface and the sodium is released into solution. Samples were again mixed and centrifuged as above, 3 times. The decanted solution was filtered through a 0.2µm nylon syringe filter then retained for

analysis by ion chromatography (IC). All samples were prepared in triplicate.

Exchangeable Cations

The exchangeable cations (EC) test serves to characterize the ion exchange surface of the material. Each clay particle has an available charged surface; this charge is satisfied by the adsorption of ions onto the surface. The exchangeable cations give an indication of the initial composition of the exchange surface. In this test, the sample was mixed with an excess of ammonium in the form of 1N ammonium acetate, the ammonium displaced ions present on the exchange surface so that they may be measured. The sample was mixed, shaken and centrifuged as with the CEC test above. This process was repeated 3 times and the decanted solution was filtered with a 0.2µm nylon syringe filter and analyzed using IC. All samples were prepared in triplicate.

Reagents CEC/EC

1N sodium acetate was prepared by dissolving sodium acetate salt in deionized water (DI). 1N ammonium acetate was prepared by mixing 99.5% glacial acetic acid with concentrated ammonium hydroxide. In the CEC test, 2-propanol was used to rinse the remaining pore water from the sample between the sodium and ammonium equilibration steps.

Ion Chromatography

Separate analytical instrumentation systems were used to measure anion and cation concentrations. Anion analysis was done using the integrated ICS 2500 system from DIONEX Corp. Samples were injected using an AS50 autosampler (injection volume = 25µL). A CD25A electrochemical conductivity detector measured conductivity of test samples and a GP50 gradient pump provided flow at a rate of 1mL/min. The mobile phase consisted of 8.0mM Na_2CO_3/1.0mM $NaHCO_3$ solution. The IonPac AS14 separator column provided isocratic separation of seven common inorganic anions at ambient temperature. Cation analysis was performed using the ICS 2000 with a conductivity detector system (DIONEX Corp.) interfaced with a PC running CHROMELEON v.6.5.

Sedimentation Tests

The segregation index and the fines capture index are used to characterize the tailings sedimentation behaviour. The segregation index may be computed based on the solids content of each layer or the fines content of each layer. The fines capture is defined as 100% minus the segregation index. The average solids content at the end of the test is determined by the weighted average of the solids content of each layer. The segregation index is based on the solids content in each layer and is determined by the following equation:

$$SI = \frac{\sum \left| (s_n - s_{ave}) * (H_n - H_{n+1}) \right|}{s_{ave}} * 100\% \quad [1]$$

Where S is solids content and H is the normalized height. Fines capture index is 100% minus the segregation index. Segregation index can also be determined by fines content in each layer. The equation can be written as below

$$SI = \frac{\sum \left| (f_n - f_i) * (H_n - H_{n+1}) \right|}{f_i} * 100\% \quad [2]$$

where f = initial fines content.

For high sand-to-fines ratio mixtures such as 5:1 and 6:1, determination of the segregation index using the solids content is preferred. For lower sand-to-fines ratios, such as 4:1, calculation of the segregation index based on fines content is preferred because it provides a better understanding of the fines capture in each layer.

RESULTS

Mixed clay mineral CEC

Kaolin was mixed with bentonite in the following percentages: 1, 2, 5 and 10% and the CEC were measured on each mixture. Pure kaolin and bentonite were also tested, and their mean CECs were measured as 6.98 meq/100g and 74.91 meq/100g respectively. The measured CEC values are presented in Table 1. Based on the measured CEC of kaolin and bentonite, the CEC of the mixtures was predicted using the arithmetic sum of the parts. Figure 1 compares the predicted CEC values to the measured values.

Table 1 EC and CEC (mean values)

Sample	Ca	Na	Mg	K	Total Ex	CEC
			meq/100g			
Kaolinte 2007	1.25	0.15	3.51	.24	5.36	12.2
Kaolinte 2008	1.4	0.52	1.95	0.0	3.87	9
Kaolinite WISEST	1.4	0.42	2.1	n/a	4.0	7.0
1% Bentonite	2.1	0.39	2.8	n/a	5.2	7.6
2% Bentonite	2.6	0.38	3.5	n/a	6.4	8.4
15% Bentonite	4.3	0.38	5.71	n/a	10	11
10% Bentonite	7.4	0.37	9.7	n/a	17	15
Bentonite	58	0.37	77	0.31	136	75
MFT 2007	5.9	5.3	1.6	0.3	13.1	29
MFT N	8.8	12	2.0	0.07	23	31
MFT S	4.1	16	1.4	0.10	22	40

Kaolinite 2007, 2008 and WISEST tests were conducted by different researches to calibrate their experimental methods.

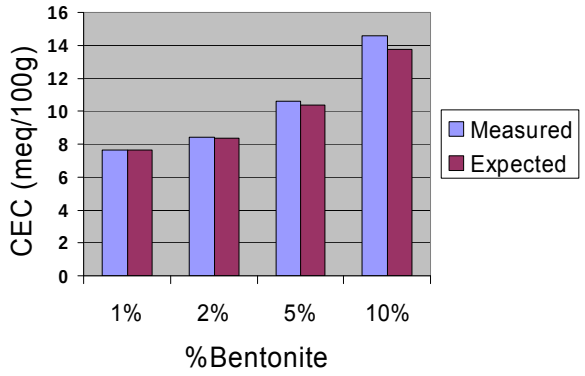

Figure 1. Cation exchange capacity of kaolin/bentonite mixtures: measured vs. expected

At low bentonite concentrations, the arithmetic sum of CECs of the two clays is an accurate predictor of the total CEC. The trend shown here indicates that as bentonite concentration increases the %error of the predictions also increases: from 0.5% error at 1% bentonite content to 5.6% error at 10% bentonite content. The likely cause of the increasing %error in CEC is the dissolution of soluble mineral phases that result in increased Ca and Mg concentrations in the sodium acetate solution. Saturated paste extracts of bentonite showed substantial masses of Ca and Mg. Further testing at higher bentonite contents would provide better insight into the interaction between the two clays and the subsequent effect on CEC.

CEC of MFT

MFT samples were centrifuged and pore water was separated prior to equilibration with sodium acetate solution. Two different MFT samples were used in the test. Separated water was analyzed using ion chromatography and the results are shown in Table 1. Samples were prepared in triplicate; two dilutions were prepared from each. All MFT samples were filtered using 0.2µm nylon syringe filters for particulate matter and an OnGuard II RP 2.5cc cartridge from DIONEX to remove organics.

Mixed Clay Mineral EC

For the kaolinite-bentonite clay mixtures, the measured EC was generally less than the measured CEC. At low bentonite content, the total EC accounted for less than the measured CEC. At 10% bentonite, the measured total EC exceeds the CEC, and at 100% bentonite the total EC is nearly double the CEC. Figure 2 displays the measured exchangeable cations as a percentage of the total cation exchange capacity. The difference between the CEC and EC is shown in grey. In the last two cases (10% and 100% bentonite) the EC exceeds the CEC. The % difference is indicated separately.

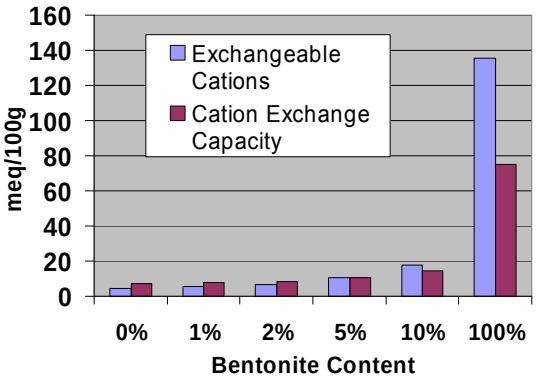

Figure 2. Total EC vs. CEC and varying bentonite content

Magnesium and calcium are the dominant cations in all tested bentonite contents. Sodium concentrations did not increase with bentonite content, while potassium increased slightly from ~21meq/100g in pure kaolin to ~30meq/100g. Changes in anion concentration in the saturated paste extraction indicate that mineral solubility is

interfering with EC determination. Chloride content in the saturated extracts are relatively constant at 0.2 meq/100 g of soils decreasing to 1.5 meq/100g at 10% bentonite which suggests that there is chloride salt in kaolinite, probably halite (NaCl).

Conversely, sulphate concentrations increase with increasing bentonite concentration which suggests that a sulphate mineral is present in the bentonite. The sulphate content increases from 8 meq/100g at 5% bentonite to 15 meq/100g at 10%. If calcium sulphate is present within the bentonite, then as more bentonite is added it would be expected that calcium and sulphate content should increase accordingly. Sulphate content was observed with increasing bentonite. The calcium content did not increase at the same rate because of ion exchange reactions. As the calcium sulphate mineral (gypsum) dissolves and calcium solubilizes, some of the Ca exchanges for Mg on the kaolinite and bentonite exchange sites, increasing the Mg content in solution.

EC of MFT

There is a substantial difference between the total EC and the CEC of both MFT samples and differences between individual MFT samples. 2008 MFT samples S and N had different amounts of calcium on their exchange sites. Sodium, potassium, and magnesium contents were similar (see Table 2). A sample of MFT N collected in 2007 samples also had different Ca and Na content. Work by Islam in 2008 indicated that the distribution of cation on the MFT N samples was consistent between 5 samples analyzed the average results are presented in Table 2.

NaOH Treated Kaolinite

A major component of the oil sands bitumen extraction process is the addition of caustic (NaOH) or sodium citrate to create a surfactant so that bitumen releases from the sediment surfaces into the water phase for recovery. The sodium ions from the sodium hydroxide and sodium citrate cause ion exchange reactions with the clay minerals present in the ore.

The addition sodium hydroxide to the clay mixtures results in the release of exchanged Mg from the exchange sites. The untreated kaolinite has 28% of surface exchange sites filled with Mg, but after NaOH addition 30% of the sites exchange sites are filled with Na and negligible Mg is present on the kaolinite surface (Table 2).

The exchangeable cations in MFT samples are similar in that negligible Mg is present on the exchange sites (4 to 6 meq/100). Sample MFT S has a distribution of exchangeable cations similar to the NaOH treated kaolinite, but with higher exchangeable sodium (10 meq/100g) and CEC.

Table 2 Exchangeable cations

Sample	Ca-Ex	Na-Ex	Mg-Ex	K-Ex	EC/CEC
	% of Sites Filled				
Kaolinite 2007	10	1	28	1	42
Na-Kaolinite 2007	10	30	0	2	47
Kaolinte WISEST	21	6	30	0	57
Kaolinte 2008	15	6	22	0	43
MFT N 2007	20	18	5	1	45
MFT S	10.2	39.7	3.6	0.2	56
MFT N	28.6	38.9	6.4	0.2	76

Sedimentation Test Results

A series of sedimentation tests were conducted on synthetic tailings prepared from kaolinite and mixed clay minerals. The tailings solids contents were varied, but the fines content was kept constant at 20%. In some of the tests the clay minerals were treated with NaOH to pH 9.5 prior mixing to mimic extraction conditions. The NaOH treatment had a profound impact on the sedimentation characteristic of the synthetic tailings mixtures. For untreated kaolinite, the segregation boundary occurred at approximately 55% solids. When the kaolinite was treated with NaOH, the synthetic tailings completely segregated at 64% solids Synthetic kaolinite tailings were prepared with 56% solids and 20% fines as a standard mix; the mixed clay mineral test was prepared with 60% solids and 20% fines as a standard mix.

Mixed Clay Minerals

Standpipe sedimentation test results at 60% solids content, with 20% fines mixed at 2, 5 and 10% bentonite content are presented in Figure 3. Pure kaolinite (not shown) and mixtures of 2 and 5% bentonite all exhibited segregating behaviour at 60% solids content with Na-loaded exchange sites (see Table 2). At 10% bentonite content the synthetic tailings mixtures became non-segregating.

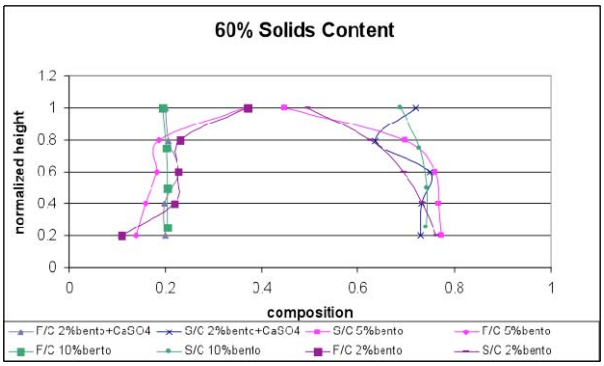

Figure 3. Results of mixed clay minerals sedimentation tests at 60% solids content and NaOH treated clay minerals

The addition of bentonite to the fines appears to improve sedimentation behaviour. The bentonite used in this experiment contained Ca and Mg on its exchange sites (Table 2) and contained some soluble sulphate salts. The addition of bentonite to kaolinite clays may have introduced some divalent cations into solution so that when the clay, sand and DI water were mixed for the sedimentation test, cation exchange reactions redistributed the divalent cations onto the clay surfaces. At lower ionic strengths, the divalent cations would be preferred on the exchange sites over monovalent cations. At 10% bentonite addition, sufficient divalent cations are present to change the clay surface properties, causing the clay particles to aggregate. The aggregates are able to support the sand grains so that the mixture does not segregate. We were unable to differentiate between cations generated from exchange reactions and cations that may be from soluble sulphate salts in the bentonite with the data gathered during this experimental program. The addition of bentonite in these experiments does appear to lower the solids content segregation boundary.

The importance of the divalent cation on sedimentation behaviour was investigated via the addition of gypsum ($CaSO_4$:$2H_20$) (13 mg/L) to the mixed clay minerals sedimentation tests. The addition of gypsum to the 2% bentonite mixture produced a non-segregating tailings. The 10% bentonite mixture and the 2% bentonite mixture with gypsum amendment produced similar sedimentation behaviour with a fines capture of >98%.

Synthetic Kaolinite Tailings

As series of standpipe sedimentation tests were conducted on synthetics tailings using NaOH-treated kaolinite and tailings sand at 56% solids content, 20% fines, and fines/(fines+ water) ratio of 0.2. Successive amounts of gypsum (Table 3) were added to the standpipe tests to determine the amount of gypsum addition required to convert the slurries to a non-segregating mixture.

Table 3. Kaolinite sand clay mixtures for synthetic tailings sedimentation tests

Mix #	Pore fluid amendments
4	DI water + washed sand
11	20.2 mmoles/L NaOH
12	NaOH treated Kaolinite + 4.7 mmoles/L $CaSO_4$
13	NaOH treated Kaolinite + 7.0 mmoles/L $CaSO_4$
14	NaOH treated Kaolinite + 9.4 mmoles/L $CaSO_4$
15	NaOH treated Kaolinite + 14.7 mmoles/L $CaSO_4$

Results for the synthetic tailings sedimentation tests are presented Figure 5 and Table 4. Mix 11 was an un-amended sedimentation test on NaOH-treated clay and it segregated completely. The segregation boundary was not determined for the un-amended NaOH-treated clay because sedimentation tests at 64% solids content and 20% fines completely segregated and a solids content of 64% is greater than what can practically be pumped in an oil sands tailings operation.

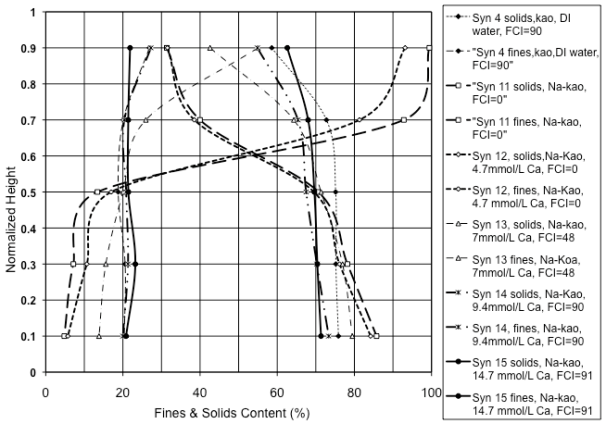

Figure 4. Normalize height and fines and solids content for kaolinite sand synthetic tailings sedimentation tests.

Progressively higher gypsum amendment content were added to Mixes 12, 13, 14 and 15. Mix 12 segregated completely, while Mix 13 (7.0 mmoles gypsum amendment) starts to show the impact of calcium adsorption. Mixes 14 and 15 were

essentially non-segregating mixtures, with little difference in segregation index. It is apparent that gypsum addition improves sedimentation behaviour, but more is not necessarily always better. In some of the preliminary sedimentation testing (not shown) using the untreated kaolinite with 14.7 mmoles of gypsum amendment increased segregation behaviour. The addition of Ca to a kaolinite that already had a surface dominated by adsorbed Ca and Mg increased segregation behaviour. This suggests that it may be the distribution of charged species on the surface and not the species itself that influences segregation behaviour.

Table 4. Exchangeable cations on Kaolinite in sand Clay slurry sedimentation tests

Tailings		E-Ca	E-Na	E-Mg	E-K	Fines Capture Index
		% Sites Filled				
4	Initial	10.28	1.16	28.75	1.99	90
	Final	9.22	1.96	30.88	2.12	
11	Initial	10	30	0	2	0
	Final	10	39		2	
12	Initial	10	30	0	2	0
	Final	35	16	0	1	
13	Initial	10	30	0	2	48
	Final	44	12	0	1	
14	Initial	10	30	0	2	90
	Final	51	7	0	1	
15	Initial	10	30	0	2	91
	Final	63	2	0	1	

Table 4 presents a summary of the calculated distribution of exchangeable cations on the kaolinite surfaces for the sedimentation tests.

The sedimentation tests indicate that the slurries do not become non-segregating until at least 50% of the exchange sites are occupied by calcium. Also of interest is that the segregation index does not increase significantly with increasing calcium adsorption. It is apparent that sedimentation behaviour is a function of the Ca/Na ratio or divalent to monovalent cation ratio on the clay surfaces. For the synthetic kaolinite tailings, the Ca/Na ratio for non-segregating behaviour needs to be around 7:1. Mix 4, using the untreated kaolinite washed sand and deionized water, which had a divalent to monovalent cation ratio of 10:1 also had non-segregating behaviour for 56% solids and 20% fines mixture. Analysis of the various MFT samples indicates adsorbed Ca/Na ratios of 1:4 to 3:4 which also suggests that segregating behaviour is a function of the distribution of adsorbed cations.

Table 5 presents a summary of the final water chemistry (recycled water) for the sedimentation tests. The final water chemistry was used to calculate the changes in adsorbed cation species. For Mix 11, the NaOH-treated clay, the sodium solution concentration increased when the clay, sand and water were mixed (see Table 5). It appears that the kaolinite may contain sodium chloride and calcium sulphate salts.

Table 5. Water chemistry for kaolinite synthetic tailings experiments

	Stock Solution							Recycled Water							
Mix No.	I	pH	Ca	Na	SO4	Cl	Mix No.	I	pH	Ca	Na	Mg	K	SO4	Cl
			mmol/L							mmol/L					
4	-	-	-	-	-	-	4	0.01	6.9	1	0.9	0.8	0	2.02	1
11	0.02	11	-	20.2	-	-	11	0.02	11		23		0	1.5	0
12	0.02	5.9	4.7	-	6.2	-	12	0.02	9.3	0	18	-	0	5	0
13	0.03	6.2	7	-	6.6	-	13	0.03	9.3	0	19	-	0	6.6	0
14	0.04	6.5	9.4	-	10.3	-	14	0.03	8.7	1	20	-	0	8	0
15	0.06	6.5	15	-	15.5	-	15	0.04	9.2	2	22	-	0	12.4	0

Table 6 present a summary of some saturated paste extracts from the kaolinite and sands used in the sedimentation experiments. The DI water extraction of the kaolinite indicates that there are soluble salts present within the clay. Sulphate and chloride are present in the recycled water, which supports the presence of soluble salts. Ca, Na, Mg and K are also present in solution. Approximately 1 mole of chloride and 0.9 moles of Na were measured suggesting the presence of NaCl contamination. The solution also contained 2 moles of sulphate and 1.8 moles Ca and Mg,s which suggest a mixture Ca and Mg sulphate. The sands supplied for the sedimentation test also contained soluble salts, to the extent that they were washed with DI water prior to use. The washed sand contained some residual Na, Ca and Mg and sulphate. The problem with determining the source of the salts is that once the DI water, sand and kaolinite are mixed, cation exchange reactions occur, altering the distribution of cations on the clay surfaces. The changes in adsorbed cations were calculated based on the changes in water chemistry and the addition of Ca, Na, and Mg from both the clays and the washed sand.

Table 6. Chemistry of Extracted Solutions.

	pH	Ionic Strength	Na	Ca	Mg	NH4+	K	SO4-2	Cl
			Cations					Anions	
		M	meq/L						
Extraction of Kaolinite with DI	5.93	0	0.33	0.02	0.02	0.02	0.06	-	0.25
Unwashed Sand	5.6	0.01	0.11	5.2	2.58	0.12	0.04	9.68	0.05
Washed Sand	5.6	0.01	0.05	2	0.98	0.03	0.03	2.92	0.01

The recycled water chemistry also illustrates that the process are not strictly ion exchange. As calcium is added it is adsorbed until 9.4 mmmole of Ca addition is reached, the point when Ca is first measured in the recycled water. In a pure ion exchange reaction, the sodium concentration would be expected to rise in the recycled water as calcium replaces sodium on the exchange sites in a predictable fashion: one Ca^{+2} exchanged for two Na^{+}. Sulphate concentrations were observed to dd,increase as the gypsum dose increase but sodium is only increased by 1 mmole/L for each 3 mmoles/L of calcium addition. We can see from Table 5 that as the calcium is adsorbed, some the adsorbed sodium is being displaced but the total number of filled sites is also increasing. For Mix 11, about 50% of the sites are filled but in Mix 15 the exchangeable cations increases to 65% of the cation exchange capacity. Sodium concentrations are increasing in the recycled water but not at the same rate as calcium adsorption.

SUMMARY AND CONCLUSIONS

- The addition of bentonite to kaolinite increases the cation exchange capacity of the mixture by the equivalent exchange sites on the bentonite.
- Calcium (10-20%) and magnesium (22 to 30%) are the dominate exchangeable cations on the kaolinite clay surfaces.
- Treating the kaolinite clay with NaOH to mimic oil sands extraction conditions results in the complete desorption of exchangeable magnesium and replacement by sodium (30%). Exchangeable calcium was not impacted by NaOH addition.
- Exchangeable cations in kaolinite and MFT samples account for 42% to 75% of the available cation exchange capacity
- The amount of exchangeable cations appears to increase with increasing bentonite content due to the presence of soluble calcium, magnesium and sodium salt present in the kaolinite and bentonite.
- The CEC of MFT samples ranged from 29 to 40 meq/100g
- Analysis of MFT samples indicate calcium (10% to 29%) and sodium (18 to 40%) are the dominant exchangeable cations.
- The addition of bentonite to a kaolinite sand slurry reduced the solids content for the segregation boundary.
- The addition of calcium amendment to a 2% bentonite slurry produced the same segregation index as the 10% bentonite mixture.
- The segregation behaviour of NaOH treated kaolinite and sand slurry (56% solids & 20% fines) changes to non-segregating when calcium occupies 50% of the available cation exchange capacity.
- Segregation behaviour does not improve with increasing calcium adsorption after 50% of the sites are occupied by calcium

ACKNOWLEDGMENTS

This work was funded by The Oil Sands Tailing Research Facility and by The Applied Environmental Geochemistry Research Facility at the University of Alberta. The Summer Student was funded by an NSERC Discovery Grant and the two grade 11 students were sponsored by the Women in Scholarship Science Engineering and Technology. This work would not have been possible without the training and support of the analytical chemist Jela Burkus.

REFERENCES

Boratynec, D. (2003). Fundamentals of Rapid Dewatering of Composite Tailings. Department Civil & Environmental Engineering. Edmonton, University of Alberta. MSc.: 267.

Caughill, D. L., N. R. Morgenstern, and Scott J. D. (1993). "Geotechnics of nonsegregating oil sands tailings." Canadian Geotechnical Journal 30(5): 801-811.

ERCB (2008) Tailings Performance Criteria and Requirements for Oil Sands Mining Schemes, Energy Resources Conservation Board, Calgary, June 26 2008, 11 pages.

Hollander, E. How the clay particle beat the 104tph process (interaction of colloidal chemistry and process engineering). Shell Canada Energy. CONRAD clay conference 2008 presentation slides.

Islam, N. (2008) The role of cation exchange on the sedimentation behavior of oil sands tailings. . Civil & Environmental Engineering Edmonton, University of Alberta. MEng.

Scales, P. (2008) Rheology of clay suspensions, CONRAD clay conference 2008 presentation slides. Melbourne Engineering Research Institute. 23 pages

Shaw, B. (2006). Alternative Composite Tailings Chemicals: Lime 1999 Laboratory Tests. Edmonton, Syncrude Research.

Sofra, F. and D. V. Boger (2002). "Environmental rheology for waste minimization in the minerals industry." Chemical Engineering Journal 86: 319-330.

Tang J. (1997) Fundamentals Behaviour of Composite Tailings. M.Sc., University of Alberta.

CATION EXCHANGE CAPACITY OF CLAY FRACTIONS FROM OIL SANDS PROCESS STREAMS

Peter Uhlik[1,2], Ali Hooshiar[1], Heather A.W. Kaminsky[1], Thomas H. Etsell[1], Douglas G. Ivey[1] and Qi Liu[1]
1 Department of Chemical and Materials Engineering, University of Alberta, Edmonton
2 Department of Geology of Mineral Deposits, Comenius University in Bratislava, Slovakia

ABSTRACT

Understanding the clay minerals in oil sands is vital to oil sands processing as they influence water chemistry and interact with bitumen to reduce bitumen recovery and froth quality, as well as control the settling behaviour of fine tailings. Cation exchange capacity (CEC) and total surface area (TSA) are important properties that characterize clay minerals. In the past, relatively high values of both properties indicated the presence of expandable clay minerals along with kaolinite and illite, the two dominant clay minerals in oil sands. The presence of mixed-layer illite-smectite and kaolinite-smectite has been confirmed by XRD and HRTEM in recent years. In this study, the CEC of the clay fractions obtained from the clay lenses interbedded within the oil sands, the oil sands ore and extraction products (froth, middlings and tailings) has been determined. Two cation-exchange capacity measurement techniques (using methylene blue and Cu (II) triethylenetetramine) were chosen to evaluate the impact of organic matter and nano-sized iron oxides on the CEC of the clay fractions. Simultaneously, both CEC measurement techniques were mutually compared.

INTRODUCTION

Clays should be considered in any oil sands bitumen extraction process for several reasons. First, interactions between clays and organic materials, especially bitumen, have a great influence on both froth quality and extraction efficiency. It has been shown that the interactions between clays and bitumen result in clay-organic complexes. The presence of different cations on clays influences the formation of these complexes. These interactions alter both oil composition and clay surfaces (Clementz, 1976; Czarnecka & Gillott, 1980; Ignasiak et al., 1983; Wallace et al., 2004). Different clays such as montmorillonite and kaolinite play various roles in the bitumen extraction process in the presence of different cations. For example, montmorillonite decreases the bitumen liberation rate dramatically in a system containing calcium ions, while kaolinite does not (Kasongo et al., 2000). Second, the settling behaviour of tailings is directly controlled by the flocculation/dispersion behaviour of existing clays. Even a small amount of smectite, either as a discrete mineral or as smectitic layers in a mixed-layer mineral, has a great influence on settling and consolidation of tailings. Third, mutual interactions between clay characteristics and water chemistry have major influences on the extraction process. None of these interactions can be studied successfully without having a sufficient knowledge about the types, microstructures and properties of existing clays in the oil sands industry. Therefore, several studies have been done to determine the types of existing clays in oil sands. Kaminsky et al. (2008a) have performed a review on previous studies of clay mineralogy in oil sands. Based on such studies, the most abundant clays are kaolinite and illite. Smectite, chlorite, vermiculite and mixed layer clays were also reported in the oil sands in smaller quantities. Surprisingly, surface area and cation exchange capacity of tailings are considerably higher than the expected values for kaolinite and illite. Omotoso & Mikula (2004) and Kaminsky et al. (2008a, b) showed that this is due to the smectite mixed layering in kaolinite and illite.

This paper is focused on CEC as one of the fundamental properties of clay minerals. “The CEC is defined as a measure of the ability of a clay or a soil to adsorb cations in such a form that they can be readily desorbed by competing ions” (Bache in Dohrmann, 2006). Ions typically are absorbed in the interlayer spaces as a result of neutralization of the charges arising from substitutions in silicate layers. In addition to interlayer cations due to isomorphous substitutions, cations also can be absorbed via broken bonds along edges replacing the hydrogen in exposed hydroxyls. Broken bonds are the main cause of cation exchange capacity in kaolinite, and also provide a significant portion of the cation exchange capacity in illite and chlorite. In contrast, isomorphous substitutions

play the major role in the CEC of smectites. Cation sorption and distribution vary greatly among different clay minerals (Grim, 1962; Moore & Reynolds, 1997; Table 1). Soluble salts and nanosize oxides, especially Fe, make the measurement of clay's CEC complicated (Cornell and Schwertmann, 2000; Dohrmann, 2006; Hendershot et al., 2008). Organic matter also influences the total CEC of soils (Lax et al., 1986; Kaiser et al., 2008). Studying the influence of organic matter and iron oxides on CEC of clays obtained from various samples connected with oil sands is the main objective of this paper. The influence of both groups of these materials on CEC, as one of the most important properties of clays used for characterization of clay fraction in oil sands, has been studied.

Table 1: Cation exchange capacity of some clay minerals (Grim, 1962).

Clay mineral	CEC(meq/100g)
Kaolinite	3-15
Illite	10-40
Smectite	80-150
Vermiculite	100-150
Chlorite	10-40

MATERIALS AND METHODS

Samples

Four samples including high and low grade oil sands ores were used in this study (Table 2). Two of them (IS-8 and HK) were processed in a Syncrude-style batch extraction unit using the CANMET procedure that has been reported to represent hydrotransport conditioning at 50˚C (Wang & Mikula, 2002). The primary froth, middlings and tailings streams were then collected. Descriptions of sample preparation for the HK samples and their detailed characterization were published by Kaminsky et al. (2008a, b). Streams of IS-8 were directly used for separation of the <2 μm fraction by sedimentation using Stokes's law.

Two ores, 3A and 3B were processed using solvent extraction. In this process approximately 40 g of the oil sands ores were mixed with 200 ml of toluene for 2 minutes and then centrifuged, using a Sorvall RC6 Plus centrifuge (rotor type SLA-1500, 3500 rpm, 30 min), in order to separate solids from solvents and bitumen. Fresh toluene was added after supernatant removal and the procedure was repeated three times. Solids were then mixed with deionized water and the <2 μm fractions were separated by sedimentation.

Three clay lenses from the same area of the Syncrude lease (Table 2) as samples 3A and 3B were also used in this study since separation of the clay size fraction from these samples was easer compared to clay separation from oil sands ores. The clay lenses were manually separated from sands and mixed with deionized water. An ultrasonic bath was used for dispersing the larger pieces and aggregates of clays. The <2 μm fraction was prepared by sedimentation. Finally, the ultra fine clay fraction, <0.2 μm, was obtained by centrifuging the <2 μm fraction.

The modified Jackson treatment by Šucha et al. (1991) was applied to a portion of each separated clay fraction from each sample. In this procedure, sodium acetate was used to remove carbonates, hydrogen peroxide to remove organic materials, and sodium dithionite ($Na_2S_2O_4$) and citrate buffer to remove iron oxides. After extraction of iron oxides, the samples were centrifuged in order to remove the solids from the extract. Solids were washed with deionized water and centrifuged again. The extract was analyzed by atomic absorption spectroscopy (AAS) for iron. Na labelled samples are those saturated with sodium, after residual organic matter and iron oxide removal. Some slurries of the HK sample were selected to determine the amount of amorphous iron oxides by the ammonium oxalate procedure (Smith, 1984).

Two samples, mixed layered illite-smectite (IS Cz-1) and hectorite (smectite, SHCa-1), from the Source Clay Minerals Repository of the Clay Minerals Society were used as standards to control our procedures.

XRD analysis

Oriented clay slides of size fractions 0.2–2 μm and <0.2 μm were prepared by the Millipore transfer method (Moore & Reynolds, 1997). All samples were run on a Rigaku RU-200B X-ray diffractometer with Co Kα radiation. Oriented samples were run from 3° to 58° 2θ with 0.02° steps per second. All tests were run in two conditions: overnight saturation at 54% relative humidity (RH) and, subsequently, additional over night saturation with ethylene glycol (EG).

Table 2: Basic characterization of studied samples.

Sample	Bitumen (%)	Fines (%)	Water (%)	Characterization
IS-8	13.1	9	1.2	high grade*
HK	8.5	32		low grade, Suncor lease
3A	12-14	20	4-5	high grade, good processability*
3B	7-8	35	5-6	low grade, poor processability*
4A	2-3	40-50	8-10	Imbedded (mm to cm scale) sand or silt and clay, poor processability*
4B	2-3	40-50	8-10	Imbedded (mm to cm scale) sand or silt and clay, poor processability*
5	0-1	80-90	8-10	nearly 100% clay, poor processability*

*Syncrude samples

Determination of CEC

Two methods were used to determine the CEC of the clay samples. The first method was methylene blue titration. In this method 0.2 g of the dried solids were dispersed into 50 ml of 0.015M $NaHCO_3$ along with 2 ml of 10% w/w NaOH. The resultant mixture was stirred using a magnetic stir bar and sonicated, until the sample was completely dispersed. Once the samples were dispersed, 2 ml of 10% v/v H_2SO_4 was added and the pH measured to ensure it was below pH 3. The sample was then titrated in 1 ml or 0.5 ml intervals with a fresh solution of 0.006N methylene blue (MB). After each addition of methylene blue, a transfer pipette was used to place one drop of the titrated mixture onto Whatman #4 qualitative filter paper. The droplet was examined for the presence of a blue halo which would indicate the end point of the titration. When a light blue halo appeared around the drop, the sample was left to stir for two more minutes and then another drop was placed on the filter paper to make sure the drops had been taken from a homogenized, fully dispersed solution. The end point was reached when the halo was still present after the second drop. At the end point of the titration, the volume of methylene blue added to the slurry was recorded and used to calculate the methylene blue index and methylene blue surface area (SA) according to the methods of Hang and Brindley (1970): MBI (meq/100 g) = [(volume of MB x normality of MB)/(weight solids)] x 100 and SA (m^2/g) = MBI x 130 x 0.0602.

used for the exchange solution. 1.463 g of triethylenetetramine was dissolved in 100 ml of deionized water and mixed with an identical amount of copper (II) sulphate. The solution was then appropriately diluted (Meier & Kahr, 1999). At least two specimens with different weights (120 and 80 mg) per sample were added to 30 ml deionized water and dispersed in an ultrasonic bath. Afterwards, 6 ml of Cu-trien was added and the suspensions were shaken for one hour by a rotary machine (B&B SA-12) at 60 rpm. The suspension was then centrifuged. The concentration of Cu (II) complex in the supernatant was determined by ultraviolet-visible (UV-VIS) spectrophotometry (Cary, Varian). The difference between the adsorption of the diluted Cu-trien reagent and the adsorption of the supernatant of a sample was used for the CEC calculation.

RESULTS

XRD analysis

The main clay minerals in all studied samples are kaolinite and illite with a very small amount of chlorite and probably mixed-layered illite-smectite (Figures 1-3). From the XRD patterns of sample 3A and all slurries of IS-8, it can be concluded that these samples consist of more kaolinite than the rest of the samples. According to the XRD patterns after EG saturation, the IS-8 sample contains very little or no expandable phase compared to the other studied samples (Figure 3), especially HK (Kaminsky et al., 2008a, b).

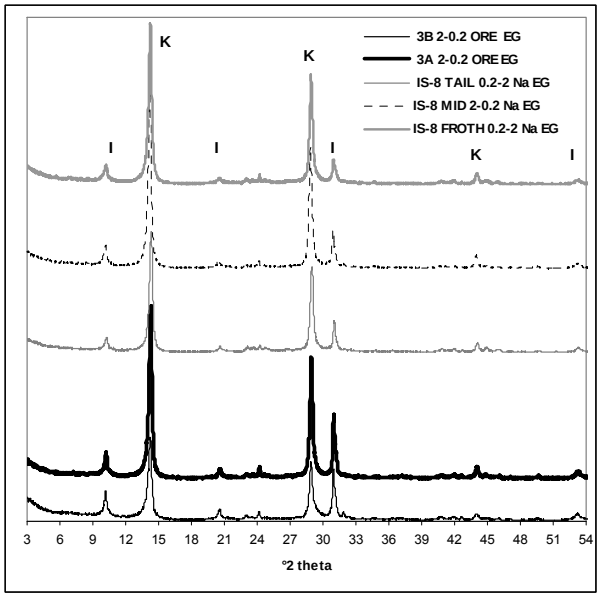

Figure 1: XRD patterns of oriented specimens of the clay fraction from the oil sands. I- illite, K- kaolinite.

The mineralogy of the clay fractions obtained from the clay lenses is very similar to the mineralogy of HK, including the presence of lepidocrocite (Figure 3).

Determination of iron content from amorphous and crystalline Fe oxides

Sodium dithionite extraction provides information about the presence of Fe in both amorphous phases and crystalline oxides. As depicted in Table 3, a relatively wide range of iron content was obtained from the studied samples. The smallest amount of dithionite extractable Fe was determined for IS-8 slurries, with values between 0.1 and 0.2% of Fe. Clay fractions of clay lenses and sample HK contain from 0.3 to 2.4% of soluble Fe. According to data from Table 3, it seems that Fe oxides are concentrated in the coarser fraction of the primary froth. This concentration of iron oxides in the coarser fraction is most obvious for the HK samples. The similarity of ammonium oxalate and dithionite extraction results indicates that major form of soluble Fe is amorphous matter and microcrystalline iron oxide hydroxides such as lepidocrocite. Significant variations in the amount of soluble Fe have been obtained from both procedures only for the HK unseparated ore. For this sample the Fe content was much higher from sodium dithionite extraction. This value was much higher than the value of iron obtained for all other samples, except for the HK primary froth 0.2-2 μm fraction. This is probably because the procedure with sodium dithionite extracts some crystalline iron (i.e., carbonate iron) in addition to the amorphous iron, whereas the ammonium oxalate procedure only removes the amorphous iron. Since the crystalline iron concentrates in the coarse fraction, this makes a large difference for the samples containing the coarse fraction (Kaminsky et al., 2008a).

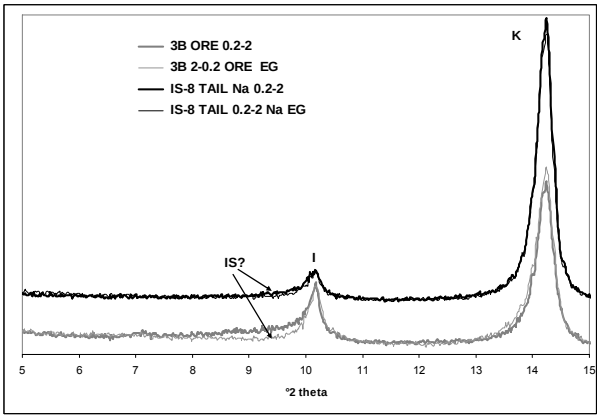

Figure 2: Comparison of XRD patterns of oriented specimens before and after ethylene glycol (EG) saturation. I- illite, K-kaolinite, IS- mixed-layered illite-smectite.

CEC measurements

CEC results for clay fractions of clay lenses from both methods, MB and Cu-trien, show that they are not affected by either the method or the presence of Fe and/or organic matter in the samples (Table 4). Results show a similar trend for IS-8 slurries except for the froth and the tailings (0.2-2 μm) from Cu-trien. These two values are considerably higher than all the other of IS-8 samples. Generally, CEC results, as well as SA values, are very low for IS-8 samples. Significant differences were not observed between the CEC of the <0.2 and 0.2-2 μm fractions of IS-8 slurries. On the contrary, the HK ultrafine fraction has a higher CEC value than the 0.2-2 μm fraction.

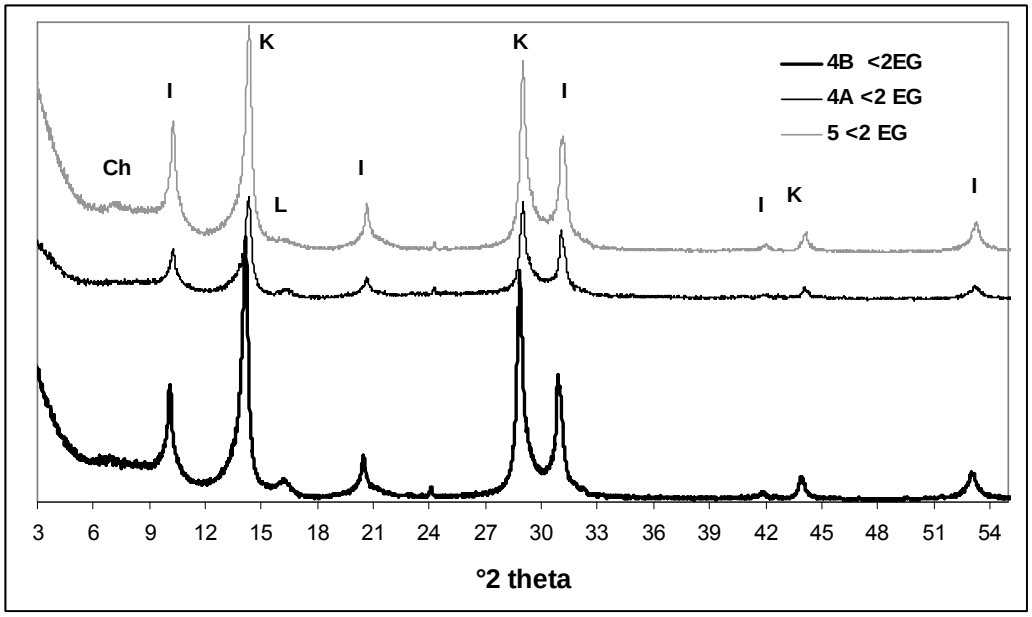

Figure 3. XRD patterns of oriented specimens of the clay fraction from clay lenses. CH – chlorite, I- illite, K- kaolinite, L- lepidocrocite.

Table 3: Amount of soluble Fe (mg/g of used sample) after sodium dithionite extraction (1) and after ammonium oxalate procedure (2).

Sample	1	2
IS-8 Froth 0.2-2	2.44	
IS-8 Middlings 0.2-2	1.42	
IS-8 Tailings 0.2-2	1.66	
IS-8 Froth <0.2	1.19	
IS-8 Middlings <0.2	0.98	
IS-8 Tailings <0.2	1.08	
5 <2	5.97	
4A <2	10.61	
4B Clay <2	14.40	
IS Cz-1 <2	1.36	
HK <0.2 Ore	6.21	4.39
HK <0.2 Middlings	4.01	
HK <0.2 Tailings	6.38	
HK 0.2-2 Ore	10.17	9.28
HK 0.2-2 Primary Froth	23.97	
HK 0.2-2 Middlings	9.52	8.01
HK 0.2-2 Tailings	3.04	
HK Unseparated Ore	24.58	4.16

Table 4: All measured data of CEC and SA.

		Before Jackson Treatment				After Jackson treatment (Na)		
Fraction (mm)	**Sample**	**SA** calculated from MBI (m^2/g)	**CEC MBI** (meq/100g)	**CEC Cu-trien** (meq/100g)		**SA** calculated from MBI (m^2/g)	**CEC MBI** (meq/100g)	**CEC Cu-trien** (meq/100g)
<2	5	148	19	19		151	19	19
<2	4A	153	20	20		147	19	19
<2	4B	154	20	20		157	20	15
<2	IS Cz-1	316	40	39		295	38	42
<2	SHCa-1	567	73	74		-	-	-
0.2-2	IS-8 Froth	63	8	7		-	-	19
0.2-2	IS-8 Middlings	55	7	8		47	6	8
0.2-2	IS-8 Tailings	-	-	-		-	-	16
<0.2	IS-8 Froth	94	12	11		70	9	12
<0.2	IS-8 Middlings	102	13	13		94	12	13
<0.2	IS-8 Tailings	78	10	-		94	12	14
0.2-2	HK Primary Froth	172*	22*	32		-	-	22
0.2-2	HK Middlings	86*	11*	10		-	-	-
0.2-2	HK Tailings	70*	9*	11		-	-	10
<0.2	HK Primary Froth	243*	31*	39		-	-	-
<0.2	HK Middlings	290*	37*	41		-	-	35
<0.2	HK Tailings	297*	38*	33		-	-	35
<0.2	3B Ore	125	16	27		-	-	-
0.2-2	3B Ore	94	12	15		-	-	-
0.2-2	3A Ore	-	-	20		-	-	-

- not measured because of sample deficiency
* published by Kaminsky et al. (2008a)

A more important discrepancy between the values obtained from the two CEC techniques has been found for only two of the samples, the HK primary froth and the ultrafine fraction of the 3B ore before removing the Fe oxides and organic matter. Cu-trien values are higher by about 10 meq/100g, or 20-40%, than MBI values.

DISCUSSION

The CEC data and XRD results of the studied clay fractions are in accordance with the general trend that expandable phases increase the value of CEC. The HK sample has the highest CEC within the studied samples. Kaminsky et al. (2008a, b) reported a significant amount of expandable mixed-layered phases: illite-smectite (I-S) and kaolinite-smectite in this sample. The high CEC is primarily due to the high content of I-S, almost 30% in the 0.2-2 μm fraction and almost 50% in the <0.2 μm fraction. On the other hand, IS-8 had the lowest CEC value and contained a negligible amount of expandable phases. Another difference between HK and IS-8 is the ratio of kaolinitic to illitic phases. Kaolinite is the dominant phase in sample IS-8. It is worth noticing that HK is a fines-rich ore and IS-8 is an ore with low fines.

There are some concerns as to the accuracy of the MB results arising from published uncertainties about the adsorption of MB by glass surfaces, excess adsorption of the dye cations, MB sensitivity to the type of exchangeable cations and

the strong dependence of MB adsorption on the dispersion of clay minerals (Hang and Brindley, 1970; Kahr and Madsen, 1995; Czímerová at al., 2006). Despite these concerns, there is good aggreement between CEC values from the MB and Cu-trien methods (Figure 4). However, there are three samples significantly above and two samples significantly below the linear trend line. At present there is no satisfactory explanation for the lower positioned samples (4B Na and HK Tailings <0.2 μm fraction). It could be measurement error or another unknown reason. The three points positioned above the trend line (3B ore <0.2 μm fraction, HK primary froth 0.2-2 μm fraction and <0.2 μm fraction) are discussed in the next paragraph.

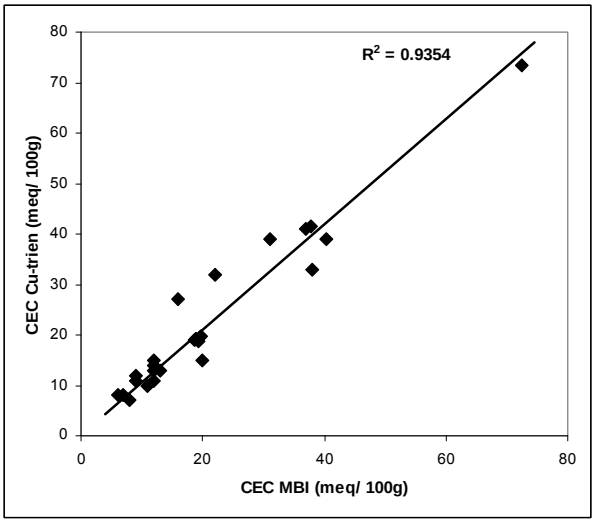

Figure 4. Relationship between values of CEC from both used techniques.

According to previous work (Meier and Kahr, 1999; Ammann et al., 2005; Czímerová et al., 2006), the determination of CEC with Cu-trien has the same accuracy as and is much faster than traditional methods such as the ammonium acetate or $BaCl_2$ method. Therefore, Cu-trien was chosen as the basic method for the CEC determination. The MB method was chosen as the second method because it has been frequently used in industry. Although more consistent results were expected from Cu-trien, the MB values were more consistent before and after organic and iron oxide removal indicating that MB is less affected by the presence of organic matter and/or iron oxides (Figure 5).

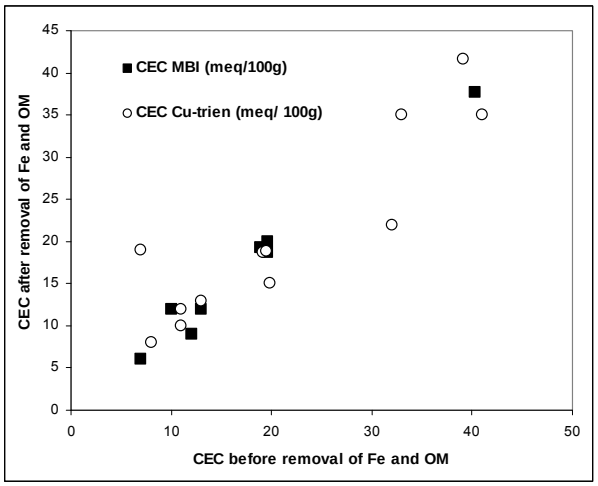

Figure 5. Relationship between values of CEC from studied samples before and after removal of iron oxides and organic matter.

This explains the occurence of three samples that were above the trend line in Figure 4. Grygar et al. (2007) have mentioned a risk of chemisorption of Cu^{2+} on hydrous ferric oxide admixtures. This may explain the extremely high Cu-trien result for the HK primary froth 0.2-2 μm fraction sample, which had a high content of Fe oxides noted by the sodium dithionite treatment (Table 3) as well as by TEM observation (Kaminsky 2008b). The Cu-trien CEC of the same sample after dithionite treatment (HK Primary Froth 0.2-2 Na) was significantly lower and was the same as the CEC measured by the MB method (Table 4). However, this value is still higher than other data for HK slurries. The SA calculated from MBI is higher than the SA calculated from the XRD result for the HK primary froth 0.2-2 μm fraction (Kaminsky et al., 2008). Based on this discrepancy the higher CEC of the HK primary froth 0.2-2 μm fraction Na may not be caused by either clay minerals or Fe oxides, but is probably due to the presence of residual organic matter that was not affected by either toluene or H_2O_2. The amount of this residual organic matter is greatest in the primary froth (Kaminsky, 2008).

CONCLUSIONS

Three conclusions can be drawn from the above results. First, in spite of the good results obtained by the halo MB method, this method is not optimal. It requires a person familiar with determination of the end point associated with the halo method, optimum dispersion and knowledge of the sample.

Cations, other than Na, could cause difficulties with this method as could the presence of highly charged clay minerals (Kahr and Madsen, 1995). Second, the occurence of amorphous or nanosize iron oxides in the oil sands is known (Kotlyar et al., 1988, 1990), but they are not particularly well characterized. This is probably because they are not easy to study due to their low quantities, very small size and poor crystallnity. The nanosize Fe oxides with their high sorption activities may play a role in oil sands processing difficulties despite their low concentration. For this reason it is suggested that a greater focus be placed on the role of Fe oxides in oil sands. Third, it seems that high amounts of Fe oxides and/or organic matter increase the CEC. On the other hand, when the amounts of Fe oxides and/or organic matter do not exceed some critical value they do not affect measured values of CEC; e.g.,, samples from clay lenses. Good agreement for most CEC results before and after application of the modified Jackson treatment indicate that this procedure does not influence the cation exchangeable properties of clay minerals.

ACKNOWLEDGEMENTS

The authors are grateful to the Centre for Oil Sands Innovation (COSI) for providing research funding and to Syncrude and Imperial Oil for providing samples.

REFERENCES

Ammann, L., Bergaya, F. & Lagaly, G. (2005) Determination of the cation exchange capacity of clays with copper complexes revisited. Clay Minerals, **40**, 441-453.

Clementz, D.M. (1976). Interaction of petroleum heavy ends with montmorillonite. Clays and Clay Minerals, **24**, 312-319.

Cornell, R.M. & Schwertmann, U. (2000). The iron oxides. 2nd edition Wiley-VCH GmbH & Co. KGaA.

Czarnecka, E. & Gillott J.E. (1980). Formation and characterization of clay complexes with bitumen from Athabasca oil sand. Clays and Clay Minerals, **28**, 197-203.

Czímerová, A., Bujdák J. & Dohrmann, R. (2006) Traditional and novel methods for estimating the layer charge of smectites. Applied Clay Science, **34**, 2-13.

Dohrmann, R. (2006). Cation exchange capacity methodology I: An efficient model for the detection of incorrect cation exchange capacity and exchangeable cation results. Applied Clay Science, **34**, 31-37.

Grim, R. E. (1962) Applied clay mineralogy, McGraw-Hill Book Company, Inc., USA.

Hang, P. T. & Brindley, G. W (1970). Methylene blue adsorption by clay minerals. Determination of surface areas and cation exchange capacities. Clays and Clay Minerals, **18**, 203-212.

Hendershot, W.H., Lalande, H. & Duquette, M. (2008). Ion exchange and exchangeable cations. In Soil sampling and methods of analysis, edited by Carter, M.R & Gregorich E.G, 2nd edition. Canadian Society of Soil Science.

Ignasiak, T.M., Kotlyar, L.S., Longstaffe, F., Strausz, O.P. & Montgomery, D. (1983). Separation and characterization of clay from Athabasca asphaltene. Fuel, **62**, 353-362.

Kaiser, M., Ellerbrock, R.H., & Gerke H.H. (2008). Cation exchange capacity and composition of soluble soil organic matter fractions. Soil Science Society of America Journal, **72**, 1278-1285.

Kahr, G. & Madsen, F.T. (1995). Determination of the cation exchange capacity and the surface area of bentonite, illite and kaolinite by methylene blue adsorption. Applied Clay Science, **9**, 327-336.

Kaminsky, H.A.W. (2008). Characterization of an Athabasca oil sands ore and process streams. [PhD. Thesis]. University of Alberta, Edmonton, Alberta.

Kaminsky, H.A.W., Etsell, T.H., Ivey, D.G., & Omotoso, O. (2008a). Distribution of clay minerals in the process streams produced by the extraction of bitumen from Athabasca oil sands. Canadian Journal of Chemical Engineering, in press.

Kaminsky, H.A.W., Hooshiar A., Uhlik, P., Shinbine A., Etsell, T.H., Ivey, D.G., Liu, Q. & Omotoso, O. (2008b). Comparison of morphological and chemical characteristics of clay minerals in the primary froth and middlings from oil sands processing by high resolution transmission electron microscopy. Proceedings from International Conference on Oil Sands Tailings, Edmonton, submitted.

Kasongo, T., Zhou, Z., Xu, Z. & Masliyah J.H. (2000). Effect of clays and calcium ions on bitumen extraction from Athabasca oil sands using flotation. The Canadian Journal of Chemical Engineering, **78**, 674-681.

Kotlyar, L.S., Kodama, H. & Ripmeester J.A. (1990) Possible identification of poorly crystalline inorganic matter present in Athabasca oil sands. Applied Clay Science, **5**, 1-12.

Kotlyar, L.S., Sparks, B.D., Kodama, H. & Grattan-Bellew, P.E. (1988). Isolation and characterization of organic-rich solids present in Utah oil sand. Energy & Fuels, **2**, 589-593.

Lax, A., Roig, A. and Costa, F. (1986) A method for determining the cation-exchange capacity of organic materials. Plant and Soil, **94**, 349-355.

Meier, L.P. & Kahr, G. (1999) Determination of the cation exchange capacity (CEC) of clay minerals using the complexes of copper(II) ion with triethylenetetramine and tetraethylenepentamine. Clays and Clay Minerals, **47**, 386-388.

Moore, D. M. & Reynolds, J. R. C. (1997). *X-ray diffraction and the identification and analysis of clay minerals.* Oxford University Press, Oxford, UK.

Omotoso, O. E. and Mikula, R. J. (2004). High surface areas caused by smectitic interstratification of kaolinite and illite in Athabasca oil sands. *Applied Clay Science*, **25**, 37-47.

Smith, B.F.L. (1984). The determination of silicon in ammonium oxalate extracts of soils. *Communications in Soil Science and Plant Analysis*, **15**, 199-204.

Šucha, V., Środoń, J., Zatkalíková, V. & Franců, J. (1991). Mixed layered illite/smectite: separation, identification, use. *Mineralia Slovaca*, **23**, 267 - 274.

Wallace, D., Tipman, R., Komishke, B., Wallwork, V., & Perkins, E. (2004). Fines/water interactions and consequences of the presence of degraded illite on oil sands extractability. *The Canadian Journal of Chemical Engineering, 82*, 667–677.

Wang, N., & Mikula, R.J. (2002). Small scale simulation of pipeline or stirred tank conditioning of oil sands: Temperature and mechanical energy. *Journal of Canadian Petroleum Technology*, **41**, 8-10.

POLYMER AIDS FOR SETTLING AND FILTRATION OF OIL SANDS TAILINGS

Xiaoyan Wang, Zhenghe Xu and Jacob Masliyah
NSERC Industrial Research Chair in Oil Sands Engineering
Department of Chemical and Materials Engineering
University of Alberta, Edmonton, Alberta, Canada

ABSTRACT

Commercial Magnafloc 1011 (Percol 727) polymer and in-house synthesized Al-PAM polymer were used to flocculate oil sands tailings that were derived from a low fines oil sand ore. The polymers were tested for their flocculation ability in terms of tailings settling and filtration. Both polymers showed excellent ability to enhance tailings settling.

Al-PAM performed very well as a filtration aid. The moisture of the cake obtained from tailings derived from the high fines ore was 6.6 ± 1.2wt%. This class of polymers can provide an alternative approach for oil sands tailings disposal that can eliminate tailings ponds.

However, the commercial Magnafloc 1011 (Percol 727) polymer was found ineffective as a filtration aid for the two tailings tested.

INTRODUCTION

Although Alberta is enjoying success story of unlock oil sands resources for oil, the environmental consequences of oil sands operations also brings Alberta to the radar of environmentalists world wide. One of the challenges facing oil sands industry is large land disturbances and huge tailings ponds. When discharged to the tailings ponds, the coarse sands settle quickly, while much of the fines and residual bitumen in tailings remain suspended, leading to the eventual formation of so-called mature fine tailings (MFT). The MFT typically contains about 30wt% of solids after two to three years settling with further consolidation taking hundred years [1]. The accumulation of large volume of MFT not only trap large amount of water, but its storage causes environmental concerns. To reduce this environmental concern and minimize fresh water in-take for oil sands processing, it is natural to treat tailings as they are produced. The immediate treatment of tailings will allow warm process water to be recycled quickly, while dry solids to be used for backfill so that tailings ponds could be eliminated. Clearly, the success of this approach will also contribute to greenhouse gas reduction and reduced chemical cost for processing.

In this study, we will focus on finding a suitable polymer which can effectively flocculate and enhance filtration of whole oil sands tailings. Although filtration as applied to oil sands tailings management has been attempted [2, 3], use of polymer as flocculants to enhance filtration of whole tailings has not been reported.

EXPERIMENTAL

Materials

The whole tailings were produced by laboratory extraction tests using a low fines ore. Bitumen extraction was conducted using Aurora process water. The tailings samples were assayed using industrial standard procedure (Dean Stark). They contained 76.4 wt% water, 1.1 wt% bitumen and 22.5 wt% solids. The solids contained 4.2% fines defined as -44 um.

Two polymers (flocculants), Magnafloc 1011 (Percol 727) purchased from Ciba Specialty Chemicals and in-house synthesized Al-PAM polymer, were used as settling and filtration aids. Magnafloc 1011 is a partially hydrolyzed polyacrylamide with a high molecular weight of about 17.5 million Daltons and of a medium charge density of around 27%. The synthesized Al-PAM is a hybrid $Al(OH)_3$-polyacrylamide, with ionic bond between $Al(OH)_3$ colloids and polyacrylamide chains[4].

Settling tests

For each settling test, 100g of tailings slurry were placed into a 250-ml beaker and mixed at 500 rpm for 2 minutes, followed by flocculant addition to the slurry under mixing at 300 rpm. After mixing, the slurry was transferred into a

100-ml graduated cylinder. After settling for 10 minutes, the photographs were taken to show the effectiveness of flocculant in promoting solids settling. The turbidity of the supernatant was measured using Turbidimeter (HF Scientific DRT-15CE Portable Turbidimeters, Fisher Scientific). It should be noted that flocculant dosages in this paper are expressed on the basis of slurry weight of tailings. Flocculant stock solutions of 500 ppm were prepared in deionized water one day prior to their use.

Filtration tests

The filtration tests were carried out using a laboratory filtration unit (LPLT300, Fann Instrument Company) shown in Fig.1. An especially hardened filter paper of 2-5 μm pore size (N87000, Fann Instrument Company) was used as filter media. The slurry was mixed in a similar manner as in the settling test, but performed in the filtration cell. After mixing, the tailings slurry was immediately filtered under 15kPa pressure. The weight of filtrate was monitored continuously by an electric balance interfaced with a computer.

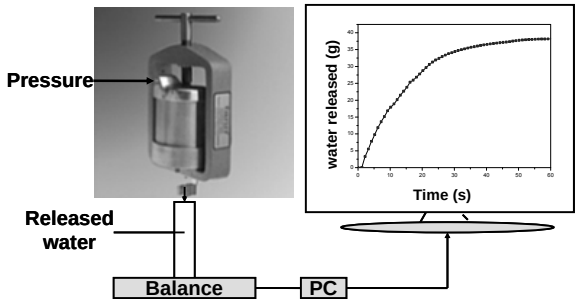

Figure1. Filter press used in this study

RESULTS AND DISCUSSION

Settling test results

The results of the two tailings settling tests with the addition of Magnafloc 1011 and Al-PAM are shown in Fig.2. For raw tailings (Blank), supernatant remains muddy after 10-minute settling, although coarse solids settled quickly to the bottom. Clearly the fine solids were stable in raw tailings and remained suspended. After addition of 10 ppm Magnafloc 1011, the supernatant became quite clear, indicating flocculation of fine solids that led to quick settling. With the addition of 10 ppm Al-PAM, the supernatant became almost crystal clear, indicating a slightly more effective flocculation of fine solids by Al-PAM than by Magnafloc 1011 at the same polymer dosage.

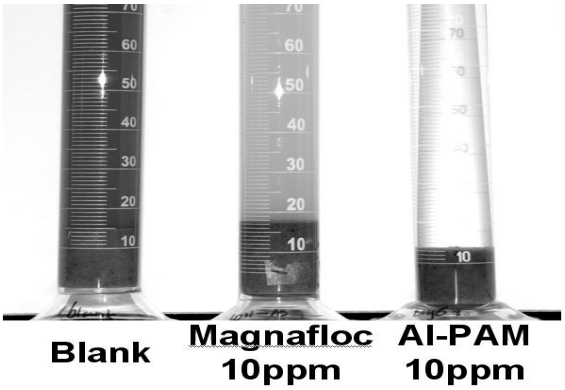

Figure 2. Comparison of tailings settling results with the addition of Magnafloc 1011 and Al-PAM after 10-minute settling

To quantify the quality of supernatant, the turbidity of the supernatant was measured after settling for 10 minute. The results in Fig.3 show that the supernatant for blank case is less turbid than the supernatant obtained with 10 ppm Magnafloc 1011 addition, which was surprising to us. It appears that Magnafloc 1011 stabilized some ultrafines at the same time of flocculating the majority of the fine solids. The supernatant obtained with 10 ppm Al-PAM addition is much clearer with almost no solids. Clearly, Al-PAM is a better flocculant for solids settling of oil sands tailings of low fine ores produced in our laboratory.

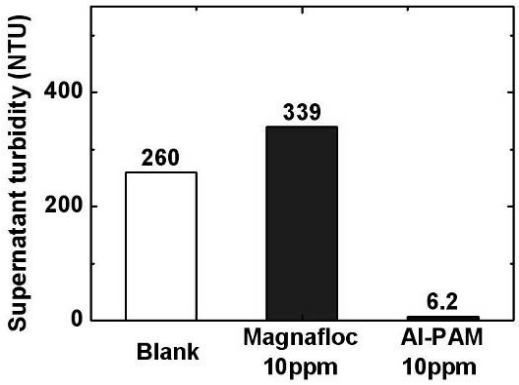

Figure 3. Turbidity of supernatant obtained from laboratory-generated tailings with and without flocculant addition

Filtration test results

The results of the filtration tests are shown in Fig.4. The y-axis in Fig.4 represents the moisture in the slurry above the filter paper, which is calculated by

$$\text{Moisture} = \frac{\text{Mass of water in filter press at t}}{\text{Mass of slurry in filter press at t}}$$

$$\text{Moisture} = \frac{W_{slurry} + W_F - W_{ft}}{M_{slurry} + M_F - W_{ft}} \times 100\%$$

where W_{slurry} is the mass of water in the slurry at time zero; W_F is the mass of water in the added flocculant solution; W_{ft} is the mass of filtrate at time t, which is monitored by computer; M_{slurry} is the mass of slurry at time zero; M_F is the mass of added flocculant solution. Without flocculant addition, the filtration rate of the raw tailings is extremely slow. It is surprising that the filtration rate with the addition of 10 ppm Magnafloc 1011 is worse than the case without flocculant addition. The presence of stable ultrafines determined by supernatant turbidity appears to be responsible for such an observation. It should be noted that without flocculant addition or with Magnafloc 1011 addition, a filter cake did not form after 180-second filtration.

However, Al-PAM addition significantly improved filtration rate as shown in Fig.4. The moisture of the cake obtained after 180-second filtration with 10 ppm Al-PAM addition was only 6.6±1.2wt%.

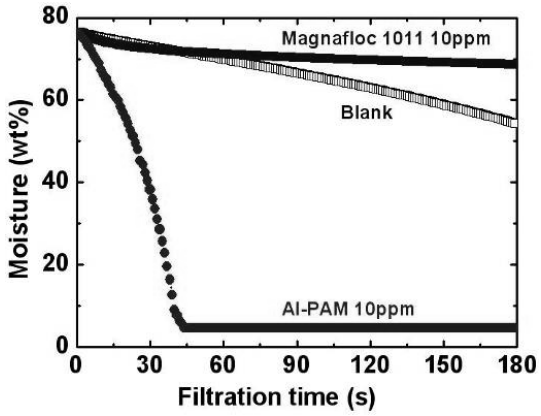

Figure 4. Comparison of tailings filtration with the addition of Magnafloc 1011 and Al-PAM polymers

The photograph in Fig.5 shows that the cake is really dry. Such a dry cake can be directly disposed to the mined areas for backfill with little trapped water. From this study, we demonstrated that oil sands tailings can be managed in recycling process water while producing dry filter cake for backfill and eliminating the need for tailings pond. Fig.6 shows a schematic of such a process.

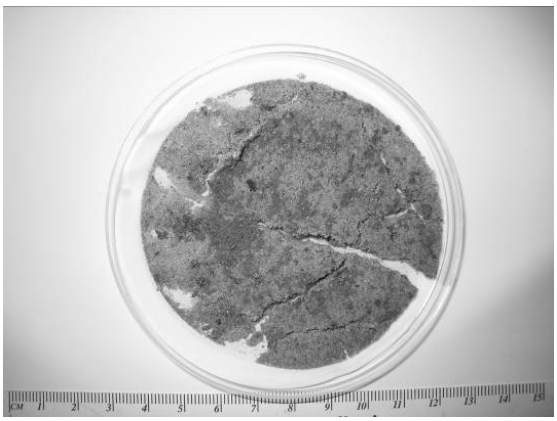

Figure 5. A photograph of filter cake showing very dry cake

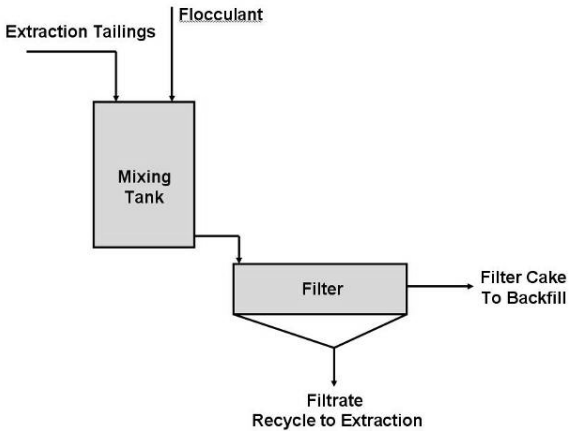

Figure 6. Schematics of filtration process for oil sands tailings management

CONCLUSIONS

From this study, the following conclusions are drawn.

1. Both Magnafloc 1011 (Percol 727) and synthesized AL-PAM polymer were found to be effective as settling aids.

2. The commonly used commercial flocculant Magnafloc 1011 was not effective as a filtration aid for the tested oil sands tailings.

3. The synthesized Al-PAM polymer was found to be a very effective filtration aid for the tested oil sands tailings.

4. The flocculant-assistant filtration was demonstrated by laboratory tests to be a viable solution to oil sands tailings management.

REFERENCES

FTFC, (Fine Tailings Fundamentals Consortium): Advances in Oil Sands Tailings Research. Alberta Department of Energy, Oil Sands and Research Division: 1995.

Xu, Y., Cymerman, G., Flocculation of fine oil sand tails. Polymers in Mineral Processing, Proceedings of the UBC-McGill Bi-Aunnual International Symposium on Fundamentals of Mineral Processing, 3rd, Quebec City, QC, Canada, Aug.22-26, 1999, 591-604.

Liu, J. K.; Lane, S. J.; Cymbalisty, L. M. Filtration of hot water extraction process whole tailings. CA 1103184, 1981.

Yang, W. Y.; Qian, J. W.; Shen, Z. Q., A novel flocculant of $Al(OH)_3$-polyacylamide ionic hybrid. Journal of Colloid and Interface Science 2004, 273, (2), 400-405.

COMPARISON OF POLYMER APPLICATIONS TO TREATMENT OF OIL SANDS FINE TAILINGS

Haihong Li, Joe Zhou and Ross Chow
Alberta Research Council, Edmonton, Alberta, Canada

ABSTRACT

The challenges in oil sands fine tailings treatment lie in two aspects: fast solids/water separation and maximum water recovery, and consolidation of the final sediment. Polymeric flocculants are now used in the oil sands industry, alone or in combination with electrolyte coagulants, to achieve the above purposes. This paper compares the application of three types of polymeric flocculants: a conventional polyacrylamide (PAM), an $Al(OH)_3$-PAM hybrid polymer and a thermal-sensitive poly(*N*-isopropyl acrylamide) (PNIPAM) for the treatment of fine solids and oil sands tailings. Experimental results show that using PAM formed large and loose flocs of fines or oil sands tailings, which have high settling rate but with a low solids content in the formed sediment (-30% in case of oil sands tailings, similar to MFT). $Al(OH)_3$-PAM formed medium sized and dense flocs, which also have high settling rate with less water in the formed sediment. PNIPAM achieved almost the same flocs settling rate as PAM or $Al(OH)_3$-PAM, but released much more water and formed more consolidated sediment (by up to 50%) compared to PAM. Mechanistic studies indicate that the above different performances originated from the difference in inter-particulate interactions. The PAM flocculates fines via "hydrophilic hydrogen bonding" that maintains a stable sediment structure; the $Al(OH)_3$-PAM added an extra "electrostatic force" to the PAM and denser flocs were formed. Both PAM and $Al(OH)_3$-PAM can not induce further water release in sediment consolidation, due to carried surface charges. For the PNIPAM, fine solids flocculates via "hydrophobic interaction". Therefore the formed flocs contain less water at a high temperature. Once the temperature was cooled down, the PNIPAM destroys the structure stability of sediment via "repulsive force", resulting in more water release in sediment consolidation. However, its application to oil sands fine tailings remains to be explored. Development of innovative and smart polymers is the key for successfully tackling the specific issues of oil sands fine tailings processing.

INTRODUCTION

Issues of fine solids dewatering

Canadian oil sands production has reached 1.2 million barrels per day during 2006. The operations of bitumen extraction from mineable oil sand ores in Alberta consume huge amounts of water (2-4 barrels fresh water for producing 1 barrel bitumen) and produce the same huge amount of tailings slurry, which is discharged to tailings ponds and cause direct environmental impact on land, air, water and wildlife. On the other hand, since the use of fresh water from the Athabasca River is reaching its limit, it is important and crucial to use as much as possible the recycled water from tailings ponds in the bitumen extraction.

The challenges preventing industrial operations from efficiently using the recycled water came from the difficulties of tailings treatment (i.e. solids dewatering). Because of the slow settling of fine solid (mostly clay) particles due to Brownian movement (random movement), it takes a few years for the slurry to reach only about 30% solid content without further consolidation (the MFT even contains 60-70% water in volume). An effective solid dewatering technology is demanded with potentially two benefits: volume reduction of tailings ponds and usage increase of recycled water.

Polymer applications

Efforts have been devoted to address the oil sands fine tailings problem for the last three decades, including applying process aids to enhance solids dewatering such as polymeric flocculants, plus three process steps: solids flocculation, sediment thickening, and filtration.

In solids flocculation, polymeric flocculant is added and mixed with tailings slurry. The polymer molecules attach onto solid surface and bind the fine particles together into flocs (aggregates) that have much larger size than individual fine particles (Figure 1). These flocs then settle down by gravity

at a speed much quicker than that of single fine particle (Figure 2). After the settling reaches its end (balance), the clear supernatant above solid sediment is recovered as recycled water and reused for bitumen extraction.

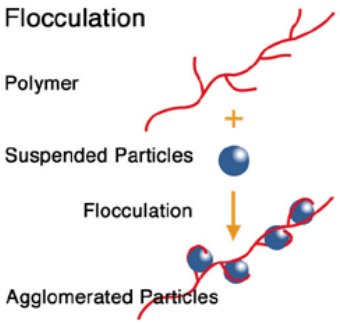

Figure 1. Flocculation of solid particles with polymeric flocculant.

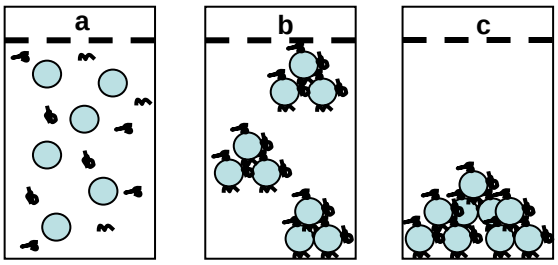

Figure 2. Flocculation and settling of solid particles induced by polymeric flocculant: a. mixture of slurry and polymer; b. flocculation; c. settling.

Following solids settling, sediment consolidation is commonly carried out in a slurry thickener. It is the step whereby the settled flocs are concentrated and compacted on the floor and the volume reduction of sediment occurs in response to natural overburden loading. As void space is reduced, solid particles within the consolidating sediment undergo rearrangement, including downward displacement and reduction in inclination angle. More water could be released during this step and the released water amount is dependent on the sediment structure and flocs properties such as shape, size and density. Finally, if necessary, the thickened sediment will go through a filtration step to reduce the cake moisture to the lowest possible level. In this step, the separation of solids from liquid is achieved by passing a suspension through a filter medium, such as cloth, membrane, or sintered metal, which retains the particles. The filter medium is characterized by its filtration properties like permeability and retention. Therefore, filtration is best achieved by large, strong flocs with low surface charges.

It has been found that polymer properties such as molecular weight and charge density play important roles in promoting effective flocculation of fine solid particles. However, the polymer effect on the whole dewatering process (flocculation, consolidation and filtration) is not clear or not satisfactory with consolidation and filtration.

This paper compares the effect of three types of polymers on the solids dewatering and their action mechanisms. These polymers include a conventional polyacrylamide (PAM), an $Al(OH)_3$-PAM hybrid polymer (Al-PAM) and a thermal-sensitive poly(*N*-isopropyl acrylamide) (PNIPAM). The aim is to find a way for screening out a better polymeric flocculant (or dewatering process aid).

EXPERIMENTAL

All test results presented here came from the publications that authors were involved. Detailed test set-up and conditions can be found from the references (Li et al., 2008a, b; 2007).

In general, the three tested polymers were one commercial PAM product and two synthesized products of Al-PAM and PNIPAM.

The solid samples of either pure minerals (silica and kaolinite) or oil sands tailings were used for testing. Deionized water or process water were used for preparing solid slurries.

Testing was consisted of settling and consolidation tests.

RESULTS AND DISCUSSION

Test results with polyacrylamide (PAM)

PAM's role of flocculating fine mineral particles has been intensively reported (Moddy, 1992; Chen et al., 2003; Pearse, 2005). In treating oil sands tailings, the results of using six polymers were presented in Figure 3 to demonstrate the effect of polymer molecular weight on flocculation (Li et al., 2008a). These polymers have the same negative charge density of 30% but different MWs (0.01, 1,

15, 17.5, 20, and 40 million Daltons). Their dosage is 20ppm based on slurry volume.

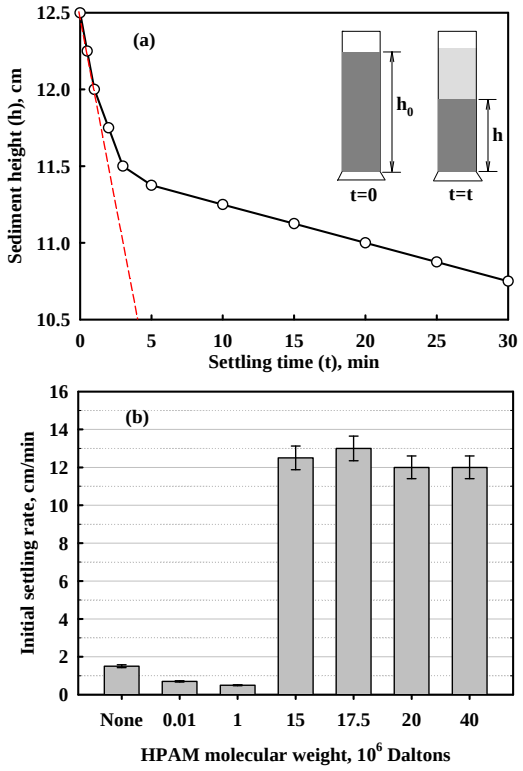

Figure 3. Effect of polymer molecular weight on initial settling rate of tailings: (a) A typical settling curve as a function of settling time; (b) The settling results at 30ppm.

It can be seen that the effect of polymer molecular weight on tailings settling is obvious. The initial settling rate with no polymer addition is very low (around 2 cm/min or 1.2 m/hr). No improvement was obtained with the addition of a PAM polymer at a low MW of 0.01 or 1 million Daltons. The low-MW polymers acted as dispersant keeping the fine solid particles in a dispersed state. However, the polymers with a high MW (≥15 million Daltons) induced fast tailings settling (about 12 cm/min or 7.2 m/hr) because the polymers acted as a flocculant. These polymers impose bridging effect between the fine solid particles and result in the formation of large flocs. Figure 4 compares the size enlargement of flocs with the dispersed particles. The flocs size is about 50 micron and the particles are about only 5 micron. It is a ten times increase in size induced by PAM and thus the flocs sink down at a faster settling rate. Another character of the flocs formed by the PAM is that they are in irregular shapes as shown in Figure 4. This is determined by the polymer properties such as molecular structure and action mechanism.

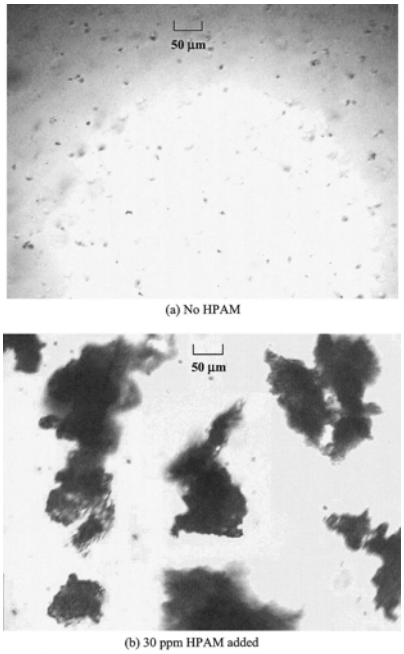

Figure 4. Images comparing the dispersion and flocculation of kaolinite slurry (0.6 wt%, 23°C) with (a) no PAM and (b) PAM added at a dosage of 30 ppm.

Test results with $Al(OH)_3$-PAM hybrid polymer (Al-PAM)

The flocculation efficiency of Al-PAM in treating kaolin suspension was found much better than using a commercial polyacrylamide (PAM) and a PAM/$AlCl_3$ blend (Yang et al., 2004). Figure 5 shows the effect of Al-PAM addition on the settling of fine oil sands tailings (Li et al., 2008b).

It can be seen that adding Al-PAM induced effective flocculation of the fine tailings compared with the case of no polymer addition. There is no obvious difference of the settling rates between the al-PAM and PAM.

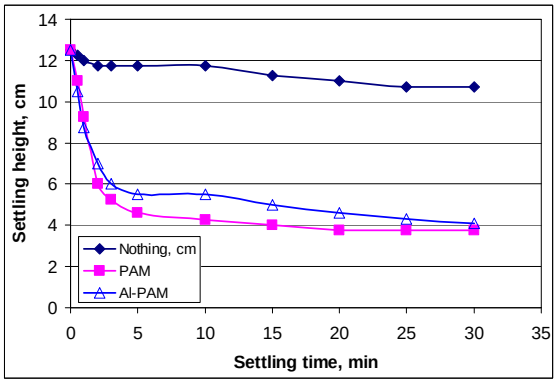

Figure 5. Flocculation induced by Al-PAM and PAM with tailings at 20ppm.

Although the flocs formed by Al-PAM settle as quickly as the flocs formed by PAM, they have different flocs characters. As shown in Figure 6 (Yang et al., 2004), they have more regular shapes or are denser than the flocs formed by PAM, which could be helpful to the following filtration process.

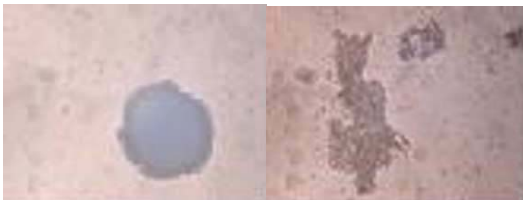

Figure 6. Comparison of flocs formed by Al-PAM (left) and PAM (right).

Test results with poly(*N*-isopropyl acrylamide) (PNIPAM)

The most significant findings in solids dewatering are to use stimuli-sensitive polymers. This type of polymer was found to achieve both rapid solid sedimentation and low sediment moisture. The difference of applying this polymer from conventional ones is that it can transfer the inter-particle forces, such as from repulsive to attractive to form solids aggregates at one stimuli condition and after finishing settling, back to repulsive at another stimuli condition to release more water from the sediment (Franks, 2005).

Tests of using a temperature-sensitive polymer, PNIPAM, in the flocculation followed by consolidation of silica suspension were conducted (Li et al., 2007). PNIPAM has a critical solution temperature (CST around 32°C), above which PNIPAM can induce attractive inter-particle force and transfer to repulsive force when temperature is below CST.

During the test campaign, four PNIPAMs with different MW were added; they are 0.23, 0.71, 2.00 and 3.6 million Da (Li et al, 2008c), and two temperatures were used at room temperature and 50°C. Figure 7 presents the settling results at room temperature (below CST). It can be seen that at the doses higher than 10 20 ppm PNIPAM additions, all of the four PNIPAMs acted as dispersants as the settling rates are close to zero. Slight flocculation might take place at dosage below 10ppm with two high-MW PNIPAMs. They induced 2.5-3.5 m/hr settling rates at around 5ppm. If the PNIPAM is designed for solids-dispersing purpose at room temperature, the most suitable molecular weight range should be smaller than 1M Da (i.e., 0.23 and 0.71 million Da). However, since the PNIPAM needs to perform both settling and consolidation, it is necessary to study its flocculating ability at 50°C before any conclusions on MW-dependent PNIPAM can be made.

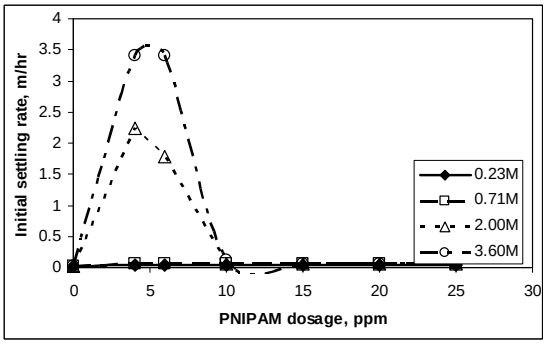

Figure 7. Effect of PNIPAM dosage on silica settling at room temperature below CST.

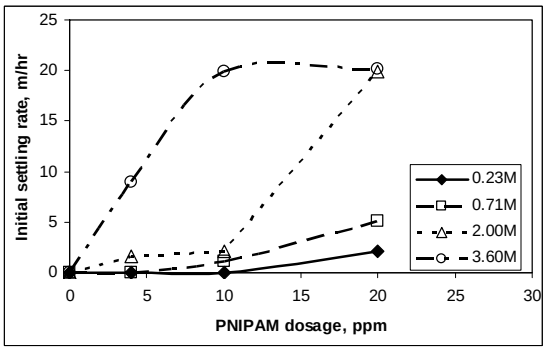

Figure 8. Effect of PNIPAM dosage on silica settling at 50°C above CST.

Figure 8 presents the settling results at 50°C (above CST). It can be seen that the PNIPAM induced silica flocculation and its effectiveness is dependent on polymer MW and dosage. At 4ppm, the high-MW PNIPAMs (2 and 3.6 million Da) induced silica settling (aggregation). Much better settling was obtained with 3.6M Da PNIPAM than with 2M Da. No obvious flocculation was observed from the settling tests done with the low MW PNIPAMs (0.23 and 0.71M Da). At 10ppm, the PNIPAM with 0.71M Da MW induced almost the same settling as the 2M Da PNIPAM. The PNIPAM with the lowest MW (0.21 M Da) did not induce any silica settling until its dosage was increased to 20ppm, a slow silica settling rate was obtained. At the same 20ppm addition, the PNIPAMs having high MWs (3.6M and 2M Da) induced very quick solid settling and found to have a minimum sediment volume in less than 1 min. These results clearly demonstrate that the ability for a PNIPAM to perform efficient solids flocculation at 50°C rely on its molecular weight and dosage. The higher the molecular weight, the lower the dosage needed for solids flocculation.

Following the settling tests, consolidation tests were conducted to study the water release from sediment. Figure 9 presents the results of the water released during sediment consolidation under the conditions of PNIPAM MW and dosage. The sediment flocculated by the PNIPAM with high MW (3.6 M Da) released much high water of 34%v/v at a low polymer dosage of 10ppm, whereas only 13% water was released from the sediment flocculated by the PNIPAM with low MW (0.21 M Da). Thus in order to produce effective flocculation and consolidation, a PNIPAM with large MW is a good choice.

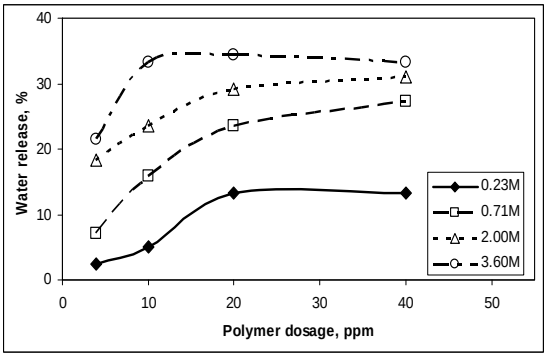

Figure 9. Effect of PNIPAM dosage on silica consolidation at room temperature below CST.

As shown in Figure 10, the advantages of using PNIPAM as a dewatering aid are evident. First in flocculation, the sediment by PNIPAM occupied less volume than that by PAM (Figure 10B vs. 10A). That is a volume ration of 6ml vs. 12ml, meaning the PNIPAM sediment has only half of the PAM sediment volume; second in consolidation, the volume of the PNIPAM sediment was further reduced to 4ml (Figure 10D), indicating 25% more released water. The PAM sediment did not release any water at this stage. The performance difference between these two polymers lies in their difference of molecular structure as shown in Figure 11. Compared with PAM, The PNIPAM molecule has an extra carbonhydrogen chain connecting onto the nitrogen element. It is the carbonhydrogen chain that determines PNIPAM performance better than PAM.

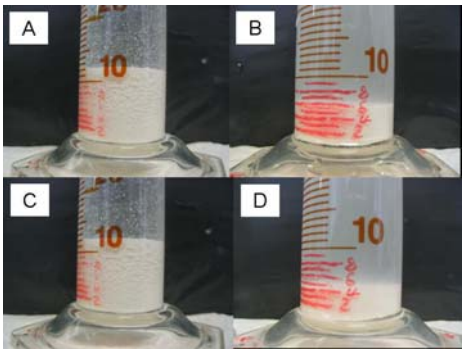

Figure 10. Comparison of dewatering performance between PAM and PNIPAM at 10ppm.

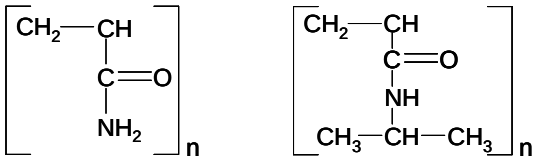

Figure 11. Different molecular structures between PAM and PNIPAM.

Polymer action mechanisms

From above results, Al-PAM was found to induce more spherical and denser flocs than PAM, and PNIPAM produced more packed sediment than PAM. Different action mechanisms of these three polymers should account for their solids dewatering performance, i.e., they induce inter-particle forces in different ways.

It has been confirmed that PAM induces attractive inter-particle force via "hydrogen bond" (Xiao et al., 1996), in which the hydrogen atoms of one molecule is attracted to an electronegative atom, usually of another molecule. Figure 12 presents the AFM results of the effect of PAM molecular weight on the interaction forces between clay and silica surface. The long-range interaction forces for no polymer addition as shown in Figure 12a were measured to be purely repulsive. The repulsion became stronger when the polymer addition at a lower MW of 0.01 million Da was used (circles). There is almost no difference among the force profiles (squares and diamonds) at a MW of 1 and 15 million Da. A further increase of the MW from 17.5 to 20 and 40 million Da caused a noticeable decrease in the repulsion (hexagons to inverted triangles) or even resulted in an attractive force between clay and silica (inverted triangles and crosses).

The attractive forces appeared within the separation distance of about 10 nm due to hydrogen bonding and van der Waals forces during the approach process in the force measurements. It is the attractive forces that cause a flocculation between fine particles, leading to a fast tailings settling.

Figure 12b clearly shows the clay-silica adhesion forces as a function of MW. The effect of polymer MW can be divided into two categories. For the cases of no polymer addition and low-MW polymers (MW=0.01 and 1 million Daltons), the adhesion forces were very weak (below 0.3 mN/m) and the solid-solid long-range interaction forces were purely repulsive (Figure 12a). As a result, the fine solid particles in the tailings slurries would remain in a well-dispersed state. Thereby, their settling rate becomes very slow. However, with high MW polymers (≥15 million Daltons), strong solid-solid adhesion forces were measured (Figure 12b), for example, a 1.2 mN/m force was measured with the 17.5 million Da PAM. The corresponding long-range forces were either weakly repulsive or even attractive (Figure 12a). Thus, flocculation among the fine particles would take place, leading to fast settling.

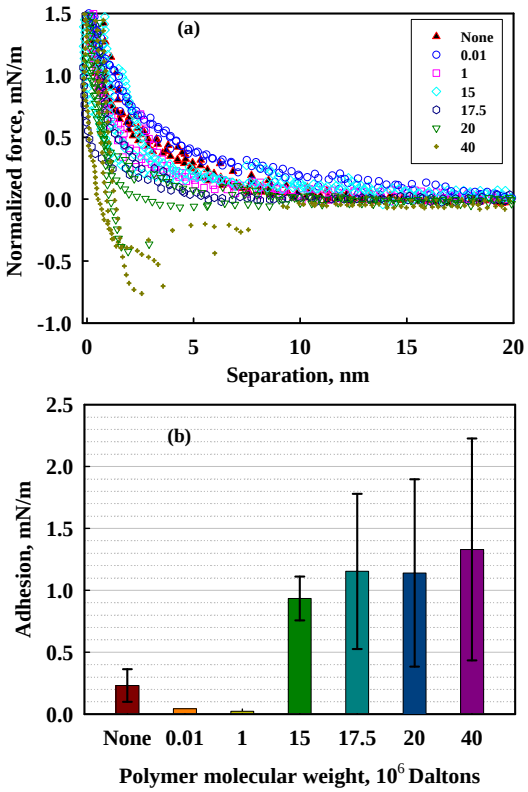

Figure 12. Effect of polymer molecular weight on interaction forces between clay and silica surface. (a) Long-range forces as a function of separation distance; (b) Effect of MW on the clay-silica adhesion forces.

Different from PAM, Al-PAM brings synergetic effect in bonding solid particles together. In addition to the common adsorption between the PAM chains and solid particles by hydrogen binding, the cationic $Al(OH)_3$ cores in Al-PAM also attract the negatively charged particles by electrostatic interactions, which result in the formation of dense spherical floccules (Yang et al., 2004). Figure 13 presents the AFM results of the effect of Al-PAM dosage on the clay-silica long-range interaction forces.

The inset of Figure 13 shows the adhesion forces between clay and silica. Near zero adhesion force was measured with no polymer addition. Attractions were measured with Al-PAM addition in a very short separation distance of about 2 nm may. They result from the electrostatic attraction between the aluminum cores of Al-PAM and the

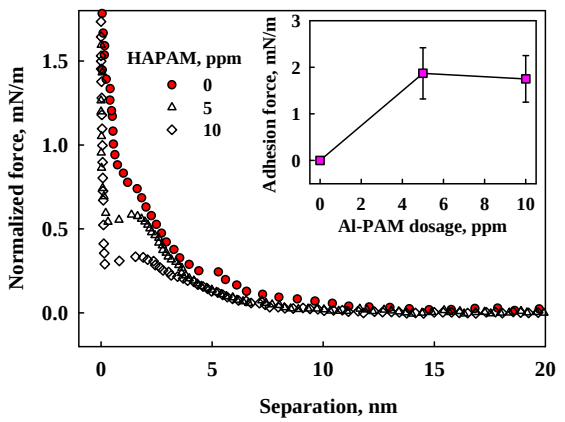

Figure 13. Effect of Al-PAM dosage on the clay-silica long-range interaction forces. The inset shows the clay-silica adhesion forces as a function of Al-PAM dosage.

negatively charged sites of the silica or clay surface, or from the van der Waals or other interactions. Although the measured long-range interaction forces are purely repulsive in all cases, the repulsions are depressed by the increasing addition of Al-PAM. The combination of a strong long-range repulsion and a zero adhesion indicates that the solid particles in the tailings slurry remain in a well-dispersed state, resulting in very slow settling. When Al-PAM was used, the adhesion force was substantially increased to about 2 mN/m. This value is higher than the force of 1.2 mN/m induced by PAM (Figure 12). Such strong adhesion forces leads to the formation of spherical flocs and effective flocculation.

The action mechanism of PNIPAM is unique. It invokes the transaction between attractive and repulsive interactions to response the change of outside stimuli conditions such as temperature (Sakohara et al., 2002). Figure 14 shows this kind of transaction of a PNIPAM solution. Starting at low temperature (T<CST), the PNIPAM aqueous solution is transparent, meaning it is hydrophilic and well soluble (Figure 14A). When the temperature is increased to around the CST at 32°C, the PNIPAM molecules begin to precipitate out from the solution as some white fog was observed in Figures 14B and 14C, indicating the molecular conformation and its hydrophobic transition. Finally when the temperature is maintained above the CST, the whole solution becomes totally opaque (Figure 14D). It can be indicated that the silica flocculation induced by a PNIPAM at 50°C is the result of "hydrophobic" inter-particle attractive forces.

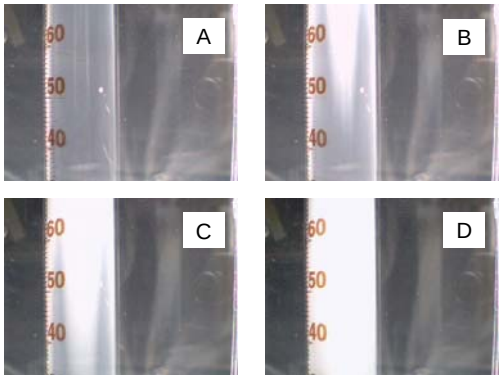

Figure 14. Photos show the effect of temperature on PNIPAM transition between hydrophilic and hydrophobic: A. Below 32°C; B and C: Around CST at 32°C, D: Above 32°C.

CONCLUSIONS

Polymers, particularly the ones high MW, play an important role in promoting solids dewatering, such as settling and consolidation.

PAM is good at inducing solids flocculation but the flocs shape is irregular; Al-PAM induced stronger flocculation of particles with formed dense spherical flocs; PNIPAM performed better than the previous twp polymers as it enhanced dewatering in both flocculation and consolidation.

Difference of action mechanisms of the three tested polymers explained their performance differences. PAM has a function of hydrogen bond; Al-PAM adds extra electrostatic attraction on it and enhances the inter-particle forces; PNIPAM manipulates inter-particle forces with the help of external stimuli conditions to obtain sediment with less volume.

The findings from these studies can be helpful for screening and developing novel dewatering aids.

REFERENCES

Franks, G. V. (2005), Improved solid/liquid separation using stimulant sensitive flocculation and consolidation, Journal of Colloid and Interface Science, 292, 598-603;

Li, H., Long, J., Xu, Z. and Masliyah, J.H., Effect of molecular weight and charge density on the performance of polyacrylamide in low-grade oil sand ore processing. The Canadian Journal of Chemical Engineering, V86, 177-185, April 2008(a);

Li, H., Long, J., Xu, Z. and Masliyah, J.H., Novel polymer aids for low-grade oil sand ore processing. The Canadian Journal of Chemical Engineering, V86, 168-176, April 2008(b);

Li, H., O'Shea, J.P. and Franks, G., Solid hydrophobic aggregation and sediment consolidation with novel polymers. Submitted to Minerals Engineering. 2008(c);

Li, H., O'Shea, J.P. and Franks, G., Role of smart polymers in solids dewatering, Chemeca 2007, Melbourne, Australia, 2007;

Sakohara, S., Kimura, T. and Nishikawa, K. (2002), Flocculation mechanism of suspended particles using the hydrophilic/hydrophobic transition of a thermosensitive polymer, KONA, 20, 246-250;

Xiao, H., Liu, Z. and Wiseman, N., Synergetic effect of cationic polymer microparticles and anionic polymer on fine clay flocculation, J. Colloid & Interface Sci. Vol. 216, 409-417(1999).

Yang, W.Y., Qian, J.W. and Shen, Z.Q., A novel flocculant of Al(OH)3–polyacrylamide ionic hybrid, Journal of Colloid and Interface Science 273 (2004) 400–405;

APPLICATION OF TEMPERATURE RESPONSIVE POLYMERS FOR WATER RECOVERY FROM MINERAL TAILINGS

Haihong Li,[1] George V. Franks,[2] John Paul O'Shea[2] and Greg G. Qiao[2]
[1] Alberta Research Council, Edmonton, AB, Canada
[2] Australian Mineral Science Research Institute, University of Melbourne, Melbourne, Vic, Australia

ABSTRACT

A novel method of flocculation resulting in both rapid sedimentation and low sediment moisture will be presented. It relies on inducing an attractive inter-particle force so that aggregation and fast settling result. The clarified liquid can be removed for example in a continuous thickener as is common practice. The novelty of the method is that the interaction force is then changed back to repulsive such that additional consolidation of sediment and expression of water will occur such as in a tailings pond. The inter-particle force can be reversibly changed by a change in temperature when the temperature sensitive polymer poly (*N*-isopropyl acrylamide) (PNIPAM) is used as the stimulant sensitive flocculant. At temperatures between about 40 and 90°C, the polymer acts as a flocculant while at temperatures below about 30°C the polymer acts as a consolidation aid. The polymer properties such as molecular weight are important in controlling the sedimentation rate, supernatant clarity and consolidation. The highest molecular weights produce the best results in terms of sedimentation rate, supernatant clarity and consolidation. In the laboratory, tests with silica indicate that the sediment bed volumes can be reduced by up to about 35 percent when compared to conventional polyacrylamide flocculants. The process has potential for use in oil sands tailings management due to the inherent chance in temperature in the tailings during processing.

INTRODUCTION

In mineral industry, the common practice of fine solids dewatering is that the particles are aggregated to allow more rapid settling and easy removal of the solids by gravity (Healy, 1973; Hiemenz and Rajagopolan, 1997; Bolto, 1995). This process is achieved in most cases by the addition of a high molecular weight polymer as a flocculant. In fact, the desired or the ultimate goal in treating mineral tailings is to obtain a rapid sedimentation plus minimum moisture content in the sediment consolidation from an economic and environment point of view. Unfortunately current solids dewatering focuses more on sedimentation optimization with less consideration of the consolidation by using polymeric flocculants such as polyacrylamide. A large amount of water is found trapped in the flocs formed by the flocculants. This has an adverse effect on the water release during the stage of sediment consolidation and filtration (Besra et al., 2004).

The solution to the problem presented here is to test novel polymers that optimize the suspension properties and behavior for each step in the processes of settling, consolidation and even filtration. Recent progress has been made in using stimuli-sensitive polymers (Franks, 2005; Li et al, 2008) to manipulate the inter-particle interactions (forces), which control the behavior of suspensions of the particles such as the settling rate and final sediment moisture, by the use of controlling stimulus such as either pH or temperature. These stimuli are used to invoke the actions of these novel polymers to change the inter-particle forces between repulsion and attraction.

The stimuli-sensitive polymers work by changing the inter-particle forces between particles in each process step. At first, they induce the forces to be attractive, and thus the particles can be made to aggregate, rapidly settle and be removed within a thickener. Then, when the inter-particle forces are changed back to be repulsive, the particles in the sediment or filter cake will undergo further consolidation, resulting in additional release of water from the sediment (Franks, 2005).

This paper is to present the novel solid/liquid separation method that can improve dewatering efficiency by producing both fast sedimentation of fine particles (by aggregation) and dense (low moisture) sediments. This paper focuses on the use of a temperature-sensitive polymer, poly (*N*-isopropyl acrylamide) (PNIPAM), in treating mineral particle suspensions.

EXPERIMENTAL

Minerals

Three mineral samples were used for the testing. They are silica, kaolin and alumina. A silica powder (Silica 400G, >98% pure) was obtained from Unimin Australia Limited. It has a density of 2.62 g/cm^3. The particle size distribution is about 53% minus 10 micron. A pure kaolinite (Snobrite 55) sample (kaolinite 98%) was obtained from Unimin Australia too. It has a median particle size of 0.7 micron, 94.5% minus 10 micron. The particle density is 2.60 and the surface area is 16 m^2/g. A high purity α-Alumina powder (AKP-15) was purchased from Sumitomo. It has average size about 0.3 microns, a BET surface area of 7 m^2 g^{-1}, density of 3.97 g cm^{-3} and an isoelectric point (iep) at pH ~9.2. The alumina has a positive or negative charge below or above the iep respectively (Franks and Meagher 2003).

Polymers

The temperature-sensitive polymer, poly(N-isopropylacrylamide) (PNIPAM), with different molecular weights and charge density were synthesised as described elsewhere (O'Shea, et al, 2007). They are non-ionic, positively charged or negatively charged in surface charge density. All polymers were dissolved in deionised water at room temperature and at pH = 6.0 as a 0.1wt% solution. They have a critical solution temperature (CST) of 32°C (Sakohara et al., 2002), at higher temperatures the polymer becomes insoluble.

A cationic commercial Ciba ZETAG polyacrylamide (PAM) flocculant was tested at a 0.1wt% solution with deionised water at pH = 6.0.

Settling tests

Settling tests were carried out in 100-ml cylinders at a number of combinations of polymer type, molecular weight and dosage. For each settling test, the solid suspension was prepared with 5g mineral sample and deionised water containing 0.01M $NaNO_3$. The appropriate amount of polymer solution (0.1wt%) was added to make a final suspension concentration of 5 wt% solids. The pH value of the suspension was 6.0±0.2. Polymer dosages were chosen to the total suspension volume. After filled with suspension, the cylinder was sealed by a sealing film and gently shaken upside down for several times to mix the suspension. As soon as the cylinder was placed on a flat solid surface, the settling test began and no further disturbances were allowed. The descent of the solids/liquid interface (mud line) was carefully observed, recorded as a function of settling time. The slope of the settling curve at time zero was obtained as the initial settling rate. To investigate the performance of PNIPAM at temperatures below and above the critical transition temperature (CST around 32°C), each settling test was conducted at two temperatures, room temperature (near 22°C) and a temperature higher than CST (usually 50°C). The settling test was first conducted at room temperature for 24 hr. Then the cylinder was shaken again to disperse the particles and immersed into a water bath with controlled temperature higher than CST for 5 min to warm up. After the cylinder was gently shaken upside down several times and was put back into the water bath and the settling test at the pre-set temperature started immediately.

Consolidation tests

After 2 hrs of settling test at 50°C the sediment volume reached an apparent equilibrium and showed no more variation; the sediment volume was recorded. The cylinder was taken out from the water bath and allowed to cool down to room temperature. The height of the sediment/solution interface was monitored for 24 hrs until another apparent equilibrium was noticed where no additional consolidation was observed. This sediment volume was also recorded. The final sediment density (volume fraction of solids) was determined by conservation of mass based on the relationship:

$$\phi_{init} h_{init} = \phi_{fin} h_{fin} \quad (1)$$

where ϕ_{init} and h_{init} are the initial volume fraction of solids and suspension height and ϕ_{fin} and h_{fin} are the final volume fraction of solids and suspension height. To evaluate the polymer performance on sediment consolidation, the water release percentage was calculated based on the sediment volume changes recorded at 50°C and 22°C:

$$\mathrm{Re}\,lease = \frac{(V_{50} - V_{22})}{V_{50}} \times 100 \quad (2)$$

where, V_{50} is the sediment volume at 50°C and V_{22} is the volume at 22°C.

RESULTS AND DISCUSSION

PNIPAM induced flocculation with various mineral particles

Starting with silica, a non-ionic PNIPAM with a MW of 3.6million Da was used for the flocculation. Figure 1 presents the settling results at 22 and 50°C.

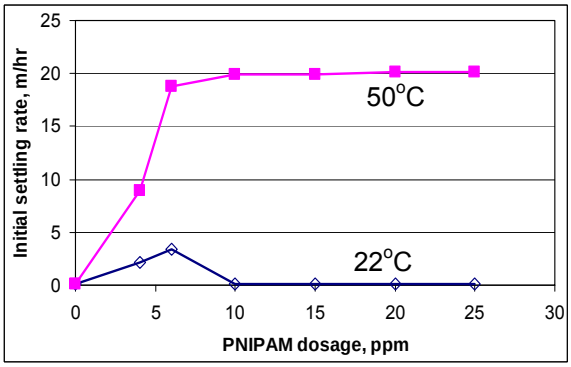

Figure 1. Silica settling results with PNIPAM (3.6MD) at 22 and 50°C (20ppm).

It can be seen that PNIPAM maintained the silica particles in a dispersed state as the settling rates at tested polymer dosages were smaller than 5m/hr. However, much higher settling rates were produced at 20m/hr after 10ppm PNIPAM addition when the suspension temperature was increased to 50°C. This indicates that an effective flocculation was induced by PNIPAM. These settling results clearly demonstrated that PNIPAM has absolutely different performance from PAM flocculant, because PAM has no response to the change of stimuli such as temperature in this case.

The flocculation of kaolinite by PNIPAM was a little more complicated than silica. These fine clay particles need to be dispersed first before PNIPAM is added and a dispersant Calgon was added at 10ppm for that purpose. The PNIPAM with a molecular weight of 3.6MD used for silica flocculation was found unable to disperse kaolinite particles at 22°C, instead, it flocculated the particles at the dosages from 4 to 40ppm. In this case, a PNIPAM with a molecular weight of 0.71MD was tested. Figure 2 shows the kaolinite flocculation induced by this PNIPAM at 200ppm at 22 and 50°C. At 22°C, the solids were actually in a dispersed state as they displayed a very slow settling curve (0.1m/hr settling rate) against settling time over a period of 30min. However, the formation of solid flocs by PNIPAM produced a pretty quick settling curve as we can see from the figure (or about 13.4m/hr settling rate), which is totally different from that obtained at 22°C. In fact, this settling difference between 22°C and 50°C demonstrates PNIPAM's role in promoting flocculation of clay fine particles.

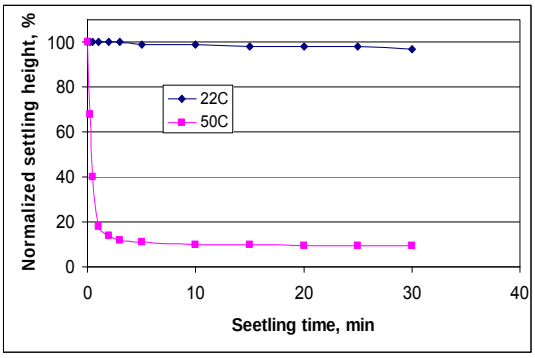

Figure 2. Kaolinite settling results with PNIPAM (0.71MD) at 22 and 50°C (Calgon 10ppm, PNIPAM 200ppm).

Furthermore, from the pictures shown in Figure 3, it can be observed that the PNIPAM addition at 50°C induced a clear supernatant after 30min compared to the PNIPAM addition at 22°C.

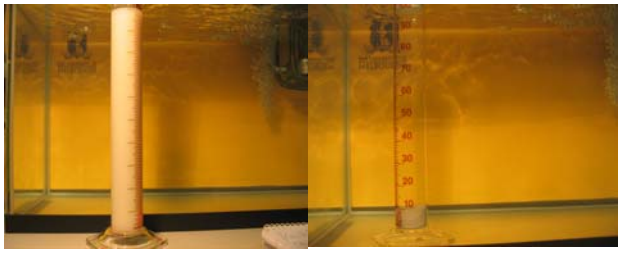

Figure 3. Photos compare the supernatants at 22 and 50°C (left/right) (Calgon 10ppm, PNIPAM 200ppm).

Figure 4 present the alumina settling results with three types of temperature-sensitive polymers: a non-ionic PNIPAM (MW 1.0MD), a 1.2MDa 15% cationic co-polymer (CPNIPAM) and a 1.84MDa 15% anionic co-polymer (APNIPAM) at 50°C.

It can be seen that the non-ionic polymer produced the fastest settling rates (14m/hr after 10ppm). The anionic polymer produced a slow settling rate (4m/hr after 50ppm) and the cationic polymer produced less than 0.01 m/hr sedimentation. The cationic polymer was unable to cause any significant aggregation in the alumina suspension. This is because polymer with the same charge

sign as the surface charge of the particles induced and even enhanced the dispersion of the alumina particles. It can not be used when aggregation and sedimentation of that particular type of particle is expected even at elevated temperature.

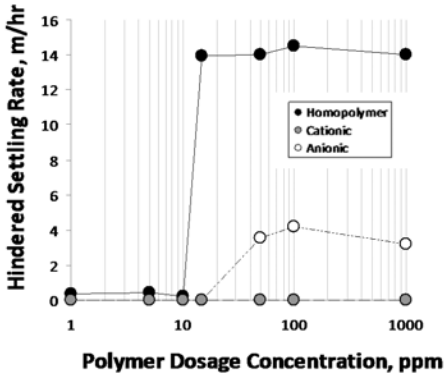

Figure 4. Alumina initial settling rates with the additions of PNIPAM with different charge density.

The silica flocculation with PAM was also found sensitive to the polymer surface charge, i.e., anionic or cationic. Figure 5 shows two pictures of silica flocculation by an anionic and a non-ionic PAM.

Figure 5. Comparison of supernatant clarity with PAMs of an anionic (left, 4, 10 and 20ppm) and a non-ionic (right 10ppm).

It can be seen that the anionic PAM (left) can not induce any obvious flocculation at tested dosages. This can be explained by the electrostatic repelling force induced by this PAM, because the silica surface is negative charged at pH 6. However, a very good flocculation was induced by the non-ionic PAM (right).

The above settling results using PNIAPM as a flocculant demonstrate that PNIPAM is effective in flocculating various mineral particles. It is therefore possible to use this type of polymer in treating tailings of oil sands, as the main components of the tailings are clay and silica.

Effect of PNIPAM MW and dosage on solid dewatering

In addition to the PNIPAM performance in solids settling, the more important advantages of this type polymer over PAM are its ability to enhance water release from sediment consolidation and this ability is MW and dosage dependent.

First, the PNIPAM was found to be strongly dependent on its MW and dosage when used to flocculate the silica suspension. Figure 6 compares the PNIPAMs with various MWs and the PAM flocculant (Li, et al, 2008).

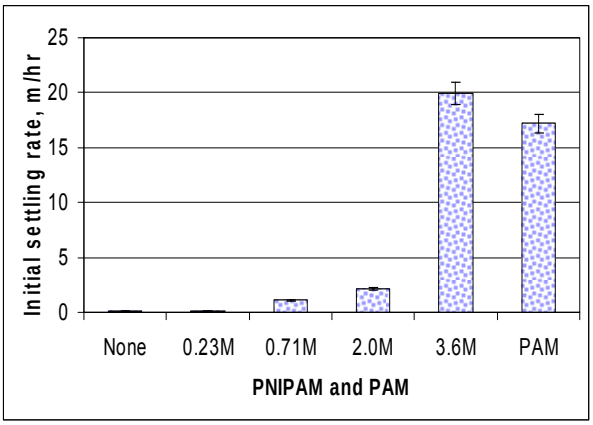

Figure 6. Comparison of different MW PNIPAM performance in silica settling at 50°C and 10 ppm.

It can be seen that the settling rates were very slow without or with PNIPAMs of low MW. The settling rates are below 5m/hr. High settling rate of 20m/hr was obtained with the high MW PNIPAM (3.6MD), which is even higher that that induced by the PAM flocculant (17m/hr).

This PNIPAM MW effect on the supernatant clarity is also significant as it can be seen from Figure 7. Starting from left two cylinders, the supernatants appeared opaque with low-MW PNIPAM additions. When the PNIPAM MW was increased, the improvement in supernatant clarity was more and more strong. It was almost transparent with the most right cylinder in which the highest-MW PNIPAM (3.6MD) was added.

Second and more interesting, the addition of PNIPAM promoted more water release after sediment cooling from the sediment consolidation as shown in Figure 8.

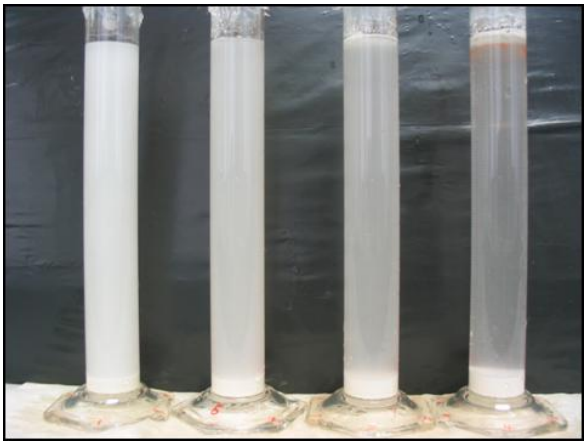

Figure 7. Comparison of supernatant clarity with PNIPAMs at various MW and 50°C. PNIPAM MW from left to right: 0.23, 0.71, 2.0 and 3.6 MD at 30ppm.

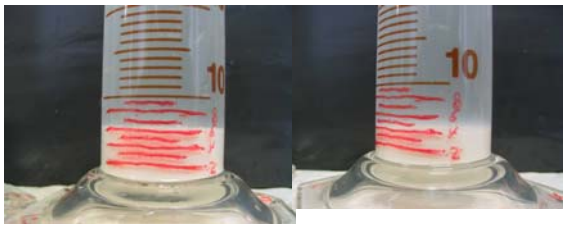

Figure 8. Photos showing the sediment volume after settling at 50°C for 2 hours (6 ml) (left) and after 22 hours additional sediment consolidation at 22°C (4 ml) (right) for a 3.6 MDa PNIPAM dosage of 20ppm.

The sediment volume at the end of settling is about 6ml (left), and the volume at the consolidation end is about 4ml (right). That is a volume reduction difference of 33% according to equation (2), i.e., more water was released.

This PNIPAM water release ability is also MW and dosage dependent. Figure 9 presents the dosage effect on the water release in sediment consolidation.

It can be seen that 4ppm PNIPAM addition produced about 22% water release and the maximum water release was observed to be 35% from 4 to 10ppm. After 10ppm addition, no more increase was obtained. The effect of PNIPAM dosage on sediment consolidation is quite consistent with the results of its effect on the settling. 10ppm PNIPAM addition seems the optimum point for both best solids flocculation and highest water release.

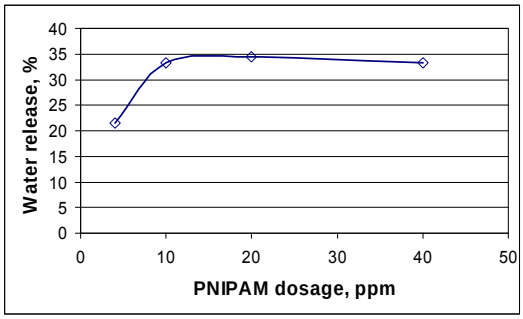

Figure 9. Dosage effect on water release from sediment consolidation for 3.6 M Da PNIPAM.

PNIPAM dewatering mechanisms

It is believed that PNIPAM plays a better role in solids dewatering than conventional PAM flocculants, particularly because of its ability to induce water release from the sediment during consolidation. This ability lies in its unique molecular structure and mechanism.

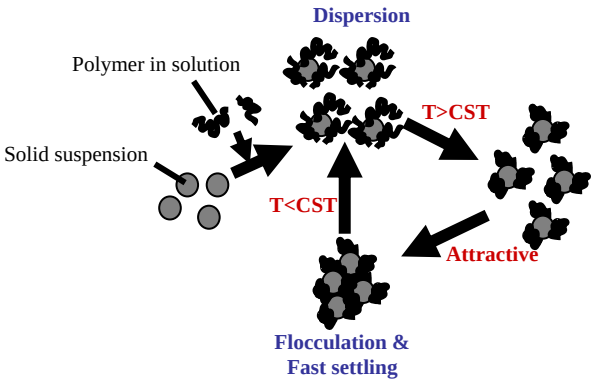

Figure 10. Schematic of PNIPAM mechanism in solids dewatering.

When used in solids dewatering, the PNIPAM is applied to work in such a way that it plays a dual-role as a flocculant and consolidation aid. Figure 10 illustrates how this temperature induced change in particle interactions can be used to cause aggregation (rapid sedimentation) and sediment consolidation. First the PNIPAM is added into the slurry and mixed with the solid suspension at room temperature which maintains the solids in dispersion state. Later, at a temperature higher

than the PNIPAM CST, the PNIPAM induces aggregation of the solid suspension. As a result, the solid flocs settle down at a rapid rate producing a clear liquid which can be removed for example in a thickener. After the solid settling is completed, the slurry temperature is reduced to below the CST so that the repulsion between the solid particles is then re-established and the sediment consolidation can be achieved to minimize the water content in the sediment bed. It is the temperature change that promotes the PNIPAM to work in a way of manipulating inter-particle interactions between repulsive and attractive.

CONCLUSIONS

Based on the results presented, the following summaries can be made:

1. The temperature-sensitive polymer, PNIPAM, was found to play a dual-role in fine solids (silica, kaolinite, and alumina) settling and sediment consolidation by cycling the temperature around the CST (Critical Solution Temperature). Therefore it induced rapid sedimentation and highly efficiency solids dewatering. The conventional flocculant, PAM, has not such ability;
2. The PNIPAM performance was found to be dependent of polymer molecular weight and dosage;
3. The action mechanism of PNIPAM in playing the dual-role is to manipulate the inter-particle forces (repulsive/attractive) via a hydrophilic/hydrophobic polymer transition when temperature is cycled below/above the CST;
4. The findings from these studies can be useful in treating oil sands tailings.

ACKNOWLEDGEMENTS

The authors acknowledge financial support from the Australian Research Council, AMIRA International, BHP/Billiton, RioTinto, Orica, Anglo Platinum, Xstrata and Phelps Dodge through the Australian Mineral Science Research Institute (AMSRI) (LP0667828).

REFERENCES

Besra, L., Sengupta, D. K., Roy, S. K. and Ay, P., Influence of polymer adsorption and conformation on flocculation and dewatering of kaolin suspension, Separation and Purification Technology, 37, 231-246(2004).

Bolto, B.A., Polymeric Flocculants in Water and Wastewater Treatment in Modern Techniques, in: Water and Wastewater Treatment, CSIRO Publishing (L.O. Kolarik, A.J. Priestley (Eds.)), Melbourne, 1995, p. 65.

Franks, G. V., and Meagher, L., The isoelectric points of sapphire crystals and alpha-alumina powder, Colloids and Surfaces A: Physicochemical and Engineering Aspects, 214, 99-110(2003).

Franks, G. V., Improved solid/liquid separation using stimulant sensitive flocculation and consolidation, Journal of Colloid and Interface Science, 292, 598-603 (2005).

Healy, T.W., Principles of Polymer Flocculation, in: Polymer Flocculation Principles and Applications, Royal Australian Chemical Institute, Melbourne, 1973, p. 1.

Hiemenz, P.C. and Rajagopolan, R., Principles of Colloid and Surface Chemistry, third ed., Dekker, New York, 1997.

Li, H. O'Shea, J. P. and Franks, G. V. Effect of Molecular Weight of Poly (N-isopropyl acrylamide) (NIPAM) Temperature-Sensitive Polymeric Flocculants on Solids Dewatering, submitted to AIChE Journal, (2008).

O'Shea J-P, Qiao GG, Spiniello M, Franks GV. Temperature mediated adsorption of poly(N-isopropylacrylamide) onto α-alumina, Proceedings of Chemeca 2007, Melbourne, Au. 23-26, Sept. (2007).

Sakohara S, Kimura T, Nishikawa K. Flocculation mechanism of suspended particles using the hydrophilic/hydrophobic transition of a thermosensitive polymer, KONA, 2002;20:246-250

Session 3

New Tailings Concepts

DISTRIBUTION OF MINERALS IN PROCESS STREAMS AFTER BITUMEN EXTRACTION BY THE HOT WATER EXTRACTION PROCESS

Heather A.W. Kaminsky[1], Thomas H. Etsell[1], Douglas G. Ivey[1,] and Oladipo Omotoso[2]
1. Department of Chemical and Materials Engineering, University of Alberta, Edmonton
2. Natural Resources Canada, CETC–Devon, Alberta, Canada

ABSTRACT

Significant research has been done to examine the composition of the solids in the different streams produced by the hot water extraction process. However, very little work has been published showing how the minerals are distributed around the extraction process. This work takes a single ore and details how the minerals partition to the froth, middlings, and tailings streams after batch extraction. Size separation, X-ray fluorescence analysis, and X-ray diffraction combined with quantification by the Rietveld method, are used to provide a detailed breakdown of how elements and minerals are affected by the hot water extraction process.

Results show that the primary froth is enriched in kaolinite, iron oxide-hydroxides, zircon, and titanium oxides compared with the other streams. The middlings stream, on the other hand, is enriched in all the clay minerals but especially illite-smectite. Also of interest is the observation that the majority of the titanium and iron in all streams is found in the <45 μm size fraction. These results will hopefully lead to an increased understanding of the challenges and opportunities associated with the disposal of the solid waste produced by the hot water extraction process.

INTRODUCTION

The mineralogy of the oil sands has been the subject of many different studies ranging from geological deposit characterization (Bayliss & Levinson, 1976) to studies on how valuable minerals deport around extraction in a pilot plant (Alberta Chamber of Resources, 1996). The short coming of these studies is that no attempt has been made to provide a mineralogical balance around extraction. This paper fills that gap in the literature.

MATERIALS AND METHODS

Sample Preparation

A low-grade oil sand ore (1.5 kg), containing 8.5% bitumen from a Suncor lease, was processed in a Syncrude-styled batch extraction unit using the CANMET procedure that has been reported to represent hydrotransport conditioning at 50˚C (Wang & Mikula, 2002). The primary froth, secondary froth, middlings, and tailings streams were collected and the solids cleaned and separated from the residual water and organics by the Dean-Stark procedure (Syncrude, 1979). Immediately after extraction and prior to Dean Stark analysis, the total tailings stream was allowed to sit for 2 minutes, after which the supernatant was decanted as the middling fraction. While the technique for middling/tailing separation is arbitrary, the middling fraction generally represents the fine tailings stream that ends up as MFT for a given extraction water chemistry. The cleaned solids were then homogenized and separated into 3 coarse fractions (>250 μm, 106 - 250 μm, and 45 – 106 μm) by wet sieving in a Ro-tap™ sieve shaker, using deionized water. The sub-sieve fraction was separated into fines (<45 μm), clays (0.2 – 2 μm), and ultrafine clays (<0.2 μm) by centrifugation. The ultrafine clay (<0.2 μm) component of the secondary froth was not obtained, due to insufficient material.

X-ray Diffraction Analysis-Oriented Clay Slides

Oriented clay slides of the 0.2 – 2 μm and <0.2 μm material were produced by the millipore transfer method (Moore & Reynolds, 1997) and pre-treated as outlined by Chichester et al. (1969), using calcium saturation instead of magnesium saturation. All samples were run on a Bruker D8 Advance x-ray diffractometer with an incident beam parabolic mirror (using Co Kα radiation), a 35 mm sample diameter, and a VANTEC-1™

linear detector. A 0.2 mm exit slit was used to improve the resolution of the mirror-linear detector geometry. Oriented samples were run from 4˚ (2θ) to 36˚ (2θ). All tests were run at ambient temperature and humidity (~22˚C and 25% relative humidity (RH)). For the tests where humidity was a concern (potassium-saturated samples and the calcium-saturated 54% RH samples), the samples were removed from their humidity-controlled containers and tested one at a time. Also, duplicate tests were done on some samples, after exposure for various lengths of times to the atmosphere. The calcium-saturated samples showed no signs of dehydration, even after being exposed to the atmosphere for up to 72 hrs.

X-ray Diffraction Analysis-Non Oriented Slides

Sub-samples of approximately 3 g, from each coarse fraction, were micronized in a McCrone micronizing mill loaded with corundum grinding balls and isopropyl alcohol. Sub-samples of each clay fraction were freeze dried.

The freeze dried and the micronized solids were analyzed by random powder XRD. Sample preferred orientation was minimized by passing the samples through a 400-mesh sieve onto a horizontal sample holder (Omotoso 2007). The excess material was then removed by passing a straight edge over the surface of the sample holder. The random powder samples were analyzed from 4˚ (2θ) to 99.6˚ (2θ) using a Bruker D8 Advance θ- θ diffractometer with an incident beam parabolic mirror (Co Kα), a 25 mm sample diameter, and a VANTEC-1™ linear detector. A 0.2° θ exit slit was used to limit the incident beam size and resolution of the linear detector. The samples were quantified with AUTOQUAN™.

X-ray Fluorescence Analysis of Samples

After XRD analysis, approximately 0.6 g of each of the micronized solids were taken and ashed at 1000°C for 4 h to burn off any residual hydrocarbons, fully oxidize the elements, and decompose any carbonate minerals. The ashed solids were then prepared into fused beads for X-ray fluorescence (XRF) analysis using a Katanax™ fuser with a platinum crucible and pan. The fused beads were analyzed with a Bruker S4 Explorer XRF equipped with a wavelength dispersive spectrometer (WDS). Calibration standards based on certified reference materials were used for elemental quantification.

RESULTS AND DISCUSSION

Distribution of Bitumen, Solids, and Water

The mass balance of bitumen, solids, and water around extraction is shown in Table 1. As shown in the table, the ore contains 8.5 wt% bitumen, corresponding to a mid-grade ore. These values also correspond to an average 89% recovery of bitumen into the primary froth and an average 92% overall bitumen recovery, confirming that this ore sample is a good processing ore.

Table 2 shows the mass balance around extraction of the different particle sizes of solids. All assays in this paper are given as weight percentages. As shown, the middlings comprise only 16% of the total solids, but 70% of the total clays and 73% of the total ultrafine clays. This means that the clay minerals present in the ore will have a much larger impact on the properties of the middlings stream than on the properties of any other stream.

A break down of the particle size distribution for the sand (>45 μm) is shown in Table 3. As shown, the majority of the sand is in the 106–250 μm size range, which is ideal for most mineral processing techniques.

Table 1: Mass balances of bitumen, solids, and water around extraction

		ASSAY				DISTRIBUTION			
	Wt% of total feed	Bitumen	Solids	Water	Dean Stark Loss	Bitumen	Solids	Water	Dean Stark Loss
Water	68.5%	0%	0%	100%	0%	0%	0%	99%	0%
Ore	31.5%	8.5%	89.1%	1.7%	0.7%	100%	100%	1%	100%
Total Feed	100.0%	2.7%	28.0%	69.1%	0.2%	100%	100%	100%	100%
Primary Froth	5.3%	44.6%	22.3%	32.3%	0.8%	88.8%	4.2%	2.5%	9.0%
Secondary Froth	0.6%	15.2%	26.4%	57.1%	1.3%	3.2%	0.5%	0.5%	1.6%
Middlings	65.7%	0.2%	9.8%	89.4%	0.6%	5.7%	22.9%	85.0%	82.5%
Tailings	27.0%	0.3%	74.6%	25.0%	0.1%	3.2%	72.0%	9.8%	6.9%
Sum of Streams	98.6%	2.7%	28.3%	68.5%	0.5%	101.0%	99.6%	97.7%	100.0%
Losses	1.9%	-1.4%	5.3%	83.7%	24.0%	-1.0%	0.4%	2.3%	100.0%

Table 2: Distribution of sand, fines, clays, and ultrafine clays around extraction

		ASSAY				DISTRIBUTION			
	Wt% of all streams	>45 µm	<45 µm	<2 µm	<0.2 µm	>45 µm	<45 µm	<2 µm	<0.2 µm
Primary Froth	4.2%	52%	48%	14%	4%	3%	7%	7%	6%
Secondary Froth	0.5%	68%	32%	14%	0%	0%	0%	1%	0%
Middlings	15.8%	2%	98%	39%	12%	1%	53%	70%	73%
Tailings	79.6%	86%	14%	2%	1%	96%	39%	22%	21%
Ore	100%	68%	32%	10%	3%	100%	100%	100%	100%
Sum of Streams	100%	71%	29%	9%	3%	100%	100%	100%	100%

Table 3: Distribution of particle sizes in sand fractions around extraction

		ASSAY			DISTRIBUTION		
	Wt% of all streams	>250 µm	106-250 µm	45-106 µm	>250 µm	106-250 µm	45-106 µm
Primary Froth	4.2%	0%	37%	15%	3%	3%	4%
Secondary Froth	0.5%	0%	52%	16%	0%	0%	0%
Middlings	15.8%	0%	1%	1%	16%	0%	1%
Tailings	79.6%	0%	65%	21%	81%	96%	95%
Ore	100%	0%	50%	17%	100%	100%	100%
Sum of Streams	100%	0%	53%	17%	100%	100%	100%

Distribution of Titanium, Zirconium, and Iron

Of the elements present in the oil sands, the three most interesting for secondary uses are titanium, zirconium, and iron. Furthermore, all three elements are preferentially enriched to the primary froth, with the primary froth accounting for 53% of the total titanium, 29% of the total iron, and 33% of the total zirconium (Table 4). The enrichment is most pronounced for the titanium, especially in the sand fraction (>45 µm) where a ten fold increase in titanium assay is noted between the ore and primary froth (Table 5). This enrichment indicates that the titanium-containing minerals in the sand fraction are effectively collected by the bitumen. The enrichment of the zirconium and the iron, while substantial, is not as complete as the enrichment of the titanium minerals.

It is also interesting to note how the three minerals distribute among the different size fractions. Titanium and iron exhibit similar distributions, with the majority concentrated into the fines (<45 µm) fraction of each stream. The fines account for 83% of the total iron and 74% of the total titanium. The two elements differ most in distribution within the clay size fraction, where only 20% of the total titanium is found in the clay size fraction as compared with 44% of the total iron. Unlike the titanium and iron, the zirconium is primarily concentrated in the sand fraction (>45 µm) of the oil sands, with only 30% contained in the fines fraction and less than 1% concentrated in the clay size fraction.

The combination of size and stream distributions indicates that the limiting factor for zirconium reclamation is likely the ability of the coarser zircon particles to float with the bitumen during the bitumen extraction. Titanium's effective flotation is apparently achieved in the primary separation vessel; however, a large portion of the titanium is concentrated in the fines, which are much more difficult to process. Furthermore, the iron enrichment in the fines means that any titanium recovered from the fines is more likely to be contaminated with iron than the titanium in the coarser streams.

Table 4: Total element balance around extraction

TOTAL	**ASSAY**								
Stream	**Sample Weight**	**SiO_2**	**Al_2O_3**	**Fe_2O_3**	**K_2O**	**MgO**	**TiO_2**	**ZrO_2**	**Other**
Primary Froth	100.0%	66.9%	11.2%	8.7%	1.1%	0.7%	6.2%	1.2%	4.1%
Secondary Froth	100.0%	75.3%	10.9%	5.4%	1.0%	0.7%	3.3%	0.5%	3.0%
Middlings	100.0%	68.5%	21.9%	3.5%	2.7%	0.6%	0.8%	0.0%	2.1%
Tailings	100.0%	93.7%	3.6%	0.4%	0.7%	0.0%	0.1%	0.1%	1.4%
Ore	100.0%	83.0%	9.5%	1.8%	1.3%	0.3%	0.6%	0.3%	3.0%
Sum of Streams	100.0%	88.5%	6.8%	1.2%	1.0%	0.1%	0.5%	0.2%	1.6%
TOTAL	**DISTRIBUTION**								
Stream	**Sample Weight**	**SiO_2**	**Al_2O_3**	**Fe_2O_3**	**K_2O**	**MgO**	**TiO_2**	**ZrO_2**	**Other**
Primary Froth	4%	3%	7%	29%	5%	19%	53%	33%	11%
Secondary Froth	0%	0%	1%	2%	0%	2%	3%	1%	1%
Middlings	16%	12%	51%	44%	42%	62%	26%	0%	20%
Tailings	80%	84%	42%	25%	54%	17%	18%	67%	68%
Ore	100%	100%	100%	100%	100%	100%	100%	100%	100%
Sum of Streams	100%	100%	100%	100%	100%	100%	100%	100%	100%

Table 5: Element balance for >45 µm size fraction

>45 µm	ASSAY								
Stream	**Sample Weight**	**SiO_2**	**Al_2O_3**	**Fe_2O_3**	**K_2O**	**MgO**	**TiO_2**	**ZrO_2**	**Other**
Primary Froth	100.0%	84.3%	5.2%	2.1%	0.6%	0.2%	3.9%	1.4%	2.4%
Secondary Froth	100.0%	90.2%	4.9%	0.9%	0.6%	0.0%	1.6%	0.4%	1.5%
Middlings	100.0%	56.1%	31.6%	4.5%	2.8%	1.4%	1.0%	0.1%	2.6%
Tailings	100.0%	95.0%	2.7%	0.2%	0.5%	0.0%	0.0%	0.1%	1.4%
Ore	100.0%	92.6%	2.8%	0.4%	0.5%	0.0%	0.3%	0.5%	2.9%
Sum of Streams	100.0%	94.5%	2.9%	0.3%	0.5%	0.0%	0.2%	0.2%	1.4%
>45 µm	**DISTRIBUTION**								
Stream	**Sample Weight**	**SiO_2**	**Al_2O_3**	**Fe_2O_3**	**K_2O**	**MgO**	**TiO_2**	**ZrO_2**	**Other**
Primary Froth	3%	3%	5%	21%	3%	34%	68%	28%	5%
Secondary Froth	0%	0%	1%	1%	0%	0%	4%	1%	0%
Middlings	1%	0%	6%	8%	3%	47%	3%	0%	1%
Tailings	96%	97%	88%	69%	93%	19%	25%	71%	93%
Ore	100%	100%	100%	100%	100%	100%	100%	100%	100%
Sum of Streams	100%	100%	100%	100%	100%	100%	100%	100%	5%

The minerals can be considered in four broad categories: – clay minerals, other silicates, iron-containing minerals, and titanium-containing minerals.

Clay Mineral Balances

As expected, the majority (>60%) (Table 6) of the clay minerals detected are concentrated in the clay-size fraction of the different streams. The clay minerals not found in the clay size are generally found in the silt-size fraction, so that the vast majority of the clay minerals are in the fines. The only stream that had any appreciable quantity of clay minerals in the sand-size fraction was the tailings, where 14% of the total clay minerals detected were in the >45 µm fraction (Table 6). This may be due to the large quantity of material in this size fraction, which makes complete clay dispersion and separation more difficult. It is no surprise, therefore, that the majority of the clay minerals (73%) partition, along with the majority of the clay size fraction, to the middlings stream, while only 7% of the total clay minerals partition to the primary froth. Chlorite, kaolinite, and kaolinite-smectite make up the bulk of the clay minerals that partition to the primary froth, with the primary froth accounting for 10% of the total chlorite, 8% of the total kaolinite, and 8% of the total kaolinite-smectite. The primary froth accounts for only 4% of the total illite-smectite, while the middlings accounts for 75% of the total illite-smectite, indicating that the illite-smectite has a preference for the aqueous middlings stream (Table 7)

Table 6: Total clay balance around extraction

Clay Minerals	**ASSAY)**				
Stream	**<0.2 µm**	**<2 µm**	**<45 µm**	**>45 µm**	**Total**
Primary Froth	97.7%	91.0%	42.5%	1.2%	21.2%
Secondary Froth		88.6%	60.6%	1.0%	20.2%
Middlings	98.9%	93.6%	60.7%	68.0%	60.9%
Tailings	99.8%	78.5%	19.2%	0.5%	3.2%
Sum of Streams	99.0%	90.0%	43.1%	0.9%	13.1%
Ore	98.1%	95.0%	62.0%	0.8%	20.4%
Clay Minerals	**DISTRIBUTION**				
Stream	**<0.2 µm**	**<2 µm**	**<45 µm**	**>45 µm**	**Total**
Primary Froth	17%	62%	97%	3%	100%
Secondary Froth		63%	97%	3%	100%
Middlings	19%	60%	97%	3%	100%
Tailings	21%	60%	86%	14%	100%
Sum of Streams	19%	60%	95%	5%	100%
Ore	14%	48%	97%	3%	100%

Table 7: Distribution of clay minerals around extraction

TOTAL	**ASSAY (wt %)**						
Stream	**Chlorite**	**Illite**	**Illite-smectite**	**Kaolinite**	**Kaolinite-smectite**	**Total Non-Clay**	**Total Stream**
Primary Froth	1.6%	5.8%	2.5%	9.4%	1.9%	78.8%	100.0%
Secondary Froth	1.2%	4.4%	1.4%	11.0%	2.2%	79.8%	100.0%
Middlings	3.5%	18.3%	12.0%	22.1%	4.9%	39.1%	100.0%
Tailings	0.1%	1.2%	0.7%	1.0%	0.2%	96.8%	100.0%
Sum of Streams	0.7%	4.1%	2.5%	4.7%	1.0%	86.9%	100.0%
Ore	1.1%	5.2%	3.3%	9.1%	1.6%	79.6%	100.0%
TOTAL	**DISTRIBUTION**						
Stream	**Chlorite**	**Illite**	**Illite-smectite**	**Kaolinite**	**Kaolinite-smectite**	**Total Non-Clay**	**Total Stream**
Primary Froth	10%	6%	4%	8%	8%	4%	4%
Secondary Froth	1%	0%	0%	1%	1%	0%	0%
Middlings	80%	70%	75%	74%	74%	7%	16%
Tailings	10%	24%	21%	17%	17%	89%	80%
Sum of Streams	100%	100%	100%	100%	100%	100%	100%
Ore	100%	100%	100%	100%	100%	100%	100%

Table 8: Distribution of non-clay minerals around extraction

TOTAL	ASSAY												
Stream	**Anat.**	**Brook.**	**Ilm.**	**Mic.**	**Pyr.**	**Q**	**Rut.**	**Sch.**	**Sid.**	**Zr.**	**Total Clays**	**Other**	**Total Stream**
Primary Froth	1.8%	1.2%	1.1%	3.7%	1.2%	60.5 %	2.0%	2.0%	3.2%	1.6%	21.2 %	0.4%	100.0%
Secondary Froth	0.9%	0.2%	0.2%	1.9%	0.2%	71.4 %	1.3%	1.0%	2.0%	0.4%	20.2 %	0.2%	100.0%
Middlings	0.1%	0.0%	0.0%	0.0%	0.0%	36.4 %	0.1%	0.1%	1.0%	0.0%	60.9 %	1.3%	100.0%
Tailings	0.0%	0.0%	0.0%	2.6%	0.0%	93.8 %	0.0%	0.0%	0.1%	0.0%	3.2%	0.3%	100.0%
Sum of Streams	0.1%	0.0%	0.0%	2.2%	0.1%	83.2 %	0.1%	0.1%	0.4%	0.1%	13.1 %	0.5%	100.0%
Ore	0.3%	0.0%	0.0%	2.0%	0.0%	76.6 %	0.0%	0.0%	0.5%	0.0%	20.4 %	0.2%	100.0%
TOTAL	**DISTRIBUTION**												
Stream	**Anat.**	**Brook.**	**Ilm.**	**Mic.**	**Pyr.**	**Q**	**Rut.**	**Sch.**	**Sid.**	**Zr.**	**Total Clays**	**Other**	**Total Stream**
Primary Froth	68%	98%	98%	7%	81%	3%	74%	81%	38%	93%	7%	3%	4%
Secondary Froth	4%	2%	2%	0%	1%	0%	5%	5%	3%	2%	1%	0%	0%
Middlings	20%	0%	0%	0%	6%	7%	16%	15%	45%	5%	73%	42%	16%
Tailings	8%	0%	0%	93%	12%	90%	5%	0%	14%	0%	19%	54%	80%
Sum of Streams	100 %	100%	100 %	100 %	100 %	100%	100 %	100 %	100 %	100 %	100%	100%	100%
Ore	100 %	100%	100 %	100 %	100 %	100%	100 %	100 %	100 %	100 %	100%	100%	100%

*Anat. = anatase, Brook. = brookite, Ilm. = ilmenite, Mic. = microcline, Pyr. = pyrite, Rut. = rutile, Sch. = schorl, Sid. = siderite, Zr. = zircon.

Other Silicates

The majority of the feldspar present in this ore is potassium feldspar, primarily microcline; however, in the middlings the "best" refinement was obtained when plagioclase feldspar is included in the refinement. For the purposes of the mineral balance discussion, the two feldspars are combined to give a total distribution of feldspars around extraction. Both quartz and feldspar are concentrated in the >45 µm fraction; this fraction accounting for 82% of the quartz and 71% of the feldspars, with microcline being slightly finer than the quartz. It is, therefore, not surprising that the majority of both the microcline and quartz ended up in the tailings stream, as larger particles have more difficulty floating than smaller particles. Quartz showed no affinity for the primary froth, as all quartz present is likely the result of entrainment or association with other minerals that were attracted to the froth. Overall, it seems that the distribution of these minerals is dominated by the difficulty in suspending large hydrophilic particles.

Zircon

Zircon is strongly enriched in the primary froth, with 93% of the detected zircon partitioning to this stream. This is a significantly higher figure than predicted by elemental analysis. This is most likely due to the difficulty of detecting the small concentrations of zircon that remain in the other streams. As well, in contrast to the elemental results, most (61%) of the detected zircon was found in the fines fraction as opposed to the sand fraction (Table 9). Once again, this is likely due to the detrimental effects of a large quantity of quartz on the detectability of zircon by Rietveld analysis.

Titanium-Bearing Minerals

As predicted by XRF results, the majority (76%) of the titanium minerals detected were in the <45 µm fraction. This trend was consistent for all the detected titanium-bearing minerals (rutile, anatase, brookite, and ilmenite). Ilmenite was the coarsest, with only 61% of the ilmenite found in the <45 µm fraction (Table 9), and brookite was the finest, with 88% in the <45 µm fraction (Table 9). Also, as predicted, the titanium minerals were strongly

enriched in the primary froth, with 79% of the total titanium minerals detected reporting to the froth. Of the titanium-rich minerals, brookite and ilmenite were only detected in the froth streams. They were, however, present in quantities close to the lower detection limit. Rutile and anatase were detected in all streams, although not in all size fractions of every stream. Of the detected anatase, 68% reported to the primary froth, compared with 74% of the rutile (Table 8). This is expected, since rutile is known to have a higher contact angle with water than anatase does (Wu & Nancollas, 1998), and so is likely to be more easily collected by the bitumen.

Iron Bearing Minerals

Like the titanium-bearing minerals, the iron-bearing minerals are concentrated in the <45 µm fraction (74%) and in the primary froth (56%). Of the five iron–bearing minerals detected (ilmenite, lepidocrocite, schorl, siderite, and pyrite), all except schorl had the majority of their weight in the <45 µm fraction, whereas 57% of the schorl was >45 µm. In addition, all the minerals except siderite had more than 75% of their detected weight in the primary froth. Only 38% of the siderite was detected in the primary froth. This distribution is expected of pyrite, which is more hydrophobic than the other iron-bearing minerals detected (Wills, 1997). Ilmenite, on the other hand, is expected to be less hydrophobic than siderite. As such, it is interesting that ilmenite is strongly enriched in the froth, while the siderite is not as strongly enriched in the froth.

Table 9: Distribution of selected minerals by particle size

	ASSAY				DISTRIBUTION			
	Ultrafine Clay (<0.2 µm)	Clay (<2 µm)	Fines (<45 µm)	Sand (>45 µm)	Ultrafine Clay (<0.2 µm)	Clay (<2 µm)	Fines (<45 µm)	Sand (>45 µm)
Anatase	0.05%	0.36%	0.32%	0.03%	1%	28%	82%	18%
Brookite	0.00%	0.00%	0.15%	0.01%	0%	0%	88%	12%
Ilmenite	0.00%	0.00%	0.10%	0.03%	0%	0%	61%	39%
Lepidocrocite	0.1%	0.2%	0.0%	0.0%	25%	100%	100%	0%
Pyrite	0.0%	0.1%	0.2%	0.0%	0%	8%	78%	22%
Rutile	0.01%	0.27%	0.29%	0.28%	0%	20%	72%	28%
Schorl	0.0%	0.0%	0.2%	0.1%	0%	0%	43%	57%
Siderite	0.1%	0.9%	1.0%	0.1%	0%	22%	82%	18%
Zircon	0.00%	0.00%	0.15%	0.04%	0%	0%	61%	39%
Total Titanium Bearing	0.06%	0.63%	0.86%	0.35%	5%	52%	71%	29%

CONCLUSIONS

The mass, element, and mineral balances around extraction reveal several interesting trends. As reported by other researchers, the titanium and zircon-bearing minerals are enriched in the primary froth, with 53% of the total titanium and 33% of the total zirconium reporting to this fraction. The limiting factor for zirconium enrichment seems to be an incomplete affinity for the primary froth, likely due to the fact that zirconium is among the least hydrophobic minerals. The enrichment of the titanium is more complete, likely because most titanium minerals are more hydrophobic and smaller than the zircon bearing minerals. Iron is also enriched in the froth, but not as strongly as the zircon and titanium, because iron is a minor constituent of many of the silicate minerals detected. Of the iron-bearing minerals, all except for siderite were found to be enriched in the primary froth.

The mineral balance of the clay minerals showed that the non-charged, less asymmetric phases of kaolinite and chlorite preferentially reported to the primary froth. The charged clay and more asymmetric clay minerals of illite-smectite and illite, conversely, preferred the middlings stream. This distribution is important, because it indicates that the more highly active clay minerals, i.e., the ones that will have a negative impact on settling behaviour, tend to concentrate in the stream where settling behaviour is most important (the middlings).

REFERENCES

Alberta Chamber of Resources. (1996). Mineral developments agreement co-products study [Report], Alberta: Author.

Bayliss, P., & Levinson, A.A. (1976). Mineralogical review of the Alberta oil sand deposits (Lower Cretaceous, Mannville Group). Bulletin of Canadian Petroleum Geology, 24 (2): 211–224.

Moore, D. M. & Reynolds, J. R. C. (1997). X-ray diffraction and the identification and analysis of clay minerals. Oxford, UK: Oxford University Press.

Omotoso, O. (2007). [Personal communication].

Syncrude Research, (1979). Determination of Bitumen, water and solids content of oil sand, reject and slurry samples (Classical). Method 2.7. Syncrude analytical methods for oil sand and bitumen processing. Syncrude Canada Limited.

Wang, N., & Mikula, R.J., (2002). Small scale simulation of pipeline or stirred tank conditioning of oil sands: temperature and mechanical energy. Journal of Canadian Petroleum Technology 41 (1), 8–10.

Wills, B. (1997). Mineral processing technology (6th Ed.). London: Butterworth-Heinemann.

Wu, W., & Nancollas, G. H. (1998). Kinetics of heterogeneous nucleation of calcium phosphates on anatase and rutile surfaces. Journal of Colloid and Interface Science, 199, 206–211.

COMPARISON OF MORPHOLOGICAL AND CHEMICAL CHARACTERISTICS OF CLAY MINERALS IN THE PRIMARY FROTH AND MIDDLINGS FROM OIL SANDS PROCESSING BY HIGH RESOLUTION TRANSMISSION ELECTRON MICROSCOPY

Heather A.W. Kaminsky[1], Peter Uhlik[1,3], Ali Hooshiar[1], Alyssa Shinbine[1], Thomas H. Etsell[1], Douglas G. Ivey[1], Qi Liu[1] and Oladipo Omotoso[2]
1 Department of Chemical and Materials Engineering, University of Alberta, Edmonton, Alberta, Canada
2 Natural Resources Canada, CETC–Devon, Alberta, Canada
3 Department of Geology of Mineral Deposits, Comenius University in Bratislava, Slovakia

ABSTRACT

Understanding the interaction of clay minerals with bitumen in the oil sands is of great interest in developing water-free or water-reduced bitumen extraction processes. Previous work by Kaminsky et al. has shown, by x-ray diffraction, that there is a difference in clay minerals that partition to the froth stream versus the clays that remain in the middlings. However, x-ray diffraction analysis was insufficient in determining why the different minerals partitioned the way they did. This work examines the clay minerals in each stream by high resolution transmission electron microscopy, combined with energy dispersive x-ray analysis, to examine the characteristic chemical and morphological differences in the clay particles in each stream.

INTRODUCTION

Clay mineral characterization is important for several reasons. First, although mixed layer clay minerals have been identified as a component of the oil sands, their structure is not well known. This characterization should lead to a better understanding of the structure of the mixed layer clay minerals. The structure of the mixed layer clay minerals can, in turn, be used by others to improve models of clay behaviour in thickeners, tailings ponds or in processing. Second, knowledge of where iron and other colour inducing chromophores are located will help with the development of bleaching techniques, so that the kaolinite found in the oil sands can be theoretically used in high-value applications such as paper making, concrete admixtures or fine ceramics. Finally, exploring the relationship between particle thickness, charge distribution and the degree of mixed layering seen in XRD patterns will substantially add to the body of knowledge in clay science and may help address problems seen with other unusual clay mineral deposits such as the Birdwood kaolinite in Australia (Zbik, 2006).

Previous work by Kaminsky et al. (2008) has shown that kaolinite and chlorite are preferentially distributed to the froth stream during processing, while illite-smectite is preferentially distributed to the middlings. This work also showed that the illite-smectite in the primary froth exhibited a higher degree of low angle asymmetry after ethylene glycol solvation than the illite-smectite in the middlings. This paper provides some possible explanations for the difference in the illite-smectites observed in the middlings and froth.

MATERIALS AND METHODS

Sample Preparation

A low-grade oil sand ore (1.5 kg), containing 8.5% bitumen from a Suncor lease, was processed in a Syncrude-styled batch extraction unit using the CANMET procedure that has been reported to represent hydrotransport conditioning at 50˚C (Wang & Mikula, 2002). The primary froth, secondary froth, middlings and tailings streams were collected and the solids cleaned and separated from the residual water and organics by the Dean-Stark procedure (Syncrude, 1979). Immediately after extraction and prior to Dean Stark analysis, the total tailings stream was allowed to sit for 2 minutes, after which the supernatant was decanted as the middling fraction. While the technique for middling/tailing separation is arbitrary, the middling fraction generally represents the fine tailings stream that ends up as MFT for a given extraction water chemistry. The cleaned solids were then homogenized and the >45 μm particles were removed by sieving in a Ro-tap™ sieve shaker,

using deionized water. The sub-sieve fraction was separated into fines (2-45 μm), clays (0.2–2 μm), and ultrafine clays (<0.2 μm) by centrifugation. The particle size distribution of the clay fractions was assessed using a Mastersizer 2000™ to confirm that proper separation was achieved during centrifugation.

TEM Analysis

Two types of samples were used in TEM analysis – dispersed samples and ultrathin sections. The preparation of the dispersed samples involved diluting clay solids with deionized water to an approximate 40:1 dilution. The resulting slurry was sonicated to fully disperse the clays in the slurry. One drop of the solution was then placed on a lacey, carbon-coated, copper grid.

The dispersed samples were examined in both JEOL 2022 FS and JEOL 2010 transmission electron microscopes (TEMs). The length and width of the clay particles in the images obtained were then measured and compiled.

Ultrathin sections were prepared using fragments of the dried specimens that were coated with agar and saturated with water. The samples were then embedded in resin using the method of Tessier, 1984; and Elsass et al., 1998. In this method the water was replaced by methanol, then by propylene oxide and finally by Spurr resin to ensure all pores and free spaces had been impregnated. After polymerization of the resin, ultrathin sections (~70 nm thick) were cut using a Reichert Ultracut E microtome and a diamond knife. The microtome slices were captured on a lacy, carbon-coated, copper grid.

High-resolution TEM images were taken with a JEOL 2010 microscope operated at 200 kV and equipped with a CCD camera and an energy-dispersive x-ray (EDX) spectrometer. The camera settings were adjusted so as to enable real-time low-light imaging. The electron beam was defocused to minimize specimen damage, so that the image was barely visible on the phosphorescent screen, and the magnification was increased to between 400 000 and 1MX. Fringe images were obtained by adjusting the sample height to the point of minimum contrast and then adjusting the focus until fringes were obtained. Selected area diffraction (SAD) patterns were recorded on film.

The number of interlayers per particle and particle thickness were used for calculation of expandability of illite-smectite according to the equation by Środoń et al. (1990):

$Exp_{MAX}=(T+NoD_S) – (N+No) / (N+No)(D_S-D_I) * 100$

No is the number of crystal measured for a given sample. T is a "total" measured thickness and N is a "total" number of measured interlayers. D_S and D_I are interlayer spacings for smectite (1.35 nm) and illite (1 nm). Expandability means the percentage of smectitic interlayers per illite-smectite crystal.

RESULTS

Particle Size Distribution by Mastersizer

Particle size analysis of the clay size samples was performed using a Mastersizer 2000™. As shown by the particle size distribution (Figure 1), the centrifugation was successful at separating out particles less than 0.2 μm in size. The middlings stream had a few larger particles present, but overall the average particle size was in the expected range (Table 1).

Table 1: Particle size distribution numbers for d_{10}, d_{50}, and d_{90}[1]

	d_{10}	d_{50}	d_{90}
Primary Froth, <0.2	0.08	0.14	0.23
Middlings, <0.2	0.08	0.13	0.22
Tailings, <0.2	0.07	0.13	0.22
Secondary Froth, <2	0.11	1.93	12.58
Primary Froth, 0.2-2	0.08	0.29	3.35
Middlings, 0.2-2	0.08	0.14	1.16
Tailings, 0.2-2	0.13	3.70	17.86

The distribution in particle size was much more varied for the 0.2–2 μm fractions, as shown in Figure 2. This may be due to the fact that the Mastersizer uses the equivalent projected spherical diameter as a measure of particle size. Therefore, for highly asymmetrical particles (such as clays) undergoing Brownian motion, the projected spherical diameter is likely to be dominated by the largest dimension of the particle.

[1] $d_{10,}$ d_{50} and d_{90} represent the sizes at which 10%, 50% and 90% of the particles are smaller than the size given.

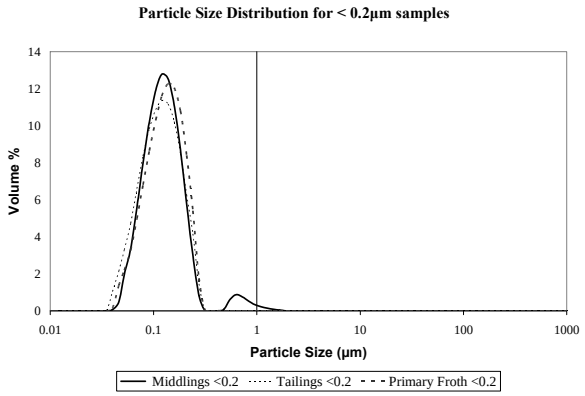

Figure 1: Particle size distribution for <0.2 µm fraction.

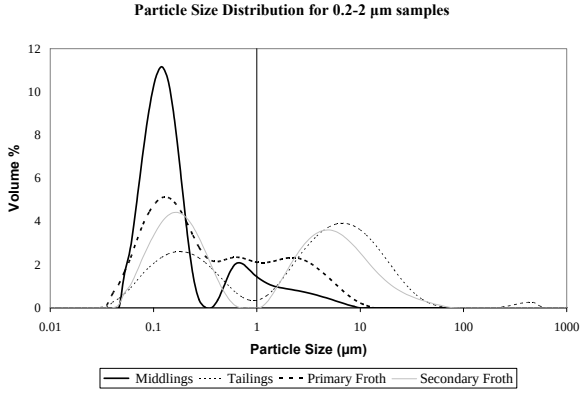

Figure 2: Particle size distribution for the 0.2–2 micron streams.

This dimension, however, will not dominate as strongly for particle size by settling. Even with the large variation in sizes, the d_{50} for most streams, with the exception of the tailings stream, was under the 2 µm cut-off. Furthermore, the refractive index of kaolinite was used as the refractive index for all particles, but does not take into account differences in mineralogy or the presence of residual organics. These differences may cause a slight overestimate of the particle size, meaning that all the samples were satisfactorily separated into the <0.2 µm and <2 µm streams.

Basal Particle Morphology by TEM

The compiled measurements of particle length and width are shown in **Table** 2. Two interesting trends are observed based on these measurements. The first is that the middlings have a slightly higher average length-to-width ratio than the primary froth, for both the 0.2–2 µm and the <0.2 µm fractions. This is consistent with the XRD results (Kaminsky et al., 2008), which show that the middlings contain more illite and illite-smectite (i.e., lath like particles) and less kaolinite (i.e., pseudohexagonal particles) than the primary froth. The difference in average particle size measured in the primary froth and the middlings was also interesting. In the 0.2–2 µm fractions, the middlings had particles that were substantially longer and wider than the primary froth particles of the same size fraction. On first glance this appears to contradict the Mastersizer results, which showed that the middlings had a smaller particle size than the primary froth. However, the Mastersizer measures the equivalent projected spherical diameter as a measure of particle size, which means that for platy particles such as clays, the particles may be counted as both very small particles when observed edge on, and as very large particles when observed on the basal surface. The middlings encompassed a very pronounced bimodal distribution of particle size, whereas the primary froth covered a wider range. This could indicate that the primary froth samples had particles that were more uniform in size and thickness, resulting in a larger overall size relative to the middlings, as the middlings is composed of particles with high surface area-to-volume ratios (thin, elongated structures). This hypothesis is consistent with the XRD crystallite measurements of the middlings, which showed the average crystallite size of the primary froth to be larger than that of the middlings (Table 3). In the <0.2 µm fraction the middlings were smaller than the primary froth, which is consistent with the Mastersizer results. The morphology of the middlings noted here exemplifies why the rheological behaviour of the middlings is so undesirable from a tailings management perspective, as increased aspect ratios and decreased particle sizes both increase the yield strength of a slurry of particles (Brenner, 1974).

Table 2: Length and width measurement for dispersed particles in primary froth and middlings samples

Size Fraction	Stream	Average Length (nm)	Average Width (nm)	Average L/W Ratio	# of Particles
< 0.2 µm	Middlings	182	113	1.75	184
	Primary Froth	375	244	1.67	887
0.2-2 µm	Middlings	889	529	1.82	515
	Primary Froth	515	303	1.74	166

Table 3: Crystallite size (thickness) measurements for clay minerals determined by XRD

Size Fraction	Stream	Chlorite (nm)	Kaolinite-smectite (nm)	Kaolinite (nm)	Illite-smectite (nm)	Illite (nm)	Average Particle Thickness (nm)
0.2-2 µm	Primary Froth	14	8	28	11	21	21
	Middlings	17	7	25	6	25	18
< 0.2 µm	Primary Froth		4	10	4	10	6
	Middlings		4	10	3	8	5

A final trend noted in the examination of the dispersed particles was the prevalence of fine iron oxides. These areas were prevalent in both the middlings and the primary froth, but were more common in the primary froth samples. Feroxyhite and other iron-oxide hydroxides were identified from selected area diffraction patterns of these areas. Feroxyhite and most of the other iron-oxide hydroxides were not detected in any of the XRD patterns, but the extremely fine nature of these particles would likely cause the broadened peaks to be lost in the background of the patterns.

Fundamental Particle Thickness by HRTEM

No kaolinite lattice images were detected in these samples, due to the extreme sensitivity of the kaolinite to the electron beam. Of the particles that were observed, most had the characteristic 1.0 nm d-spacing of illite; however, there were others with measured spacings closer to 1.2 nm, possibly indicating the presence of smectitic layers within a particle. Particles exhibiting inconsistent layer spacings, as shown in Figure 3, were further indications of this possibility. Both phenomena may be due to an incorrect amount of defocus during imaging. However, the presence of well resolved layers, exhibiting 1.0 nm spacing close to the areas of inconsistency, suggests that it is a sample phenomenon rather than an experimental artefact. It is significant to note that no monolayers were found in any of the samples, further confirming the absence of discreet smectite in these samples. Many particles exhibiting frayed edges were also observed in the samples. It is possible that the layers at the frayed wedge are de-potassified, similar to the phenomenon reported for hydrous mica or degraded illite (Wallace et al., 2004).

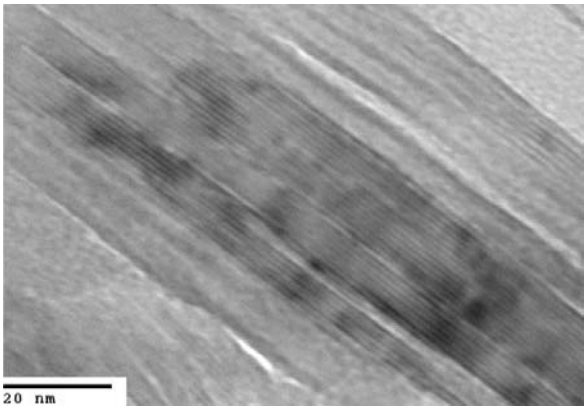

Figure 3: HRTEM image of 0.2-2 µm middlings sample showing inconsistent layer spacings.

Table 4 depicts a summary of the measurements on the lattice fringe images obtained for the middlings and primary froth. As shown, the average number of layers observed per particle remained constant for both primary froth samples and the <0.2 μm middlings at four layers per particle. This value is consistent with the initial TEM results previously described by Kaminsky et al., (2006), as well as with the fundamental crystallite size measured by XRD for the <0.2 μm. The 0.2–2 μm middlings sample had a slightly higher average of five layers. These results for the 0.2–2 μm sample are significantly different from the thickness values predicted by XRD. There are two probably causes of this discrepancy. Firstly, the scattering domains detected in the XRD can come from multiple particles stacked together to form domains larger than the true particle thickness. Alternatively, the HRTEM may underestimate the fundamental thickness of this stream as the smaller particles are the ones most easily observed in HRTEM. Therefore, they may be statistically overrepresented in the images analyzed. Calculated % smectite from HRTEM data is about 10% higher than Kaminsky et al., (2008) reported from XRD data (Exp_{XRD}). This discrepancy is in agreement with previous work, as Exp_{MAX} is higher than Exp_{XRD} because of the assumption of smectitic crystal edges (Środoń et al., 1990).

Table 4: Average particle thickness and d-spacings for particles observed by HRTEM

Stream	Size Fraction	Average d-spacing	# of Particles	Average # of Layers	% Smectite in illite/smectite
Middlings	**<0.2**	1.02	121	4	33
	0.2-2	1.12	209	5	41
	Total	1.09	330	4	38
Primary Froth	**<0.2**	1.07	286	4	36
	0.2-2	1.08	204	4	36
	Total	1.07	490	4	36

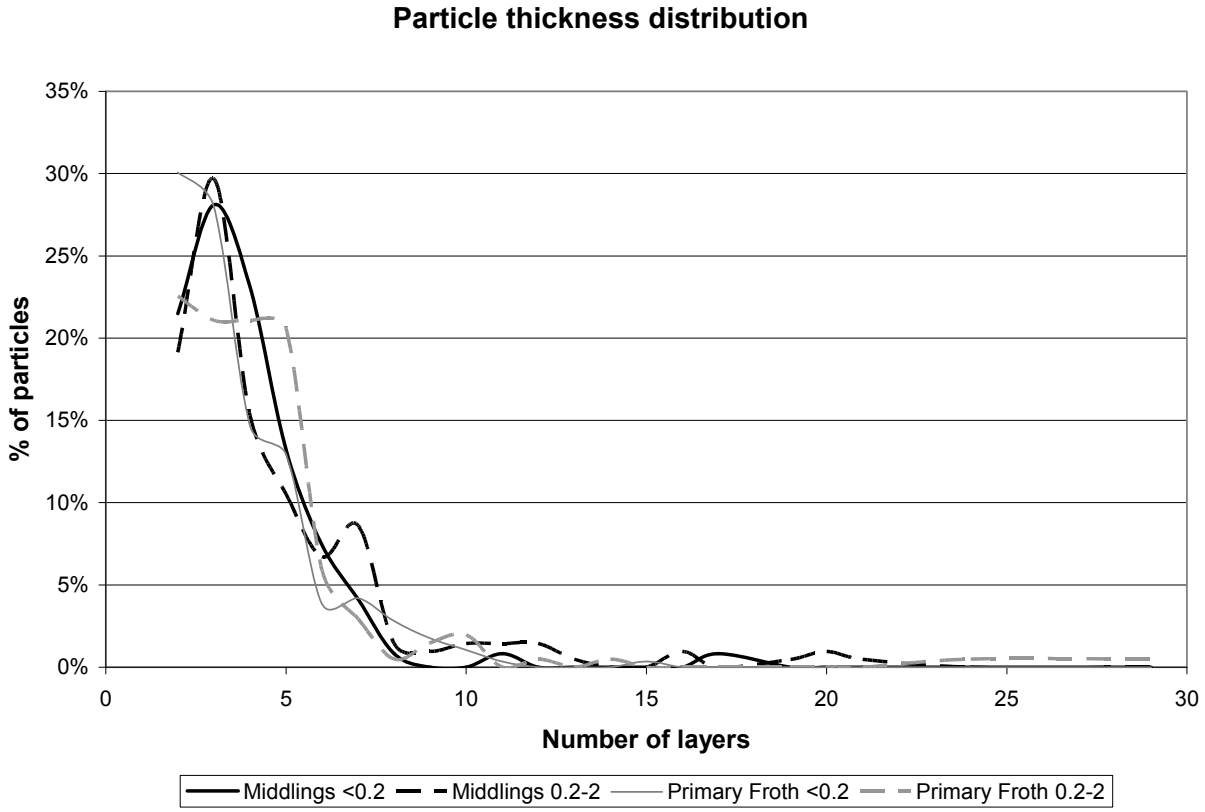

Figure 4: Thickness distribution of particles from HRTEM images.

Differences were observed between the thickness distribution of the primary froth and the middlings particles. As shown in
Figure 4, the <0.2 µm primary froth appears to have a bimodal distribution with one average between three and four layers and the other at seven layers. Conversely, the <0.2 µm middlings sample exhibits a single peak at four layers, with a slight shoulder at around six layers. This difference in particle thickness distribution may explain the difference in sample response to ethylene glycol noted in the XRD results. The slightly lower average of the major peak (between three and four layers, as opposed to four layers) would indicate a larger degree of smectitic character for some particles and, hence, a larger degree of swelling with ethylene glycol. This larger swelling for some particles would, in turn, lead to the low angle asymmetry observed in the XRD profiles. It may also explain why the methylene blue absorption was higher in this fraction.

Charge Distribution by TEM-EDX

EDX analysis on individual clay particles was performed using a JEOL 2200FS TEM equipped with an INCA energy dispersive X-ray (EDX) spectrometer. A very small number of particles were analyzed using this method, due to the difficulty of isolating the areas of interest. Attempts at improving the dispersion of the clay particles were unsuccessful, resulting only in more isolated clusters of particles.

The results were further broken down into four types of particles, according to the shape of the particle observed, i.e., kaolinite (pseudohexagonal, no potassium detected), illite (lath type with potassium), other (pseudohexagonal, with potassium) and uncategorized. These results are shown in Table 5. It is interesting to note that pseudohexagonal particles containing potassium (and iron) were detected in the primary froth; pseudohexagonal particles are generally assumed to be kaolinite. Since these particles contain potassium and iron, they are potentially kaolinite-smectite.

Table 5: TEM-EDX results for 0.2–2 µm middlings and primary froth classified by type

Stream	Middlings		Primary Froth		
Classification	**Illite**	**Unclassified**	**Illite**	**Other**	**Unclassified**
Al	12.7%	16.3%	15.1%	21.4%	20.9%
Si	27.0%	26.8%	24.1%	23.1%	24.1%
K	2.4%	1.4%	2.2%	0.2%	1.6%
Fe	2.8%	1.1%	2.4%	0.9%	1.0%
Mg	1.3%	0.7%	1.2%	0.0%	1.7%
Ca	0.5%	0.6%	0.0%	0.2%	0.0%
Cl	0.0%	0.0%	0.7%	0.3%	0.0%
Na	0.0%	0.0%	0.5%	0.2%	0.0%
O	53.0%	53.2%	53.5%	53.5%	50.6%
S	0.3%	0.0%	0.0%	0.1%	0.0%
Ti	0.0%	0.0%	0.3%	0.0%	0.0%
Si/Al ratio	2.25	1.64	1.68	1.08	1.15
Number of particles	2	1	7	2	3

Table 6: Layer charge calculations for 0.2–2 µm primary froth illite particles

Element	Wt%	Gram Eq.[2]	Normalized Gram Eq.	Tet.[2] Layer	Oct.[2] Layer	Interlayer	Tet. Layer Charge	Oct. Layer Charge	Interlayer charge
Mg	1.20	0.10	0.20		0.20			0.40	
Al	15.10	1.68	2.29	0.47	1.82		1.40	5.47	
Si	24.10	3.43	3.51	3.51			14.04		
K	2.20	0.06	0.23			0.23			0.23
Fe	2.40	0.09	0.18		0.00	0.18		0.00	0.35
Ca		0.00	0.00			0.00			0.00
Ti	0.30	0.03	0.03	0.03			0.10		
Mn		0.00	0.00						
Na	0.04	0.00	0.01			0.01			0.01
Sum Gram Equivalents		5.38	6.44			**Layer Charge**	**-0.47**	**-0.12**	**0.59**

[2] Eq= Equivalents, Tet. = Tetrahedral, Oct. = Octahedral

Table 7: Layer charge calculations for 0.2–2 µm middlings illite particles

Element	Wt%	Gram Eq.	Normalized Gram Eq.	Tet. Layer	Oct. Layer	Interlayer	Tet. Layer Charge	Oct. Layer Charge	Interlayer Charge
Mg	1.3	0.11	0.21		0.21			0.42	
Al	12.7	1.41	1.87	0.19	1.68		0.57	5.03	
Si	27	3.84	3.81	3.81			15.24		
K	2.4	0.06	0.24			0.24			0.24
Fe	2.8	0.10	0.20		0.11	0.09		0.22	0.17
Ca	0.5	0.02	0.05			0.05			0.10
Sum Gram Equivalents		5.55	6.38			**Layer Charge**	**-0.19**	**-0.32**	**0.51**

From the EDX results, the structural formulae for the illite particles in the 0.2–2 µm primary froth (Table 6) and 0.2–2 µm middlings (Table 7) were calculated according to the method of Laird (1994). Assumptions made in this process included the following: all detected elements were part of the structure, the anion charge was 22 (11 atoms of oxygen), the tetrahedral occupancy was 4 gram-equivalents, the octahedral occupancy was 2 gram equivalents, the iron had a charge of +2, magnesium preferentially filled the octahedral layer and residual iron could exchange in the interlayer to balance the charge on the molecule. It should be noted that having iron preferentially fill the octahedral layer with the magnesium balancing the interlayer charge is also possible and that the different choice would have no effect on the total charge balance. The presence of Fe^{3+} instead of Fe^{2+} in the octahedral layer would reduce the overall charge on the particle.

Based on the calculated formulae, the primary froth particles have a slightly higher charge than the middlings. Furthermore, the charge on the primary froth particles seems to be concentrated more in the tetrahedral layer, leading to a more localized charge. Conversely, the charge in the middlings seems to be concentrated in the octahedral layer. This distribution noted in the primary froth is consistent with clay that would interact easily with organic molecules having some polar (charged) functional groups and some non-polar sections (Moore & Reynolds, 1997). The polar sections would interact with the strong localized charges provided by the tetrahedral substitution, while the non-polar regions would interact with the pure siloxane surface of the unsubstituted portions of the clay. The charge distribution of the middlings, on the other hand, is consistent with a clay that would be surrounded easily by hydrated cations and attract a large amount of water to its surface.

Another observation from the calculated charge distribution is that iron associated with the primary froth particles is mostly associated with the interlayer, rather than the octahedral layer as it is with the middlings. This may explain the higher degree of low-angle asymmetry observed in the XRD results, as the particles with iron substitution in the interlayer will have more interlayer space and will, therefore, be detected at lower angles in the XRD.

DISCUSSION

The clay minerals found in the middlings were different from the clay minerals found in the froth. Firstly, the froth solids were enriched in chlorite and kaolinite and were depleted in illite-smectite. Liendo (2005) found that kaolinite absorbed bitumen products more readily than montmorillonite or illite. This indicates that the enrichment of the kaolinite and chlorite to the froth solids is due to an affinity of these minerals for the bitumen rather than due to the rejection of the illite-smectite. The mechanism for this affinity remains unclear. Since the bitumen seems to have an affinity for these minerals, it is likely that ores containing large amounts of these minerals will have a larger amount of solids reporting to the froth and, hence, will cause more difficulty with down stream processes such as froth upgrading

and coke production. Depending on the mechanism of kaolinite interaction with the bitumen, these minerals may also be problematic in solvent extraction processes. If the kaolinite interaction is a relatively weak interaction between a neutral surface and a non-polar molecule, then solvent extraction may not be a concern. However, if the interaction is more complex, then the kaolinite may still prefer the hydrophobic bitumen over the hydrophobic solvent. Work by Ward & Brady (1998) suggests that the adsorption of organic acids on kaolinite occurs primarily on aluminum sites on exposed edges of the kaolinite. This is significant as it may explain why the clay minerals in the froth had a smaller basal surface area in TEM analysis than the middlings clay minerals. The smaller basal surface area would mean an increased number of edges and, therefore, an increased number of sites for the organics to adsorb on.

Apart from the preferential enrichment of kaolinite and chlorite to the froth, there are other ways in which the froth clay minerals are different from the middlings clays. The middlings clays exhibit a higher aspect ratio than the clays in the primary froth both in terms of their length-to-width ratio and in terms of the surface area-to-thickness ratio. The high aspect ratios cause slurries of these particles to have higher yield strengths and higher relative viscosities, making the slurry more resistant to flow. (Brenner, 1974) The increased resistance to flow means that settling of the particles is more difficult.

The illitic particles in the middlings also appeared to have a lower total charge than the illitic particles in the primary froth. Furthermore, the charge was more concentrated in the octahedral layer meaning that the effect of the charge would be more diffuse at the surface of the clay. The presence of this diffuse charge means that a similarly diffuse charge is required in the interlayer in order to balance the diffuse charge on the clay surface. In practice this means a hydrated cation is present where the layers of water surrounding the cation act to diffuse the charge present. Consequently, the charge distribution of the middlings is indicative of a clay that would trap more water than the clay in the primary froth. The tetrahedral charge on the primary froth, on the other hand, is indicative of a clay that is closer to pure illite where the charge can be balanced by a cation that is not heavily hydrated. The localized charge could also be balanced by negatively charged functional groups present in the bitumen. In fact, the presence of a few localized charges, combined with relatively large expanses of neutral surfaces, is ideal for the interaction with large organic molecules having polar and non-polar segments, as is the case with some of the organic molecules present in the bitumen.

The most interesting difference between the clay size fraction of the middlings and that of the froth is the amount of iron in the froth stream. Iron accounts for 15 wt% of the elements detected in the clay size fraction of the froth. Some of this iron appears to be present in the form of iron oxide-hydroxides which are not detected by XRD. Furthermore, iron is found associated with many of the clay mineral particles in the TEM. The exact nature of the iron associated with the clay minerals is unknown. In some instances, it is clear that there are discrete dots on the surface of the clay minerals that are rich in iron; in other cases the clay surface appears to be completely uniform indicating that the iron is structural. Kessick (1979) reported the presence of tightly bound organic matter complexed with iron (III) on the surface of clay minerals in the oil sands. He believed that this complexed organic matter provided a critical link between the clay particles and the bitumen. This is particularly interesting in light of the large amounts of residual organics found in the primary froth clays. It is quite possible that the iron is playing some role in affiliating the clay surfaces with the organics – whether humic acids or residual bitumen.

CONCLUSIONS

Several interesting conclusions can be drawn from the TEM analysis shown here. Firstly, the thickness distribution of the particles observed in the primary froth reveals a bimodal distribution with one set of particles slightly thicker than the particles found in the middlings and one set of particles slightly thinner, which may explain the asymmetry in the XRD pattern upon solvation with ethylene glycol. The potential association of iron with the interlayer of the illite-smectite may also contribute to this asymmetry.

Secondly, the middlings contain the largest concentration of illite–smectite in all streams. As well, the middlings clays appear to have a larger basal surface area and a smaller thickness, on average, than the particles present in the other streams. These features indicate the middlings

clay will be more active and have higher rheological strengths.

Finally, the charge distribution of the middlings clays is consistent with a clay that would capture a large quantity of water, whereas the charge distribution in the primary froth is consistent with a clay that would strongly interact with organic molecules having some polar functional groups.

REFERENCES

Brenner, H. (1974). Rheology of a dilute suspension of axisymmetric Brownian particles, International Journal of Multiphase Flow, 1, 195-341.

Elsass F., Beaumont A., Pernes M., Jaunet A.-M. & Tessier D. (1998) Changes in layer organization of Na- and Ca-exchanged smectite materials during solvent exchanges for embedment in resin. Canadian Mineralogist. 36, 1475-1483.

Johnston, C. (Speaker). (2008, May 1¬2). Surface chemistry of clay minerals [Presentation]. CONRAD-Clay workshop. Calgary, AB.

Kaminsky, H.A.W., Etsell, T. H., Ivey, D.G., & Omotoso, O. (2006). Fundamental Particle Size of Clay Minerals in Athabasca Oil Sands Tailings. Clay Science 12 (supplement 2), 217–222

Kaminsky, H.A.W., Etsell, T.H., Ivey, D.G., & Omotoso, O. (2008). Distribution of clay minerals in the process streams produced by the extraction of bitumen from Athabasca oil sands. Canadian Journal of Chemical Engineering, in press.

Kessick, M.A., (1979). Structure and properties of oil sands and clay tailings. Journal of Canadian Petroleum Technology, 18 (1), 49–52.

Laird, David. (1994). Evaluation of the structural formula and alkylammonium methods of determining layer charge. In A.R. Mermut (Ed), CMS Workshop lectures, volume 6, Layer Charge Characteristics of 2:1 silicate clay minerals. Colorado, USA: Clay Minerals Society.

Liendo, J. (2005). Fundamental study on the role of fines in upgrading [M.Sc. Thesis], Edmonton, AB: University of Alberta.

Moore, D. M. & Reynolds, J. R. C. (1997). X-ray diffraction and the identification and analysis of clay minerals. Oxford, UK: Oxford University Press.

Środoń. J., Andreoli, C., Elsass, F. & Robert M. (1990).Direct high-resolution transmission electron microscopic measurement of expandability of mixed-layer illite/smectite in bentonite rocks. Clays and Clay Minerals, **38**, 373-379.

Syncrude Research, (1979). Determination of bitumen, water and solids content of oil sand, reject and slurry samples (Classical). Method 2.7. Syncrude analytical methods for oil sand and bitumen processing. Syncrude Canada Limited.

Tessier D. (1984) Étude experimentale de l'organisation des mate´riaux argileux. [PhD Thesis], Paris, France: University of Paris VII.

Wallace, D., Tipman, R., Komishke, B., Wallwork, V., & Perkins, E. (2004). Fines/water interactions and consequences of the presence of degraded illite on oil sands extractability. The Canadian Journal of Chemical Engineering, 82, 667–677.

Wang, N., & Mikula, R.J., (2002). Small scale simulation of pipeline or stirred tank conditioning of oil sands: temperature and mechanical energy. Journal of Canadian Petroleum Technology 41 (1), 8–10.

Ward, D. & Brady, P. (1998). Effect of Al and Organic Acids on the Surface Chemistry of Kaolinite. Clays and Clay Minerals, 46, 453-465.

Zbik, M. (2006). Micro-structural explanation for differences in gelation properties of kaolinites from Birdwood (S. Australia) and Georgia (U.S.A.).Clay Science, 12 (Supplement 2), 31–36

TAILINGS SEGREGATION FUNDAMENTALS FROM FLOW BEHAVIOR PERSPECTIVE

Yetimgeta Mihiretu[1], Rick Chalaturnyk[2], J.Don Scott[2]
1 Energy Resources Conservation Board, Fort McMurray, Alberta, Canada
2 University of Alberta, Edmonton, Alberta, Canada

ABSTRACT

Segregation has been a major challenge in tailings management. Studies have been made to understand the fundamental mechanics involved in the segregation process. Rheological tests were used to characterize flow behaviour of the tailings material. Surrogate materials and representative tailings samples were used in the experimental program. Comparison of flow characteristics of the tailings material with that of the surrogate materials was presented. The surrogate materials were found representative enough to characterize the physical processes. Rheological characterization data were used to explain the fundamental physics of segregation in standpipes. It was demonstrated that segregation was affected by grain size distribution, slurry solid content and rheological properties of the fines-water matrix. It was postulated that rheological properties can predict the segregation potential of tailings slurry. Recommendations for further study are presented.

INTRODUCTION

Tailings disposal commonly involves a mixed deposition of solids and liquid phases in a slurry form. The discharging scheme involves tailings transportation and then deposition into a storage facility. The most common methods of tailings disposal are conventional tailing disposal (single point discharge or spigot discharge), thickened tailings (paste), and dry stacking. It is not in the scope of this paper to discuss details about the different types of tailings disposal methods. The emphasis here is the conventional tailing disposal which is commonly used in the oil sands industry.

The most common conventional tailings deposition methods of hydraulic fill construction are: (1) spigotting and single point discharge, (2) cycloning, and (3) cell construction. Details of these methods are discussed in the literature (Morgenstern and Scott 1999). The hydraulic fill process results in a segregating type of tailings where coarse grained particles settle out and form a beach profile while the fine and slow settling particles flow into the pond as thin fluid fine tailings. These thin fluid fine tailings settle and consolidate through time to a complex slurry form commonly called mature fine tailings. The current volume of MFT impounded in the tailings ponds is estimated to be more than 700Mm^3 and the projected volume could reach to 10Bm^3 at the end of mining with the current trend of oil sands processing.

Tailings segregation results in grain size distribution down the beach and a variability in permeability. Grain size distribution is the most fundamental property of the tailings that controls the basic properties such as permeability and rheology. In tailings studies, it is the grain size distribution variation that is prevalent and segregation is defined as a tendency for certain sizes to preferentially collect in one or another physical zone.

This large volume of tailings presents a major environmental concern and necessitates the application of environmentally sustainable disposal methods (Fine Tailings Fundamentals Consortium 1995). At present, environmental regulations are getting more and more stringent.

Another concern with conventional tailings disposal is the resulting loose deposit formation which is highly susceptible to liquefaction when subject to high static stress (accumulating self weight) or load or dynamic stress induced by earth tremors (Robinsky 1999). Moreover, stratification of beach deposited tailings is highly anisotropic and adversely oriented resulting in undesirable drainage path conditions.

The MFT transforms through time to a very stable gel form that is also very poor in self-weight consolidation (dewatering) (Carrier, Scott et al. 1987), (Eckert, Masliyah et al. 1996) posing a major challenge to the closure and reclamation plan of the mine operators.

The waste material from processing occurs mostly in the form of slurry. Disposal of these materials

requires construction of large impoundments. The disadvantage of such impoundments includes deep burial of potential ore bodies, high cost of construction and maintenance of the dam, slow rate of consolidation of the fines and lack of environmental appeal (Scott and Cymerman 1984).

Different research efforts have been undertaken by the industry and research institutions to understand the tailing properties and to produce a tailing material with favorable qualities for closure and reclamation. The mixing of coarse and fine tailings with a coagulent to form nonsegregating tailings, injection of flocculants, introduction of new tailings technologies, and improved extraction processes to reduce the formation of fines are some technologies currently used and/or under active research.

The role of geotechnical engineering in tailings management has been mainly safe storage of the waste materials and the study of short-term and long-term sedimentation and consolidation properties of the fluid fine tailings to meet environmental, closure and reclamation requirements. Therefore, the primary subjects of interest are stability of impoundment structures, depositional methods, sedimentation-consolidation of fluid fine tailings, liquefaction potentials, seepage and closure and reclamation landforms. These challenges in mine waste management are under-recognized and the role of geotechnical engineers to meet these challenges has been under-appreciated (Morgenstern 2001).

The two main factors that affect the segregation mechanism are the grain size distribution and the type of fluid medium. When a solid phase and a liquid phase mix at a certain proportion they form slurry. The slurry is a fluid that can be transported in pipes or open conduits. The rheological behaviour of the slurry is of utmost importance because it reflects the resistance of the slurry to flow.

The rheological properties of slurry characterize its resistance to flow, deformation and structural changes. The fundamental physics of segregation lies in the rheological response of the slurry

The purpose of this paper is to demonstrate the relationship between the rheological characteristics of slurries with the sedimentation/segregation mechanisms within the slurry.

Experimental Methodology

The surrogate materials used for the slurry preparation in the testing program were chosen based on the criteria: material availability, quality and repeatability of the working samples, and the similarity to the real material, in particular tailings from the oil sand industry. Material properties, procedures for sample preparation and testing methodology are provided in detail in Mihiretu, Chalaturnyk and Scott (2005).

For the fine tailings, the actual tailings sample was treated with release water from the tailing ponds to achieve a desired solid content.

For sedimentation tests different size standpipes and a modified standpipe with capacities of 1 litre, 2 litres and 5 litres were used. Details about the modified standpipe test apparatus are given in Mihiretu, Chalaturnyk and Scott (2006).

RESULTS AND DISCUSSION

A viscosity measurement on a representative kaolinite slurry at 30% solids by mass is shown in Figure 1.

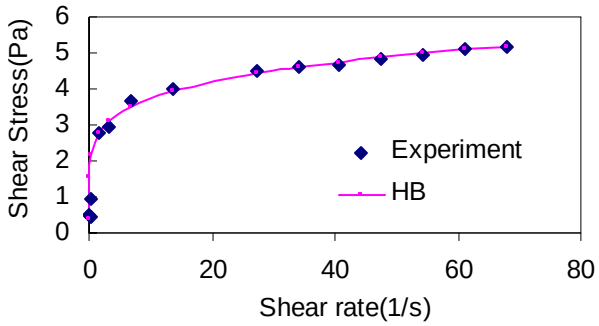

Figure 1. Shear stress versus shear rate diagram for kaolinite slurry at 30% solids content.

A Mature Fine Tailing (MFT) sample at about the same solids content was also tested for comparison. Figure 2 shows the rheogram of the MFT at 30% solids content.

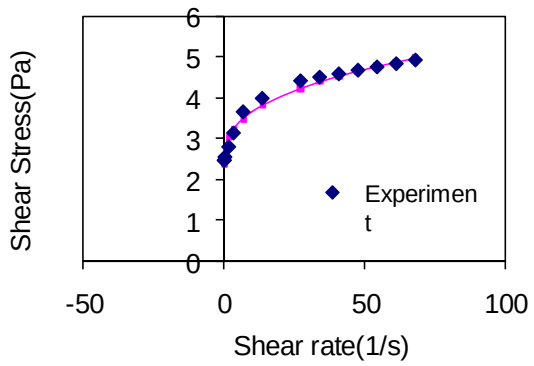

Figure 2. Shear stress versus shear rate diagram for mature fine tailings at a solids content of about 30%.

Figures 1 and 2 were also fitted with a Hershel-Bulkley rheological model which is given by the following equation:

$$\tau = \tau_y + K\,(sr)^n \qquad [1]$$

Where τ_y is the yield stress, K is the Consistency index, sr is the shear rate and n is the flow index. The Hershel-Bulkley parameters are summarized in Table 1.

Table 1 Summary of rheological model parameters.

Sample Type	τ_y	K	n
Kaolinite Slurry	1.0	1.60	0.23
MFT (Suncor)	2.4	5.45	0.37

The representative comparison between the surrogate material (Figure 1) and the tailings material (Figure 2) shows that the surrogate material represents the tailings material very well. Minor differences close to zero shear rate are more or less attributable to test conditions or material difference. The similarity is due to common mineralogy. Fine tailings in the oil sands operation are about 76 % kaolinite.

It is therefore possible to mimic the physical properties of tailings with the help of surrogate kaolinite slurry with little compromise. The visible difference in materials could be the effect of trace bitumen which is about 6 to 9 % by mass of the tailings material.

Direct measurement of yield stress is the quickest method of characterizing slurries. Yield stress provides information about the flow initiation, sand capture, flow profile and depositional conditions.

Figures 3 and 4 respectively show the yield stress measurement of a kaolinite slurry at 30% solids content and of a kaolinite + sil flour (silt sized material) slurry at the same solids content.

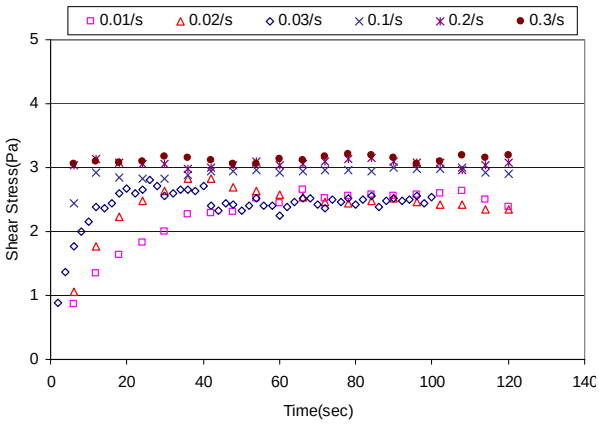

Figure 3. Variation of shear stress with time for kaolinite slurry (30%s) at different rates.

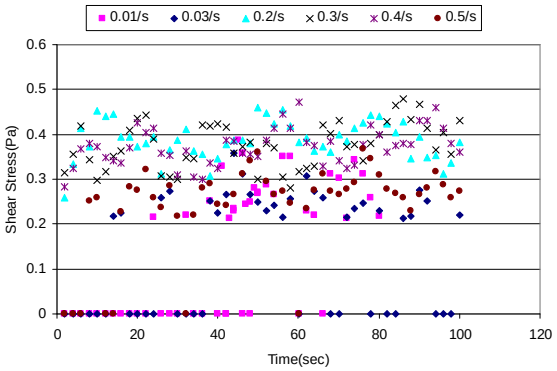

Figure 4. Variation of shear stress with time for kaolinite-sil flour slurry(1:1), 30% s, at different rates.

The different composition of the slurry materials is reflected in the rheological responses shown in Figures 3 and 4. The scatter in data plots in Figure 4 is an indication that the slurry is relatively unstable and has a tendency of settling/segregating as a result of changes in grain-size composition. The addition of a silt size to kaolinite slurry affects the rheological properties or the flow behaviour of the fine clay size slurry. The test duration is a maximum of 120sec (2 minutes).

When a similar test was conducted on slurry made of kaolinite and sand size at 30% solids by weight, the sand particles were observed settling to the bottom of the beaker. As the solid content increased the slurry attained some stable form.

Yield stress measurements thus show whether a slurry is stable or not within a few minutes. When calibrated, it can serve as a quality control for the segregation potential of a slurry with some degree of confidence.

Size composition and sedimentation

In soil mechanics, clay and silt sizes are generally grouped as fine soils. Such a classification was examined in rheological characterization in a separate study (Mihiretu, Chalaturnyk et al. 2005).

The presence of silt size is observed to decrease the yield strength of the fines matrix. As yield stress is more attributed to the ultra fine clay particles, inclusion of larger sizes tend to minimize the bonding of clay particles and consequently reduce the yield strength. The different mixtures of clay and silt at an initial total solids content of 33.3% is shown in Figure 5. The clay and silt size particle composition is varied at 100% clay, 80% clay & 20% silt size, 65% clay & 35% silt size and 50% clay & 50% silt size. Figure 5 clearly shows that despite the same solids content in all tests, the sedimentation results in a segregating concentration profile both in solids content and sand profiles. This kind of phenomena is indirectly observed in the rheological characterization of slurries. Thus we may attribute the sedimentation process to be directly related to the rheological property of the suspension (slurry). There is a clear demonstration that the fine clay size presence quite significantly contributes to the settling properties depending upon the concentration level. In dilute concentration ranges (about FWR < 20) the effect is not that clearly visible. As the fine concentration gets higher the dominant effect of clay particle presence comes into play.

Scott, Dusseault et al. (1985) observed over the range of their study that the addition of sand reduces the apparent viscosity and yield stress. They remarked that the development of gel strength can be beneficial if it is desirable to suspend a granular phase such as sand in the sludge by mixing.

The measurement of yield stress has become a very significant parameter in evaluating the geotechnical suitability of deposits. This application further extends to the proper characterization of the rheological behaviour of soft soils and slurries in tailings management.

The presence of fines (clay size particles) is a very important factor that affects the yield stress of the slurry. At the same time the addition of larger sizes made the slurry flow easily at high solid contents, indicating that slurries with a coarse filler addition is more workable than kaolinite slurry alone.

Another significant contribution of yield stress is the minimization of settling of larger grains suspended in the fine matrix. Scott, Dusseault et al. (1985) have discussed such an application in their study of oil sand sludge. They indicated that the yield stress development is beneficial to suspend a granular sand phase when it is mixed into sludge. They noted that a more profound understanding of the microscopic behaviour of the sludge system is worthy of pursuit.

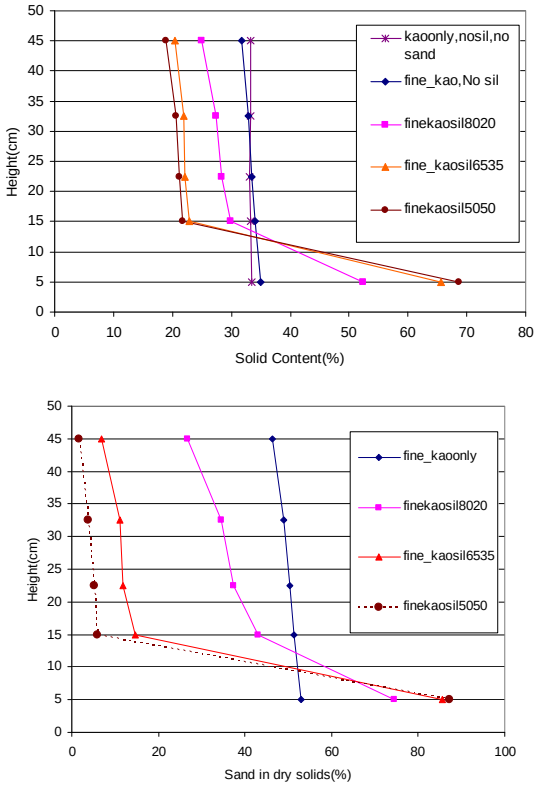

Figure 5. Solid and sand content profiles in different mixtures of clay and silt size composition after 15 minutes in the standpipe.

(Klein, Partridge et al. 1990) stated that yield stress has been attributed to the formation of a structure resulting from interparticle interaction. The strength of these interparticle interactions is related to the interparticle distance. The increased yield stress can therefore be explained by the increased strength of these interactions resulting from smaller distances between the particles at higher solids concentration. The interparticle interaction may be due to hydrodynamic, surface chemical or magnetic forces. Increase in solid concentration is shown to result in reduced distance between particles and an increase in yield stress.

Pore fluid medium effects

The pore fluid medium in tailings is generally water. The chemistry of the water directly influences the fluid-particle and particle-particle interactions which then affect the sedimentation and segregation processes.

The pore water chemistry predominantly affects the fine material namely the clay particles. Figure 6 shows the yield stress response of the thickener underflow fines (less than 45 micron) with the pH adjusted to 12 using $Ca(OH)_2$ and NaOH.

The data plot with CAO treated fine tailings exhibit a distinct yield stress of about 5.8Pa whereas the one treated with NaOH shows no yield stress but rather a dilatant behaviour during shearing. A similar test conducted on kaolinite slurry at 50% solids by mass showed a minimized shear stress with time and somewhat plastic deformation. This phenomenon is more attributable to the clay mineralogy than a difference in solid concentration.

As Zhou, Scales et al. (2001) pointed out the nature and magnitude of forces acting in the flow system and the resulting microstructure are responsible for the complicated rheological responses. They also explained the existence of three kinds of forces which coexist to various degrees in flowing suspensions: hydrodynamic forces, Brownian force and Colloidal force. It is believed that the complex interaction of these forces account for the remarkably different rheological behaviour at higher pH.

The effect of pore water chemistry on the sedimentation process is simply demonstrated with several standpipe tests on 20%s kaolinite slurry prepared with distilled water (pH = 7) and Edmonton City tap water (pH = 7.7± 0.2) and allowed to settle. The process of sedimentation with time is shown in Figure 7.

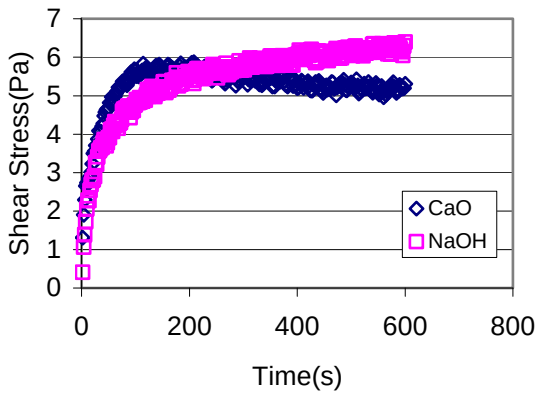

Figure 6. Yield stress measurement of thickener underflow fines (<44 micron) at 35% solids by mass and pH of fluid medium at 12.

The overlap between the 1 litre and 2 litre standpipe data indicates that there is negligible wall effect on the sedimentation process.

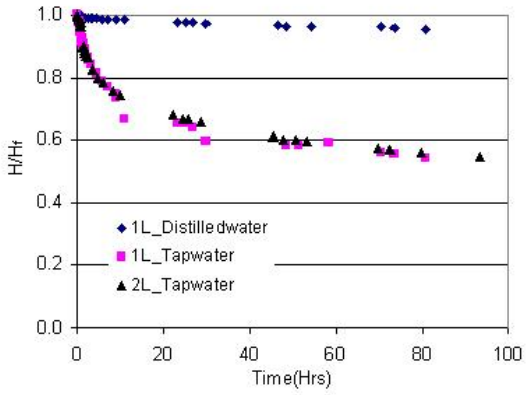

Figure 7. Sedimentation of kaolinite slurry (20%s) prepared with different pore water mediums.

The fast settling rate in the tap water is better explained by the presence of cations mainly Ca^{2+} and Mg^{2+} in the tap water that could bond with clay particles to flocculate and then settle in larger groups.

Yield Stress and Sand Capture Mechanism

Figure 8 shows a free-body diagram of a single sphere suspended in a fluid with yield stress τ_y.

Integration of the tangential force over the surface is given by:

$$F_t = \int_0^{2\pi}\int_0^{\pi} (\tau \sin\theta) R^2 \sin\theta \, d\theta \, d\phi \qquad [2]$$

which can be simplified to

$$F_t = \pi^2 \tau_y R^2 \qquad [3]$$

The buoyant weight of the sphere is given by

$$F_b = \frac{4}{3}\pi R^3 (\rho_s - \rho) g \qquad [4]$$

Where ρ_s is the density of the sphere and ρ is the density of the fluid.

Equating the equations (3) and (4) at equilibrium results in

$$R = \frac{3\pi}{4}\frac{\tau_y}{(\rho_s - \rho)g} \qquad [5]$$

Or in terms of Diameter

$$D = \frac{3\pi}{2}\frac{\tau_y}{(\rho_s - \rho)} \qquad [6]$$

Equation (6) shows the maximum theoretical size of diameter D that can be captured by a slurry with a yield stress of τ_y. A formulation similar to equation (6) has been also developed by Dedegil (1986). This relationship has been tested for kaolinite slurry suspending sand particles. It was observed that the theoretical size capture overestimates the sand size that is captured by the yield stress. Correction factors depending on test conditions were applied (Mihiretu, Chalaturnyk et al. 2006).

For settling of a sphere in a Newtonian Fluid the Reynolds number is indicated by

$$\mathrm{Re}_1 = \frac{\rho d v}{\eta} = \frac{\rho v^2}{\eta \frac{v}{d}} \qquad [7]$$

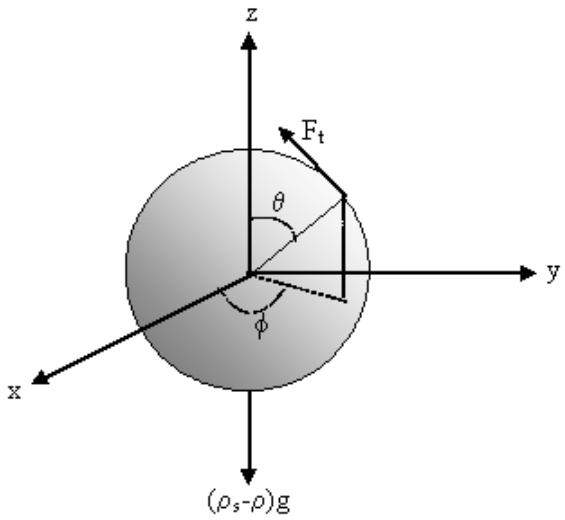

Figure 8. Free body diagram of a sphere of radius R suspended in a fluid.

And the drag coefficient for Newtonian Fluid Is provided as

$$C_{D1} = \frac{4}{3}\frac{(\rho_s - \rho)}{\rho v^2} dg \qquad [8]$$

According to Dedegil (1986), the calculation of the Reynolds number for Bingham fluids should include the yield stress τ_y and the modified Reynolds number (Re_m) is given by (Ansley and Smith 1967):

$$\mathrm{Re}_m = \frac{\rho v^2}{K\tau_y + \eta_B v/d} \qquad [9]$$

Where K is a constant related to yield stress and viscous stress contributions. Dedegil (1986) took K=1.

The drag coefficient is given by

$$C_D = \frac{2}{\rho v^2}\left(\frac{2}{3}(\rho_s - \rho) dg - \pi\tau_y\right) \qquad [10]$$

Equations 7 and 8 versus 9 and 10 were evaluated by Dedegil (1986) with Bingham fluid data from Valentik and Whitmore (1965) and are presented in Figures 9 and 10 respectively.

Figures 9 and 10 demonstrate the significance of yield stress in the proper understanding of the flow condition when the fluid exhibits non-Newtonian flow behavior.

The fine particles in the whole slurry system exhibit particle to particle interaction forming a fine matrix that can support larger size particles. In their study of oil sands sludge, Scott, Dusseault et al. (1985) stated that the sand grains remain suspended due largely to gel strength (yield stress). They presented the rheological characteristics of the material they investigated. From their results it is observed that the material showed pseudo-plastic behaviour.

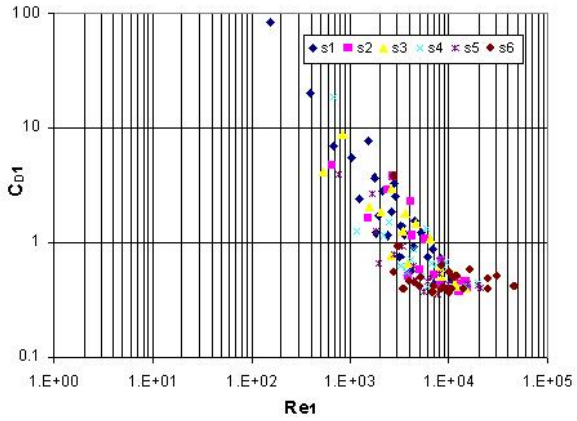

Figure 9. Drag coefficient versus Reynolds number without taking yield stress into account (Data from Dedegil, 1986, Valentik and Whitmore, 1965)

The significance of understanding the sedimentation and strength characteristics of slurry has also been discussed by Tan, Yong et al. (1990). They observed that at the end of settling, the water content of a slurry is still much higher that the liquid limit (a soil in the soil mechanics sense) and the slurry is still fluid-like. They further noticed that fine slurry exhibited non-Newtonian behaviour with some threshold yield strength. They demonstrated the significance of yield stress by pouring sand on to the surface of sediments and observing retained sand particles. They also emphasized that yield strengths, though small in a conventional soil mechanics sense, are significant in soil treatment.

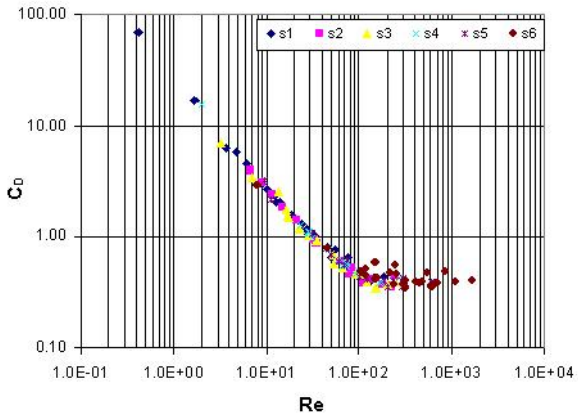

Figure 10. Drag coefficient versus Reynolds number taking yield stress into account (Data from Dedegil, 1986, Valentik and Whitmore, 1965)

The application of the theoretical formulation as given by Equation (6) requires some caution. For example, some experimental results indicate that the theoretical formulation generally gives a larger size. A correction factor in the range of 0.15 to 0.25 needs to be applied for the sand particle size ranges in this experiment

The settling of different coarse grain particles in non-Newtonian fluid is still in the realm of obscurity with challenges from the complex mechanisms involved. Some of the mechanisms that are not yet well explained are the formation of channeling during sedimentation when a solid concentration gets higher, usually above 40% solids. Moreover, it is believed that during deposition or sediment build-up there is complex mechanism of restructuring taking place. The restructuring is responsible for the development of a concentration gradient within the deposit profile and some form of degradation at the interface with fine slurry or release water.

In oil sand tailings, there are traces of bitumen that could contribute to the complexity of the sedimentation/consolidation process. The degree of their influence is worthy of further study.

As an ubiquitous phenomena, segregation also occurs during slurry flow or granular flow in both man-made and natural processes. Detailed discussion in these areas is not in the scope of this paper.

SUMMARY AND CONCLUSIONS

The segregation process during sedimentation has been examined with the perspective of the application of flow behaviour. Rheological characterizations were used to explain the flow behaviour of slurries containing fine and coarse particles.

By use of a surrogate slurry, studies have been made to understand the fundamental mechanics involved in the segregation process. Comparison of flow characteristics of the tailings material with that of the surrogate materials showed that the surrogate materials were representative enough to characterize the physical and chemical processes. It was demonstrated that segregation was affected by grain size distribution, slurry solid content and rheological properties of the fines-water matrix. It was postulated that rheological properties can predict the segregation potential of tailings slurry.

ACKNOWLEDGEMENTS

The writers would like to thank Steve Gamble for the laboratory assistance. Also the writers are grateful to Roxby Hughes with Suncor for the MFT samples and Albian Sands for thickener underflow samples.

REFERENCE

Ansley, R. W. and T. N. Smith (1967). "Motion of Spherical Particles in a Bingham Plastic." AIChE Journal 13(6): 1193-1196.

Carrier, W. D., III, J. D. Scott, et al. (1987). Reclamation of Athabasca Oil Sand Sludge. Geotechnical Practice for Waste Disposal' 87, Ann Arbor, Michigan, ASCE.

Dedegil, M. Y. (1986). Drag Coefficient and Settling Velocity of Particles in non-Newtonian Suspension. International Symposium on Slurry Flows, Anaheim, California, ASME.

Eckert, W. F., J. H. Masliyah, et al. (1996). "Prediction of Sedimentation and Consolidation of Fine Tails." AIChE Journal 42(4): 960-972.

Edwards, S. F. and D. V. Grinev (2003). "Statistical mechanics of granular materials:stress propagation and distribution of contact forces." Granular Matter 4(4): 147-153.

Fine Tailings Fundamentals Consortium, F. (1995). Clark Hot Water Extraction Fine Tailings. Advances in Oil Sand Tailings Research. Edmonton, Alberta Department of Energy, Oil Sands and Research Division. I.

Klein, B., S. J. Partridge, et al. (1990). "Rheology of Unstable Mineral Suspensions." Coal Preparation 8: 123-134.

Mihiretu, Y. T., R. J. Chalaturnyk, et al. (2005). Slurry Characterization Using Yield Stress Measurements. Proc. Canadian Geotechnical Conference, Saskatoon, Saskatchewan.

Mihiretu, Y. T., R. J. Chalaturnyk, et al. (2006). Settling of Sand through Clay Slurry. Proc. Canadian Geotechnical Conference, Vancouver, B.C.

Morgenstern, N. R. (2001). Geotechnics and Mine Waste Management -Update. Safe Tailings Dam Constructions Seminar, Gaellivare, Sweden.

Morgenstern, N. R. and J. D. Scott (1999). Geotechnics of Fine Tailing Management. Professional Development Course on Liquid Solid Separation, Aug. 21-22 1999. Quebec City.

Robinsky, E. I. (1999). Thickened Tailings Disposal in the Mining Industry. Toronto, E.I.Robinsky Associates Limited.

Scott, J. D. and G. J. Cymerman (1984). Prediction of Viable Tailing Disposal Methods. Proceeding of a Symposium: Sedimentation consolidation models: Prediction and Validation., San Fransisco, California, ASCE.

Scott, J. D., M. B. Dusseault, et al. (1985). "Behaviour of the clay/bitumen/water sludge system from oil sands extraction plants." Applied Clay Science 1: 207-218.

Tan, T.-S., K.-Y. Yong, et al. (1990). "Behaviour of Clay Slurry." Soils and Foundations 30(4): 105-118.

Valentik, L. and R. L. Whitmore (1965). "The terminal velocity of spheres in Bingham Plastics." Brit.J.Appl.Phys/ 16: 1197-1203.

Zhou, Z., P. J. Scales, et al. (2001). "Chemical and physical control of the rheology of concentrated metal oxide suspensions." Chemical Engineering Science 56: 2901-2920.

COMPUTATIONAL FLUID DYNAMIC SIMULATION OF STANDPIPE TESTS

Junwen Yang[1], Rick J. Chalaturnyk[2]
1 Energy Resources Conservation Board, Fort McMurray, Alberta, Canada
2 University of Alberta, Edmonton, Alberta, Canada

ABSTRACT

Standpipe tests are widely used in evaluating the sedimentation, segregation and even consolidation properties of the oil sands tailings and other slurry due to their defined boundary conditions. Numerical simulation also was carried out to model the standpipe tests in literature (Burger et al. 2000). In this paper, the application of the computational fluid dynamic (CFD) method in simulating the sedimentation of bidisperse and polydisperse suspension was evaluated. The CFD simulation results were compared with the results from Burger's shock-capturing schemes as well as with experimental results. Then the technique was used to simulate the segregation boundary tests for oil sand tailing slurry with continuous distribution of solid particles. The issues related to conducting computational fluid dynamic simulation on the oil sands tailing are presented.

INTRODUCTION

Evaluation of the sedimentation, segregation, and consolidation properties of oil sands tailings and other slurry was often carried out in the standpipe or column. Large amount of data can be found in literature or reports. Then attempts have been made to predict the settling velocity and volume fraction profile of the solid particles with time using numerical methods. The attempts started from the simplest cases where a single sphere particle settles in an infinite liquid. With increase in the solid particle volume fraction, hindered settling occurs where the settlement of one particle is influenced by the presence of other particles. The complexity of the prediction further escalated with the increasing number of size groups for the solid particles and with increasing Reynolds number.

Analytical solution for the settling velocity of a particle in an infinite liquid was given by Stokes Law (1851). Since then various empirical formulas have been developed to relate the settling velocity of the particle to their sizes in which Reynolds number ranges from laminar flow, transitional flow to turbulent flow (Schiller et al., 1933; Rubey, 1933; Dallavalle, 1943; Dallavalle, 1948; Lapple, 1951; Torobin, 1959; Olson, 1961). Based on the assumption that the local settling velocity or solid phase velocity is a function only of the local volume fraction, Kynch (1952) developed the theory for one-dimensional settlement of monosized spheres under the influence of gravity. Burger et al (2000) extended the theory to polydisperse suspension and solved the non-linear conservation law equations using shock-capturing numerical schemes. Xue and Sun (2002) presented a model to model the sedimentation of polydisperse agarose beads with a broad particle size distribution. Later, Burger et al. (2008) further extended the theory to the centrifugal settling of a suspension with continuous distribution of sizes. None of them used computational fluid dynamics (CFD) method to simulate the settling of the suspension with polysized solid particles.

In this paper, computational fluid dynamics (CFD) method is applied to simulate the settling of suspension with two and four sizes of solid particles first. The intention is to evaluate the feasibility of CFD method to model the sedimentation of polydisperse suspension. Then sensitivity analysis is conducted to evaluate the influence of various parameters on the settling behavior of the oil sands tailing suspension with continuous size distribution. The CFD packages used in this paper are CFX 11 (Ansys, 2006), FLUENT 6.2 (Fluent, 2005) and open-source CFD code MFIX (Syamlal et al. 1994).

VERIFICATION OF SEDIMENTATION EXPERIMENTAL DATA USING CFD METHOD

Binary Solids Suspension

The data used in this verification was reported by Schneider et al. (1985) and was used by Burger et al. (2000). The material used in the experiment was glass beads with density of 2790 kg/m^3. The particles with diameters d_1= 0.496 mm and

d_2 = 0.125 mm, respectively were settled in a settling column of height L = 0.3 m. The density and viscosity of the fluid are 1208 kg/m^3 and 0.02416 kg/m.s, respectively. The initial solid volume fractions for coarse and fine particles are 0.2 and 0.05, respectively.

Both MFIX and FLUENT were used to simulate the experiment. The simulation results were shown in Figure 1 along with Burger's simulation results. Reasonable agreement between MFIX simulation, FLUENT simulation and Burger's simulation was shown in the figure.

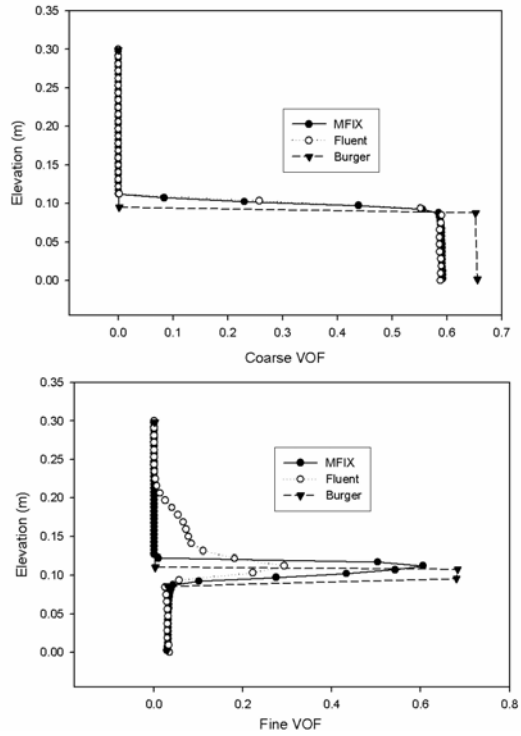

Figure 1. Comparison of fine particle volume fraction at time = 599.7 seconds

CFD Modeling the Settling of Suspension with Particles of Four Different Sizes

Greenspan and Ungarish (1982) compared their theoretical results for a mixture of four size species with the experimental data cited by Smith (1966) and found that the results agree closely with the experimental data. Burger et al (2000) applied the shock-tracking techniques to simulate the experiment in Greenspan and Ungarish's paper (1982). Their simulation results showed a very close agreement with the experiment data cited by Greenspan and Ungarish (1982), therefore by Smith (1966).

The four particle species have the same density of 2790 kg/m^3 with sizes of 0.496 mm, 0.3968 mm, 0.2976 mm and 0.1984 mm respectively. The density of the liquid is 1208 kg/m^3 and the viscosity

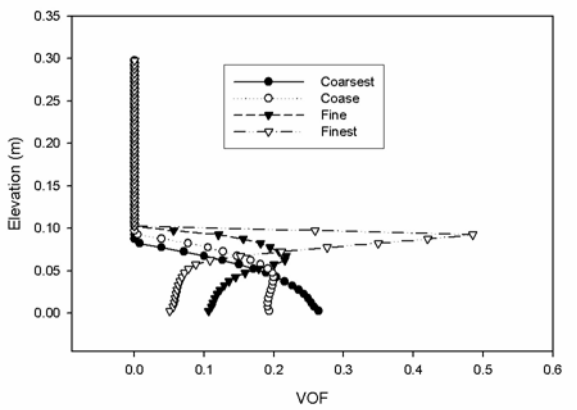

Figure 2. VOF Profile for Four Particle Sizes at Time = 615.07s (MFIX)

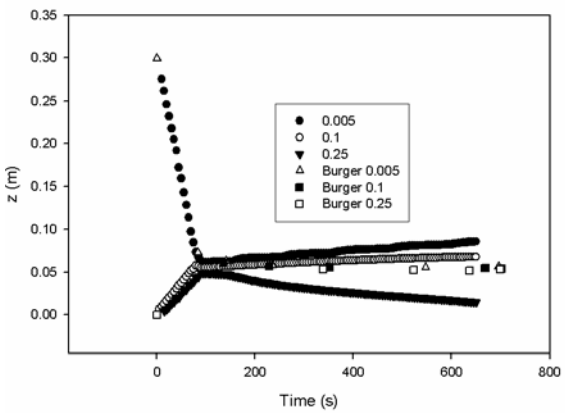

Figure 3. Comparison of Shock Wave Line for Heaviest Particles at Time = 615.07s (MFIX and Burger's)

is 0.02416 kg/m.s. The initial volume fractions of all the four species are 0.05. The sedimentation of particles with four particle sizes was first simulated using MFIX. The volume fraction profiles at 615 s were shown in Figure 2. The figure showed that segregation occurred for the polydisperse suspension with the largest particles settling at the bottom and the smallest particles at the top of the solid sedimentation. The shock wave line generated from the MFIX simulation results were compared with Burger's (2000) in Figure 4 – Figure 6. It can be seen that close agreement was achieved between those two simulations.

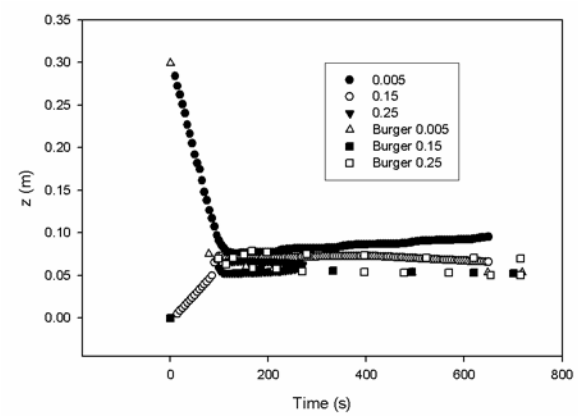

Figure 4. Comparison of Shock Wave Line for Heavy Particles at Time = 615.07s (MFIX and Burger's)

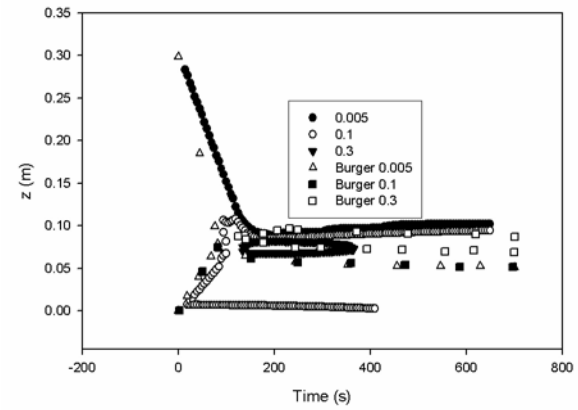

Figure 5. Comparison of Shock Wave Line for Light Particles at Time = 615.07s (MFIX and Burger's)

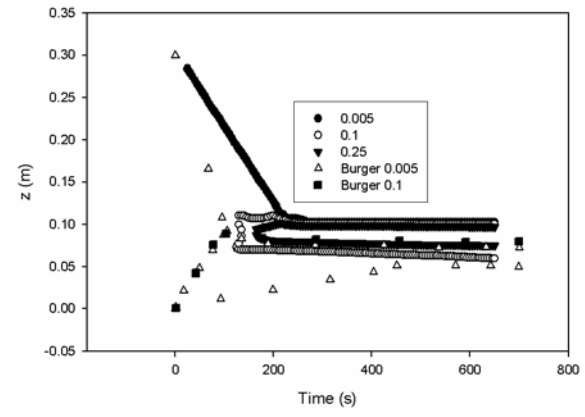

Figure 6. Comparison of Shock Wave Line for Lightest Particles at Time = 615.07s (MFIX and Burger's)

The same sedimentation experiment mentioned above was modeled in Fluent 6.2. For each solid phase, Gidaspow Model is selected for granular viscosity, Lun-et-al Model for granular bulk viscosity, Schaffer Model for frictional viscosity, Based-ktgf for frictional pressure, algebraic granular temperature, Lun-et-al Model for solids pressure and radial distribution function. A constant internal friction angle of 30 degree was assigned. Friction packing limit and packing limit are 0.61 and 0.63 respectively. The drag models for solid-liquid and solid-solid were Gidaspow and Syamlal-Obrein-Symmetry model respectively.

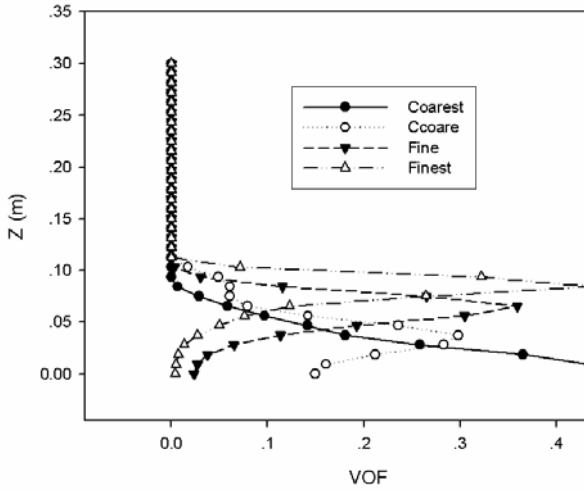

Figure 7. VOF Profile for Four Particle Sizes at Time = 750s (Fluent)

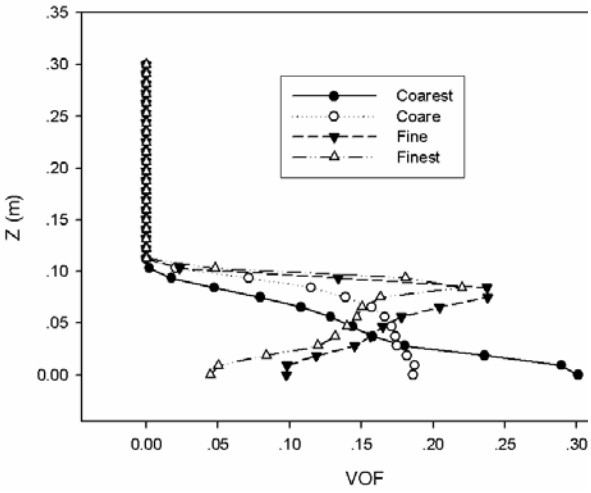

Figure 8. VOF Profile for Four Particle Sizes at Time = 1200s (Fluent)

The volume fraction of four particles at time of 750 and 1200 s were shown in Figure 7 and Figure 8. From these figures it can be shown that the coarsest particles settle first at the bottom, followed by the coarse particles. There are no apparent changes in VOF profiles for the coarsest and

coarse particles from 750 s to 1200 s. However, most fine particles settle on the top of other particles with time.

The simulation of polydisperse of four particles with varied particle size using MFIX and Fluent demonstrates that the settling of the polydisperse suspensions can be modeled using CFD method.

CFD SIMULATION OF SETTLING OF OIL SANDS TAILINGS SLURRY

Segregation Boundary Tests

Batch standpipe tests were conducted on tailing slurry with a wide range of solid content (i.e. percent of solid mass) and fine content (i.e. percent of fine mass in solid components), where 44 micron is selected as the cutoff between fine and coarse particles. After the slurry was uniformly mixed in mixer then placed into standpipe, an interface between upper clear water and lower suspension develops. The variation of the elevation of the interface with elapsed time was recorded and was used to characterize the properties of the tailing slurry. The observation was ended when the elevation of the interface changed extremely slowly. Then the profiles of the solid content and fine content were obtained by measuring the mass fraction of water, sand and fine. The fine capture is calculated based on the formula proposed by (Chalaturnyk and Scott, 2001) and the slurry is classified as non-segregating if the fine capture exceeds 95%.

In order to determine the segregation boundary of the oil sands tailing slurry, three standpipe tests were conducted on the oil sand tailing with solid and fine content combination shown in the table below. The particle size distribution of the solid particles is shown in Figure 9. It contains 24.8% fine particles and 75.2% coarse particles. The bitumen content was not measured in these experiments. Segregation index for the three CT mixture were also included in the table. It can be seen that SB1 is segregating slurry while SB3 is non-segregating slurry.

Simulation of Segregation Boundary Tests Using CFD Method

SB1 and SB3 are chosen to verify the Euler-Euler Multiphase model in CFX 11, Fluent 6.2 and MFIX as SB1 is segregating matrix and SB3 is non-segregating. Euler-Euler multiphase simulation was conducted for the dense solid-liquid flow. The tailing slurry used in the experiments SB1 and SB3 was assumed to be composed of water, coarse and fine particles. The flow in viscous regime was evaluated using kinetic theory describing the flow of smooth, slightly inelastic, spherical particles. The friction between solid particles which occurs in the plastic regime was evaluated based on the concepts from critical soil mechanics.

Table 1. Segregation index

Test #	Initial Solids Content (%)	Initial Fine Content (%)	Sands Fine Ratio (SFR)	Calculated Segregation Index
SB1	45	25	1.8	44.5
SB2	55	25	2.2	8.2
SB3	65	25	2.6	1.6

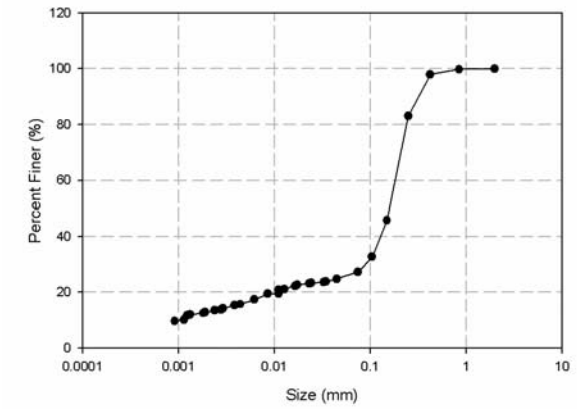

Figure 9. Size Distribution of Solid Particles Used in Segregation Tests

Simulation of SB1 and SB3 Using CFX 10

CFX 10 was first used to simulate SB1 and SB3 tests using default settings. The densities of the liquid, coarse particles and fine particles are 1000, 2700 and 2700 kg/m^3 respectively. The diameters are assumed to be 120 micron for coarse particles and 20 micron for fine particles. The change of interface between suspension and clear water in the simulation result was compared with that in experiment (Figure 10 and Figure 11). Those two figures showed that slower settling occurs in SB3 compared with SB1 while those simulation results are not in close agreement with the experimental results.

Sensitivity Analysis Using FLUENT

Impacts of the following factors on the sedimentation of SB1 and SB3 were evaluated: granular temperature model, solid pressure model, solid bulk and frictional viscosity model, packed bed settings, granular viscosity, solid friction angle, particle diameter and density.

Sixteen tests were conducted for SB1 using Fluent. In all the cases, simulation time of 30 seconds was reached. The influence of some of the parameters on the simulated solid and fine contents was shown in Figure 12 to Figure 19.

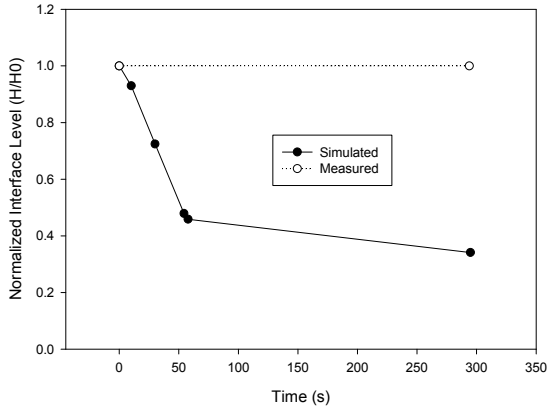

Figure 10. Comparison of Interface Development for SB1

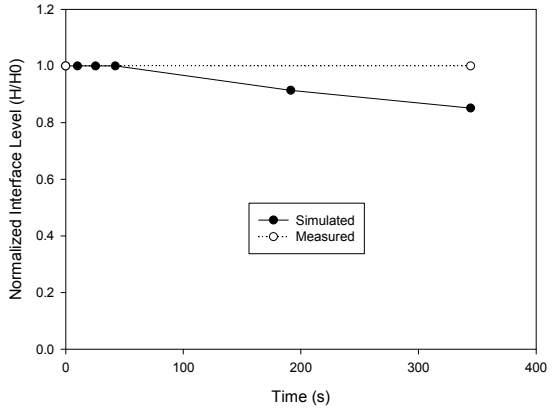

Figure 11. Comparison of Interface Development for SB3

Figure 12 showed the effects of granular temperature model and solid pressure on the solid and fine contents at the time of 30s. The influence of bulk viscosity was shown in Figure 13. It can be seen from these figures that selecting granular temperature model, solid pressure model and bulk viscosity have very limited effects on the solid and fine content profile at the time of 30s.

Figure 14 showed the significant influence of frictional viscosity on the solid and fine content profile at the time of 30s. This is expected as the frictional viscosity will dominate among all the viscosities when the volume fraction for solid phases increases, especially when the solid volume fraction exceeds 0.5.

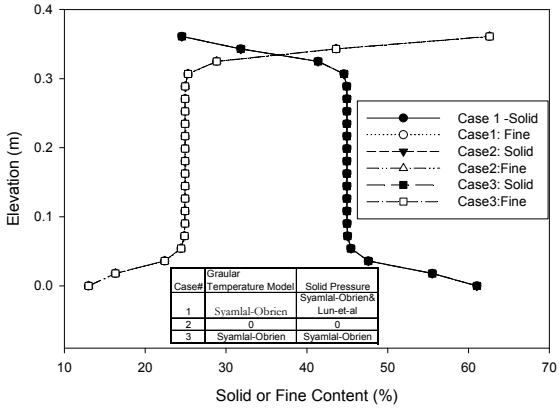

Figure 12. Effects of granular temperature model and solid pressure on solid and fine contents

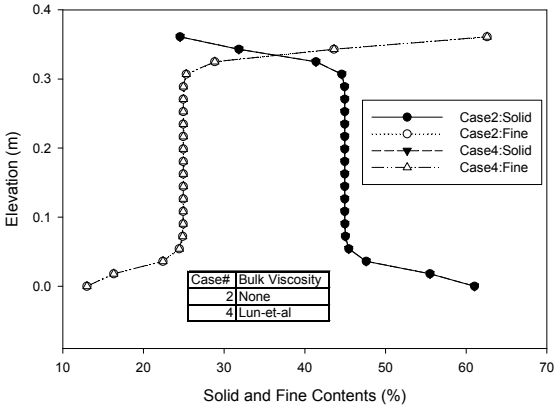

Figure 13. Effects of bulk viscosity on solid and fine contents

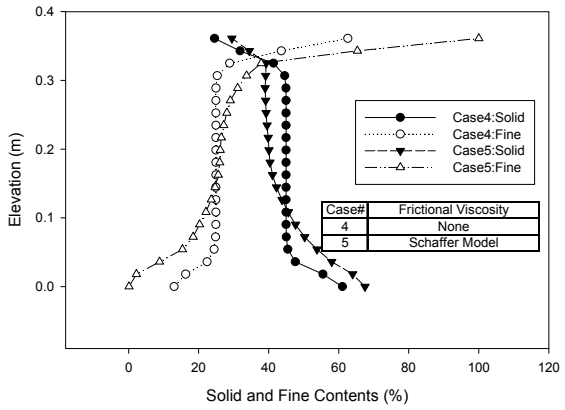

Figure 14. Effects of frictional viscosity on solid and fine contents

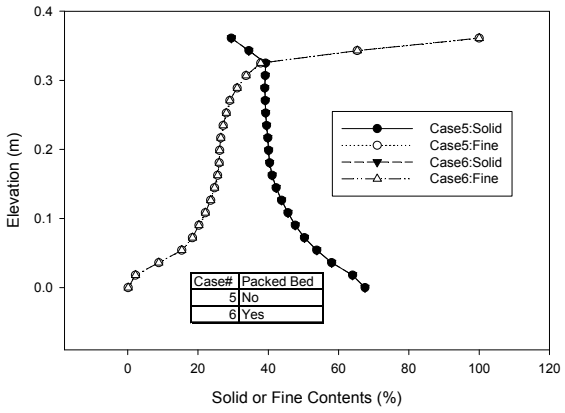

Figure 15. Effects of Packed Bed on solid and fine contents

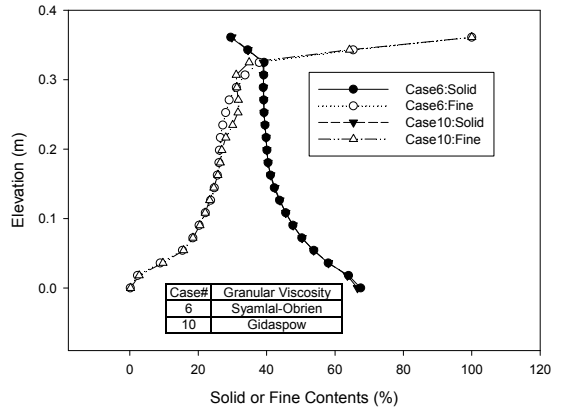

Figure 16. Effects of granular viscosity on solid and fine contents

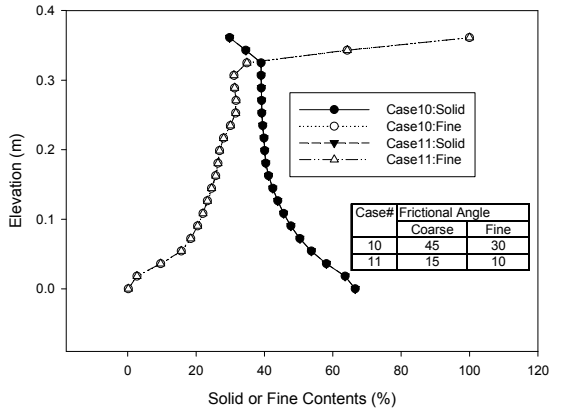

Figure 17. Effects of frictional angle on solid and fine contents

The effects of Packed Bed were shown in Figure 15. The figure demonstrated that whether choosing Packed Bed does not change the solid and fine content at the final simulation stage. Figure 16 showed the effects of choosing granular viscosity model on the solid and fine content profile.

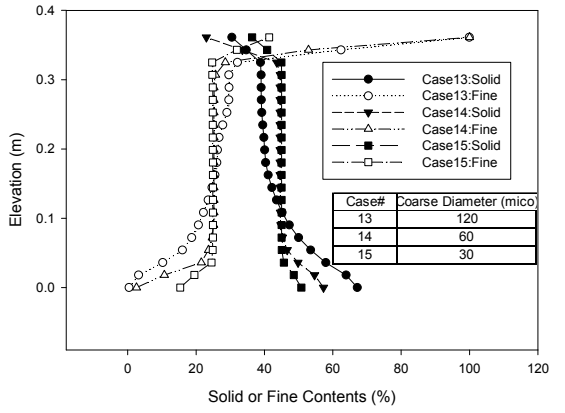

Figure 18. Effects of particle diameter on solid and fine contents

Figure 17 showed the effects of internal angle of friction for solid phases. It was seen that granular viscosity model has certain influence and frictional angle does not affect the solid and fine contents at the time of 30s.

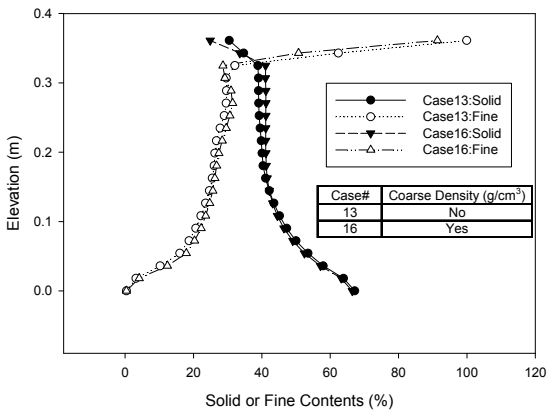

Figure 19. Effects of particle density on solid and fine contents.

The effects of diameter and density for coarse particles on the final solid and fine contents were shown in Figure 18 and Figure 19. It can be seen that settling rate was reduced as the coarse particle diameter and density decrease.

Effects of Particle Size Division for Fine and Coarse Particles

In the above simulations, 44 micron was chose to divide fine and coarse particles. Division of solid particles in fine and coarse particles is in agreement with industry standard and also simplifies the CFD simulation. Theoretically, the mixture was composed of infinite number of sizes of particle to form a continuous distribution. However, the number of particle groups allowed in Euler-Euler simulation in Fluent, CFX and MFIX is limited by the memory of the machine as well as the solution schemes. Therefore, the continuous distribution of solid particles was divided into two groups with each group represented by an effective diameter.

Loth et al. (2004) studied the effective diameter for the two-phase flow in which the gravity and drag force determine the particle motion. They found that the volume-width diameter shown in the following equation is the effective diameter for the flow where particle Reynolds number is much less than 1:

$$D_{31}^2 = \frac{\int_0^\infty f(D)D^3 dD}{\int_0^\infty f(D)DdD} \quad [1]$$

Where *f(D)* is the number Probability Distribution Function (PDF) and *D* is the diameter of the particles. The number Probability Distribution Function is the Probability Distribution Function in term of the number of particles within certain size range as shown in the following equation:

$$n_i = \frac{m_i}{\rho_{di}\frac{\pi D_i^3}{6}} \quad [2]$$

Where m_i is the mass fraction of particles in Group *i*, ρ_{di} the dry density of the particles which is assumed to be 2700 Kg/m^3, D_i the diameter of particles and n_i the number of the particles in Group i. The number PDF can be calculated by the following equation:

$$f(D_i) = \frac{n_i}{\sum_{i=1}^{N} n_i} \quad [3]$$

Where N is the number of particle group.

As stated above, several assumptions were made in calculating the probability distribution of particle numbers. The assumption involved in particle shape is prone to errors. Moreover, it is more convenient to determine the fraction of mass for certain sizes of particles than to determine the number distribution in practice. Therefore, the mass Probability Distribution Function was used to calculate the effective particle size D31 for fine and coarse particles, as shown in the following equation:

$$f(D_i) = \frac{m_i}{\sum_{i=1}^{N} m_i} \quad [4]$$

Where m_i is mass fraction of particles in Group i. The number of the particles was calculated based on the assumption that the particles in each particle group are spherical and have uniform size. Here the number Probability Distribution Function was changed to the mass Probability Distribution Function.

Figure 20 and Figure 21 showed the change in the solid and fine content profiles with various coarse-fine divisions. Greater variation in solid content for the simulation in the upper 20 cm of the standpipe domain can be observed for the simulation using the coarse-fine division of 44 micron than those using 22 and 5.5 micron as a division which is confirmed in Figure 20 and Figure 21.

The influence of different division on modeling the non-segregating slurry SB3 was shown in Figure 22 and Figure 23. It can be observed that solid and fine content remain almost constant for the simulation using 5.5 micron as a coarse-fine division.

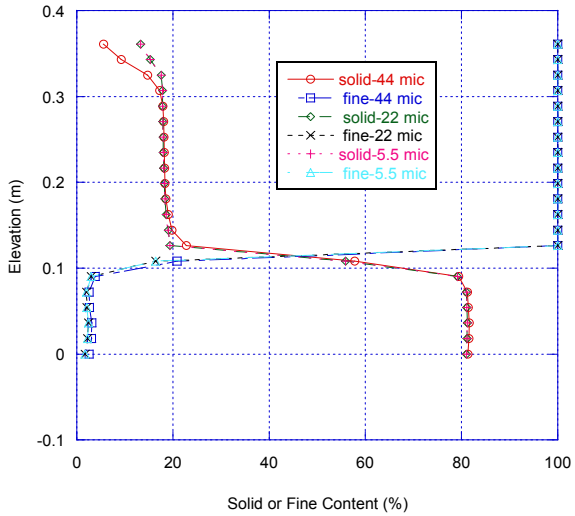

Figure 20. Effects of coarse-fine division on solid and fine content profiles at 200s for SB1. D31 was calculated based on mass PDF.

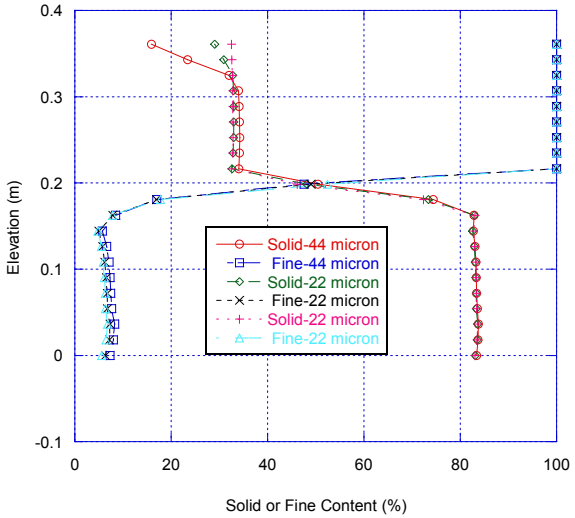

Figure 22. Effects of coarse-fine division on the solid and fine content profiles at 200s for simulation of SB3. D31 was calculated based on mass PDF.

PROPOSED SOLUTION

Segregation Slope

Apparently, above simulations using Fluent and CFX are not able to model the real-time sedimentation process for both segregating slurry SB1 and non-segregating slurry SB3. The non-segregating slurry was predicted to be segregating within a short time.

Gera et al. (2004) reviewed the literature on the segregation prediction. They found that the prediction in the models by Goldschmidt et al. (2001) and Chen et al. (2002) is contrary to experiment results which show that segregation will not occur at low velocities for the binary system. In order to make the model to predict no segregation at low velocities, they added a new term into the particle-particle drag coefficient. The modified particle-particle drag coefficient is shown in the following equation:

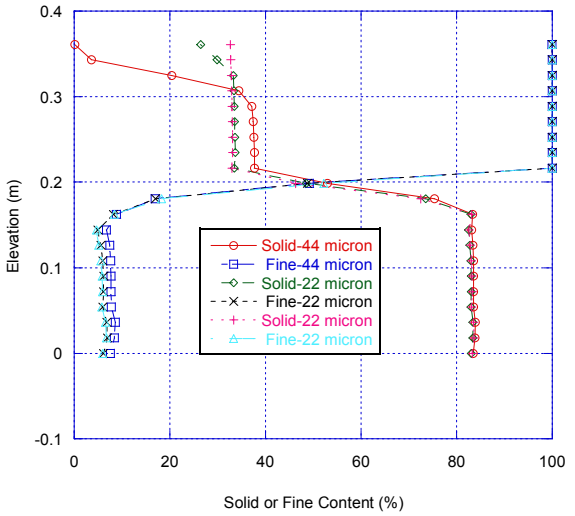

Figure 23. Effects of coarse-fine division on the solid and fine content profiles at 2000s for simulation of SB3. D31 was calculated based on mass PDF.

$$F_{ml} = \frac{3(1+e_{lm})(\pi/2 + C_{flm}\pi^2/8)\varepsilon_l\rho_l\varepsilon_m\rho_m(d_{pl}+d_{pm})^2 g_{0,lm}|\vec{v}_l - \vec{v}_m|}{2\pi(\rho_l d_{pl}^3 + \rho_m d_{pm}^3)} + C_1 P^* \quad [5]$$

Where F_{ml} is the drag coefficient. In the first term, e_{ml} and C_{fml} are the coefficient of restitution and coefficient of friction, respectively, between l^{th} and m^{th} granular-phase particles; g_{0ml} is the radial distribution function at contact, ε, ρ, d and $\vec{v}$ are the fraction of volume, density, diameter and velocity, respectively. The subscripts l and m indicates the variables for l^{th} and m^{th} granular-phase particles respectively. In the second term which is the added term by the author, P^* is the solids pressure. The authors showed both non-segregation at lower velocity and the rate of segregation at intermediate velocity were correctly predicted by the modified model. The performance of this modified model will be evaluated for segregating (SB1) and non-segregating oil sand tailing slurry (SB3).

The standpipe was assumed to be 40 cm high with a diameter of 4 cm. Cylindrical symmetricalness was assumed, thus only length of the domain in x (radial) direction was 2.0 cm. Two-dimensional simulations were conducted for all the cases by assigning the number of grid in z (Azimuth) direction as 1. With exception of the case Sb1-Run6 in which 4x40x1 grid was used, a grid of 8x80x1 uniform grid was used for all the other simulation cases. The parameters of Segregation Slope were varied from 0 to 0.9 for the simulation of segregating slurry, SB1. As for the non-segregating slurry, SB3, the influence of the segregation slope and the solid viscosity models on the volume fraction of coarse and fine particles were verified.

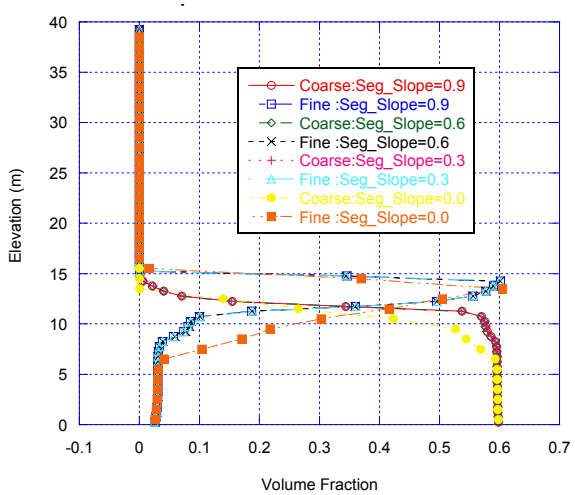

Figure 24. Effects of Segregation Slope on Coarse and Fine Volume Fraction for SB1 at Time of 1000s

The effect of segregation slope on the volume fraction profiles of SB1 at 1000 s is shown in Figure 24. The comparison indicates that its effects on the profiles at 1000 seconds seems to be relatively significant as indicated by the discrepancy between the curve representing the segregation slope of zero with those of non-zeros. The influence of the segregation slope on the volume fraction profile of SB3 is shown in Figure 25. It seems that the influence is insignificant as almost the same curves were obtained for different segregation slopes.

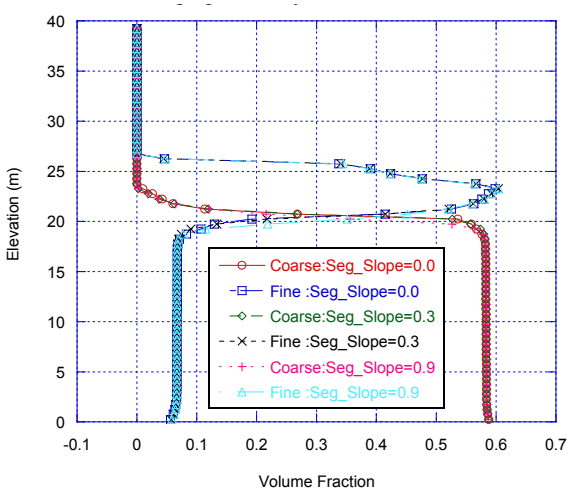

Figure 25. Effects of Segregation Slope on Coarse and Fine Volume Fraction for SB3 at Time of 1000s.

Two-Phase Simulation

Above simulations demonstrated that some interactions between solid and solid as well as between solid and liquid were not captured in the current models. In order to circumvent the considerations of the clay-clay and clay-water interactions, clay and water can be considered as a single phase with varying viscosity and density, which can reflect the distribution of clay particles in water due to segregation or non-segregation. For non-segregation mixture, the clay volume fraction almost remains constant, which simplify the simulation.

The slurry viscosity was measured using a Brookfield DV-II+ Programmable Viscometer. Cylindrical spindles were used for these tests. Logarithmic model in the following form was used to correlate viscosity with shear strain rate:

$$\mu = 10^{(a+b*\log(\dot{\gamma}))} \quad [6]$$

in which μ and $\dot{\gamma}$ are viscosity and shear strain rate respectively, a and b are curve-fitting parameters which are functions of solid content. The parameters can be related to solids content by regression as follows:

$$a = -2.3885 + 0.12102s - 0.0008079s^2 \quad [7]$$

$$b = -0.7666 - 0.002714s \quad [8]$$

where *s* is the solid content of the slurry (%). The simulation result was shown in Figure 26. It can be seen that the sand volume fraction remain almost constant even at time of 2500 seconds.

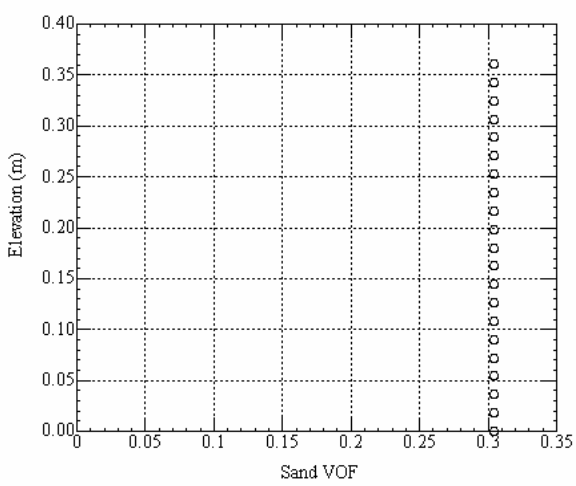

Figure 26. Sand volume fraction at flow time of 2500 s

SUMMARY AND CONCLUSION

CFX 10, FLUENT 6.2 and MFIX were used to model the sedimentation of suspension composed of two or more uniform sizes of solid particles. The simulated volume fraction profiles reasonably agree with those obtained by Burger's using modern shock capturing numerical schemes. Since Burger (2000) compared his simulation results with the results from measurements by Schneider et al. (1985) and claimed that their simulation results agrees with the experiment, it is concluded that the CFD are valid tools to model the sedimentation of the bidersperse and polydisperse suspension.

A serial of sensitivity tests were numerically done to verify the capability of CFX-10, MFIX and FLUENT 6.2 in modeling the sedimentation process of oil sand tailing slurry. Simulation results indicate that all these software packages are not able to model the sedimentation process of the tailing slurry in which the particle sizes have a continuous distribution.

In summary, these CFD packages are able to capture the time sequence of sedimentation process for suspensions with uniform particle sizes while they fail to follow the settling process of continuously distributed solid particles suspended in liquid. Logically, the difference between the former and latter contributes to the discrepancy.

A suspension containing two or four sizes of particles was modeled using CFD successfully by simulating each group of particles as a separate solid (disperse) phase. On the other hand, the continuous distribution of solid particles in oil tailing slurry has to be approximated using bidisperse suspension, which introduced significant error no matter which method was used to calculate the effective particles size for each group.

The ultra-fine solid particles, bitumen and chemistry of the oil tailing slurry make oil sand tailing slurry unique in solid-liquid suspension. Interactions between ultra-fine particles are not accounted in any of these software packages. Therefore, the uniqueness of the oil sand tailing slurry partially resulted in the failure of these packages to capture the extremely slow process of the sedimentation of the tailing slurry.

Compared with segregation, non-segregation behavior of the solid-liquid system brought more challenge in numerical simulation. The interactions between clay and clay as well between clay and water are critical to solution of this problem. One solution to this is to modify the suspending medium viscosity to reflect the influence of the interactions. Considering the clay-water as a single phase can be another way to evade the complexity of the interactions.

ACKNOWLEDGEMENTS

The authors would like to acknowledge the financial and technical support provided by Suncor Energy Ltd. through the Oil Sands Tailings Research Facility.

REFERENCES

ANSYS Inc., 2006. CFX 11 Solver Theory.

Bürger, R. and García, A., 2008. Centrifugal Settling of Polydisperse Suspensions with a Continuous Particle Size Distribution: A Generalized Kinetic Description. Drying Technology, 26:8, pp. 1024 - 1034.

Burger, R., Concha, F., Fjelde, K.K., and Karlsen, K.H. Numerical Simulation of the Settling of Polydisperse Suspensions of Spheres. Powder Technol. 113 (2000), 30-54.

Chen, A., Grace, J.R., Epstein, N. and Lim, C.J., 2002. Steady state dispersion of mono-size, binary and multi-size particles in a liquid fluidized bed classifier. Chem. Eng. Sci. 57, pp. 991-1002.

Dallavalle, J.M., 1943. Micromeritics. Pitman, New York, N.Y.

Dallavalle, J.M., 1948. Micromeritics. Pitman, New York, N.Y., 2nd ed.

Fluent Inc., 2005. Fluent 6.2 User Guide.

Gera, D., Syamlal, M., and O'Brien, T.J., 2004. Hydrodynamics of Particle Segregation in Fluidized Beds. International Journal of Multiphase, 30, pp. 419-428.

Goldschmidt, M.J.V., Kuipers, J.A.M., van Swaiij, W.P.M., 2001. Segregation in dense gas-fluidised beds: validation of multi-fluid continuum model with non-intrusive digital image analysis measurements. In: 10th Engineering Foundation Conference on Fluidization, Beijing, China, May 20–25, pp. 795–802.

Greenspan, H. P. and Ungarish, M., 1982. On Hindered Settling of Particles of Different Sizes. Int. J. Multiphase Flow, 8:6, pp. 587--604.

Kynch, G.J., 1952. A theory of sedimentation. Trans. Farad. Soc., 48, pp.166-176.

Lapple, C.E., 1951. Fluid and Particle Mechanics. University of Delaware Publ., Newark,Del., p284.

Olson, R., 1961. Essentials of Engineering Fluid Mechanics. International Textbook, Scranton, Chapter 11.

Rubey, W.W., 1933. Settling velocities of gravel, sand and silt particles. Am. J. Sci., 225:325.

Smith, T. N., 1966. The sedimentation of particles having a dispersion of sizes. Trans. Inst. Chem. Engrs, 44, pp.153-157.

Syamlal, M., Roger, W., and O'Brien, T.J., 1994. MFIX documentation: theory guide, Technical Note, DOE/METC-94/1004, TIS/DE94000087, National Technical Information Service, Springfield, VA.

Torobin, L.B. and Gauvin, W.H., 1959a. Fundamental aspects of solid-gas flow. Part 1 and 2. Can. J. Chem. Eng., 37: 129-141, 167 - 176.

Xue, B., and Sun, Y., 2003. Modeling of sedimentation of polydisperse spherical beads with a broad size distribution. Chemical Engineering Science, 58 pp.1531 – 1543.

CHARACTERIZATION OF OIL SANDS THICKENED TAILINGS

S. Jeeravipoolvarn[1], J. D. Scott[1] and R. Donahue[1], B. Ozum[2]
1. Department of Civil and Environmental Engineering – University of Alberta, Edmonton, AB, Canada
2. Apex Engineering Inc, Edmonton, AB, Canada

ABSTRACT

Oil sands tailings material is composed of sand, fines, residual bitumen and process water whose properties influence the segregation, sedimentation and consolidation behavior of this material. Tailings properties are determined by the extraction process operating conditions; specifically by the use of additives to alter the *pH* of the ore-water slurry system. These additives control the extent of clay dispersion. Detailed characterization of the tailings is essential to understand the effect of the different extraction processes as well as the settling, consolidation and nonsegregating behavior of the tailings materials. To predict the tailings field behavior, the tailings characterization tests should be performed with similar physical and chemical conditions that are in the extraction process. This paper presents the characterization of the Albian Sands Muskeg River Mine's thickened tailings when the extraction plant was operating in a non-additive process mode. The particle size distribution, pore water chemistry and morphology are emphasized. Dispersed and non-dispersed particle size distribution tests showed considerable differences in the amount of clay size material because of the extent of clay dispersion in the extraction process. Comparisons of scanning electron micrographs of the non-dispersed Albian Sands thickened tailings and the dispersed Clark Hot Water Extraction (CHWE) process tailings also show considerable differences in clay structures. These findings indicate that particle size distribution and water chemistry measurements made under the extraction process conditions can be used as tools to understand and predict the effectiveness of the extraction process and, as well, the tailings geotechnical properties.

INTRODUCTION

In northern Alberta bitumen is produced by surface mining of oil sands ore followed by ore-water slurry based extraction processes. Almost all plants are using some versions of the Clark's Hot Water Extraction (CHWE) process. In this process, as implemented at Syncrude Canada Ltd.'s and Suncor Energy Inc.'s plants, caustic *NaOH* is used. Use of *NaOH* increases the *pH* of the ore-water slurry, increases the solubility of asphatic acids which act as surfactant reducing the surface and interfacial tensions. Therefore, addition of *NaOH* disperses the clay-shale stringers and seams and breaks the clay-shale down to small booklets and clay flakes. Because of the dispersion of clay, CHWE process tailings possess poor geotechnical characteristics which cause the formation of mature fine tailings (MFT). As an alternative to the CHWE process; low energy, non-additive extraction processes were developed and implemented at Albian Sands Energy Inc.'s Muskeg River Mine. In this process clay particles are not dispersed as much as that in the CHWE process. As a result, CHWE and low energy, non-additive extraction processes yield different tailings behavior.

Albian Sands' plant was designed to recover the process water in the tailings stream as warm as possible because of unavailability of low grade heat produced as a by-product of bitumen upgrading. For this purpose, Albian Sands' whole tailings stream discharged from the extraction plant was separated by the use of cyclones into Cyclone Underflow tailings composed of high solids content with low fines content (>55% s and <7% f) and Cyclone Overflow tailings composed of low solids content with high fines content (<30% s and >50% f). Cyclone Overflow tailings was thickened to a tailings stream with higher solids contents by the use of thickeners from which the Thickener Overflow (warm process water) could be recovered and recycled to the extraction process. The use of cyclones and thickeners could also reduce the production of MFT since the production of nonsegregating tailings (NST) became possible by blending the Cyclone Underflow and Thickener Underflow (>40% s) tailings and treating the blended tailings product with a flocculent to improve its settling, consolidation and nonsegregating characteristics.

Formation of a yield stress in the water-clay (<2 μm) matrix of the tailings is needed to prevent segregation. Such a yield stress is formed at a certain clay content (or clay/(clay+water) ratio) of the water-clay matrix. Therefore, clay content

measurement is important for tailings management. Clay content measurements made by different test methods, however, produce inconsistent results (SOSG 1996, Tang 1997); as a result of which further evaluation of the particle size distribution measurements is required.

Clay structures in the oil sands tailings are dependent on mineralogy and pore water chemistry, especially on divalent cation concentrations and *pH*. To examine clay structures in tailings, the Scanning Electron Microscope (SEM) is generally used. SEM images for NST samples indicated that a more aggregated and finer card-house structure of the fine tailings reflects a better ability to hold sand grains. It was also concluded that the segregation behavior of the tailings can be evaluated from the clay-water ratio and the morphology of the clay structure (Tang et al. 1997).

Understanding tailings behavior is challenging due to the complex physical and chemical processes involved in the extraction and tailings treatments. Material characterization is essential to understand the material changes and relate the changes to the material sedimentation and consolidation performance. This paper performs a comparative analysis to investigate test preparation effects on tailings particle size distributions, specifically clay size material, and recommend a guide for material characterization. Discussion and analyses in this study emphasizes the characterization of Albian sands thickened tailings. Different particle size determination methods are investigated. The water chemistry of the tailings is measured and morphology comparisons of the thickened tailings with Syncrude CHWE fine tailings are presented through SEM images.

ORIGIN OF CLAYS IN TAILINGS

Oil sand contains minor amounts of clay particles in the water layer surrounding the quartz sand grains. The great majority of clay minerals in the tailings come from the indurated clay-shale discontinuous seams and layers in the oil sands ore bodies. These dense but weak clay-shale materials are broken up during the mining process and the larger more indurate pieces are screened out as reject materials. In the bitumen extraction process, the clay-shale pieces are further broken down into clay aggregates and lumps and some clay lumps are dispersed into small clay booklets and flakes. The amount of dispersion depends on the extraction process. The sodium hydroxide dispersing agent in the CHWE process effectively disperses much of the clay aggregates into clay flakes smaller than 2 μm which have large active clay surfaces. The low energy extraction process such as the Albian Sands process has been developed to prevent dispersion of the clay aggregates.

TAILINGS MATERIALS

Tailings materials chosen in this study included thickened tailings (Albian sands' low energy extraction tailings) and fine tailings (Syncrude's CHWE tailings). These two types of tailings are selected as they can be regarded as two extreme cases; thickened tailings represent a flocculated system while the CHWE tailings exhibit a dispersed system.

Albian sands thickened tailings, TT, will be the main study subject for various particle size determination methods while the Syncrude CHWE fine tailings, FT, are included for comparison. Properties of TT and FT are presented in Table 1.

Solids content (% s) was determined by drying the sample at 110°C for about 24 hours. Therefore, %s also contains the residual bitumen in the tailings sample. Fines content (% f) was determined by wet sieving of the tailings sample. Like solids content (%s), fines content (% f) data also includes the residual bitumen in the fines.

Table 1 Tailings properties

Samples	Solids % of total mass	Fines % of solids	Bitumen % of total mass	Bitumen % of fines mass	FWR	e	e_f	G_s	G_f
Thickened Tailings	39	54	1.8	8.6	26	3.8	6.6	2.44	2.28
Fine Tailings	33	94	1.9	6.1	31	5.1	5.2	2.48	2.47

Bitumen content of the tailings sample was determined by the Dean-Stark extraction method. In this extraction method the solids are dried and some heavy hydrocarbons may tend to cement the finer particles together. As it is difficult to fully disperse these cemented aggregates it is inadvisable to use such extracted tailings in other testing.

The TT contains almost 50% sand which has an influence on the physical properties, such as void ratio (e), specific gravity (Gs) and the Atterberg Limits. As the fines/fines+water ratio (FWR) of the tailings not the total tailings material controls the geotechnical properties of the tailings, values are also given in terms of the fines (<45 μm), such as fines void ratio (e_f) and specific gravity of the fines (G_f).

The sand, silt and clay particles in the oil sands have a specific gravity close to 2.65. The bitumen which is attached to or trapped in the fines is considered as part of the solids and has a specific gravity of about 1.03. The low values of G_s and G_f are a result of the combination of mineral particles and bitumen.

Atterberg Limits

Atterberg limits were determined on the TT and FT with a modification to ASTM Standard D2487 (2008). All samples were prepared the same way. The slurries were not bitumen extracted or oven dried. They were allowed to settle; the release water was decanted and then was air dried with continuous mixing to the liquid limit and plastic limit water contents. The drying procedure increases the concentration of the chemicals in the pore water but at these low water contents, the different water chemistries do not appear to have different influences.

Table 2 Atterberg limits

Samples	Fines content %	w_L %	w_P %	I_p %	<2 μm dispersed %	*Ac*
TT	54	35	16	19	22	0.86
TT < 45 μm	100	57	27	30	39	0.77
FT	94	52	27	25	49	0.51

Included in Table 2 are calculated Activity values. The Activity is the Plasticity Index divided by the clay fraction (<2 μm) and reflects how the type and amount of clay influences the properties of the tailings slurry. Although the thickener underflow was not dispersed with a dispersing agent for the Atterberg limit tests, the small lumps and pieces of clay-shale remaining in the thickener underflow appeared to have been broken down and dispersed by the considerable mixing required to reduce the water content to the liquid limit and plastic limit values. Therefore, the Activity has been calculated using the < 2 μm fractions measured in the dispersed particle size determination (PSD) hydrometer-sieve tests.

The higher the Activity of a tailings, the more the properties of the tailings are influenced by the clay fraction and type of exchangeable cation and pore fluid chemistry. The Activity of all oil sand tailings is increased by the presence of bitumen (organic matter) and is high for the predominate kaolinite clay in the tailings. Kaolinite clay is generally a low Activity clay around 0.5. The higher Activity of TT compared to that of FT appears to be caused by the greater amount of bitumen in the TT fines (Table 1) as the clay mineralogies are similar in both materials (Tables 4).

PARTICLE SIZE ANALYSIS

In order to investigate chemical and physical effects on particle size distribution, several particle size determination methods are performed and evaluated. These methods include modified dispersed and non-dispersed hydrometer-sieve tests, a dispersed hydrometer-sieve test with bitumen removal, methylene blue tests and x-ray diffraction (XRD) measurements. Effect of shearing due to pipelining on particle size determination is also presented.

Philosophy of Determining Particle Size Distribution

Research on oil sands tailings have shown that sample preparation and testing methods can influence the measurement of the size distribution of the fine particles. The philosophy that has been developed in the University of Alberta Geotechnical Centre to conduct particle size distribution tests is to prepare and test tailings samples so the sample properties remain the same as the material deposited in the tailings ponds. Changes to bulk properties, clay particle sizes, clay surface charges and pore water chemistry are prevented as much as possible.

Modified Hydrometer-Sieve Test

The ASTM standard hydrometer-sieve test method (ASTM D422-63) has been developed for standard soil materials and the presence of bitumen in the sample and the possibility of dispersing clay aggregate during testing have required modifications to the test methods. The presented method is similar to the ASTM standard with some modification for oil sands tailings as followings.

The Dean Stark bitumen removal process requires driving off all the water from the sample as well as removing the bitumen. It has been found that this process may not remove all the heavy asphaltenes from the sample. When the sample is dried, the asphaltenes tend to cement some of the fine particles together and the resulting particle size distribution underestimates the amount of clay size material in the samples. Also the bitumen removal process may affect the clay surface chemistry. For these reasons, bitumen is not removed from the sample.

Drying of the sample, even if the bitumen is successfully removed, results in a dry lump of soil. The dry lump is pulverized by mixing in a blender and using an ultrasonic bath or by some other grinding or dispersion processes. As the effect of this pulverizing or dispersing on the clay aggregates is not quantifiable, the sample is not dried in the modified sample preparation.

During the bitumen extraction process an equilibrium between the exchangeable cations on the clay surfaces and the sodium enriched process water occurs. For the hydrometer tests the tailings need to be diluted to 5% or 2.5% solids content. Tailings water is used for dilution in the modified test procedure to reduce changes in clay surface charges. Using deionized water for this dilution would result in cations leaving the clay surfaces to establish a new equilibrium. Change in surface chemistry of the clays tends to change their structure.

Using a dispersing agent in the water to ensure that the soil particles are far enough apart so the assumptions in Stokes law are satisfied, will break down and disperse the clay aggregates. As well, in the ASTM methods the sample is blended in distilled water containing the dispersive agent to ensure that the sample is dispersed as much as possible. This blending and dispersion will increase the percent of material finer than 2μm. For this reason, if a dispersion agent is not used in the bitumen extraction process in the extraction plant, the non-dispersive ASTM hydrometer-sieved test method (ASTM D4221-99) is used in the laboratory. This ASTM method does not use a dispersing agent and does not disperse the sample in a blender. To ensure that the settling particles will not flocculate and are far enough apart so they will not interfere with one another, the solids content is diluted to 2.6% to 1.5%. For the CHWE process tailings whose clay aggregates are already dispersed by the sodium hydroxide, using distilled water with a dispersing agent does not cause any significant further dispersion of the clay aggregates (Miller 2008).

Dispersed Hydrometer-Sieve Test

Three dispersed tests varying the amount of solids in the hydrometer-sieve samples were conducted (Figure 1). The purpose of using lower solids amounts than the standard 50g was to allow comparisons with the lower solids non-dispersive tests. The three test results are similar. The amount of fines (<44μm) was determined by wet sieving following the hydrometer tests and averaged 54%. The amount of clay size material was determined by hydrometer and averaged 24%. The term clay size is used, not clay, as some rock forming minerals, usually quartz, can be finer than 2μm. Also, as not all clay aggregates are dispersed in the extraction plant and the laboratory test procedure, there can be considerable clay mineral in the form of aggregates and booklets coarser than 2μm. Kaolinite commonly exists in booklets larger than 2μm, and even if the clay aggregates are dispersed the clay size particles may be coarser than 2μm. Such large clay booklets have a small surface area compared to their mass so do not behave like the finer clay flakes but behave more like silt-size rock forming materials.

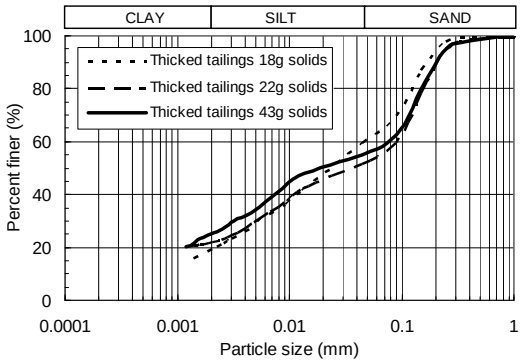

Figure 1. Dispersed hydrometer-sieve test on thickened tailings

Non-Dispersed Hydrometer-Sieve Test

Four non-dispersed tests varying the amount of solids in the hydrometer-sieve samples were conducted (Figure 2). The objective of the non-dispersed tests is to not disperse the clay lumps and aggregates anymore than they are in the mining, extraction and tailings treatment processes. The non-dispersed tests should more accurately reflect the particle size distribution of the thickener underflow material in the tailings pond.

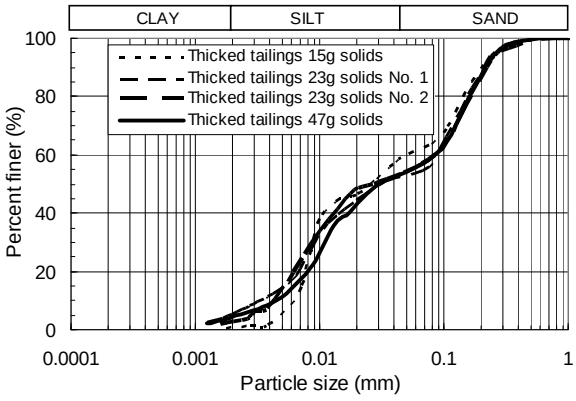

Figure 2. Non-dispersed hydrometer-sieve tests on thickened tailings

As no dispersing agent is used, there is a possibility of particles in the hydrometer jar flocculating and settling out rapidly. For this reason, smaller amounts of solids are used in the non-dispersed tests in order that the particles are farther apart and reduce a chance of floc formation. Solids content from 4.7% down to 1.5% were used. The four test results are similar. The amount of fines was determined by sieving and averaged 54%, the same value found in the dispersed tests. This is to be expected as the dispersing process would have no effect on the quartz sand grains coarser than 45μm. The amount of clay size material was determined by hydrometer and averaged only 4%. As 35% of the sample is composed of clay mineral, most of the clay mineral in the thickener underflow is in the form of aggregates and booklets coarser than 2μm and are not active clay minerals.

For fine tailings, results from dispersed and non-dispersed hydrometer tests are given by Miller et al. (2008) and are shown in Figure 3. The results show that dispersed and non-dispersed tests give similar particle size distributions. Unlike the thickened tailings, the fine tailings from CHWE process have already been extensively dispersed and have not been treated with any coagulant or flocculant. As a result, an addition of a dispersing agent does not significantly change the grain size distribution of this material.

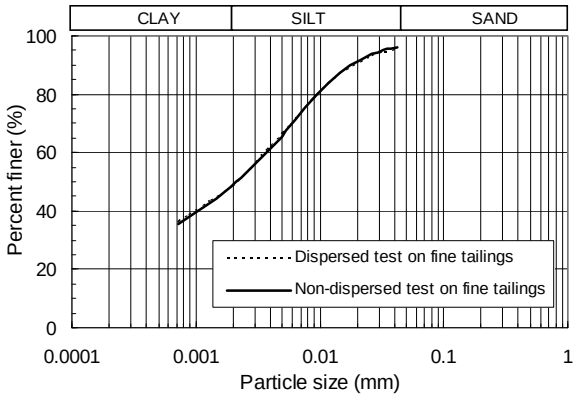

Figure 3. Dispersed and non-dispersed hydrometer-sieve tests on CHWE fine tailings

Hydrometer-Sieve Test with Bitumen Removal

For this test, the thickened tailings sample had the bitumen removed by the Dean Stark method, was dried and pulverized, then was dispersed in distilled water with a dispersing agent in a blender and an ultrasonic bath following the procedure in the standard hydrometer-sieve test (ASTM D422-63).

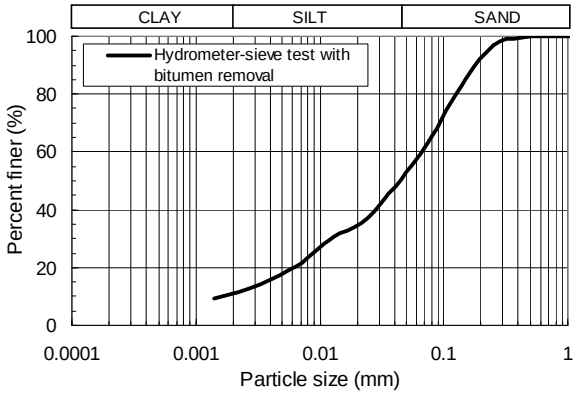

Figure 4. Hydrometer-sieve tests with bitumen removal on thickened tailings

The particle size distribution obtained is shown in Figure 4. The amount of fines was determined by

sieving and was 51% similar to that measured by the two previous methods. The amount of clay size material determined by hydrometer, however, was 12%, considerably less than the 24% found in the modified dispersed tests. The difference may have been caused by the drying process cementing fine particles together with residual asphaltenes.

Shearing Effect on Particle Size Determination

To investigate effects of pumping and pipeline shearing on particle size distribution, a simulation of shearing effort was performed using a Philadelphia Mixer Model 745-5033 apparatus. The mixer was used to shear 0.8L tailings samples at 1080 rpm for 24 minutes.

Hydrometer-sieve tests were performed on non-sheared and sheared thickened tailings samples to determine if pumping and pipelining shear resulted in finer tailings from a breakdown in particle sizes. Figure 5 shows dispersed hydrometer-sieve test results on thickened tailings samples. No significant difference in grain size distribution is apparent in the material. Non-dispersed hydrometer-sieve tests could not be performed because of flocculation inducing hindered sedimentation.

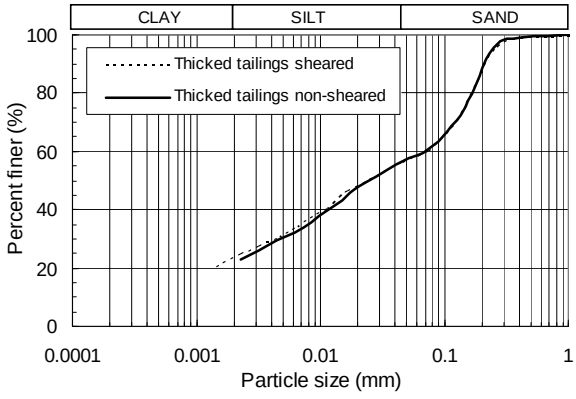

Figure 5. Dispersed hydrometer sieve tests on sheared and non sheared thickened tailings.

Methylene Blue Test

The Methylene Blue test is a determination of the dye adsorption of clay. The principle of this test is based on the chemical reactions triggered by an excess in negative charges on clay surfaces and/or the ionic exchanges phenomena taking place between the easily exchangeable cations of the clay and the methylene blue cations (Chiappone et al. 2004). The adsorption capacity of clay increases as a function of the clay particle specific surface and charge.

The Standard Methylene Blue test on oil sands tailings follows the procedure in ASTM Standard C837-99 (2003). This procedure is generally modified to extract the bitumen first by the Dean Stark method and then the dried mass is pulverized, blended and dispersed in deionized water with a dispersing agent in an ultrasonic bath (Sethi 1995). Morin (2008) gives a similar procedure as in the ASTM Standard except the sample is not bitumen extracted or dried first. The sample, however, must have a low amount of bitumen contamination. The samples are fully dispersed in this procedure by stirring at 250 RPM at a temperature of 120ºC. If the samples are not fully dispersed they are then transferred to a sonicator for 20 minutes. The cycle of heating/stirring and sonication is continued until the sample is completely dispersed.

For oil sands tailings, the quantity of exposed clay mineral can be calculated using the empirical relationship expressed in Equation 1 (Morin 2008).

$$\%Clay = \left(\frac{MBI + 0.04}{0.14} \right) \quad [1]$$

Where %Clay is the clay mineral fraction in the total solids and MBI is the methylene blue index.

The %Clay measurements from methylene blue tests on TT and FT are given in Table 3. Also included is the amount of clay sized material measured in parallel hydrometer tests. Sample TT1 and the FT samples were bitumen extracted and then tested according to ASTM Standard C837-99. The other TT samples were not bitumen extracted or dried.

Dispersed tests were performed by raising the pH to 9 with sodium bicarbonate ($NaHCO_3$) then adding sulfuric acid to lower the pH within a range of 2.4 to 3.8 as required in the ASTM procedure. The mass of solids used was varied to use about 2g of fines. The wet sample was dispersed in 300mL of deionized water with 15 milliequivalents/L of $NaHCO_3$. One sample was also subsequently dispersed in an ultrasonic bath heated to 80°C for 20 minutes.

Table 3 Methylene blue test results

Material	MBI Treatment	%Clay (MBI)	%Clay (Hydrometer)
TT1	bitumen extracted, dried, dispersed	25	24
TT2	dispersed	25	21
TT3	non-dispersed	25	4
TT4	sheared, dispersed	27	23
TT5	sheared, non-dispersed	25	4
TT6	sheared, dispersed, sonicated	29	N/A
FT1	bitumen extracted, dried, dispersed	44	43
FT2	bitumen extracted, dried, non-dispersed	43	43
FT3	bitumen extracted, dried, dispersed	51	49
FT4	bitumen extracted, dried, non-dispersed	41	49

The non-dispersed methylene blue tests were performed by mixing the samples in process water and lowering the pH with sulfuric acid to the desired range. The samples, however, were initially mixed with a drill mixer to become homogeneous and then during the test stirred for 20 minutes with a magnetic mixer.

All the MBI tests on the TT samples in Table 3 are similar and all appear to be dispersed as the %Clay is similar to that in the dispersed hydrometer tests. The FT samples also appear to be dispersed which is not surprising as the fine tails in the CHWE extraction process become dispersed.

The methylene blue test is an effective tool to determine the total amount of clay material but does not provide any information regarding the form of clay particles in the tailings prior to dispersion. When the bitumen extraction process in the extraction plant does not disperse the clay lumps and peds, a methylene blue test needs to be developed and used which also does not disperse the clay. The present test procedure that disperses the clay more than the extraction plant results in an overestimation of the percent of active clay material in the tailings.

Mineralogy Tests

Although determining particle sizes is not an objective of mineralogy testing, the results can be used to interpret the total amount of clay in the tailings. For the mineralogy tests, tailings were dried and pulverized and dispersed in distilled water with a dispersing agent in an ultrasonic bath. The dispersion process is very thorough to separate the different minerals to allow for their accurate measurement.

Table 4 gives the mineralogy of the thickened tailings, desanded thickened tailings and fine tailings determined by AGAT laboratories. About 35% of the thickened tailings sample is clay mineral. As the dispersed particle size distribution showed only 25% of the sample was finer than 2 μm, the remainder of the clay must be in the form of aggregates and booklets coarser than 2 μm. The desanded TT sample shows that the clay minerals comprise 71% of the fines. The more vigorous dispersion techniques used in the mineralogy testing therefore result in more clay being broken down to become finer than 2 μm. As the finer clay flakes have a relatively large surface area to their mass, they are more active and can change the geotechnical properties of the tailings samples. It is, therefore, fundamental that sample preparation techniques not disperse the clays more than they are when the tailings come form the extraction plant or thickener and are deposited in the tailings pond.

Table 4 Mineralogy of tailings

Sample	Fines content %	Mineral percent							
		Rock forming minerals				Clay minerals			
		Quartz	Plagioclase	K-Feldspar	Siderite	Kaolinite	Illite	Mixed layer	Smectite
TT	54	63	0	2	0	26	9	0	0
TT <45 μm	100	28	0	1	0	56	15	0	0
FT	94	19	1	1	3	55	20	1	0
FT <5 μm	100	2	0	0	0	76	18	4	0

The fine tails sample contained 76% clay material. As the fine tails was 94% fines, the clay minerals comprise (0.94)(76%)=71% of the fines. Both the TT and FT, therefore, from the mineralogy tests, had fines composed of 71% clay minerals. The methylene blue tests showed that the TT fines were composed of (25%)/(0.54)=46% clay minerals and the CT fines were composed of (44%)/(0.94)=47% clay minerals. Sethi reported that the clay minerals to fines percent in most oil sands tailings was 44% which agrees with the findings in this study. As the clay minerals to fines percent of 44% has been determined by methylene blue tests, it would appear that the fines contain indurated clay-shale particles that are not dispersed in the methylene blue test procedure and cannot become active clay flakes.

WATER CHEMISTRY

This section presents and discusses the results of the analytical testing of tailings pore fluids.

Pore fluid and sediment samples were collected at the completion of sedimentation tests by decanting fluids from the standpipes into 250mL sample containers. Pore fluid and tailings sediment samples were submitted for analytical testing to the Applied Environmental Geochemistry Research Facility (AEGRF) at the University of Alberta to characterize tailings sediment and pore fluid chemistry from the experimental program. Major cations and ions in the pore fluid samples were quantified using a Dionex IC-2000 ion chromatography system. A bicarbonate concentration was determined by potentiometric titrations. Water chemistry measurement of the thickened tailings and the fine tailings are shown in Table 5.

From Table 5, the pH and conductivity values of both tailings are quite similar with the pore water of fine tailings having a slightly higher pH and conductivity than that the thickened tailings. This is due to higher total dissolved ions in the fine tailings and the bicarbonate in the fine tailings is about five times larger than that of the thickened tailings. The biggest difference between the two water samples is the monvalent to divalent cations ratios. The monovalent to divalent cation ratio is 3 for the thickened tailings and 27 for the fine tailings.

The difference in the water chemistry in the two tailings samples changes the surface charge on the clays by changing the distribution of Ca^{2+} and Na^{+} on the clay surface. The thickened tailings sample has a low monovalent to divalent cation ration and low bicarbonate concentration which results in the clay surfaces having an abundance of exchangeable Ca^{2+} cations. The fine tailings has a very high monovalent to divalent cation ratio and very high bicarbonate concentration which results in the clay surfaces being dominated by sodium cations. The high bicarbonate concentrations in the fine tailings sample further exaggerates the monovalent to divalent cation ratio because divalent cations tend to form bicarbonate complexes ($CaHCO_3^-$) in solution and would then not be available for cation exchange reactions. When the clay surfaces are dominated by sodium the clays become dispersed as in the bitumen extraction process when *NaOH* is added. When calcium ions exchange for sodium ions on the clay surfaces, the clay particles aggregate and flocculate which is the reason that calcium amendments are added during CT production.

Exchangeable Sodium Ratio (ESR) is often used to indentify possible clay structure status in salt impacted soils. ESR relates the compositions of the solution phase to the compositions of the absorbed phases. It provides a prediction of adsorbed phases based on the concentration of ions in the solution. ESR can be calculated by the Gapon equation (Equation 2).

$$ESR = \frac{0.015[Na^{+}]}{\sqrt{\frac{[Ca^{2+}]+[Mg^{2+}]}{2}}} \quad [2]$$

Table 5 Water chemistry measurements

Sample	pH	Conductivity (µS/cm)	HCO_3^-	Anions (mg/L)			Cations (mg/L)					
				F^-	Cl^-	SO_4^{2-}	Li^+	Na^+	NH^{4+}	K^+	Mg^{2+}	Ca^{2+}
TT	7.9	865	172	1.3	63	89	0.15	127	2.2	16	18	30
FT	8.2	1200	846	8.2	94.0	4.8	BDL[1]	257.8	8.8	7.8	4.1	5.9

[1]BDL = below detection limit

Based on ions in pore water in Table 5, it is found that the ESR values of thickened tailings and fine tailings are 0.07 and 0.30 respectively. According to Dawson et al. (1999), for ESR values of 0.1 or more, sodium ions will occupy adsorption sites on the clay resulting in a high potential for dispersion. The calculated ESR values imply that the thickened tailings clay structure is non-dispersed while the fine tailings clay structure is dispersed. This is in agreement with the findings from SEM image comparison.

SCANNING ELECTRON MICROSCOPY

SEM images of thickened tailing and fine tailings are shown in Figures 6 through 9 respectively. Both materials have approximately the same solids content and fines content to allow this comparison. It can be seen that the Albian Sands thickened tailings has a much more aggregated, face to face association of clay particles (Mitchell 1993), and flocculated structure, edge to edge and edge to face association of aggregates, than the Syncrude fine tailings. The Syncrude fine tailings has substantial more edge to edge associations and has substantially less aggregation

The morphology of tailings thickened by organic polymers and tailings treated by calcium amendments, that is CT, is different. This is because the mechanisms of coagulation by calcium amendments is quite different from the polymeric flocculation process. The polymeric flocculation process is expected and found to be less structured due to the randomly bonding polymers with clay particles while the calcium amendments would promote the creation of aggregated and flocculated soil structure stabilized by electrostatic forces between the clay particles. Shearing of polymeric flocculated tailings by pumping and pipe flow tend to destroy the flocculated structure prior to deposition while shearing has little effect on calcium amended tailings.

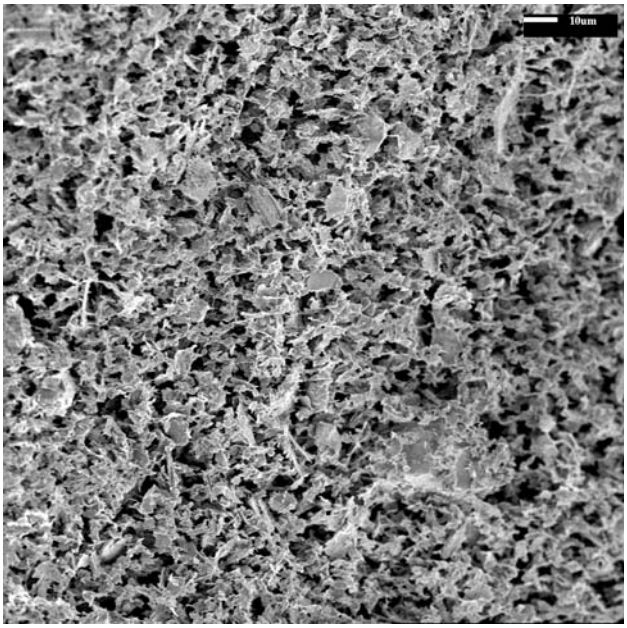

Figure 6. SEM of desanded thickened tailings 34% solids 100% fines (× 500)

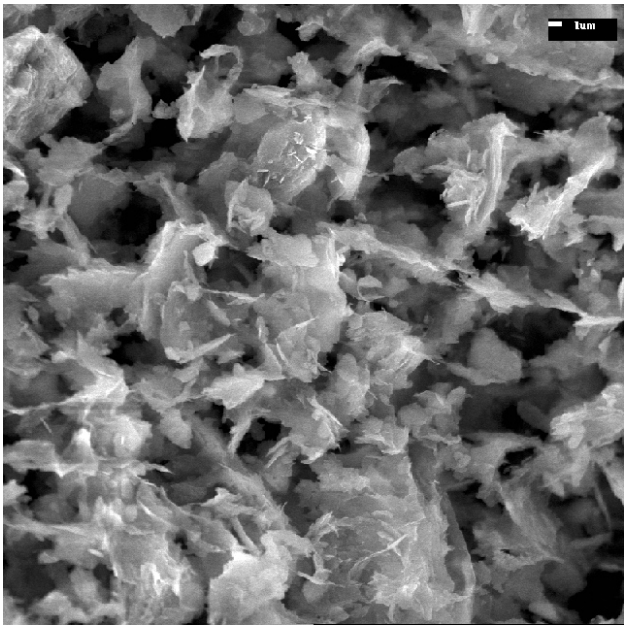

Figure 7. SEM of desanded thickened tailings 34% solids 100% fines (× 2000)

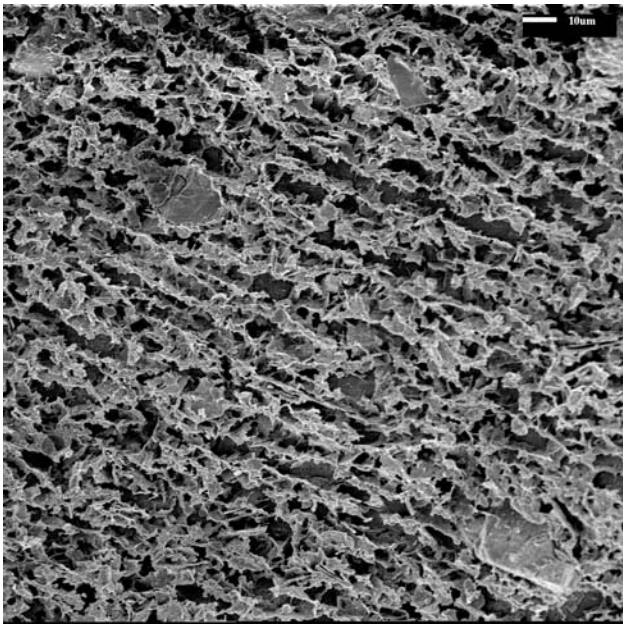

Figure 8. SEM of fine tailings 37% solids 93% fines (× 500)

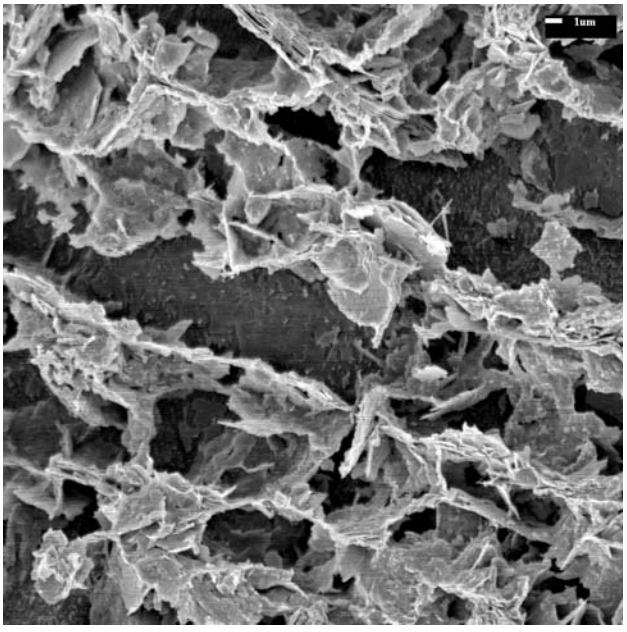

Figure 9. SEM of fine tailings 37% solids 93% fines (× 2000)

DISCUSSION AND CONCLUSIONS

This study highlighted particle size determination methods related to oil sands tailings characterization. Several methods are presented and evaluated on oil sands thickened tailings. Pore water chemistry of the thickened tailings was also measured and morphology was investigated via SEM images.

It was found that the dispersed and non-dispersed hydrometer tests showed considerable differences in the amount of clay size material for thickened tailings. If the philosophy of treating the tailings material in the laboratory the same way it is treated in the field is accepted, then the non-dispersed tests would give the best interpretation of the amount of clay size material.

The influence of the polymeric flocculent used in the thickener on the resulting particle size distribution of the thickened tailings has not been studied. It was observed that the large visible flocs formed by the flocculent have been destroyed in the thickener compaction process, subsequent pumping and particle size distribution sample preparation procedures. This influence, however, needs to be evaluated.

Effect of shearing during pipeline transportation was partly investigated due to the occurrences of hindered sedimentation in the non-dispersed hydrometer-sieve test. The dispersed and non-dispersed methylene blue tests give similar clay-size measurements on both sheared and non sheared materials. It would appear that all the methylene blue samples are dispersed.

When the bitumen extraction process in the extraction plant does not disperse the clay lumps and peds, a methylene blue test needs to be developed and used which also does not disperse the clay. The present test procedure that disperses the clay more than the extraction plant results in an overestimation of the percent of active clay mineral in the tailings.

It has been recognized that it is the clay minerals in the fines which control the performance of the fines and the viscosity of the fines-water matrix. It, therefore, has been suggested that the clay content be used to define segregation not fines content. However, not only is the fines content easier to measure and monitor in the laboratory and field but the clay content of the fines in oil sand tailings appears to be quite consistent.

Atterberg limits for all oil sand tailings, which take into account not only the clay amount and mineralogy but also tailings water chemistry and exchangeable cations, are quite consistent. The Atterberg limit values plot in a band parallel to the

A-line on the Plasticity Chart showing consistent properties for these sand-fines-clay mixtures. So the use of fines content is acceptable in practice.

Different pore water chemistry causes the tailings to form different soil fabrics during deposition. The low monovalent to divalent cation ration and ESR values in the thickened tailings compared to the fine tailings suggests that the distribution of cations on the clay surfaces is different for the two tailings. The SEM observations of the aggregated and flocculated structure for the thickened tailing and a dispersed structure for the fine tailings suggest that soil fabric is a function of pore fluid chemistry. It is believed that this aggregated structure is contributing to the smaller clay size measurement obtained from the non-dispersed hydrometer-sieve method.

The combination of all the discussed factors indicates that extraction chemistry in conjunction with tailings processing impacts water chemistry which in turn influences the soil fabric formed after deposition. The formation of aggregated and flocculated soil fabric will control hydraulic conductivity and sedimentation-consolidation behavior.

Further research on methods to determine the particle size distribution of tailings from extraction and tailings treatment processes which do not disperse the clay-shale lumps and aggregates is required. The aim of such research would be to develop a standard particle size distribution test procedure for this class of materials.

ACKNOWLEDGEMENTS

The authors are grateful for the financial support from the University of Alberta and APEX Engineering Inc.

REFERENCES

ASTM C837-99, 2003. Standard Test Method for Methylene Blue Index of Clay, *ASTM International*, West Conshohocken, PA, www.astm.org.

ASTM D2487-06el, 2008. Standard Practice for Classification of Soils for Engineering Purposes, *ASTM International*, West Conshohocken, PA, www.astm.org.

ASTM D4221-99, 1999. Standard Test Method for Dispersive Characteristics of Clay Soil by Double Hydrometer, *ASTM International*, West Conshohocken, PA, www.astm.org.

ASTM Standard D 422-63, 1998. Standard Test Method for Particle-Size Analysis of Soils, *ASTM International*, West Conshohocken, PA, www.astm.org.

Chiappone, A., Marello, S., Scavia, C. and Setti, M. 2004 Clay mineral characterization through the methylene blue test: comparison with other experimental techniques and applications of the method. *Canadian Geotechnical Journal*, 41:1168-1178.

Dawson, R. F., Sego, D.C., and Pollock, G.W. 1997. Freeze Thaw Dewatering of Oil Sands Fine Tails, *Canadian Geotechnical Journal*, 36:587-598.

Miller, W., Scott, J.D. and Sego, D.C., 2008. Physical and Chemical Characteristics of OSLO/Clark Fine Tailings, Submitted to Canadian Geotechnical Journal.

Mitchell, J. K. (1993). Fundamentals of soil behavior. New York, John Wiley and Sons Inc.

Morin, M. 2008. AST Methylene Blue Procedure: Sludge & Slurries. *Natural Resources Canada*, Canada Energy Technology Centre, Advanced Separation Technologhies, Tailings & Emulsions.

Sethi, A. 1995. Methylene Blue Test for Clay Activity Determination in Fine Tails. MRRT Procedures.

SOSG (Suncor Oil Sand Group Limited) 1996. Suncor Steepbank Mine Application Second Request for Supplemental Information. *Report to Alberta Environmental Utility Board*.

Tang, J. 1997. Fundamental Behaviour of Composite Tailings. *MSc thesis*, University of Alberta, Edmonton, AB, Canada.

Tang, J., Biggar, K.W., Scott, J.D. and Sego, D.C. 1997. Examination of mature fine tailings using a scanning electron microscope, *Canadian Geotechnical Conference*, Ottawa, Ontario, 746-754.

PROPERTIES OF NONSEGREGATING TAILINGS PRODUCED FROM THE AURORA OIL SANDS MINE TAILINGS

R. Donahue[1], S. Jeeravipoolvarn[1] J. D. Scott[1] and B. Ozum[2]
1. Department of Civil and Environmental Engineering – University of Alberta, Edmonton, AB, Canada
2. Apex Engineering Inc, Edmonton, AB, Canada

ABSTRACT

Oil sands tailings disposal practice in northern Alberta causes accumulation of mature fine tailings (MFT) at about 33% solids with 98% fines (<45 μm) content, which possesses very poor settlement and consolidation properties. Accumulation of MFT over the four decades is an environmental liability, solution of which is an engineering challenge to be faced. To reduce MFT volumes, Composite (or Consolidated) Tailings (CT) is produced by mixing and depositing a blend of Cyclone Underflow and existing MFT with gypsum ($CaSO_4$). This process has been implemented by major oil sands players; however, this tailings disposal practice has low energy efficiency, produces additional MFT from Cyclone Overflow tailings and deteriorates release water chemistry in terms of high Ca^{2+}, Mg^{2+} and SO_4^{2-} concentrations. As an alternative to CT production, Nonsegregating Tailings (NST) production by mixing a blend of Cyclone Underflow and Thickener Underflow with *CaO* (lime) or $CaO+CO_2$ has been investigated. Experiments performed on several tailings samples, including the Albian Sands' Muskeg River Mine tailings samples produced by non-additive and additive extraction process modes, showed that treatment of an NST mix with *CaO* or $CaO+CO_2$ improves the geotechnical behavior of the NST and simultaneously improves the release water chemistry. The present paper summarizes the performance of the *CaO* or $CaO+CO_2$ additives on NST mixes prepared from Syncrude Canada Ltd.'s Aurora Mine tailings material. Experiments were performed on NST mixes with a sand-fines ratio (SFR) of 5 prepared from the Aurora Mine tailings material. Static segregation tests performed on NST mixes showed that addition of *CaO* at 0.6 g/L dosage moves the segregation boundary to 53% solids content from the no additive 63% solids content. Release water chemistry was monitored to ensure that recycle of release water would not detrimentally affect the bitumen extraction process. It was observed that the use of *CaO* at a 0.6 g/L dosage improved the settling, consolidation and nonsegregating behavior of the NST mix and simultaneously improved the release water chemistry by reducing its Ca^{2+}, Mg^{2+} and Na^{+} concentrations.

INTRODUCTION

In northern Alberta bitumen is produced from surface mineable oil sands by using some version of Clark's Hot Water Extraction (CHWE) process. Oil sands plants produce large volumes of tailings as a waste steam; properties of which are influenced by the use of caustic *NaOH* or other chemicals to promote bitumen extraction efficiency. Conventionally, the whole tailings, composed of sands, clay, water, and residual bitumen, are discharged into a tailings pond. In this tailings disposal practice, sand particles segregate and settle out to form beaches, while the fine particles (<45 μm) are carried with the run off water into the ponds. Over a two year period the fine particles settle and form Mature Fine Tailings (MFT), a stable suspension of fluid fine tailings that has undergone settlement and compression to about 33% solids content (by mass).

Accumulation of MFT is accepted as an environmental liability, the solution of which has been studied by many researchers. To reduce the MFT inventory, the production of Composite (or Consolidated) Tailings (CT) was investigated at the University of Alberta in 1993 (Caughill et al. 1993) and implemented commercially by almost all major oil sands players (Matthews et al. 2002). Production of CT with a sufficiently high solids contents is accomplished by using cyclones which separates the whole tailings into Cyclone Underflow tailings composed of high solids contents and with a low fines content (>55% s and <7% f) and Cyclone Overflow low solids content tailings with a high fines content (<30% s and >50% f). After cycloning, CT with the desired solids and fines contents is produced by blending Cyclone Underflow and MFT usually at sand-fines ratios (SFR) of 4 or 5. In this process gypsum

($CaSO_4$) is used as a chemical coagulant additive to prevent segregation.

Although CT production technology can accelerate tailings densification and reclamation, the continuous accumulation of Ca^{2+} and SO_4^{2-} ions in the recycle water will eventually negatively affect bitumen extraction. Production of CT doesn't significantly reduce the MFT inventory since additional MFT is produced from the Cyclone Overflow effluent. As well, energy efficiency of the plant is not improved because of the discharge of warm Cyclone Overflow water into the tailings ponds. Furthermore, CT production may cause H_2S emissions from the tailings ponds by anaerobic reduction of SO_4^{2-} by the residual bitumen in the tailings.

To overcome the short fallings of the CT technology, production of nonsegregating tailings (NST) by treating the blend of Cyclone Underflow and Thickener Underflow and/or MFT with *CaO* or *CaO* and CO_2 was developed (Ozum et al. 1999, Chalaturnyk et al. 2002). Experiments performed using Albian Sands' Cyclone Underflow and Thickener Underflow effluents produced by both non-additive and additive extraction process modes showed that the use of *CaO* at about 0.6 g/L (i.e. 600 g/m^3) dosages improved settling, consolidation and nonsegregating properties of the NST mix and simultaneously produced release water with less Ca^{2+}, Mg^{2+} and Na^{+} ions (Scott et al. 2007).

Experimental data generated for the production of NST using Albian Sands' tailings material and Syncrude tailings material showed that the use of process aids such as sodium citrate or caustic in the extraction process controls the extent of clay dispersion in the ore-water slurry and, therefore, it controls the geotechnical characteristics of the tailings as well. It was experimentally demonstrated that when the Albian Sands' extraction plant was operating in non-additive process aid mode the dispersion of the clay particles was much less than that of the tailings produced when the extraction plant was operating in additive mode or the tailings produced by the Syncrude and Suncor CHWE process. This finding on clay dispersion dependency on the operating conditions of the extraction plant is significant for future oil sands extraction processes.

In the present study, production of NST with *CaO* or *CaO* and CO_2 additives, from Syncrude Canada Ltd.'s Aurora mine tailings was tested. Aurora Mine tailings material is somewhere between the tailings material produced by the Albian Sands' Muskeg Rive Mine when the extraction plant was operating in non-additive mode and the Syncrude CHWE tailings material. Experiments were performed to determine the effect of the *CaO* additive on the settling and segregation behavior of the NST mix and on the release water chemistry.

NST PRODUCTION

Objectives of the Experimental Program

The objective of the experimental program was to demonstrate the performance of *CaO* additive to produce NST from Syncrude Canada Ltd.'s Aurora Mine tailings.

To achieve this objective, experiments were performed to determine: (i) the segregation boundary of the NST mix with an SFR of 5; (ii) the effect of the *CaO* dosage on the segregation boundary of the NST mix with an SFR of 5; and, (iii) the effect of the *CaO* dosage on the release water chemistry.

Material Used for the Experiments

Cyclones can be adjusted to obtain desired cyclone underflow and overflow solids and fines contents. The material for the testing program came from an Aurora Mine's cyclone with an underflow at a solids content of approximately 65% and fines content of 10% and with an overflow at a solids content of about 36% and fines content of 46%. The cyclone overflow was thickened in an experimented thickener using a polymeric flocculant to a solids content of 50% and a fines content of 46%. Mixing the cyclone underflow (CU) with the thickener underflow (TU) to obtain an NST with a SFR of 5 would require blending 77 parts of CU with 23 parts of TU. The resulting NST would have a solids content of 61.5% and a fines content of 16.7%.

As the cyclone underflow was not available, tailings sand at a 90% solids content and 1% fines content was used. The NST mixes were then prepared from blends of tailings sand, thickener underflow and process water.

Mix Designs for the NST

Thirteen NST mixes at different solids contents all with an SFR of 5 were prepared from the combination of tailings sand, thickener underflow and process water. Recipes for the preparation of the NST mixes are presented in Table 1.

Experimental

Thirteen NST mixes with an SFR of 5 were used in all experiments. Effects of *CaO* dosage on the NST properties and on the release water chemistry was determined by setting *CaO* additions to 0 (no additive), 0.2, 0.4, 0.6, 0.8 and 1.0 g/L dosages. A summary of these tests are presented in Table 1.

Standpipe tests were performed using 2 L graduate cylinders. During the settling tests the tailings-water interface was recorded as a function of time. After settling was complete (after about two days), the release water was siphoned and submitted to the Applied Environmental Geochemistry Research Facility at University of Alberta for water chemistry analysis. A summary of the water chemistry results are presented in Table 2.

The sediments were sampled in eight layers and their solids contents were measured. The percent fines captures were determined by calculating the amount of variation of the solids content profile from the average solids content (since solids and fines contents profiles are mirror images of each others). A fines capture of 95% is taken as the segregation boundary. The fines capture is defined as the percent of fines retained or captured in the pores of the sand after settlement of the tailings is completed.

Table 1 Recipes for Aurora NST mixes with SFR of 5 and results of static segregation tests

Test No	Tailings Sand mass (g)	Thickener Underflow mass (g)	Process water (g)	CaO addition (g/L NST)	NST mix design			NST initial mix		NST final	Fines capture (%)
					Solids content (%)	Fines content (%)	SFR	Solids content (%)	Fines content (%)	Average solids content (%)	
SCL-1	721	688	406	0	55	16.7	5	54.1	20.4	64.2	70.9
SCL-2	825	787	291	0	60	16.7	5	58.2	19.4	67.9	93.0
SCL-3	939	896	165	0	65	16.7	5	63.5	20.1	69.8	96.7
SCL-4	721	688	406	0.2	55	16.7	5	51.1	16.9	62.7	67.8
SCL-5	721	688	406	0.4	55	16.7	5	52.5	21.9	72.7	92.7
SCL-6	721	688	406	0.6	55	16.7	5	54.0	18.4	69.6	97.9
SCL-7	721	688	406	0.8	55	16.7	5	53.6	18.7	70.4	97.4
SCL-8	721	688	406	1.0	55	16.7	5	53.4	19.4	69.4	95.1
SCL-9	825	787	291	0.2	60	16.7	5	56.6	18.1	66.0	73.1
SCL-10	825	787	291	0.4	60	16.7	5	55.8	19.6	65.6	94.6
SCL-11	825	787	291	0.6	60	16.7	5	56.9	18.2	66.2	98.1
SCL-12	825	787	291	0.8	60	16.7	5	56.3	19.5	69.5	98.2
SCL-13	825	787	291	1.0	60	16.7	5	56.5	21.6	71.0	97.0

Table 2 Summary of water chemistry test results for Syncrude Aurora NST

Test No	Initial pH	Final pH	Conductivity (μs/cm)	CaO (g/L)	Ca^{2+} (mg/L)	Mg^{2+} (mg/L)	$Ca^{2+}+Mg^{2+}$ (mg Ca^{2+}/L)	Na^{+} (mg/L)	HCO^{3-} (mg/L)	CO^{3-} (mg/L)	Cl^{-} (mg/L)	SO_4^{2-} (mg/L)
PW[1]	8.5	8.5	-	-	18.3	18.5	48.8	660	489	0	442	364
SCL-1	7.5	8.3	3130	0	21.1	18.7	51.9	627	465	12	436	377
SCL-2	7.5	8.5	3120	0	21.5	19.4	53.6	627	435	15	421	391
SCL-3	7.4	8.5	3070	0	21.1	19.5	53.3	618	215	50	444	367
SCL-4	7.9	9.1	2810	0.2	7.0	7.6	19.5	588	52	72	442	362
SCL-5	8.2	9.8	2600	0.4	4.5	1.3	6.6	525	10	156	433	358
SCL-6	8.6	10.4	2700	0.6	6.8	0.3	7.3	536	0	132	439	359
SCL-7	8.6	11.3	3070	0.6	9.1	0.2	9.4	573	0	72	436	347
SCL-8	8.8	12.0	5140	1.0	88.3	0.2	88.6	659	212	40	421	364
SCL-9	7.5	9.0	2750	0.2	8.2	7.9	21.2	558	96	20	419	368
SCL-10	7.7	9.1	2530	0.4	5.8	3.1	11.0	510	0	140	414	365
SCL-11	7.9	10.6	2660	0.6	7.4	0.4	8.0	521	0	114	418	364
SCL-12	8.3	11.2	2940	0.8	12.3	0.2	12.7	543	0	82	416	351
SCL-13	8.6	11.9	4690	1.0	62.6	0.1	62.9	634	523	6	459	305

[1]Process water

SEGREGATION RESULTS AND DISCUSSION

No *CaO* Segregation Boundary

The final solids content profiles for the three samples with 55%, 60% and 65% initial solids contents with an SFR of 5 without any additive are presented in Figure 1. It can be seen from Figure 1 that the NST mix with 55% initial solids content is segregating. Nonsegregating behavior of the NST mix improves as the solids content increases to 60% and 65% solids. The segregation boundary defined as 95% fines capture is located at about 62% solids content.

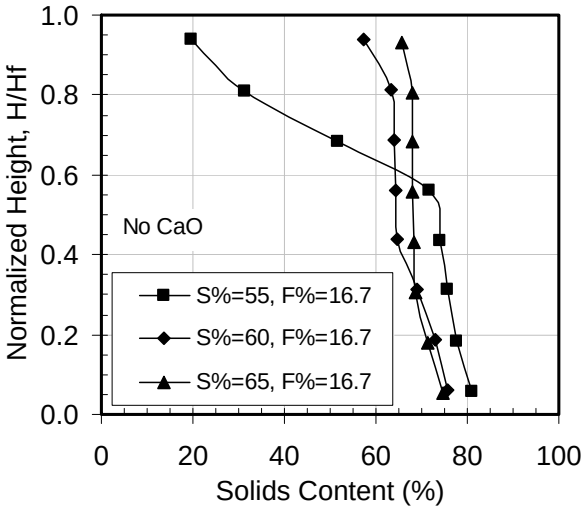

Figure 1. Solids content profiles, no *CaO* additive.

Effect of *CaO* Dosage on Segregation Boundary

Experimental investigation and analysis showed that the segregation boundary of the Aurora Mine tailings mix with SFR of 5 is at about 62% solids content. Addition of Ca^{2+} ions into the NST mix results in the formation of a yield stress in the clay-water matrix, which prevents the settling and segregation of the sand particles.

The effect of *CaO* dosage on the final solids content profiles for the NST mixes at 55% and 60% initial solids contents with SFR of 5 are presented in Figures 2 and 3 respectively. The percent fine capture for these tests is given in Table 1. It can be seen from Figures 2 and 3 and Table 1 that final solids content profiles at 0.2 g/L *CaO* dosage negatively affects the nonsegregating behavior. Further increase in *CaO* dosage beyond 0.2 g/L improves the nonsegregating property of the NST mixes.

The effect of *CaO* dosage on the segregation boundary (95% fines capture) is plotted in Figure 4. Below the dashed line the NST mixes are nonsegregating. At 0.2 g/L *CaO* dosage, a higher solids content is required to produce NST. The reduction in nonsegregating behavior of the NST mix at about 0.2 g/L *CaO* dosage is related to decomposition of water soluble bicarbonates ($(Ca,Mg)(HCO_3)_2$) to water insoluble carbonates ($(Ca,Mg)CO_3$).

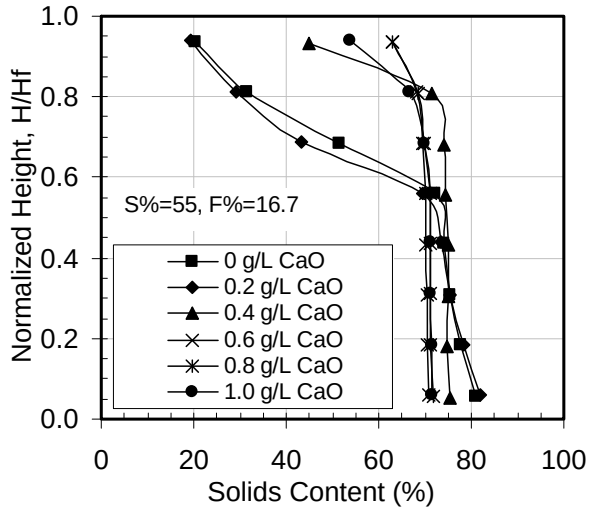

Figure 2. Effect of *CaO* dosages on final solids content profiles, initial solids content of 55%.

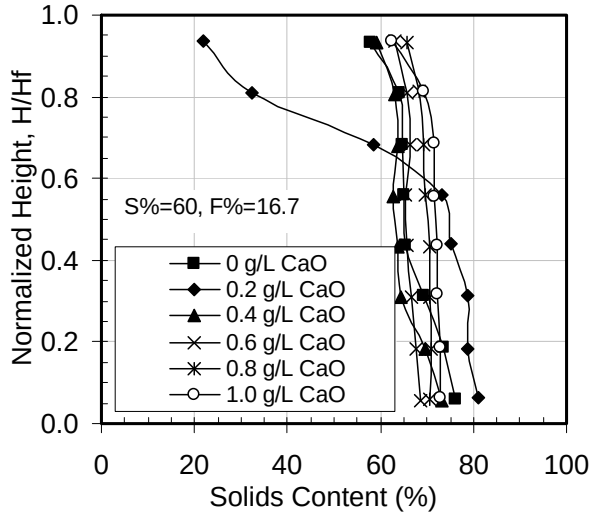

Figure 3. Effect of *CaO* dosages on final solids content profiles, initial solids content of 60%.

A further increase in *CaO* dosage from 0.2 g/L to 0.6 g/L improves the nonsegregating behavior of the NST mix by shifting the segregation boundary to a lower solids content, that is, to lower than 55% solids content. The segregation boundary for the NST with SFR of 5 without *CaO* addition was at about 62% solids content. This shift in segregation boundary from 62% solids content to lower than 55% solids content is a significant advantage for the commercial production of NST from the Aurora Mine tailings.

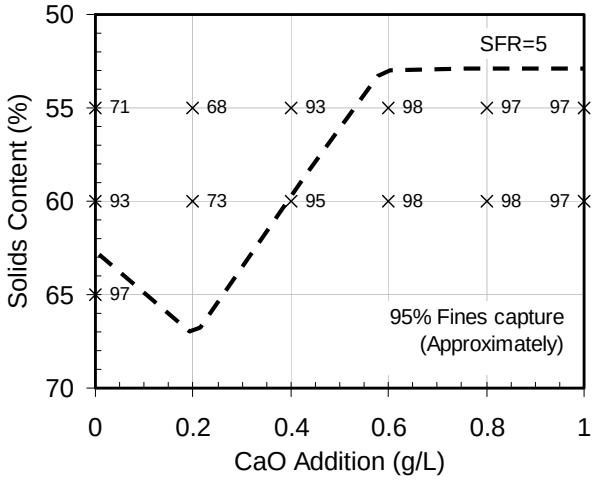

Figure 4. Effect of *CaO* dosages on segregation boundary.

Further increases in *CaO* dosage, that is, *CaO* dosages larger than 0.6 g/L has no significant effect on the segregation boundary. This observation suggests that 0.6 g/L *CaO* dosage is likely a minimum value for preventing segregation. Additional use of *CaO* additive beyond 0.6 g/L dosage, however, would not have a detrimental effect on the release water chemistry. Excessive amounts of *CaO* (or $Ca(OH)_2$) in the release water would soften the bicarbonate hardness of the fresh make-up water, which would improve the extraction efficiency.

Void Ratios of the NST Mixes, No *CaO* additive

The changes in the average void ratios (in the whole sample) as a function of time for the NST mixes with 55%, 60% and 65% initial solids contents with SFR of 5 without any additive are presented in Figure 5. The changes of void ratio reflect the water drainage rates from the NST mixes. During the early period (about 14 hours after starting), the void ratio in Sample SCL1 (55% initial solids) decreased more rapidly than those in samples SCL 2 (60% initial solids) and SCL3 (65% initial solids). This was mainly due to the higher initial void ratio in Sample SCL1 therefore it had a higher initial hydraulic conductivity.

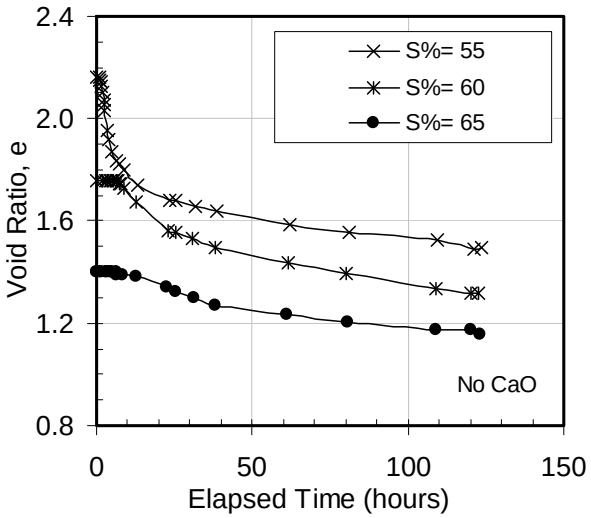

Figure 5. Change in void ratio as a function of time, no *CaO* additive.

Effect of *CaO* Dosage on Void Ratios of the NST

Effect of *CaO* dosage on the average void ratios as a function of time for the NST mixes with 55% and 60% initial solids contents with SFR of 5 are presented in Figure 6 and in Figure 7 respectively.

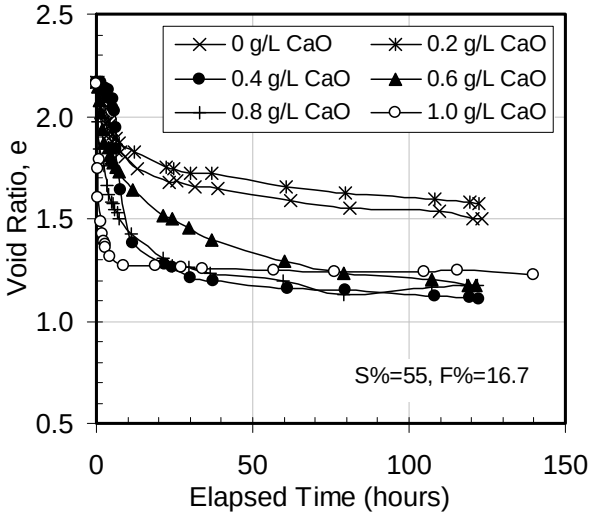

Figure 6. Effect of *CaO* dosages on the change of void ratio as a function of time, 55% solids content.

As seen from Figure 6, the interfaces of Sample SCL1 (0 g/L *CaO*) and Sample SCL4 (0.2 g/L *CaO*) settled at much slower rates relative

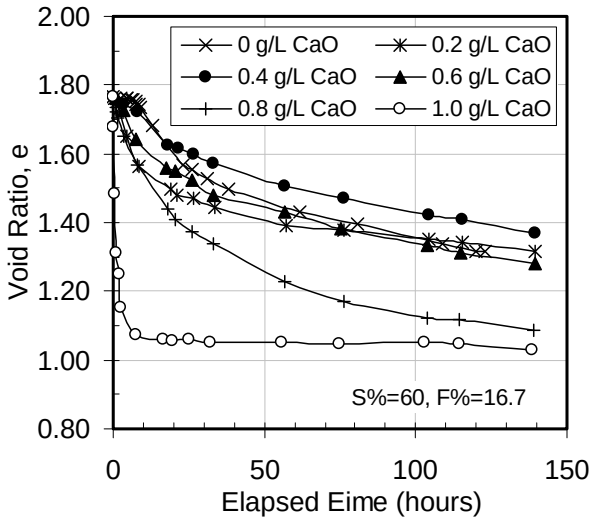

Figure 7. Effect of *CaO* dosages on the change of void ratio as a function of time, 60% solids content.

to samples with greater than 0.2 g/L *CaO* addition. It appears that a *CaO* addition greater than 0.2 g/L obviously improves the dewatering rate of the NST samples. No such effect is seen for the low *CaO* additions to the 60% solids NST (Figure 7). The lower initial void ratio for the 60% solids NST masks this effect.

Of importance to water release rates; the 1.0 g/L *CaO* addition greatly increases the initial rate of settlement and results in complete water release in a short time for both the 55% and 60% solids content NST.

The segregating behaviour of SCL1 and SCL4 will make a more compressible material as the fine particles will stay at the top while a less compressible material (the coarse particles) will settle to the bottom causing ineffective use of self-weight stress (Sridharan and Prakash 2001). As a result, the low *CaO* dosages mixes will result in a higher final tailings volume.

RELEASE WATER CHEMISTRY RESULTS AND DISCUSSION

Water Chemistry Analysis

After the settling tests were finalized, the release waters from each column were sampled and submitted to the Applied Environmental Geochemistry Research Facility at University of Alberta for chemical analyses. The water samples

were analyzed to determine the concentrations of dissolved species and to determine the changes in dissolved species as a result of *CaO* addition. The fluid samples were analyzed for major cations (Ca^{2+}, Mg^{2+}, Na^{+}, K^{+} and Li^{+}) and major anions (SO_4^{2-}, PO_4^{3-}, Cl^{-}, Br^{-}, NO_2^{-} and NO_3^{-}) by Ion Chromatography (IC). The concentrations of inorganic carbon species (CO_3^{2-}, HCO_3^{-} and H_2CO_3) in the samples were measured by standard alkalinity titration. The concentrations of transition metals in some selected samples were measured by Inductive Coupled Plasma Mass Spectrometry (ICP/MS). The analysis of transition metals was conducted to investigate dissolved *Al, Fe* and *Zn* concentrations.

Effect of *CaO* Dosage on *pH* and Electric Conductivity of the Release Water

Effects of *CaO* dosage on *pH* and electric conductivity of the release water are presented in Figures 8 and 9 respectively. Release water pH increases as *CaO* dosage increases almost in linear fashion. The *pH* value of the sample with 1 g/L *CaO* addition was close to 12. Electric conductivity slightly decreases as *CaO* dosage increases up to 0.4 g/L and then increases as *CaO* dosage becomes greater than 0.6 g/L.

Effect of *CaO* dosage on release water Ca^{2+}, Mg^{2+}, Na^{+} and HCO_3^{-} concentrations

Effects of *CaO* dosage on the release water Ca^{2+}, Mg^{2+}, Na^{+} concentrations are presented in Figures 10, 11 and 12 respectively. The calcium

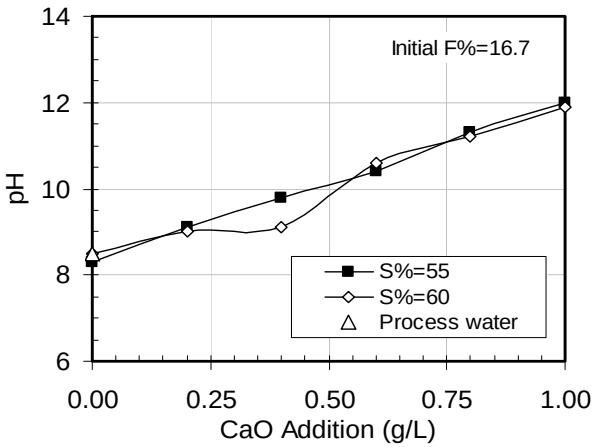

Figure 8. Effect of *CaO* dosages on release water *pH*.

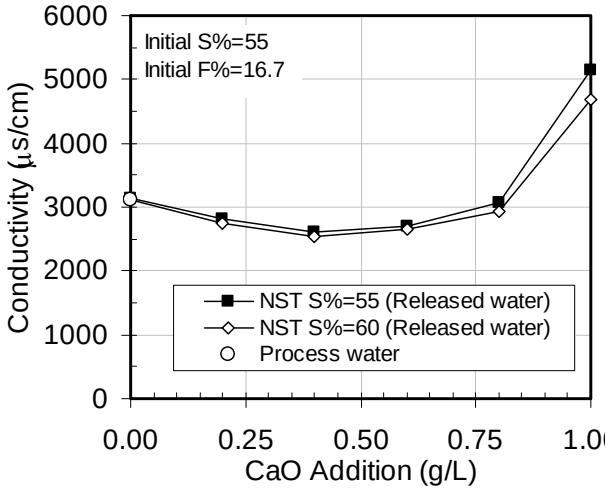

Figure 9. Effect of *CaO* dosages on release water electric conductivity.

concentration decreases as the *CaO* dosage increases from 0 to 0.4 g/L. The calcium concentrations increase slightly as the *CaO* dosage is increased to 0.8 g/L then increases significantly above initial concentrations with further addition. The initial decrease in Ca^{2+} concentration with *CaO* addition is due to the precipitation of carbonate minerals. Calcite minerals are oversaturated in the process water at the start of the experiments. The addition of *CaO* adds calcium and consumes protons raising the pH of the water (Equation 1). As the *pH* rises the inorganic carbon species change from HCO_3^{-} to CO_3^{2-} and the alkalinity is consumed by the precipitation of calcite. Once the alkalinity is consumed and the *pH* is above 10.4, calcite no longer precipitates and the addition of *CaO* at greater than 0.6 g/L rapidly increases the Ca^{2+} concentration.

$$CaO + H+ = Ca^{2+} + OH^{-} \quad [1]$$

Release water Mg^{2+} concentration decreases as *CaO* dosage increases. The decrease in Mg^{2+} concentration is due to the co-precipitation of Mg^{2+} with calcium carbonate minerals and at a higher *pH* (*pH*>10.5) by the precipitation of Brucite ($Mg(OH)_2$).

Sodium pore fluid concentrations have a similar response to the addition of *CaO* as Ca^{2+} but for different geochemical mechanisms. Sodium concentrations decrease with the initial addition of *CaO* until 0.4 g/L of *CaO* is added. Sodium concentrations increase with further *CaO* addition

and are slightly higher than original pore fluid concentrations at 1.0 g/L. Changes in sodium concentrations are likely the result of cation exchange reaction with clay minerals in the tailings. The initial drop in calcium concentration due to calcite precipitation drives calcium off exchange sites allowing sodium to occupy exchange sites reducing their solution concentration. As the tailings sediments have low cation exchange capacity (4 to 12 meq/100g) only a small amount of exchange can occur resulting in a relatively small decease in sodium concentration. As the calcium concentration begins to increase in solution at 0.6 g/L *CaO* addition, sodium pore fluid concentration increases as calcium replaces sodium on the exchange sites. Sodium pore fluid concentrations end up slightly higher than the original tailings fluids due to the sodium that was bound to exchange sites at the original neutral pH conditions. As the sediments have low exchange capacity and no highly soluble sodium and mineral phases, concentrations of sodium are unlikely to rise significantly with further *CaO* addition.

Release water Na^+ concentration slightly decreases with an increase in *CaO* dosage up to the 0.4 to 0.6 g/L level. As the *CaO* dosage increases beyond the 0.6 g/L level the release water Na^+ concentration slightly increases. Using the current NST process, Na^+ concentration could be reduced from 620 mg/L to about 520 mg/L. Reduction in Na^+ concentration in the amount of about 100 mg/L is an important trend to improve the quality of the recycle water. Addition of chemical aids (caustic or organic acids salts, the hydrolysis of which causes the *pH* increase) into the extraction process results in the accumulation of Na^+ ions in the recycle water, which has a detrimental effect on the efficiency of the extraction process.

Release water HCO_3^- concentration decreases sharply by an increase in *CaO* dosage up to 0.4 g/L level then apparently increases in concentration as *CaO* dosage increases above 0.8 g/L (Figure 13). These measurements are an artifact of the alkalinity titration method and at *CaO* dosages above 0.6 g/L all the carbonate alkalinity has been consumed in the precipitation of calcite minerals. At *CaO* dosages of 1.0 g/L the *pH* rises to 12 and all inorganic species would be in the CO_3^{2-} species form. At *pH* conditions above 10.4 the non carbonate species $Ca(OH)_2$ accounts for

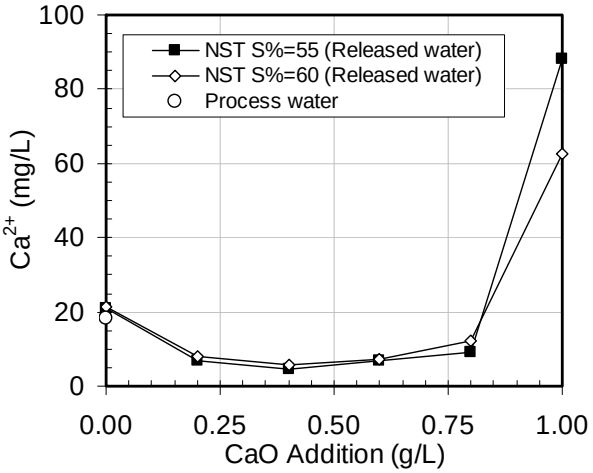

Figure 10. Effect of *CaO* dosages on release water Ca^{2+} concentration.

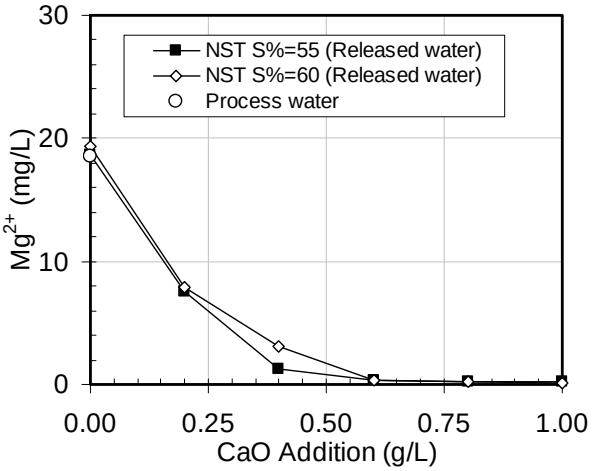

Figure 11. Effect of *CaO* dosages on release water Mg^{2+} concentration.

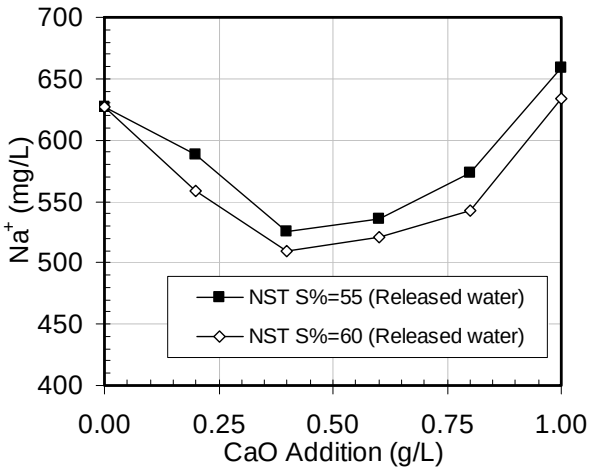

Figure 12. Effect of *CaO* dosages on release water Na^+ concentration.

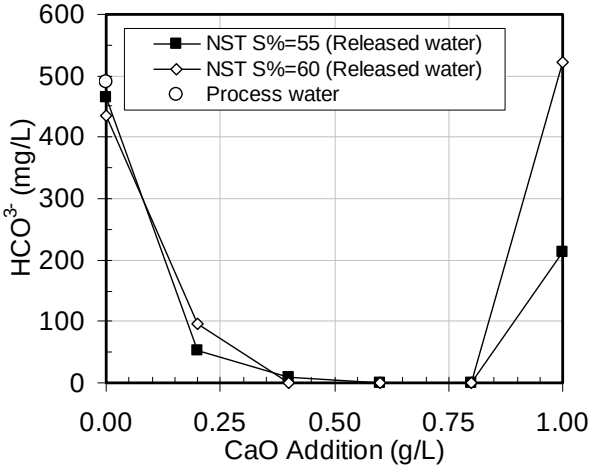

Figure 13. Effect of *CaO* dosages on release water HCO_3^- concentration.

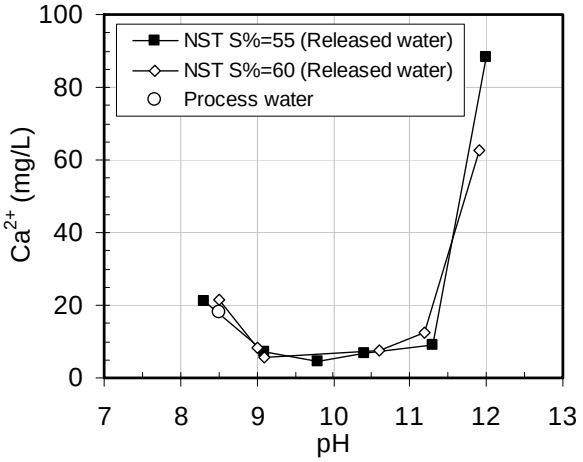

Figure 14. Release water Ca^{2+} concentration as a function of *pH*.

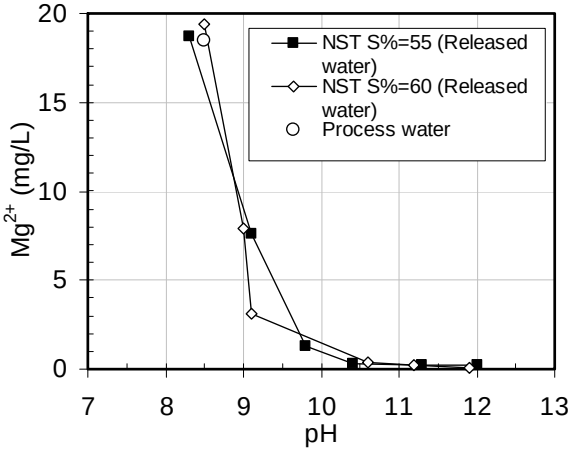

Figure 15. Release water Mg^{2+} concentration as a function of *pH*.

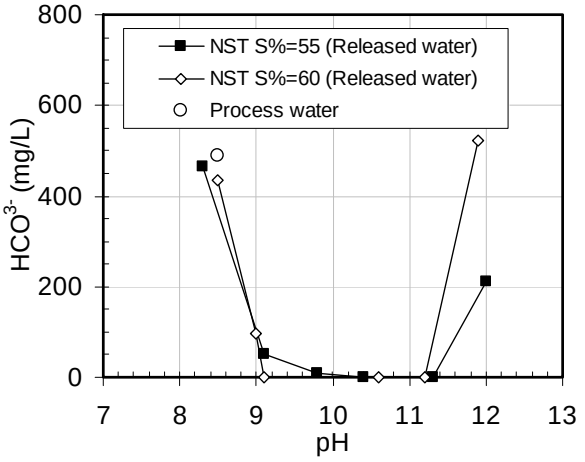

Figure 16. Release water HCO_3^- concentration as a function of *pH*.

the majority of the acid titratable alkalinity in the pore fluids. PHREEQC analysis of the pore fluids confirms that the alkalinity measurement for samples SCL8 and SCL-13 are the result of non-carbonate alkalinity.

Effect of *CaO* dosage on release water chemistry can be detected by measuring the pH of the NST mix. Considering the importance of *pH* measurement as an example, plots of release water Ca^{2+}, Mg^{2+} and HCO_3^- concentrations as a function of pH are presented in Figures 14, 15 and 16 respectively.

In summary, the proposed NST process uses low cost *CaO* ($130/ton) for the production of NST from the blend of cyclone underflow and thickener underflow and simultaneously improves the release water quality. Preliminary extraction tests performed using the release water produced by this NST process (containing lesser amounts of Ca^{2+}, Mg^{2+} and Na^+ concentrations) showed significant improvement in the efficiency of the extraction process. Further studies on this NST have to be performed to confirm this effect in greater detail.

SUMMARY AND CONCLUSIONS

Based on thirteen standpipe tests and water chemistry analyses the following conclusions are arrived:

- The NST production process with *CaO* additive can produce nonsegregating tailings from the

blend of Aurora Mine's Cyclone Underflow and Thickener Underflow tailings.

- Laboratory observation suggests that 0.6 g/L *CaO* dosage is likely a minimum value for preventing segregation of the NST.
- For the production of NST, *CaO* should be used at a minimum of 0.6 g/L dosage as *CaO* addition greater than 0.6 g/L improves the dewatering rate of the NST.
- *CaO* dosages of 1.0 g/L greatly increases the initial rate of water release from the NST and results in complete water release in a short time.
- Release water produced from the NST contains lower concentrations of Ca^{2+}, Mg^{2+} and Na^{+} ions, which makes it more acceptable for the extraction process.
- Excess amounts of *CaO* (or $Ca(OH)_2$) present in the release water could be used for the softening of the bicarbonate hardness of the fresh make-up water.

ACKNOWLEDGEMENTS

The authors are grateful for the financial support from the University of Alberta and APEX Engineering Inc.

REFERENCES

Caughill, D.L., Morgenstern, N.R., and Scott, J.D. 1993. Geotechnics of Nonsegregating Oil Sand Tailings. Canadian Geotechnical Journal, 30: 801-811.

Chalaturnyk, R.J., Scott, J.D., and Ozum, B. 2002. Management of Oil Sands Tailings. Petroleum Science and Technology, 20(9&10): 1025-1046.

Matthews, J.G., Shaw, W.H., MacKinnon, M.D., and Cuddy, R.G. 2002. Development of composite tailings technology at Syncrude. International Journal of Surface Mining, Reclamation, and Environment, 16(1): 24-39.

Ozum, B., Chalaturnyk R.J., and Scott J.D. 1999. Production of Nonsegregating Tailings. CONRAD's Tailings Management Workshop, July 7, Fort McMurray, Alberta Canada.

Scott J.D., Donahue, R., Blum, J.G., Paradis, T. G., Komishke, B., and Ozum, B. 2007. Production of Nonsegregating Tailings with *CaO* or *CaO* and CO_2 for Improved Recycle Water Quality. CONRAD's Water Usage Workshop, November 21 & 22, Calgary, Alberta Canada.

Sridharan, A., and Prakash, K. 2001. Consolidation and Permeability Behavior of Segregated and Homogeneous Sediments. Geotechnical Testing Journal, 24 (1): 109-120.

ELECTROKINETIC SEDIMENTATION AND DEWATERING OF CLAY SLURRIES

Eltayeb Mohamedelhassan
Dept. of Civil Engineering, Lakehead University, Thunder Bay, Ontario, Canada

ABSTRACT

An experimental study was conducted on the effectiveness of electrokinetic sedimentation and dewatering of two laboratory-prepared clay slurries. The two slurries were kaolinite clay slurry and kaolinite/bentonite mixture slurry. Two identical Plexiglas columns, 200 mm inside diameter and 900 mm high, were designed and manufactured for the study. One column was used for electrokinetic testing and the other for a control test. The solids content of the slurry at mixing was 20% (mass/mass). After poured in the column, the slurry was allowed to settle and drain by gravity for 24 hr, which resulted in a solids content of 76% for the kaolinite slurry and 28% for the kaolinite/bentonite slurry. An electric field intensity of 100 V/m was then applied in the electrokinetic testing column via pair of graphite electrodes. The test was performed in two phases: sedimentation and dewatering. The duration of the test was 76 hr for the kaolinite slurry and 52 hr for the kaolinite/bentonite slurry. The volume reduction in the kaolinite slurry by electrokinetic treatment was 58.7% compared to 25.7% in the control. The corresponding average solids content in the electrokinetic column was 306% compared to 114% in the control. The volume reduction in the kaolinite/bentonite slurry by electrokinetics was 66.3% while the reduction was only 2.9% in the control. The corresponding average solids content after electrokinetic treatment was 105% compared to 29% in the control.

INTRODUCTION

There are numerous engineering applications that required settling acceleration, dewatering, and volume reduction. Such applications include the dewatering of dredged river sediments, dewatering of phosphatic waste clays from phosphate industries, primary and secondary settling processes in waste water treatment plants, and dewatering of mine tailings. In recent years, accelerating the settling of soil particles and recovering water from oil sand tailings has received increasing attention from the oil sand industry in Canada.

The application of a direct current electric (dc) electric field to a soil-water-electrolyte system incites three distinct electrokinetic transport mechanisms: electromigration, electrophoresis, and electroosmosis. Electromigration is the migration of ions in the soil pore fluid toward the opposite charged electrode; electrophoresis the transport of charged particles (become significant when the techniques is employed in the treatment of slurries or when surfactants are introduced in the pore fluid to form charged particles); and electroosmosis is the transport of soil pore fluid, generally toward the negative electrode (cathode).

The research of using electrokinetic sedimentation and dewatering started in the 1960's. The United States Bureau of Mines pioneered the research and development of electrokinetic dewatering of tailings from minerals and coal processing as reported in the successful field and laboratory applications by Sprute and Kelsh (1975, 1976). Electrokinetic dewatering of clayey suspensions from sand washing plants and mineral processing suspensions has been studied over the past years (Lockhart 1986; Sunderland 1987). Shang (1997) investigated in a laboratory study electrokinetic sedimentation and dewatering of clay slurries as engineered soil cover. The use of electrokinetic in the sedimentation and dewatering of contaminated sediments was investigated in laboratory studies by many researchers over the last fifteen years (e.g. Sauer and Davis 1994; Buckland et al. 2000; Mohamedelhassan and Shang 2001; Chung and Kamon 2006).

The sedimentation velocity of a soil suspension can be expressed as (McRoberts and Nixon 1976):

$$U = \beta \, u \, n^r \qquad (1)$$

where U (m/s) is the suspension settling velocity, u (m/s) is the particle settling velocity, β is a factor representing the statistical average of velocities of all particles, n is the porosity of the suspension, and r is the coefficient of sedimentation.

Electrokinetics can potentially enhance the dewatering of fine suspensions by two mechanisms: accelerating the sedimentation by increasing the movement of solid particles suspended in water (i.e. electrophoresis); and by transporting the water molecules in the soil pores (i.e. electroosmosis). Based on the principles of electrochemistry, most surfaces of solids become negatively charged when they are in contact with water. Further, clay particles carry negative charges due to isomorphous substitution. Therefore, when dc electric field is applied on a clay suspension, clay particles will move toward the positive electrode (anode) by electrophoresis. The velocity of individual particle induced by electrophoresis is given by (Russel et al. 1989):

$$u_{ep} = \frac{\varepsilon_w \zeta E}{\mu} \quad (2)$$

where u_{ep} (m/s) is the particle velocity induced by electrophoresis, ε_w (F/m) is the permittivity of water, ζ (V) is the zeta potential, μ (N s/m^2) is the viscosity of water, E (V/m) = - ∇P is the electric field intensity in the sediment, and P (V) is the electric potential. In electrokinetic enhanced sedimentation process, the particle settling velocity (u in equation 1) is given by:

$$u = u_g + u_{ep} \quad (3)$$

where u_g is the settling of individual particle by gravity. If the electric potential is maintained after the electrokinetic sedimentation process has been completed, electroosmosis will drive the water in the soil pores toward the cathode. For open drainage condition, the electroosmotic flow is expressed by the empirical relationship (Mitchell 1993):

$$Q_{eo} = k_e E A \quad (4)$$

where Q_{eo} (m^3/s) is the electroosmotic flow rate, k_e (m^2/sV) is the electroosmotic permeability, and A (m^2) is the cross-sectional area of the soil normal to the direction of flow.

In this study, the effectivness of electrokinetics in terms of accelerating the sedimentation by electrophoresis and then enhancing the dewatering and consolidation by electrososmosis for two clay slurries was investigated. For each of the electrokinetic tests performed in the study, an identical control test with no applied electric field was conducted to provide based line date for comparison.

EXPERIMENTAL PROGRAM

Material Properties

Two clay slurries were prepared for the study. The slurry was prepared at an initial solids content of 20% (mass of dry soil/mass of water) using tap water. The first clay slurry was prepared using inorganic clay obtained from Plainsman Clay in Lethbridge, Alberta. The predominant clay mineral of the soil is kaolinite (hereafter referred to as kaolinite clay). The second slurry was prepared by a clay mixture of 87.5% Plainsman clay and 12.5% commercial bentonite clay (hereafter referred to as kaolinite/bentonite mixture. Table 1 summarises the geotechnical properties of the two clays.

Table 1. Characteristics of the kaolinite clay and kaolinite/bentonite mixture

Property	Kaolinite clay	Kaolinite/bentonite mixture
Specific gravity	2.63	2.62
Liquid limit	39	258
Plastic limit	19	89
Sand (%)	4	3
Silt (%)	59	55
Clay (%)	37	42

Experimental Apparatus

Two identical sedimentation/dewatering columns were designed and constructed for the study. One column was used for electrokinetic testing and other was used as a control. The column was made of a 6 mm thick and 200 mm inside diameter Plexiglas cylinder and is 900 mm high with a total volume capacity of 28.3 litre. Figure 1 shows the schematic of the two columns. The length of the column will allow for accurate measurement and observation during the sedimentation and dewatering processes. The diameter of the column was designed to be large enough to eliminate the boundary effect during the sedimentation and dewatering processes. The electrode were made of 2 mm thick flexible graphite cut to the inside diameter of the column. Graphite was selected for the electrodes for its resistant to corrosion and oxidation. The electrodes were perforated with 6 mm diameter holes to allow gases formed

around the electrode form electrochemical reactions to escape and to allow water to pass through during the dewatering process. Styrofoam disc of similar diameter to the electrode was attached to top electrode to allow it to float over the slurry as shown in Figure 1. The electrodes were

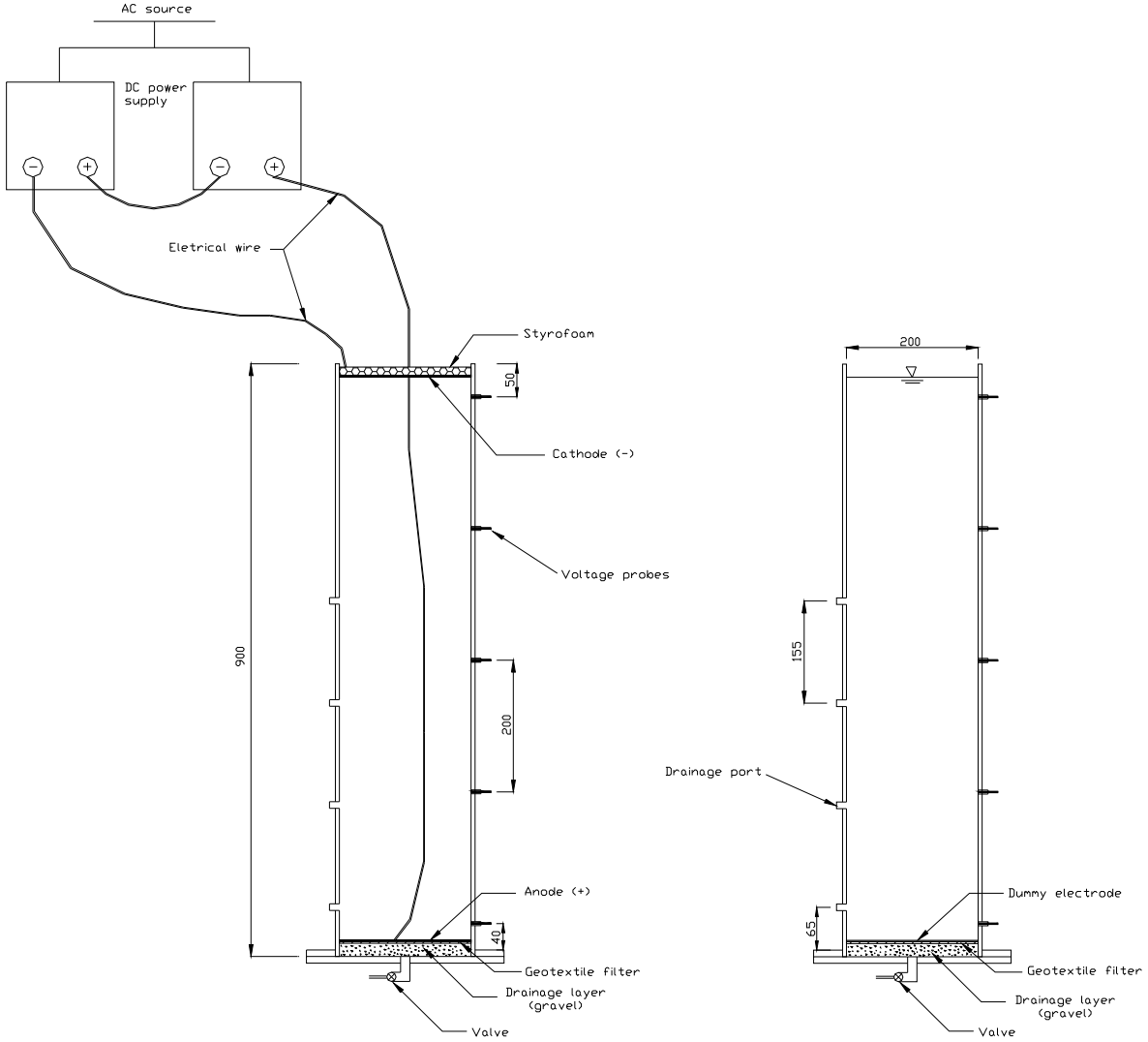

(a) Electrokinetic test (b) Control test

Figure 1. Schematic of the sedimentation/dewatering columns – sedimentation phase configuration

arranged in parallel to generate an approximately uniform electric field along the axis of the column. Five voltage probes were installed at 200 mm intervals to measure the electric potential along the column. In addition, four sampling ports were also installed along the column at 155 mm intervals to allow sampling along the column height. Two dc power supplies each with a ratings of 60 V and 4 A were contacted in series, as shown in Figure 1, for a maximum ratings of 120 V and 4 A.

Testing Procedure

A 20-mm drainage layer of clean gravel, 4 to 6 mm in grain size diameter, was placed at the bottom of the column and was overlain by a geotextile filter as shown in Figure 1. A perforated graphite electrode was placed on the top of the geotextile filter in the column used for the electrokinetic test. A dummy electrode made of high density polyethylene (HDPE), with identical dimensions and perforated pattern to that of graphite electrode, was used in the column of the control test (see

Figure 1). The slurry was prepared by mixing dry clay and tap water at a ratio of 20% (mass of dry soil/mass of water). A mechanical mixture was used to insure a uniform and consistent slurry. The slurry was then poured into the two columns placed side-by-side. The clay slurry was allowed to settle and drain by gravity for 24 hr, after which the drainage valve at the bottom of the column was closed. At end of this period, the height of the samples in the columns were 220 and 219 mm for the kaolinite clay slurry and 515 and 517 mm for the kaolinite/bentonite mixture slurry, compared with their original height of about 700 mm. This corresponded to an average solids content of ~76% for the kaolinite clay slurry and ~28% for the kaolinite/bentonite mixture slurry.

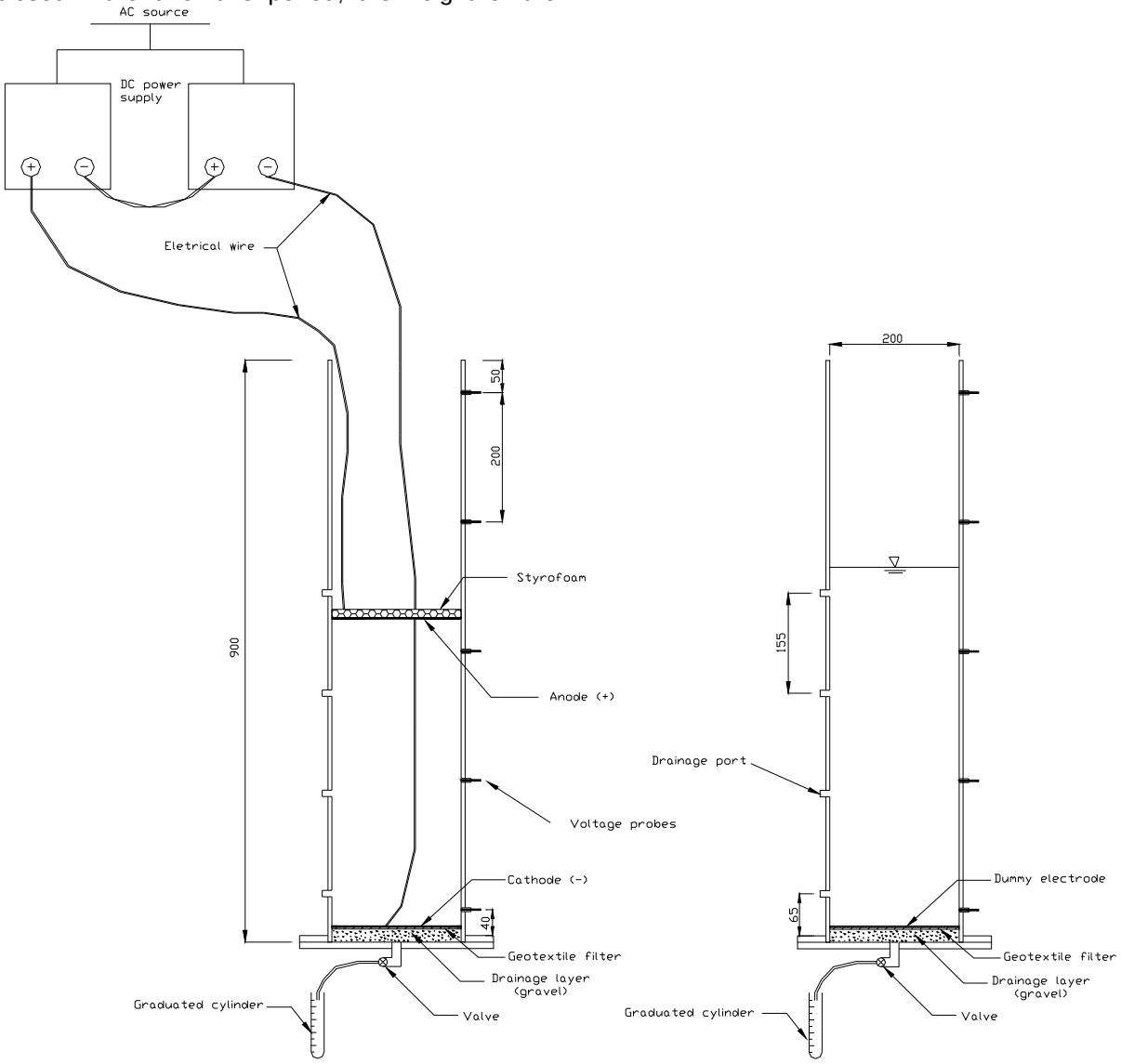

(a) Electrokinetic test (b) Control test

Figure 2. Schematic of the sedimentation/dewatering columns – dewatering phase configuration

The tests were conducted in two phases, namely, sedimentation and dewatering (or consolidation). In the electrokinetic testing column, a continuous electric field intensity of 100 V/m was applied on the slurry, directed upward (top cathode (-) and bottom anode (+)), as shown in Figure 1. Since clay particle are in general negatively charged, the

movement of particles is expected to be downward (toward the anode) due to electrophoresis. The settlement with time was recorded through reading the mudline height. When the consecutive mudline readings taken over a 4 hr period were identical, electrokinetic sedimentation was considered complete. The sedimentation phase lasted 28 hr in the kaolinite slurry and lasted 40 hr in the kaolinite/bentonite slurry.

In the second phase (dewatering or consolidation), the surface water above the mudline was first decanted and the drainage value at the bottom of the column was opened. In the electrokinetic testing column, the electrode configuration was reversed to top anode (+) and bottom cathode (-) as shown in Figure 2 and then an electric field intensity of 100 V/m was applied. Under this electrode configuration, the water flow induced be electroosmosis was downward (similar to the flow by gravity) and expelled from the drainage valve. The drained volume of water was collected in a graduated cylinder and recorded during the test. As the soil settled and consolidated, the distance between the electrodes decreased and the electric field intensity was maintained at 100 V/m by adjusting the applied voltage every two hours during the test. The electrokinetic dewatering phase was considered completed when no water was collected in the graduated cylinder over a 4 hr period. The dewatering phase lasted 48 hr in the kaolinite clay slurry test and 12 hr in the kaolinite/bentonite mixture slurry test.

RESULTS AND DISCUSSION

Figure 3 shows the mudline height versus time during the sedimentation phase of the kaolinite clay slurry. As shown in the figure, the mudline height decreased from 219 mm at the beginning of the sedimentation phase to 142 mm in electrokinetic test and decreased from 220 mm to 193 mm in the control test after 28 hr. This represented a decrease of 35.1% in mudline height of the electrokinetic test compared to 12.4% in the control. The settlement in the electrokinetic test is attributed to gravitation settlement (similar to the control test) and electrophoresis, which enhanced the movement of the negative clay particles toward the positively charged anode in the bottom of the column, as shown in Figure 1. Figure 3 clearly shows that most of the sedimentation occurred in the first 20 hr of testing.

Figure 4 shows the volume of water collected in the graduated cylinder during the dewatering (or consolidation) phase for the kaolinite clay slurry. The figure shows that 1618 cm^3 of water was drained in the electrokinetic test compared to 924 cm^3 for the control test during 48 hr of testing. The volume of water drained in the electrokinetic test is attributed to gravity (similar to the control) and electroosmosis, which transported the water in the soil toward the negatively charge cathode in the bottom of the column as shown in Figure 2.

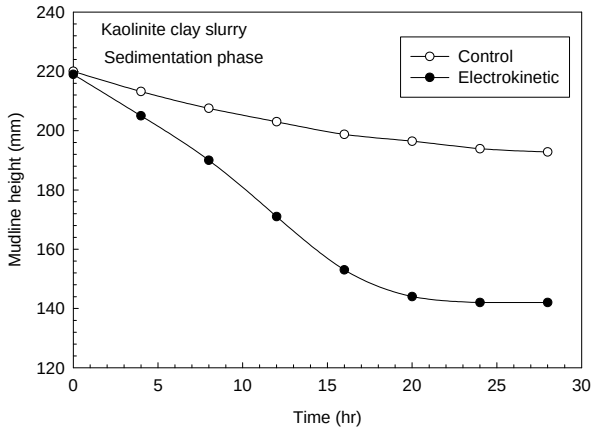

Figure 3. Mudline height vs. time for the kaolinite clay slurry during the sedimentation phase

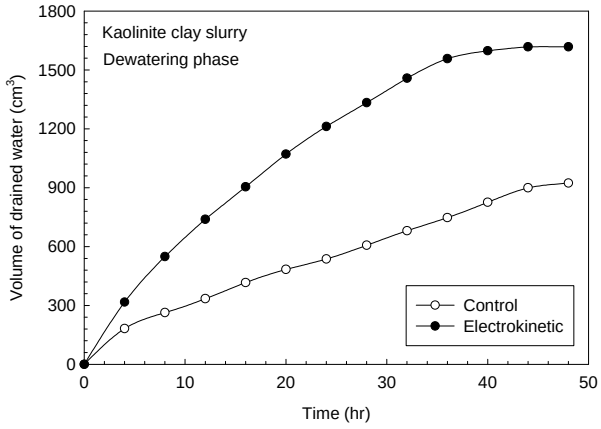

Figure 4. Volume of drained water vs. time for the kaolinite clay slurry during the dewatering phase

The change in volume of the kaolinite clay slurry during the sedimentation and dewatering phases is shown in Figure 5. The volume change is calculated as the volume of water above the mudline during the sedimentation phase and the

volume of drained water during the dewatering phase. Figure 5 show that the total volume of the slurry in the electrokinetic test decreased by 58.7% due to sedimentation by electrophoresis and gravity (35.2% in 28 hr) and due to dewatering by electroosmosis and gravity (23.5% in 48 hr). In the control test, the volume decreased by 25.7% due to gravitational sedimentation (12.4%) and gravitational dewatering (13.3%). The final average solids content was ~306% in the electrokinetic test column and ~114% in the control test column compared to the initial solids content of 76%.

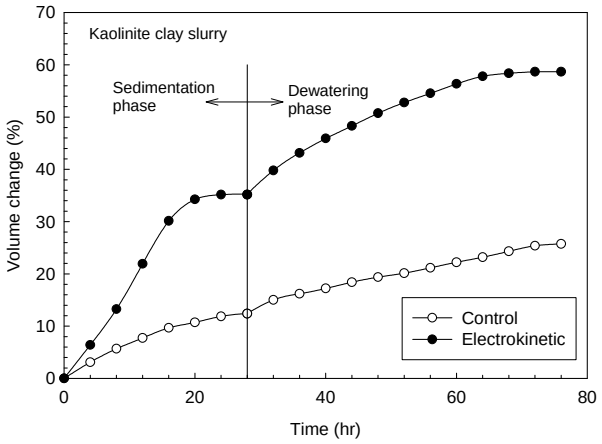

Figure 5. Volume change in the kaolinite clay slurry vs. time

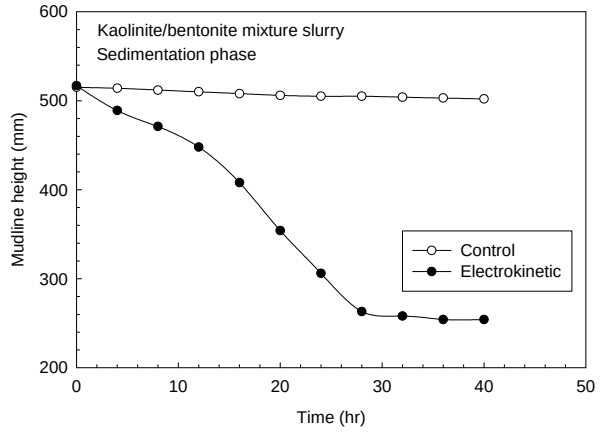

Figure 6. Mudline height vs. time for the kaolinite/bentonite mixture slurry during the sedimentation phase

Figure 6 shows the mudline height versus time during the sedimentation phase of the kaolinite/bentonite mixture slurry. As shown in the figure, the mudline height decreased from 517 mm at the beginning of the sedimentation phase to 254 mm in electrokinetic test and from 515 mm to 502 mm in the control test after 40 hr of testing. This represented a decrease of 50.9% in electrokinetic test compared to only 2.5% in the control test. Thus, the settlement in the electrokinetic test is attributed primarily to electrophoresis since the gravitation settlement was very small as seen by the control test result.

Figure 7 shows the volume of water collected in the graduated cylinder during the dewatering phase for the kaolinite/bentonite clay slurry. The figure shows that 2500 cm^3 of water was drained in the electrokinetic test compared to 66 cm^3 for the control during 12 hr of testing. The volume of water drained in the electrokinetic test is attributed primarily to electroosmosis since the gravitation drainage contribute to 66 cm^3 only.

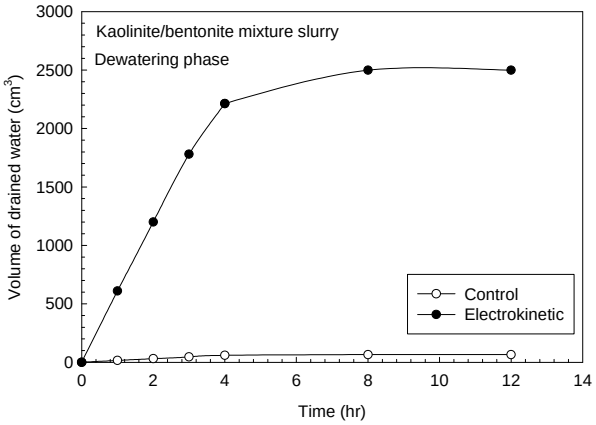

Figure 7. Volume of drained water vs. time for the kaolinite/bentonite mixture slurry during the dewatering phase

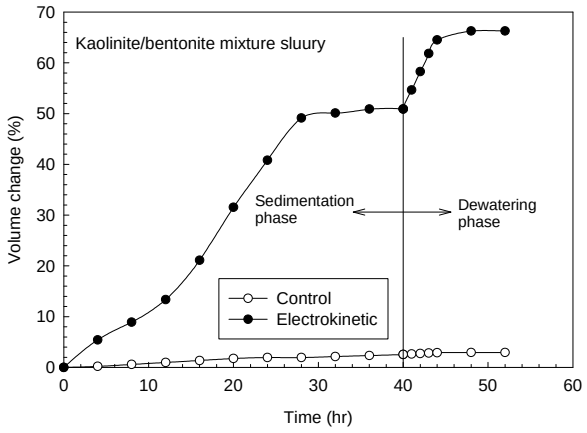

Figure 8. Volume change in the kaolinite/bentonite mixture slurry vs. time

Figure 8 shows the change in volume of the kaolinite/bentonite slurry during the sedimentation and dewatering phases. As seen in the figure, the volume of the slurry decreased by 66.3% due to sedimentation (50.9% in 40 hr) and dewatering (15.4% in 12 hr). It is obvious from Figure 8 that the contribution of gravity in volume change of the electrokinetic test was very small as the control test shows that the volume change by gravity was 2.9% (2.5% by sedimentation and 0.4% by dewatering). Therefore, the sedimentation in electrokinetic test was primarily due to electrophoresis and the dewatering was primarily due to electroosmosis. The final average solids content was ~105% in the electrokinetic test column and ~29% in the control test column compared to the initial solids content of 28%.

CONCLUSIONS

An experimental study was performed on the effectiveness of electrokinetic sedimentation and dewatering of laboratory-prepared kaolinite clay slurry and kaolinite/bentonite mixture slurry. The electric field intensity during the electrokinetic test was 100 V/m. The results of the study have shown that:

- The volume of the kaolinite slurry in the electrokinetic test column decreased by 58.7% compared to a decrease of 25.7% in the control test after 76 hr.
- The average solids content of the kaolinite slurry increased from initial value of 76% to 306% in the electrokinetic test and 114% in the control test.
- The volume of the kaolinite/bentonite slurry in the electrokinetic test decreased by 66.3% compared to a decrease of 2.9% only in the control test after 52 hr.
- The average solids content of the kaolinite slurry increased from initial value of 28% to 105% in the electrokinetic test and only 29% in the control test.
- As compared with the control, electrokinetic sedimentation and dewatering was effective for both slurries. However, its effectiveness was superior in the sedimentation and dewatering of the kaolinite/bentonite mixture slurry.

ACKNOWLEDGEMENTS

The author would like to acknowledge the contribution of J. Bromwich, M. Dokic, and A. Menard to performing the experiments.

REFERENCES

Buckland, D.G., Shang, J.Q., and Mohamedelhassan, E. 2000. Electrokinetic sedimentation of contaminated Welland river sediment. Canadian Geotechnical Journal, 37: 735-747.

Chung, H.I., and Kamon, M. 2006. Electrokinetic dewatering and sedimentation of dredged contaminated sediment. Journal of ASTM International, 3(6): 268-273.

Lockhart, N.C. 1986. Electro-dewatering of fine suspensions. Advances in Solid-Liquid Separation, pp. 241-274.

McRoberts, E.C., and Nixon, J.F. 1976. A theory of soil sedimentation. Canadian Geotechnical Journal, 13: 294-310.

Mitchell, J.K. 1993. Fundamental of soil behaviour. 2nd ed. John Wiley & Sons, New York.

Mohamedelhassan, E., and Shang, J.Q. 2001. Analysis of electrokinetic sedimentation of dredged Welland river sediment. Journal of Hazardous Materials, 85: 91-109.

Russel, W.B., Saville, D.A., and Schowalter, W.R. 1989. Colloidal dispersions. Cambridge University Press, Cambridge, U.K.

Sauer, J.E., and Davis, E.J. 1994. Electrokinetically enhanced sedimentation of colloidal contaminants. Environmental Science and Technology, 28: 737-745.

Shang, J.Q. 1997. Electrokinetic dewatering of clay slurries as engineered soil covers. Canadian Geotechnical Journal, 24: 78-86.

Sprute R.H., and Kelsh, D.J. 1975. Limited field test in electrokinetic densification of mill tailings. US Department of the Interior, US Bureau of Mines Report of Investigations 8034.

Sprute R.H., and Kelsh, D.J. 1976. Dewatering and densification of coal waste by direct current-laboratory tests. US Department of the Interior, US Bureau of Mines Report of Investigations 8197.

Sunderland, J.G. 1987. Electrokinetic dewatering and thickening. II. Thickening of ball clay. Journal of Applied Electrochemistry, 17:1048-1056.

EXPERIMENTAL MEASUREMENTS OF TURBULENT SAND AND SLURRY JETS

Neil Hall, Mohammed Elenany, Dr. David Zhu, Dr. N Rajaratnam

ABSTRACT

This paper presents the results of experiments with turbulent sand and sand – water slurry jets impinging vertically into a stagnant water body. The sand jets had initial concentrations of 60 % by volume, and the slurry jets had initial concentrations between 11.6 and 21.0 % by volume. The sand used for the experiments was silica sand with a D50 of 206 ± 54 um. The concentration and velocity profiles of the jets were measured at a distance of 10 to 65 jet diameters, using a novel fibre optical probe capable of making simultaneous concentration / velocity measurements. Concentrations measured within these experiments varied from approximately 12 to .1%, with the highest concentrations found on the jet centreline, and the lowest found at the exterior of the jet. Both jets were found to have self-similar Gaussian profiles. The axial sand velocity profile decreased significantly before reaching a plateau region. The 'terminal' axial sand velocity within this region varies somewhat depending upon sand mass flux, and is between .32 and .43 m/s. The sand velocity profiles were wider than the sand concentration profiles. This may be due to the inertia of the sand particles affecting the concentration profile. The momentum flux of the sand within the sand jets was found to decrease sharply, followed by a constant flux below a depth of 25 to 30 jet diameters. The slurry jets were found to behave similarly, with a constant momentum flux below 20 jet diameters.

INTRODUCTION

Turbulent jets have many applications in engineering, and have been extensively studied. When a second solid phase (e.g. sands) is added to the jet, it is termed a two phase jet, and its properties change significantly. The understanding of two phase jets is important for activities such as the pumping of tailings into settling tanks, dredging and island building operations, the discharge of industrial or urban waste, spray injections, and pulverized coal combustion. As a result, many studies have been carried out on this subject (Brush, 1962; Parthasarathy and Faeth, 1987; Muste et al., 1998; Mazurek et al., 2002; Jiang et al., 2005; Virdung and Rasmuson, 2007). However, the difficulty in measuring and modelling the properties of these jets has limited the studies to particle concentrations of less than a few percent. At such low concentrations, it is assumed that the particles have no significant interactions. Also, traditional measurement techniques such as particle image velocimetry do not work at higher concentrations. Studies of two phase jets with high concentrations are very limited, and lack detailed measurements.

This paper is a study of the properties of highly concentrated two phase sand–water jets. An optical probe used for studying particle movements in fluidized bed reactors (Jinzhong et al. 2003a,b) was adapted for this study. The probe was developed to be capable of making simultaneous measurements of concentration, velocity and flux within these conditions.

This paper presents the results of sand concentration and velocity measurements within sand and slurry jets. Two sand jets are studied,with a sand concentration of 60 % by volume and with nozzle diameters of 8.2 mm and 13.7 mm. Four slurry jets are studied, with initial sand concentrations varying between 11.6 and 21 % by volume, and with nozzle sizes of 15.5 mm and 9 mm.

EXPERIMENTAL DESIGN

Setup

Sand jet and slurry jet experiments were conducted in a rectangular glass tank, 1.25 m wide, 2.50 m long and 1.20 m deep. The tank was filled with tap water. For the sand jet experiments, a metal cone, 0.50 m in upper diameter, 0.20 m in lower diameter and 0.5 m in length, fitted with a conical shape hopper at the bottom, was used as a sand feeder. See Figure 1 for the tank and sand feeder

arrangement. The cone was filled with dry sand; sand with a median diameter D_{50} equal to

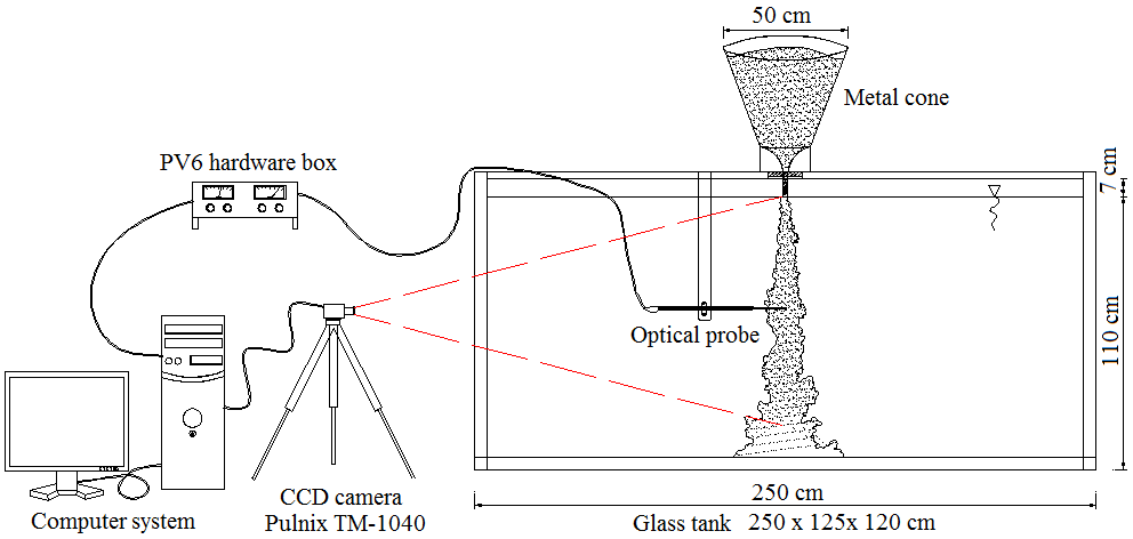

Figure 1: Experimental arrangement for the sand jet experiments.

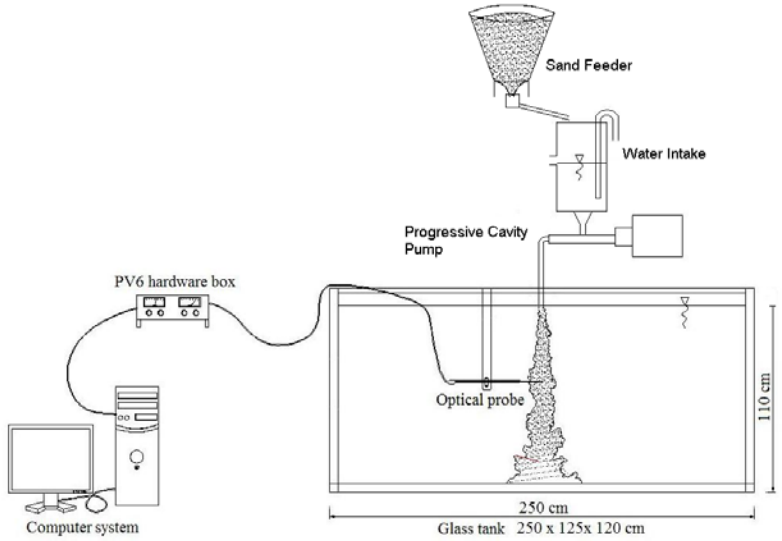

Figure 2: Experimental arrangement for the slurry jet experiments.

206 ± 54 μm was used. Two different nozzles with diameters, d, of 12.6 and 19.2 mm were fixed to the bottom of the hopper. The sand feeder was mounted above the water tank with the bottom of the nozzle located 75 mm above the water surface. Measurements were taken by releasing the plug in the bottom of the hopper, and allowing the sand to jet into still water in the tank. After allowing the sand jet to fully develop in the tank (about 30 seconds), the simultaneous measurement of concentration and velocity at each point took 40 seconds. Between measurements, the jet was stopped, a board was inserted into the water, and the water was allowed to settle for 4 minutes. This prevented the development of a secondary flow, and ensured that the jet did not meander.

To form the slurry jet, sand was fed from a syntron C2R3S sand feeder into a cylindrical mixing chamber and combined with tap water. The turbulence of the tap water jet entering the mixing chamber ensured effective sand mixing. An overflow pipe maintained a constant water level. This slurry was gravity fed into a 1Hp Seepex 1-6L-BN progressive cavity pump. A knuckle joint, combined with a 1 m vertical pipe fed the slurry to the water surface. See Figure 2 for a diagram of the setup. The slurry jet was discharged into the centre of the tank, with the nozzle 5 mm below the water level. To ensure that a vortex did not develop around the jet nozzle, a piece of hog's hair was cut to fit in the water on two sides of the nozzle.

A novel fibre optic probe, used in fluidized bed studies at UBC by Jinzhong l. (2003a), was used to make simultaneous measurements of both the sand particle velocities and concentrations. The probe's tip is 4 mm in diameter. Each fibre bundle is 1 mm wide, and the two bundles are separated by 2 mm. The length of the probe's tip is 40 cm. The probe's electronics create a light source, which travels along the fibre bundle to the tip of the probe and is emitted. Reflections from passing particles return to the fibre bundle and travel back to a photo diode. The voltage spike from this reflection is amplified within the probe, and transmitted to the PV6 hardware box for digitization.

The average particle concentration within a fluid can be calculated as the average voltage from one photo diode and fibre bundle. To calculate particle velocities, two sets of fibre bundles are required. The particles must be travelling perpendicular to the axis of the probe, and along the same plane as the two fibre bundles. Velocities are computed by cross correlating the two voltage signals from the two fibre bundles. The resulting mean time delay provides an accurate velocity measurement if the probe is properly calibrated.

Calibrations

Calibration is a vital component of taking measurements with the fibre optic probe. There are two components to the probe's calibration. A velocity calibration is done to correct the probe's velocity measurements. This is required since the separation distance between the two fibre bundle's measurement volumes is not well defined, and cannot be accurately measured. This calibration only needs to be done once, assuming that the probe is not altered. The result of this calibration is a single calibration coefficient, used to adjust all the velocity data.

A concentration master calibration is done to provide a relationship between the average voltage output of the probe, and the volumetric particle concentration. This calibration was done regularly to ensure that it remained valid. The calibration is done by taking a series of measurements of sand slurries of known, constant concentration flowing past the probe tip (the calibration curve is non-linear, and requires 5 to 6 points to accurately define). The method used to calibrate the probe involved placing the probe, tip down, into a flask of evenly mixed sand and glycerine. The sand was kept evenly suspended and moving using a propeller mixer, rotating at a low rpm in the bottom of the flask (far from the probe tip to avoid reflection).

Glycerine was used instead of water because of the difficulty in evenly mixing sand and water. To correct for the difference between the reflective index of glycerine/sand and water/sand, all sand jet measurements were performed as profiles across the jet, so that the sand mass flux could be computed. Since the true mass flux is known, the concentration measurements were then corrected with a correction factor.

A secondary calibration procedure was implemented to ensure that the probe's measurements did not vary due to suspended particles in the tank water (a slight cloudiness created from the sand). This involved taking probe measurements in still water before and after each series of measurements (typically 10 to 15 measurements in a horizontal profile across the jet). These measurements were compared to the zero measurement in the concentration master calibration to provide a small correction.

Measurement Procedures

The characteristics of the sand and slurry jets were measured using two methods. The first method was to measure the vertical centreline profile. This was achieved by taking point measurements down the centreline of the jet, with a spacing of 5 cm near the water surface, and 10 cm farther from the water surface. The

second method involved measuring horizontal profiles of the jet at different depths below the water surface, with measurements taken every 1 or 2 cm, to allow for 10 to 20 samples per profile. The results from the horizontal profiles (peak value, and jet width) are more accurate than the vertical profile data, since the results from the horizontal profiles are calculated from a least squares fit of the data.

For the sand jet experiments, each data point is the average of 5 measurements. Each measurement is a file of continuous sampling for 8 seconds at a sampling rate of 3.9 kHz. For the slurry jet experiments, each data point is the average of 10 measurements. Each measurement is a file of continuous sampling for 2 seconds at a sampling rate of 15.6 kHz. The sampling time and sampling frequency is important for three reasons: (1) A large sample of data improves the accuracy of the result. (2) A high sampling frequency is required to obtain an accurate velocity measurement without aliasing. (3) The measurement file must be long enough to encompass numerous turbulent eddies, to allow for an accurate average measurement.

Six horizontal cross sections were selected for the 12.5 mm sand jet. They were located at: 20, 33.5, 40, 50, 60 and 70 cm below the water surface. Cross sections for the 19.2 mm jet were located at 20, 30, 40, 60, 70 and 80 cm below the water surface. To test repeatability, one profile was repeated from each experiment (a distance of 40 cm from the water surface for the smaller nozzle and 30 cm for the larger nozzle). Cross sections for all slurry jet experiments were located at 10, 20, 30, 40, 50, and 60 cm below the water surface. To measure repeatability with the slurry jet, one horizontal profile, at 20 cm depth, was repeated 10 times over two days. The depth of the measurements was limited by the size of the jet tank. Measurements were not taken within 30 cm of any surface (the bottom of the tank, or the sand mound) to ensure that the measurements were not affected by the boundaries. The measurements closest to the surface were limited by two factors. The concentration was primarily limited by the maximum measurable concentration for the probe's calibration. The velocity and concentration measurements in the sand jet were limited by air bubbles entrained in the flow in the first 10 to 15 cm. These bubbles resulted in inaccurate and unrepeatable measurements.

The primary details of the experiments are shown in Table 1 for the sand jets, and Table 2 for the slurry jets, where d_n is the jet diameter at the nozzle, d_o is the jet diameter at the water surface, U_n is the average velocity at the nozzle, and U_o is the average velocity at the water surface. C_o is the initial sand concentration of 60 % mass by volume (due to a void space of 0.4), m_o is the sand mass flux, ρ_s is the sand density, and F_r is the densimetric Froude number. Here $F_r = U_o/(gd_o(\rho_s - \rho_w)/\rho_w)^{.5}$, ρ_s is the sand density, and ρ_w is the water density. The experiments for the slurry jets are labelled according to the nozzle size and the sand flow rate, where L is large (15.5 mm), S is small (9 mm), and 90 is a higher sand flow rate than 70.

The diameter of the sand jet at the water surface was calculated using the initial sand concentration of 60 % mass by volume at the nozzle (due to void space), using the mass flux for an initial velocity, and assuming that the jet narrowed as it accelerated through the air. As a result of the narrowing of the jet through the air, the concentration at the water surface is the same as the concentration at the nozzle. The acceleration of the jet through the air was measured by the probe in a previous study (Hall, 2008).

Table 1: List of sand jet experiments

Sand Jet	d_n (m)	d_o (m)	m_o (g/s)	U_n (m/s)	U_o (m/s)	Fr
12.5 mm	0.0125	0.0082	55.5	0.30	0.69	1.95
19.2 mm	0.0192	0.0137	161.4	0.37	0.72	1.58

Table 2: List of slurry jet experiments

Slurry Jet	d_o (m)	m_o sand (g/s)	m_o slurry (g/s) / (m^3/s)	Conc (% vol)	Conc (% wt)	Velocity (m/s)	Fr
L70	0.0155	26.3	203.9 / 0.000183	11.6	12.9	0.97	2.00
L80	0.0155	40.55	209.4 / 0.000178	16	19	0.95	1.96
L90	0.0155	58.4	220 / 0.000176	21	26	0.94	1.94
S80	0.009	43.2	165.5 / 0.000132	21	26	2.1	5.69

ERROR ESTIMATION

One horizontal concentration / velocity profile was repeated twice for each sand jet, to measure the probe's repeatability (the 40 cm profile for the smaller nozzle and the 30 cm profile for the larger nozzle). Table 3 tabulates the results of the repeatability. The variation in the calculated axial concentration, the calculated axial velocity, the calculated concentration profile width and the calculated velocity profile width is very low, with the exception of the variation in the calculated axial concentration of the 12.5 mm sand jet.

Table 3: A comparison of the repeated profiles for both jets. The values are the % difference between the two repeats

Jet	12.5 mm	19.2 mm
Concentration Peak	16.8 %	4.1 %
Velocity Peak	2.4 %	3.8 %
Concentration Width	3.1 %	2.6 %
Velocity Width	3.8 %	7.9 %

To measure the repeatability of the slurry jet measurements, one profile was repeated 10 times over two days. Figures 4 and 5 show the results of the measurements. For concentration measurements, the standard deviation of the measurements is approximately constant for all the different measurement locations and is 15 % of the average value. When the data were least squares fit to a Gaussian distribution, the standard deviation of the amplitudes remained 15 % of the average value, indicating that the majority of the error is associated with systematic errors. For the velocity measurements, the standard deviation of the measurements within the inner 60 % of the jet was 4 % of the average value. Outside this region, the errors were much larger, due to measurement difficulties within and between large eddies of particles. For the profile width measurements, the standard deviation in the average measurement was 8%.

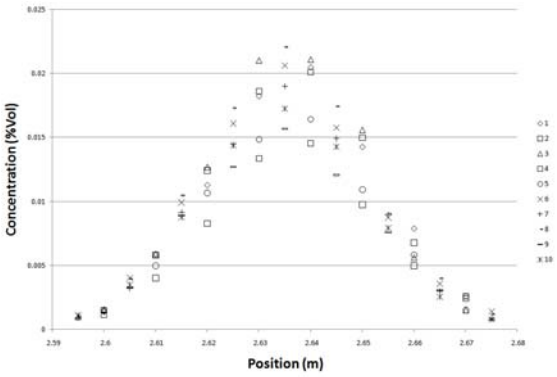

Figure 4. Concentration repeatability for a cross section at 20 cm, repeated 10 times over 2 days.

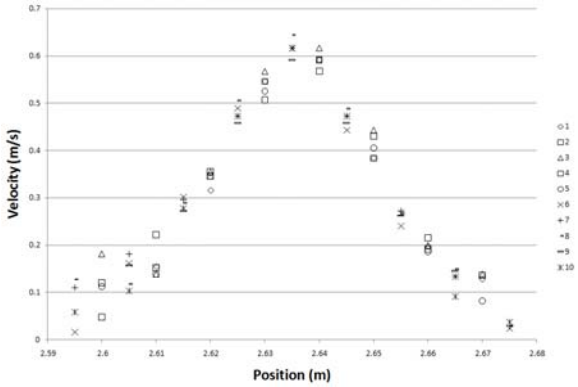

Figure 5. Velocity repeatability for a cross section at 20 cm, repeated 10 times over 2 days.

PROBE MEASUREMENT RESULTS

When a jet exits the nozzle, it is assumed that the flow velocity is constant across jets diameter.

The profile of the flow velocity of a developed jet, however, is Gaussian. There is a region, after a jet exits the nozzle, where the flow develops, and is called the zone of flow establishment.

The zone of flow establishment can be calculated based on the observations of Jiang et. al., (2005). The formula from the paper is as follows:

$$(z/D) = 5.42 + 67.85\,(u_{ss}/u_o) \qquad [1]$$

Where z is the length of ZFE; u_{ss} is the particle settling velocity (0.033 m/s); D is the nozzle diameter and u_o is the initial disperse phase velocity. From this expression, the zone of flow establishment was calculated as 10.82 cm for the 12.5 mm diameter sand jet, and 16.4 cm for the 19.2 mm diameter sand jet, 12.0 for the 'L70' slurry jet, 12.1 for the 'L80' and 'L90' slurry jets, and 5.8 cm for the 'S80' slurry jet. These results show that the jets are fully developed within the region of our measurements, with the exception of the measurements taken in the large slurry jets above a depth of 12 cm.

To confirm the validity and quality of the measurements, the concentration and velocity profiles were all normalized according to the peak concentration/velocity, and the profiles width (the width at which the concentration/velocity is ½ the maximum). These results are shown in Figures 6 and 7.

The normalized concentration profiles show that the measurements are accurate over the whole range of measurements, from high concentration in the centre of the jet, to the low concentration eddies at the outer edge of the jet. The concentration profiles are all self-similar, and fit a Gaussian profile. The concentrations measured ranged from 12 % by volume at 20 cm depth in the centre of the 19.2 mm sand jet to about 0.1 % by volume at 80 cm depth in the outer edge of the sand jet.

The normalized velocity profiles are different from the concentration profiles, since the velocity of the sand does not approach zero at the outer edge of the jet. Irrespective of this, the velocity profiles are all self-similar and fit a Gaussian profile. The accuracy of the velocity measurements decreases at the outer edges of the jet. This is shown in Figure 7 with the increased scatter in the data. There are two reasons for this decreased accuracy: (1) The probe's voltage spikes from passing sand particles at very low concentrations (relative to the calibrated maximum concentration) are weak and disperse. This makes the correlation of the two voltage signals less accurate, due to the reduced resolution. (2) The turbulent eddies at the outer edges of the jet means that the probe measures periods of large sand flux, followed by periods of no sand flux. The absence of sand flux for significant portions of each measurement makes an accurate sand velocity calculation more difficult.

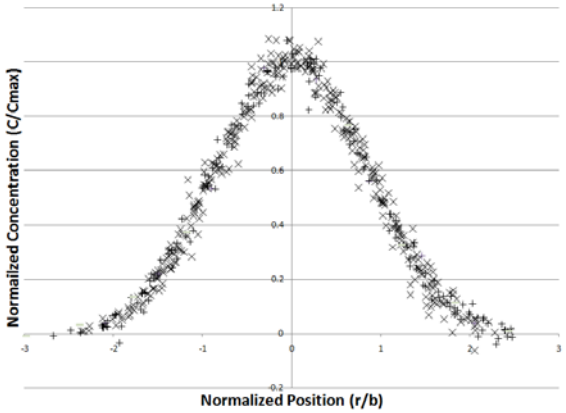

Figure 6. Normalized concentration profiles for the sand (+) and slurry (x) jets. b is the width at which the concentration is ½ the maximum

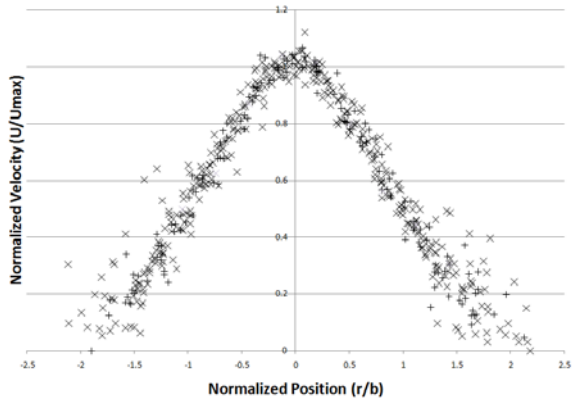

Figure 7. Normalized velocity profiles for the sand (+) and slurry (x) jets. b is the width at which the velocity is ½ the maximum

The velocity and concentration data for each separate horizontal profile were fit to Gaussian distributions in order to allow for accurate calculations of the local axial concentration, the

axial velocity, the concentration profile width, and the velocity profile width. The vertical axial profiles that were measured were used to augment the calculated axial concentration and velocity data.

Dimensional considerations were used to predict the main characteristics of the jets, and to create a non-dimensional plot of the results. For the axial average velocity of the jet, we can write:

$$U = f_1[M_o, B_o, \rho_o, L, \upsilon] \quad [2]$$

where f denotes a functional relation. M_o is the initial sand momentum flux, B_o is the initial sand buoyancy flux, ρ_o is the initial slurry density, L is the depth, and υ is the slurry kinematic viscosity. The sand momentum and buoyancy are defined as:

$$M_o = \frac{\pi d_o^2}{4}(1-n)U_o^2\rho_s \quad [3]$$

$$B_o = \frac{\pi d_o^2}{4}(1-n)U_o g\Delta\rho_o \quad [4]$$

where n is the porosity of the sand (0.4), ρ_s is the sand density, $\Delta\rho = \rho_s - \rho_w$, and ρ_w is the water density.

Using dimensional considerations, Eq. 2 can be reduced to:

$$\frac{M_o}{\rho L^2 U^2} = f_2[\frac{B_o}{\rho U^3 L}, \frac{UL}{\nu}] \quad [5]$$

If we neglect the effect of the Reynolds number, then we can reduce the relationship to the following:

$$\frac{UF_r}{U_o} \propto \frac{L}{d_o F_r} \quad [6]$$

Data for concentration and momentum were plotted in a non-dimensional form using the initial the following relations:

$$M_o \frac{C}{C_o} \propto \frac{L}{d_o} \quad [7]$$

$$\frac{M}{M_o} \propto \frac{L}{d_o} \quad [8]$$

Figures 8 and 9 show the normalized local axial concentration profiles for the sand jets and the slurry jets. The figures contain data from both the horizontal profile calculations, and the data from the vertical axial jet measurements. The concentration is normalized by the maximum concentration at the water surface (60 % by volume), and the depth is normalized by the jet diameter at the water surface.

Figures 10 and 11 show the normalized axial velocity profile for the sand jets and the slurry jets. The figures contain data from both the horizontal profile calculations, and the data from the vertical axial jet measurements. The velocity is normalized by the maximum sand velocity at

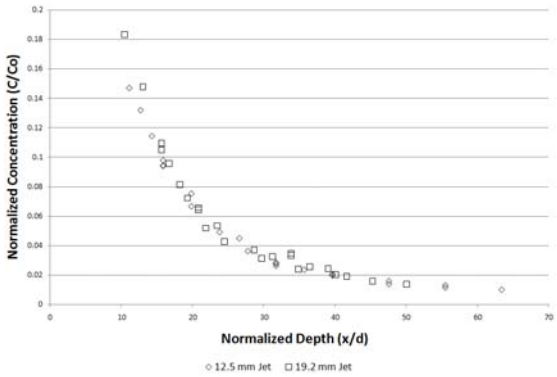

Figure 8. The normalized local axial concentration profile for sand jets, demonstrating that the jet is self-similar.

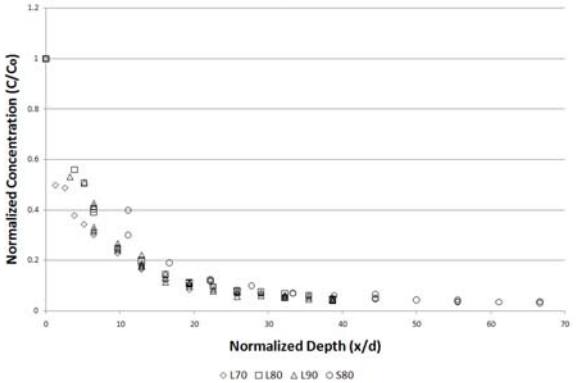

Figure 9. The normalized local axial concentration profile for slurry jets, demonstrating that the jet is self-similar.

the water surface divided by the densimetric Froude number, as calculated previously. The depth is normalized by the jet diameter at the water surface and the densimetric Froude number. The velocity data for the sand jet does not normalize as well as the concentration data,

and there is a small shift between the two data sets. This may be due to the difficulty in calculating the velocity of the sand at the water surface. The velocity used to normalize the data is the velocity of the same sand jet in air, without considering the deceleration of the sand as it strikes the water surface. The data for the small sand jet shows a significant decrease in velocity to a normalized depth of approximately 15 - 20, where the axial velocity then stays constant at a value of about 0.32 m/s (roughly 10 times the settling velocity of the sand - 3.3 cm/s). It is not clear whether the profile of the large sand jet has reached a plateau at that normalized depth, since it is very near the bottom of the measurement zone. The velocity for the large sand jet at this normalized depth is about 0.4 m/s.

The velocity data for the slurry jet normalizes well in the zone of established flow, but not above this zone. This data also shows a significant decrease in velocity close to the water surface, but the velocity continues to decrease slightly out to the measurement boundary. It appears that the velocity profiles of the slurry jets have reached a plateau similar to that of the sand jets at the end of the measurement zone. The different sand loading between the four slurry jets L70, L80, L90, and S80 has a small but noticeable effect on the velocity of the jet. The increased loading of the higher concentration jets increases the negative buoyancy, and thus increases the axial velocity throughout the measurement region (0.1 to 0.6 m). The axial velocities of the slurry jets within the plateau region vary between 0.35 to 0.43 m/s.

The axial velocities of both sand and slurry jets are similar within the plateau region. This may be a result of the buoyancy forces of the jet dominating the flow. The 'terminal velocity' reached at the plateau might result from an effect similar to the cloud velocity of a group of particles. Once the jets spread out enough, it is expected that the particles would slow down and settle at their individual settling velocities.

Figure 12 shows the spreading of the sand jet's concentration and velocity profiles. The paper by Mazurek et al, 2002, indicates that the spreading rate of the concentration profile of a sand jet is a function of the particle Froude number. Since both jets have similar particle Froude numbers, they have similar spreading rates, as shown in the figure. A comparison of the spreading rate of these sand jet results with other researchers buoyant jet results demonstrates the significance of the particle diameter and particle density.

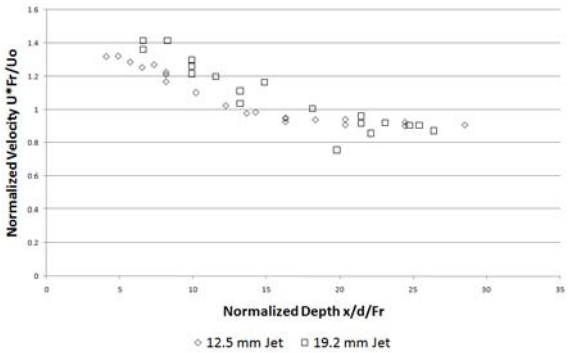

Figure 10. Normalized axial velocity profile for sand jets, demonstrating that the jet is self-similar.

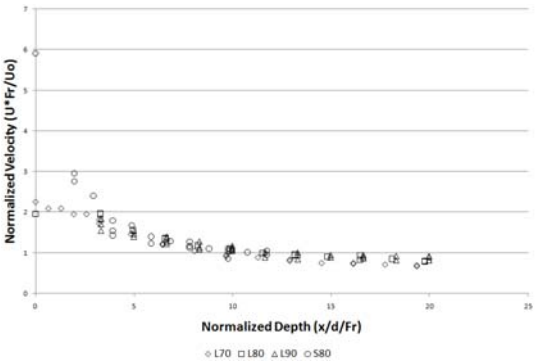

Figure 11. Normalized axial velocity profile for slurry jets, demonstrating that the jet is self-similar.

Other researchers use much smaller particles, with smaller density differences from the ambient fluid (Papanicolaou and List 1988), and their results indicate that the concentration profile is significantly wider than the velocity profile. As the particle size and density difference increases, the added inertia and buoyancy of each particle results in a decreased concentration profile width. Our results, and the results of Brush, 1962, who used similar sized glass particles, indicate that the concentration profile width is significantly smaller than the velocity profile width.

Figures 13 and 14 show the spreading of the slurry jet's concentration and velocity profiles, respectively. The slurry jets L70, L80, L90 all

have similar densimetric Froude numbers, and, as expected, all have similar spreading rates. The slurry jet S80 has a larger densimetric Froude number, and has a significantly larger spreading rate. For all the slurry jets, except the higher Froude number 'S80' jet, the concentration spreading is almost equal to the velocity spreading. The higher Froude number jet has the same property as the sand jets, with the velocity spreading larger than the concentration spreading.

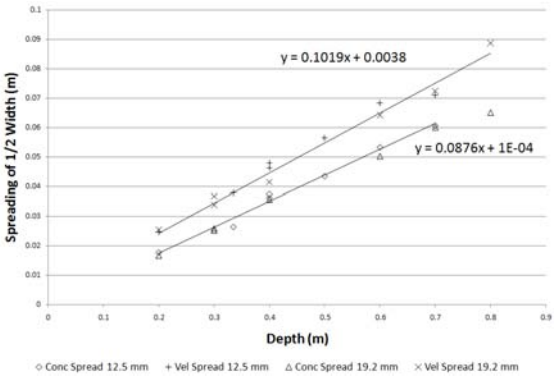

Figure 12. Jet spreading for the two sand jets. The spreading is calculated from the profile width at ½ the maximum value. The velocity spreading is larger than the concentration. The two jets exhibit similar spreading, as expected since their Froude numbers are similar.

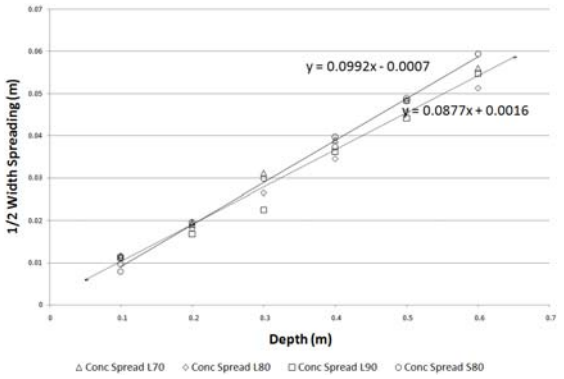

Figure 13. Concentration spreading for the slurry jets. The solid line is for the 'S80' jet, and the dashed line is the average of the other jets.

The momentum flux of the sand phase of a jet can be calculated at each horizontal profile using the following integral:

$$M = U\int_0^{\infty} m^* e^{(\frac{r}{b2})^2} dr = 2\pi\rho C U^2 \int_0^{\infty} e^{(\frac{r}{b1})^2} [e^{(\frac{r}{b2})^2}]^2 r dr \quad [9]$$

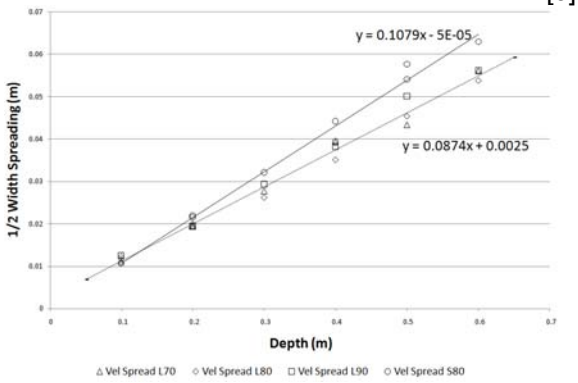

Figure 14. Velocity spreading for the slurry jets. The solid line is for the 'S80' jet, and the dashed line is the average of the other jets.

In this integral, m^* is the mass flux per unit area, C is the peak concentration of the horizontal profile, U is the peak velocity of the horizontal profile, and b1, b2 are the Gaussian spreading coefficients of the concentration and velocity profiles, respectively. Since the total mass flux of the sand and slurry jets is constant (considering only the sand), any change in the momentum flux can be attributed to a change in the velocity profile.

Figure 15 is a normalized plot of the momentum flux for the sand jets. The momentum is normalized by the initial momentum of the sand at the water surface, and the depth is normalized by the diameter of the nozzle. As expected, the momentum fluxes of the sand jets are self similar. The plot shows that the momentum flux decreases initially, up to 25 to 30 diameters from the nozzle, where it becomes constant.

Figure 16 is a normalized plot of the momentum flux for the slurry jets. The plot show that the momentum flux decreases until about 20 diameters from the nozzle, where it becomes constant. This terminal momentum flux for the slurry jet is lower than for the sand jet. This results from the slurry jet losing more momentum, at a faster rate, than the sand jet.

As the sand particles exit the jet nozzle, buoyancy forces act to increase the momentum, drag forces act to decrease the momentum, and particle interaction forces are expected to have a varying effect, depending upon particle size, specific density, and turbulent eddy size. For sand and slurry jets, the drag forces dominate initially (jet-like flow), and the sand particles lose momentum, transferring their energy to turbulence and increased water momentum. The plots of momentum flux for both sand and slurry jets show that the three forces quickly balance out. Beyond this point, the energy created from the particle buoyancy equals the energy lost to water momentum and water turbulence, and particle interactions. This balance will be maintained as long as the jet has a high enough particle density to flow as a cloud (plume). Once the jet spreads out far enough to decrease the particle density beyond some limiting point, the sand particles will settle separately, and the system will decrease its momentum flux further.

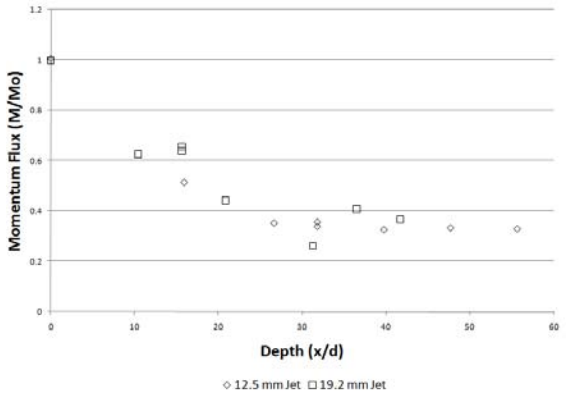

Figure 15. The normalized momentum flux of the sand within the sand jet.

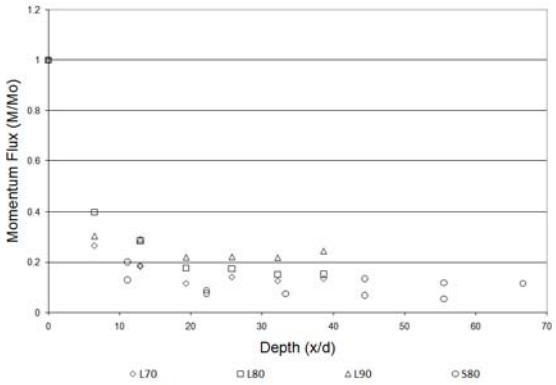

Figure 16. The normalized momentum flux of the sand within the slurry jet.

CONCLUSIONS

Experimental measurements of particle concentration and velocity within sand jets and highly concentrated slurry (sand – water) jets were presented. The measurements indicate that the decay profiles (radially and axially) are self similar. The axial sand concentration profiles for all jets decay rapidly throughout the measurement zone (approx. 10 to 60 jet diameters). The axial particle velocity profiles for all jets decay rapidly, and then reach a plateau region, where the velocity remains constant. The 'terminal velocity' is between .32 and .4 for sand jets, and between .35 and .43 for slurry jets. This velocity appears to vary depending upon the sand mass flux of the jet. The spreading rates of the jets appear to be dependent upon the densimetric Froude number. These experiments indicate that the spreading rate of the velocity profile is larger than that of concentration, probably due to the inertia of the particles.

The momentum flux of the sand within the jet has been calculated, and it appears to quickly decrease towards a constant value, as the drag forces, buoyancy forces, and particle interaction forces balance out.

REFERENCES

Brush, L. M. J., (1962). "Exploratory study of sediment diffusion." *Journal of Geophysical Research*, Vol. 67, No. 4, pp 1427-1433.

Jiang, J. S., Law, A. W. K., Cheng, N. S., (2005). "Two-phase analysis of vertical sediment-laden jets." *Journal of Eng. Mechanics*, 131(3), 308-318.

Jinzhong, Lui, Grace, John R., Bi, Xiaotao, (2003) "Novel Multifunctional Optical-Fiber Probe: I. Development and Validation" *AICHE Journal*, 49(6), 1405-1420.

Jinzhong, Lui, Grace, John R., Bi, Xiaotao, (2003) "Novel Multifunctional Optical-Fiber Probe: II. High-Density CFB Measurements" *AICHE Journal*, 49(6), 1421-1432.

Hall, Neil, (2008). *Thesis – In Progress*

Mazurek, K. A., Christison, K., Rajaratnam, N., (2002). "Turbulent sand jet in water" *Journal of Hydraulic Research*, Vol 40, No. 4, 527-530.

Muste, M., Fujita, I., Kruger, A., (1998). "Experimental comparison of two laser-based velocimeters for flows with alluvial sand." *Experiments in Fluids*, Vol 24, pp 273-284.

Papanicolaou, P.N., List E.J., (1988). "Investigations of round vertical turbulent buoyant jets."*Journal of Fluid Mechanics* 195 , pp. 341–391.

Parthasarathy, R.N., Faeth, G.M., (1987). "Structure of particle-laden turbulent water jets in still water." *Int. J. Multiphase Flow*, 13(5), 699-716.

Virdung, T., Rasmuson, A., (2007). "Hydrodynamic properties of a turbulent confined solid-liquid jet evaluated using PIV and CFD." *Chemical Engineering Science.* 62, 5963-5979.

PRELIMINARY STUDY OF SAND JETS IN WATER-CAPPED ARTIFICIAL AND REAL MFT

Jianan Cai, David Z. Zhu, N. Rajaratnam
University of Alberta, Edmonton, Alberta, Canada

ABSTRACT

Mature fine tailings (MFT) has a high concentration of fines and behaves like a Bingham plastic. This study aims to improve our understanding of physical processes related to MFT and sand/slurry operations in tailings ponds. Because of the opacity of MFT, Laponite® is used to make transparent gels that also behave as Bingham plastic fluid. Parallel experiments were carried out to study the dynamics of sand jet in water-capped Laponite gel and real MFT. It was observed that sand jets from nozzles smaller than 5.5mm in diameter can be trapped by water-capped gel, while those from larger nozzles were able to penetrate through the gel. However, in water-capped MFT, sand jets even as big as 10 mm in diameter failed to penetrate into the MFT. Additional observational results were analyzed and physical mechanisms were explored in this paper.

INTRODUCTION

In oil sands operations, large amounts of mature fine tailings (MFT) are disposed as by-products, and tailings ponds need to be reclaimed after the operations. Generally, there are two categories of methods proposed for tailings ponds reclamation: water capping and soil capping. In water capping, fresh water is added to cap MFT, and an end pit lake is created which is expected to support a healthy aquatic ecosystem. While in soil capping, sand and soil are used to cap the MFT and the reclaimed areas would be possible to support vegetation. The challenges in tailings pond management are to reduce the volume of the MFT and to increase the MFT's yield stress for soil capping. A better understanding of the dynamics of sand and slurry jets in tailings ponds will be important in optimizing our tailings management.

MFT are mainly comprised of fine solids, water, and residual bitumen (Luo, 2004). Due to its high solids concentration (>30% by weight), MFT has a high viscosity but it cannot easily sustain any loads (Masliyah, 2006). Banas (1991) reported that oilsands tailings sludge can be classified as a non-Newtonian fluid, which behaves like a Herschel-Bulkley model material in undisturbed state and a Bingham model fluid when remoulded. Based on this, MFT can be treated as a visco-plastic fluid, especially a Bingham plastic.

A number of studies on rigid particle movements in visco-plastic media have been reported in the literature. However, most of the studies were concentrated on the behaviour of single particles or suspensions (Atapattu et al., 1990; Hariharaputhiran et al. 1998; Ferroir et al., 2004; Merkak et al., 2006); and few studies analyzed agitated movements or particle movements as groups.

Our understanding of physical processes in MFT has been hampered by the opacity of MFT, not allowing observations of movements inside it. So in our experiments, Laponite® dispersion is used as an artificial MFT material. Laponite is a rheological additive to make transparent clay, which also behaves like a visco-plastic fluid and can be made by mixing Laponite with tap water or deionized water at different concentrations (Southern Clay Products, Inc., 2006). Figure 1 is an example of the flow curve for Laponite gels at 2.5% concentration by weight (Morrison, 2008).

This research is composed of a series of parallel experiments studying sand jets behaviour in artificial and real MFT with or without water capping. It aims to improve our understanding of physical processes related to MFT and sand/slurry operations in tailings ponds. The study will have potential applications in recycling processed water and decommissioning of tailing ponds using water capping and revegetation. In addition, the study can also provide validated data for CFD modeling calibration and furthermore detailed study in this field.

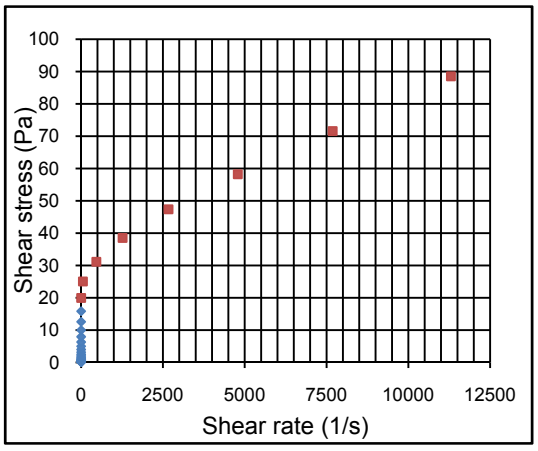

Figure 1. Laponite 2.5% RD flow curve

In our experiments, vertical sand/slurry jets are placed above the surface of water-capped MFT and Laponite gel. The following four parameters are varied in our experiments: the diameter of the sand jet, the height (thus the velocity) of the sand jet, water capping depth, and the viscosity of Laponite gel or real MFT. Section 2 and 3 present the results of sand jets in artificial MFT (i.e. Laponite gel) and real MFT, respectively. The summary and future studies are presented in Section 4.

SAND JETS IN ARTIFICIAL MFT

Experimental Setup

This set of experiments was carried out in a Plexiglas container, which is 61cm high and 19cm by 19cm in cross-section (see Figure 2). In this tank, gel was made from Laponite powder well mixed with water, and was capped by another layer of water to create a two-layer system. A feeder with a stopper inside the nozzle was utilized to hold sands, and was attached to a fixed beam. By moving the feeder up and down along the centerline, the heights of sand jets can be changed. All sands used have a median size of 0.2 mm (D_{50}=0.2mm). Food color was added into the gel to distinguish it from the upper water layer. A digital video camera was used to record the experiments.

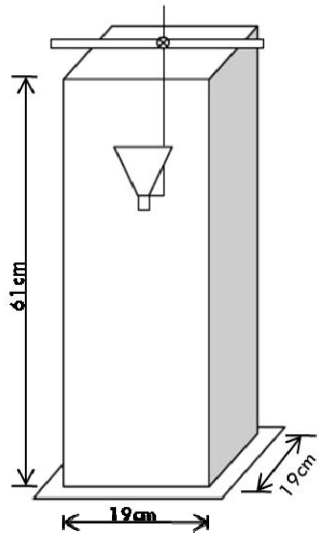

Figure 2. Experimental setup for sand jets in water-capped Laponite gel

In order to make the gel transparent, tap water and deionised water (Di water) at a 2:1 ratio were used to mix with Laponite in 0.7% concentration by weight. Rigorous mixing using a mechanical blender is needed to fully mix the powder during preparation for at least 20 minutes. Typically one hour is needed for dispersion, but the process could take longer depending on the temperature of water added and the amount of gel needed.

Table 1 summarizes all experimental parameters. The ones with crossing lines were not conducted as similar behaviour was expected from those with the same nozzle diameter.

Table 1 List of sand jet experimental parameters

Jets in Gel	Nozzle (mm)	Heights (cm)	Jets in gel-water	Nozzle (mm)	Height (cm)
A	2.3	~~4~~	~~G~~	~~5.5~~	~~1~~
B	2.3	13	H	5.5	8 cm
C	2.3	26	I	5.5	20 cm
D	3.0	4	J	10	1 cm
E	3.0	13	~~K~~	~~10~~	~~8~~
F	3.0	26	L	10	24

Observations

Sand jets in gel

Figure 3 is a picture taken after sands was spread on the surface of the gel layer. It is shown that single sand particles can be trapped at the gel surface. However, with accumulated sands at the surface, a few drops of sand started to form, and penetrate into the gel and eventually become trapped at a certain depth. The positive yield stress of the gel is the reason for the trapping of the sand particles. In this experiment, the gel was made with 0.7% of Laponite, which is much smaller than about 2.5% needed to simulate real MFT. A larger yield stress will reduce or prevent the penetration of sand particles inside the gel.

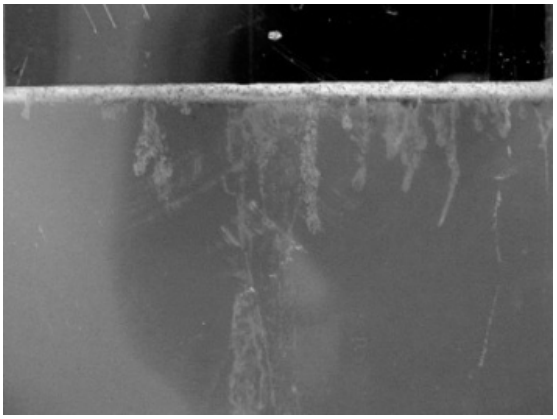

Figure 3. Picture of sands staying on gel surface

Sand jets in gel were then studied where sand jets of various diameters were produced from different heights. Figure 4 shows the sand jets from a nozzle of diameter 2.3mm into gel from a height of (a) 4 cm, (b) 13 cm and (c) 26cm above the gel surface. All three jets had similar behaviour: the jet shape was broken into drops in the gel before sands reached the bottom. The higher jet, however, was able to maintain its jet-like shape longer given its larger jet velocity. Moveover, in higher jets the sand drops descended more quickly than those formed in lower jets, but drops in lower jets showed more randomness during falling.

Sand jets shown in Figure 5 are from a nozzle of 3mm in diameter located at a height of (a) 4 cm, (b) 13 cm and (c) 26cm above the gel surface. Unlike jets presented in Figure 4, these larger jets were able to penetrate the gel layer without forming drops.

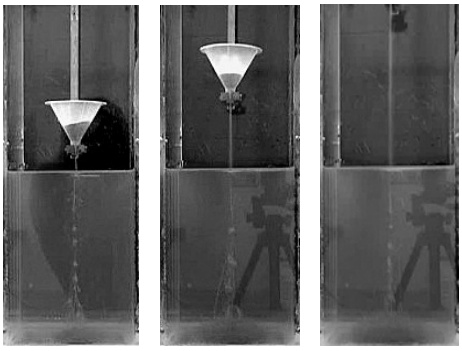

(a) (b) (c)

Figure 4. 2.3 mm sand jets in gel from different heights

(a) (b) (c)

Figure 5. 3mm sand jets in gel from different heights

Sand jets in water-capped gel

When the gel was capped with a layer of water, sand jets were observed to be trapped in the gel. Figure 6 shows the feature of a 5.5 mm jet from 8 cm above the water surface that the sand jet gradually lost its shape and finally got trapped at certain depth where a lot of sand clumps appeared and drops began to come out. The jet shown in Figure 7 has the same diameter as those in Figure 6, but it was located 20 cm above the water surface. Figure 7(b) also shows the ultimate deformation of this 5.5 mm jet.

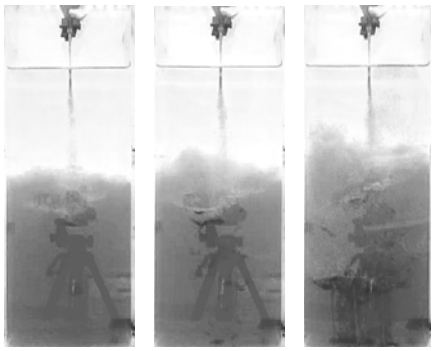

(a) (b) (c)

Figure 6. A 5.5 mm sand jet in water-capped gel from a height of 8 cm

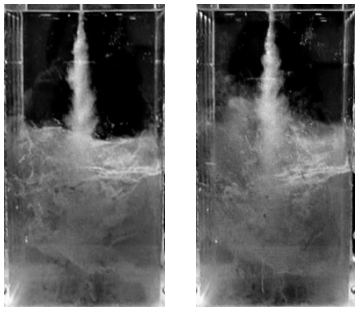

(a) (b)

Figure 7. A 5.5 mm sand jet in water-capped gel from a height of 20cm

Figure 8 shows the development of a 10 mm jet placed 1cm above the water surface. Different from those shown in Figure 6 and Figure 7, sand jets from a larger nozzle had enough momentum to easily penetrate the gel. Compared with jet of 5.5 mm in diameter, this jet entrained more air into the upper water layer as well as the gel layer. Some of these air bubbles escaped from the gel due to turbulence induced by jet, while the others got trapped after the jet stopped.

At the same time, water was also entrained into the gel by the jets. In this run, the amount of water entrained from Figure 8(c) to 8(d) can be estimated as the difference of the gel volume between these two pictures. After the jet stopped, a cavity was created along the gel layer, which was filled with the mixture of air, water, gel and a few of sand particles. Then as shown in Figure 9, this kind of mixture was squeezed out from the cavity since it is lighter than the gel around it.

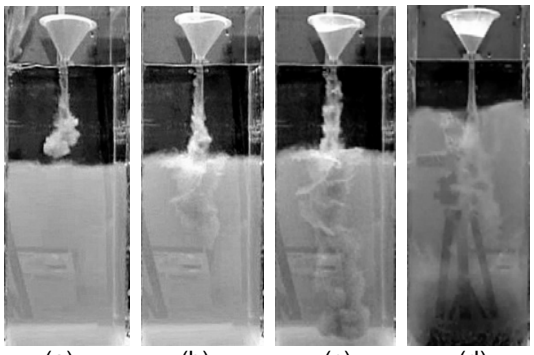

(a) (b) (c) (d)

Figure 8. A 10 mm sand jet in water-capped gel from a height of 1cm

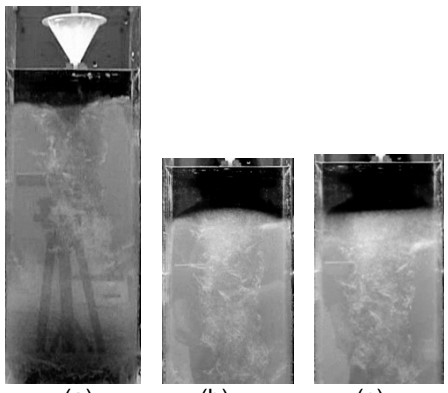

(a) (b) (c)

Figure 9. Water entrained into and released from the gel layer

More air bubbles got entrained into the water layer when the jet was placed higher. Figure 10 shows the development of a 10 mm sand jet 24 cm above the water surface. In this case, both water and air got entrained into the gel, and some of the air bubbles were trapped in the gel after the jet stopped. It may be noticed that lots of sand particles in the outer layer of the jet are lifted to the water surface by released air bubbles. When the sand jet stopped, this part of sand sank slowly until stopped by the gel.

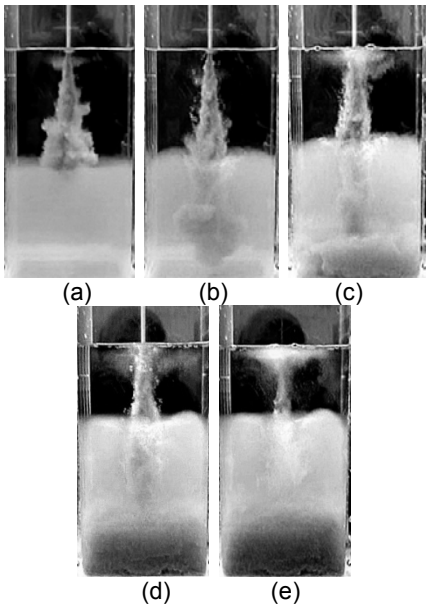

Figure 10. A 10 mm sand jet in water-capped gel from a height of 24cm

Discussion

Water entrainment

To estimate the volume change in water and gel layers, pictures taken at different times in the 10mm sand jet experiments are compared. As shown in Figure 11, solid lines indicate the water-gel interface before and after the experiments; broken lines are used to indicate the differences. The results are summarized in Table 2 and Table 3. In each table, D stands for depth and V stands for volume. Initial time indicates the time it took for the jet front to reach the water-gel interface, measured from the start of the experiment; and the final time refers to the time the experiment was finished.

For both 10 mm jets from a height of 1cm and 24cm, 100ml of sand was added into the feeder. Assume the porosity of the sand (D_{50} = 0.2 mm) is 0.4, then the total amount of the sand can give rise to 60 ml volume change in the container, which gives 1.7 mm increase in total depth. The experimental results give us only 0.9 mm for the jet from 1 cm and -0.5 mm for the one from 24 cm. This discrepancy is most likely caused by the relatively low resolution of the images used for measuring the depths. As each pixel in our images represents 1.1 mm in physical scale, uncertainties in detecting the water surface and tank bottom can cause a combined error of 1 to 2 pixels, or 1 to 2 mm.

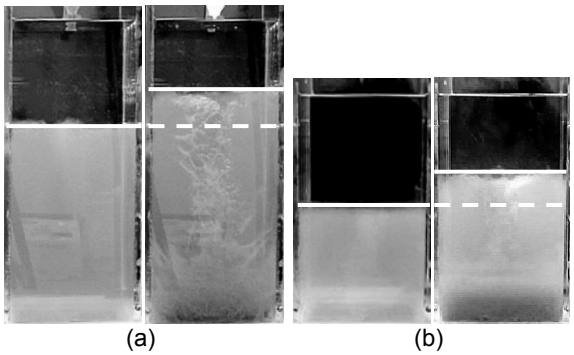

Figure 11. Volume exchange between water and gel (a) 10 mm jet from 1cm (b) 10 mm jet from 24 cm

Unlike the total depth, the interface between water and gel went through a large change. The interface rises by 4.9 cm and 4.5 cm for the lower and higher jet experiments, respectively. This corresponds to 1776 ml and 1636 ml, respectively, increase in the volume of the gel layer. Notice that this volume change is caused by the sand jets, which itself has a volume of only 60 ml. Thus the sand jet induces about 26 times of the gel volume change compared to the volume of the sand jet itself.

For sand jets in water, the sand jets entrain the ambient water into the jets and dragged the entrained water along into the gel. A significant portion of the water was mixed with the gel and resulted in the increase of the volume of the gel layer and the reduction of the water layer. It is observed in the experiments that the water/gel interface is not horizontal. There is a water cavity in the gel layer created by the sand-water jets. Given the three-dimensional shape of the cavity, we roughly estimated its volume to be around 130ml. After taking this into consideration, however, the increase of the volume of the gel layer is still about 25 times of the pure sand volume. In conclusion, sand jets are extremely effective in entraining water and in mixing the water in the gel layer.

Air entrainment

Figure 12 is a typical view after sand jet experiments stopped. In this picture large amount of small air bubbles were trapped by the viscous gel. From our observation, these air bubbles could stay there for at least 24 hours without escaping. Notice that these trapped air bubbles will also increase the volume of the gel, thus its volume

Table 2. Volume changes in water and gel layers for 10 mm sand jet from 1 cm

(a)	Water		Gel		Total		Time (s)
	D (cm)	V (ml)	D (cm)	V (ml)	D (cm)	V (ml)	
Initial	15.98	5769	30.53	11021	46.51	16790	1.03
Final	11.16	4029	35.45	12797	46.60	16823	6.83
Difference	-4.83	-1740	4.92	1776	0.09	33	5.80

Table 3. Volume changes in water and gel layers for 10 mm sand jet from 24 cm

(b)	Water		Gel		Total		Time (s)
	D (cm)	V (ml)	D (cm)	V (ml)	D (cm)	V (ml)	
Initial	18.02	6505	16.43	5931	34.45	12436	1.57
Final	13.44	4852	20.96	7567	34.40	12418	7.00
Difference	-4.58	1653	4.53	1636	-0.05	-18	5.03

needs to be estimated. At the moment, we are not able to estimate this volume, though it appears to be relatively small.

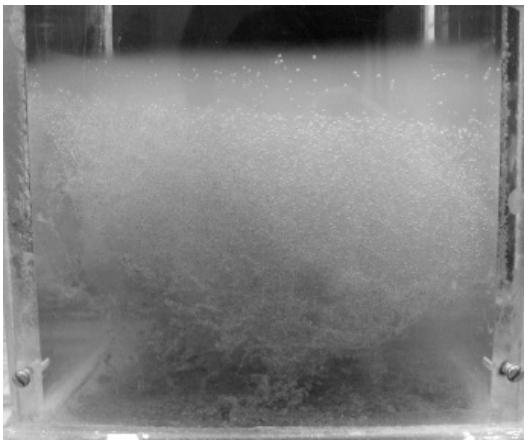

Figure 12. Air entrained into gel by a 5.5mm sand jet

The depth of water layer was found to have remarkable influence on the air bubble volume. In a relatively deep water layer, most air bubbles were able to escape before they were entrained into the gel.

Trapped depth in water-capped gel

Earlier sand jet studies are mostly concerned with the motion of spheres in non-Newtonian media. It was observed that in a non-Newtonian visco-plastic fluid, the flow field created by a falling sphere will not extend beyond several sphere radii. Once the prevailing stress level drops below the value of the yield stress, the sphere will no longer move and it will behave like an elastic solid (Chhabra, 2007).

In our experiments, it has been observed that there was a trapped depth for 5.5 mm sand jets. When sand jets move down into gel, they will mix with gel and create a mixture of sand, water and gel. Those sand particles in outer layer around the jet have lower velocities but higher shear stresses than those in the central part. For a Bingham plastic, the rheological equation can be written as

$$\tau = \tau_0 - \mu \frac{\partial u}{\partial r} \quad (\tau > \tau_0) \qquad (1)$$

Just like sand jets in water, we might assume Gaussian velocity distribution within a jet in MFT,

which can be represented by the following equation:

$$u = u_m exp\,(-\alpha \frac{r^2}{b^2}) \quad (2)$$

where u_m is the maximum velocity at the centerline; b is the radial distance away from the centerline where local vertical velocity $u = \frac{1}{2}u_m$; α is a constant to describe the curve and is equal to 0.693. This assumption has not been verified, but it still may be used for a preliminary analysis.
We also assume such relationships as $u_m = k_1\, z^p$ and $b = k_2\, z^q$ at each section.

Substitute Equation (2) into (1), we get

$$\tau = \tau_0 + \frac{2\,\mu u_m}{b^2} \cdot r \cdot exp\left(-\alpha \frac{r^2}{b^2}\right) = \tau_0 + \frac{2\,\mu k_1}{{k_2}^2 z^{(2q-p)}} \cdot r \cdot exp\,(-\frac{\alpha r^2}{{k_2}^2 z^{2q}}) \quad (3)$$

which is the shear stress distribution in radial direction.

The location of the maximal shear stress can be calculated by letting $\frac{\partial \tau}{\partial r} = 0$. From Equation (3), we obtain that at $r = \frac{k_2 z^q}{\sqrt{(2\alpha)}} = \frac{b}{\sqrt{(2\alpha)}}$ away from the centerline, the shear stress will reach its maximum: $\tau_m = \tau_0 + \frac{\mu k_1 \sqrt{(2/e)}}{k_2 \sqrt{\alpha}}\, z^{(p-q)} = \tau_0 + \sqrt{\frac{2}{\alpha e}} \cdot \frac{\mu u_m}{b}$. Let $k = \frac{\mu k_1 \sqrt{(2/e)}}{k_2 \sqrt{\alpha}}$, the maximum shear stress at each transversal section can be expressed as

$$\tau_m = \tau_0 + k\, z^{(p-q)} \quad (4)$$

This might be applied in the analysis of sand jets deformation in the gel.

Liquid-like and Solid-like Regions

Figure 13 is a sketch of two different types of motions induced by sand jets in gel. Figure 13 (a) illustrates the processes of sand jets which can be trapped by gel; while (b) illustrates that sand jets can penetrate the gel. In our experiments, sand jets from smaller nozzles (≤5.5mm in diameter) are type (a) and larger jets (=10mm in diameter) are type (b).

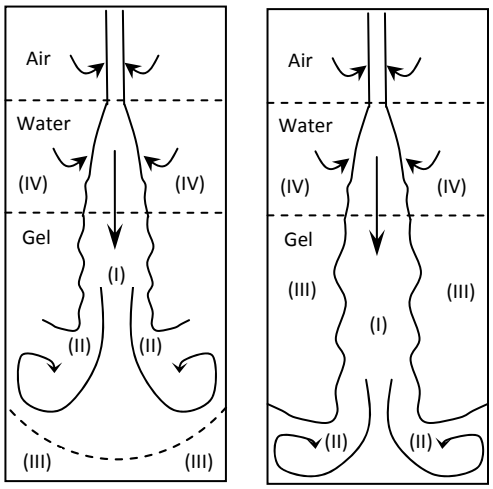

(a) trapped (b) untrapped

Figure 13. Different regions in a sand jet mixing proecess: (I) & (II) liquid-like zones; (III) solid-like zone

For both types, in the air and water, all sand jets could entrain a lot of ambient materials (air and water) and transport them into the gel layer. But once jets fell into gel, those from smaller nozzles can be trapped. Thus at the bottom of the container there was a region where the gel never got mixed with sands and water. Sand jets from larger nozzles penetrated the gel and such a region was observed as well. In Figure 13, this region was named as Zone (III). Gel within this region was not affected by the jet at all, simply behaving like solid material. In type (a) Zone (III) are stationary, while in type (b) this zone rose gradually because water in Zone (IV) was continuously entrained into the jet then mixed with sands and gel in the bottom of the container.

For both types, however, Zone (I) and (II) behaved like liquid. Water and air were entrained to Zone (I), transported to Zone (II) and fully mixed with gel there. Here Zone (I) and (II) are liquid-like regions.
For type (b), we can take a reasonable guess that if all of the water in Zone (IV) gets mixed into the lower gel layer, finally the gel in Zone (III) will arrive at the surface, and then the sand jet might have some influence on this solid-like region.

SAND JETS IN REAL MFT

Experimental Setup

In these sets of the experiments, MFT was loaded to a glass-sided tank with 59cm long, 52cm high and 28cm wide, instead of gel in the lower layer. Water was added to make a layer above MFT. A sand feeder was fixed to a metal frame to produce sand jets. The diameter of the sand is the same as that used in gel-water experiments. The experimental setup is shown in Figure 14, and MFT properties are listed in Table 4. Syncrude MFT collected on Feb 15/08 Dean Stark Solids was used in our experiments. Table 5 is a list of parameters of this set of sand jets experiments.

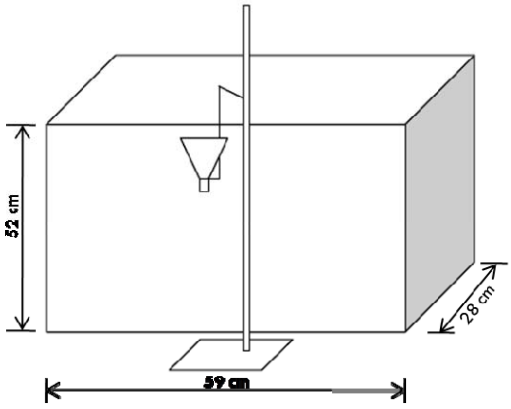

Figure 14. Experimental setup for sand jets in water-capped MFT

Table 4. MFT properties

Sample	Dean Stark			% Solid on Raw Slurry
	% Bitumen	% Water	% Mineral	
Untreated	1.75	63.16	34.92	35.93
Treated	0.78	60.00	33.61	35.62

Table 5. Sand jets parameters in water-capped MFT

Jets in MFT-water	Nozzle sizes (mm)	Heights of jets (cm)
M	2.3	24
N	3.0	24
O	5.5	23

Observations

When it comes to water-capped MFT, observations are not the same as sand jets in water-capped gel. Figure 15 and Figure 16 are pictures of a 3 mm sand jet in sequence; Figure 17 presents those of a 5.5 mm jet. Both jets failed to penetrate the lower MFT layer at the start; they got accumulated as a hump staying right above water-MFT interface. But as it became bigger and heavier, the hump began to descend and got into MFT, leaving a cavity above.

It is found that a bigger jet creates a wider cavity. In addition, a bigger jet created a hump with two peaks, while the smaller one only has a single peak (see Figure 15 and 17). This might be caused by different jet parameters.

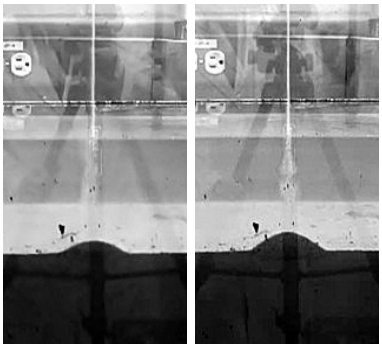

Figure 15. A 3 mm sand jet in water-capped MFT from a height of 24 cm

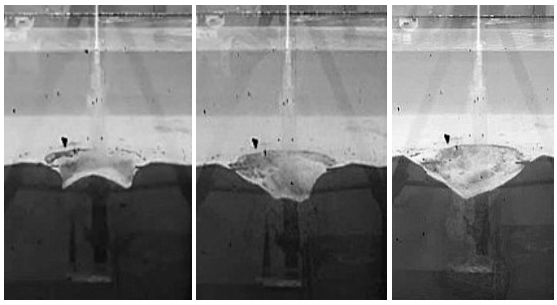

Figure 16. Interface deformation in a 3 mm sand jet

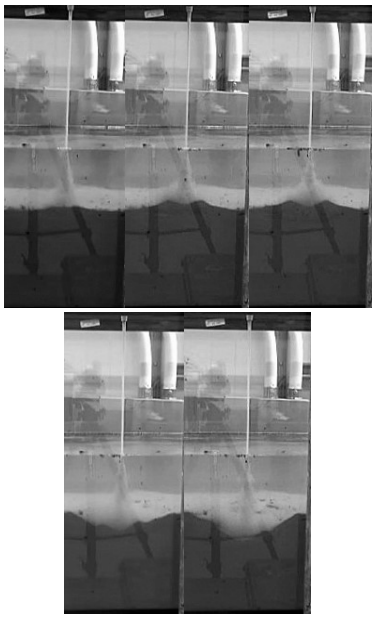

Figure 17. Evolvement of a 5.5 mm sand jet in water-capped MFT from a height of 24 cm

Discussion

Trapped depth in MFT

During the experiments of water-capped MFT, sand jets were not able to penetrate into MFT layer. At the very beginning all of sand particles just piled at the interface and built a hump above it. As more sands accumulated, the interface below the hump started to deform and slowly sank into MFT.

Figure 18 gives a description of forces on the sand hump when it is sinking very slowly. This equilibrium status can be expressed by Equation (5).

$$G - B - F_{\tau_0} + T = 0 \quad (5)$$

Where *G* is gravitational force; *T* is the thrust caused by approaching sand jet; *B* is buoyancy force; F_{τ_0} is the supporting force due to yield stress τ_0.

Each force in Equation (5) is calculated as shown in Equation (6) to Equation (9). The deformed interface is assumed to fit a spherical curve with

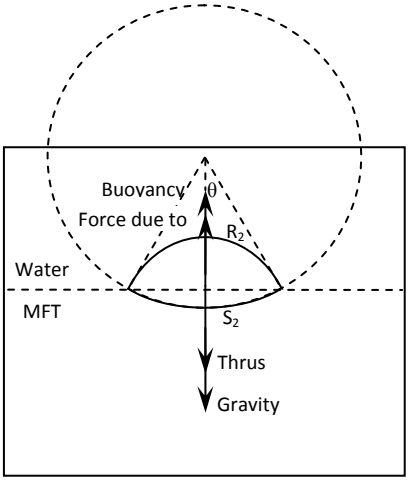

Figure 18. Sketch of forces acting on the sand hump

radius of R_2 and a central angle of 2θ, and F_{τ_0} is considered as the vertical component of the force by τ_0 actting over the sphere surface S_2 (Chhabra, 2007).

$$G = \rho_s g \int_0^t \gamma Q_1 dt \quad (6)$$

$$B = \rho_w g \int_0^t (\gamma Q_1 - Q_2) dt + \rho_M g \int_0^t Q_2 dt \quad (7)$$

$$F_{\tau_0} = \int_0^\theta \tau_0 \sin\theta \, dS_2 = \tau_0 \int_0^\theta 2\pi R_2^2 \sin^2\theta \, d\theta \quad (8)$$

$$T = \frac{dM}{dt} \quad (9)$$

Where *g* is the gravity acceleration; ρ_s, ρ_w, ρ_M are density of pure sands, water and MFT respectively; Q_1 is jet discharge, γ is the percentage of sands in it thereby γQ_1 represents the pure sand discharge from the jet to the hump; Q_2 is the sand discharge from water to MFT; and M is the momentum of the incoming sand jet.

For the case that the height of this hump is much smaller than the depth of the water, we can assume a fixed location of the crest, where the jet discharge is constant all the time. Consequently, Equation (6) ~ (9) can be rewritten as Equation (6') ~ (9'):

$$G = \rho_s g \gamma Q_1 t \quad (6')$$

$$B = \rho_w g \gamma Q_1 t + (\rho_M - \rho_w) g \int_0^t Q_2 dt \quad (7')$$

$$F_{\tau_0} = \pi R_2^2 \tau_0 \left(\theta - \frac{1}{2}\sin 2\theta\right) \quad (8')$$

$$T = \frac{dM}{dt} = \rho_{sw} \frac{Q_1^2}{\pi R_j^2} \quad (9')$$

Substitute Equation (6') ~ (9') into (5):

$$(\rho_s - \rho_w) g \gamma Q_1 t - (\rho_M - \rho_w) g \int_0^t Q_2 dt - \pi \tau_0 \left(\theta - \frac{1}{2}\sin 2\theta\right) R_2^2 + \rho_{sw} \frac{Q_1^2}{\pi R_j^2} = 0 \quad (10)$$

Where $\rho_{sw} = \gamma \rho_s + (1-\gamma)\rho_w$, which is the composite density of sand and water within the jet section at the hump crest; R_j is the jet radius at this section.

Then Q_2 can be solved as

$$Q_2 = \frac{\rho_s - \rho_w}{\rho_M - \rho_w} \gamma Q_1 - \pi \tau_0 \frac{d\left(\left(\theta - \frac{1}{2}\sin 2\theta\right) R_2^2\right)}{dt} \quad (11)$$

Our experiments suggested that $\theta \leq \frac{\pi}{2}$, $\frac{dR_2}{dt} \geq 0$ and $\frac{d\theta}{dt} \geq 0$, in this case it can be shown that $\frac{d\left(\left(\theta - \frac{1}{2}\sin 2\theta\right) R_2^2\right)}{dt} < 0$, so Q_2 will increase with time t. As soon as the value of Q_2 exceeds that of Q_1, there will be more sands sinking into MFT than received from the jet. This can be a good explanation for why the whole hump got trapped into MFT eventually.

SUMMARY AND FUTURE STUDY

A series of experiments were conducted on sand jets in pure gel, water-capped gel and water-capped MFT. In pure gel experiments, sand jets with smaller diameter lost the jet shape and were broken into drops before they reached the bottom, while bigger jets kept on running without deformation. When a water layer was added above the gel, it is more difficult for sand jets to penetrate. Although sand jets from larger nozzles were able to get to the bottom of the container, those from smaller nozzles always got trapped in the gel. With respect to jets in MFT-water layers, it is getting even harder for jet to penetrate due to larger yield stress in MFT (vs. gel in 0.7% concentration).

Either in gel-water or MFT-water system, sand jets went through three different media: air, water and gel or MFT. Air and water both are Newtonian, but MFT and gel are non-Newtonian fluids, which need to be treated in a different way. Our study is currently on-going, and the results are still very preliminary. In the next stage, we plan to continue our study in following aspects.

- Density correction: our transparent MFT (i.e. gels) has a density close to water, while real MFT has a density about one and half times of that of water. Buoyancy plays an important role in mixing process, so it is significant to find a laboratory method of density amendment.

- Viscosity adjustment: gel used in our experiments was in a concentration of 0.7% by weight. The volume of water entrained by sand jets is as much as 25 times that of sand jets itself. It is a concern that how much water can be entrained into the gel and how sand jets behave when gel of a higher concentration get involved.

- Sensitivity analysis: as we can see in this preliminary study, sand jets behaved in different ways with different parameters, such as diameter and velocity. Additionally, we believe the thickness of water layer is also a factor affecting the sand jets behaviour. Detailed study will be focused on critical parameters having an effect on sand jets: the condition for MFT to support sands, the influences of different parameters on sand jets and so on.

REFERENCES

Atapattu, D. D., Chhabra, R. P., & Uhlherr, P. H. T. (1990). Wall effect for spheres falling at small reynolds number in a viscoplastic medium. Journal of Non-Newtonian Fluid Mechanics, 38(1), 31-42.

Baghdadi, H. A., Parrella, J., & Bhatia, S. R. (2008). Long-term aging effects on the rheology of neat laponite and laponite - PEO dispersions. Rheologica Acta, 47(3), 349-357.

Banas, L. C. (1991). Thixotropic behaviour of oil sands tailings sludge. (M.Sc., University of Alberta (Canada)).

Chhabra, R. P. (2007). Bubbles, drops, and particles in non-newtonian fluids [electronic resource] (2nd ed.). Boca Raton, FL: CRC Taylor & Francis.

Ferroir, T., Huynh, H. T., Chateau, X., & Coussot, P. (2004). Motion of a solid object through a pasty (thixotropic) fluid. Physics of Fluids, 16(3), 594-601.

Luo, G. (2004). Investigation of CT beneath MFT deposition for oil sands tailings disposal. (M.Sc., University of Alberta (Canada)).

Masliyah, J. H. (2006). Tailings and water management. Unpublished manuscript.

Merkak, O., Jossic, L., & Magnin, A. (2006). Spheres and interactions between spheres moving at very low velocities in a yield stress fluid. Journal of Non-Newtonian Fluid Mechanics, 133(2-3), 99-108.

Morrison, S. A. (2008). Unpublished manuscript.

Southern Clay Products, Inc. (2006). Product Bulletin/Laponite®. Retrieved March, 2008, from http://www.laponite.com/index.asp

NUMERICAL SIMULATION OF SAND JET IN WATER

Amir Hossein Azimi, David Zhu and Nallamuthu Rajaratnam
University of Alberta, Edmonton, Alberta, Canada

ABSTRACT

Understanding the dynamics of sand jet in water is important in many engineering applications, including oil-sands tailings operations. The interaction of sand phase and water phase, commonly known as two-phase flows, requires advance experimental and computational studies. The objective of this paper is to evaluate the capability of the available numerical models for simulation of two-phase turbulent jet and examine the impacts of domain resolution on simulation results. The results indicate that the available CFD model (CFX 11.0) is able to simulate the mean properties of two-phase turbulent sand/water jets but, care must be taken to design a proper mesh structure to obtain reliable results.

INTRODUCTION

When a continuous phase flow contains a particulate phase such as solid particles, it is referred to as liquid-solid two-phase flow field. Mass, momentum and energy transfer of the system significantly change by the effect of suspended particles interactions. Existence of the solid phase in the system creating a considerable impact in the flow's nature such as time average velocity, the turbulent intensity, and the Reynolds stresses.

Two-phase turbulent jet flows have many applications in science and engineering fields, such as spray combustions, engine injections, exhaust plumes, pulverized coal burners (Sheen et al., 1994). Recently, a series of experiment has been carried out to study the effect of highly concentrated particulate phase in turbulent jet. (Hall et al., 2008) Although, the applications of two-phase turbulent jets are very extensive in engineering filed, but a comprehensive understanding of the relationship between each phase is not complete and requires more investigation. Presence of the second phase (solid particles) in the fluid system increases the complexity of the mixing phenomena in turbulent jets flow.

One of the earliest investigations on liquid-solid turbulent jets was conducted based on dimensional analysis to the zone of established flow (ZEF) by Singamsetti (1966). The observations indicated that the axial velocity distribution across the jet follows the Gaussian distribution and is self-similar.

The structure of (solid-liquid) turbulent jets was also studied both experimentally and theoretically by (Parthasarathy and Faeth, 1987). The study was limited to nearly mono-disperse particles with particle Sauter mean diameter (SMD) of 505 μm. The particle volume fraction in their experiment was less than 5%. Mean and fluctuating particle velocities were measured with LDA system. They concluded that the turbulent solid-liquid jets exhibited higher relative turbulent intensities of the particles which resulted in significant increases in particle drag from estimates based on the standard drag curve.

Particle Image Velocimetry (PIV) is one of the efficient and effective measurement techniques which used to measure both liquid and solid velocities and turbulent levels in two-phase flow systems. PIV technique also used for measuring the structure of two-phase (liquid-solid) turbulent jets and it was studied by many researchers.

A careful experiment was carried out for studying the effect of sand particles on turbulent jets using the PIV technique (Jiang et. al., 2005). Polyamid particles with a neutral buoyancy and nominal diameter of 50 μm were used as seeding particles for tracking the fluid motion and fluorescent particles (MF-Rhodamin B-particles) with a nominal diameter of approximately 75 μm and density of 1.51 g/cm^3 were selected as dispersed phase solid particles. The initial concentration of the solid phase was fixed at 0.19% in order to eliminate the effect of particle/particle interaction. Their analysis shown that, the mean particle velocity can be taken as the sum of fluid velocity and the settling velocity. They also found that the decay rate of the centreline concentration in dispersed phase increases with the particle settling velocity while decrease with the initial discharge velocity. The zone of flow establishment (ZFE) for the dispersed phase velocity was also found to be longer than that of the fluid.

In recent decays, development of powerful computers and improvement of programming skills enables researchers to simulate the complex phenomena using numerical methods. Different computational schemes and methods such as CFD codes, Large Eddy Simulation (LES) and Direct Numerical Simulation (DNS) were developed based on the level of complexity of the fluid system, required accuracy, and programming skills.

An advance simulation of the two-phase turbulent jets in three dimensional spaces was performed using Direct Numerical Simulation (DNS) by Yuu et. al., (1999). They used the discretized form of the Navier-Stokes equations in compressible form to study the effect of particle phase on the free jet flow. They observed that, presence of particles in the system generate many small-scale disturbances and they grow, deform and disrupt regular large-scale vortices, and eventually they change the whole flow field to turbulence. They mentioned that, because the Kolmogorov micro-scale motion in the turbulent flow pattern is much smaller than that the computational cell size, DNS method for simulation of highly turbulent structures is still not possible even if the present supercomputer is used.

Large Eddy Simulation (LES) could be one approach to simulate particles in this regime. Yuu *et al.,* (2001) simulated the effect of particle existence using the LES. The gas-particle jet flow was simulated at high Reynolds number ($R_e=10^4$). Obtained results of air and particle turbulent characteristics were mean velocity, turbulent intensity and Reynolds stress distributions. They used the drag interaction term based on Squires and Eaton (1990) expression and used the drag curve for calculation of drag coefficient based on Schiller and Naumann model.

Both DNS and LES require significantly small cell size and high level of programming efforts which directly increases the computational time and expenses of the simulation. Hence, for engineering purposes, using CFD codes for simulation of flow structures could save a lot of time and expenses.

A recent investigation in the developing region of a confined solid-liquid turbulent jets was conducted by Virdung and Rasmuson (2007). In this study, the behaviour of two-phase turbulent jets and the effect of dispersed phase volume fraction were investigated both experimentally and numerically. Relatively large particle size was selected in this study (1500 μm) and the volume fraction was varied from 0 (single phase) to 1.9%. The experimental domain with dimensions of 900 x 1000 x 20 mm indicated that the experiment was only able to observe the 2D behaviour of the jet. Measurements were obtained using PIV technique and simulations were performed using the CFD solver Fluent 6. They concluded that, in the dispersed phase, the rate of decrease in centreline velocity decreased with increasing volume fraction. They have also shown, for both phases, the widths of the jet increased with increasing volume fraction.

The initial dispersed phase volume fractions of the turbulent jets in the most of previous experiments were limited to less than 5%. In these cases, the effect of particle-particle interaction ignored and the flow structure treated as homogeneous two-phase flow system. In many environmental problems such as marine construction, deep ocean mining and discharge of sewage sludge into water bodies, the initial volume fraction of the turbulent jets could be up to 60%. Therefore, the behaviour of two-phase (solid-liquid) turbulent jets in high concentration requires more investigation.

Based on the mentioned requirements, a recent series of experiments were carried out at University of Alberta Hydraulic Laboratory in order to examine the effect of highly concentrated (solid-liquid) turbulent jets (Hall et. al., 2008). The dispersed phase time-averaged mean velocity and concentration were measured using the optical probe.

The objective of this paper is to present a detailed and careful comparison of the simulations performed using a CFD commercial code with the physical experiments. The calibrated CFD model can then be applied for modeling other sand/water two phase flows.

MODELING BACKGROUND

Based on the properties of phases in multi-phase flow system and concentration of the dispersed solid phase in the system the governing models for multi-phase flow systems could be classified into three categories (Manninen et al., 1996). Mixture models are used for simulation of liquid-liquid systems. In relatively low dispersed phase concentration and dilute systems homogenous model simulate the phenomenon and in presence of highly concentrated dispersed phase the interactions between particles plays an important

role in mass, momentum and energy transfer. The last category amongst the mentioned models is theoretically more advanced as it fully describes the mechanics of each phase. Each phase in inhomogeneous model has its own velocity field and is described by an individual set of continuity and momentum equations.

The interactions of both phases on each other considered as inter-phase relations which significantly change the structure of the flow system. Adding the inter-phase forces to the momentum equations of each phase requires more closure relations. Due to the complexity of the problem and limited knowledge of physics in the phase interaction, many empirical expressions were involved to the equation of motion. Therefore, uncertainties due to presence of empirical equations, in some special cases, reduces the reliability of the model compare to the simpler models.

The formulation for the continuity equation of both homogeneous and inhomogeneous models is identical. By volume averaging over a small control volume as shown by Wörner (2003), one can obtain continuity equation for phase α

$$\frac{\partial(r_\alpha \rho_\alpha)}{\partial t} + \frac{\partial(r_\alpha \rho_\alpha u_{\alpha i})}{\partial x_i} = 0 \qquad (1)$$

Herein, r_α is the volume fraction of phase α, and the volume conservation equation

$$\sum_\alpha r_\alpha = 1 \qquad (2)$$

ρ_α = density of phase α; $u_{\alpha i}$ (i=1,2,3) represent the velocity of phase α. According to Drew (1983) and Wörner (2003), the momentum equation for phase α can be presented as

$$\frac{\partial(r_\alpha \rho_\alpha u_{\alpha i})}{\partial t} + \frac{\partial(r_\alpha \rho_\alpha u_{\alpha i} u_{\alpha j})}{\partial x_j} = r_\alpha \rho_\alpha g_i - r_\alpha \frac{\partial p_\alpha}{\partial x_i} + \frac{\partial}{\partial x_j}\left(r_\alpha \mu_\alpha \frac{\partial u_{\alpha i}}{\partial x_j} \right) + M_\alpha \qquad (3)$$

Where M_α describes the interfacial forces acting on phase α due to the presence of the other phases and examples include drag force, lift force, virtual mass force, turbulent dispersion force, etc. Obviously, closure relations are required for the inter-phase momentum transfer term M_α.

As mentioned above for closing the system of equations of motion the constitutive equations are required for simulation of turbulent in each phase. The standard k-ε model was selected for continuous phase and dispersed phase zero equation model was chosen for dispersed phase. In this study, the major source of the inter-phase momentum transfer is inter-phase drag force which expresses as

$$M_\alpha^D = \frac{C_D}{8} A_{\alpha\beta} \rho_\alpha \left| u_\beta - u_\alpha \right| (u_\beta - u_\alpha) \qquad (4)$$

Where M^D is the drag force per unit volume (vector); u is the velocity vector; C_D is the dimensionless drag coefficient and $A_{\alpha\beta}$ is the interfacial area density (the interfacial area per unit volume between phase α and phase β). There are several models available for calculation of dimensionless drag coefficient (C_D). In the present simulation, a well-known Schiller and Naumann (Wörner 2003) drag model was used for calculation of drag coefficient.

$$C_D = \frac{24}{R_e}(1 + 0.15\, R_e^{0.687}) \qquad (5)$$

In vertical downward slurry jets the particles accelerates from their initial velocities by the effect of gravity. Hence, the virtual mass force with the coefficient of 0.5 was applied for the simulation.

Turbulent dispersion is the most important mechanism for the mixing of dispersed phases in turbulent flows. Turbulent velocity fluctuations of the carrier fluid are the major generators of the motion on the dispersed elements. Based on the various range of eddy sizes on the continuous phase, different responses would expected from the particles. The reaction of the particulate phase to the turbulent fluctuations could simulate with different models.

In this study, Favre Averaged Drag Model was used for simulation of the turbulent dispersion. This model has been shown to have a wide range of universality (Ansys, 2003).

$$F_\alpha^{TD} = -F_\beta^{TD} = C_{TD} C_D \frac{\nu_{t\alpha}}{\sigma_{t\alpha}} \left(\frac{\nabla r_\beta}{r_\beta} - \frac{\nabla r_\alpha}{r_\alpha} \right) \qquad (6)$$

Where F^{TD} is the Favre Averaged Drag Force; C_{TD} is the turbulent dispersion coefficient; $\nu_{t\alpha}$ is the turbulent viscosity of phase α; $\sigma_{t\alpha}$ is the turbulent Schmidt number for continuous phase volume fraction, currently taken to be 0.9.

LABORATORY EXPERIMENT

A series of experimental and numerical study were carried out at University of Alberta Hydraulic Laboratory for analyzing the effect of nozzle diameter and variation of dispersed phase concentration in highly concentrated turbulent jets (Hall et. al., 2008). The experiments were conducted in a rectangular glass tank with the dimensions of 2500 x 1250 x 1200 mm. Sand particles with an average diameter of D_{50}=210 μm were vertically fallen through different nozzle diameters (12.5 and 19.2 mm) into the water bodies. The velocity and concentration of the sediment particles of the steady sand jet were measured using fibre optic probe. There was 7 cm air space between the nozzle and the water surface that changed the initial diameter of the jet from 12.5 and 19.2 to 8.2 and 13.7 mm at the water surface. Six cross sections (20, 33.5, 40, 50, 60 and 70 cm from the water surface) were selected for the sand jet through 12.6 mm nozzle. The locations of cross sections for the sand jet through 19.2 mm nozzle were also located at 20, 30, 40, 60, 70 and 80 cm from the water surface. For the sake of consistency, one profile was chosen from each experiment (40 cm from the smaller nozzle and 30 cm from the larger nozzle). The initial concentration of the sand jet was obtained 55% based on measuring the porosity of the sand particles (n=0.45). The disperse phase velocities and concentrations were measured twice in different times and maximum 5% variation on measurement was observed. The initial velocity and the settling velocity were measured at 30.5 cm/sec and 3.3 cm/sec, respectively. Base on Jiang et. al., (2005) observations, the position of ZEF (Zone of Established Flow) calculated as follow

$$(z/D) = 5.42 + 67.85\,(u_{ss}/u_o) \qquad (7)$$

Where z is the length of ZEF; u_{ss} is the particle settling velocity; D is the nozzle diameter and u_o is the initial disperse phase velocity. Regarding to the above expression the zone of established flow was calculated as 20 cm.

NUMERICAL SIMULATION

Figure 1 shows the numerical domain of this study. The domain has a 100 cm height and the jet nozzle located at top of the domain which has a diameter of 8.2 mm for simulation of small nozzle and 13.7 mm for simulation of the large nozzle. In order to save the computational memory and time, the width and depth of the domain were limited to 30 cm on both directions which selected base on the experimental observation. Four different mesh sizes were used for examining the effect of cell size. Table 1 shows the mesh size, number of nodes and number of elements.

Table 1: Mesh characteristics and sell size.

	Coarse mesh	Medium mesh	Fine mesh	Very fine mesh
Cell size (mm)	10.00	8.75	7.62	7.00
No. of nodes	145,838	218,865	328,793	427,079
No. of elements	811,242	1,221,682	1,845,952	2,398,471

Number of nodes was increased by 50% in each step and 30% for the finest structure. The last mesh structure is the maximum number of nodes that present solver (CFX) version 11 can handle. The simulation domain was discretized into small control volumes using a mesh generated by CFX-Mesh. Figure 1 illustrates the geometry and mesh structure of the domain in both three dimension and top view. The nozzle located at the centre of the top plane (*XZ* plane) and all profiles were selected in the *Z* direction. Computational domain was divided in four regions which classified as: inlet (nozzle), walls, top and the bottom. For the sake of simplicity and to reduce the CPU time of simulation in this study, small part of the experimental tank was simulated as a computational domain. Hence, for preventing the effect of walls on the turbulent jet, it was assumed that the domain was cut by four imaginary planes that both carrier phase and dispersed phase can enter and exit through the computational domain. The solver package (CFX 11.0) has an option called opening boundary condition that allows the fluid to cross the boundary surface in either direction. This option was selected for walls of the domain. Relative pressure was specified in opening boundary condition to satisfy the conservation equations. Direction of the flow is also accounted normal to the boundary. The boundary condition for top selected as non-slip wall condition and for the bottom boundary condition a zero static pressure option was selected. The model adjusts the pressure at bottom of the domain equals to the hydrostatic pressure. Water density was selected for continuous phase equal to

998 kg/m^3 and sand was selected as dispersed phase with the density of 2540 kg/m^3.

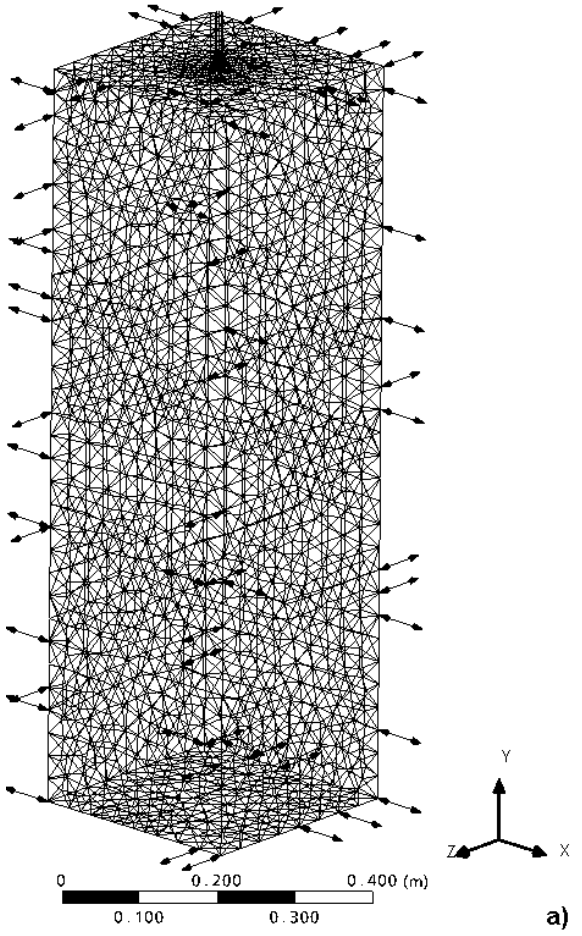

Figure 1. Simulation domain of the sand jet. a) Three-dimensional view; b) Top view.

Proper selection of turbulence models is crucial in using commercial CFD codes.In this simulation, the well-known k-ε model was chosen for continuous phase. For dispersed phase, there is only one option available in turbulent regime (Dispersed Phase Zero Equation) which was selected for dispersed phase. Drag coefficient was predicted using the well known Schiller & Neumann mode. All sand particles assumed spherical hence, the virtual mass coefficient was set equal to 0.5. Regarding to the influence of velocity fluctuations on particle dispersion the Favre Averaged Drag Force coefficient was selected equal to 0.75. In all setups, the mass flow rate of sand was identical and equal to 55.5 g/sec for small nozzle and 161.4 g/sec for large nozzle. Because of the unsteady behaviour of the turbulent sand jet the total numbers of iteration were limited to 150 iterations. The simulation domain was discretized into finite control volumes. The mentioned governing equations were integrated over each control volume. Then, the discretized integral equations were numerically solved using CFD solver (CFX 11.0) and solution variation within a control volume were computed within finite element shape functions (Ansys 2003). This approach is generally referred as to the finite-element-based finite volume method. In present simulation, the second order center difference Eulerian-Eulerian scheme was used. The residual target was chosen at 10^{-5} which gives a reasonable degree of convergence.

RESULTS AND DISCUSSION

The present investigation was conducted to study in detail the capability of available numerical model for simulation of the two-phase turbulent jet flow in water.

For reference and to present a general view of the flow structure, a contour plot of the dispersed phase velocity in YZ plane is displayed in Figure 2. For verification of the computational domain and all boundary conditions, a preliminary simulation was performed. A vertical water jet with the diameter of 12.6 mm was simulated through water bodies. The output results of simulation were compared with the analytical solution (Rajaratnam, 1976). Figure 3 shows the variation of time averaged water velocities of impinging water jet in different horizontal cross sections which indicates that the velocity distribution across the jet follows the Gaussian distribution and is self similar.

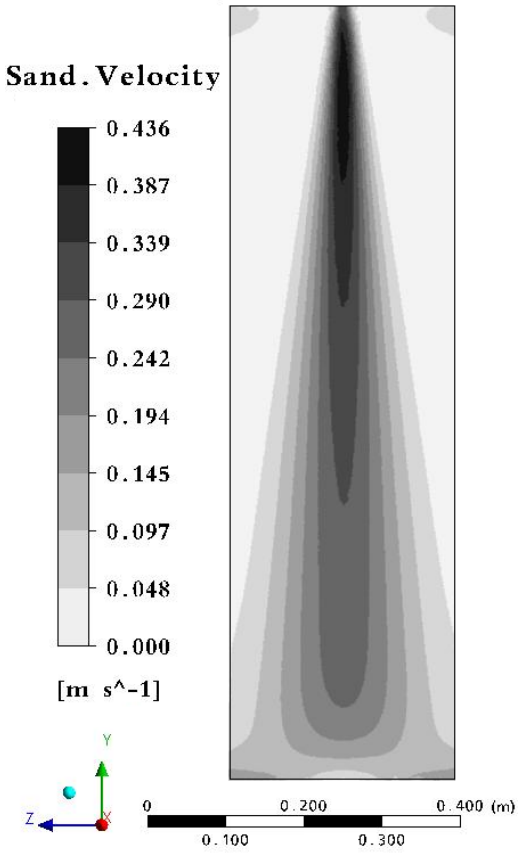

Figure 2. Sand velocity contour with the larger nozzle diameter *D*=13.7 mm.

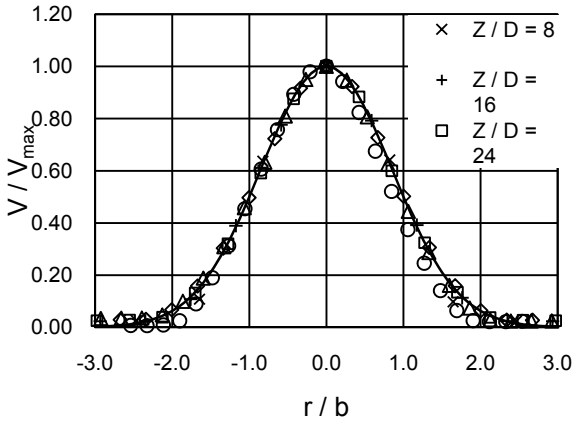

Figure 3. Normalized time-averaged water velocities of water jet in water bodies.

In order to examine the effect of mesh size and reduce the numerical errors, the model was simulated with four different mesh structures (Table 1). Figure 4 illustrates the variation of axial dispersed velocity and concentration of turbulent jets with 8.2 mm nozzle diameter. In general, predictions agree very well with the experiments both for the mean velocity and concentration.

Obtained results from simulation indicate that the computed concentrations were in good agreement with experimental observations and the accuracy of the results are independent from the domain resolution in a range from x/d=20 near the bottom of the tank (x/d=60). Error of simulation increases close to the nozzle and it reduces by increasing the number of nodes in domain (Figure 4a). For the sand velocity profile (Figure 4b), acceptable results obtained from the nozzle up to the middle of the tank (x/d = 40) but the obtained results from numerical simulation was relatively inaccurate at the bottom area of the tank compare to laboratory measurement (x/d > 40).

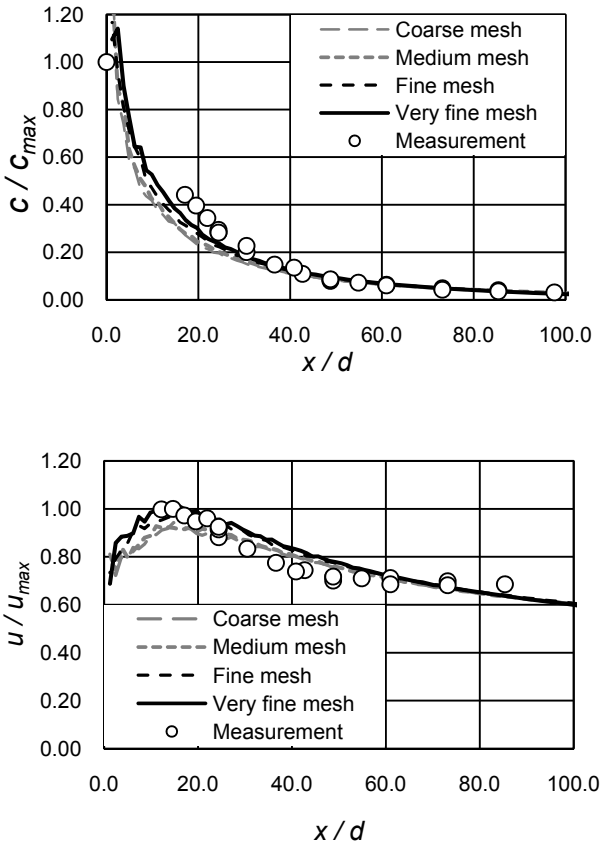

Figure 4:. Axial normalized concentration and dispersed phase velocity of turbulent sand jet. Nozzle diameter = 8.2 mm.

Approximately constant velocities observed from experimental measurement which indicates that sand particles reach the terminal velocity at the

location of x/d = 30. The simulation outputs shows a reduction in velocities in this region which may relate to the effect of bottom boundary.

The impact of the cell size on the accuracy of dispersed phase velocity indicates that, small cell size gives more precise results in the area from the nozzle up to the location of x/d = 30 but, all mesh structures give the same level of accuracy from x/d =30 near to the bottom of the tank.

In the region that the effect of mesh refinement is significant, errors of simulation for sand concentration were calculated and compared to the laboratory measurements. Table 2 presents the calculated errors and standard deviations of numerical simulation at 10< x/d <20. Comparing the average error of simulation with laboratory experiment indicates that, the error of simulation reduces for concentration measurement from 35.7±7.2 %, using coarse mesh, to 15.6±6.6 %, using very fine mesh. Considering the complexity of the flow system and experimental uncertainties obtained error by using very fine mesh could be accepted.

Table 2: Comparison of the calculated errors and standard deviation for axial dispersed velocity and concentration.

	Coarse mesh	Medium mesh	Fine mesh	Very fine mesh
Average error (%)				
Concentration	35.7	31.0	21.8	15.6
Standard deviation (%)				
Concentration	±7.20	±7.70	±7.60	±6.60

Three cross sections were selected from the small nozzle sand jet with the diameter of 8.2 mm. Model outputs were compared to the experimental observation for evaluation of the simulation accuracy and effect of mesh refinement. The nearest measured profile in laboratory experiment was located at 20 cm from the nozzle and the farthest profile was chosen 80 cm from the nozzle. For investigation of computational error and validation of simulation through entire jet, three profiles with the locations of 20, 40, and 80 cm from the nozzle were selected. Figure 5 illustrated the comparison of sand velocity measurements and simulation outputs in different sections.

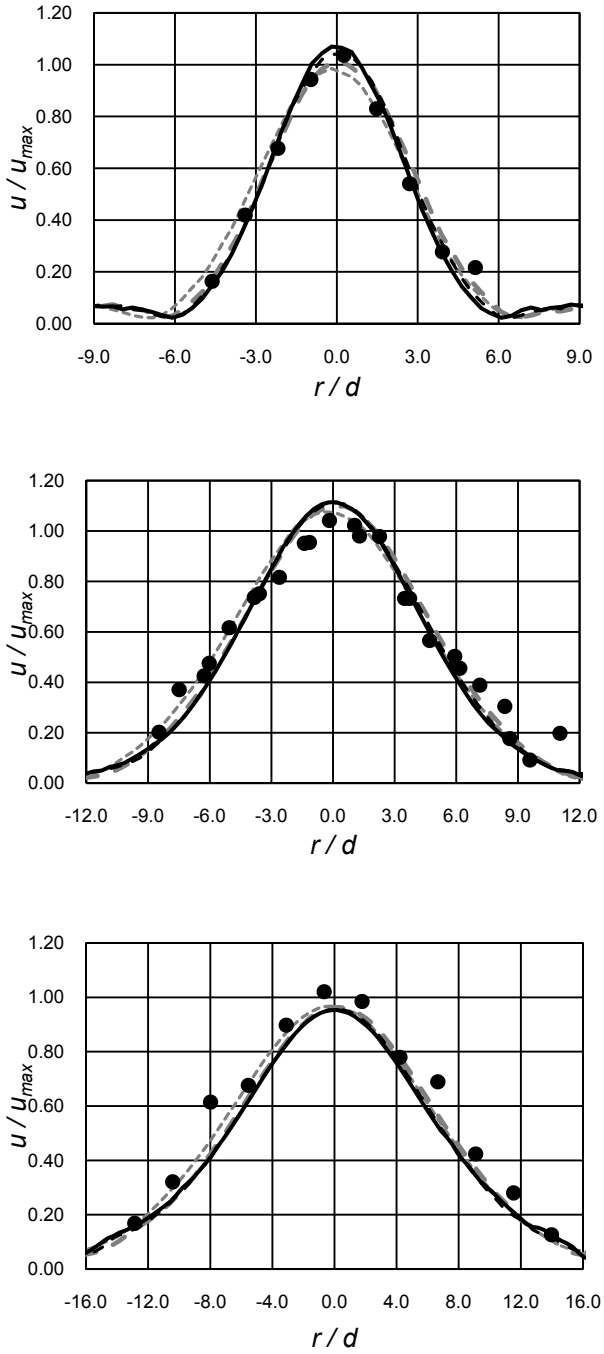

Figure 5. Comparison of measured dispersed velocity of turbulent sand jet with simulation outputs using different mesh set up. a) Profile located 20 cm from nozzle. b) Profile located 40 cm from nozzle. c) Profile located 80 cm from nozzle.

Numerical results are in good agreement with observations at 20 cm and 40 cm profiles (Figure 5a, and b).

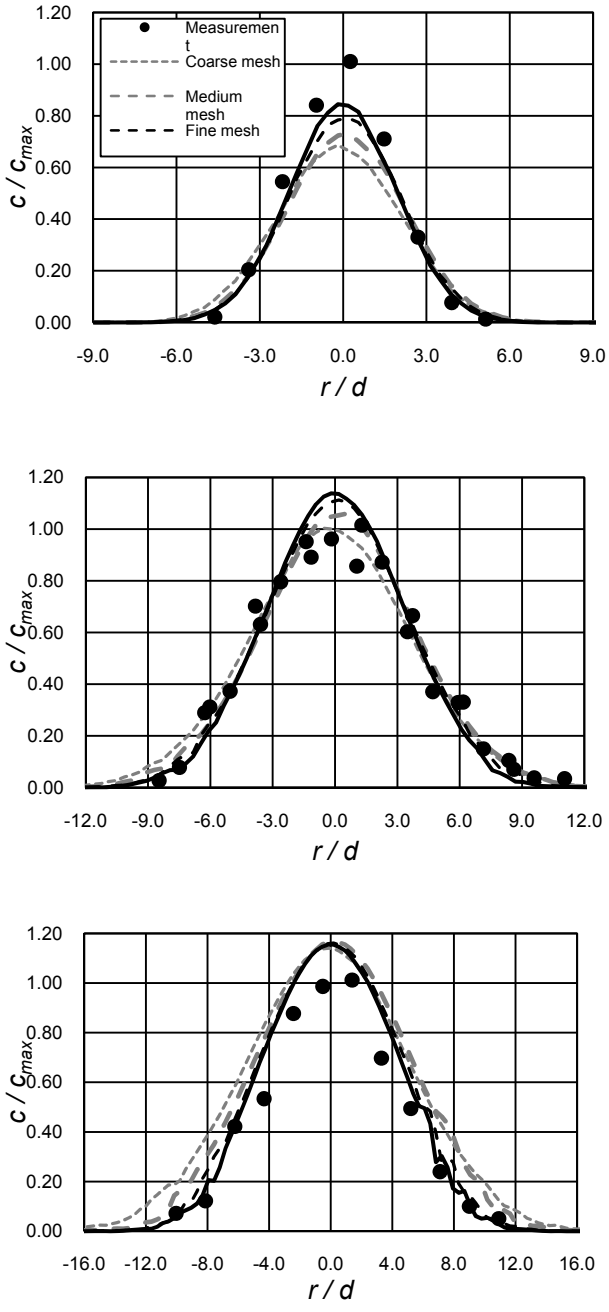

Figure 6. Comparison of measured concentration of turbulent sand jet with simulation outputs using different mesh set up. a) Profile located 20 cm from nozzle. b) Profile located 40 cm from nozzle. c) Profile located 80 cm from nozzle.

Near the bottom of the tank the model was able to predict the sand velocity with underestimation. Considering the effect of mesh resolution on flow structure shows that the solid particle velocity profile has been nearly unchanged by different mesh structure. Capability of numerical simulation for computation of turbulent jet concentration was also studied and the results were presented in Figure 6. Our model predicted the concentration near the nozzle accurately when using a highly dense mesh structure. Unreliable estimation was observed for simulation of peak concentration by using a coarse mesh structure (Figure 6a). At 40 cm from the nozzle, our model was not able to predict the peak concentration properly using the very fine mesh. Relatively accurate results were observed at outer region at this location (Figure 6b). Near the bottom tank (Figure 6c) acceptable results were obtained for concentration when very fine mesh applied.

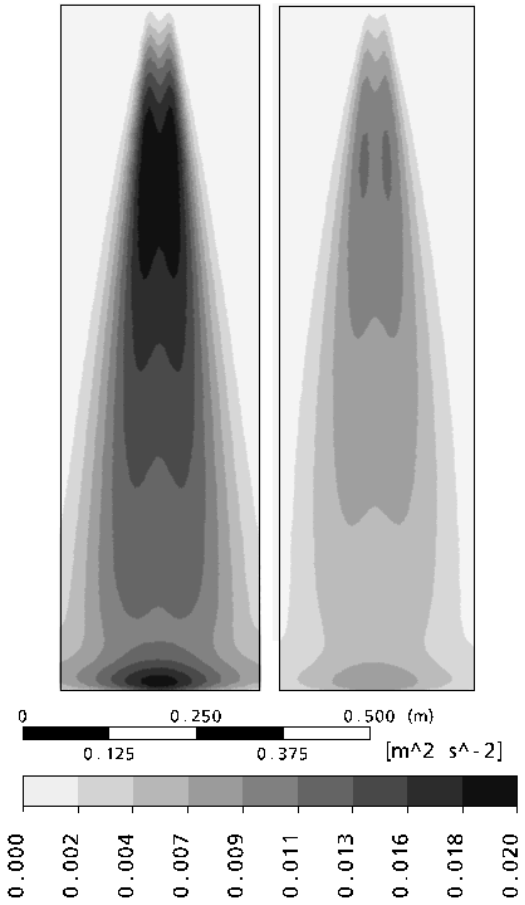

Figure 7. Contour plot of turbulent kinetic energy for different nozzle diameter: (Left) 13.7 mm nozzle and 8.2 mm nozzle (right).

Contour plot of turbulent kinetic energy was shown here in order to study the effect of dispersed mass flow rate on turbulent structure (Figure 7). Significant increase in turbulent kinetic energy was observed as expected due to increasing the mass flow rate.

The maximum kinetic energy of the system in first case (sand mass flow rate =161.4 g/sec) was obtained equal to 0.02 m^2/sec^2 and for the second case (sand mass flow rate=55.5 g/sec) the turbulent kinetic energy was found equal to 0.013 m^2/sec^2. More investigation will require to capture the effect of mass flow rate on the energy of the flow system.

CONCLUSIONS

A two-phase (solid-liquid) turbulent sand jet was investigated numerically using CFX 11.0 solver package. Two characteristics of turbulent jet, particle velocity and concentration were compared with laboratory experiments. The simulation in general performs well compared to the measurements. Model gives reliable results for prediction of sand velocity. It was found that, the simulation outputs for dispersed velocity were not sensitive to mesh resolution. In general, prediction of sand concentration was sensitive to the mesh size and more accurate results can be obtained when very fine mesh structure is used.

Model performance was evaluated at different vertical sections. The results indicate that, model performs accurately near the nozzle when highly dense mesh structure was used. Also, relatively acceptable results observed in the concentration near the bottom of the tank using high density mesh structure. It was concluded that, the accuracy of simulation for prediction of concentration was not improved using the fine mesh structure at the middle of the jet $20< x/d <60$. Effect of particle mass flow rate on turbulent kinetic energy was also studied. It is found that, the kinetic energy of the system increases with the increase in sand mass flow rate.

REFERENCES

Ansys. (2003). *CFX-5* solver theory, *ANSYS* Canada Ltd.

Drew, D. A., (1983). “Mathematical modeling of two-phase flow.” *Annu. Rev. Fluid Mech.*, 15, 261-291.

Hall, N., Zhu, D., Rajaratnam, N., (2008), “Experimental Study of Sand and Slurry Jets in Water”, *1st International Oil Sand Conference, Edmonton, Canada.* Submitted,

Jiang, J. S., Law, A. W. K., Cheng, N. S., (2005). “Two-phase analysis of vertical sediment-laden jets.” *Journal of Eng. Mechanics*, 131(3), 308-318.

Manninen, M., Taivassalo, V., and Kallio, S. (1996). “On the mixture model for multiphase flow.” *Technical Research Centre of Finland*, Espoo, Finland, VTT Publications 288.

Parthasarathy, R. N., Faeth, G. M., (1987). “Structure of particle-laden turbulent water jets in still water.” *Int. J. Multiphase Flow*, 13(5), 699-716.

Rajaratnam. N., (1976). “Turbulent jets.” Elsevier, Netherlands, 304 p.

Sheen, H. J., Jou, B. H., Lee, Y. T., (1994). “Effect of particle size on a two-phase turbulent jet.” *Experimental Thermal and Fluid Science* 8, 315-327.

Singansetti, S. R., (1966). “Diffusion of sediment in submerged jet.” *J. Hydraul. Div., Am. Soc. Civ. Eng.*, 92(2), 153-168.

Squires, K. D., Eaton, J. K., (1990). “Particle response and turbulence modification in isotropic turbulence.” *Physics of Fluids A*, 2, 1191-1203.

Virdung, T., Rasmuson, A., (2007). “Hydrodynamic properties of a turbulent confined solid-liquid jet evaluated using PIV and CFD.” *Chemical Engineerin Science.* 62, 5963-5979.

Worner, M. (2003). A compact introduction to the numerical modeling of multiphase flows, Forschugszentrum Karlsruhe GmbH, Karlsruhe, Germany.

Yuu, S., Katamaki, S., Kohno, H., Umekage, T., (1999). “Effect of particle existence on low Reynolds number gas-particle free jet (Re=800).” *JSME International Journal.* 42(1), 9-15.

Yuu, S., Ueno, T., Umekage, T., (2001). “Numerical simulation of the high Reynolds number slit nozzle gas-particle jet using subgrid-scale coupling large eddy simulation.” *Chemical Engineering Science*, 56, 4293-4307.

DEVELOPING A DYNAMIC SIMULATION MODEL FOR TAILINGS MANAGEMENT AND PLANNING

Nicholas Beier, David Sego, and Norbert Morgenstern
University of Alberta, Edmonton, Alberta, Canada

ABSTRACT

Mining and mineral processing ultimately lead to the production of waste by-products including waste rock and a finer grained slurry called "tailings". Management of the tailings and waste rock currently results in environmental challenges and financial burdens for operators. The volume of tailings generated and associated environmental hazards depend upon the individual ore bodies and the physical/chemical extraction processes. These tailings are managed through the implementation of a tailings management system (TMS), consisting of tailings treatment/dewatering at the mill, thickening, transport to and construction of storage impoundments, natural dewatering within the impoundments, water recovery and recycle, effluent treatment, and restoration of the site.

Evaluating all the options available to develop a sound management system or understanding the implications of modifications to an existing TMS can be time consuming and expensive. A sound, well thought out TMS will help fulfill the mining industry's commitments to achieve sustainability and to apply the best available technologies. The objective of this study is to develop a model/tool that will guide the tailings planner/regulator through the process of tailings management to attain the most practical, economical, and environmentally sound solution. The proposed research will use an object orientated, systems dynamic modeling software called GOLDSIM to develop the "tool". Development of the model will entail a review of the physical, chemical and natural processes experienced by the tailings and associated best management practices beginning from the initial formation through deposition and finally closure of the tailings storage facility. The goal of the review is to extract and/or to develop theoretical, empirical, process-based and qualitative formulations for each of the TMS to form the building blocks of the GOLDSIM model. Combining and linking all of the TMS components into one simulation model in a public manner has not been completed to date.

The model will allow the tailings planner to simulate the tailings system over time, demonstrate various outcomes by alternating management practices, and conduct sensitivity analyses to determine which options have the largest impacts on the system.

INTRODUCTION

Background

Mining and mineral processing ultimately lead to the production of waste by-products including waste rock and a finer grained slurry called "tailings". Management of the tailings and waste rock currently results in environmental challenges and financial burdens for operators. The typical tailings production rates have increased steadily over the last century as the demand for minerals and metals increased and technology advanced, allowing lower and lower grades of ore to be mined and processed. Tens of thousand of tonnes of tailings were produced each day in the 1960's which has increased to 100's of thousands by 2000 (Jakubick et al. 2003). The volume of tailings generated and associated environmental hazards for a particular mine depend upon the individual ore bodies and the physical/chemical extraction processes. For example, annual tailings production at the Kidd Creek copper-zinc mine is 2.92 million tonnes (Fitton, 2007) while a typical oil sands mine operating at 200,000 barrels per day could produce up to 235 million tonnes a year (Allen, 2008).

Mine operators manage these tailings through the implementation of a tailings management system (TMS). In a recent technical publication, the Australian Government, (2007) defined tailings management as "managing tailings over their life cycle, including their production, transport, placement, storage, and the closure and rehabilitation of the tailings storage facility." Therefore, one can see the management of tailings consists of several components including tailings treatment at the mill including dewatering/ thickening, transport to and construction of

geotechnically sound impoundments, water recovery and recycle, effluent treatment, and restoration of the site (Ritcey, 1989).

The selection and operation of individual TMS components and their associated tailings impoundments can have a dramatic impact on the environment. During the period of 1979 to 1999, there have been on average two to five major tailings impoundment failures per year (Dixon-Hardy and Engels, 2007). Dixon-Hardy and Engels reviewed several tailings management plans from mines in North America, Australia, and South Africa to try and understand why problems that lead to these failures are being overlooked. They generally found that tailings management systems did not actually manage the tailings to sustain safety and stability but rather focused on reducing and upholding commitments to third parties and regulators. They recommend that "a suitable tailings management system should successfully manage a wide range of risks associated with tailings storage and not just focus on satisfying the regulations/licenses" Dixon-Hardy and Engels (2007). A successful TMS should optimize in-pit storage, minimize the area of disturbance, and ensure deposition of tailings is coordinated with the construction of sound, geotechnically stable structures. Additionally, the TMS should strive to minimize long-term storage of fluid fine tailings, ultimately minimizing the time for reclamation and closure (Ritcey, 1989). Adequately designed facilities can operate at high risk if they are not managed sufficiently during construction, operation and closure (Dixon-Hardy and Engels, 2007).

OBJECTIVE

Evaluating all the options available to develop a sound management system or understanding the implications of modifications or upsets to an existing TMS can be time consuming and expensive. A sound, well thought out TMS will help fulfill the mining industry's commitments to achieve sustainability and to apply the best available technologies to minimize the risk of failures. There currently is no single simulation model available to assist the planner or regulator in evaluating the management options quickly and efficiently.

The objective of the proposed research is to develop a model/tool that will guide the tailings planner/operator/regulator through the process of tailings management to attain the most practical, economical, and environmentally sound solution. The model will allow the tailings planner to simulate the tailings system over time, demonstrate various outcomes by alternating management practices, and conduct sensitivity analyses. Essentially, the simulation model is a *what if* tool to experiment with various operating strategies or design alternatives (Scaffo-Migliaro, 2007). The intent of the TMS modeling is not to predict and design the exact behaviour but rather to identify the properties and processes (i.e. consolidation, solids content, treatment options) that are most significant. These significant processes would have the greatest impact on the overall success of the tailings management system and would be the target of further research, or more detailed design.

The modeling process will also help quantify uncertainty in the model parameters and processes through sensitivity analyses. Understanding the level of uncertainty, even if it is quite large still has utility, because it identifies elements that require further study or careful attention during detailed design and operation. The results of the modeling effort will guide the judgment of TMS decision makers (designers/regulators), as they determine the relative influence of various parameters and processes on the TMS behaviour. For example, the impact of clay content of the deposited tailings on the required containment volume and footprint and deposit stability could be determined. Understanding the TMS will not only minimize costs, it will reduce the quantity of fresh water consumption through improved water management. It will also reduce the risk of environmental damage through increased stability and performance of the tailings impoundment facility. Ultimately, the goal is to manage the tailing streams practically and economically ensuring the protection of human health and the environment.

SIMULATION MODEL

Code Selection

Mining applications have inherent uncertainties due to changing ore bodies, extraction processes and mill upsets. Dynamic simulation modeling (DSM) is therefore appropriate to accurately simulate the evolving system through time. Goldsim, a highly graphical, object orientated

simulation platform can simulate dynamic systems such as a TMS. It allows flexible inputs, outputs, time stepping, and coupling of processes (Wickham et al. 2004). The Goldsim platform is like a "visual spreadsheet". The user can visually and explicitly create and manipulate data, equations and relationships (Kossik and Miller, 2004). The simulation model can be constructed from process-based, empirical or even qualitative formulations based on a tentative relationship between two parameters. Probability can even be incorporated within the model to represent uncertainty in processes, parameters and events.

In addition to dynamic uncertainties, a TMS is highly multidisciplinary. In a typical TMS, sub models for each discipline or component are not usually linked. Therefore, a user may loose site of the "big picture" (the ultimate problem that the modeling is trying to address). The interdependencies of the different elements of the subsystems are often ignored or poorly represented. To integrate all of the TMS components, Goldsim is highly suited for top down, total system modeling approach, keeping the "big picture" in focus. This facilitates documentation of the complex model and allows one to see how all the components of the model fit together, ensuring they are reasonable and logical. Goldsim also has the ability to dynamically link with external programs such as excel to enhance the simulation capability (Kossik and Miller, 2004). The DSM modeling approach using GODSIM will assist the planner to understand the TMS and its boundaries, identify key variables and clarify complex interrelationships.

Model Structure

It is obvious that a typical TMS is multifaceted, interrelated and complex. Therefore, the simulation model will be a simplification of the real system and include only the important processes. The accuracy of the model will depend on the level of detail and parameters available to the modeler.

Various methods, ranging from empirical estimates to direct measurements and theoretical formulations are available to the modeler. Their use depends on the degree of accuracy required and cost for implementation. A hierarchical level of detail is proposed for the simulation modeling which fits well with the proposed "top down systems" approach of the model structure. For example, the lowest level of detail would include database "Mining" of the literature or professional judgment for a quick estimate of a particular parameter (particle size distribution, PSD). Correlations may then be implemented based on this estimation such as the use of the Kozeny-Carmen equation to estimate hydraulic conductivity, k, of tailings (Chapuis and Aubertin, 2003). The next level would base estimations of a particular parameter or property on some direct measurement of simple properties. In this scenario, the range of PSD would be measured and k would be estimated from these measurements. This approach is commonly used for most preliminary tailings and mine waste studies (Fredlund et al., 2003). Finally, direct measurement of properties and parameters may be conducted either in a laboratory or in situ and used in conjunction with theoretical or empirical formulations. An example of this detail level would be the measurement of large strain consolidation relationships of tailings. The challenge to the modeler is then to apply the appropriate level of detail that will result in a suitable engineering simulation satisfying the objective of the model process. Attempt should be made to use the highest possible level of detail that is necessary. Therefore, nearly any parameter or process can be determined whether it is based on crude empirical correlations or direct in situ measurements (Fredlund et al. 2003).

TAILINGS MANAGEMENT MODEL

Approach

The proposed research will use the object orientated, systems dynamic modeling software called GOLDSIM as the "simulation engine" and will be linked with external modeling software including spreadsheet models, consolidation models, design data/charts, computer assisted drawing (CAD), and geographic information systems (GIS) to develop the tailings simulation model (Figure 1).

A spreadsheet will be used as the data entry/interface for all model inputs such as site properties, tailings properties, mining and extraction rates, environmental data and pertinent management decision variables (i.e. constraints on the system). The user will have the option to utilize built in functions and sub-models or implement their own models. Implementation of user specific models/data would be completed either in the data input spreadsheet or the Goldsim model directly. Model output will be displayed in a

spreadsheet and can be visualized via GIS where needed (i.e. deposition modeling).

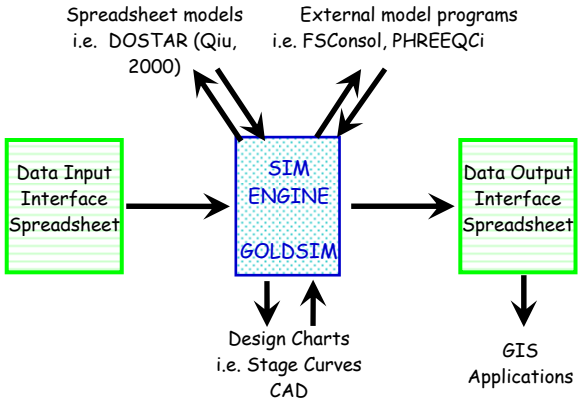

Figure 1. Tailings Simulator Schematic

Conceptual Model

A dynamic systems model will be developed for the simulation and evaluation of tailings management systems. The systems model will track the stocks and flows of mass (ore, solids [mineral including both fine and coarse], water, and chemicals) throughout the TMS. A simplified conceptual model of a typical TMS is depicted in Figures 2a and 2b and will represent the highest level of the TMS simulation model. The TMS model will be composed of a suite of sub-models representing individual components such as the mine pit, extraction plant, tailings treatment, impoundment and the environment. Critical processes (such as consolidation, evaporation or seepage) within each component will dictate mass transfer between components.

The systems model will be designed to capture and represent the major processes and relationships in each sub model. The relevant processes, variables and operating parameters will come from existing operating data, water balance modeling (including tailings impoundment and site wide), seepage analyses, deposition models, and impoundment design (stability and seepage) (Botham, 2008). For existing mine sites, this information would be contained in a typical tailings plan as outlined in the Mining Association of Canada (2005) “Developing an Operation, Maintenance, and Surveillance Manual”. In the oil sands industry, this information will be required by the Energy Resources Conservation Board (ERCB) on a yearly basis as part of the Draft Directive (2008) Tailings Performance Criteria and Requirements for Oil Sands Mining Schemes. Where detailed information is unavailable, estimations will be incorporated using the hierarchy level of detail approach described earlier.

Mine Pit and Extraction Plant

The sub-model components representing the mine pit and extraction plant will essentially drive the model. For example, the ore reserve, production schedule and associated plant availability will dictate and influence the tailings production rate and properties (grain size, specific gravity, and slurry density).

Tailings Treatment

The tailings treatment model will incorporate the potential dewatering and handling processes experienced by the tailings after extraction but prior to deposition. Dewatering might be achieved through a combination of physical, chemical and natural processes by utilizing hydrocyclones, mechanical thickeners, filter presses, chemical amendments, etc. In the case of non-segregating oil sand tailings, re-handling and mixing of various streams (fine/coarse) would be simulated at this stage. Regardless of the treatment method used, the user must ultimately specify a relationship between the inflows (tailings from extraction) and the outflows (tailings for deposition and overflow recycle/release).

Impoundment or In-pit

The impoundment component will consist of several interrelated sub-models encompassing the impoundment structure itself, the tailings deposit and the free water pond. Stage/area/volume relationships will be developed for the impoundment structure based on existing or proposed designs. Implementation of a second impoundment or in pit deposition and therefore a different stage/area/volume relationship can be triggered by date (based on mine plan) or event (impoundment is full). Reservoir elements, unique to Goldsim, will be utilized within each sub-component to track the volume of water stored through time, including inflows, outflows and potential overflows. Inflows to the impoundment include tailings solids and pore fluid, direct and indirect precipitation, site runoff, and miscellaneous flows (emergency dump). Impoundment outflows will include evaporation, pond recycle, and seepage (basal and dyke). Inflows, outflows and available storage will be

influenced by the tailings deposition method, deposit dewatering characteristics (seepage, consolidation, and evaporation), and climate (precipitation/ evaporation).

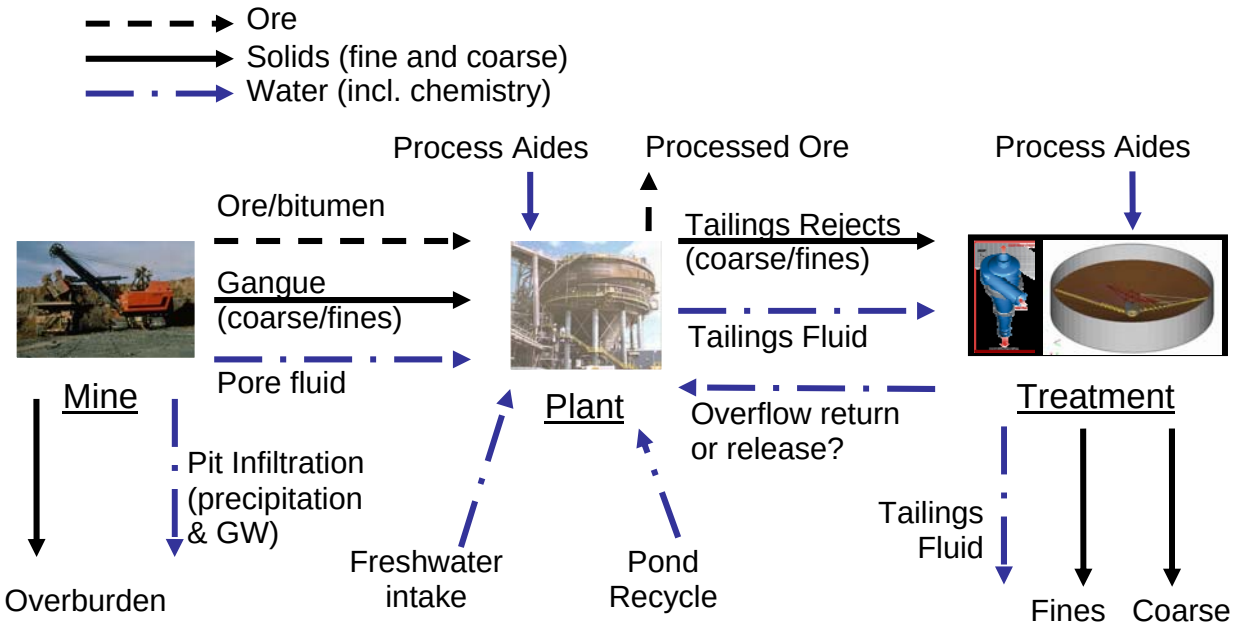

Figure 2a. Tailings Conceptual Model (Mine – Mill – Treatment flows to impoundment/in pit)

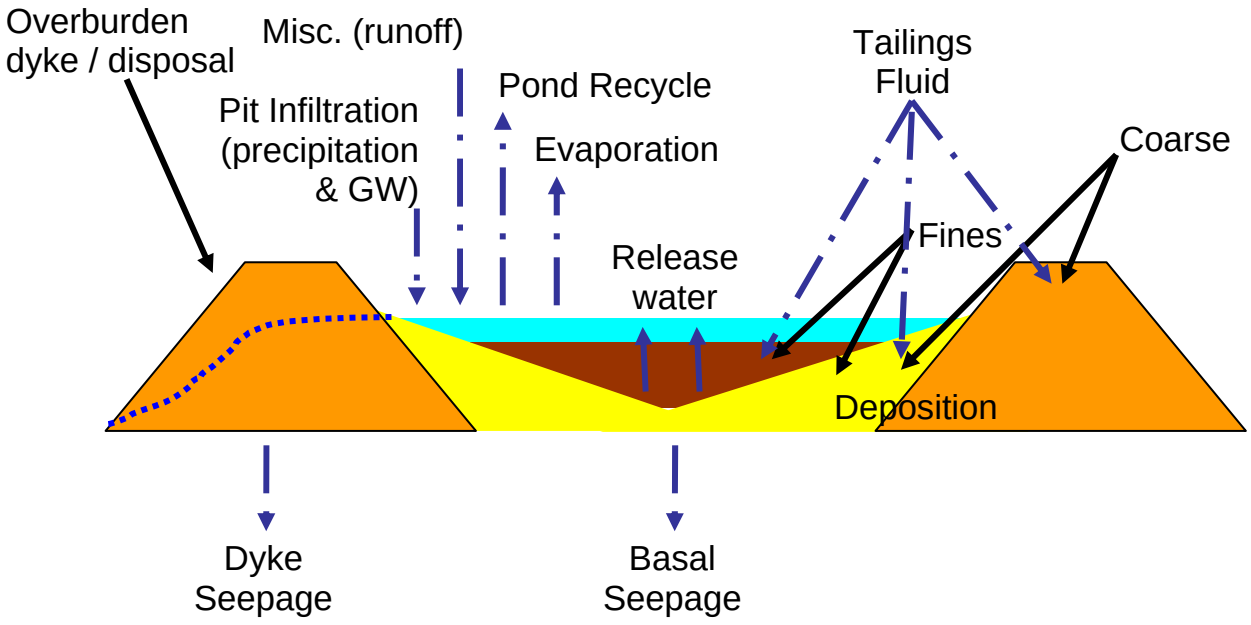

Figure 2b. Tailings Conceptual Model (Impoundment/in pit flows from Mine-Mill-Treatment)

Water - Chemistry System

Many processes can influence the water-chemistry system of a TMS. Simple mixing of various water and tailings streams will lead to dilution and accumulation of mass. There can also be charge exchange reactions, precipitation and other chemical or biological processes leading to addition or removal of mass from the water stream. Several processes including extraction and tailings dewatering behaviour can be significantly impacted by the chemical make up of the recycle water or pore fluid. Therefore it is important to understand the chemistry in the TMS. The initial scope of TMS model will only look at dilution/accumulation of ions. This should be sufficient to understand the major trends of chemical mass flow between the many components of the TMS. Future research could fine tune the water chemistry system to include more complicated reactions such as surface exchange with clays and solubility/precipitation reactions.

MODEL DEVELOPMENT AND APPLICATION

The following approach will be used to develop the dynamic system model for tailings management (Halog and Chan, 2008). The initial and most important stage will be to define or frame the TMS system and modeling goals. This includes outlining the questions that need to be answered by the model exercise. For example:

- What is the required impoundment storage volume (for both solids and water)?
- What is the available storage volume?
- What is the available recycle water volume and quality?
- Time frame to produce a stable tailings deposit?
- What is the seepage rate to the environment and its quality?

Once the system is framed, it must be decomposed into a series of linked sub-systems to define key variables, relationships and feedbacks. State variables or stocks (reservoirs) should be identified. These variables will define the status of the system (tailings deposit volume, pond level). Control variables and parameters which impact the rate of flow of material into and out of the stocks are then defined (hydraulic conductivity). Variables should be chosen such that they can be quantified initially by available data. As the model develops, the user can add more variables were required. Mathematical functions then need to be formulated to express the relationship between the variables and relevant feedback mechanisms.

Once assembled the model will be run to verify it does not violate natural mathematical or engineering laws (negative mass). Sensitivity analyses will be conducted to ensure there are no abnormalities or errors with the model. After the model has been verified, model validation can begin. The operational data from a “real system” will be used by the model to determine whether there is an observable difference in the expected results. Refinements to the model will likely be required to ensure these differences are within acceptable tolerances.

Due to the complexity of oil sands operations, initial validation will be conducted with a typical open pit copper mining operation utilizing an external tailings facility. Data will be provided from previous University of Alberta research (Qiu, 2000). The complexity and scale of the tailings management plan at this mine is suitable for development and calibration stages of the TMS model structure and components. To ensure the model can handle more complex TMS plans that include fine grained tailings deposits, a typical Alberta Coal mine operation will then be simulated. Validation data will again come from extensive research conducted at the site by the authors (Beier and Sego, 2008; Stahl and Sego, 1995). Finally, after the model has been proven robust for these simple TMS cases, an oil sands mine will be simulated. Fine tuning of the model will be required to reflect the management scheme and material flows at oil sands operations. Model validation will be based on data provided in publicly available sources such as ERCB applications and educational research (theses and journals).

The initial dynamic TMS simulator will be developed as a descriptive model. It will simply describe the tailings system and provide data for evaluation and sensitivity analyses. Once fully operational, it will be used as a predictive model to explain the behaviour of the TMS system under certain operating conditions (extreme precipitation events, plant upsets). It can also be used to aid decision makers in evaluating new technology. To illustrate predictive capabilities of the model, novel tailings dewatering processes will be implemented into the TMS model. For example, in-situ

freeze-thaw dewatering and structural enhancement will be evaluated as an alternative for management of fine coal tailings. The ultimate goal would be to introduce a novel technology (such as centrifuge dewatering) into the oil sands TMS simulation to understand the overall impact on the system. This modeling process would help elucidate where further research is required to advance the technology. An example technology to be run is cross flow filtration of total tailings based on the preliminary work by Beier and Sego (2008) and ongoing research.

CONCLUSION

Tailings management is a complex issue, especially for large operations such as the oils sands. The proposed dynamic systems-modeling approach will assist TMS decision makers (designers/regulators) to determine the relative influence of various parameters and processes on the tailings system behaviour. It will also allow the user to forecast and compare outcomes by alternating management practices and investigating the impact of novel and innovative tailings technologies.

ACKNOWLEDGEMENTS

The authors are thankful for the financial assistance from National Sciences and Engineering Research Council of Canada, Alberta Research Council, Oil Sands Tailings Research Facility, and Prairie Mines an Royalty Ltd.

REFERENCES

Allen, E. 2008. Process water treatment in Canada's oil sands industry: I. Target pollutants and treatment objectives. Journal of Environmental Science, **7**: 123-138.

Australian Government. 2007. Tailings Management. Leading practice sustainable development program for the mining industry. Commonwealth of Australia. www.ret.gov.au/sdmining, accessed Aug 8, 2007.

Beier, N.A., Sego, D.C., Cyclic freeze–thaw to enhance the stability of coal tailings, Cold Regions Science and Technology (2008), doi:10.1016/j.coldregions.2008.08.006

Beier, N. and Sego, D. (2008). Dewatering of Oil Sands Tailings Using Cross Flow Filtration. 61st Canadian Geotechnical Conference and 9th joint IAH-CNC Groundwater Specialty Conference, Edmonton, Alberta, September 22-24, 2008. 8 pp

Botham ,L.C. 2008. Modeling tools for Mine waste planning. CIM Conference and Exhibition, Edmonton, Alberta, May, 2008.

Chapuis, R. and Aubertin, M. 2003. On the use of the Kozeny-Carmen equation to predict the hydraulic conductivity of soils. Canadian Geotechnical Journal, **40**: 616-628.

Dixon-Hardy, D.W. and Engels, J.W. 2007. Guidelines and recommendations for the safe operation of tailings management facilities. Environmental Engineering Science, **24**:5 625-637.

Fitton, T. 2007. Tailings beach slope prediction. PhD Thesis, School of Civil, Environmental and Chemical Engineering, RMIT University, Melbourne, Australia, May 2007.

Fredlund, M.D., Fredlund, D.G., Houston, S.L., and Houston, W. 2003. Assessment of unsaturated soil properties for seepage modeling through tailings and mine waste. Tailings and Mine Waste '03: Proceedings of the Tenth International Conference on Tailings and Mine Waste, 12-15 October 2003, Vail, Colorado, USA.

Halog, A. and Chan, A. 2008. Developing a dynamic systems model for the sustainable development of the Canadian oil sands industry. International journal of Environmental Technology and Management, **8**:1, 3-22.

Jakubick, A., McKenna, G., and Robertson, A. 2003. Stabilisation of Tailings Deposits: International Experience". In proceedings of Mining and the Environment III, Sudbury, Ontario, Canada, 25-28 May, 2003.

Kossik, R and Miller, I. 2004. A probabilistic total system approach to the simulation of complex environmental systems. Proceedings of the 2004 Winter Simulation Conference.

Qiu, Y. 2000. Optimum deposition for sub-aerial tailings deposition. PhD thesis, Department of Civil and Environmental Engineering, University of Alberta, Edmonton, Alberta.

Ritcey, G.M. 1989. Tailings Management: Problems and Solutions in the Mining Industry. Elsevier Science Publishers, Amsterdam. pp 970.

Scaffo-Migliaro, A. 2007. Modeling and simulation of an at-face slurry process for oil sands. MSc thesis, Department of Mechanical Engineering, Univeristy of Alberta, Edmonton, Alberta.

Stahl, R.P. and Sego, D.C. 1995. Freeze-thaw dewatering and structural enhancement of fine coal tails. Journal of Cold Regions Engineering, **9**:3 135-151.

Wickham, M., Johnson, B., and Johnson, D. 2004. Dynamic systems-modeling approach to evaluating hydrologic implications of backfill designs. Mining Engineering, **56**:1 52-56.

POSSIBLITY OF USING CENTRIFUGAL FILTRATION FOR PRODUCTION OF NON-SEGREGATING TAILINGS

Reza Moussavi Nik, David C. Sego, Norbert R. Morgenstern
University of Alberta, Edmonton, Alberta, Canada

ABSTRACT

The feasibility of using a filtering centrifuge to achieve a more concentrated MFT, as a component for making CT/NST is reviewed. A series of plant scale centrifugal filtration tests have been conducted using untreated and treated fine tailings. The cake formed on the filter cloth has an average solids content ranging from 43%wt to 65%wt and can be used for making concentrated CT/NST. For untreated tailings, partial segregation of the fine particles has been observed inside the filtering centrifuge and methods to reduce the level of segregation were examined. Initial results indicate that centrifugal filtration has the potential as an approach for improving the quality of Non-Segregating Tailings.

INTRODUCTION

One method for management of oil sands tailings in northern Alberta has been production of composite/consolidated tailings (CT) or Non-Segregating Tailings (NST). CT or NST is composed of MFT (mature fine tailings) plus a coagulant (gypsum) and the cyclone underflow (tailing sand). This waste stream is non-segregating when discharged, but in practice it is not particularly robust and partial segregation has been observed resulting in fines release at the surface following deposition.

Figure 1 shows the slurry properties diagram, a convenient tool for describing the properties of slurries composed of fine and coarse mineral matter (Scott and Cymerman 1984, Morgenstern and Scott 1995, FTFC 1995). The points that locate below a segregation boundary are representative of non-segregating mixtures. It should be noted that the segregation boundaries presented on this diagram have been determined using static test conditions. Based on this diagram, the CT produced in the field (with an average solids content of 60%wt) is close to the segregation boundary and a small decrease in its solids concentration results in segregation. In the field, a common reason for variations in concentration of CT is the fluctuations in solids content of the sand from cyclone underflow. Making a CT with higher solids content located at a reasonable distance below the segregation boundary will prevent segregation due to these fluctuations.

Dewatering MFT

One approach for making a concentrated CT would be dewatering the MFT before mixing it with the underflow sand. In this research project use of a filtering centrifuge has been studied for this purpose.

Review of the published research work and patented material shows that previously either filtration or centrifugation has been considered as possible methods for treatment of oil sands fine tailings. Baillie and Malmberg (1969) have proposed centrifugation of chemically flocculated pond sludge. Similarly Corti and Falcon (1989) have considered multi stages of centrifugation for treatment of oil contaminated sludge. Hepp and Camp have used vacuum pre-coat filtration for chemically treated tailings (1970). According to Kasperski (1992) most of the mechanical and physical methods of treatment including centrifugation and filtration have had difficulty to design a feasible and economic process that would be acceptable to the industry.

It should be mentioned that a challenge for filtration of oil sands tailings has been the presence of bitumen and its tendency to clog the filter pores. As will be discussed later, this is less likely to occur when using centrifugal filtration.

CENTRIFUGAL FILTRATION

Concept

A schematic view of the batch filtering centrifuge used in this research is illustrated in Figure 2. The basic components of this centrifuge are a perforated drum (basket) and a filter cloth that is placed inside the drum. This combination spins around a vertical axis, resulting in a centrifugal

gravity field. An observer in the rotating frame attached to the drum experiences a centrifugal acceleration directed radially outward from the axis of rotation. The magnitude of this acceleration can be expressed as following:

$$a = r\omega^2 \quad (1)$$

where ω is the angular velocity of the centrifuge drum and r is the radius from the axis of rotation. Usually the centrifugal gravity (G) is measured in multiples of earth gravity *g*:

$$\frac{G}{g} = \frac{r\omega^2}{g} \quad (2)$$

With the spinning speed in *rpm* and radius of the drum in *cm,* we can write:

$$\frac{G}{g} = 0.00001118 r\omega^2 \quad (3)$$

As soon as the slurry is introduced, the coarser solid particles settle on the filter cloth and gradually form a cake. While the solids are retained by the filter, the liquid flows through the cake and the filter cloth. This liquid that passes through the filter medium is known as the filtrate (Figure 2).

The driving force that causes filtration is due to a hydrostatic pressure difference across the drum wall and the free liquid surface:

$$P_c = \frac{1}{2}\rho_l \omega^2 (r_a^2 - r_i^2) \quad (4)$$

In the above equation, ρ_l is the density of the liquid; r_i is the inner radius of the free liquid surface and r_a is the radius of the cloth and drum, as illustrated in Fig. 2 (Purchas 1977).

The resistance against filtration depends on the thickness and permeability of the cake layer and the filter medium, along with density and viscosity of the liquid. The filtration rate can be determined according to the driving and resistive forces. Detailed equations defining these parameters are available from chemical engineering handbooks and will not be detailed here. (Purchas 1977; Perry et al. 1997; Richardson et al. 2002).

Figure 3 shows a schematic diagram of the pressure distribution in the cake and the free liquid above it. As it is illustrated, the pressure increases from zero to a maximum at the cake surface, and then drops consistently within the cake to overcome the resistance against flow. Additional pressure drop occurs across the filter medium (Perry et al. 1997).

EXPERIMENTAL PROCEDURE

Materials

The mature fine tailings used in this study were from Syncrude Canada Ltd. Average solids content of the MFT was 35.93%wt with a bitumen content of 1.76%wt. About 97.7% of the solids are finer than 45 microns. The grain size distribution (GSD) of the material obtained using a 152H hydrometer is presented in the results section.

Test Setup

Different components of the test setup are illustrated in Figure 4. In order to mix gypsum with MFT, a drill mixer was used. A Variable Frequency Drive (VFD) was used to control the rate of acceleration/deceleration and the spinning speed of the centrifuge. A centrifugal slurry pump with an adjustable flow rate fed the slurry into the centrifuge.

The filtering centrifuge used in this study has a maximum nominal angular velocity of 1750 rpm. Diameter of the drum is about 600 mm. The filter cloth that was used for this stage of research had a pore size of 0.8 microns. The filter cloth has a special coating which reduces blockage of the pores (by the bitumen present in the MFT) and facilitates removal of the cake.

Operating Cycle

The advantage of using a batch centrifuge system for the plant scale tests is that duration of the filtration period and the level of centrifugal gravity are adjustable. This facilitates qualitative optimization of the final products and adjustment to varying product requirements (Perry et al. 1997).

Figure 5 illustrates a typical operating cycle of the batch filtering centrifuge used in this study. During the first stage, the stationary drum is accelerated to the loading speed (~600 rpm to 800 rpm) in less than a minute while it is empty. Then MFT is introduced into the system by means of the pump. After loading is complete in couple of minutes, the centrifuge is accelerated to higher speed

(>900 rpm) spinning for the desired duration and finally it is decelerated in about a minute.

In a typical filtration operation in other industrial fields, the filtration continues until no filtrate is left inside the cake and it is almost dry. This would not be the case in the present study, since the aim is to achieve a thicker MFT (preferably pumpable) to be used in production of CT. In other words the state of the final product would be the main criteria to determine the duration and acceleration during centrifugal filtration.

Products

The MFT introduced into the filtering centrifuge produces three products:

- *Cake:* A thicker slurry or paste like material which is collected from the filter cloth. Figure 6-a shows a picture of the thick cake scraped from the filter.
- *Filtrate:* The water passing through the filter medium which is almost clear and has low percentage of solids. Figure 6-b shows a sample of filtrate.
- *Thin tailings:* Part of the liquid that has not passed through the filter medium and is not collected within the cake, remains inside the basket and includes fine particles in a suspension.

In order to evaluate performance of the centrifugal filtration, weight and solids content of the feed MFT and each of the above mentioned products are measured. Also hydrometer tests have been conducted on the feed MFT, the cake and the thin tailings left inside the drum for selective tests to assess the amount of the fines collected in the cake compared to the source MFT and in the thin tailings.

RESULTS AND OBSERVATIONS

Summary of the test conditions are presented in Table 1 for seven tests. In this table the period mentioned as “delay before centrifugal filtration” is the time that material has been left aside after mixing with gypsum and before being fed into the centrifuge. It should be noted that for the two tests SD-300-C and SD-300-D the material was circulated through the pump during this period to simulate the conditions of shearing along the pipeline in the field.

The amounts of gypsum are calculated for one cubic meter of CT, with a sand to fines ratio of 4 and a solids content of 62%wt.

The solids content of the cake, thin tailings and filtrate for each of the tests is presented in Table 2. Table 3 summarizes the weight of each of these three products as a percentage of weight of the MFT fed into the system.

Figure 7 shows the grain size distribution (GSD) for the original MFT fed into the system, the cake and the thin tailings in test SD-0. Results indicate that segregation of the coarse and fine particles has occurred, i.e. the cake is composed of coarser particles while the thin tailings include a large percentage of the fine particles. In this test only 29% of the total fine particles in the MFT were captured in the cake.

Although the cake has a high solids content, the majority of the fine particles still form a suspension (thin tailings). Considering this issue, it was decided to treat the MFT with gypsum as a coagulant before centrifugal filtration.

Figure 8 presents the GSD of the cake and thin tailings from test SD-900 with respect to the feed material. In this case the test conditions have been similar to test SD-0, except for using 900 ppm gypsum. It is observed that GSD of the cake is similar to the source material in comparison to the previous test. About 58% of the fines are captured within the cake. The solids content of the thin tailings remaining inside the basket is about 18.5% which is high.

Test SD-600 in Table 1 is a case that after 600 ppm of gypsum is mixed with MFT, the material was left aside for about 30 minutes before being fed into the pump. The interesting observation made after this test is the low solids content of the thin tailings (about 5.4%) and the large amount of the material collected as cake (77.5% of the total weight). The cake has a solids content of about 48% and is a suitable material for making a robust NST. It should be noted that the amount of gypsum used is less than the current practice in the industry, resulting in less Ca^{2+} ions present in the filtrate and the water later released from NST deposit.

To confirm the observation from the previous test, two tests SD-300-A and SD-300-B were conducted. In test SD-300-A, the MFT was mixed with gypsum and left aside for one hour before

being introduced into the filtering centrifuge, while in test SD-300-B, it was instantly fed into the filtering centrifuge after mixing. The thin tailings in test SD-300-A have significantly lower solids content and majority of the solids are collected within the cake. As it is shown in Figure 9, hydrometer analysis of the cake reveals that no segregation occurred in test SD-300-A and GSD of the cake is similar to the source material.

Test SD-300-C is similar to the two pervious tests, but the MFT mixed with gypsum has been circulated through the pump for 37 minutes before starting the centrifugal filtration. Tables 2 and 3 indicate that about half of the material is still in the form of a suspension with high solids content, a case which is not desired. In this test and test SD-300-D, circulating the MFT before feeding filtering centrifuge has lead to less capture of the fine particles within the cake.

It can be seen that the amount of the filtrate achieved from the tests is a small percentage of the total weight. As it was stated before, rate of filtration depends on permeability of the cake and the level of centrifugal gravity. Tables 1 and 3 indicate that although duration of the test is shorter for test SD-300-D, the amount of filtrate is more in comparison to the other tests. This is due to the higher spinning velocity which results in a larger relative centrifugal acceleration.

Advantage of Centrifugal Filtration

One significant advantage of using centrifugal filtration for thickening MFT is that bitumen, due to its lower specific gravity, forms an internal layer close to the centre of rotation and has less opportunity to touch the filter medium. This significantly reduces blockage of the filter pores contained in the filter cloth.

STUDY IN PROGRESS

The thick MFT obtained from previous tests will be used to make NST and the segregation and flow behaviour of this material will be studied. Just to mention a case as an example, the cake from test SD-600 with a S.C. of 48%wt was mixed with sand (S.C.=75%wt) at a SFR=4 and resulted a NST with 67%wt S.C. This NST when deposited in a laboratory flume test, showed a deposition slope about 1% steeper than a CT made with the source MFT that had a S.C. of 63%. Detailed results of studying the behaviour of CT/NST made from thickened MFT will be presented in a separate publication.

Review of the results presented in the previous section indicate that leaving the MFT mixed with gypsum for a period of time before starting the centrifugal filtration, has a significant effect on the amount of fine particles that can be captured within the cake. To determine the minimum required time for an acceptable level of flocculation and fines capture, a series of tests are in progress. The aim of these tests are to find a correlation between the amount of coagulant that is mixed and the shear strength (or viscosity) of the MFT at certain time intervals after mixing.

CONCLUSION

Initial results of the filtering centrifuge tests indicate that this method of dewatering can be considered as an approach for management of oil sands tailings. The thick MFT achieved in this method of dewatering can be mixed up with sand from cyclone underflow for production of robust Non-Segregating Tailings. In addition, the filtrate produced is a potential source of recycle water to be utilized in the extraction process, after a minor treatment if required. Meanwhile since a large percentage of the fine particles can be captured within the cake, the amount of flocculant agents required for treatment of the thin tailings remaining inside the basket will be reduced, resulting in a significant reduction in the costs associated with management of the tailings during the next stages.

ACKNOWLEDGEMENT

The financial support from the Oil Sands Tailings Research Facility (OSTRF) which made this research possible is highly appreciated.

REFERENCES

Baillie R.A., and Malmberg, E.W. (1969). “Removal of Clay from the Water Streams of the Hot Water Process by Flocculation”, U.S.Patent. No. ,3,487,003.

Corti, A. and Falcon, J.A. (1989) “Method and Treatment for Contaminated Oil Sludge.”, U.S. Patent No. 4,812,225.

FTFC. (1995). Advances in Oil Sands Tailings Research. Alberta Department of Energy, Oil Sands and Research Division.

Hepp, P.S., and Camp, P.W. (1970). “Treating Hot Water Process Discharge Water by Flocculation and Vacuum Precoat Filtration.”, U.S. Patent No. 3,502,575.

Kasperski, K. L. (1992). "A Review of Properties and Treatment of Oil Sands Tailings." AOSTRA Journal of Research, 8 11-53.

Morgenstern, N. R., and Scott, J. D. (1995). "Geotechnics of fine tailings management." Geoenvironment 2000, ASCE, 2 1663-1673.

Perry, R.H., Green, D.W., and Maloney, J.O. (1997) Perry’s Chemical Engineers’ Handbook. Mc-Graw Hill., 7th ed.

Purchas, D. B. (1977). Solid/Liquid Separation Equipment Scale-Up. Uplands Press Ltd.

Richardson, J.F., Harker, J.H., and Backhurst., J.R. (2002) Coulson and Richardson’s Chemical Engineering. Butterworth Heinemann., 5th ed.

Scott, J. D., and Cymerman, G. J. (1984). "Prediction of viable tailings disposal methods." Symposium on Sedimentation and Consolidation Methods, American Society of Civil Engineers, 522-544.

Table 1 – The Test Conditions

Test	Spinning Velocity (rpm)	Duration (min)	Gypsum (ppm)	Delay before centrifugal filtration (minutes)
SD-0	940 rpm	09:10	0	0
SD-900	898 rpm	09:30	900	0
SD-600	900 rpm	09:02	600	30
SD-300-A	925 rpm	09:00	300	60
SD-300-B	925 rpm	08:50	300	0
SD-300-C	925 rpm	08:48	300	37*
SD-300-D	1250 rpm	05:20	300	34*

* Circulated through the pump during this period

Table 2 – Solids content of the test products

Test	Cake SC	Thin Tailing SC	Filtrate SC
SD-0	64.9%	20.7%	0.75%
SD-900	48.5%	18.5%	0.42%
SD-600	48.1%	5.40%	0.74%
SD-300-A	43.1%	2.15%	1.12%
SD-300-B	61.4%	22.6%	0.66%
SD-300-C	58.7%	24.7%	0.60%
SD-300-D	56.7%	22.3%	0.51%

Table 3 – Weight percentage of each product

Test	Cake %wt	Thin Tailing %wt	Filtrate %wt
SD-0	36.7%	55.8%	---
SD-900	65.6%	29.7%	4.76%
SD-600	77.5%	18.1%	4.35%
SD-300-A	86.3%	9.7%	4.01%
SD-300-B	40.6%	53.4%	6.01%
SD-300-C	46.5%	48.1%	5.38%
SD-300-D	42.1%	49.5%	8.40%

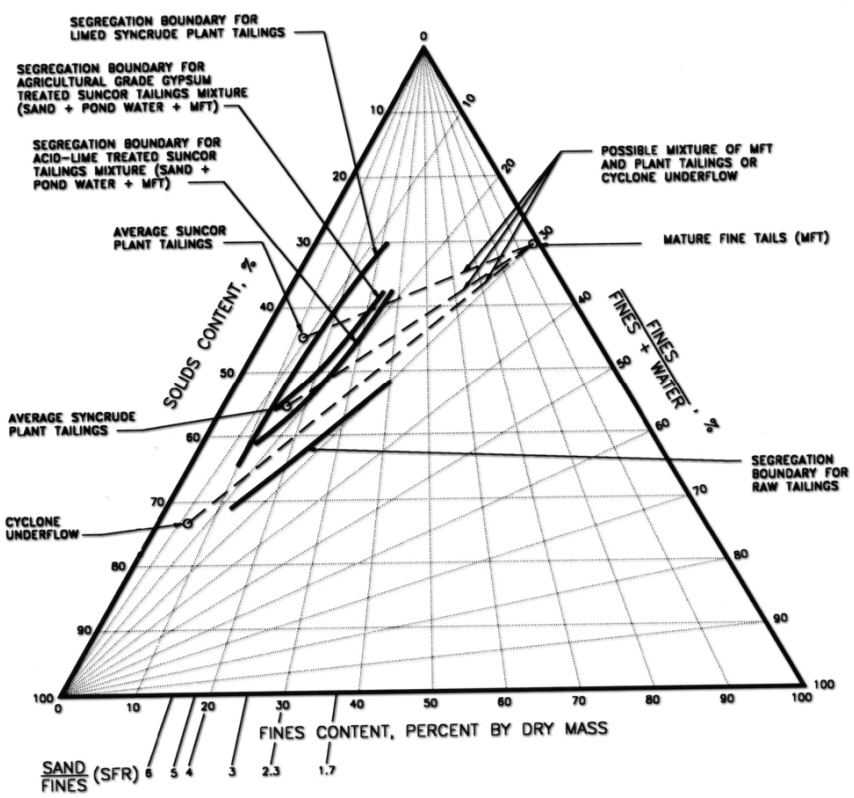

Figure 1. The Slurry Properties Diagram

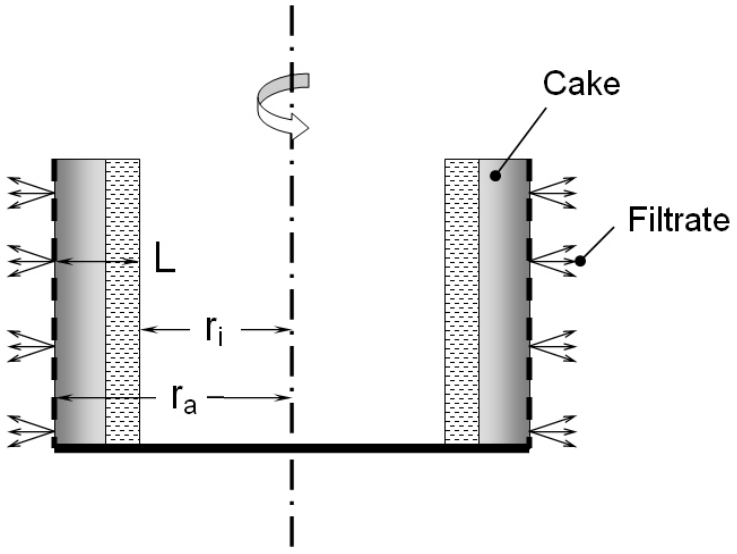

Figure 2. Schematic View of the Batch Filtering Centrifuge

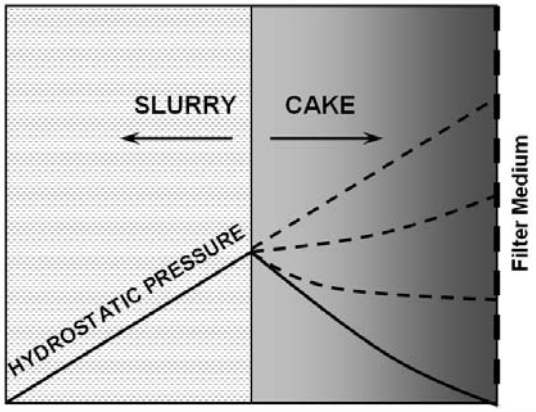

Figure 3. Pressure distribution in the cake and slurry

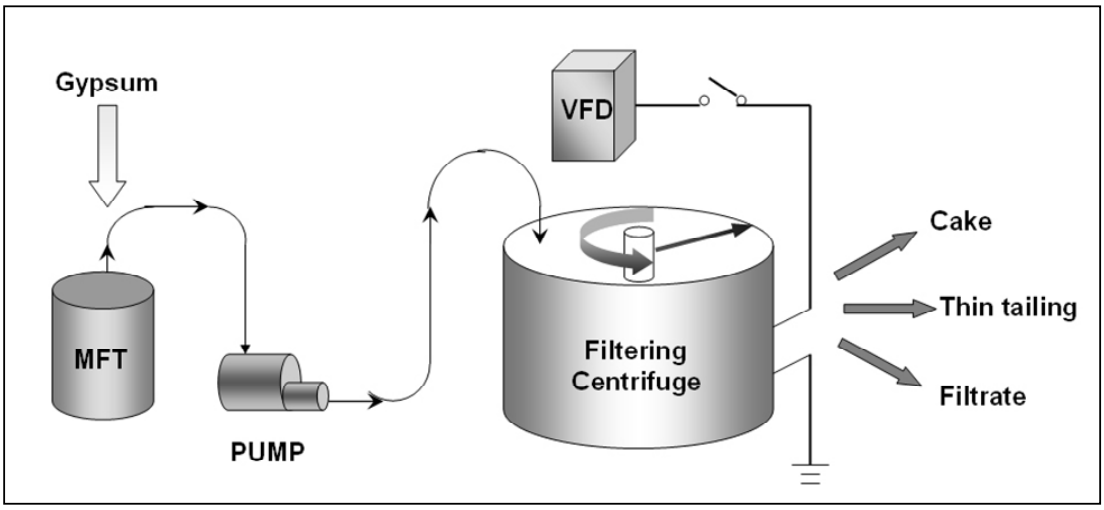

Figure 4. Filtering Centrifuge Test Setup

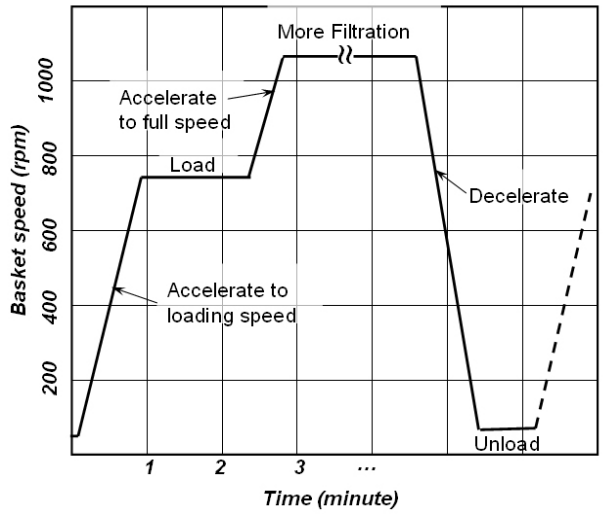

Figure 5. Typical operating cycle of the batch filtering centrifuge

(a) (b-1) (b-2)

Figure 6- Products of the centrifugal filtration for a sample test:

a- Cake with a solids content of about 67%,
b- Filtrate with a solids content of about 0.7% : (1) - right after the test ; (2) - after sitting for couple of days

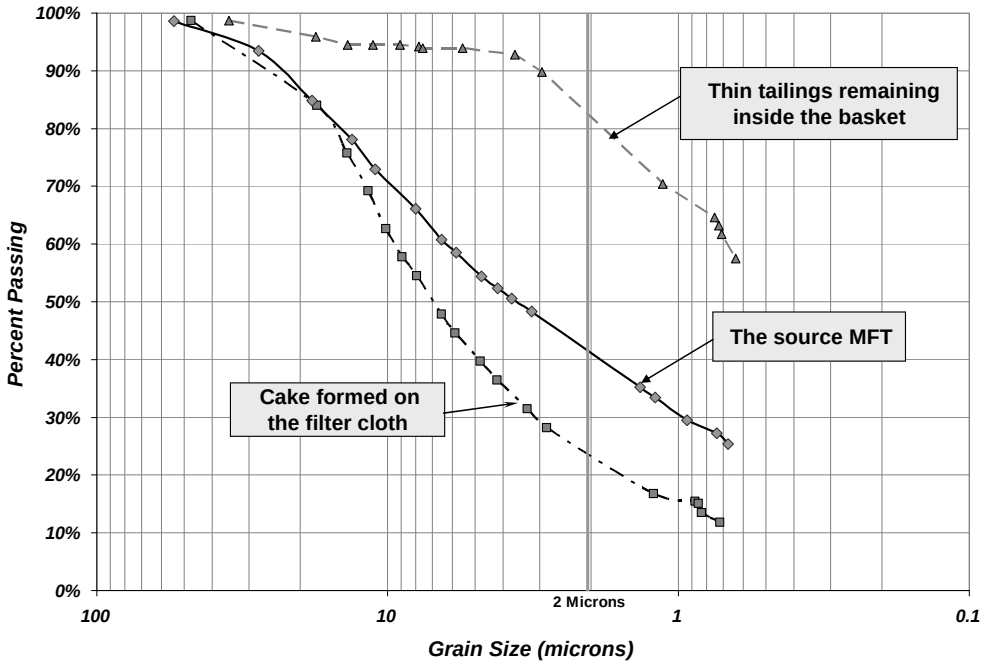

Figure 7. Results of hydrometer analysis for the test SD-0. The diagrams indicate segregation of the source MFT into a coarse (cake) and a fine fraction (thin tailings). About 29%wt of the fines are collected within the cake.

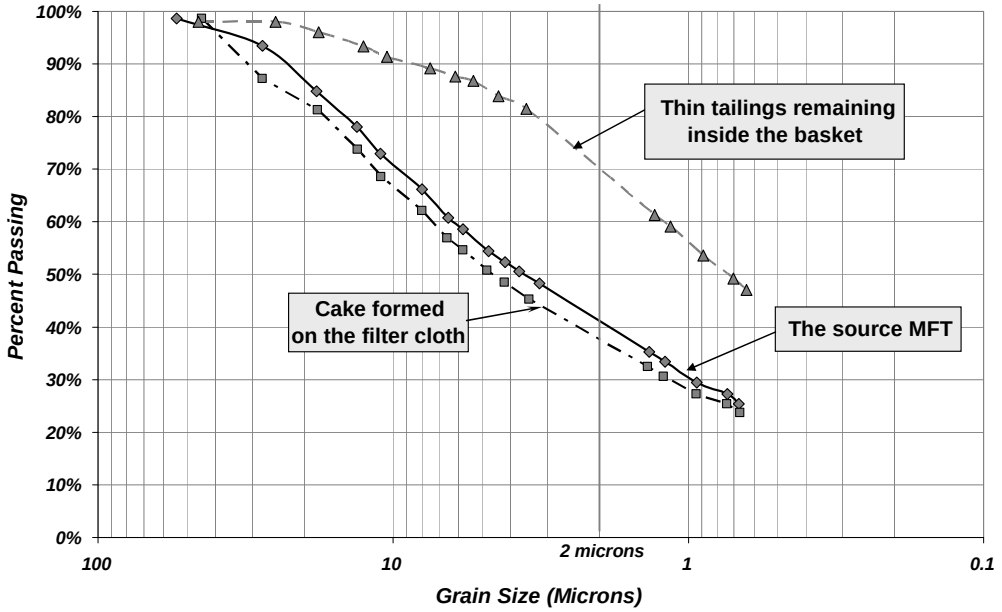

Figure 8. Results of hydrometer analysis for the test SD-900. The diagrams indicate segregation of the source MFT into a coarse (cake) and a fine fraction (thin tailings). About 58%wt of the fines are collected within the cake.

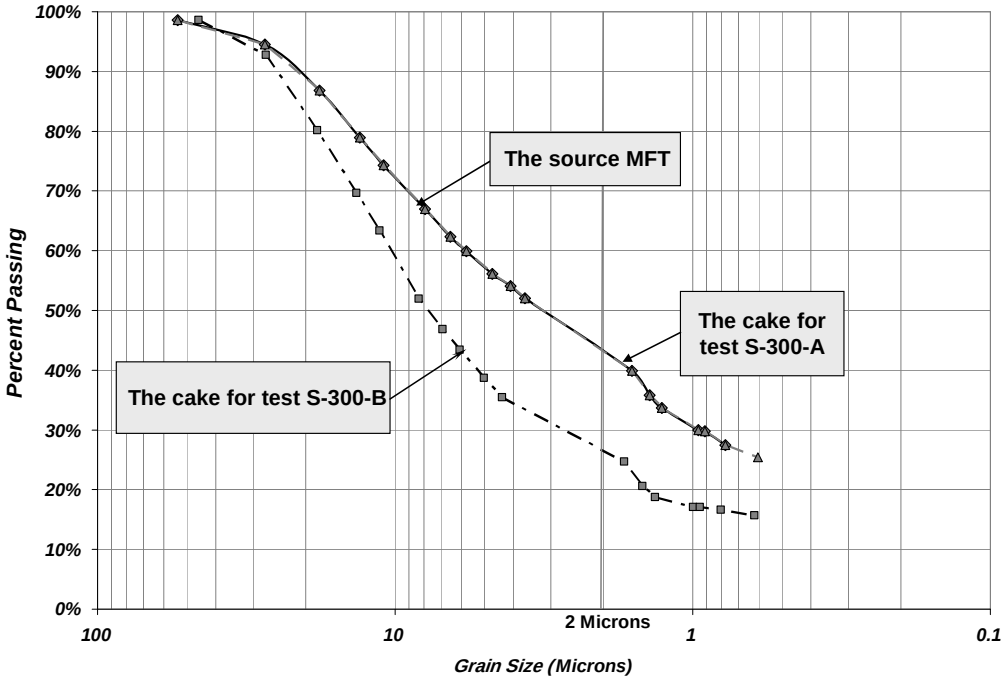

Figure 9. Results of hydrometer analysis for the tests S-300-A and S-300-B. The GSD of the cake for test S-300-A resembles the one for the source MFT.

SEDIMENTATION AND CONSOLIDATION OF IN-LINE THICKENED FINE TAILINGS

S. Jeeravipoolvarn[1], J. D. Scott[1] and R.J. Chalaturnyk[1], W. Shaw[2], N. Wang[3]
1. Department of Civil and Environmental Engineering – University of Alberta, Edmonton, AB, Canada
2. WHS Engineering Ltd., Calgary, AB, Canada
3. Syncrude Canada Ltd., Fort McMurray, AB, Canada

ABSTRACT

An alternative technology to improve oil sands tailings settling behavior, an in-line thickening process (ILTT), was investigated. To achieve these new tailings, flocculants and coagulant are mixed with cyclone overflow tailings in an in-line multi stage fashion. Conceptually by binding fine particles at low solids content into flocs, the hydraulic conductivity is increased, tortuousity is decreased and the mass of the falling flocs is increased. Field and laboratory studies were carried out and preliminary findings indicate that the field in-line thickening process produces tailings that undergo rapid hindered sedimentation from fines void ratios of 67 to 5 followed by consolidation and segregation phenomena at lower void ratios. Shearing during deposition is believed to cause the segregation. History matching of the field pilot pond was performed to determine the geotechnical consolidation properties of the field deposits and these properties were compared to untreated cyclone overflow consolidation properties, which forms new MFT, and to consolidation properties of laboratory remolded ILTT samples. Production of Composite Tailings using ILTT instead of MFT was examined and it is postulated that ILTT CT would be far superior to MFT CT as ILTT's permeability is more than 20 times the permeability of MFT.

INTRODUCTION

The oil sands mining operations in Northern Alberta produce large volumes of tailings composed of sand, silt, clay and a small amount of bitumen. Upon deposition, the tailings segregate with the sand dropping out forming dykes and beaches and about one-half of the fines and most of the bitumen flowing into the tailings pond as thin fine tailings (TFT) which have about 8% solids and 90% fines. In the pond, sedimentation occurs and in about two years reaches approximately 30% solids. At this solids content the process of sedimentation ceases and the process of self-weight compression fully governs. Field measurements show that the material does not appear to be compressing further in the tailing ponds and the fine tailings at this point is called mature fine tailings (MFT).

The slow compression behavior of the MFT causes major problems for oil sand companies to manage containment ponds and to increase the amount of the recycle water for bitumen production. This led to considerable research on alternative solutions for tailings deposition and dewatering. Major tailings developments include production of composite tailings (CT), nonsegregating tailings (NST), and the use of thickeners and centrifuges.

To search for an alternative to MFT formation, a new type of tailings called in-line thickened tailings (ILTT) is being developed. The process is aimed to improve settling and strength behavior of thin fine tailings. This will result in a reduction of MFT formation and storage by rapidly dewatering the cyclone overflow tailings stream which is a high fines stream and the main source of new MFT. The schematic implementation of ILTT into the conventional oil sands operation is shown in Figure 1. After extraction, the oil sands tailings are passed through cyclones which produce coarse and fine tailing streams. Cyclone overflow tailings, the fines tailings stream, is thickened via the in-line thickening process. Rapid water release results in hot water which can be returned to the extraction plant reducing energy costs.

After deposition in a containment pond the ILTT reaches a solids content of about 30% in about 10 days and a solids content up to 50% in a few months. At this higher solids content, the ILTT can be pumped out and mixed with the cyclone underflow to produce a superior Composite Tailings than that produced with cyclone underflow and MFT. This CT process is also shown in Figure 1.

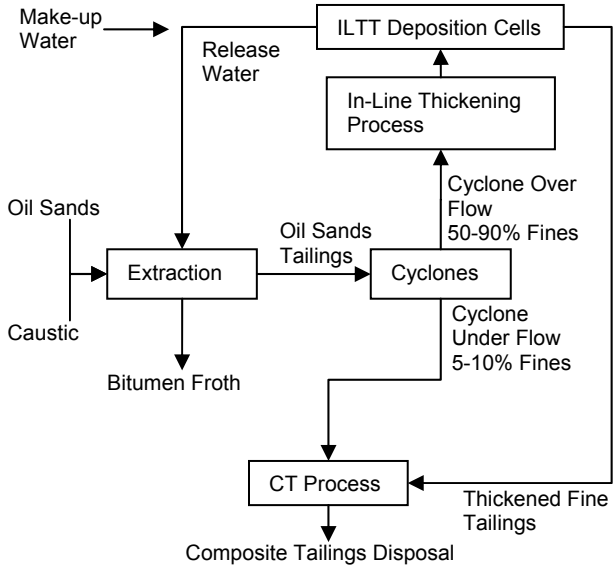

Figure 1. Syncrude ILTT production

To achieve these new tailings, chemical additives are used to increase size of clay flocs, settling rate, hydraulic conductivity and shear strength of the cyclone overflow tailings. This new method uses a multi-stage flocculation and coagulation mixing process which is also known as tapered flocculation (Yuan and Shaw 2007). The process is illustrated in Figure 2. During the first stage (Figure 2(*a*)), a flocculant solution is added and distributed into the cyclone overflow tailings. The long chain molecules of the flocculant, which has various charges along the chain, attach to coarse and fine particles and brings these particles together to form a floc. Some clays particles are not captured during this stage. In the second stage (Figure 2(*b*)) the coagulant solution is added into the tailings from the first stage. The coagulant alters surface charges on the clay particles and results in coagulation of the particles. The final stage (Figure 2(*c*)) is to add a flocculant solution into the product of the second stage to bind the coagulated clay with the flocs to form large aggregates.

By following the above process, the hydraulic conductivity of the mixtures is significantly increased because the aggregates are far apart, tortuousity is decreased and the mass of the falling aggregates is increased. This results in tailings that can sediment quickly to the end of sedimentation. Moreover, as some consolidation occurs, a suitable shear strength is obtained which allows a large variety of reclamation methods.

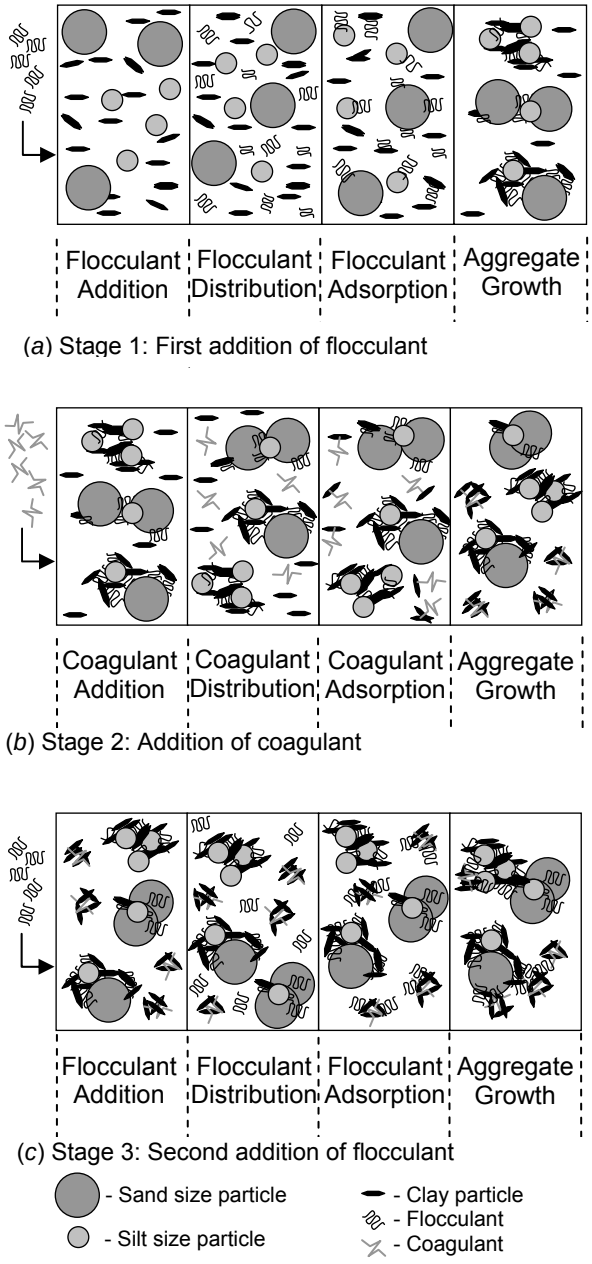

Figure 2. The ILTT process (Modified from Yuan and Shaw 2007)

To be able to engineer this new type of tailings, a study of the sedimentation and consolidation behavior of the ILTT is essential. This paper presents some early findings of field investigations of ILTT pilot scale ponds and laboratory research on remolded ILTT samples. Field sedimentation and compression mechanisms are shown and history matching of the field behavior by a finite strain consolidation theory is given.

FIELD INVESTIGATIONS

ILTT pilot ponds were started in late 2005 to demonstrate the pilot scale behavior of tailings produced from the in-line thickening process. Geotechnical field investigations including pore pressure measurements, solids and fines content measurements and vane shear strength measurements were performed to monitor the compression behavior of the deposits.

In-Line Thickened Tailings Pilot Ponds

The Syncrude ILTT pilot project was composed of two pilot ponds; the west pond and the east pond. Although the tailings stream is produced from extraction of ore bodies from many mining locations; in the pilot operations the west pond ILTT was mainly from marine oil sands ore and the east pond ILTT was mainly from estuarine oil sand ore. Marine ore contains a higher percentage of highly active clay minerals which detrimentally affect extraction and the resulting tailings contain more active clay minerals and bitumen. Flocculation and coagulation of these tailings may also be less efficient because of these properties.

Two distinct discharging methods were used for each pond. The ILTT was discharged down a half-pipe chute (Figure 3) into the west pond (located at the west side of the ILTT mixing plant). This type of discharge results in high energy dissipation which causes shearing of the ILTT aggregates. The relationship between shearing effort and aggregate size is postulated in Figure 4. This shearing of the aggregates results in a smaller aggregate size which is believed to have detrimental effects on the ILTT settling, compression and segregation behavior. To avoid aggregate breakage as much as possible, another type of ILTT deposition, a sub-TT discharge was used for the east pond (Figure 5). This discharging method utilized an inverted spill box which was located lower than the mixing plant. The third ILTT stage (Figure 2(*c*)) was also moved to this box. This type of discharge provides a lower energy dissipation technique.

The plan view of both ponds is illustrated in Figure 6. The pond is equally divided into three sections for sampling and pore pressure monitoring. Each section contains a center station for monitoring and there are also two extra stations at the inlet and outlet of the pilot ponds.

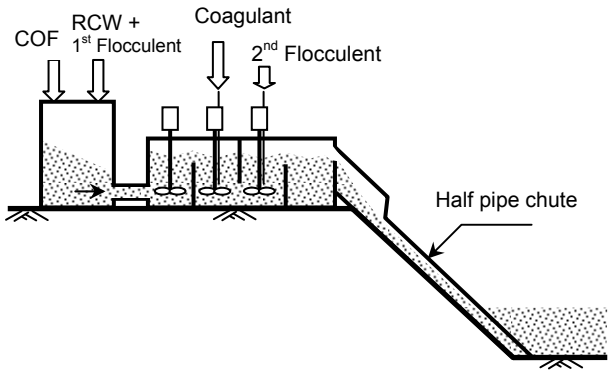

Figure 3. Half-pipe chute deposition in the west pilot pond

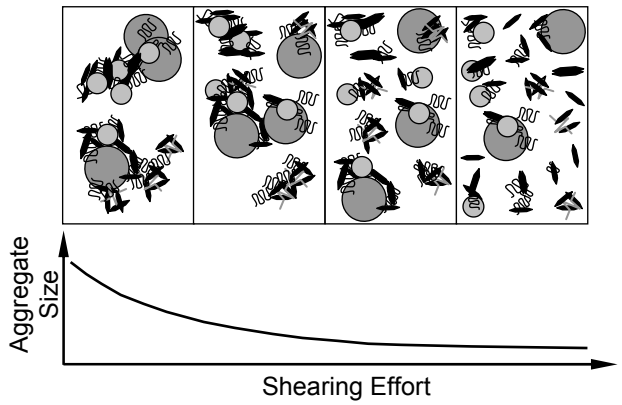

Figure 4. Aggregate rupture (Modified from Shaw and Wang 2005)

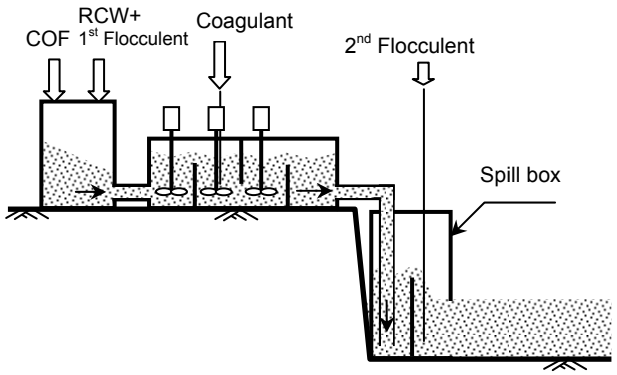

Figure 5. Sub-TT deposition in the east pilot pond

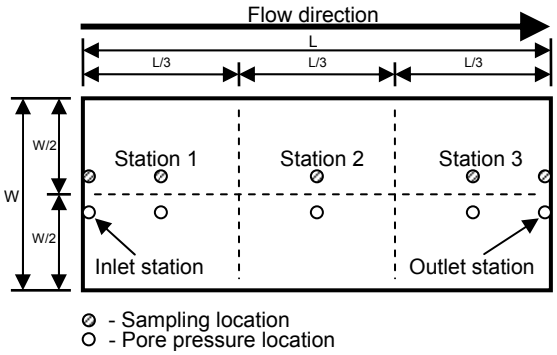

Figure 6. Plan view of an ILTT pilot pond

Field Investigation Results and Discussion

This discussion is divided into four sections which are tailings-water interface measurements, solids and fines content measurements, pore water pressure measurements and vane shear strength measurements. The results will be focused on the east pilot pond as it better represents the ILTT tailings behavior from a lower energy deposition technique.

Tailings-Water Interface Measurements

In November 2005, the ILTT east pilot pond was filled continuously for approximately 10 days at a solids content of about 3.7% (void ratio of 65.6) and a fines content of 89%. The average solids content at the end of the 10 day filling period was 32.6% (void ratio of 5.2). Then it was left to settle under its own weight for approximately 230 days. The tailings-water interface height of ILTT in this pond is shown in Figure 7.

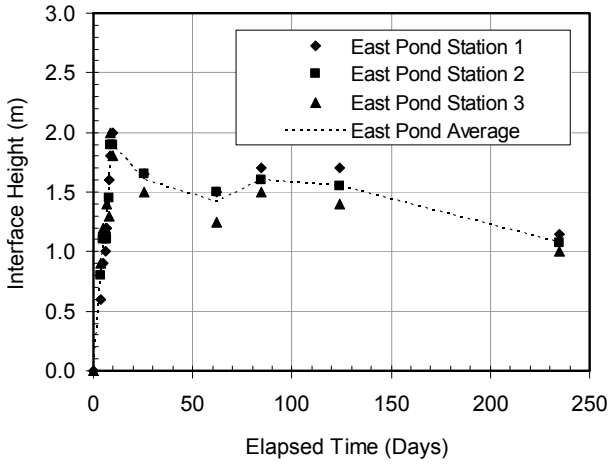

Figure 7. Interface height vs. time of the east pilot pond

An incongruity in the interface height measurements was observed at 70 days. This was during the winter period where accurate measurement was difficult. The last measurement was performed at 235 days. At this time, the surface was desiccated by a winter freeze-thaw process and natural drying. The average interface height was 1.1 m and an average crust thickness was about 0.2 m.

Solids and Fines Content Measurements

Sampling for the solids and fines contents were done by using a thin walled sampler provided by GeoForte Services Ltd. This sampler was designed to retrieve a core sample from a tailings pond. The core sample was extruded out of the sampler and divided into several sections for solids and fines content profile determinations.

The measurements of solids content profiles at different elapsed times at the three sampling stations from the east pilot pond are shown in Figures 8(*a*), 8 (*b*) and 8(*c*). The fines content profiles at the three stations are given in Figures 8(*d*), 8(*e*) and 8(*f*).

The solids content profiles in Figure 8 indicate that there is a rapid increase in solids content from an initial solids content of 3.7% to an average solids content of 35.8% within 26 days. After filling, the pond was allowed to compress under self-weight stress. The surface of the pond has gone through freezing, thawing and drying during the quiescent period which developed a crust approximately 0.2 m thick. Below the crust the average solids content was about 50% (void ratio of 2.5).

The fines content profiles are shown in Figure 8. The average fines content of the ILTT was found to be 89% and the profiles indicate that the ILTT is a nonsegregating mix showing minimal changes in the fines content profiles during the observation period of 235 days. This finding is also confirmed by the slurry properties diagram in Figure 9. The diagram reveals that the ILTT samples obtained from the east pilot pond show small segregation. In contrast to this finding, samples obtained from the west pilot pond indicate segregation behavior by showing a reduction of fines content at a constant fine/(fines+water) ratio. The difference between the two pilot ponds was the discharge method and the tailings ore type. The higher energy deposition method in the west pond is believed to be the main reason for aggregate breakage and the segregation behavior of the ILTT in this pond.

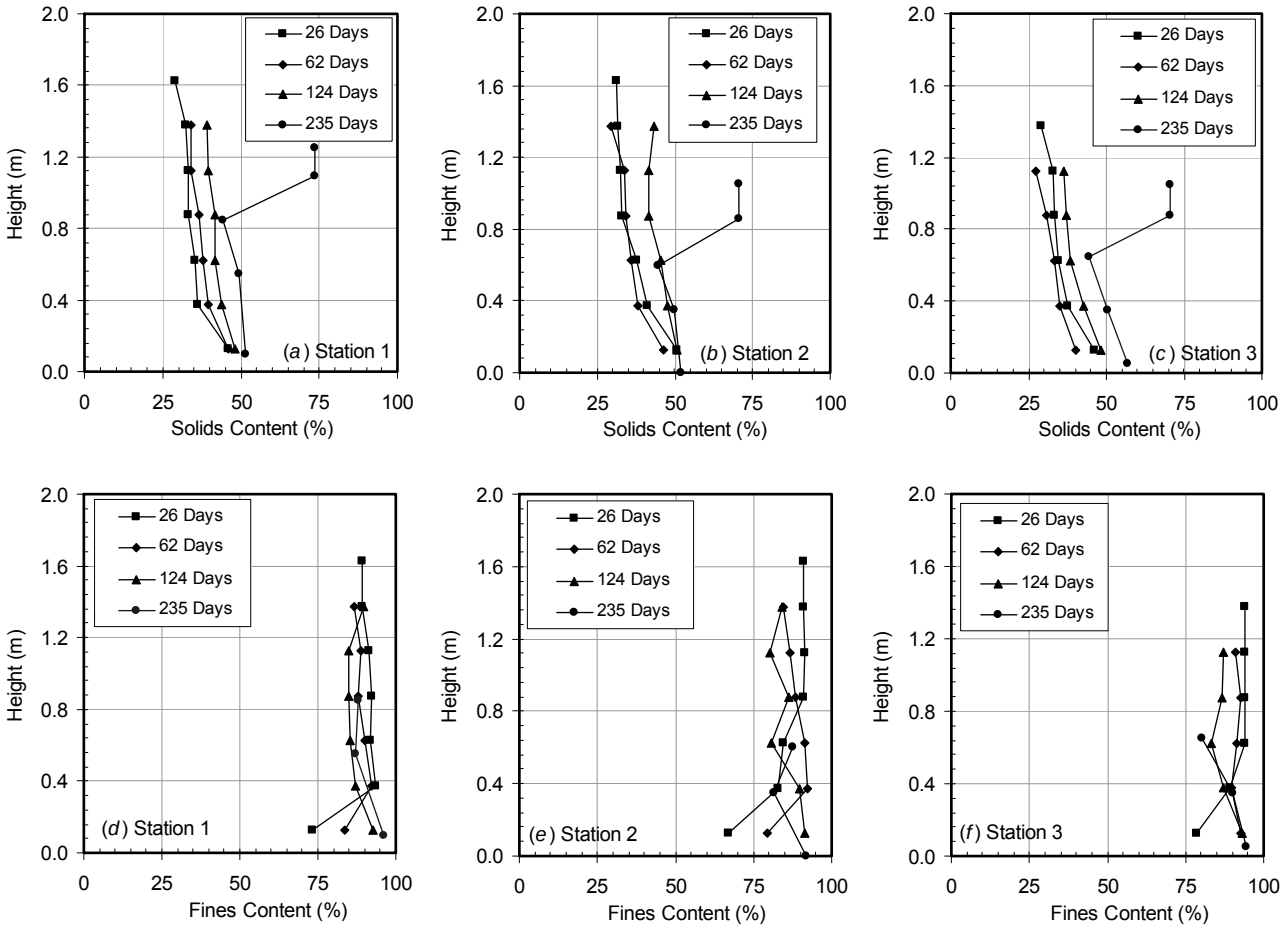

Figure 8. Solids and fines content profiles of the east pilot pond

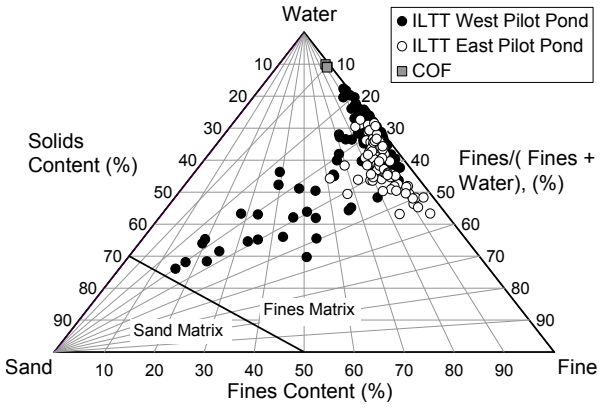

Figure 9. Slurry properties diagram

To summarize the processes that occured in the east ILTT pilot project, a mechanistic diagram of the ILTT process is illustrated in Figure 10. First the cyclone overflow is mixed with recycle water and chemical additives via the in-line thickening process. This produces an ILTT material at a solids

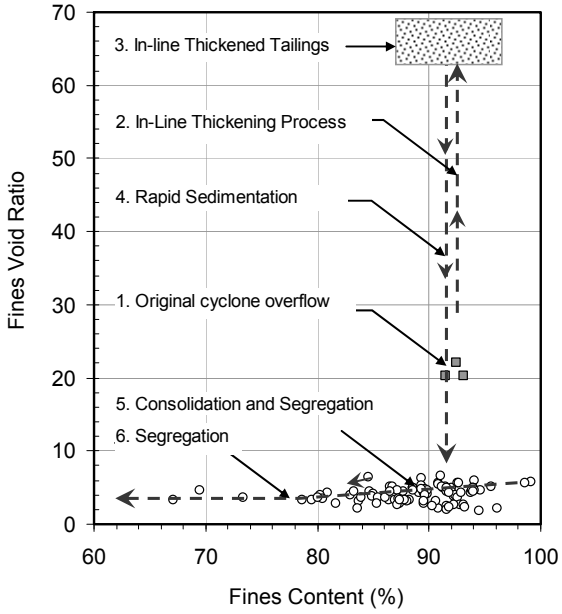

Figure 10. The ILTT process

content of about 4% (void ratio of 66 and fines void ratio of 67). The ILTT then undergoes rapid sedimentation releasing more than 90% of its original water volume as it reaches a fines void ratio of about 5. At this point both consolidation and segregation phenomena can occur simultaneously in the material causing both a reduction in the fines void ratio and the fines content. Generally the ILTT continues to undergo consolidation to a lower void ratio while some whose structure was broken during the deposition process showed a small amount of segregation.

Pore Water Pressure Measurements

Pore water pressure measurements in a pond are essential to monitor dissipation of excess pore pressure which is an indication of the consolidation progress in a tailings deposit. The pore pressure measurements were performed by using Roctest, model PWP, push-in piezometers with a vibrating wire readout unit, model MB-6TL. In the pilot ponds, four piezometers were pushed in the pond simultaneously to different elevations. The piezometers were kept in place until the pore water pressure measurements became stable when the pressure values were taken.

The last pore pressure measurements at 235 days in the east pond are shown in Figures 11(*a*), 11(*b*) and 11(*c*) for Station 1, 2 and 3 respectively. The total stresses shown were calculated from the solids content profiles from Figure 8. The pore pressure measurements at Stations 1 and 2 indicate that double drainage conditions prevailed in these locations as the pore pressure was equal to the hydrostatic pressure at the bottom of the stations. While at Station 3 the pore pressure at the bottom was equal to zero. A possible explanation for Station 3 was that the underlying sand foundation was fully drained in this particular location. This bottom pore pressure would create a draw down condition on the tailings in the pond. The pore pressures being approximately equal to the total stress above the pond bottom indicate that any downward drainage must have consolidated a layer of tailings at the bottom which somewhat sealed the pond bottom and prevented further significant downward drainage.

Vane Shear Strength Measurements

The vane shear strength of the ILTT materials was measured by pushing in a field vane apparatus directly into the deposits. The vane was pushed down 25 cm at a time to obtain shear strength with depth. The measured vane shear strength values of the east pilot pond at the last field investigation program at 235 days are shown in Figure 12.

The vane shear strength of the east pond varied from 1.6 kPa (solids content of 44% and void ratio of 3.2) under the crust to 5.2 kPa (solids content of 52% and void ratio of 2.3) near the bottom of the pond. The dry crust of the east pond had a surface vane shear strength of about 97 kPa at a solids content of about 72% (void ratio of 1.0). The vane shear strength profiles of the east pond indicate good shear strength consistency between all stations. This is because the settling processes are similar at all stations and the ILTT materials are quite homogeneous throughout the pond.

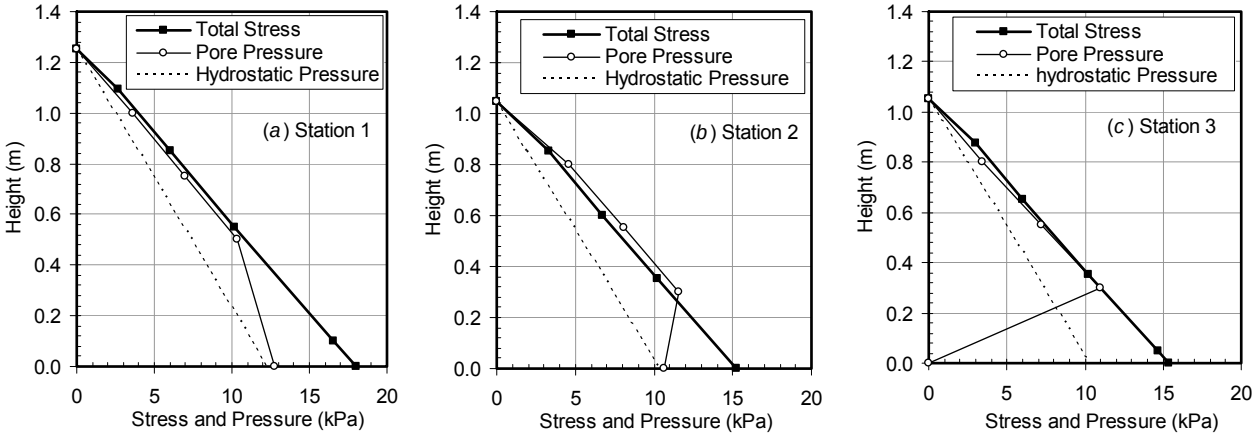

Figure 11. Total stress and pore pressure profiles of ILTT east pond at 235 days

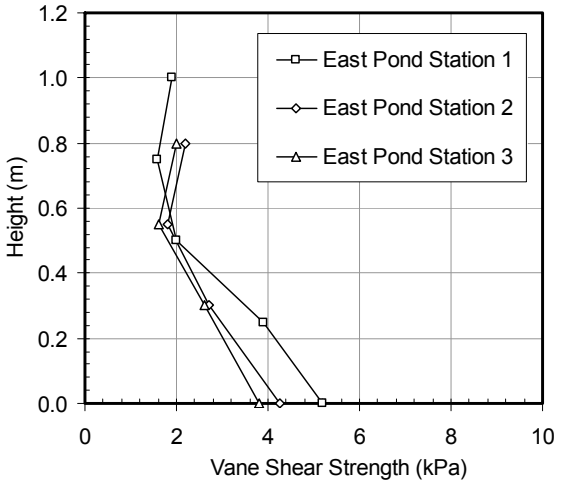

Figure 12. Vane shear strength profiles of ILTT east pond at 235 days

LABORATORY EXPERIMENTS

ILTT samples obtained from the pilot scale test pond were delivered to the University of Alberta and tested in the summer of 2006. The objectives of the laboratory test program were to obtain particle size distributions, index properties and consolidation characteristics of the ILTT materials.

As well as testing the ILTT materials; samples of cyclone overflow, taken at the same time as the ILTT was made and deposited, were similarly tested. The difference in material properties should show the influence of the flocculation and coagulation processes. As well, the untreated cyclone overflow is the same as new MFT and should indicate the differences between ILTT and MFT. Samples of MFT from the MFT tailings pond were not tested as ageing of MFT has a significant effect on its thixotropic properties which affect its consolidation properties (Jeeravipoolvarn et al. 2008 (*a*) and (*b*)). Comparing ILTT and MFT of the same age was preferred.

Material Index Properties

Figure 13 provides particle size distributions of ILTT and cyclone overflow. The cyclone overflow tailings consist of 8% sand, 92% fines and 52% clay size materials similar to that of ILTT. The particle size distributions were obtained by a standard hydrometer-sieve test (ASTM D422-63). The test is therefore a dispersed test and results in identical particle size distributions of the two tailings as the ILTT flocculated aggregates are completely dispersed.

Figure 14 shows a plasticity chart containing data from the east pond ILTT, west pond ILTT, cyclone overflow and 1982 MFT. The east pond ILTT has an average liquid limit of 50 and an average plasticity index of 29. These values are in the same range as the cyclone overflow and 1982 MFT. The west pond, however, has an average liquid limit of 71 and an average plasticity index of 47.

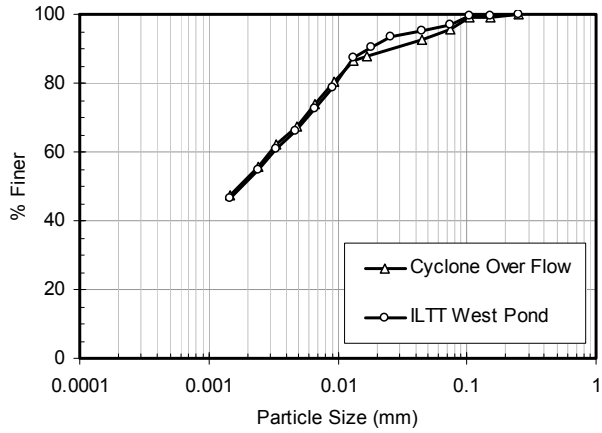

Figure 13. Particle size distribution

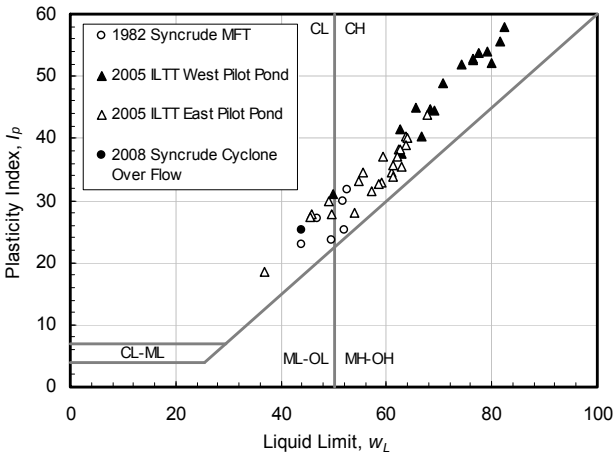

Figure 14. Plasticity chart of various oil sands tailings

The relatively higher values of w_L and I_p of the west pond ILTT could indicate two possibilities. One is a variation in bitumen content and another is the variations in the ore type of cyclone overflow used for the two ponds.

The segregation of the material in the west pond provided samples with higher fines content which in turn also indicates a higher bitumen content. This will generally increase both w_L and I_p of the

tailings. The tailings with more bitumen (usually finer tailings) tend to have a higher liquid limit (Scott et al. 1985). Estuarine and marine ores may pose differences in both the extraction and the in-line thickening process efficiency. Future research is essential to investigate the ILTT production from the two different ores.

Large Strain Consolidation Tests with Hydraulic Conductivity and Vane Shear Strength Measurements

The large strain consolidation test performed at the University of Alberta is a multi-step loading test. The test apparatus and procedures have been slightly modified for the in-line thickened tailings to allow vane shear tests to be performed at different void ratios.

The consolidation cell is 140 mm inside diameter and can accommodate samples up to 200 mm high. The wall friction is minimized by choosing the appropriate initial height of the samples so that the sample at the high stresses (10 kPa and over) has a diameter to height ratio of approximately 2.5 to 3. Also the height of the sample should be kept as high as possible to minimize errors in measuring the thickness of the sample and in hydraulic conductivity tests. The ILTT samples are tested at effective stress ranges from about 0.5 kPa to 300 kPa to cover the stress range that the ILTT might experience in the field.

The hydraulic conductivity is measured at the end of consolidation for each loading step. The upward gradient in the test is controlled to be as small as possible so the seepage force will not exceed the applied stress. The shear strength is then measured after the hydraulic conductivity test by a laboratory vane apparatus before the next load is applied.

Three materials were tested; cyclone overflow, east pond ILTT and west pond ILTT. Sample preparations required the samples to be mixed thoroughly therefore all the samples are remolded samples. The properties of each tailings are listed in Table 1. The lower value for specific gravity (Gs) of the west pond ILTT results from the higher bitumen content.

Figures 15, 16 and 17 show comparisons of the compressibility, hydraulic conductivity and vane shear strength of all the tested materials

Table 1 Tailings properties

Tailings	Solids Content (%)	Water Content (%)	e_i	Gs	Fines Content (%)
COF	30.9	223.6	5.66	2.53	93.9
East pond ILTT	35.5	181.7	4.61	2.52	87.4
West pond ILTT	29.7	236.7	5.80	2.45	95.3

respectively. From Figure 15, the west pond ILTT has essentially the same compressibility as the cyclone overflow. In Figure 16, the hydraulic conductivity of the west pond ILTT is lower than the cyclone overflow at the same void ratios while the east pond ILTT has the highest hydraulic conductivity. As fines void ratio is used in Figure 16 to eliminate an influence of different fines contents, the higher hydraulic conductivity of the east pond ILTT than the cyclone overflow indicates the influence of the in-line thickening process on the tailings permeability.

As mentioned in the introduction to the laboratory experiments, cyclone overflow materials were tested as they, when deposited, will settle and form new MFT. This new MFT will have the same mineralogy and initial water chemistry as the ILTT as both the cyclone overflow and ILTT samples were obtained at the same time. The comparisons of ILTT and cyclone overflow geotechnical properties will then not be influenced by different initial material properties. Figure 16 also shows the hydraulic conductivity of typical old MFT. As found in other testing programs, the hydraulic conductivity of old MFT is considerably smaller than that of new MFT (new cyclone overflow) and ILTT. This observation is important when considering the properties of composite tailings made with the high solids, high permeability ILTT.

For vane shear strength, the west pond ILTT has higher strength compared to the cyclone overflow at effective stresses above 10 kPa (Figure 17). At the higher effective stresses, there appears to be no difference in the vane shear strength between the two tailings. It is believed that the physical forces dominate the behavior of the soils at effective stress above 10 kPa and the chemical effects are minor. As mentioned earlier, the ILTT pilot samples have gone through sample preparation processes. The structure of these

samples may not be representative of the original field material.

For the east pond ILTT, the laboratory vane shear strength is much smaller compared to the field vane strengths at effective stresses lower than 10 kPa. This could be caused by structural changes from the laboratory sample preparation. At higher effective stress than 10 kPa, shear strengths of both field and laboratory east pond ILTT are similar.

In natural sedimentary clay deposits the undrained shear strength has been found to increase with depth and is proportional to the increase in effective stress with depth (Holtz and Kovacs 1981). A relationship between plasticity index and a ratio between undrained shear strength and effective stress, τ_u/σ'_{vo}, for normally consolidated clays was established by Bjerrum and Simons (1960). This relationship provides a τ_u/σ'_{vo} ratio of about 0.25 for oil sands fine tailings with plasticity index of about 30. However, the large strain consolidation test results (Figures 15 and 17) show that this ratio is not constant at all fines void ratio but increasing linearly with fines void ratio (Figure 18). The large values at high void ratios are indicative of the strong bonds in the flocs. As the flocs are compressed during consolidation the flocs break and lose strength.

The research hypothesis of comparing ILTT and cyclone overflow properties was that the difference in the behavior of both materials would be directly related to the effect of the flocculants and coagulant added in the in-line thickening process. The function of the additives is to bind soil particles together to form large aggregates of soil particles that will settle quickly during deposition at low solids content. The hypothesis is that as the additives flocculate the soil particles together, the shear strength of the soil will increase as breaking the structure requires additional energy. The soil structure therefore becomes stronger. Compared to the parent materials, the treated tailings would not compress as much when subjected to the same applied stress. This appears to be insignificant in our preliminary test results. The hydraulic conductivity should also be affected by the process because the additives change the structure of the soil reducing the tortuous channels of the soil resulting in greater hydraulic conductivity.

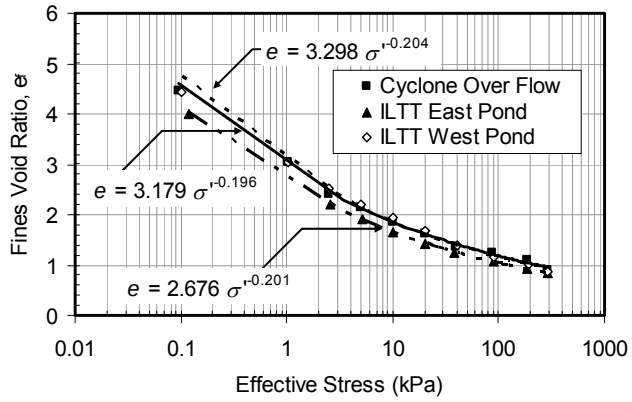

Figure 15. Compressibility of COF, east pond ILTT and west pond ILTT

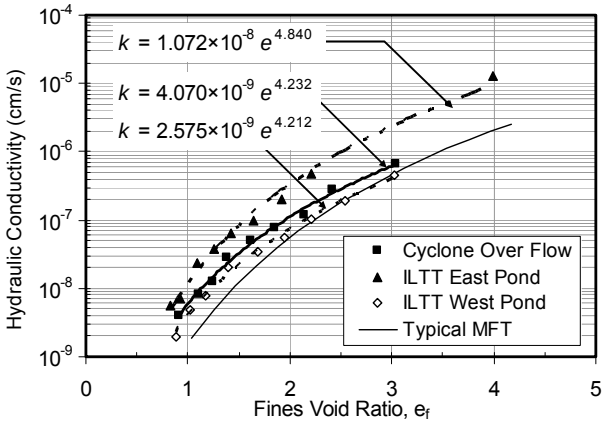

Figure 16. Hydraulic conductivity of COF, east pond ILTT and west pond ILTT

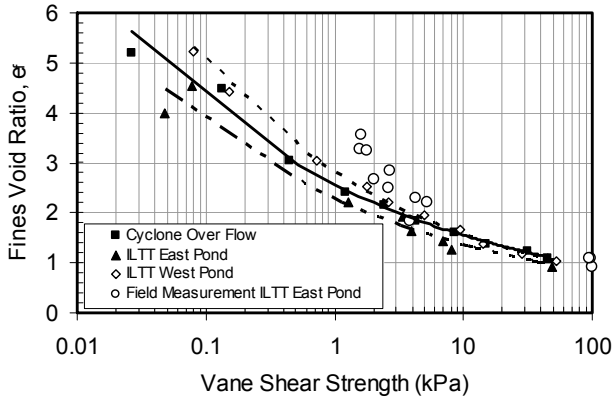

Figure 17. Vane shear strength of COF, east pond ILTT and west pond ILTT and field ILTT

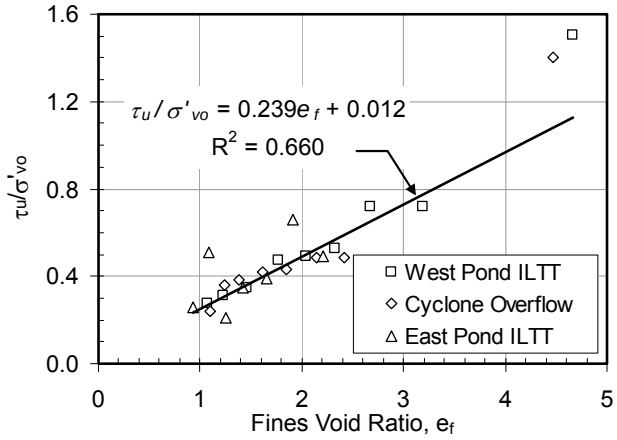

Figure 18. Laboratory determined shear strength-effective stress relationship

COMPARISON OF THE FIELD AND LABORATORY RESULTS

In order to compare field performance and laboratory consolidation characteristics of the ILTT from the east pilot pond, a finite strain consolidation theory (Gibson et al. 1967) was utilized to history match the field interface height measurements. A one dimensional condition is assumed due to the much larger width and length of the pond compared to the height of the slurry. A one dimensional finite strain consolidation governing equation in terms of excess pore pressure is given by Somogyi (1980) as in Equation 1.

$$\frac{\partial}{\partial z}\left[\frac{k(e)}{\gamma_w(1+e)}\right]\frac{\partial u}{\partial z}+\frac{k(e)}{\gamma_w(1+e)}\frac{\partial^2 u}{\partial z^2} + \frac{de}{d\sigma'}\frac{\partial u}{\partial t}-\frac{de}{d\sigma'}\left[(Gs-1).\gamma_w\frac{d(\Delta Z)}{dt}\right]=0 \quad [1]$$

Where u is excess pore pressure, z is a material coordinate, k is hydraulic conductivity, σ' is effective stress, e is void ratio, γ_w is unit weight of water, Gs is specific gravity and t is time.

To demonstrate an effect of the in-line thickening process by increasing solids content with time especially during a filling period, a quiescent condition was assigned in the model. For a filling period, according to Carrier et al. (1983), a prediction of an interface settlement is essentially independent on filling history but follows the total amount of solids filled in a pond and the interface height is also essentially linear during the filling period. This is true when the filling rate is constant and the one dimensional pond condition is satisfied. These conditions are justified for the current simulation and the interface during the filling period was therefore obtained from this approach. Boundary conditions for the simulation are depicted by Figure 11. The pilot pond clearly shows a double drainage condition. Therefore a Dirichlet boundary condition of u = 0 is assigned for both top and bottom boundaries.

The history match was done by searching compressibility and hydraulic conductivity functions based on the power law relationships given in Figures 15 and 16. The mathematical formula of the relationships remain the same, however, the compressibility function was assigned to have a bi-power form as at effective stress lower than 10 kPa, large amounts of oil sands tailings compressibility data suggest little to no variations (Jeeravipoolvarn 2005). Therefore the form of the compressibility is chosen as Equation 2 while a hydraulic conductivity-void ratio function remains a conventional power law functions expressed as Equation 3.

$$e=\begin{cases} A_1\sigma'^{B_1} & for \quad \sigma' < 10kPa \\ A_2\sigma'^{B_2} & for \quad \sigma' \geq 10kPa \end{cases} \quad [2]$$

$$k = Ce^D \quad [3]$$

It is noted that the A_1 and B_1 are laboratory determined parameters while the A_2, B_2, C and D are history matching parameters. An initial height of the pond was back calculated from the final solids content profiles in Figure 8 and the initial solids content of 3.7%. The initial height was found to be 20.4 m. The simulation period was allowed to go up only to 70 days. This period was chosen due to the fact that the pilot pond experienced freezing, thawing and drying after this period.

A consolidation computer program was coded in Visual BASIC. A fully implicit finite difference scheme with upwind in a convection term is used to solve the governing equation. The scheme was selected due to its stability and numerical parameters n = 40 and $\Delta t = 10^{-4}$ are used in the model (n and Δt denote a total node number and incremental time respectively).

A result of an interface height simulation with time is shown with the average field measurements in Figure 19 while Figure 20 shows the increase in

solids content with time due to the in-line thickening process in the east pilot pond.

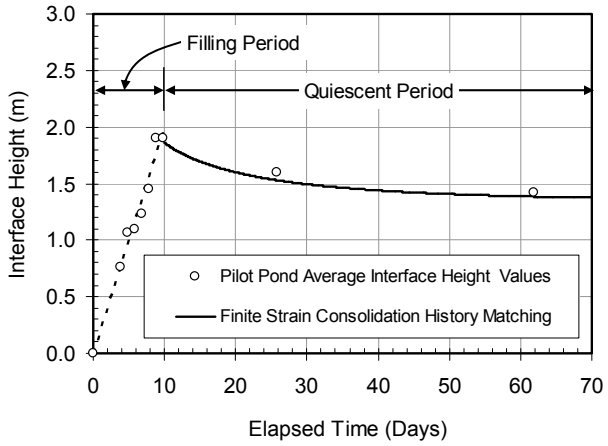

Figure 19. History matching of interface height vs. time

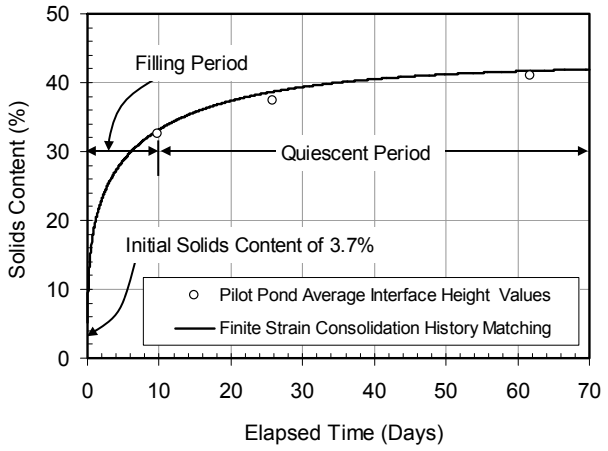

Figure 20. History matching of increase in solids content with time

In Figure 19, the ILTT material was filled into a pond in a period of 10 days. During this period, Figure 20 provides that ILTT has changed its solids content from the initial value of 3.7% to 33.2% (void ratios of 65.6 and 5.1 respectively). After it released more than 90% of its water during this period, the ILTT was allowed to undergo self-weight compression up to 70 days when the simulation period was over. Further increase in solids content slows dramatically as the hydraulic conductivity reduces and excess pore pressures dissipate slowly.

The good agreement between the history match simulation and the field data shown above was performed by the incorporation of void ratio-effective stress and hydraulic conductivity-void ratio relationships shown in Figures 21 and 22 respectively. The laboratory experimental data from the large strain consolidation tests in Section 3.2 is also included for relationship comparisons.

For the compressibility, it requires compressibility of the field ILTT to be more compressible by having a higher value of compression index. The history matching compressibility function also indicates that it would take a higher effective stress to compress the ILTT material to the same void ratios in the pond compared to the laboratory remolded ILTT sample. The field ILTT was more difficult to compress than the remolded laboratory samples because of the fairly strong large flocs in the field. Mixing the field ILTT in the laboratory would break these flocs making the material easier to compress.

The hydraulic conductivity-void ratio relationship of low solids or high void ratio materials is the most important property governing the rate and magnitude of settlement and consolidation (Suthaker and Scott 1994). For this reason it is important to examine and compare the hydraulic conductivities in Figure 22. At 50% solids content (void ratio of 2.5) the field hydraulic conductivity is 2.5 times larger than the laboratory hydraulic conductivity. This is a result of the breakdown of the floc structure in the laboratory samples as they were remolded. Of even more importance, at 50% solids the field ILTT is 12 times more permeable than the cyclone overflow (or new MFT) and even larger than that of typical old MFT (Figure 16). So even after compressing to 50% solids, the field ILTT still processes sufficient floc structure to have a relatively large permeability.

At 30% solids (void ratio of about 5.9), a typical MFT solids content, the field hydraulic conductivity is 22 times more permeable than that of the cyclone overflow (new MFT). This great difference in permeability at the same solids content is caused by the difference in structure of the flocculated ILTT vs. the dispersed MFT.

Future research on hydraulic conductivity and compressibility behavior of undisturbed in-line thickened tailings is required to further investigate these properties.

A comparison of vane shear strengths from the field history matching, field measurements and

laboratory measurements on ILTT and cyclone overflow is given in Figure 23. History matching vane shear strengths were obtained from the relationship between τ_u/σ'_{vo} and fines void ratio in Figure 18 with the compressibility data in Figure 21. The results show that the predicted undrained shear strengths are closer to those data measured in the field than to the laboratory determined shear strengths. At higher void ratios above 2.5 the field ILTT has a higher shear strength than the cyclone overflow. As discussed above, this is a result of the strong bonds in the ILTT flocs. Future research on a relationship between undrained shear strength and effective stress of the undisturbed ILTT is required.

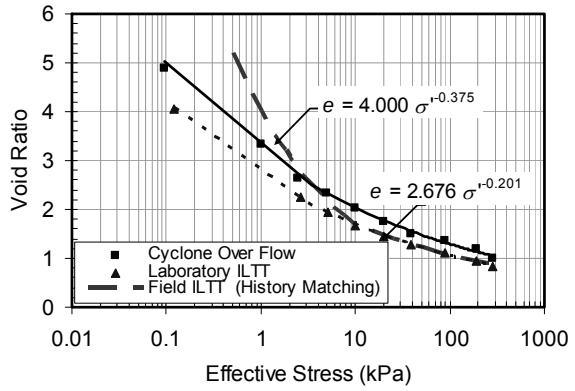

Figure 21. Comparison of the field history matching and laboratory compressibilities

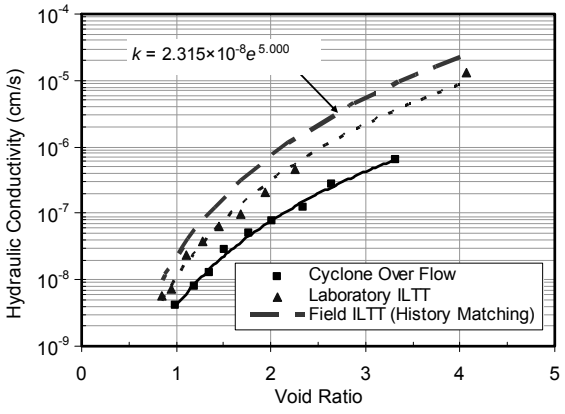

Figure 22. Comparison of the field history matching and laboratory hydraulic conductivity

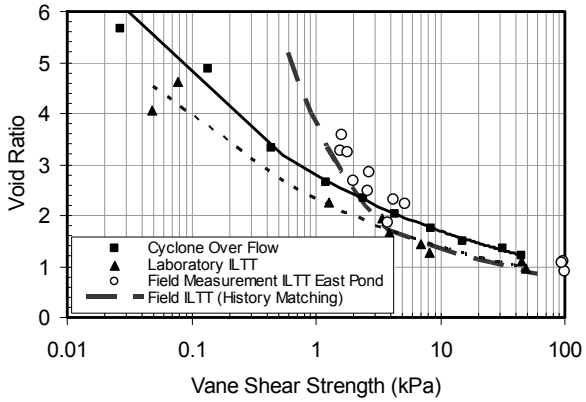

Figure 23. Comparison of the field history matching, field measurements and laboratory shear strengths

COMPOSITE TAILINGS USING ILTT

Composite tailings, CT, is presently produced by mixing and depositing a blend of cyclone underflow and MFT with a coagulant, generally gypsum, added to make the mix nonsegregating. The MFT is pumped from the existing tailings ponds where it has accumulated over the years. This procedure is consuming some of the current inventories of MFT and it releases water fairly rapidly for make-up water for the extraction plant (Matthew et al. 2002). Dewatering rates, however, are lower than expected and careful engineering of the CT process is required to prevent segregation during deposition. Another drawback is that the amount of MFT which can be added to the cyclone underflow is limited as too much fines in the CT reduces its permeability and the dewatering rate will be too slow. Generally the sand-fines ratio, SFR, of CT is only 4 or 5, that is, the fines content is from 17% to 20%.

As the oil sands tailings on average contains about 17% fines and the cyclone overflow which contains most of the fines is deposited in a tailings pond and forms more MFT, the CT process can not keep up with the formation of more MFT and MFT volumes continue to increase. Another problem with the present CT process is that the dosages of gypsum to prevent segregation are quite large resulting in the build up of Ca^{2+} and SO_4^{2-} ions in the recycle water which in time will negatively affect bitumen extraction.

Figure 24 shows the present CT process. All mixes of MFT and cyclone underflow, CU, will lie on the straight line joining the MFT and cyclone underflow materials. The segregation boundary for untreated tailings blends is also shown. All tailings above this segregation boundary will segregate so all untreated mixes of MFT and CU will segregate. The segregation boundary for gypsum treated tailings is also shown. All tailings below the gypsum segregation boundary will be nonsegregating so the CT mixes of MFT and CU will become nonsegregating with the addition of a coagulant such as gypsum. Figure 24 also shows all possible mixes of ILTT and CU which lie on the line that joins these two materials. Possible CT mixes of ILTT and CU lie below the untreated segregation boundary which indicates that these CT mixes would require no or little coagulant addition with a resulting increase in the quality of the recycle water for bitumen extraction.

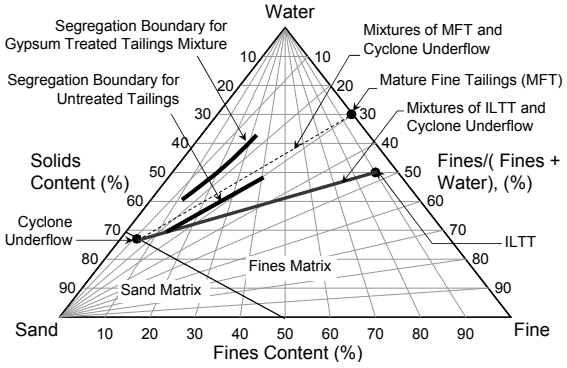

Figure 24. Tailings properties diagram

The greatest advantage of CT made from ILTT and CU is the large hydraulic conductivity of the ILTT fines. As shown in Figures 16 and 22, at solids content of 30% the field hydraulic conductivity of ILTT is more than 20 times the hydraulic conductivity of new MFT (cyclone overflow) and even greater than that of old MFT. This means the ILTT CT will release water and consolidate more than 20 times faster than MFT CT allowing more rapid CT disposal. The greater ILTT hydraulic conductivity will also allow a larger amount of fines in the ILTT CT than the 20% maximum in the MFT CT. This would assist in the reduction of fine tails volume stored in tailings ponds.

OBSERVATIONS AND CONCLUSIONS

An in-line thickening process was developed to provide a method that can rapidly recover hot water and produce thickened tailings without the aid of a thickener. Field pilot programs were conducted and were successful.

Two ILTT pilot ponds were filled. The major difference between the ponds was the discharge method. The west pond had a half-pipe chute discharge while the east pond had a sub-TT discharge. The latter discharging method was a lower energy deposition technique which did not cause segregation of the ILTT.

In the east pilot pond, it was found that the tailings compressed from an initial solids content of 3.7% to 32.6% (void ratios of 65.6 and 5.2 respectively) in 10 days and to about 50% (void ratio of 2.5) at a depth of 1 m in 4 months. The fines content profiles were consistent with depth and have an average value of 89%. The pore pressure measurements in this pond showed some consolidation at the bottom at all stations as the pond had a permeable foundation. It appeared that a layer of tailings consolidated at the bottom and sealed it preventing further significant downward drainage.

Evident segregation was found in the west pilot pond. A hypothesis on the cause of segregation was that the high discharging energy to this pond broke floc structure allowing the sand to settle out. Further research is required to confirm the influence of shearing on ILTT segregation behavior.

Material index properties show that the cyclone overflow and ILTT similarly consist of 8% sand, 92% fines and 52% clay size materials. The east pond ILTT has an average liquid limit of 50 and an average plasticity index of 29. These values are in the same range as the cyclone overflow and typical MFT.

The field pilot ponds were history matched by utilizing a finite strain consolidation theory and by searching compressibility and hydraulic conductivity functions based on power law relationships. Good agreement was obtained with matching the field interface height with time and the increase in solids content with time. Field compressibility and hydraulic conductivity functions were obtained.

The field ILTT was more difficult to compress than the remolded laboratory samples because of the fairly strong large flocs in the field.

The field ILTT was more permeable than the laboratory ILTT samples at the same solids contents because of the breakdown of the floc structure in the laboratory samples as they were remolded.

At 30% solids content the field hydraulic conductivity was 22 times more permeable than that of the new MFT (cyclone overflow). This great difference in permeability was caused by the difference in structure of the flocculated ILTT vs. the dispersed MFT.

Possible Composite Tailings mixes of ILTT and Cyclone Underflow lie below the untreated segregation boundary which indicates that these CT mixes would require no or little coagulant addition with a resulting decrease in cost to make CT and an increase in the quality of the recycle water.

At solids contents of 30% the field hydraulic conductivity of ILTT is more than 20 times the hydraulic conductivity of new MFT and even greater than that of old MFT. The ILTT CT will release water and consolidate more than 20 times faster than MFT CT. It will also allow a larger amount of fines in the ILTT CT than is presently used in the MFT CT.

Shearing of the field ILTT by thorough mixing in the laboratory changed its compressibility and permeability properties as shearing tends to breakdown the floc structure. The ILTT became more compressible under the same effective stress which had the advantage that it compressed more and released more water. A major disadvantage, however, was that its permeability decreased. A challenge exists, when making CT with ILTT, to develop procedures to pump ILTT from depositional ponds and mix it with cyclone underflow without a significant breakdown of the floc structure.

ACKNOWLEDGEMENTS

The authors are grateful for the financial support from the University of Alberta and Syncrude Canada Ltd. The authors also appreciate the technical support from Gerry Cyre, Geoforte Services Ltd., Edmonton and Steve Gamble, Department of Civil and Environmental Engineering, University of Alberta.

REFERENCES

Bjerrum, L. and Simons, N.E., 1960. Comparison of Shear Strength Characteristics of Normally Consolidated Clays, 1st PSC, ASCE, 711-726.

Carrier, W.D., III, Bromwell, L.G., and Somogyi, F., 1983. Design Capacity of Slurried Mineral Waste Ponds. Journal of Geotechnical Engineering, 109(5): 699-716.

Gibson, R.E., England, G.L. and Hussey M.J.L. 1967. The Theory of One-dimensional Consolidation of Saturated Clays. I. Finite Non-linear Consolidation of Thin Homogeneous Layers. Géotechnique, 17(3): 261–273.

Holtz, R.D. and Kovacs, W.D., 1981. An Introduction to Geotechnical Engineering. Prentice-Hall, Englewood Cliffs, NJ, 733 p.

Jeeravipoolvarn, S. 2005. Compression behavior of thixotropic oil sands tailings. MSc thesis, University of Alberta, Edmonton, AB, 223 p.

Jeeravipoolvarn, S., Chalaturnyk, R.J. and Scott, J.D., 2008 (*a*). Consolidation Modeling of Oil Sands Fine Tailings: History Matching, Proceedings of 61st Canadian Geotechnical Conference, Edmonton, AB, September 22-24, 190-197.

Jeeravipoolvarn, S., Chalaturnyk, R.J. and Scott, J.D., 2008 (*b*). Three ten meter standpipes: experimental and prediction, submitted to Canadian Geotechnical Journal.

Matthews, J.G., Shaw, W.H., MacKinnon, M.D., and Cuddy, R.G., 2002. Development of composite tailings technology at Syncrude. International Journal of Surface Mining, Reclamation, and Environment, 16(1): 24-39.

Scott, J. D., and Dusseault, M.B. and Carrier III, W.D., 1985, Behaviour of the clay/bitumen/water sludge system from oil sands extraction plants, Journal of Applied Clay Science, 1: 207-218.

Yuan, S. and Shaw, W. 2007. Novel Processes for Treatment of Syncrude Fine Transition and Marine Ore Tailings. Canadian Metallurgical Quarterly, 46(3): 265-272.

Shaw, W. and Wang, N., 2006. In-Line Thickened Tailings Pilot Program. CIM Fort McMurray, Oil Sands Discovery Center Auditorium, Fort McMurray, Alberta, February 21, 2006.

Somogyi, F. 1980. Large Strain Consolidation of Fine Grained Slurries. Presented at the Canadian Society for Civil Engineering, Winnipeg, Manitoba, Canada, May 29-30.

Suthaker, N.N., and Scott, J.D. 1994. Large Strain Consolidation of Oil Sand Fine Tails in a Wet Landscape. 47th Canadian Geotechnical Conference, Halifax, Nova Scotia, 514-523.

Session 4

Water and Heat Considerations

WATER AND HEAT INTEGRATION IN OILSANDS PROCESSING

Vince Wallwork, Mike Rogers and Alberto Alva-Argaez

ABSTRACT

The public is constantly bombarded about the vast quantities of water used in the processing of oilsands. Practioners in the industry however, continue to strive to optimize its use. Consequently, this theme presentation attempts to set the record straight on how water is used, why it is used, where it is used and what happens to it after it has been used.

At the same time, the presentation looks at the crucial role water plays in the transfer of waste heat from one part of the process to others. The energy savings derived from such activities as well as the impact on greenhouse gas equivalent emissions are examined.

The challenges and issues to satisfy the goals of managing scaling, corrosion and fouling, while limiting fresh water used, is examined for both the open-pit mining, extraction and integrated Upgrader operations as well as each of these processes in a stand-alone configuration. In addition, a similar examination is made for stand-alone SAGD operations as well as SAGD integrated with an Upgrader and SAGD integrated with an open-pit and extraction operation.

OZONE TREATMENT OF NAPHTHENIC ACIDS IN ATHABASCA OIL SANDS PROCESS-AFFECTED WATER

Hongjing Fu[1], Mohamed Gamal El-Din[1], Daniel W. Smith[1],
Michael D.MacKinnon[2], Warren Zubot[2]
1.Department of Civil and Environmental Engineering, University of Alberta. Edmonton, Alberta, Canada
2. Syncrude Canada Ltd., Edmonton Research Centre, Edmonton, Alberta Canada

ABSTRACT

Naphthenic acids (NAs) are the main resource responsible for the aquatic toxicity of oil sands processed-affected water (OSPW), and the treatment of NAs is critical for OSPW water reclamation and potential discharge options. NAs are natural low molecular weight cyclic and acyclic carboxylic acids released from the bitumen extraction process, which is based on caustic hot water digestion, with concentrations ranging from 40 to 120 mg/L in OSPW, depending on the ore quality and extraction process. The semi-batch ozonation approach has been conducted as an option to degrade NAs in OSPW from Syncrude Canada Ltd. Using a simple non-optimized treatment, in which ozone was bubbled through an OSPW sample for different ozone doses ranging from 50 to 1500 mg/L, 70-99% reductions of NAs were achieved. In the same samples, the reductions in dissolved organic carbon (DOC) and chemical oxygen demand (COD) were only 32% and 53%, respectively. This indicates that ozonation processes through de-carboxylation rather than complete dissolved organic matter (DOM) re-mineralization. The biochemical oxygen demand (BOD_5) was 24 mg/L with the used ozone dose of 80 mg/L, rising from the original value of 4 mg/L. This preliminary data shows that ozone offers a promising treatment for the NAs removal and a potential of combination of biological treatment after the ozonation in OSPW water management options. Further research will focus on optimizing ozone treatment efficiency, and understanding the mechanisms of NAs degradation pathways and the effects on toxicity of OSPW.

INTRODUCTION

The Northern Alberta oil sand region contains 174 billion barrels of oil in the form of bitumen, which ranks Canada the second largest crude oil reserves, 15% of world reserves, after Saudi Arabia (Alberta Energy, 2008). Different from the conventional oil process, hot water extraction is currently used to extract bitumen from oil sands, which are mixtures of bitumen, sands and clays. The extraction process consumes a large volume of water, and an average of 3 barrels of fresh water is required to produce 1 barrel of oil (Allen, 2008). As a result, an estimated 1 billion m^3 of OSPW will have accumulated in the Athabasca oil sands region by 2025 (Herman et al., 1994), and water treatment technologies are required to enhance the water quality for recycle without compromising the bitumen extraction efficiency, and for further discharge.

Naphthenic acids, which are natural low molecular weight surfactants released from bitumen during extraction of oil sands ore, have been shown to contribute most of the acute toxicity of OSPW. Currently, bitumen extraction is based on a caustic hot water digestion, which results in low molecular weight carboxylic acids, known as naphthenic acids (NAs), being released into the resulting process waters (OSPW) at concentrations ranging from 40 to 120 mg/L, depending on the age of OSPW, ore quality and extraction processes (Quagraine et al., 2005). NAs are closely related cyclic and alicyclic aliphatic carboxylic acids, with the general chemical formula $C_nH_{2n-z}O_2$, where n indicates the carbon number and Z is zero or a negative, even integer that specifies the hydrogen deficiency resulting form the ring formation. In fresh OSPW, the naphthenic acids are dominated by the ones with carbon number of 13 to16, while in aged OSPW, the carbon number of dominated naphthenic acids shifts to larger molecules (i.e. C_{22}).

Naphthenic acids were proven to be main components responsible for the toxicity of OSPW to aquatic organisms by the fact that the acute lethality of OSPW to rainbow trout and water fleas was significantly reduced under the condition that the naphthenic acids in OSPW were removed (MacKinnon and Boerger, 1986). The degradation of naphthenic acids in OSPW occurs naturally in the process of natural degradation, and the acute toxicity of OSPW

decreased with the decreased relative abundance of smaller naphthenic acids (C_{13-16}) (Holowenko et al., 2002), while naphthenic acids with multiple rings are less toxic and more resistant to microbial degradation (Lo et al., 2006). Therefore, the persistence of chronic toxicity resulting from the more resistant fraction of naphthenic acids is still a concern. Considering the resistance of the fraction of naphthenic acids contributing chronic toxicity and the long time required for natural degradation of naphthenic acids in OSPW, the treatment of OSPW, especially the removal of naphthenic acids from OSPW becomes a critical issue for further water discharge and environmental acceptability. Peng et al. (2004) applied the nanofiltration to water softening and removal of naphthenic acids, and more than 95% of the hardness and naphthenic acids were reported to be reduced. The sorption of naphthenic acids from OSPW was evaluated in a laboratory scale, and the naphthenic acids with carbon numbers ranging from 13 to 17 showed preferential sorption (Janfada et al., 2006).

Ozonation can also effectively oxidize organic pollutants in conventional wastewater because of ozone's high oxidation ability (Zhou and Smith, 2001; Ikehata and El-Din, 2005; El-Din et al., 2006), and likewise, it can potentially be applied to the OSPW, in which naphthenic acids contribute most heavily to environmental toxicity. In this work, a semi-batch ozononation system has been applied to OSPW received from Syncrude Canada Ltd., and the residuals of naphthenic acids, DOC, COD and BOD_5, were measured to assess the ozone treatments and the relationship between ozone doses and the residuals were discussed.

Method

The process-affected waters used in this work were collected in December 2007 in the West In-pit Pond by Syncrude Canada Ltd. Figure 1 shows the schematic of the semi-batch ozonation system built up in the lab for the treatment of OSPW using ozone. An ozone generator (WEDECO, GSO-40, Herford, Germany) was utilized to produce ozone gas using extra dry, high purity oxygen. The ozone contactor was constructed of a Pyrex Brand bottle with a capacity of 2000 mL. Ozone gas was introduced from the bottom though a glass diffuser, and the ozone concentrations in feeding gas were monitored using a high concentration ozone monitor. The ozone concentrations in the off gas were monitored with ozone monitors or by trapping ozone using KI wash bottles. The ozone residual in the reactor was measured using the Indigo method. The gas flow rate was measured by wet test meter. The used ozone dose for this system can be calculated by subtracting both the waste ozone dose and the residual ozone dose from the applied ozone dose. After treatment with ozone, the OSPW was purged by a purify nitrogen flow to strip the ozone residual off the reactor for 5 mins.

The content of naphthenic acid in water samples was measured using FI-IR in the Edmonton Research Centre of Syncrude Canada Ltd., and both the COD (chemical oxygen demand) and DOC (dissolved organic carbon) were measured by Maxxam Analytic's Inc. (Calgary). The BOD_5 was measured using the standard method. The water samples were filtered with membrane with a pore size of 0.45 μm (Millipore Corporation, Billerica, Massachusetts) for DOC testing.

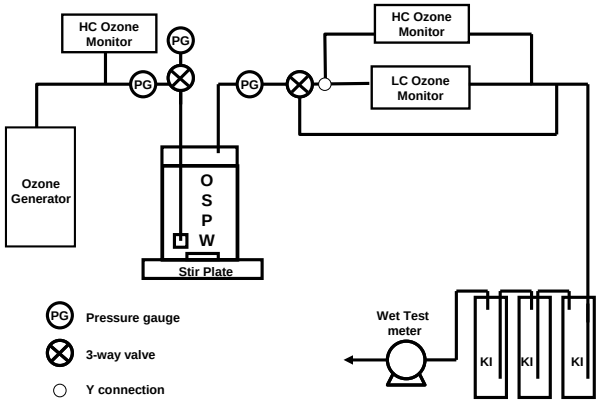

Figure 1. The schematic of semi-batch ozonation system

Results and Discussion

Figure 2 shows the relationship between the applied ozone dose and the residual naphthenic acids. The naphthenic acid residuals decreased rapidly as the applied ozone dose increased. With the applied ozone dose of 50 mg/L (1 min of ozone exposure), 73% of the initial naphthenic acids in the OSWP have been deducted, dropping from 68.2 mg/L to 18.6 mg/L. The reduction of 97% was achieved with the applied ozone dose of 500 mg/L (exposure time of 10 mins), and 1 mg/L naphthenic acids were tested with the applied ozone dose of 1500 mg/L (exposure time of 30 mins), which is close to the detection limit of the FT-IR methods for naphthenic acids. Based on the data above, ozone has shown a promising effect on the

degradation of naphthenic acids in OSPW from Athabasca oil sands industry.

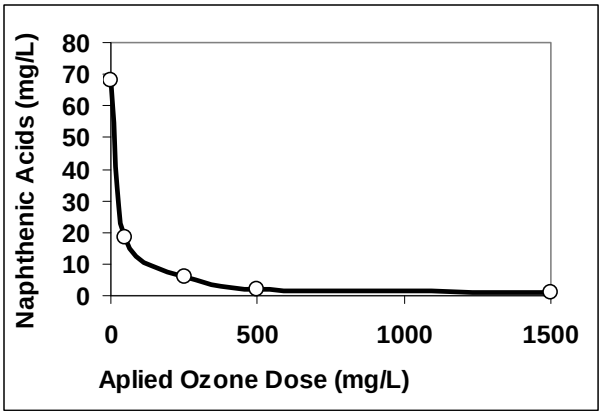

Figure 2. The relationship between naphthenic acids degradation and the applied ozone dose

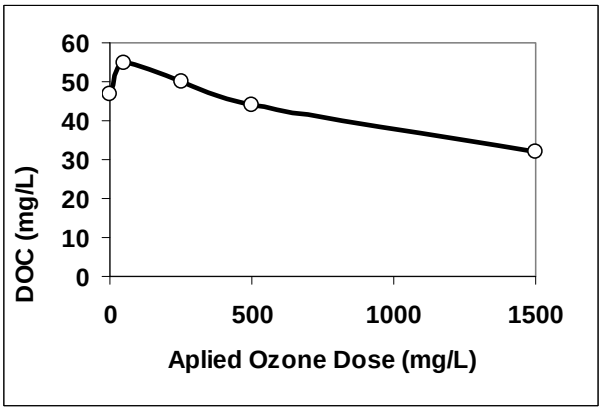

Figure 3. The effect of applied ozone d on DOC removals

The relationship between the DOC residual and the applied ozone dose is shown in Figure 3. The DOC residual increased from 47 mg O_2/L to 55 mg O_2/L with the applied ozone dose of 50 mg/L (exposure time of 1 min) and then dropped to 50 mg O_2/L with the applied ozone dose of 250 mg/L (exposure time of 5 min). The DOC residual of 32 mg O_2/L, 32% of original DOC, was achieved with the ozone exposure time. Comparing the deductions of both naphthenic acids and DOC, it is easy to find that the naphthenic acids reduction (97%) is much higher than the DOC reduction (32%) after the OSPW was treated with ozone for 30 mins. This indicates that ozonation is proceeding through de-carboxylation rather than complete dissolved organic matter (DOM) re-mineralization.

Figure 4 shows the effect of the ozone exposure time on the COD residuals. The COD decreased gradually, dropping from the original COD of 180 mg O_2/L to 154, 128, 110 and 86 mg O_2/L with the applied ozone doses of 50, 250, 500 and 1500 mg/L, respectively. A COD reduction of 53%, which is much lower than the naphthenic acids reduction, was obtained. The low COD reduction may be explained by the assumption that the large organic matters break into small organic molecules, which also contribute COD. However, the mechanism of the naphthenic acids degradation pathways is still unclear, and further experiments are needed to prove this assumption.

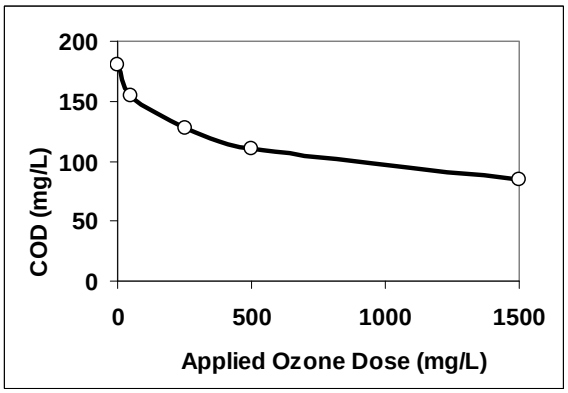

Figure 4. The effect of ozone exposure time on COD removals

Scott et al. (2005) reported that the naphthenic acids in Athabasca OSPW were less biodegradable than commercial naphthenic acids by measuring the naphthenic acids residuals after being incubated with microorganisms under aerobic conditions. The BOD_5 values of OSPW being treated with different the used ozone doses are shown in Figure 5. The initial BOD_5 of OSPW was 4 mg/L, which indicated that the biodegradability of OSPW is low. With increasing used ozone doses, the BOD_5 values of OSPW increased, reaching 25 mg/L with the used ozone dose of 80 mg/L, and keeping constant with higher used ozone doses. The fact that ozone treatment of OSPW resulted in higher BOD_5 values of OSPW indicates that ozone treatment has the potential to increase the biodegradability of OSPW, which may facilitate the process of bioremediation of OSPW after ozonation.

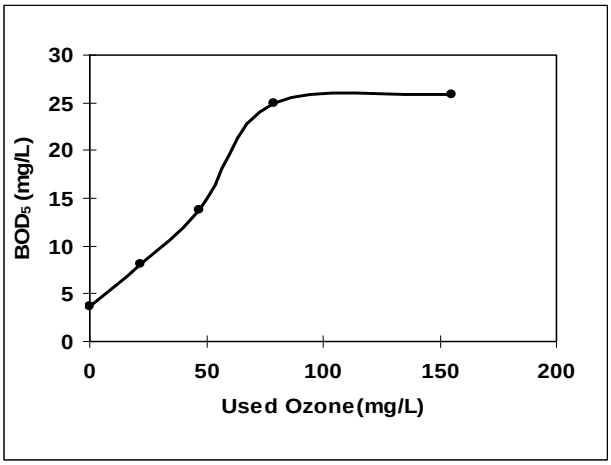

Figure 5. The effect of used ozone dose on BOD_5

CONCLUSION

The results of degradation of naphthenic acids in OSPW using ozone indicated that ozone is a promising advanced wastewater treatment technology for the naphthenic acids removal and have great potential application in the water management in oil sands industry. Further research will focus on optimizing ozone treatment efficiency, assessing of the dose-relationship, and understanding the mechanisms of NAs degradation pathways and the effects on toxicity of OSPW.

REFERENCE

Allen, E.W., "Process water treatment in Canada's oil sands industry: I. Target pollutants and treatment objectives" Journal of Environmental Engineering and Science 7(2): 123-138 (2008).

Gamal El-Din, M., D.W. Smith, F. Al Momani and W.X. Wang, "Oxidation of resin and fatty acids by ozone: Kinetics and toxicity study" Water Research 40(2): 392-400 (2006).

Herman, D.C., P.M. Fedorak, M.D. Mackinnon and J.W. Costerton, "Biodegradation of Naphthenic Acids by Microbial-Populations Indigenous to Oil Sands Tailings" Canadian Journal of Microbiology 40(6): 467-477 (1994).

Holowenko, F.M., M.D. MacKinnon and P.M. Fedorak, "Characterization of naphthenic acids in oil sands wastewaters by gas chromatography-mass spectrometry" Water Research 36(11): 2843-2855 (2002).

Ikehata, K. and Gamal El-Din, M., "Aqueous pesticide degradation by ozonation and ozone-based advanced oxidation processes: A review (Part II)" Ozone-Science & Engineering 27(3): 173-202 (2005).

Janfada, A., J.V. Headley, K.M. Peru and S.L. Barbour, "A laboratory evaluation of the sorption of oil sands naphthenic acids on organic rich soils" Journal of Environmental Science and Health Part a-Toxic/Hazardous Substances & Environmental Engineering 41(6): 985-997 (2006).

Lo, C.C., B.G. Brownlee and N.J. Bunce, "Mass spectrometric and toxicological assays of Athabasca oil sands naphthenic acids" Water Research 40(4): 655-664 (2006).

MacKinnon, M.D. and H. Boerger, "Description on two treated methods for detoxifying oil sands tailings ponds water" Water Pollution Research Journal of Canada 21(4): 496-512 (1986).

Peng, H., K. Volchek, M. MacKinnon, W.P. Wong and C.E. Brown, "Application of nanofiltration to water management options for oil sands operations" Desalination 170(2): 137-150 (2004).

Quagraine, E.K., H.G. Peterson and J.V. Headley, "In situ bioremediation of naphthenic acids contaminated tailing pond waters in the Athabasca oil sands region-demonstrated field studies and plausible options: A review" Journal of Environmental Science and Health Part a-Toxic/Hazardous Substances & Environmental Engineering 40(3): 685-722 (2005).

Scott, A.C., M.D. MacKinnon and P.M. Fedorak, "Naphthenic acids in athabasca oil sands tailings waters are less biodegradable than commercial naphthenic acids" Environmental Science & Technology 39(21): 8388-8394 (2005).

Zhou, H. and D.W. Smith, "Advanced technologies in water and wastewater treatment" Canadian Journal of Civil Engineering 28: 49-66 (2001).

COAGULATION-FLOCCULATION PRETREATMENT OF OIL SANDS PROCESS AFFECTED WATERS

Yingnan Wang, Parastoo Pourrezaei, Mohamed Gamal El-Din
Department of Civil and Environmental Engineering, University of Alberta,
Edmonton, Alberta, Canada, T6G 2W2

ABSTRACT

Process affected water generated from oil sands industry is mainly composed of natural organic matters (NOM), suspended and dissolved particles, hydrocarbons, trace metals and many other toxic compounds such as naphthenic acids that need to be treated using conventional and advanced treatment methods. Coagulation-flocculation is a conventional physical-chemical pre-treatment process to remove the fine suspended and dissolved particles. In this study, jar test apparatus was used to simulate the expected conditions for coagulation-flocculation. Aluminum sulphate (alum), one of the most common coagulants, was used at 0-300 mg/L to destabilize particles. Cationic polymer (CTI TL) was also applied to enhance the flocculation process. The optimum dosage of alum was 200 mg/L at sample natural pH of 8.5. When 20 mg/L cationic polymer CTI TL was used as a flocculant, TOC and turbidity removal were increased from 6% and 94% to 16% and 99%, respectively. When CTI TL was used as a sole coagulant without alum, TOC and turbidity removal ratios were 8% and 97%, respectively but the optimum polymer dosage was only 5 mg/L which is more economical for the industry application. The effect of sample pH was also studied. TOC and turbidity removal efficiencies were higher at pH 6.5 than those at pH 8.5.

INTRODUCTION

Oil sand is composed of water, bitumen and mineral compounds in different proportions. As a result of different processes to extract the bitumen from oil sands, the slurry effluent which is a mixture of water, residual bitumen and sand particles are deposited in the tailings ponds (Chalaturnyk et al. 2002). The consumption rate of water per each ton of oil sand extracted is approximately in the range of 0.7-1.0 m^3 (Peng et al. 2004). More than 80 percent of the required water for surface mining can be recycled from the tailing ponds, and the remaining part is taken from the Athabasca River which is mainly used for utility requirements. Due to the enforced zero discharge policy, the produced waters from oil sands operations cannot be discharged to the environment and have to be stored in the tailing ponds. Owing to rapid growth of oil sands industry, these tailing ponds are growing faster than the available capacity. Therefore; management and reuse of the water is a major issue in development of the future processes. Water management options for oil sands process-affected waters (OSPW) are urgent to be developed, which can also reduce the amount of water to be imported from the river (Chalaturnyk et al. 2002).

Different types of wastewaters are generated from various oil sands processes that need to be treated with the conventional water treatment technologies, such as physical-chemical treatment (Chalaturnyk et al. 2002), as well as advanced treatment options (Rivas et al. 2004). OSPW comprise a variety of components such as suspended solids, hydrocarbons, salts, dissolved organics, ammonia, trace metals, and naphthenic acids that affect the choice of treatment methods (Gentes et al. 2006; Holowenko et al. 2001, 2002). Suspended particles and dissolved compounds can be removed by conventional primary treatment such as natural sedimentation and filtration. However, when the size of the suspended solids and the soluble particles are relatively small to be effectively removed by the filtration and natural sedimentation the treatment can be achieved by the application of the coagulation and flocculation processes which can increase the size of the particles by agglomeration to enhance the settling quality. Compared to other treatment technologies, sedimentation assisted by coagulation-flocculation is more cost effective and easy to operate, which can also save considerable amount of energy (Dosta et al. 2008).

Coagulation is a process used for destabilization of the suspended and dissolved particles with the addition of the coagulant to provide a condition for the particles to coalesce together and form larger flocs (Gregory et al. 2006). Flocculation is the following process with or without the addition of the

flocculant aid to facilitate the aggregation of the flocs formed in the first step. The most common and economical coagulant agent is aluminum sulphate (alum) (Gregory et al. 2006) which is added during the coagulation process to form positive ions and other hydrolysis products to neutralize the negative charges on the surface of the suspended particles which can repel them from each other and prevent the aggregation process. Other coagulants such as aluminum chloride, ferric chloride and ferric sulphate (Tatsi et al. 2003) can also be used depending on the characteristics of the water to be treated as well as the target treatment levels.

Jar testing is an effective method to simulate the desired conditions for coagulation-flocculation which consists of the rapid/flash mixing with high intensity for coagulation followed by the slow mixing with lower intensity for flocculation. After the mixing period, the formed flocs are allowed to settle (Amuda et al. 2006; Clark and Stephenson 1999). The most important factors that need to be optimized during the jar test procedure are pH, coagulant and coagulant aids type and their dosages, coagulation and flocculation mixing intensities and times (Ahmad et al. 2007; Almubaddal et al. 2008). The optimum conditions and chemicals can be obtained by sensitivity analysis approach.

The objectives of this research were to investigate whether the coagulation-flocculation is an effective and applicable process for the treatment of oil sands process affected waters and to find the optimum treatment conditions and most effective chemicals to yield the higher removal efficiencies in terms of TOC and Turbidity.

MATERIALS AND METHODS

Materials

Aluminum sulphate ($Al_2(SO_4)_3 \cdot 18H_2O$), hydrochloric acid (2N HCl), sodium hydroxide (2N NaOH) and cationic polymer (CTI TL) were used to perform the experiments. Concentrations of the prepared stock solutions for alum and polymers were 10 g/L. Alum was employed as the primary coagulant with the concentration in the range of 0-300 mg/L. Cationic polymer was also used which acted as a sole coagulant and flocculant aid in the presence of alum at the concentration range of 0-30 mg/L.

OSPW Samples

Oil sand process-affected waters (OSPWs) were collected directly from Syncrude Canada Ltd. OSPW samples were reserved in a cold room at approximately 4ºC. Each time before the testing, the samples were well mixed and allowed to reach the room temperature. Turbidity, pH, temperature and TOC of the samples were determined before treatment. The pH of the samples was adjusted to 6.5 and 10.5 by using HCl and NaOH whenever needed before the testing. Also the natural pH of the samples was used as one of the treatment conditions since it is more economical and time saving without pH adjustment in full-scale treatment operations.

Jar Tests

A classic jar test was used to perform the experiments is a bench-scale Phipps and Bird apparatus which consists of 6 units of 2.0 liter square jars with a 6-place paddle stirrer. The conditions for all the jars during the experiment were kept the same to reduce the experimental errors. Operational conditions to perform the testing were 30 seconds rapid mixing at 220 rpm followed by 30 minutes low intensity mixing for flocculation at 30 rpm. After these steps the formed flocs were allowed to settle for approximately 40 minutes. Alum and cationic polymer were added at the beginning and during the coagulation step.

Sample Analysis

After settling, pH, turbidity and the TOC of the supernatant drained from the discharge line of the jars were tested to evaluate the removal rate of organic carbons, particles and color of the samples. Total organic carbon, turbidity, and pH of the samples were analyzed using the Apollo 9000 TOC analyzer based on high temperature (680°C) combustion method, Orbeco-Helligo Digital turbidimeter, and Accumet AR20 pH meter, respectively.

RESULTS AND DISCUSSION

Sample Characteristics

The average characteristics of OSPW as well as the range of pH, turbidity, TOC and TSS are shown in Table 1. Through the jar tests, the temperature slightly increased because of the mixing, and pH was slightly decreased due to the addition of alum.

Table 1. Main physical and chemical characteristics of raw OSPW.

Parameter	Average	Range	No. of samples
pH	8.6	8.5-8.8	20
Turbidity (NTU)	115	84-124	20
TOC (mg/L)	53	48-56	20
TSS (mg/L)	35	33-37	6

Alum Coagulation

A series of jar tests were conducted by varying alum dosages from 0 mg/L to 300 mg/L. The pH of some raw samples was adjusted to 6.5 by adding concentrated hydrochloric acid and the other samples were maintained at natural pH of OSPW which was around 8.5. These jar tests were conducted to optimize the alum dosage at a specific pH to obtain higher TOC and turbidity removal efficiencies.

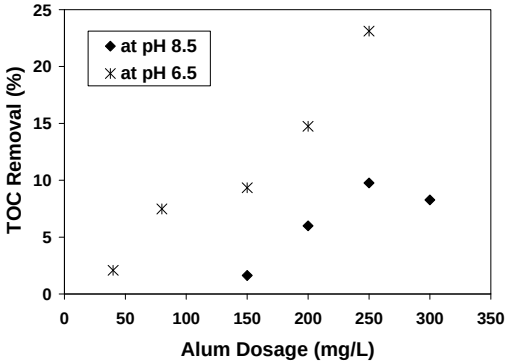

Figure 1: Effect of pH and alum dosage on TOC removal.

The results presented in Figure 1 and Figure 2 show that more TOC and turbidity were removed at pH of 6.5 than those at pH of 8.5 with the same alum dosage and other operational factors. This resulted from the most effective pH range of alum which was between 5.8 and 7.7 (Crittenden et al. 2005). With 250 mg/L alum, the TOC removal efficiencies were 23% at pH 6.5 and 10% at pH 8.5, respectively. Any alum dosage more than 250 mg/L would be an over dosage of the sample at its natural pH (~8.5) since destabilized particles could be restabilized again by the opposite charges of the coagulant, which is unfavorable for settling. Considering that simpler processes are usually favored by the industry, OSPW samples at their natural pH were used for the further treatments. 200 mg/L, in stead of 250 mg/L, of alum was used as the optimum dosage in future experiments, since 250 mg/L of alum was likely to be an over dosage if the environment or sample characteristics were slightly changed, such as temperature, pH, et al. Moreover the TOC and turbidity removals were not significant different when 200 mg/L or 250 mg/L alum was used.

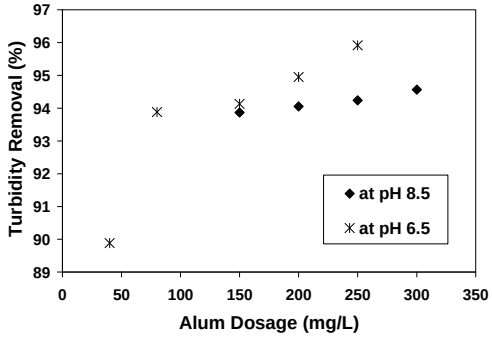

Figure 2: Effect of pH and alum dosage on turbidity removal.

As shown in Figure 2, the turbidity removal was more than 93% when the alum dosage was over 80 mg/L indicating that most suspended solids removed as a result of the coagulation and flocculation followed by sedimentation processes.

Effect of Cationic Polymer

CTI TL which is a cationic polymer was chosen to investigate the effect of the addition of flocculant aid on TOC removal. The optimum rapid mixing time for CTI TL was found by adding the polymer at different times during the rapid mixing process. The alum dosage was optimized at the concentration of 200 mg/L and with 30 seconds rapid mixing. The CTI TL dosage was fixed at 20 mg/L in all the jars.

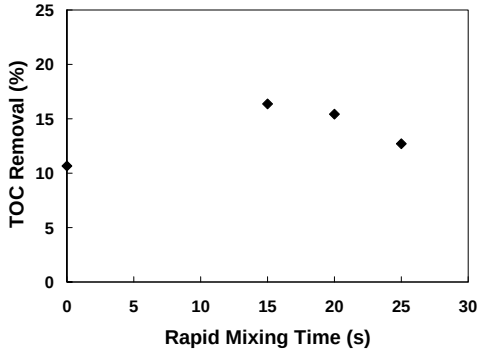

Figure 3: Effect of rapid mixing time of CTI TL at 220 rpm.

Based on the results shown in Figure 3, the optimum rapid mixing time for CTI TL in 30 seconds coagulation process was 15 seconds. Longer time rapid mixing could break the bridged floc particles, which resulted in poor settling (Peng et al. 2004).

The optimum CTI TL dosage was found by carrying out a series of jar tests with different polymer dosages and at a fixed alum dosage. The first floc formed at 3 min after alum addition. The depth of sludge at the bottom of the 2 L jar after 40 min settling was about 10 mm. The TOC removal and turbidity removal efficiencies are shown in Figure 4.

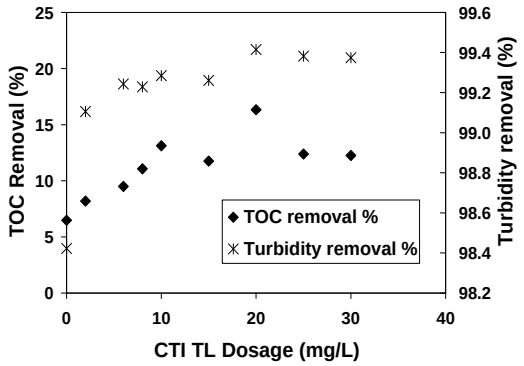

Figure 4: Effect of CTI TL dosage on TOC and turbidity removals when cationic polymer was used as a flocculant aid.

Figure 5: Picture of OSPW samples before and after coagulation-flocculation followed by sedimentation processes with 200 mg/L alum and 20 mg/L CTI TL.

More than 99% of the turbidity was removed during the coagulation-flocculantion followed by sedimentation processes. When polymer was used at 20 mg/L, it gave the highest TOC removal and turbidity removal at 16% and 99%, respectively. From the experimental data, the turbidity after treatment was less than 1 NTU. Compared with the results of 6% and 94% for TOC and turbidity removal, respectively, presented in Figure 1 and Figure 2 obtained when only 200 mg/L alum was used, it can be concluded that cationic polymer CTI TL was a flocculant aid to enhance the coagulation-flocculation process (Aguilar et al. 2003). Figure 5 shows the sample before and after coagulation, flocculation and settling processes. Most particles had been removed and the sample was much clear after treatment.

The effect of cationic polymer on the coagulation process when it is applied without any other coagulants was also investigated. TOC removal and turbidity removal were measured when different CTI TL dosages (0.5 mg/L to 20 mg/L) were applied. The first floc was formed at 2 min after coagulant addition, which was faster than that when alum was used as the coagulant. The flocs were bigger and settled faster than previous experiments. After 40 min settling, the depth of sludge at the bottom of the 2 L jar was about 3 mm. The results based on TOC removal and turbidity removal is shown in Figure 6.

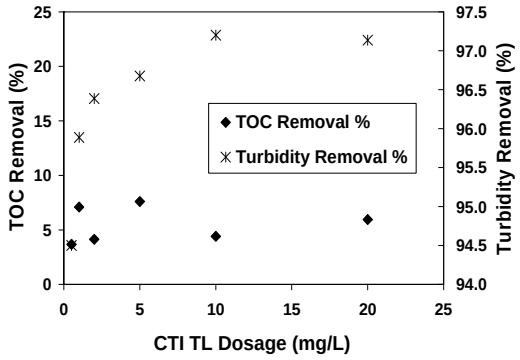

Figure 6: Effect of CTI TL dosage on TOC and turbidity removals when cationic polymer was used as a sole coagulant.

The highest TOC removal was 8% when 5 mg/L CTI TL was used, and at this point, 97% of turbidity was removed. Although the highest removal efficiencies were all less than those when alum and cationic polymer were used together, 5 mg/L of CTI TL was much less than the dosage of polymer and alum together (20 mg/L of CTI TL and 200 mg/L of alum as optimum dosages). It was

also a choice for the industry application according to the lower cost.

CONCLUSIONS

The coagulation-flocculation followed by sedimentation treatment for OSPW with alum and cationic polymer led to very high removals of turbidity (up to 99%), but the removal of TOC was low (up to 16%). OSPW pH can affect the treatment efficiency. The TOC and turbidity removal efficiencies were better at pH of 6.5 than those at pH of 8.5, since the most effective pH of alum was between 5.8 and 7.7. However, the natural pH of OSPW was around 8.5, which was out of the most effective pH range of alum, but alum treatment was proved to work. Other coagulants with larger effective pH range should be investigated in future experiments. Cationic polymer CTI TL significantly enhanced the coagulation process with alum. Cationic polymer can be used as the sole coagulant without alum as well. Although lower TOC removal was achieved (up to 8%), the coagulant dosage was much less than that when it was used with alum together. The flocs settled faster and more compacted sludge was produced. So it is recommended to use cationic polymer as the sole coagulant for OSPW pretreatment.

ACKNOWLEDGEMENTS

This work was funded by Oil Sands Tailing Research Facility (OSTRF). OSPW samples were supplied by SynCrude Canada and some instruments were funded by NSERC. We also gratefully acknowledge the technical support from Maria Demeter.

REFERENCES

Chalaturnyk, R.J., Scott, J.D., and Ozum, B. 2002. Management of Oil Sands Tailings. Petroleum Science and Technology, 20: 1025-1046.

Peng, H., Volchek, K., MacKinnon, M., Wong, W.P., and Brown, C.E. 2004. Application of Nanofiltration to Water Management Options for Oil Sands Operations. Desalination, 170: 137-150.

Rivas, F.J., Beltran, F., Carvalho, F., Acedo, B., and Gimeno, O. 2004. Stabilized Leachates: Sequential Coagulation-Flocculation + Chemical Oxidation Process. Journal of hazardous materials, 116: 95-102.

Gentes, M.L., Waldner, C., Papp, Z., and Smits, J.E. 2006. Effects of Oil Sands Tailings Compounds and Harsh Weather on Mortality Rates, Growth and Detoxification Efforts in Nestling Tree Swallows (Tachycineta Bicolor). Environ Pollut, 142: 24-33.

Holowenko, F.M., Mackinnon, M.D., and Fedorak, P.M. 2001. Naphthenic Acids and Surrogate Naphthenic Acids in Methanogenic Microcosms. Water research, 35: 2595-2606.

Holowenko, F.M., MacKinnon, M.D., and Fedorak, P.M. 2002. Characterization of Naphthenic Acids in Oil Sands Wastewaters by Gas Chromatography-Mass Spectrometry. Water research, 36: 2843-2855.

Dosta, J., Rovira, J., Gali, A., Mace, S., and Mata-Alvarez, J. 2008. Integration of a Coagulation/Flocculation Step in a Biological Sequencing Batch Reactor for Cod and Nitrogen Removal of Supernatant of Anaerobically Digested Piggery Wastewater. Bioresource technology, 99: 5722-5730.

Gregory, J., Newcombe, G., and David, D., 2006. Chapter 3: Floc Formation and Floc Structure. Interface Science and Technology. Elsevier, pp. 25-43.

Tatsi, A.A., Zouboulis, A.I., Matis, K.A., and Samaras, P. 2003. Coagulation-Flocculation Pretreatment of Sanitary Landfill Leachates. Chemosphere, 53: 737-744.

Amuda, O.S., Amoo, I.A., and Ajayi, O.O. 2006. Performance Optimization of Coagulant/Flocculant in the Treatment of Wastewater from a Beverage Industry. Journal of hazardous materials, 129: 69-72.

Clark, T., and Stephenson, T. 1999. Development of a Jar Testing Protocol for Chemical Phosphorus Removal in Activated Sludge Using Statistical Experimental Design. Water research, 33: 1730-1734.

Ahmad, A.L., Wong, S.S., Teng, T.T., and Zuhairi, A. 2007. Optimization of Coagulation-Flocculation Process for Pulp and Paper Mill Effluent by Response Surface Methodological Analysis. Journal of hazardous materials, 145: 162-168.

Almubaddal, F., Alrumaihi, K., and Ajbar, A. 2008. Performance Optimization of Coagulation/Flocculation in the Treatment of Wastewater from a Polyvinyl Chloride Plant. Journal of hazardous materials.

Crittenden, C.J., Rhodes Trussell, R., Hand, W.D., Howe, J.H., and Tchobanoglous, G., 2005. Water Treatment: Principles and Design. John Wiley & Sons, Inc., Hoboken, New Jersey.

Aguilar, M.I., Saez, J., Llorens, M., Soler, A., and Ortuno, J.F. 2003. Microscopic Observation of Particle Reduction in Slaughterhouse Wastewater by Coagulation-Flocculation Using Ferric Sulphate as Coagulant and Different Coagulant Aids. Water research, 37: 2233-2241.

Session 5

Tailings and Landscape Engineering

A REVIEW OF WETLAND RESEARCH AT SUNCOR: RE-ESTABLISHING WETLAND ECOSYSTEMS IN AN OIL-SANDS AFFECTED LANDSCAPE

Christine Daly[1] and Jan J.H. Ciborowski[2]
1 Suncor Energy Inc.
2 University of Windsor

ABSTRACT

Constructed wetlands will be a critical component of reclaimed landscapes in the oil sands region. Research wetlands at Suncor Energy Inc. (Suncor) were constructed with Consolidated Tailings (CT), Mature Fine Tailings (MFT) and oil sands process waters (OSPW), mining by-products, to investigate the remediation potential of wetlands. The reclamation research program at Suncor examines a range of biotic and chemical variables that may influence the sustainability of tailings-constructed wetlands. The program: (1) Examines the impact CT, MFT and OSPW may have on macrophytes, benthic invertebrates, amphibians, waterfowl and water quality; (2) Identifies food webs, (3) Identifies indicators of wetlands health; and (4) Describes processes controlling the ecological trajectory of natural and constructed wetlands. Results indicate that CT-affected wetlands can accumulate and support a productive and diverse invertebrate community. Birds that feed on insects emerging from wetlands with fresh OSPW and/or tailings materials exhibit few negative effects on immune function, except during harsh climatic conditions. Tree swallows (*Tachycineta bicolor*) also appear to have abundant food resources based on the large nestling biomasses quantified at reclaimed oil sands wetlands. One reclamation approach that may mitigate negative effects of CT, such as lower plant diversity, is to amend wetland sediments with a mixture of peat-and mineral soil. Covering CT sediments with peat-mineral amendments resulted in significantly increased plant diversity and colonization rates compared to non-CT capped sediments. Another reclamation strategy examines petroleum coke, a carbonaceous by-product of mining, which may stabilize clay-dominated tailings in constructed wetlands. Field studies compared trace metal concentrations in the pore waters and biota of coke-covered sediments with those of reference and CT sediments. Concentrations in pore water and associated biota (macrophytic algae *Chara vulgaris*, snail *Lymnaeidae*, invertebrate *Tanytarsus* (*Chironomidae*)) were similar in all three treatments. Tailings-constructed wetlands may be a viable, sustainable, and productive reclamation option.

INTRODUCTION

Wetlands covered between 39% and 63% of Suncor Energy Inc. (Suncor)'s lease (Suncor 1998, 2003, 2005) prior to disturbance, making them a significant component of the natural environment in the Athabasca region of northeastern Alberta. Wetlands are often created or restored to mitigate the loss of wetland function caused by anthropogenically-induced changes to the landscape (Hunter and Faulkner 2001). Significant efforts are focused on recreating wetland ecosystems within Suncor's reclaimed oil sands landscape. One approach focuses on constructing wetlands using mining by-products - tailings, process water and potentially petroleum coke, in the design.

This review paper focuses on reclaimed wetland research at Suncor. It is written for scientists, engineers and other interested parties that would like to learn more about how tailings and process waters have been used to build wetland ecosystems, and how these materials affect ecosystem function. The objective is to recommend a strategy that will help industry better manage tailings and tailings technology with the end goal, successful reclamation, in mind. We begin with an introduction of the oil sands mining industry, present case studies on wetland reclamation research complexes, discuss effects of petroleum coke, a potential reclamation strategy, on reclaimed wetlands, and conclude with a summary of the current state of knowledge on reclaimed wetland food webs.

WETLAND RECLAMATION IN THE OIL SANDS MINING LANDSCAPE

Suncor is one of several energy companies extensively mining oil sands in the Athabasca region of northern Alberta. At Suncor about 500,000 tonnes of oil sand is mined per day (Suncor 2006b) and approximately 260 thousand barrels of crude oil is produced daily (Suncor 2006a). Predictions suggest that more than half a million barrels of crude oil will be produced per day at Suncor between 2010 and 2012 (Suncor 2006a) indicating that mining activities are increasing.

Bitumen is removed from the oil sands using a combination of hot water, steam, and caustic soda (NaOH) to separate the hydrocarbons from the oil-bearing sand (The Fine Tails Fundamentals Consortium (FTFC) 1995). For each m^3 of oil sand processed, about 3 m^3 of water is required and that means 4 m^3 of fluid tailings are produced (Holowenko et al. 2002). Oil sands companies retain all extraction wastes on their leases, so process water; Mature Fine Tailings (MFT) and Consolidated Tailings (CT) are stored in large settling ponds on site. The production and storage of tailings and process water continues to increase along with crude oil production.

MFT are an aqueous suspension of sand, silt, clay, residual bitumen and naphtha at a pH between 8 and 9 (FTFC 1995). Oil sands companies mix MFT with sands and gypsum to encourage flocculation of the clays and speed up the tailings dewatering process. The resulting materials are called consolidated tailings (CT) (Fedorak et al. 2003). MFT, CT and process waters contain high levels of salts due to the ions in the raw ore, sodium hydroxide from the extraction process and gypsum added to create CT. Process waters and MFT contain high levels of dissolved organics (naphthenic acids 50-120 mg/L) (Leung et al. 2001; Quagraine et al. 2005; Toor 2008). Naphthenic acids in freshly produced process water are acutely toxic to many aquatic organisms. For example, 100% of fathead minnows (*Pimephales promelas*) exposed to fresh tailings pond water died in less than 48 h (Lai et al. 1996). However, natural degradation results in a significant reduction in toxicity within 6-18 months (Golder Associates Ltd. (Golder) 1997; Lai et al. 1996; Quagraine et al. 2005; Toor et al. 2007; Videla 2007).

In accordance with the Environmental Protection and Enhancement Act of Alberta, prior to discharge to the natural environment the original landscape function must be restored. Reclaiming wetlands may be a suitable restorative strategy since wetlands are highly valued for their ability to act as filters, sinks and transformers for sediments, nutrients and pollutants (Hook 1993). Construction of wetlands using tailings, process water and petroleum coke may serve a dual function of treating contaminants in oil sands mining by-products and providing high quality habitat.

CASE STUDY: CT RESEARCH WETLAND COMPLEX

A 34 hectare CT Research Wetland Complex (CT Wetlands) was constructed at Suncor in Reclamation Area 11 in 1999/2000 to assess approaches for reclaiming a CT landscape (Golder 2005) (Fig. 1). Reclamation of CT landscapes presents challenges: CT and process water have high concentrations of salts and naphthenic acids, elevated pH, and residual bitumen. The objective of the CT Wetlands project was to determine the optimum vegetation practices required to create ecologically viable, sustainable and productive wetland ecosystems and to examine the water treatment capacity of CT-constructed wetlands.

Three interconnected wetlands were constructed on an overburden substrate as part of the CT Wetlands: 1 m CT Wetland (1 m thickness of CT), 4 m CT Wetland (4 m CT) and Jan's Pond. The 1 m CT Wetland base is composed of 1 m of CT that was capped with 20 cm of peat-mineral soil. The 4 m CT Wetland base is composed of 4 m of CT that is uncapped with peat-mineral soils except in a few areas (20 cm deep) known as the muskeg peninsulas. The base of Jan's Pond is composed of non-sodic overburden (clays, silts and sand) with a thin layer of CT on top. It was not capped with peat-mineral soils.

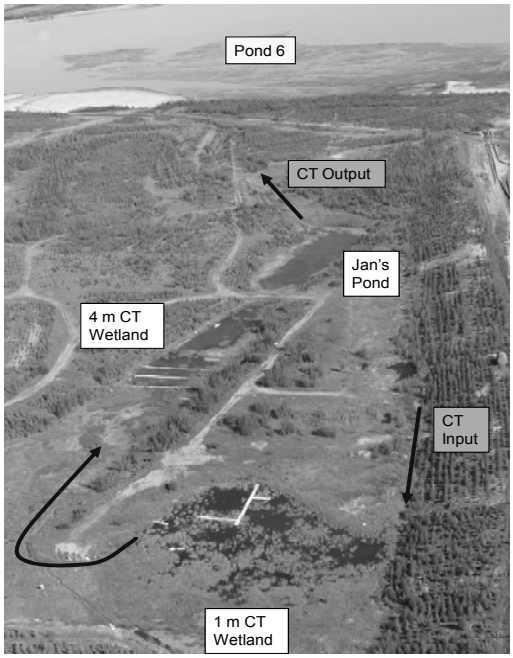

Figure 1. The CT Research Wetland Complex depicting the 3 wetlands (1 m CT, 4 m CT and Jan's Pond) and the CT process water input and output which functions to circulate water throughout the wetland system.

Process water is continuously pumped from tailings ponds into the 1 m CT at a rate of 75 L per minute. Process water flows through 1 m CT to 4 m CT to Jan's Pond before draining back along a return channel into a tailings pond, Pond 5. The residence time of process water within the CT Research Wetland Complex is approximately 30 days.

Vegetation

Thirty-three cattail (*Typha latifolia*) plots were established in 2000 in the 1 m CT (n = 6), 4 m CT (n=6), Jan's Pond (n=6) and three nearby reclaimed wetlands (Golder 2005). Plots contained 25 plants and were 1m by 1m. Plants were assessed at the end of each growing season from 2000 to 2004 for height, water depth, presence of reproductive structures, plant vigour and expansion outside the plot boundaries. Golder (2005) reported that there was a trend whereby cattail height increased in average height for the first few years after planting. However, in 2003 there was a decrease in height at maturity compared to the previous years. The decrease in height was related to the below average temperature that year, suggesting that temperature an important determinant of cattail height in the CT Wetlands.

Golder (2005) also reported that after 5 growing seasons 4 of the 6 wetlands had average cattail expansions greater than 7 m^2. The intertwining rhizomatous root structure of cattail and its ability to proliferate makes this emergent plant species an excellent candidate for reclaimed wetlands (Golder 2005). The ability of a plant to produce reproductive structures is one indicator of plant health (Kennedy and Murphy 2004). Results from the Golder study (2005) indicated that the number of flowering stems is the CT Wetlands is comparable to natural wetlands in the area and thus typical for this region. Baker (2007) quantified macrophyte growth in Jan's Pond and determined that this oil sands influenced wetland was capable of supporting cattail and bulrush growth in a capacity similar to an undisturbed wetland. Similarly, Cooper (2004) reported that isolated CT plots sediment plugs the 4 m CT Wetland were rapidly colonized when placed in a reference wetland suggesting that CT was a hospitable substrate for many plants species. Although the composition of wetland plant species in CT-constructed wetlands differed from freshwater natural wetlands (Cooper 2004; Golder 2007), likely because the saline waters in tailings-constructed wetlands are more hospitable to saline tolerant species not abundant in freshwater wetlands. Capping CT sediments with peat-mineral amendments significantly increased plant diversity compared to non-CT capped sediments (Cooper 2004). By 2008, nine years after construction commenced, virtually all of the peat-amended substrate in the 4 m C Wetland had been colonized by bulrush and cattails. However, there was little establishment of submergent vegetation in deeper areas on CT sediments (unpublished data).

Wetland Treatment Capacity

The CT Research Wetland Complex has a capacity to treat some parameters of concern in process water during the 30 days it takes for the water to cycle through the complex. Ammonia levels decrease substantially between the inlet and outlet of the wetland system (Table 1). In 2004 water quality sampling indicated that ammonia levels decreased from 8.87 mg/L at

inlet to 0.05 mg/L at the outlet. Similar trends were observed in 2004 and 2007 (Table 1). The water quality guideline for the protection of aquatic life for total ammonia is 0.499 mg/L at pH 8.0 and 20°C (Canadian Council of Ministers of the Environment (CCME) 1999). The decreased ammonia concentrations at the outlet suggest that ammonia is undergoing attenuation in the wetlands due to volatilization, oxidation or microbial decay.

In 2000 phosphorus levels decreased from approximately 300 µg/L to 60 µg/L between the inlet and outlet (Table 1). Similarly, in 2003 and 2004 phosphorus levels decreased from 159 to 33 µg/L and 197 to 20 µg/L, respectively, between the inlet and outlet. Most uncontaminated freshwaters contain between 10 and 50 µg/L (Wetzel 2001). Water quality results suggest that the CT Wetlands are capable of removing excess phosphorus.

Table 1 – Ammonia (mg/L) and phosphorus (µg/L) concentrations measured at the inlet and outlet of the CT Wetland Complex.

Year	Ammonia [] (mg/L)		Phosphorus [] (µg/L)		Reference
	Inlet	*Outlet*	*Inlet*	*Outlet*	
2000	8.00	0.05	*300*	*60*	Golder 2005
2003	7.29	<0.05	159	33	Golder 2003
2004	8.87	0.05	197	20	Golder 2005
2007	15.50	3.89	-	-	Suncor unpublished data

"-" means no data exists

Naphthenic acid concentrations did not show significant variations between the inlet and outlet of the wetland systems between 2003 and 2007, suggesting that retention time (approximately 30 days) is insufficient to allow significant degradation (paired comparison t-test; $p>0.05$) (Table 2). Similarly, Toor et al. (2007) evaluated the potential for naphthenic acid degradation and aquatic toxicity reduction in laboratory microcosms containing process water (from Suncor and Syncrude Canada Ltd.) used to mimic reclaimed wetlands. Nutrient supplementation did not influence the removal of NAs in process water. Simulated wetlands were not capable of reducing acute toxicity within a 4 month period.

Most of the toxicity in fresh process water is associated with naphthenic acids (Golder 1997). Many studies have shown that natural aging of process water reduces toxicity (Holowenko et al. 2002; Mackinnon and Boerger 1986) but that natural aging required to reduce toxicity appears to be in the order of several months (Videla 2007). Golder (1997) reported that *Ceriodaphnia dubia* survival increased from 13% to 100% for fresh (5 months) to older (8 months) CT process water. Research indicates that microbial activity in laboratory cultures also reduces the toxicity of NAs. For example, Biryukova et al. (2007) showed that the lower molecular mass naphthenic acids were preferentially degraded during a 4 month incubation period with rhizosphere microorganisms.

Table 2 – Naphthenic acid (mg/L) concentrations measured at the inlet and outlet of the CT Wetland Complex.

Date	Inlet	Outlet	Reference
2003	67	69	Golder 2003
2004	59	60	Golder 2005
2006	63	43	Golder 2005
2007	59.2	50.6	Suncor unpublished data

Golder (2005) reported that copper (Cu) levels exceeded the chronic aquatic life guideline in 2004 but were generally below this guideline between 2000 and 2003. Iron (Fe) and nickel (Ni) showed rapid reductions of concentration in the 1 m CT, which may be related to settlement of suspended solids in this wetland (Golder 2005). In 2004, iron levels were well above the chronic aquatic guideline in the 1 m CT and slightly above guidelines in the 4 m CT. However, nickel was well below the guidelines at all wetlands (Golder 2005). Molybdenum (Mo) levels were above the chronic water quality guidelines for the protection of aquatic life from 2000-2004 (Golder 2005).

In 2004, arsenic (As) levels deceased from 0.012 mg/L, which is above the water quality guideline for the protection of aquatic life, at the inlet to 0.003 mg/L at the outlet, which is below the guideline inferring that treatment of arsenic is a possibility in the CT Wetlands (Golder 2005).

Generally, the concentrations of nutrients and several metals (Cu, Fe, Ni and As) were reduced between the inlet and outlet of the CT Wetlands suggesting that reclaimed wetlands are capable

of treating process waters. However, a longer treatment period (i.e. several months) is required for NAs and some metals (i.e. Mo).

CASE STUDY: THE TRENCHES

Suncor's Experimental Trenches (Trenches) were constructed in June 1991 (Bishay 1998; Bishay and Nix 1996; Nix et al. 1993). Each trench is 50 m long x 10 m wide x 2 m from crest to base, and all 9 cover a 1.4 ha area. The Trenches are lined with a 40 mil high density polyethylene liner, capped with 0.45 m of sand and topped with 0.15 m of peat-mineral soil. The trenches are sloped to produce a difference of 25 cm in depth between upstream and downstream ends. Water depth at the downstream end of each trench is regulated by a notched weir. Three hundred *Typha latifolia* (cattail) shoots and 60 *Scirpus validus* (bulrush) culms were planted in each trench in June 1991 and monitored annually for 4 years. Control, dyke seepage water (at the base of a tailings pond) or process water (directly from a tailings pond) treatments were applied in a randomized block design.

In 2005, the Trenches were dredged and refurbished. Three were filled with fresh water from a nearby pond (<600 µS) and 3 other trenches were filled with Suncor oil sands process water (OSPW) (>1200 µS).

Treatment Capabilities

Water and sediment chemistry and emergent macrophytes were monitored in the Trenches between 1992 and 1994 (Bishay 1998). Bishay (1998) reported that average ammonia removal rates ranged from 42 to 99% for dyke water and 32 to 96% during a 3 year study suggesting that constructed wetlands receiving oil sands wastewater can effectively reduced elevated ammonia concentrations. Average inflow rates for pond and dyke waters in the Trenches ranged between 10 to 15 mg/L and outflow rates were 0.15 to 12 mg/L. Average Total Extractable Hydrocarbons (TEH) removal rates ranged from 19% to 76% for dyke water and 54% to 69% for Pond water during a 3 year study. TEH removal to the sediments accounted for less than 30% of the TEH load retained by the wetlands suggesting that other removal mechanism like volatization, plant uptake and microbial mineralization may play an important role hydrocarbon removal.

Vegetation

Macrophyte production was not significantly lower in wetlands containing dyke water or process water compared to the control, indicating that some macrophytes thrive in oil sands wastewater (Bishay 1998). Similarly, Crowe et al. (2001) measured significantly higher apparent photosynthesis in cattail exposed to oil sands process water compared to those found in natural areas.

Crowe (1999) examined the physiological effects of oil sands process water on plant species and reported that the Trenches had the lower macrophyte biodiversity compared to off-site wetlands. Although a wetland receiving dyke seepage from tailings pond, Natural Wetland, was found to be as diverse as the reference wetlands. The lower biodiversity in the Trenches was attributed to macrophyte competition and/or exposure to CT effluent.

Hornung and Foote (2007) examined the survival and growth rates of cattail grown in buckets filled with different sediment combinations (CT over CT; Soil over soil; Soil over CT; Soil over sterilized sand) and placed in the Trenches filled with either fresh or oil sands process water. All treatments exhibited macrophyte production at different rates depending on water quality. Aboveground biomass was greater in trenches filled with process water than those filled with fresh water suggesting that process water is capable of supporting productive cattail. The significantly higher macrophyte growth was attributed to higher nutrient levels inherent in process water. Reduced photosynthesis was measured in cattail grown in process water combined with CT in the rooting zone inferring that a wetland constructed with a CT substrate and containing process water may exceed macrophyte growth tolerances.

PETROLEUM COKE AMENDMENTS IN TAILINGS-CONSTRUCTED WETLANDS

One reclamation strategy is examining petroleum coke (coke), a carbonaceous by-product of mining. In its raw state, bitumen is thick and

tar-like and contains many impurities (Baker 2007). Thus, bitumen is upgraded to isolate the lighter, more valuable, energy-rich fraction. Coke, which resembles a medium grade coal, is a by-product of the refinement of bitumen (Taplin and Devenny 1998). Capping tailings ponds with coke may serve to stabilize the clay-dominated tailings, making them trafficable. Ecological studies have examined the effect coke may have on the invertebrate and macrophyte community in tailings-constructed wetlands capped with coke (Squires 2005; Baker 2007; Puttaswamy and Liber 2008). The aquatic community was examined since organisms, such as aquatic invertebrates, may act to transfer contaminants from sediments to higher trophic levels (fish, waterfowl and predatory insects) (Smits et al. 2006; Baker 2007). Several laboratory studies have shown that coke derived from Athabasca oil sands bitumen may leach significant amounts of metals (Chung et al. 1996; Scott and Fedorak 2004; Squires 2005; Puttaswamy and Liber 2008).

Baker (2007) investigated the use of coke as a wetland substrate for the colonization of macrophytes and invertebrates. Treatment patches were 40-cm diameter x 10-cm deep holes excavated in wetland sediments and layered with either 8 cm of native sediments, sand, Syncrude coke or Suncor coke and capped with 2-cm of either peat of more of the material from the bottom layer. Water chemistry parameters, percent cover of macrophytes, macrophyte (root and shoot) biomass and invertebrate richness and abundance were measured in each treatment in July/August 2005. Sampling was also conducted in reference wetlands (Syncrude's Beaver Pond and U-Shaped Cell). Squires (2005) conducted a complementary laboratory study on both Syncrude and Suncor cokes, examining the ecotoxicological response of coke leachate to invertebrates and testing for the presence of organic and inorganic contaminants, under a variety of leaching conditions, including oxygenation, pH and freeze-thaw cycles.

Baker (2007) reported that small amendments of petroleum coke in oil sands constructed wetlands containing process water and tailings did not significantly affect the abundance or richness of invertebrates in wetlands that were constructed with process water and sediments compared to treatments without coke amendments. Coke did not lead to increased tissue metal concentration in the macroinvertebrate species measured (Baker 2007). Squires (2005) also quantified that PAH concentrations were non-detectable in coke leachates. However, Squires (2005) quantified that coke leached trace metals (copper, manganese, molybdenum and particularly, vanadium) at concentrations greater than was acceptable by the Canadian Water Quality Guidelines (CCME 1999). Similarly, Puttaswamy and Liber (2008) determined in a laboratory study that concentrations of vanadium and nickel in 100% coke leachate at pH 5.5 and 9.5 were well above the 7-d LC50 values of 550 µg/L and 3.8 µg/L, respectively, suggesting that nickel and/or vanadium may cause toxicity in oil sands coke leachate.

Although laboratory studies indicated that coke leachate contains metals at harmful concentrations (Squires 2005; Puttaswamy and Liber 2008), Baker (2008) indicated that coke did not significantly increase the concentration of trace metals in sediment pore water or associated biota (macrophytic algae *Chara vulgaris*, snail *Lymnaeidae*, invertebrate *Tanytarsus* (*Chironomidae*)) in field conditions at the scale studied. Similarly, Squires (2005) found no adverse effect of coke leachates on a midge larva (*Chironomus tentans*). A larger scale study involving the spreading of coke 1 m deep over an approximately 5000 m^2 area is in progress.

WETLAND FOOD WEB IN OIL SANDS-AFFECTED WETLANDS

A consortium of oil sands companies (Canadian Oil Sands Network for Research and Development (CONRAD): Suncor, Syncrude Canada Ltd., Albian Sands, Canadian Natural Resources Ltd., Petro-Canada, Total E & P Canada Ltd. and Imperial Oil Resources Limited) and university researchers (University of Alberta, Saskatchewan, Waterloo and Windsor) have formed an integrated, collaborative group to improve understanding of the effects of tailings and mine process waters on the biological makeup, successional processes and carbon dynamics of wetland communities. The project is also supported through a Collaborative Research and Development grant from the Natural Sciences and Engineering Research Council of Canada. This collaborative research initiative is

entitled, *Carbon flow, Food web dynamics & Reclamation strategies in Athabasca oil sands Wetlands* (CFRAW; Ciborowski et al. 2006). CFRAW proposes to document how tailings (CT and MFT) and process waters in constructed wetlands modify the maturation process leading to natural conditions in a fully reclaimed landscape. This section summarizes the current state of knowledge on reclaimed wetland food webs in the Athabasca region.

Tailings-constructed wetlands are small exporters of carbon dioxide (CO_2) and methane (CH_4). Total carbon emissions (CO_2 and CH_4) from the unvegetated sediments of 9 tailings-constructed and reference wetlands in the Athabasca region averaged 15.59 mg m^2 d^{-1} (Daly 2007). Similar emission rates were quantified by Gardner-Costa (2008). Diel changes in open-water dissolved oxygen concentration were measured to determine net community production (Wytrykush 2007 [ATW]. Although most study wetlands appear to be net heterotrophs during summer, oil-sands affected wetlands are currently not on a trajectory to becoming large net sources of green house gases (Daly 2007).

Daly (2007) used a concentration-weighted stable isotope mixing model to examine assimilation of carbon into the microbial community in oil sands-affected wetlands and determined that between 62 and 97% of carbon assimilated by the microbial community in tailings-constructed wetlands was derived from residual petroleum hydrocarbons. A complementary laboratory experiment used stable isotopes to examine naphthenic acid degradation and confirmed that oil sands derived hydrocarbons were incorporated into microbial biomass (Videla 2007). Evidence was found for the transfer of carbon and nitrogen assimilated by microbes into higher trophic-level organisms (small chironomids and *Daphnia*) (Daly 2007) indicating that microbial assimilation of residual hydrocarbons from tailings materials fuel the microbial component of the food web and potentially support higher trophic levels in tailings-constructed wetland food webs.

According to the Environmental Protection and Enhancement Act and the Department of Alberta Environment, oil sands mining companies are required to recreate a landscape that is similar to the pre-disturbance landscape. This means that reclaimed wetlands must be viable, productive and sustainable and capable of supporting higher trophic level organisms such as amphibians, fish and birds. Numerous studies have indicated that as tailings-constructed wetlands age, they become more suitable for aquatic organisms. For example, Leonhardt (2003) reported that young reclaimed wetlands (those 3-5 years old) containing tailings and/or process waters supported fewer families of aquatic invertebrates compared to natural wetlands of equivalent age, but that aquatic invertebrate richness had become equivalent after 7 years. This lag possibly represents the period of time needed for microbial activity to detoxify naphthenic acids and other materials enough to facilitate macrophyte establishment (Cooper 2002) and subsequent colonization by zoobenthos (L. Barr, M.Sc., University of Windsor, in prep). The average abundance of aquatic invertebrates, however, was not affected by the presence of mining materials (Leonhardt 2003). Community composition of oil sands-affected wetlands became increasingly similar to equally-aged reference wetlands. Convergence of community composition was expected by age 14-17 (Leaonhardt 2003). Current research is testing this prediction. Similarly, Baker (2007) measured a parallel increase in macrophyte biomass and invertebrate abundance on small plots placed in older constructed wetlands. Cooper (2004) suggested that as substrates age they become more suitable for plant growth. This in turn provides increased structural complexity and provision of attachment sites for invertebrates (M.Sc., University of Windsor, in prep). Pollet and Bendell-Young (2000) examined *Rana sylvatica* (Wood Frog) and *Bufo boreas* (Western Toad) tadpoles exposed to oil sands process-affected waters and demonstrated delayed metamorphosis, decreased survival and significantly reduced rates of growth when tadpoles were held in process waters compared to reference waters. Similarly, Hersikorn (2007) reported that *Rana sylvatica* (Wood Frog) metamorphosis was significantly delayed and tadpole survival was significantly lower in young oil sands-constructed wetlands compared to older oil-sands constructed wetlands. Hersikorn and Smits (2008) indicated that wetlands constructed from tailings material may support populations of amphibians if the wetlands are allowed to age long enough.

The secondary production of insects living in wetlands can be exported as emergent adults

(Ganshorn 2002; Thoms et al. 2008) which are an important food source for local insectivores, like tree swallows (*Tachycineta bicolor*) (Smits et al., 2005; Gentes et al., 2006; Keshwani et al., 2007). Ganshorn (2002) quantified the bioaccumulation potential of Polycyclic Aromatic Hydrocarbons (PAHs) in such insects, predatory benthic dipterans, and determined that the bioaccumulation potential in reclaimed wetlands is low. Ganshorn (2003) also found that biomass and secondary production of chironomids in two oil sands-affected wetlands was greater than secondary production in two reference wetlands suggesting that from a productivity standpoint tailings-constructed wetlands are a suitable reclamation strategy.

Research has assessed the health of tree swallows nesting on reclaimed wetlands (Gentes 2006; Gentes et al., 2006; Gentes et al., 2007; Keshwani et al., 2007; Harms and Smits 2008; Thoms et al., 2008) since these upper trophic level organisms may provide a highly visible measure of reclamation success and ecosystem health (Harms and Smits 2008). Gentes et al., (2007) examined the endocrine disrupting potential of chemicals in wetlands containing process water and/or tailings by quantifying thyroid hormone concentrations in plasma and thyroid glands of nestling tree swallows. Thyroid hormones (plasma triiodothyronine and thyroxine) within thyroid glands were elevated in nestlings from oil sands affected sites compared to those from the reference site. Such changes in thyroid function may have negative effects on metabolism, behaviour, feather development, and molt, which could decrease postfledging survival (Gentes et al. 2007). Gentes et al., (2006) indicated that harsh weather conditions in 2003 caused a widespread tree swallow nestling die-off where mortality rate at a reference wetland was 48% while rates ranged between 59% and 100% at reclaimed wetlands. The greater mortality rates in reclaimed wetlands were attributed to nestlings at oil sands-affected wetlands being less able to withstand additional stresses, such as cold, wet weather, compared to the birds of natural wetland systems, which could lower the chances of survival after fledging. In contrast, Harms and Smits (2008) examined health indicators in tree swallows nesting on experimental wetlands in the oil sands region and found no negative effects on immune function in tree swallows nesting around wetlands containing process water and/or tailings. Furthermore, average tree swallow nestling weights were greater on Suncor's Natural Wetland, a wetland which receives daily fluxes of tailings pond water via dyke seepage, compared to a reference wetland suggesting abundant food resources were available to support the avian population (Harms & Smits 2008). Gentes (2006) reported that tree swallow nestlings did not exhibit symptoms of toxicity after receiving 0.1 ml/day of NAs orally for five days, suggesting that NA exposure does not appear to a great concern for some avian species reared on oil sands reclaimed sites. Research to date indicates that tree swallow populations may be a viable in reclaimed wetland ecosystems.

SUMMARY

Overall, research at Suncor has indicated that oil-sands constructed wetlands support tolerant emergent macrophytes (i.e. *Typha latifolia*) that are both production and viable. Capping CT sediments with peat-mineral amendments can increase plant diversity in these wetlands.

Reclaimed wetlands are capable of treatment and removal of hydrocarbons and excess phosphorus and ammonia in process water to concentrations below CCME water quality guidelines with a 30-day residence period. The same period markedly reduced concentrations of many metals (Cu, Fe, Ni and As) in process water, often below CCME guidelines. The 30-day residence time was not sufficient for lowering Mo concentrations to a satisfactory level. Degradation of naphthenic acids and associated toxicity reduction are achievable given a sufficient residence time (> 5months).

Laboratory studies indicate that some metals leach from petroleum coke and have the potential to cause toxicity to invertebrates. However, research in the field indicates that coke layers placed in small plots in reclaimed wetlands did not increase metal concentrations in sediment pore water or associated biota, algae and invertebrates, possibly suggesting that coke amendments can be used to stabilize tailings while not negatively influencing the aquatic community that inhabit that environment. Although a larger scale petroleum coke study in progress at a Suncor CT-constructed wetland will provide more evidence on the effects petroleum coke has on the aquatic community in the field.

Tailings and/or process water-constructed wetlands are capable of supporting a productive invertebrate community that is somewhat less diverse than reference wetlands. Tailings and/or process water-affected wetlands become more suitable for aquatic organisms (macrophytes, invertebrates, amphibians) with age. Upper trophic level organisms, like tree swallow nestlings, which feed on insects emerging from wetlands containing tailings and process waters, do not appear to have impaired immune systems, except perhaps during harsh climatic conditions. Tree swallow nestlings also appear to have abundant food resources from reclaimed wetlands based on their large biomasses compared to nestlings in reference wetlands. Reclaimed wetlands appear to be on a trajectory to becoming a viable, sustainable and productive reclamation option.

REFERENCES

Baker, L., 2007. The effects of petroleum coke amendments on macrophytes and aquatic invertebrates in northern Alberta, Canada constructed wetlands. University of Windsor M.Sc. thesis, Windsor, Ontario.

Barr, L., 2008. The relationship between sediment type and benthic macroinvertebrates mediated through aquatic macrophyte development: experimental sediment exchanges between natural and constructed wetlands on oil sands leases, near Fort McMurray, Alberta. M.Sc. Thesis. University of Windsor. Windsor, Ontario. In prep.

Biryukova, O.V., Fedorak, P.M., S.A. Quideau, 2007. Biodegradation of naphthenic acids by rhizosphere microorganisms. Chemosphere 67 (10), 2058-2064.

Bishay, F.S. 1998. The use of constructed wetlands to treat oil sands wastewater. M.Sc. Thesis, University of Alberta, Edmonton, Alberta.

Bishay, F.S., and Nix, P.G. 1996. Constructed wetlands for the treatment of oil sands wastewater. Tech. Rep. No. 5 (prepared for Suncor Inc. Oil Sands Group), EVS Environmental Consultants, North Vancouver, B.C.

Chung, K., L. Janke, R. Dureau, and E. Fumisky. (1996). Leachability of cokes from Syncrude stockpiles. Environmental Science & Engineering March: 50-53.

Ciborowksi, J.J.H., D.G. Dixon, L.N. Foote, K. Liber and J.E.G. Smits, 2006. Carbon dynamics, food web structure and reclamation strategies in Athabasca oil sands wetlands. Proc. 33rd Annual Aquatic Toxicity Workshop, Jasper, AB, 2006.

Cooper, N, 2004. Vegetation Community Development of Reclaimed Oil Sands Wetlands. M.Sc. Thesis, University of Alberta. Edmonton, Alberta.

Crowe, A.C, 1999. Physiological effects of oil sands effluent on selected aquatic and terrestrial plant species. Simon Fraser University, Nova Scotia.

Crowe, A.U., Han, B., Kermode, A.R., Bendell-Young, L.I. and A.L. Plant, 2001. Effects of oil sands effluent on cattail and clover: photosynthesis and the level of stress proteins. Environmental Pollution 113(3), 311-322.

Canadian Council of Ministers of the Environment, 1999. Canadian water quality guidelines for the protection of aquatic life: Introduction. In: Canadian environmental quality guidelines, 1999, Canadian Council of Ministers of the Environment, Winnipeg.

Daly, C.A. 2007. Carbon sources, microbial community production, and respiration in constructed wetlands of the Alberta, Canada Oil Sands Mining Area. M.Sc. Thesis. University of Windsor, Windsor, Ontario.

Fedorak, P. M., Coy D.L., M.J. Dudas, M.J. Simpson, A.J. Renneberg, and M.D. MacKinnon, 2003. Microbially-mediated fugitive gas production from oil sands tailings and increased tailings densification rates. Journal of Environmental Engineering Science 2(199-211).

Fedorak, P. M., and D. L. Coy. (2006). Oil sands cokes affect microbial activities. Fuel 85(12-13): 1642-1651.

FTFC (Fine Tailings Fundamental Consortium), 1995. Advances in oil sands tailings research, Alberta Department of Energy, Oil Sands and Research Division, Publisher.

Ganshorn, K.D., 2002. Secondary production, trophic position and potential for accumulation of

polycyclic aromatic hydrocarbons in predatory diptera in four wetlands of the Athabasca oil sands, Alberta, Canada. M.Sc. Thesis. Department of Biological Sciences. Windsor, ON. University of Windsor.

Gardiner-Costa, J. (2008). Spatial and stress-related variation in benthic microbial respiration in northeastern Alberta wetlands. Presented at the Proceedings of the 33rd Annual Aquatic Toxicity Workshop, Saskatoon, Saskatchewan, October 5-8.

Gentes, M.L., 2006. Health assessment of Tree Swallows (*Tachycineta bicolor*) Nesting on the Athabasca Oil Sands, Alberta. M.Sc. thesis. University of Saskatchewan, Saskatoon, Saskatchewan.

Gentes, M.L., Walder, C., Papp, Z., and J.E.G. Smits, 2006. Effects of oil sands tailings compounds and harsh weather on mortality rates, growth and detoxification efforts in nestling tree swallows (*Tachycineta bicolor*). Environmental Pollution 142 (1), 24-33.

Gentes, M.L., McNabb, A., Walder, C., and J.E.G. Smits, 2007. Increased Thyroid Hormone Levels in Tree Swallows (*Tachycineta bicolor*) on Reclaimed Wetlands of the Athabasca Oil Sands. Archives of Environmental Contamination and Toxicology 53 (2), 287-292.

Golder Associates Ltd., 1997. Synthesis of Environmental Information on Consoldiated/Composite Tailings. Prepared for Suncor Energy Inc. Oil Sands. Report 972-2205-6045.

Golder Associates Ltd., 2005. Consolidated Tailings (CT) Integrated Reclamation Landscape Demonstration Project: Technical Report #5 – Year 2004. Prepared for Suncor Energy Inc. Oil Sands. Report 04-1329-013.

Golder Associates Ltd., 2007. Consolidated Tailings (CT) Integrated Reclamation Landscape Demonstration Project: Technical Report #8 – Year 2007. Prepared for Suncor Energy Inc. Oil Sands. Report 07-1329-0024.

Harms, N.J. and J.E. Smits, 2008. Health assessment of tree swallows (*Tachycineta bicolor*) on the oil sands using stress, immune function and growth indicators. Presented at the Proceedings of the 33rd Annual Aquatic Toxicity Workshop, Saskatoon, Saskatchewan, October 5-8.

Hersikorn, B., 2007. Amphibian survival and development in wetlands containing oil sands process-affected material (OSPM). Proceedings from the CONRAD Environmental Reclamation Research Group Symposium, Edmonton, Alberta.

Hersikorn, B. and J.E. Smits, 2008. In-situ caging of wood frog (*Rana sylvatica*) larvae in wetlands formed from oil sands tailings materials (OSPM). Proceedings of the 33rd Annual Aquatic Toxicity Workshop, Saskatoon, Saskatchewan, October 5-8.

Hook, D. D. (1993). Wetlands - History, Current Status, and Future. Environmental Toxicology and Chemistry 12(12): 2157-2166.

Hornung, J. and L. Foote, 2007. Oil Sands as primary succession substrates and the importance of early carbon production on site. The 34th Annual Aquatic Toxicity Workshop, Halifax, Nova Scotia.

Holowenko, F.M., Mackinnon, M.D. and P.M. Fedorak 2002. Characterization of naphthenic acids in oil sands wastewaters by gas chromatography – mass spectrometry. Water Res. 36, 2843-2855.

Hunter, R.G. and S.P. Faulkner, 2001. Denitrification Potentials in Restored and Natural Bottomland Hardwood Wetlands. Soil Science Society of America Journal 65, 1865 – 1872.

Kavanaugh, R.J., 2008. Oil sands constituents and their effects on the reproductive physiology of fathead minnows (Pimephaeles Promelas). Proceedings from the CONRAD Environmental Reclamation Research Group Symposium, Edmonton, Alberta.

Kennedy, M.P. and K.J. Murphy, 2004. Indicators of nitrate in wetland surface and soil-waters: interactions of vegetation and environmental factors. Hydrology and Earth System Sciences 8 (4), 663-672.

Keshwani, H., Hersikorn, B and J.E. Smits 2007. Reproductive performance and neonatal development of tree swallows (*Tachycineta bicolor*) on reclaimed mien sites on the

Athabasca oil sands. Proc. 34th Annual Aquatic Toxicity Workshop, Halifax, Nova Scotia.

Lai, J., Pinto, LJ, and E Kiehlmann, 1996. Factors that affect the degradation of naphthenic acids in oil sands wastewater by indigenous microbial communities. Environmental Toxicology and Chemistry 15(9): 1482-1491.

Leonhardt, C.L., 2003. Zoobenthic succession in constructed wetlands of the Fort McMurray Oil Sands region: Developing a measure of zoobenthic recovery. M.Sc. Thesis. Department of Biological Sciences. Windsor, ON. University of Windsor.

Mackinnon, M. and H. Boerger, 1986. Description of two treatment methods for detoxifying oil sands tailings pond water. Water Pollut. Res. J. Can. 21, 496-512.

Nix, P.G., Hamilton, S.H. Bauer, E.D., and C.P. Gunter, 1993. Constructed wetlands for the treatment of oil sands wastewater. Tech. Rep. No. 2, Alberta Oil Sands Technology and Research Authority, Fort McMurray, Alta.

Pollet, I. and L.I. Bendell-Young, 2000. Amphibians as indicators of wetland quality in wetlands from oil sands effluent. Environmental toxicology and chemistry 19 (10), 2589-2597.

Puttaswamy, N., and K. Liber, (2008). Metal leaching from oil sands coke and associated characterization of leachate toxicity. Presented at the Proceedings of the 33rd Annual Aquatic Toxicity Workshop, Saskatoon, Saskatchewan, October 5-8.

Quagraine, E., Peterson, HG, and JV Headley, 2005. In Situ Bioremediation of Naphthenic Acids Contaminated Tailing Pond Waters in the Athabasca Oil Sands Region—Demonstrated Field Studies and Plausible Options: A Review. Journal of environmental science and health, part a, 40 (3), 685-722.

Scott, A. C., and P. M. Fedorak. (2004). Petroleum Coking: A Review of Coking Processes and the Characteristics, Stability and Environmental Aspects of Coke Produced by the Oil Sands Companies: Department of Biological Sciences, University of Alberta.

Squires, A. J. (2005). Ecotoxicological Assessment of Using Coke in Aquatic Reclamation Strategies at the Alberta Oil Sands. Master's Thesis, University of Saskatchewan, Saskatoon, Saskatchewan.

Smits, J.E.G, Bortolotti, G.R., Sebastian, M. and J.J.H. Ciborowski, 2005. Spatial, temporal, and dietary determinants of organic contaminants in nestling tree swallows in Point Pelee National Park, Ontario, Canada. Environmental Toxicology and Chemistry 24(12), 3159-3165.

Suncor, 1998. Suncor Project Millenium Application. Volume 2B.

Suncor, 2003. Application for the Suncor Energy Inc. South Tailings Pond Project. Volume 3.

Suncor, 2005. Voyageur Project: North Steepbank extension project application. Volume 5.

Suncor, 2006a. A summary of Suncor Energy's operations and strategies.

Suncor, 2006b. Big plans big ideas.

Taplin, D., and D. W. Devenny. (1998). Chemical and physical characterization of Syncrude's stockpiled coke. Komex International Limited, Calgary, AB, Report # KI-4668.

Thoms, J.L., Martin, J.P., Harms, N.J., Smits, J.E. and J.J. Ciborowski, 2008. Relating zoobenthic & emergent terrestrial insect production to tree swallow (*Tachycineta bicolor*) nestling diet in oil sands wetlands. Proceedings of the 33rd Annual Aquatic Toxicity Workshop, Saskatoon, Saskatchewan, October 5-8.

Toor, N, 2008. The degradation and aquatic toxicity of naphthenic acids present in Athabasca oil sands affected waters. Proceedings from the CONRAD Environmental Reclamation Research Group Symposium, Edmonton, Alberta.

Toor, N., Liber, K., MacKinnon, M. and P. Fedorak, 2007. Exploring the biodegradation and toxicity of naphthenic acids present in Athabasca oil sands process-affected waters using simulated wetlands. Proc. 34th Annual Aquatic Toxicity Workshop, Halifax, Nova Scotia.

Videla, P.P., 2007. Examining oil sands dissolved carbon and microbial degradation using stable isotope analysis. M.Sc. Thesis. University of Waterloo, Waterloo, Ontario.

Wetzel, R.G. 2001. Limnology. Academic Press, New York. 1006 pp.

Wytrykush, C. and J.J.H. Ciborowski, 2007. Spatial and temporal variability of net ecosystem production in Alberta oil sands wetlands. Proceedings of the 32nd Annual Aquatic Toxicity Workshop, Halifax, Nova Scotia, September 30 to October 3.

INVESTIGATING BIOLOGICAL METHANE PRODUCTION AND ITS IMPACT ON DENSIFICATION OF OIL SANDS TAILINGS

Carmen Li, Tariq Siddique, Julia Foght
University of Alberta, Edmonton, Alberta, Canada

ABSTRACT

Bitumen extraction from oil sands ores requires water that subsequently represents a significant proportion of oil sands tailings discharged to settling basins. To meet the demand for process water and reduce the total volume of tailings, recovered water from the settling basins is re-used. Densification of tailings, which is a slow process, maximizes recovery of water and compacts the tailings for inventory management. Methane production (methanogenesis), which is a biological activity accomplished by a consortium of anaerobic microbes, accelerates densification of mature fine tailings (MFT). At least two oil sands extraction operators have observed methane emissions from their tailings basins. Growth-based enumeration of microbes naturally present in MFT samples has revealed all three expected metabolic types of anaerobes (fermentative bacteria, sulfate-reducing bacteria, and methanogens) associated with methane production. However, growth-based studies can be biased towards detecting species that are readily cultivated in the laboratory while missing important species that are difficult to grow, whereas cultivation-independent (DNA-based) molecular biological methods have the potential to reveal additional microbial diversity. Two DNA-based methods currently being applied to MFT analysis, ARDRA and DGGE, are described here, with discussion of their advantages and problems. Such analyses will enable fuller understanding of the role of microbes in methanogenesis and subsequent oil sands tailings management.

INTRODUCTION

The generation of methane from oil sands tailings basins is an environmental concern; however, this phenomenon may also be beneficial for tailings management in the oil sands industry. Methane production in mature fine tailings (MFT) from Syncrude Canada Ltd. accelerates the rate of tailings densification and water release (Fedorak et al. 2003). A better understanding of methanogenesis in tailings will potentially offer options for tailings storage, water recovery, land reclamation of tailings basins, and control of methane production.

Microbiological research on oil sands tailings increased after Syncrude's main tailings basin, Mildred Lake Settling Basin (MLSB) began to release methane over two decades ago. Foght et al. (1985) revealed that MLSB tailings are microbially active and responsible for methane production *in situ* (Holowenko et al. 2000). The substrates supporting methanogenesis in MLSB tailings have now been determined to be hydrocarbon components of Syncrude's naphtha diluent, particularly short chain *n*-alkanes and BTEX compounds (benzene, toluene, ethyl-benzene, and xylene isomers). Siddique et al. (2006; 2007) demonstrated the degradation of these naphtha components with concurrent production of methane when naphtha diluent was incubated with MFT from MLSB.

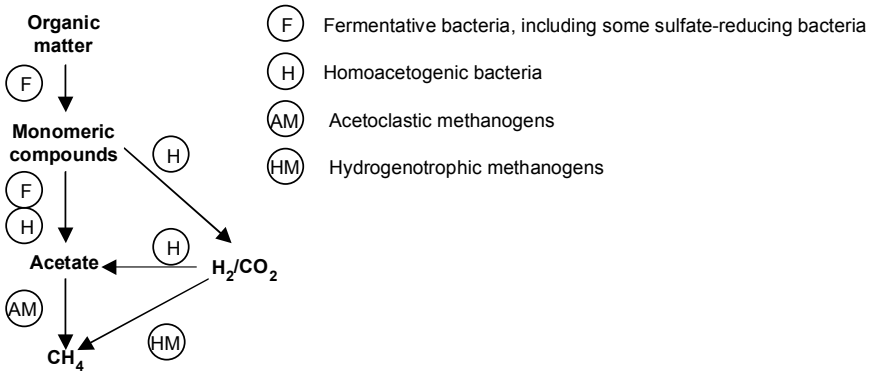

Figure 1. Simplified scheme for anaerobic biodegradation of complex organic compounds to methane.

Complex interactions between several different groups of microbes are required for the anaerobic breakdown of hydrocarbons into methane (Figure 1). The microbes involved are from two kingdoms, Bacteria and Archaea. Within the Bacteria, three main metabolic groups are responsible for the degradation of complex organic matter into simple substrates that the Archaeal methanogens require to produce methane. The first Bacterial metabolic group includes sulfate- and nitrate-reducing bacteria. They are the initial attackers; because hydrocarbon compounds are relatively stable under anaerobic conditions, these microbes are required to activate the hydrocarbons for further degradation through several enzymatic mechanisms (Callaghan et al. 2006; Elshahed et al. 2001). Following activation, the hydrocarbon is degraded into intermediate or monomeric compounds by fermentative bacteria, including some sulfate-reducing bacteria. The last group of bacteria, the acetogens, degrades the intermediate compounds further into simple substrates, such as acetate, propionate or hydrogen and carbon dioxide. Two different types of methanogens, acetoclastic and hydrogeno-trophic, then produce methane from either acetate or hydrogen and carbon dioxide (H_2+CO_2) gases, respectively. It is assumed that this general scheme of biodegradation also occurs in MFT, but the specific substrates supporting methanogenesis and the microbial species comprising the complex consortia have been the unknown factors.

Cultivation-based enumeration of microbes

When research on the microbial communities present in MFT began in the 1980's, there were few analytical techniques available for the study of microbial populations in environmental samples and none of these had been used for analysis of microbes in oil sands tailings. Plate counts, commonly used to enumerate aerobic microbes (in food samples, for example) are inappropriate and inaccurate for most anaerobic communities. One commonly used method suitable for enumerating anaerobes is the most probable number (MPN) technique. This is a cultivation-based technique that uses statistical analysis of samples diluted to extinction to estimate the numbers of different microbial metabolic groups in a sample. Its advantages include relative simplicity in execution and analysis, and broad applicability to anaerobic consortia. The MPN method was the first to be applied to study oil sands tailings. It detected all three microbial metabolic groups known to be required for the breakdown of hydrocarbons, namely fermenters, sulfate-reducing bacteria, and methanogens (Figure 1) in MFT from MLSB (Foght et al. 1985; Holowenko 2000).

The drawback to MPN analysis is that it estimates only the numbers of cultivable metabolic types, but cannot identify the species of each particular microbe within those metabolic groups. Although enumerating the groups is useful for indicating the overall potential metabolic capabilities of a microbial community, the information gleaned from this type of analysis is very broad. In theory, individual species could be isolated from the MPN tubes after enumeration, but this is very slow and tedious for anaerobic organisms, and additionally it suffers from the biases described below. Knowledge of the actual species present in MFT would offer a better understanding of how substrates such as naphtha hydrocarbons could be biodegraded into methane, and what specific factors might control the microbes' activity.

A second disadvantage of cultivation-based microbial analysis is that it requires prior knowledge of the organisms in order to provide suitable conditions for their growth in the assay. However, the preferred growth conditions for species, whether identified or not, are often unknown, or lab conditions are inadequate to supply them (Amann et al. 1995). The *in situ* environment of a microbial consortium provides very specific conditions including temperature, salinity, pH, growth substrates, availability of electron acceptors, electron sources and electron acceptors, etc. A change in any one of these conditions could either prevent or augment the growth of certain species, resulting in a biased analysis. Cultivation of microbes in oil sands MFT samples is particularly difficult because the chemical nature of tailings is not something we can replicate accurately in the lab, and without prior information about which microbial species may exist in tailings, cultivation of these microbial species would essentially be 'hit and miss'. In addition, isolation and cultivation of many anaerobes can be extremely slow because the cultures, particularly methanogens, can take weeks or months to grow.

Therefore, although the relative proportions of metabolic types in MFT can be determined by MPN methods, the identity of microbial species in MFT has remained unknown until recently when molecular methods were applied to MFT.

DNA-based identification of microbes: RFLP

Recent advances in biological techniques have focused on molecular (DNA) analysis of environmental samples. These techniques do not require cultivation of microbes from a given sample; instead, they use the total DNA from a microbial community to better predict the microbial activity within a sample. The potential advantages of forgoing cultivation include collection of more detailed results and faster analysis of slow-growing, fastidious anaerobes. One of these molecular techniques, called restriction fragment length polymorphism (RFLP) analysis (Figure 2), was used to analyze MLSB tailings (Penner 2006; Penner and Foght in preparation). The species of microbes in MLSB tailings were successfully revealed and a pathway for the degradation of naphtha hydrocarbons was proposed which involved the numerous Bacterial and Archaeal species identified.

RFLP analysis begins with extraction of DNA from all the members of the microbial community; in our laboratory, this is achieved by a physical lysis method in which a small sample (0.3mL of MFT) is shaken vigorously with tiny zirconium beads (0.1 mm and 2.3 mm diameter) in the presence of a buffer and a detergent in a dedicated 'Bead Beater' instrument. This breaks the cells open and releases their DNA, which is recovered and concentrated. The 16S rRNA gene, whose presence is common to all microbes but whose sequence is unique to each species, is amplified by the polymerase chain reaction (PCR) to generate a mixture of the amplified gene copies. To separate the individual copies for analysis, the amplified gene fragments are cloned into plasmid vectors that are inserted individually into host bacterial cells (*E. coli*) for maintenance. This is called a 'clone library', and in theory a large proportion of the clones will represent the dominant species in the original community and small proportions of clones will represent the minor components of the community.

There are two ways to analyze this clone library: the brute force method determines the sequence of amplified 16S rRNA gene in every clone in the library. This is extremely expensive, as a clone library typically consists of ≥100 clones and sometimes more. The second approach screens the clone library first, to determine how many clones are duplications of the dominant species, which only needs to be sequenced once rather than every time it occurs in the library. Screening is achieved by re-amplifying the cloned 16S rRNA gene and digesting it with 'restriction enzymes' that cleave at specific sequences to generate characteristic patterns of fragments separated by gel electrophoresis. Because each species' 16S rRNA gene sequence is unique, each digested gene will produce a characteristic 'fingerprint' of fragments. These patterns are grouped together using pattern recognition software (or visually) to form 'operational taxonomic units' (OTUs) that are almost equivalent to species but not yet identified. Representatives of each OTU can be sequenced, but in practice it is usually only the numerically dominant OTUs that are sequenced because they theoretically represent the most dominant species in the original sample. OTUs that occur only once in the library, termed 'singletons', often are not sequenced because they likely represent species that are infrequent and less important to the overall metabolic potential of the community.

The DNA sequences of the selected cloned 16S rRNA genes are compared to public databases like GenBank (http://www.ncbi. nlm.nih.gov/) or the Ribosomal Database Project (RDP; https://rdp. cme.msu.edu/) that contain millions of DNA sequences deposited by other scientists. Software found on the sites (e.g., BLASTn) compares the unknown sequence to the database using various algorithms and provides the 'best matches'. Ideally, the unknown sequence will closely match (>99%) that of a sequence obtained from a microbe previously isolated and characterized, so that the identity of the cloned sequence is quite robust at the species level and the metabolic capability of the microbe represented by the cloned sequence can be inferred with some certainty. Sometimes the match is lower (<97% identity), in which case the identity at the genus level and metabolic potential are less certain. Unfortunately, for environmental samples such as MFT, often the best match is another sequence that has been amplified from a community and has only a tenuous affiliation to a known isolate. In that case, we can only make general guesses as to the identity of the original organism and its possible metabolic activities *in situ*.

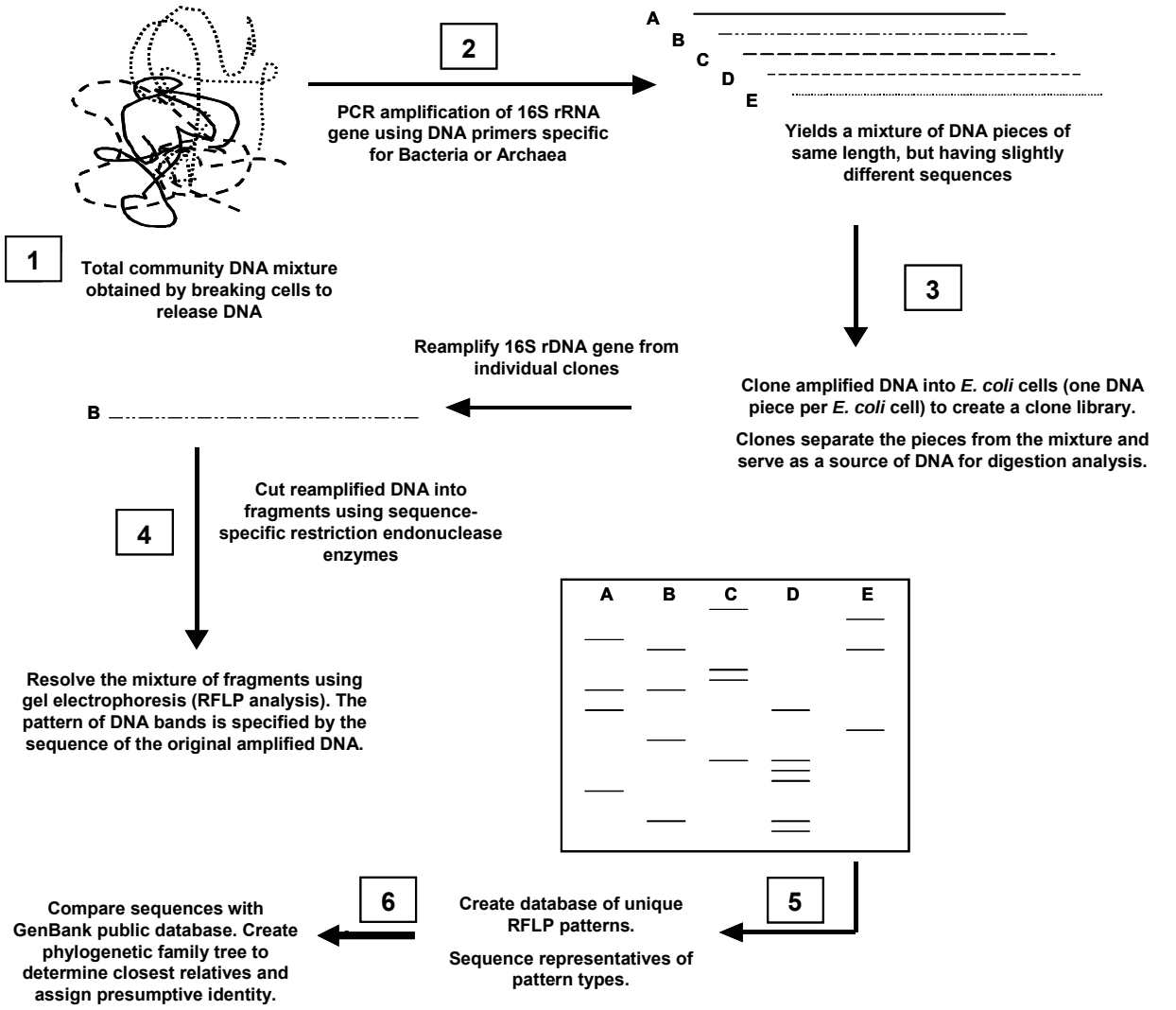

Figure 2. Schematic representation of clone library construction and RFLP analysis of microbial community composition in an MFT sample using 16S rRNA genes.

DNA-based identification of microbes: DGGE

Another cultivation-independent method used to analyze microbial diversity in environmental samples is Denaturing Gradient Gel Electrophoresis (DGGE; Figure 3). DGGE analysis involves several steps, some of which are shared with RFLP, described above: 1) isolate all microbial DNA from the sample as described above; 2) amplify the 16S rRNA genes from the DNA using PCR, but using special 'primer' sequences; 3) sort the amplified DNA into unique bands by separation on a gel prepared with a gradient of denaturant.; 4) determine the DNA sequence of each unique band; 5) compare the sequences to public databases to deduce the identity of the microbes from which the DNA was originally extracted.

DGGE begins with extracting the total genomic DNA from the microbial community of an MFT sample. Bacterial and Archaeal 16S rRNA genes are amplified by PCR using specially designed DNA primers that add nucleic acid 'tags' to the amplified DNA. These amplified PCR products are all of the same length and thus cannot be separated based on size. Instead the products are separated according to slight differences in their DNA sequences that influence their denaturing properties. Denaturing a DNA fragment refers to

separating the two DNA strands into single-stranded DNA pieces through chemical and/or heat treatment; the denaturing point of a DNA fragment (i.e., its "melting" temperature) depends on its sequence. Separation of amplified DNA

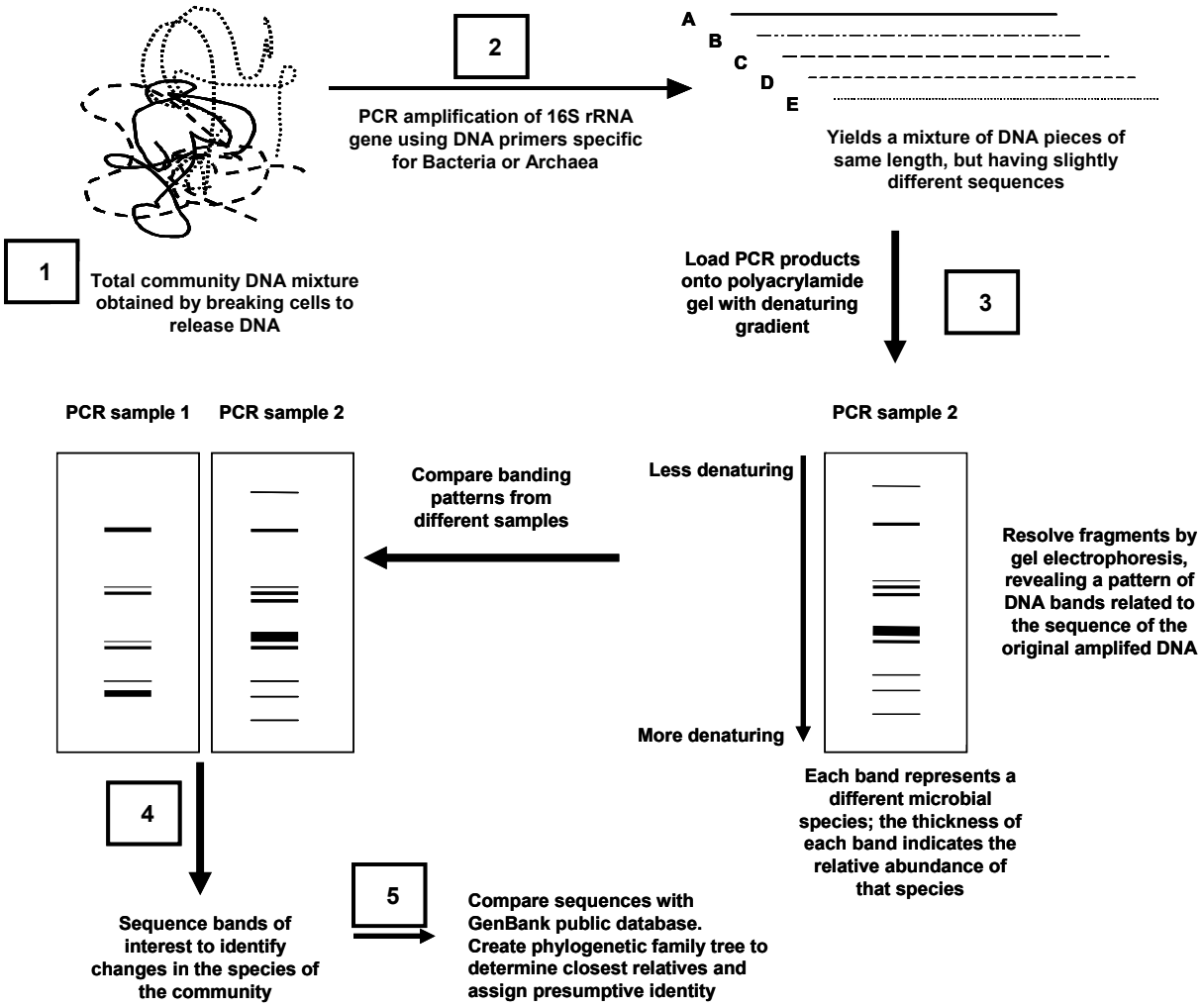

Figure 3. Schematic representation of DGGE analysis of microbial diversity in an MFT sample.

based on differing denaturing points is achieved by running the PCR products in a polyacrylamide electrophoresis gel prepared with a gradient of denaturing agent. DNA fragments stop migrating in the gel as they begin to denature. Hence unique 16S rRNA sequences will 'melt' and form discrete single bands at characteristic positions in the gel, each theoretically representing an OTU. Banding patterns between MFT samples can then be compared in order to highlight changes in predominant species or the presence or absence of particular species. Individual DGGE bands can also be excised and sequenced for presumptive identification of Bacterial and Archaeal species.

Potential problems with DNA-based analyses

DGGE analysis is rapid and efficient, which allows for information from numerous samples to be quickly gathered and compared. This is particularly convenient for the study of oil sands MFT since settling basins can be heterogeneous. Samples from different locations in a tailings basin, at different depths, or taken from different time points can vary from one another. Therefore, it is best to analyze several samples of tailings from within a single tailings basin to represent all the microbial species that exist *in situ*. DGGE analysis allows many samples to be analyzed and compared simultaneously (Figure 4). PCR, the basis of this

Figure 4. Example of a DGGE gel from MFT. Each gel lane represents a different sample and each band theoretically represents a different species of microbe.

method, can detect very small amounts of DNA which increases the likelihood that rare organisms will be detected, as opposed to cultivation techniques where many species may be missed. PCR also significantly reduces the volume of sample required for analysis (von Wintzingerode et al. 1997).

However, several of the steps in DGGE (and also RFLP) analysis of an environmental sample can bias the results, particularly for samples with low microbial biomass such as oil sands MFT. These include the efficiency of lysing all cells to release their DNA (some species are more difficult to lyse than others) and sorption of the DNA to mineral surfaces so that DNA concentrations are below minimum thresholds for efficient amplification. Also, the DNA of inactive cells (those in stasis or recently dead) can be extracted along with DNA from actively metabolizing cells, thus inappropriately influencing interpretation of results.

A caveat with any molecular technique that relies on PCR is whether amplification will occur and whether it will be biased. Chemicals such as humic acids in environmental samples are often coextracted with nucleic acids and inhibit subsequent amplification of template DNA (Tebbe and Vahjen 1993). There are also inherent problems in PCR amplification that can lead to an inaccurate representation of the actual microbial population *in situ*. For example, the DNA of certain microbial species can have a greater tendency to be amplified due to inherent chemical properties including low melting temperatures (Reysenbach et al. 1992). Other conditions of PCR amplification can heavily skew the amplification of different species' DNA, including: the primers used, primer annealing temperatures, and number of rounds of replication (Ishii and Fukui 2001; Suzuki and Giovannoni 1996). Furthermore, the amplification of contaminating DNA can also lead to erroneous results. It is important to keep these potential PCR amplification biases in mind when interpreting the results of a microbial community analysis.

It is acknowledged that the bacterial primers commonly used in DGGE analysis are not ideal for amplifying all 16S rRNA gene sequences in a sample; therefore, the intensity of bands in DGGE gels may not accurately represent the proportions of species in the original sample (Ishii and Fukui 2001). The resolution of DGGE analysis is also lower than other molecular techniques such as restriction fragment length polymorphism (RFLP) analysis due to the shorter DNA sequence that is amplified and sequenced in DGGE analysis: whereas RFLP analysis involves cloning the entire 16S rRNA gene in Bacteria and Archaea, about 1500 and 900 nucleotides respectively, DGGE amplifies a fragment of each gene that is only about 500 nucleotides long.

A significant concern in application of DGGE and RFLP analyses to microbial communities in oil sands MFT is that species that are present in low abundance may not be detected by either method. PCR amplification does not always detect rare DNA sequences, especially in complex material like MFT which contains many different microbes, some in copious quantities and others at very low amounts. In other words, if a rare species is present in a proportion of 0.1% of the total microbial diversity, its DNA is less likely to be detected by exponential PCR amplification than the DNA of another species present in a proportion of 10%. However, the assumption is that species playing an important role in degrading the methanogenic substrate will be present in quantities within the detectable limit of PCR.

Finally, even if community DNA is successfully extracted, amplified and sequenced, identification of the original organism can be limited by the public databases used to compare the gene sequences. GenBank is an enormous, global resource comprising millions of sequences, yet we routinely find that the best match to our MFT clone library or DGGE band sequence is another cloned sequence from an uncultivated, unidentified organism. In that case, we cannot with any certainty assign functions to the organisms we have detected.

CONCLUSIONS

Despite the numerous caveats that apply to DNA-based analysis of microbial communities, we are finding that these molecular methods add another dimension to investigation of microbial diversity in MFT not afforded by cultivation-based methods. By combining molecular analysis with cultivation-based enumeration techniques (MPNs) and incubation of MFT in microcosms followed by chemical analysis (Siddique et al., 2006; 2007), we are achieving a better understanding of the microbes present in MFT produced by different oil sands extraction operators and the roles that these organisms play in methanogenesis and MFT densification in the settling basins. As more organisms are identified and characterized to expand the gene sequence databases, the power of these techniques will only increase.

ACKNOWLEDGEMENTS

The authors gratefully acknowledge funding from Syncrude Canada Ltd., Canadian Natural Resources Ltd., Albian Sands Energy Inc., the Oil Sands Technology Research Facility (OSTRF) and NSERC for past and present support of this work.

REFERENCES

Amann, R., Ludwig, W., and Schleifer, K. 1995. Phylogenetic identification and in situ detection of individual microbial cells without cultivation. Microbiological reviews. 59: 143-169.

Callaghan, A.V., Gieg, L.M., Kropp, K.G., Suflita, J.M., and Young, L.Y. 2006. Comparison of mechanisms of alkane metabolism under sulfate-reducing conditions among two bacterial isolates and a bacterial consortium. Applied and Environmental Microbiology 72: 4274-4282.

Elshahed, M.S., Gieg, L.M., McInerney, M.J., and Suflita J.M. 2001 Signature metabolites attesting to the in situ attenuation of alkylbenzenes in anaerobic environments. Environmental Science & Technology. 35:682-689

Fedorak, P.M., Coy, D.L., Dudas, M.J., Simpson, M.J., Renneberg, A.J., and Mackinnon, M.D. 2003. Microbially-mediated fugitive gas production from oil sands tailings and increased tailings densification rates. Journal of Environmental and Engineering Science 2: 199-211.

Foght, J.M., Fedorak, P.M., Westlake D.W.S. and Boerger H.J. 1985. Microbial content and metabolic activities in the Syncrude tailings pond. AOSTRA Journal of Research 1:139-146.

Holowenko, F.M. MacKinnon, M.D., and Fedorak, P.M. 2000. Methanogens and sulfate-reducing bacteria in oil sands fine tailings waste. Canadian Journal of Microbiology 46: 927-937.

Ishii, K., and Fukui, M. 2001. Optimization of annealing temperature to reduce bias caused by a primer mismatch in multitemplate PCR. Applied and Environmental Microbiology 67: 3753-3755.

Penner, T. 2006. Molecular analysis of microbial populations in oil sands tailings. MSc. thesis, University of Alberta.

Reysenbach, A.L., Giver, L.J., Wickham, G.S., and Pace, N.R. 1992. Differential amplification of rRNA genes by polymerase chain reaction. Applied and Enviromental Microbiology 58: 3417-3418.

Siddique, T., Fedorak, P.M., and Foght, J.M. 2006. Biodegradation of short-chain n-alkanes in oil sands tailings under methanogenic conditions. Environmental Science & Technology 40: 5459-5464.

Siddique, T., Fedorak, P.M., Mackinnon, D., and Foght, J.M. 2007. Metabolism of BTEX and naphtha compounds to methane in oil sands tailings. Environmental Science & Technology 41: 2350-2356.

Suzuki, M., and Giovannoni, S. 1996. Bias caused by template annealing in the amplification of mixtures of 16S rRNA genes by PCR. Applied and Environmental Microbiology 62: 625-630.

Tebbe, C.C., and Vahjen, W. 1993. Interference of humic acids and DNA extracted directly from soil in detection and transformation of recombinant DNA from bacteria and a yeast. Applied and Environmental Microbiology 59: 2657-2665.

von Wintzingerode, F., Gobel, U.B., and Stackebrandt, E. 1997. Determination of microbial diversity in environmental samples: pitfalls of PCR-based rRNA analysis. FEMS Microbiology Reviews 21: 213-229.

THE INFLUENCE OF DE-COUPLING SOIL-ATMOSPHERE INTERACTION AND THE PHREATIC SURFACE WITHIN TAILINGS STORAGE FACILITIES ON RECLAMATION PERFORMANCE

Robert Shurniak[1], Mike O'Kane[1], Bonnie Dobchuk[1] and Lee Barbour[2]
1. O'Kane Consultants Inc.
2. Department of Civil and Geological Engineering, University of Saskatchewan

ABSTRACT

Oil sands tailings pore-water is typically characterized by relatively high concentrations of dissolved salts. In general, reclamation of tailings storage facilities in the oil sands involves placement of cover material to such a depth as to provide sufficient moisture holding capacity for climax vegetation communities. However, if the salts within tailings pore-water were to migrate into the cover material the potential exists for these salts to compromise both vegetation performance and soil structure.

This pore-water can enter the rooting zone as a result of inundation from a rising water table or through the advective (and possibly diffusive) transport of salts from underlying sand tailings, particularly if the water table is in close proximity to the cover material / tailings interface. Hence, the location of the water table within the tailings can have a profound impact on reclamation performance.

In general, water fluxes through the unsaturated sand tailings beneath the cover will be coupled to atmospheric demands (e.g. evapotranspiration) when the water table is close to the surface. Hence, during dry climate periods the potential exists for demand on moisture from the cover profile to be satisfied by "drawing" water from the tailings and water table. However, when the water table is below a certain depth no moisture is drawn up from the water table and consequently the moisture dynamics within the cover can be assumed to be 'de-coupled' from the water table. The depth of water table at which this occurs is dependent on a number of variables, such as the material properties of the tailings and cover material, topography, and climate.

This paper will illustrate the factors influencing the depth at which the phreatic surface de-couples from the cover moisture dynamics, and provides a methodology for determining the depth at which de-coupling will occur. A case study will be presented illustrating the methodology for determining the de-coupling depth, using analytical and numerical modelling techniques.

INTRODUCTION

A primary purpose of a reclamation cover system is to provide a suitable growth medium for proper vegetation development. When this function is properly developed it can also aid in the performance of a cover system by stabilizing the soil structure, but it can also limit the amount of water entering the underlying waste material. However, vegetative moisture demands can draw water from the underlying waste during dry climate periods. If the underlying water is "clean" (i.e. devoid of pore-water constituents detrimental to cover performance and vegetation development) then the net upward flux of water from the waste into the cover system is not of concern. Unfortunately, this is generally not the case for mine tailings.

The focus of this paper is sand tailings associated with the extraction of bitumen obtained from oil sands mining. These tailings typically contain elevated levels of sodium, chloride, sulphate and bicarbonate (Renault et al., 1999). As cited by Howat (2000), Marschner (1986) reported that, in general, plant growth becomes affected by the presence of sodium and/or salts when the sodium adsorption ratio (SAR, which describes a relationship between the relative amount of sodium ions in solution to the ratio of calcium and magnesium ions) and electrical conductivity (EC) levels exceed critical values of 15 and 4 dS/m, respectively. The soil can also become alkaline (pH 8 to 10) when sodium, magnesium and calcium combine with sulphates and carbonates, which can inhibit plant growth (Howat, 2000).

To minimize the movement of salt from tailings into the overlying cover system requires that the upward fluxes generated by atmospheric forces are de-coupled (i.e. not supplied) from the phreatic

surface. This paper provides a methodology for determining the de-coupling depth and illustrates the factors controlling this depth. The paper concludes with a case study which illustrates the methodology.

ANALYTICAL METHOD

The depth that the water table de-couples from the atmosphere is controlled mainly by the material properties of the overlying soils and the magnitude of the upward flux rate. Barbour (1990) illustrated how the suction and water content profile through a deep profile of unsaturated soil under a steady state percolation rate could be predicted using a method originally proposed by Kisch (1959). In this method Darcy's Law is applied to small increments of elevation starting at the known elevation of the water table. The water content and hydraulic conductivity for each increment of elevation is updated based on the known moisture retention curve (MRC) and hydraulic conductivity function (k-function) for the material of interest.

This same method can be used for the simplified assumption of steady state upward flow or exfiltration to determine the maximum water table depth that will still sustain a given upward flux rate.

As an example, the MRCs and k-functions for two tailings materials are presented in Figures 1 and 2, respectively. The "case study" tailings are representative of the tailings discussed in the next section of this paper, whereas the "fine" tailings are representative of tailings with a finer texture than the case study tailings. The k-functions were estimated from the MRCs using the van Genuchten (1980) method.

Using the method original proposed by Kisch (1959) the pressure profile above a water table under an upward flux rate of 0.01 mm/day can be developed (Figure 3). It is interesting to note how a limiting height above the water table is reached at which suction continues to increase without a significant advance in the elevation of the profile. This height provides an upper bound to the depth from which water can be drawn to the surface from an underlying water table.

Figure 4 shows that the case study and fine tailings can only sustain small steady state flux rates (i.e. less than 0.01 mm) and, therefore, are essentially fully de-coupled at depths of 1.5 m and 3.0 m, respectively.

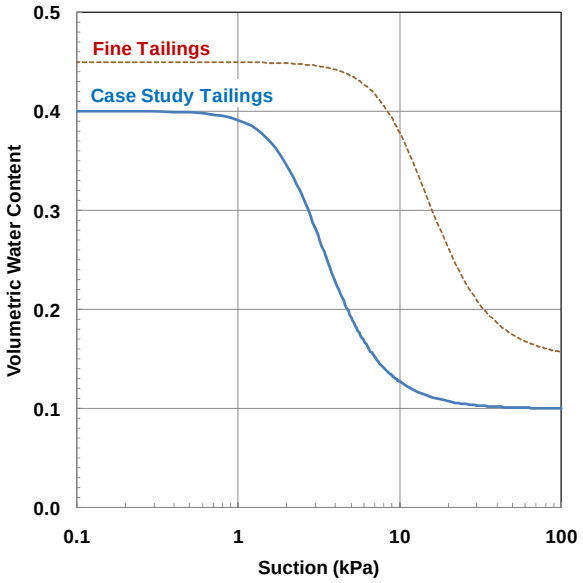

Figure 1 Moisture retention curves for example tailings.

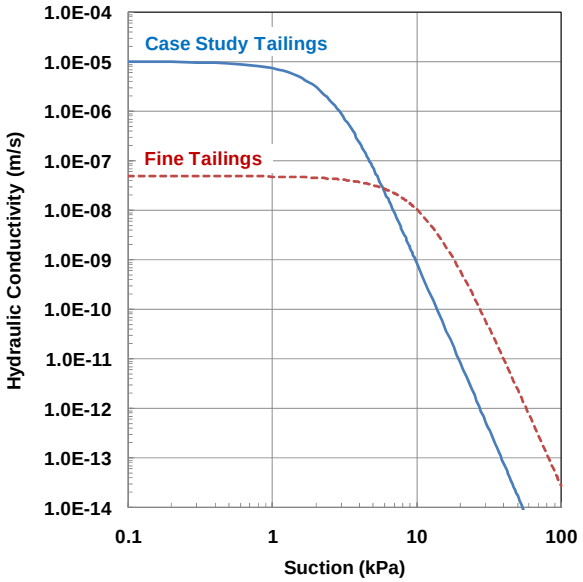

Figure 2 Hydraulic conductivity functions for example tailings.

This interpretation of 'de-coupling' depth is based on the somewhat unrealistic situation of sustained steady state, upward flux. It is likely more realistic to consider the variability in fluxes across the vadose zone above the water table due to variability in atmospheric and vegetative demands. The depth of 'de-coupling' in this case would be the depth below which there is not a cumulative annual net flux of water upwards across the water table. This type of analyses is presented in the form of a case history in the next section.

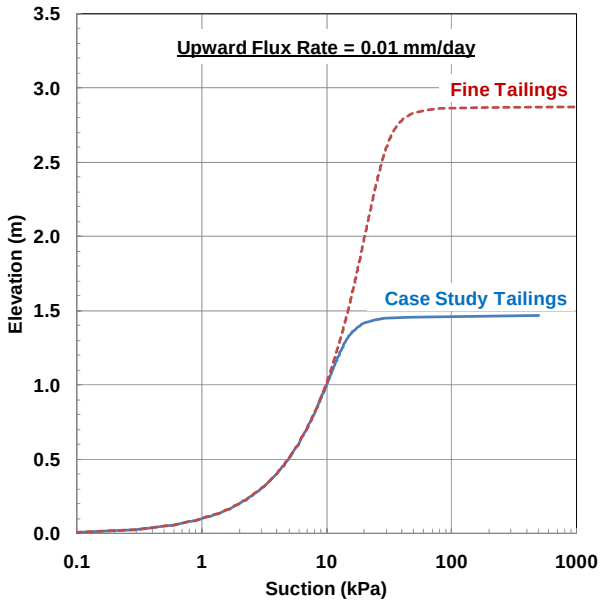

Figure 3 Suction profiles estimated for example tailings using Darcy's Law.

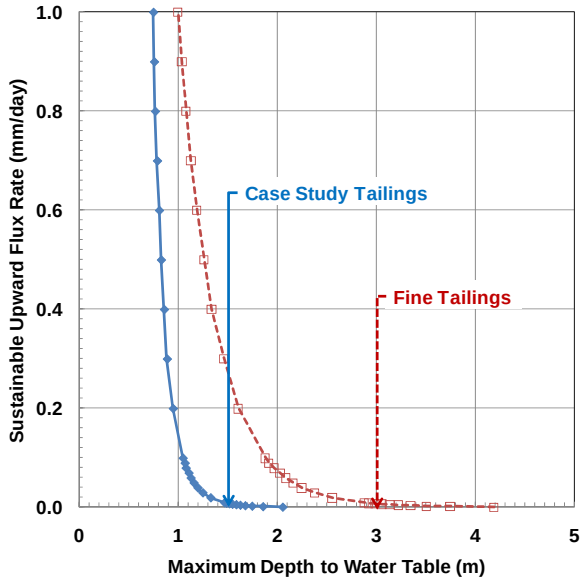

Figure 4 Graphs showing the maximum water table depths able to sustain upward flux rates between 0.001 and 1 mm/day, inclusive, for both example tailings.

CASE STUDY

A sand tailings storage facility (TSF) at one of the oil sands mines in Northern Alberta has been monitored for detailed soil-atmosphere performance and will form the basis for this case study example.

The sand tailings have a soil cover comprised of approximately 45 cm of a peat mineral mix material. A cover system model was developed, which was calibrated to the conditions measured by the field instrumentation. The results of the calibration modelling showed that the model could reasonably predict the total volume of water in the cover material, and estimate the measured responses of the cover system, in terms of the change in the volume of water to precipitation and drying events.

For the purposes of this paper, simulations using the calibrated model were undertaken to examine the moisture dynamics in the cover system and underlying sand tailings for a 51-year climate period. The database was developed from measurements gathered by Environment Canada in the Fort McMurray area.

The average annual net percolation for the 51 years simulated was used to develop probability of exceedance curves (Figure 5). These results showed that for water table depths of 1.5 m and greater, there is a 65% probability that the annual net percolation will be greater than 0 mm/yr (i.e. downward net percolation), and that there is a 45% probability that the downward net percolation will exceed 6 mm/yr. The results show that there is essentially 100% probability of a net upward flux for water tables of 1.0 m or shallower, whereas for water tables 1.5 m and deeper, the probability for a net upward flux drops to 30-35%.

It is to be expected that the net upward transport of salt from the water table in any given year could be flushed in subsequent years of net downward flux. The long-term net flux across the water table is evaluated based on the average annual net percolation over the entire 51-years of the simulation. These results confirmed that for water tables of 1.5 m and deeper, the presence of the water table ceases to impact the "cover system water balance" (Figure 6). Therefore it is reasonable to conclude, for the materials modelled, the cover system "de-couples" from the water table when the water table is at a depth of 1.5 m and greater.

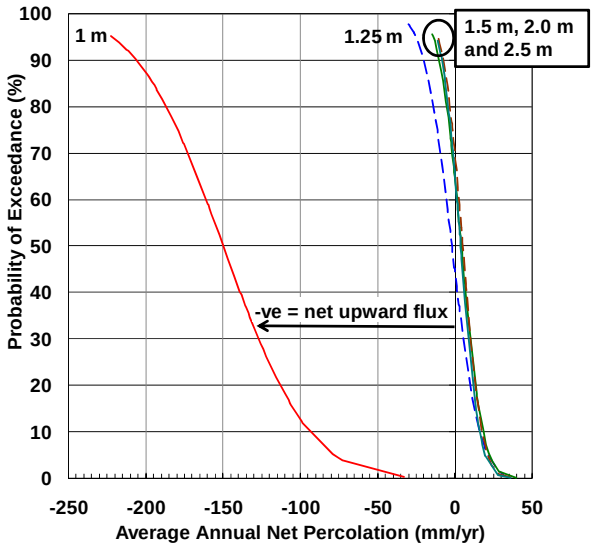

Figure 5 **Probability of exceedance showing probability of average annual net percolation exceeding a given value for different water table depths.**

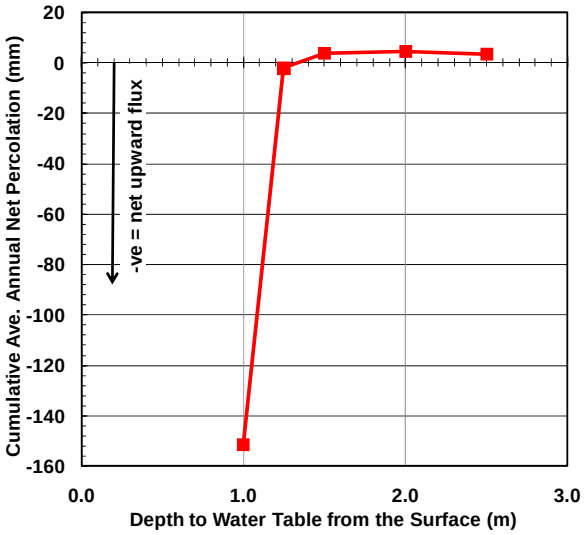

Figure 6 **Long-term average net percolation calculated at various water table depths.**

The one-dimensional steady state and transient analyses described above do not take into account the influence of two-dimensional water movement such as runoff and interflow. In order to illustrate the significance of these influences a set of two-dimensional (2D) simulations were completed using a cross-section of the TSF. Only a portion of the tailings cross-section was used in the simulation to reduce the complexity and computing time of the model. The portion of the cross-section used in the modelling is illustrated in Figure 7. The measured phreatic surface, extrapolated from piezometer measurements taken from a nearby research area, was used as an initial condition in the simulations. The pressure profile above the water table was hydrostatic at the start of the simulations. The boundary conditions for the simulation were constant head profiles at either edge of the model to define the location of the phreatic surface and a zero flux lower boundary condition. The material properties from the long-term modelling were used and a simulation was completed over the initial three-year monitoring period.

The average net percolation through the cover system over the three-year period was calculated at various locations along the cross-section, as shown in Figure 8. The overall average net percolation across the entire cover/tailings interface was 107 mm/yr for the three-year simulation period. Figure 8 also shows the initial and final water table positions.

It could be argued that the mounding of the final water table position shown in Figure 8 is an artefact of using a zero flux lower boundary condition. However, it is anticipated that the mounding would occur even if fluxes were allowed to cross the lower boundary, but that the zero flux condition exaggerates the magnitude of the mounding. Hence, the model results are more illustrative of the processes controlling net percolation than a quantitative prediction of the system's performance.

The illustrative 2D modelling clearly illustrates that net percolation varies significantly depending on the water table depth, as well as location on the slope. The bottom bench behaves most similar to the conditions predicted by the 1D decoupling models. The annual net percolation rates for this bench are 8 mm/yr and 4 mm/yr, with a corresponding water table depth of 2.1 m (at the end of the simulation). As shown in Figure 5, for a 2.0 m water table there is a 40% chance of exceeding 8 mm/yr and a 60% chance of exceeding 4 mm/yr. These results indicate that, due to the elevated position of this bench minimizing run-on and seepage effects during modelling, the slope geometry is not dominating the net percolation rate. Hence, the net percolation rate is de-coupled from the water table

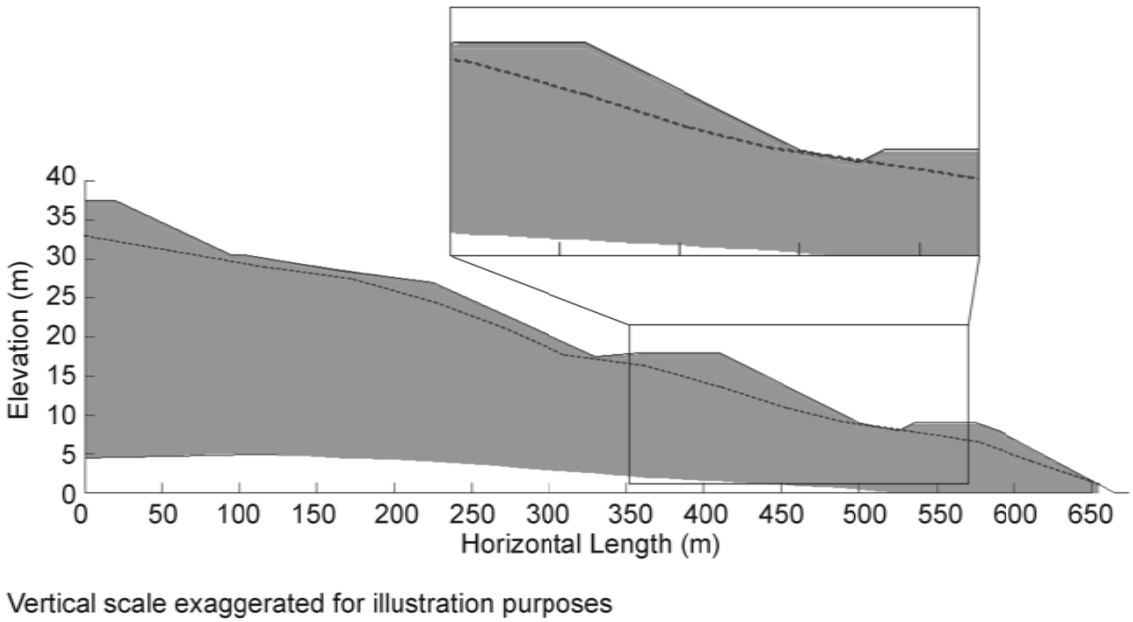

Figure 7 Cross section of the TSF embankment showing portion of cross-section used in 2D model.

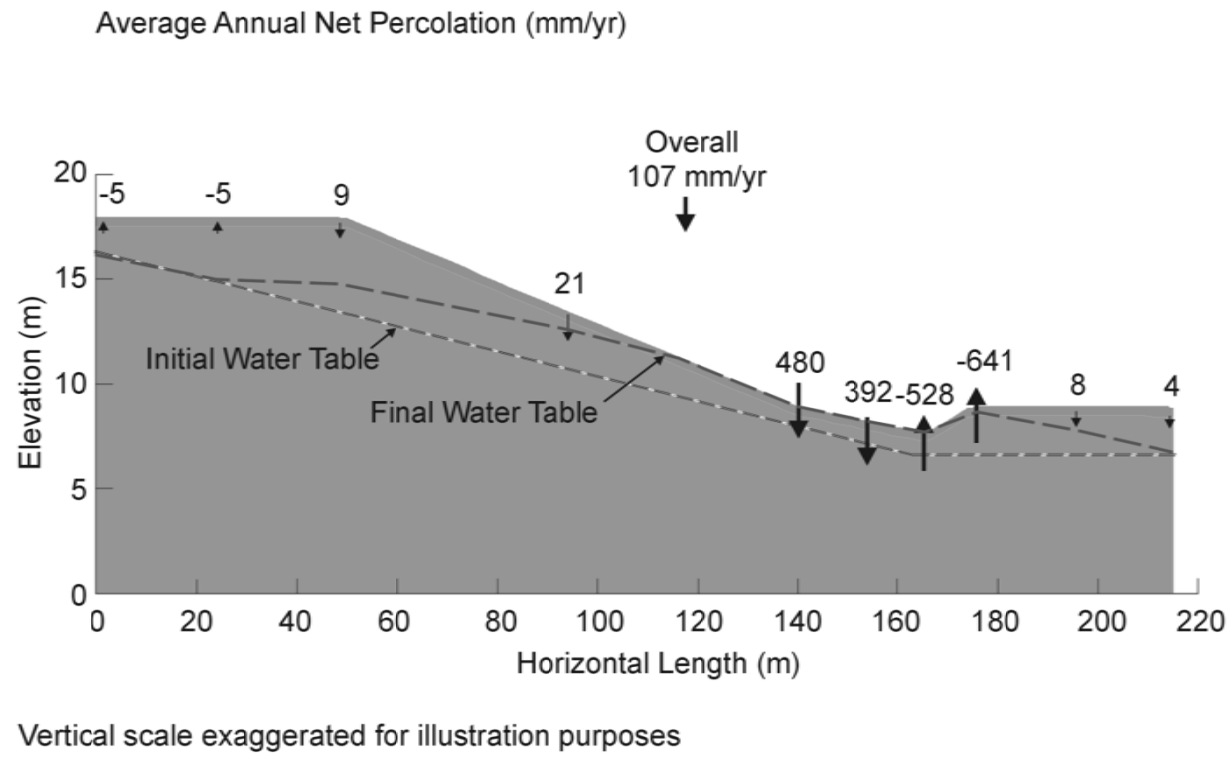

Figure 8 Average annual net percolation calculated at various locations along the cover.

at this depth, and is dependent on atmospheric fluxes.

On the upper most bench, annual net percolation rates of -5 mm/yr correspond to water table depths of 1.8 m and 2.8 m. According to the probability of exceedance curves generated from the long-term modelling (Figure 5) for water tables of 1.5 m and 2.5 m, the probability of the annual net percolation exceeding -5 mm/yr is >80%. The probability of having a net upward (negative) flux at all for these water table depths is 35%. These results indicate that at the top of the slope, factors such as lateral flow and runoff are most likely dominating the net percolation rate predicted.

On the upper slope, annual net percolation rates of 9 mm/yr and 21 mm/yr corresponded to water table depths of 4.5 m and 2.7 m (at the end of the simulation). The probability of exceedance for these net percolation rates, based on the 2.5 m water table depth in Figure 5, show a 35% chance of the net percolation exceeding 9 mm/yr and only a 5% chance of the net percolation exceeding 21 mm/yr. The probability of exceedance curves for water tables deeper than 1.5 m are similar (Figure 5); hence, these assumptions are valid for water table depths greater than 2.5 m. These results indicate that it is likely that seepage and run-on from upslope are contributing to greater net percolation in this area.

The area of dominant downward net percolation rates were just above the base of the sloping bench, with average net percolations of 480 mm/yr and 392 mm/yr, due to seepage rates, interflow, and run-on from upslope. At these locations, the water table was at a depth ranging from 1.0 m at the beginning of the simulation to 0 m at the end of the simulation. Large net upward flux rates were shown right at the base of this slope, as well as at the start of the next bench, due to seepage day lighting from upslope.

CONCLUSIONS

The upward ingress of tailings pore-water salts into reclamation materials can be damaging to plant species and the overall cover performance. As a result, it is imperative to minimize the amount of salt entering the cover. The most effective way is to minimize the potential for upward flux by de-coupling the connection between atmospheric forces and the phreatic surface. The phreatic surface becomes de-coupled from the atmosphere when the water table is too deep to supply cover moisture demand. The de-coupling depth can be determined analytically and is highly dependent on the material properties of the tailings. The analytical method is also confirmed by the case study results.

The case study also presents the results of 2D simulations. The illustrative 2D modelling was completed to examine the impact of the slopes and benches on the performance of a cover system. The results of this modelling showed that the slope geometry greatly affected net percolation rates at various locations over the model cross-section due to seepage, interflow, run-on, and runoff. The greatest impact was shown at the base of the slopes, and at the bottom of the benches, where lateral seepage created shallow water tables and the upper slopes contributed to large amounts of run-on. On the basis of this modelling alone, it is reasonable to conclude that slope geometry (i.e. “2D effects”) should be considered when evaluating performance of a cover system, particularly for areas with shallow water tables.

REFERENCES

Barbour, S.L., 1990. Reduction of acid generation in mine tailings through the use of moisture-retaining layers as oxygen barriers: Discussion. Canadian Geotechnical Journal. 27: 398-401.

Howat, D.R., 2000. Acceptable Salinity, Sodicity and pH Values for Boreal Forest Reclamation., Alberta Environment, Environmental Sciences Division, Edmonton Alberta. Report # ESD/LM/00-2. ISBN 0-7785-1173-1 (printed edition) or ISBN 0-7785-1174-X (on-line edition). 191 pp.

Kisch, M., 1959. The theory of seepage from clay-blanketed reservoirs. Géotechnique, 9:9-21.

Marschner, H. 1986. Mineral nutrition of higher plants. Academic Press, London. 674 pp.

Renault, S., Paton, E. Nilsson, G., Zwiazek, J. J., and MacKinnon, M. 1999. Responses of boreal plants to high salinity oil sands tailings water. Journal of Environmental Quality 28: 1957-1962.

van Genuchten, M.T., 1980. A Closed-form Equation for Predicting the Hydraulic Conductivity of Unsaturated Soils. Soil Science Society of America Journal 44(**5**): 892-898.

APPLICATION OF BLOCK MODELLING TO SUNCOR TAILINGS CHARACTERISATION

Patrick Sean Wells and Chengmai Guo
Suncor Energy Inc., Fort McMurray, Alberta, Canada

ABSTRACT

The proper characterisation of in-situ tailings deposits is critical to understanding the material behaviours and response to pond operations within a tailings storage facility. Active deposition of tailings with varying properties creates a dynamic environment that can be difficult to interpret and correlate to operational performance. Geological analysis is possible and has been conducted on consolidated deposits that form the static pond bottom, but the semi-fluid deposits above the bottom have not been subjected to high level analysis techniques. Classification work on these materials has been limited to basic empirical analysis and observations alone.

Suncor Energy, Inc. of Fort McMurray, Alberta has been conducting annual assessment programmes on its active tailings areas for over ten years. Innovations and improvements in both field operations and analytical techniques have resulted in gains in the understanding of the pond systems and behaviours. One such improvement is the application of block modelling and basic geostatistics to soft, semi-fluid tailings deposits. These materials have proven an almost ideal system to model geospatially, given the fairly extensive lateral continuity of their material properties. This paper describes the development of the use of block modelling of the Suncor tailings ponds, presents some of the results and observations produced, and demonstrates the significance of the results on tailings management and reclamation.

INTRODUCTION

Safe containment of soft tailings volumes and their eventual conversion into solid, reclaimable surfaces represent two of the largest challenges to the continued success of oil sands industry. These soft tailings are primarily composed of suspended clays, silts, sand, and remnant hydrocarbons resulting from the oil sands extraction process. First identified in the late 1960's, oil sands soft tailings have been the subject of intensive research programmes and the corresponding laboratory material behaviours are now well known. This is contrasted by the comparative lack of a similar understanding of the behaviour of large volumes of these materials within operating ponds. Planning parameters and predictions of operational behaviour have been based on laboratory data, and the resultant models form the basis for all long and short range tailings plans. However, there are potential shortcomings with the use of predictions made based on small scale data to predict large scale behaviours. Many of those involved in industrial operations have noted that these scale differences are often a determining factor in the success or failure of a technology. What works on a bench or in a pilot plant may not be replicable in the field, and this is nowhere more true than in oil sands tailings. This scale effect makes accurate and detailed measurements of tailings behaviour within active tailings ponds a critical component of oil sands operations management.

EARLY METHODS

Suncor's early methods of evaluating tailings ponds were based on simple volume assessments and calculations. Pond bottoms were sounded using a variety of weights, and the volumes calculated with various methods. Measuring the level of the pond surface and comparing that to simple pond peels, tables showing volumes vs. depth in a pond, were used to determine total containment remaining in the storage facility. With recycle water being an important component of the overall extraction process, measurements of the elevation of the top of the fine tailings was also important, calculating the fine tailings volumes with the same method. Some sampling with depth was conducted, but mainly to develop predictive consolidation rates by comparing the pond material to laboratory consolidation curves in order to produce basic tailings planning parameters.

As the fine tailings volumes consolidated, the term Mature Fine Tailings (MFT) came into use as a name for the material that had reached a density at which further consolidation rates were very slow. This is typically quoted as around 30% solids by

weight. In subsequent years, evaluations of the characteristics of the MFT volumes became important with the introduction of the Consolidated Tailings (CT) process. CT is a defined mixture of coarse sand from cyclone underflow, MFT from the settling ponds, gypsum or gypsum slurry, and process water. The goal is to deposit the mixture in a manner that does not segregate into its component parts, maintains the homogenous nature of the slurry as it consolidates into a trafficable surface, and releases clear water for recycle or release. In order to produce a non-segregating product, the MFT withdrawn from the ponds needs to have a clay-to-water ratio above 0.2:1. In order to designate operating depths for in-pond MFT withdrawal, an accurate profile of the MFT within the pond was required to target sufficiently dense MFT to ensure proper CT quality. Once this data was collected for this purpose, it became part of the programme to conduct tests in more sample sites and to use basic material volume calculations and pond volume vs. depth range plots to average the material properties across the pond. This was done by selecting the target pond elevation range, locating all the sample results that came from within the range, averaging the various test parameters, and applying those averages to the entire volume. In this way, a basic characterisation of the tonnage and make-up of the soft tailings was achieved.

Similar to the dawning awareness of fine tailings as a product of oil sand extraction, the CT process at full scale did not perform exactly as envisioned during the bench and pilot scale development processes. The drive for continuous improvement in CT production began, and detailed process reports began to be produced by the Suncor process team. However, there was no method of calibrating the performance outlined in these reports to the actual formation of deposits within the ponds. CT deposits can take a significant amount of time to consolidate, making assessments of solid deposits difficult and several years behind the actual deposition time. In order to produce timely assessments of the effectiveness of full scale production, predictive models for the effects of CT production on soft deposits became a more rapid method of assessment. Spreadsheet based modelling of these deposit is not detailed enough to accurately calibrate to production data. Geospatial modelling, specifically block modelling, was chosen as an improved method.

STATISTICAL METHOD

Geospatial modelling of soft tailings deposits requires the recognition of a few critical differences when comparing with traditional geological modelling. First and foremost, samples collected from active tailings ponds represent a snapshot in time, and are only valid for modelling when used with sample sites taken within the same time period. The number of sample sites usable for a model must be collected within a reasonable time frame due to the movement of fluid and semi-fluid deposits resulting from continued tailings deposition and/or withdrawal, sub-aqueous landform movements, and ongoing material consolidation. This time period is related to the material transfer rates within the pond compared to the total contained volume.

The test sites themselves represent vertical profiles within the ponds, with samples obtained at varying depth intervals and subjected to laboratory testing for bitumen/mineral/water contents, methylene blue adsorption, and particle size distributions (specifically fines content). In addition, water chemistry is analysed in selected samples. These tests are used to calculate percent solids, fines/fines plus water, clay-to-water ratios, and clay-to-fines ratios.

Suncor's current database contains 17 years of data dating from 1990, with the exception of 1991. This database consists of 481 test holes, with 9385 sample intervals. The 2007 dataset for Ponds 1, 2/3, 5, 6, and 7 contained 45 test holes with 222 sample intervals. Locations were selected to provide coverage of the pond volume, considering both depth profiles and wetted surface area.

One advantage with using geospatial techniques to model soft deposits is the strong correlation between depth and material properties. As the majority of the materials above pond bottom fall into the fluid to semi-fluid types, a fairly extensive lateral continuity has been found. The materials lack sufficient viscosity and shear strength to maintain sharp contrasts in material density or make-up, and relatively constant mixing from tailings line inputs as well as potential soft material withdrawals through dredges, syphons, or pumping barges ensures consistency in material properties across large areas of the ponds. This lateral continuity provides the opportunity for basic block modelling of the ponds with fairly widely spaced sample sites.

For this reason, the Inverse Distance Squared method was initially chosen to populate the block model. Variogram analysis of the sample set from 2007 revealed:

1. There were insufficient data points to produce reliable variograms
2. Results of the analysis on the limited variogram data indicated a directionality that did not have a physical correlation, and was likely not valid
3. The parameters obtained from the variogram analysis did not appear to be significantly different from the inverse distance squared method

A true geostatistical analysis would be useful when assessing either consolidated or sandy deposits, but is likely not necessary when working with these very soft deposits.

2007 MODELLING OBSERVATIONS

Annual pond assessments of Suncor tailings ponds provide data to tailings planning and extraction process engineering in order to reconcile the actual performance to the plan. The field and laboratory tests which are used to determine material properties and distribution in the ponds include:

- Top of MFT elevation sounding by Fisher Finder probe – used to build top of MFT surface
- Pond bottom sounding by AK97 probe (6 foot long metal spike) - determines pond bottom surface, and corresponds to in-situ shear strengths of approximately 2kPa or higher
- Piston sampling with depth above pond bottom to determine soft sediment compositional properties
- Drill sampling below pond bottom to determine fines capture and consolidation development
- Field vane shear test to determine strength distribution

Currently there are 4 tailings ponds on Suncor's Lease 86/17: Pond 1, 2/3, 5, and 6.

Pond 1 is currently in the final stages of infilling and pond closure, with tailings sand (from cyclone underflow) discharged to replace MFT.

Pond 2/3 is used as water recycle and fines settling pond, with cyclone overflow (o/f) mixed with CT recycle water.

Ponds 5 and 6 are CT deposition ponds, and both CT and densified tailings (DT) sand are discharged into these ponds.

Since different ponds are at different deposition stages, the test programme details vary from pond to pond. Figure 1 shows outlines of Suncor's Lease 86/17 tailings ponds, and the test site locations for 2007. Table 1 shows the general material classifications in Suncor tailings ponds. These include Thin Fine Tailings (TFT), Mature Fine Tailings (MFT), sand Beach, and Consolidated Tailings (CT). Two sub-classifications of CT are included and differentiate deposits that will consolidate to below pond bottom quickly (Pre-CT), and deposits with much longer consolidation times (Soft CT).

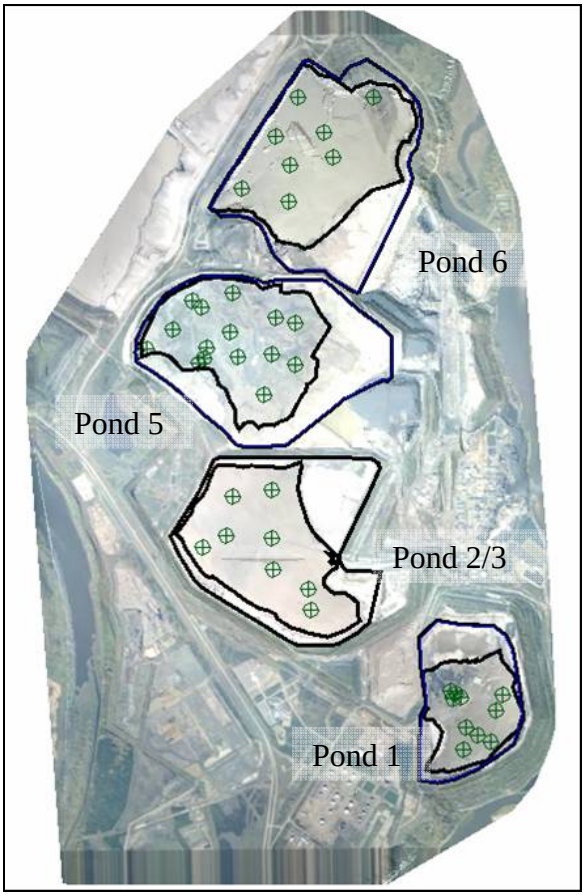

Figure 1 – Suncor Lease 86/17 '07 Test Sites

Table 1 – Suncor Tailings Material Types

Type	Lower %solids	Upper %solids	SFR Range
Water/TFT	0%	~10%	Very low
MFT	~10%	50%	< 1:1
CT	n/a (below AK97)	n/a	<7:1
Pre-CT	n/a (above AK97)	~80%	> 3:1
Soft CT	n/a (above AK97)	~75%	< 3:1 > 1:1
Beach	n/a (below AK97)	~ 80%	> 7:1

The following sections discuss the modelling and specific findings for two of Suncor's ponds.

POND 1 MODELLING OBSERVATIONS

Pond 1 is the first tailings pond commissioned in the oil sands industry, and is currently under reclamation operations. MFT volumes, built up over the course of pond operations, is being removed from the pond by dredges and replaced with sand from the extraction process. Due to material differences in deposits within the pond, a sub-aqueous sand buttress was placed around a weak deposit known as the Plant 4 beach dividing the pond into two areas, designated as Inside and outside buttress areas.

The pond bottom and top of MFT were sounded and modelled as surfaces using Surpac. Changes in the pond bottom and MFT volumes were determined by comparing to similar surfaces produced from 2006 data. Figure 2 shows the 2007 Pond 1 bottom surface contours. Figure 3 shows a cross section of the pond bottom and top of MFT surfaces. The placed sand buttress can be seen in the section, as well as a depression at the toe of the beach slope. The MFT surface slopes down from the north to the south due to MFT movement towards the removal systems.

Block modeling was used to determine the compositional properties and distribution of the soft deposits, but was limited to the area outside the buttress. This was due to the non-fluid behaviour of the Plant 4 beach material as well as difficultly in accessing the area with sampling equipment.

Most of the soft sediments within the modelled area have sand-to-fines ratio (SFR) less than 1:1 and are classified as MFT. A small portion has higher sand contents with an SFR greater than 1:1, and could be classified as soft CT with the exception that no CT has been deposited into the pond. Identification of the properties of these materials greatly assists with the selection of transfer equipment and projections of effects on operations. The majority of these soft deposits have solids contents less than 50%, but there is a small volume in select areas that have solids contents greater than 60%. This may indicate that some of the MFT may trap sufficient sand volumes to form pond bottom, thus decreasing the volume of MFT that must be removed. Figure 4 shows that the pond bottom gain between 2006 to 2007 at site 8 has an average SFR about 4:1, which is significantly lower that the 11:1 or greater SFR that a typical sand beach has.

Figure 5 shows a cross section of solids contents B-B of the soft sediments. Significant amounts of sediments above pond bottom had solids contents greater than 50%, while the MFT with solids contents less than 30% were limited to the south west portion near the dredge which is removing MFT at depth. The resultant cone in the denser MFT acts as a collection point for the lower density MFT. This profile indicates that dredging operations within the cone would encounter difficulties trying to get the dredge's cutter head below the density contrast interface, and this prediction was verified by operations.

POND 5 MODELLING OBSERVATIONS

Pond 5 is Suncor's first CT pond. The first trial CT materials were deposited here starting in 1995, and will be full in 2009. CT deposition has undergone a number of trial phases during the development of the technology, and ongoing annual assessments have resulted in a material classification system (see Table 1) based on predicted behaviour of each type.

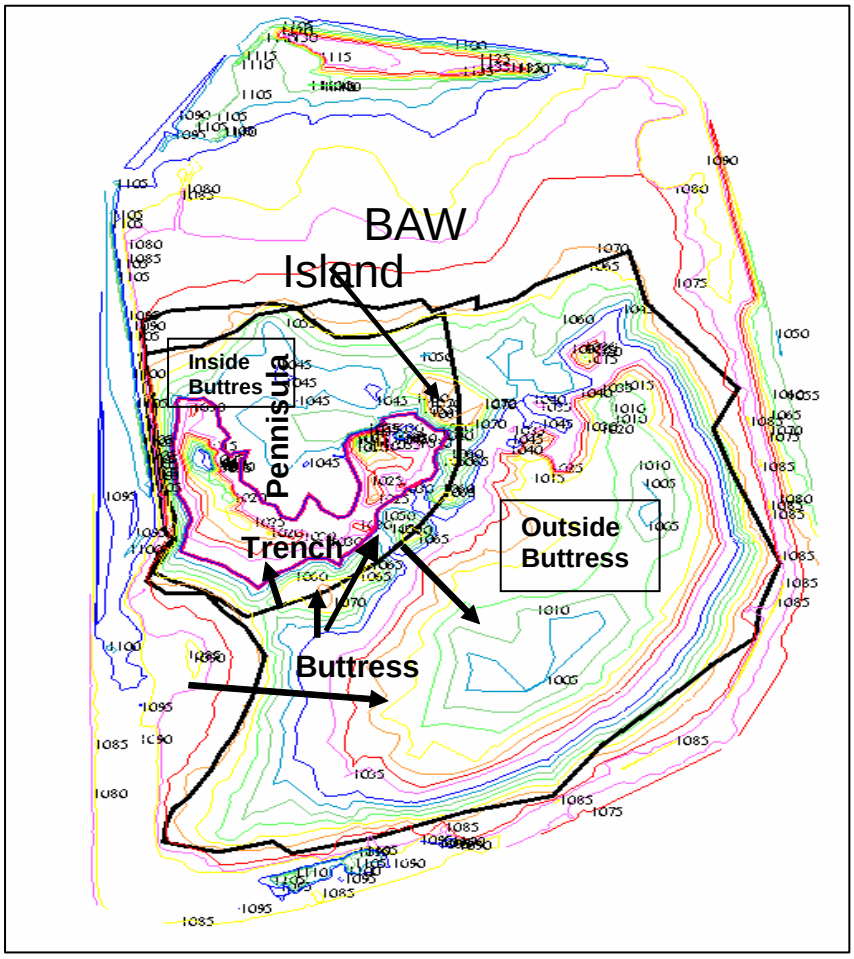

Figure 2 - Pond 1 Bottom Contours & Deposition

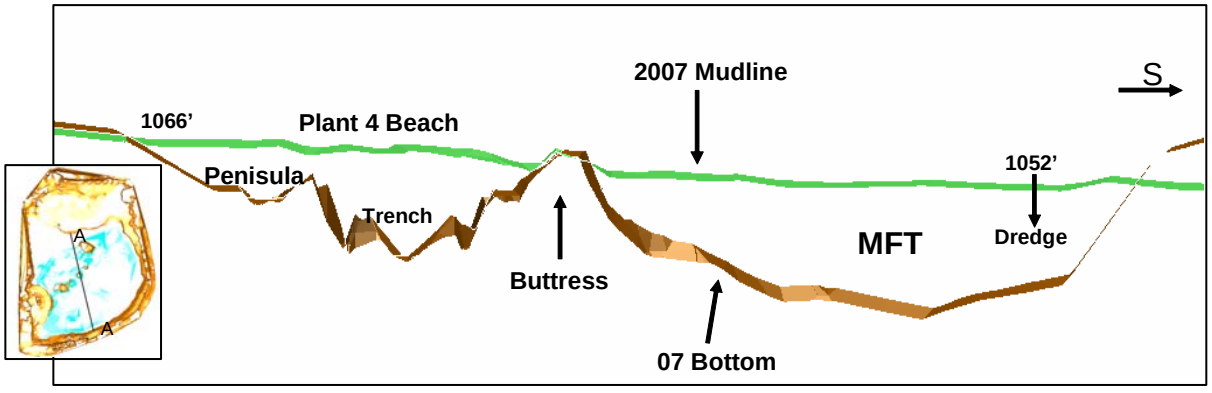

Figure 3 - Pond 1 Bottom & MFT Top

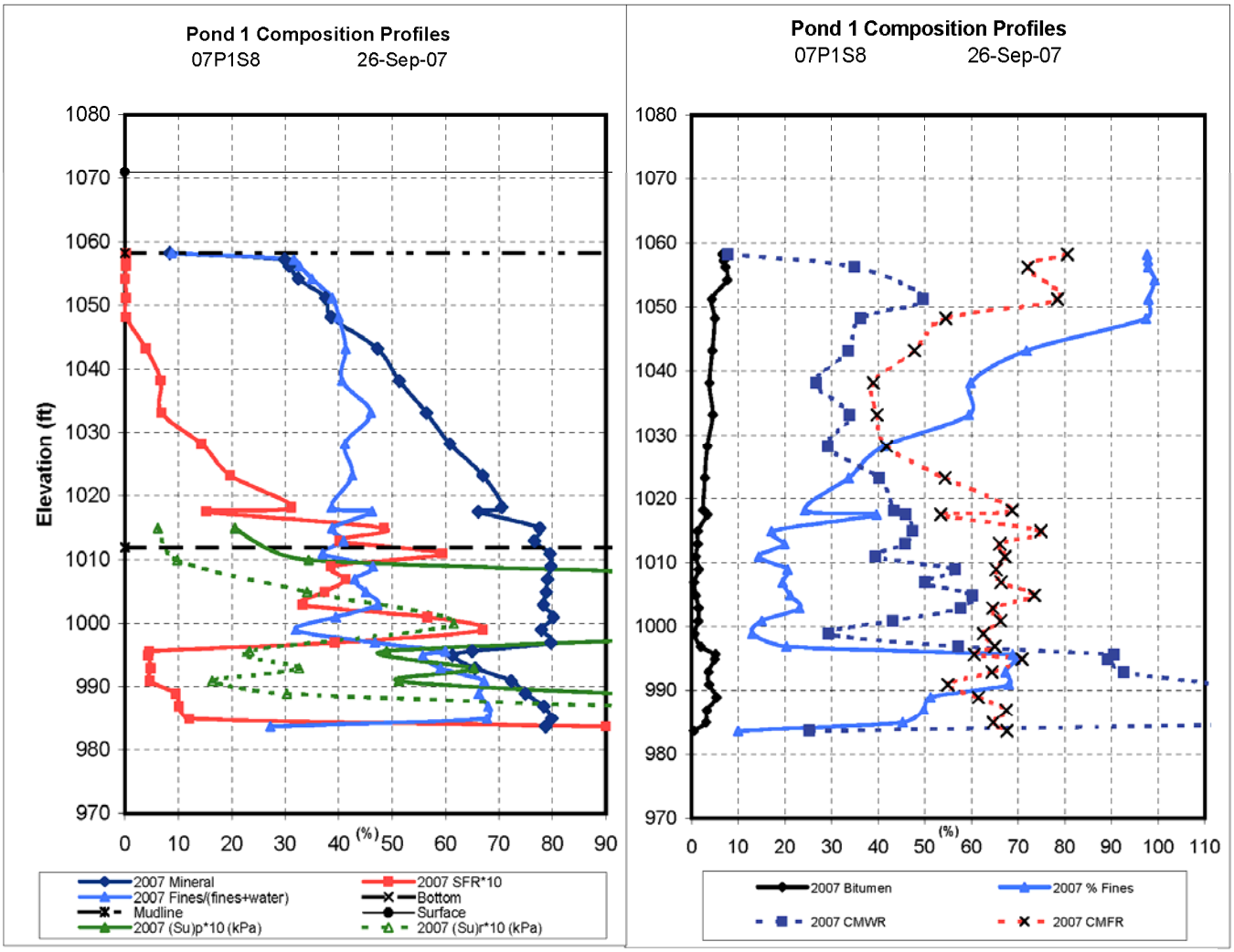

Figure 4 - Pond 1 Test Site 8

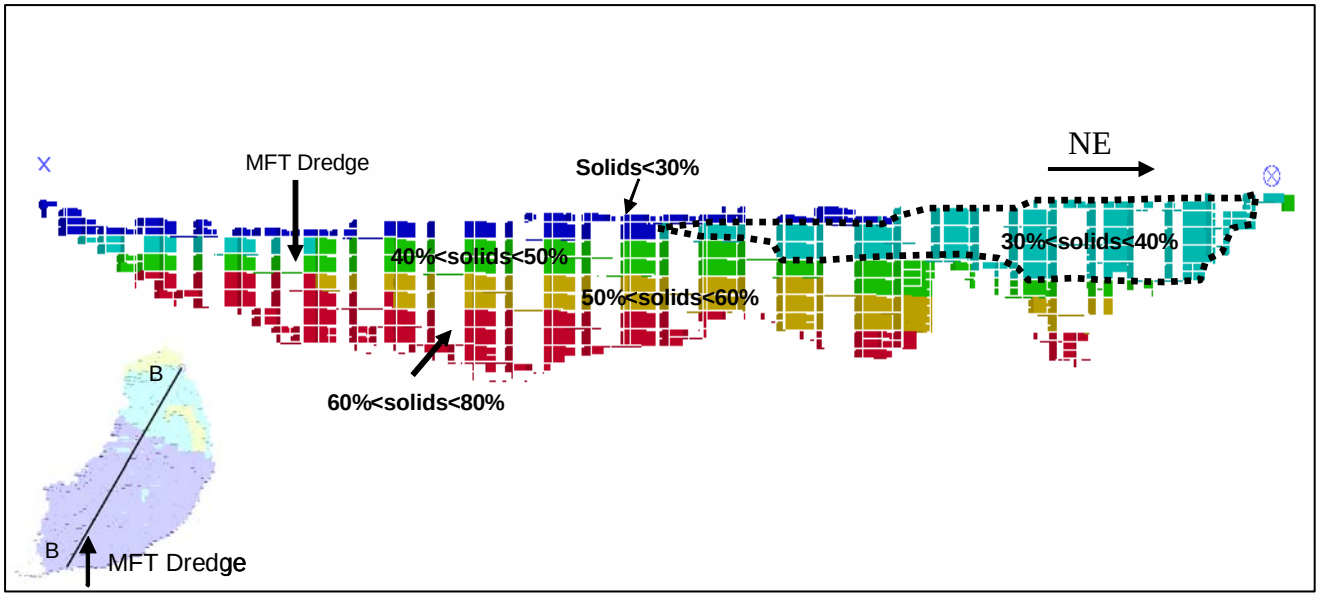

Figure 5 - Pond 1 Percent Solids – Section B-B'

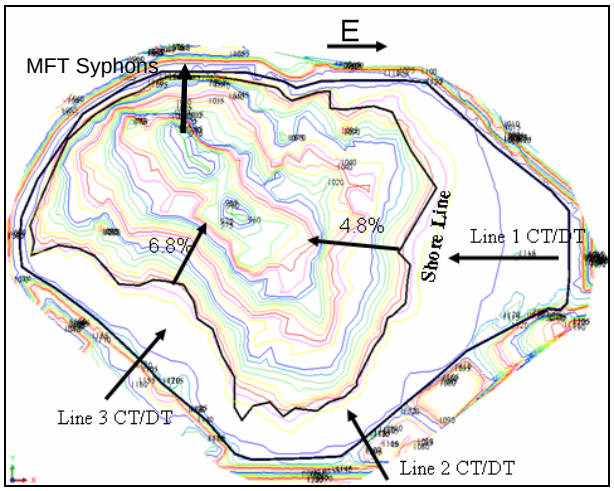

Figure 6 - Pond 5 Contours and Discharge

Several deposition methods have been trialed in Pond 5, and a description of the development of the CT deposition systems in Pond 5 was discussed by Wells at the CONRAD Tailings Seminar (2004)[1].

Figure 6 shows 2007 pond bottom contours generated in Surpac. The majority of the pond was devoid of a watercap with the exception of the area around the syphon withdrawal systems. An MFT cone forms around these intakes similar to that found around the Pond 1 dredges, and the release water and precipitation from around the pond is funnelled into this cone leaving the shorelines relatively free of surface water.

Spigot deposition of CT and densified tailings (DT) has formed broad beaches in the east and southwest. The beach below water (BBW) slope in the SW was about 6.8%, and that in the SE was about 4.8%.

[1] Advances in CT Deposition at Suncor Energy, Oilsands. Presentation. Edmonton, AB: CONRAD Tailings Workshop, Nov 8, 2004. <http://www.conrad.ab.ca/seminars/Tailings/CT_Suncor_SeanWells_081104.pdf>

Pond bottom increases have been identified as occurring from both deposition of fresh deposits as well as the continued consolidation of pre-existing materials. Some areas showed a decrease in pond bottom, likely due to consolidation of underlying material with resultant subsidence. Above pond bottom, most of the soft sediments had SFR's between 1:1 and 3:1 corresponding to the soft CT definition. Small volumes were found with SFR's higher than 3:1, designated pre-CT, found primarily close to the discharge areas or as inter-layering within deeper pond areas. Historically this material becomes pond bottom within 12 months, representing a relatively rapid consolidation rate.

The SFR distribution within the pond increases with depth generally, with areas of interfingering found within the denser areas of the pond as shown in Figure 7. Figure 8 shows the solids content cross section A-A. Significant volumes of material have solids contents between 75% and 80%. By comparing Figure 7 and 8, it can be seen that large volumes of MFT have solids contents greater than 50%. This information is used to properly identify future projects and equipment requirements to handle this material.

Figure 9 shows the SFR variations between 2006 and 2007 pond bottoms at different locations at the southwest beach. Most of the pond bottom deposits have SFR's between 3:1 and 7:1 with an average in the area of of 5.2:1. The average SFR reported as deposited in this location was 5.1. The results of this drill programme were used to verify the effectiveness of spigot deposition for CT.

Once tailings operations are complete in this pond and final assessments conducted, the block model can be used as input to predict 3D consolidation in order to develop a final surface configuration. This will be used to identify infill activities for final reclamation landform requirements, groundwater modelling, and as a design tool for capping and dewatering programmes.

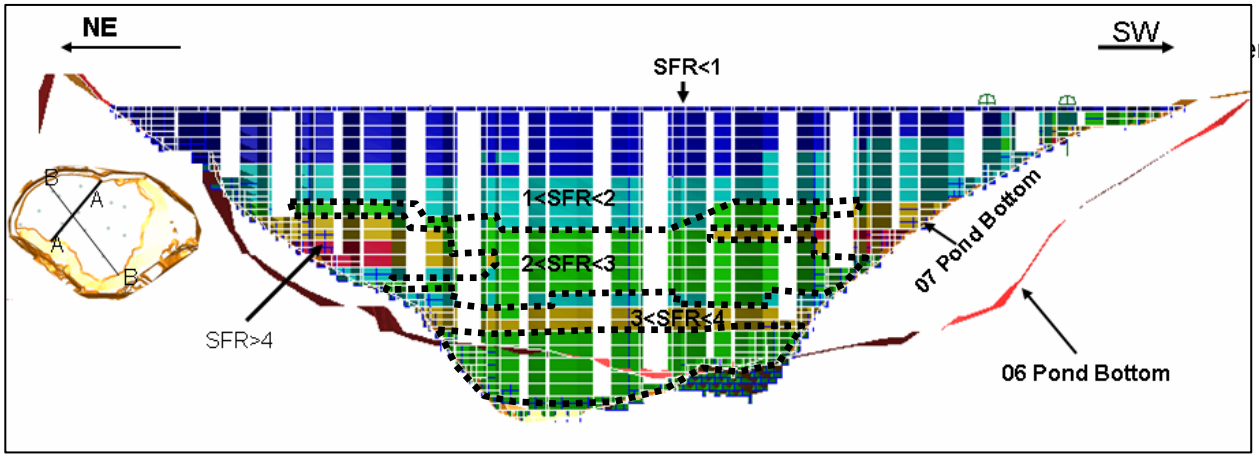

Figure 7 - Pond 5 SFR Section A-A

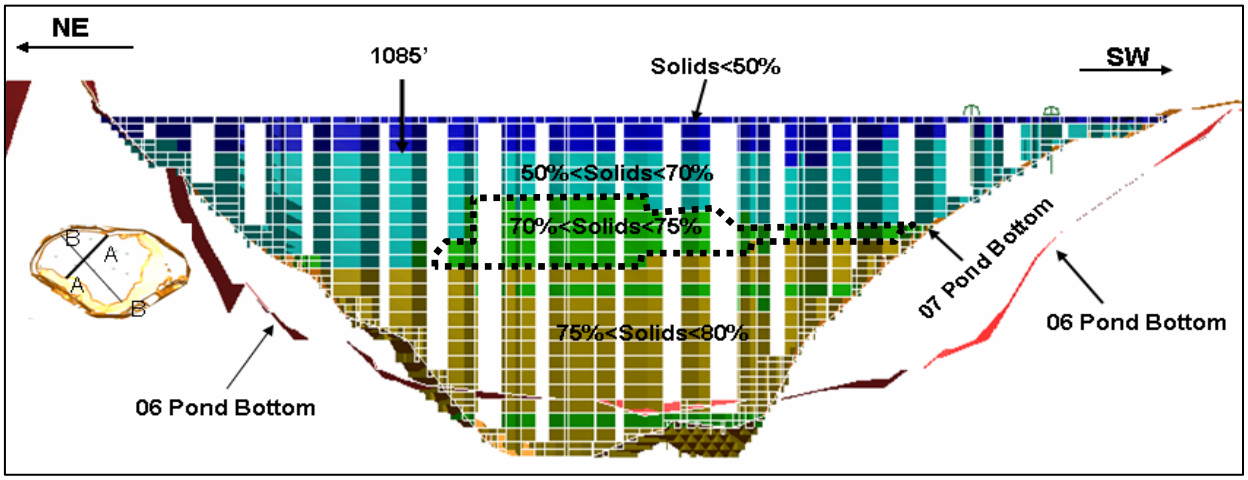

Figure 8 - Pond 5 % Solids Section A-A

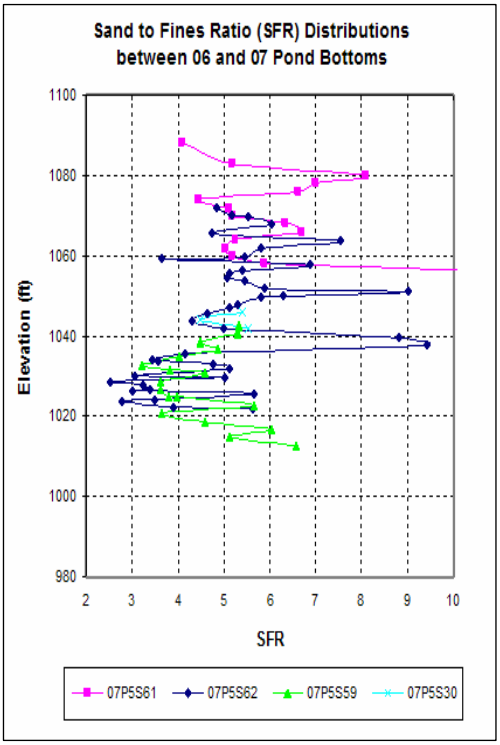

Figure 9 – Pond 5 Bottom SFR

GUIDELINES FOR SUCCESSFUL MODELLING

Similar to block modelling of geological deposits, modelling of time dependant tailings ponds requires some general guidelines in order to ensure accuracy, repeatability and validity of the results. As a starting point for development of this activity as an accepted methodology, the authors suggest the following:

1. Pond bottom testing guidelines
    a. Minimum 100m grid for pond bottom
    b. Ensure close spacing of soundings and test sites in areas of deposition and/or withdrawal

        These areas typically show the highest degrees of variability in slope profiles and material composition.

    c. Select a sounding method that minimises the effects of in-pond bitumen mats

        The AK97 sounding probe is one example.

    d. Conduct calibrations of sounding probe with both in-situ vane shears and material properties –know what the sounding probe is telling you
2. Site testing
    a. Physical samples are important

        Geophysical techniques can be difficult to calibrate in very soft materials, and widely accepted correlations are not yet available. Ensure that correlations are well established and verifications are part of the on-going programme if using testing methods such as CPT, gamma logging, resistivity, and other geophysical techniques.

    b. Follow recognised guidelines for laboratory standards

        Tests for soft tailings are less well defined and enforced than in other areas such as geotechnical testing. Ensure lab tests are confirmed for both accuracy and continuity.
3. General Items
    a. Avoid frequent changes to testing or sounding methods

        Data continuity can be more important than specific technical improvements.

        Improvements can be initiated as long as historical data is calibrated to the improved tests with a clear understanding of the effects.

    b. Tailings behaviours must be linked to deposition and transfer activities

        In order to determine if a specific tailings technology is performing as believed, comparisons between production records and the corresponding deposit behaviour are critical. This requires both detailed process records as well as tracking of deposition locations.

    c. Pond assessments and modelling should be conducted on a consistent basis, and be reconciled to annual tailings plans

        It is critical to conduct frequent assessments in order to ensure the tailings behaviour meets or exceeds projected performance targets, and planned spending profiles in support of pond operations are met. This frequency is also necessary to ensure that timely, ongoing operational optimisations can be made to achieve improved tailings performance.
4. Further development of both pond assessment and modelling techniques should be conducted as a collaborative industry effort

    A focussed industry-wide effort is recommended, with the goal being to develop these proposed techniques into an accepted and effective tool for managing large scale tailings facilities.

DESIGN CONSIDERATIONS FOR PASTE AND THICKENED TAILINGS PIPELINE SYSTEMS

Robert Cooke
Paterson & Cooke, Denver, Colorado, USA

ABSTRACT

The design of paste and thickened tailings pipeline systems is significantly more complex than conventional tailings systems. This is primarily due to the typically non-Newtonian nature of the tailings mixture.

This paper reviews engineering design considerations for paste and thickened tailings systems, focusing on the following aspects:

- Challenges associated with selecting suitable operating velocities and predicting pipeline pressure gradients for pipelines operating in laminar flow considering non-homogeneity associated with particle settling.
- Centrifugal pump performance derating.
- Interaction of pump and pipeline characteristic curves.

The paper concludes with an identification of areas where further research is required to reduce the uncertainty associated with the design of paste and thickened tailings systems.

INTRODUCTION

There has been a significant shift towards higher concentration tailings systems over the last two decades. This has been driven by the need to reduce mine water consumption in arid areas and the potential for reduced risk and environmental impact of tailings impoundments. In parallel there have been advances in the technology required to produce and transport high concentration tailings (flocculant, thickeners and pumps).

The fine particles in tailings mixtures form floc structures (either naturally or enhanced through the addition of flocculant). The interaction between the floc structures creates non-Newtonian flow properties including a yield stress. These non-Newtonian properties increase with increasing solids concentration.

Conventional tailings are un-thickened tailings or tailings thickened using conventional thickeners. Typically these tailings mixtures have yield stresses of less than 10 Pa.

Paste tailings are considered to be mixtures with a fully sheared yield stress exceeding 100 Pa. Thickened tailings covers the range between paste and conventional tailings with yield stresses in the range of 20 to 100 Pa.

The design of paste and thickened tailings (P&TT) pipeline systems is significantly more complex than conventional tailings systems. This is due to the non-Newtonian nature of the tailings mixture which impacts the pipeline operating velocity, friction losses and pump performance.

P&TT CHARACTERISTICS

Rheology

Most tailings mixtures comprise a wide range of particle sizes. The fine particles form the floc-aggregate structure. Particles too large to participate in flocculation process are considered coarse particles.

The flow behavior of most tailings mixtures can be characterized using the Bingham plastic model, i.e. the laminar flow behavior or mixture rheology is defined by the Bingham yield stress and the plastic viscosity. Both the fine and coarse particles contribute to the mixture rheology (Gillies *et al* 2002).

Shear Sensitivity

Flocculated tailings mixtures are sensitive to shear as shown in Figure 1 for freshly flocculated thickened tailings (left) and after the same mixture has been subjected to shear.

This shear effect is particularly important for the design of thickener underflow pumping systems.

Concepts and designs are being developed for shear conditioning systems to ensure that the tailings rheology has stabilized prior to pipeline transportation.

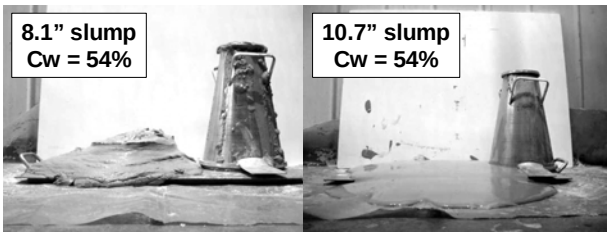

Figure 1. Shear Sensitivity

Chemistry

The addition of reagents such as lime, gypsum or CO_2 to a tailings mixture can have a significant effect on the rheology of tailings mixtures. Figure 2 shows the dramatic effect of lime addition on the rheology of a mineral sand tailings.

It is important that these factors are considered when establishing a test program to collect information for designing P&TT pipeline systems.

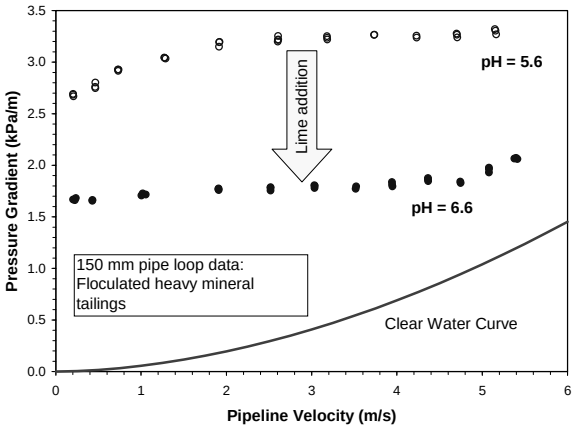

Figure 2. Effect of Lime Addition

Particle Settling and Homogeneity

Under quiescent conditions, if the immersed weight of coarse particles is supported by the mixture yield stress the particles will not settle. The mixture can be considered as homogenous (at least for time periods corresponding to typical pipeline transit periods).

During pipeline flow of Bingham plastic mixtures, the outer annulus of the flow is sheared (i.e. the region where the applied shear stress exceeds the yield stress). Thomas (1978) observed that the yield stress plays no part in supporting coarse particles in the sheared annulus as the floc structure is broken and so there is little vertical resistance to particles settling. Consequently the coarse particles settle resulting in a non-homogenous distribution of solids across the pipe section. This phenomenon is well known and has been discussed by a number of authors (Cooke 2002, Gillies *et al* 2002 and Wilson & Horsley 2004).

PIPELINE FLOW

Homogeneous Mixtures

Figure 4 illustrates a typical pipeline friction loss versus velocity curve for a homogenous Bingham plastic tailings mixture. Two flow regimes are observed: laminar and turbulent flow.

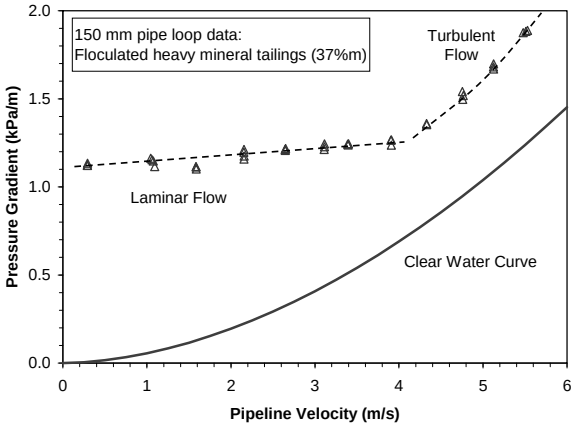

Figure 3. Pipeline Flow: Homogenous Bingham Plastic

For low velocities the flow remains laminar and the pipeline friction losses are dominated by the mixture rheology. The pipeline wall shear stress is determined using the Buckingham equation:

$$\frac{8V}{D} = \frac{\tau_o}{K_b}\left[1 - \frac{4}{3}\left(\frac{\tau_y}{\tau_o}\right) + \frac{1}{3}\left(\frac{\tau_y}{\tau_o}\right)^4\right], \qquad (1)$$

where V = average pipeline velocity (m/s)
D = internal pipe diameter (m)
τ_o = shear stress at pipe wall (Pa)
τ_y = Bingham yield stress (Pa)
K_b = plastic viscosity (Pa.s).

The pipeline friction pressure gradient is determined from:

$$\frac{\Delta P}{\Delta L} = \frac{4\,\tau_o}{D} \quad . \qquad (2)$$

The laminar flow pipeline friction losses are independent of the pipeline roughness.

At higher velocities, the flow becomes turbulent and the friction loss is strongly related to the conveying velocity and mixture density and more weakly related to the rheology and pipeline roughness. Pipeline friction losses for non-Newtonian turbulent flow are generally estimated using the Wilson-Thomas model which is based on the premise that non-Newtonian rheological properties increase the size of the micro turbulent eddies leading to an increased laminar sub-layer thickness. The thickened sub-layer results in an increase in mean velocity compared with an equivalent Newtonian liquid. The model is presented in a series of papers, the most recent being Thomas & Wilson (2007).

The transition velocity from laminar to turbulent flow is primarily a function of the mixture yield stress. Slatter and Wasp (2002) found that for large pipe diameters the transition velocity from laminar to turbulent flow is independent of pipe diameter[1] and can be estimated from the following simple but useful expression:

$$V_{trans} = 26\sqrt{\frac{\tau_y}{\rho_m}} \quad , \qquad (3)$$

where ρ_m = mixture density (kg/m^3).

P&TT Mixtures

Consider a tailings mixture with a density of 1,500 kg/m^3 and a yield stress of 20 Pa (the lower limit for thickened tailings). From Equation 3, the laminar to turbulent transition velocity is estimated as 3 m/s. If the yield stress is increased to 100 Pa (the lower limit for paste tailings), the estimated transition velocity increases to 6.7 m/s. It is apparent that if P&TT systems are operated at velocities typical for conventional tailings pipelines (2 to 3 m/s), the pipelines will operate in laminar flow.

Operating P&TT pipelines at low velocities in laminar flow is attractive from energy and wear considerations. However, most tailings mixtures contain a wide range of particle sizes and in sheared pipeline flows the coarse particles will settle. This poses interesting pipeline design challenges:

- **Operating velocity**. To ensure stable operation, slurry pipelines are designed to operate without a stationary settled bed of particles. For relatively low yield stress mixtures (less than 20 Pa), numerous loop tests have demonstrated that deposition is observed when the flow becomes laminar (i.e. the stationary deposit velocity equals the laminar to turbulent transition velocity). However, high yield stress (greater than 250 Pa) paste backfill mixtures are able to operate in laminar flow at low velocities (1 to 2 m/s) without forming a stationary deposit. Gillies *et al* 1999 suggested that a minimum pressure gradient of 1.5 to 2 kPa/m is required to ensure that coarse particles are transported in laminar flow[2]. More recently Gillies *et al* 2007 have proposed that the ratio of the mean pipe wall shear stress to the mean surficial particle stress be considered as a tentative criterion for the likelihood of stationary deposit forming in laminar flows.

- **Pipeline friction loss**. The laminar flow of mixtures containing a wide range of particle sizes will be non-homogenous due to coarse particle settling. Test data has indicated asymmetric concentration distributions and non-stable (increasing) pressure gradients in a test loop with long pipeline lengths. The Buckingham equation is not valid for these non-homogenous mixtures. It is conceivable that the actual pipeline pressure gradients will be significantly greater than the pressure gradient calculated using the Buckingham Equation and the homogenous mixture rheology. A new analysis method is required to cater for non-homogenous laminar flows.

PUMP PERFORMANCE

Centrifugal Pumps

Centrifugal slurry pumps are able to pump surprisingly viscous P&TT mixtures provided the mixture can effectively be introduced into the pump suction without inducing cavitation.

[1] This expression is valid for Hedström numbers greater than 1.5 x 10^5.

[2] Based on a investigation of sand and Newtonian oil slurries.

The performance of a centrifugal pump is reduced when pumping slurry compared with pumping water. Manufacturers provide clear water pump performance curves which must be derated to account for the effect of slurry when designing a pumping system. Derating parameters are defined for the head developed by the pump and the pump hydraulic efficiency:

$$Head\ ratio = H_R = \frac{H_m}{H_w},\ and \tag{4}$$

$$Efficiency\ ratio = E_R = \frac{\eta_m}{\eta_w}, \tag{5}$$

where H_m = head generated when pumping slurry (metres of slurry)
H_w = head generated when pumping water (metres of water)
η_m = pump efficiency when pumping slurry
η_w = pump efficiency when pumping water.

These values are determined for a fixed flow rate and pump rotational speed.

The standard industry method for derating the performance of pumps handling non-Newtonian slurries is the chart presented in Warman Technical Bulletin No 14, October 1991 (based on Walker & Goulas, 1994). The head and efficiency derating parameters are considered to be a function of impeller size and rotational speed, and slurry density and plastic viscosity (but not yield stress). These parameters are combined in the form of a pump Reynolds number:

$$Re_p = \frac{\omega\, D_i^2\, \rho_m}{K_b}, \tag{6}$$

where ω = pump rotational speed (radians/s)
D_i = impeller diameter (m).

Figures 4 and 5 show pump performance test data plotted as head and efficiency derating versus the Warman pump Reynolds number. The Warman curves provide a good prediction of the head derating, but significantly over predict the efficiency derating.

While further work is required before pump performance derating is properly understood for non-Newtonian slurries, the Warman chart is a useful design tool provided the following points are considered:

- The chart provides a reasonable estimate for head performance derating.
- The chart over predicts the efficiency derating for standard pump designs in sizes greater than the 4/3 pump used to develop the chart. However, it is prudent that the chart derating values are followed for design work due to the likely uncertainty in quantifying the mixture properties. It is expected that the efficiency derating will decrease with increasing pump size.
- Until the derating criteria are better understood, it is recommended that installations are not designed for Reynolds number lower than 10^5 without conducting test work. Similarly, the recommended upper limit for yield stress is 200 Pa.
- It is important to operate pumps close to BEP[3] (more so than for other slurry types as operation away from BEP can significantly affect the hydraulic stability of the system).

For conventional slurry pumping systems, the net positive suction head (NPSH) available must be greater than the NPSH required to avoid cavitation. Pumps can operate reliably with negative gauge suction pressure (e.g. dredging applications). However, for P&TT this issue is more complex:

- Due to the high viscosities, there is a high likelihood of air being entrained into the pump suction (particularly if the discharge into the sump is above the mixture level). The presence of air in a centrifugal pump causes a substantial reduction in the head generated by the pump. Note that this phenomenon is not cavitation, but rather a head derating effect due to the lower mixture density.
- Laboratory tests indicate that the vapor pressure for viscous high concentration water based mixtures is equal to the value for water alone.
- Bootle (2006) notes that for Bingham Plastic mixtures, due to the modified velocity distribution in the pump, the NPSH required by the pump can be significantly greater than the NPSH required when pumping water. This effect is likely to be more marked for smaller pumps.

The following guidelines should be considered:

[3] Best efficiency point

- Minimize the possibility of air entrainment into the mixture through careful sump design.
- Minimize the suction piping friction losses.
- Avoid operating with negative gauge pressures, it is suggested that a positive head of at least 2 m at the pump inlet is provided.
- Avoid using pumps smaller than 4"/3" for mixtures with yield stresses exceeding 200 Pa. The efficiency derating may be significantly higher than indicated by the Warman non-Newtonian slurry derating chart. Peristaltic pumps may be a better option for these duties.

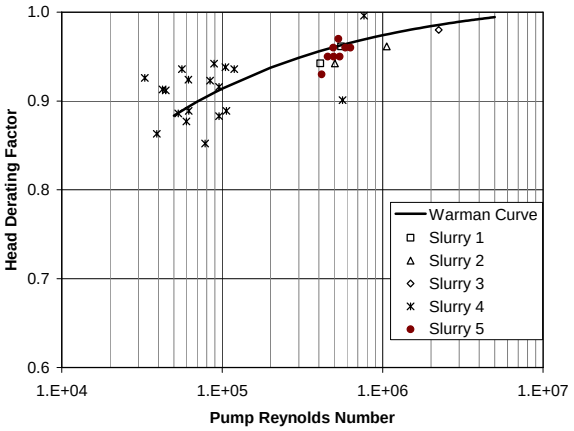

Figure 4. Pump Head Derating[4]

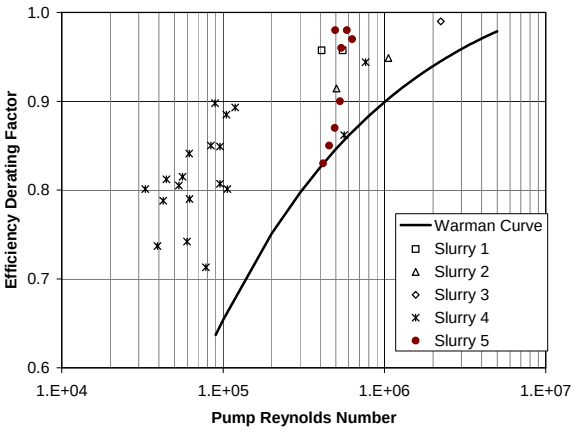

Figure 5. Pump Efficiency Derating

Positive Displacement Pumps

Positive displacement pumps require a positive gauge pressure on the suction side on the pumps. This is either provided through an elevated feed sump (concrete piston type pumps) or though the use of a charge pump (piston pumps, with and without a diaphragm). This pressure is dependant on the mixture properties and the pump configuration and it is recommended that advice is obtained from the pump vendor.

SYSTEM INTERACTION

Homogeneous Mixtures

It is often difficult to accurately control flow rate when pumping Bingham plastic slurries using centrifugal pumps. Figure 6 illustrates an example where if conventional pump selection criteria are followed 8/6 pumps will be selected for the duty. Both the pipeline system curve and the pump curve are relatively insensitive to flow rate resulting in a shallow intersection angle between the pump and pipeline system curves; a small change in the slurry properties or the pump rotational speed, will result in a large change in the underflow flow rate. Selecting smaller pumps (operating just to the right of BEP) results in a more stable operating point as illustrated for 6/4 pumps.

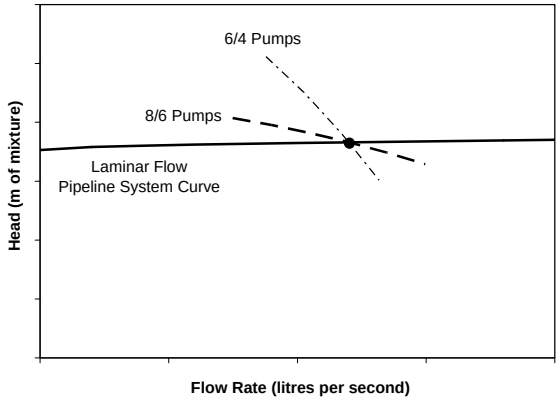

Figure 6. System Curve Interaction

P&TT Mixtures

There is evidence that pipeline pressure gradients for non-homogenous laminar flow will be greater than the pressure gradient calculated assuming a homogeneous mixture. Assuming the system is started with an empty pipeline, the pressure gradient will gradually increase until a stable value is reached. During this time a slower moving coarse-particle-rich lower layer will be formed with the resulting insitu density being greater than the delivered concentration.

This increase in operating pressure gradient can greatly affect the operational stability of centrifugal

[4] Warman curve interpolated from published curve.

pump systems. Due to their hydraulic performance characteristic positive displacement pumps are less susceptible to flow stability disruptions but care must be taken to ensure that their pressure limitations are not exceeded.

The prediction of non-homogeneous laminar flow pipeline pressure gradients is an ongoing area of research and currently there no suitable method available for predicting the ultimate stable pressure gradient.

The design of laminar flow P&TT systems requires the use of innovative monitoring and control systems to ensure reliable operation.

FUTURE RESEARCH

Significant effort is required to develop a better understanding of the flow behavior and friction losses of non-homogeneous laminar flows. This is a challenging research problem as the flow conditions can not be fully simulated in laboratory recirculation pipe loops.

CONCLUSIONS

There is uncertainty and the associated risk in the design of the non-homogeneous laminar flow P&TT mixtures. Careful attention must be placed on suitable monitoring and control systems to ensure reliable system operation.

REFERENCES

Bootle, M.J. (2006) Practical aspects of transporting pastes with rotodynamic slurry pumps. International Seminar on Paste and Thickened Tailings, Limerick, Ireland, April.

Cooke, R. (2002) “Laminar flow settling: the potential for unexpected problems”, Proc. 15th Int. Conf. on Hydrotransport, Bannf, Canada, 3-5 June.

Gillies, R., R. Sun, R.S. Sanders and J. Schaan (2007) “Lowered expectations: the impact of yield stress on sand transport in laminar, non-Newtonian slurry flows”, Proc. 17th Int. Conf. on Hydrotransport, Cape Town, South Africa, 7-11 May.

Gillies, R., R. Sun, J. Schaan and C.A. Shook (2002) “Pipeline flow of oilsand consolidating tailings slurries”, Proc. 15th Int. Conf. on Hydrotransport, Bannf, Canada, 3-5 June.

Gillies, R., K.B. Hill, M.J. McKibben and C.A. Shook (1999) “Solids transport by laminar Newtonian flows”, Powder Tech., vol 104, pp.269-277.

Thomas, A.D. (1978) “Coarse particles in a heavy medium – turbulent pressure drop reduction and deposition under laminar flow”, Proc. 5th Int. Conf. on the Hydraulic Transport of Solids in Pipes, Hanover, Germany.

Thomas A.D. and K.C. Wilson (2007) "Rough-wall and turbulent transition analyses for Bingham plastics", Proc. 17th Int. Conf. on Hydraulic Transport of Solids, BHR/SAIMM, Cape Town, South Africa, pp. 77-86.

Walker CI, Goulas A. (1984) Performance characteristics of centrifugal pumps when handling non-Newtonian homogenous slurries, Proceedings of the Institution of Mechanical Engineers, 198A, p41-49.

Wilson K.C. and R.R. Horsley (2004) "Calculating fall velocities in non-Newtonian (and Newtonian) fluids: a new view", Proc. 16th Int. Conf. on Hydraulic Transport of Solids, BHR, Santiago, Chile, pp. 37-46.

TREMIE/DIFFUSER AS A TOOL TO DREDGE AND PLACE TAILINGS

Michael Costello[1], Walther Van Kesteren[2], Dean Myers[1], Dan Nesler[1], John Horton[1], John Rowson[3], Blair Penner[4]
1. Barr Engineering Company, Minneapolis, MN, USA
2. Deltares, Delft, The Netherlands
3. AREVA Resources Canada Inc., Saskatoon, Saskatchewan, Canada
4. Petro-Canada, Calgary, Alberta, Canada

ABSTRACT

Due to shear at the outlet of a typical horizontal tailings discharge, sand deposits in a delta by the discharge point, and fines segregate farther out into the pond. Segregation leads to:

- Lost storage efficiency,
- Hard to reclaim fines areas, and
- Frequent relocation of the discharge point.

Tremie/diffuser technology can be used when placing and dredging tailings to improve all of these negative features.

As a dredge intake, a tremie/diffuser can place unamended tailings in a non-segregating mode, achieving:

- 15-20% better storage than segregated coarse and fine tailings,
- Stronger foundations more quickly,
- Deposits that can be capped for aquatic or upland reclamation,
- Less frequent relocation of discharge points, and
- Potential water and energy recycling.

In the dredging mode, tremie/diffusers can be used to minimize dilution of Mature Fine Tailings, allowing dredging, transport and placement at essentially in situ densities.

This paper presents four case studies of various applications of this versatile tool.

1. Initial full-scale application depositing fine-grained organic sediment in a non-segregating mode on a flat slope with no significant turbidity.
2. 1/3-scale with fine-grained organic sediments in Duluth, Minnesota demonstrating zero dilution during deposition.
3. Pilot- and full-scale deposition of uranium mine tailings in a pit lake in northern Saskatchewan, Canada.
4. Bench scale Oil Sand experiments on Thin Fine Tailings and Thickened Tailings.

THE CHALLENGES

Due to shear at the outlet of a typical horizontal tailings discharge, sand deposits in a delta by the discharge point, and fines segregate farther out into the pond. This happens, to a lesser degree, even with coarse and fine oil sand tailings mixed with gypsum (Composite Tailings or Consolidated Tailings (CT)). During traditional beaching, segregation occurs with the sand to fines ratio diminishing as a function of the distance from the discharge, and tailings deltas form. Segregation of tailings leads to:

- Lost storage efficiency,
- Hard to reclaim areas containing mostly fines,
- Frequent relocation of the discharge point.

The high water content of segregating tailings slurries also requires larger pipes and pumps, and misses an opportunity to recover heat from that warm water.

Alberta's Draft Tailings Directive describes these challenges in terms of its stated objectives:

"Objectives of the ERCB respecting oil sands tailings management are to

- maximize intermediate process water recycle to increase energy efficiency and reduce fresh water import,
- reduce stored process-affected waste water volumes on site,
- eliminate or reduce containment of fluid fine tailings in an external tailings disposal area during operations,
- minimize and eventually eliminate long-term storage of fluid tailings in the reclamation landscape,
- create a trafficable landscape at the earliest opportunity to facilitate progressive reclamation,
- minimize resource sterilization associated with tailings ponds, and
- ensure that the liability for tailings is managed through reclamation of tailings ponds." (ERBC 2008, Section 1.2)

The draft Tailings Directive also requires that a minimum of 45% of tailings sand be integrated with fine tailings in a non-segregating mixture by 2011 and thereafter. (ERCB 2008, Section 4.1)

Secondly, operating oil sand mines transfer Mature Fine Tailings (MFT) from basin to basin to maintain basin freeboard, and in recognition of the difficulty of consolidating, capping and reclaiming this type of tailings. Each time these tailings are transferred, they are diluted and must start their slow consolidation over again, thereby prolonging the time until they can be capped and reclaimed. The draft Talings Directive states it this way: "While operators have applied fine tailings reduction technologies, they have not met the targets set out in applications to the ERCB, and therefore the inventory of fluid fine tailings that require long-term containment continues to grow." (ERCB 2008, Section 1.1)

Tremie/diffuser technology can be used to improve oil sand tailings management and performance in all of these areas.

TREMIE/DIFFUSER PLACEMENT

A tremie is a vertical pipe designed to discharge slurries downward through a water column. A simple tremie configuration is shown in Figure 1.

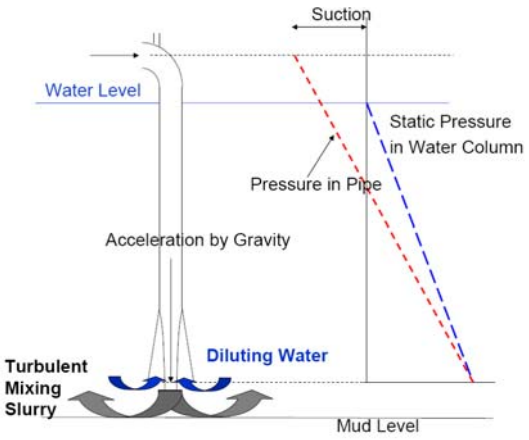

Figure 1. Simple tremie configuration (After Costello 2007).

Tremies are more effective at reducing segregation than traditional beaching (Costello 2005) and generally have spread over competent material causing a broad rise in the basin floor over time (Wells 2004). However, as the slurry flows down the tremie, it accelerates because the slurry is denser than the water column outside of the tremie. As the slurry accelerates, the cross sectional area of the flow must decrease. Constant discharge is the product of increasing velocity and necessarily decreasing cross sectional area (Discharge = Velocity x Area). This phenomenon can be observed in water flowing from the faucet, where the falling column of water is denser than the air around it. Water from outside the tremie is sucked into the tremie, diluting the slurry before it is even discharged. This dilutes MFT and reduces the strength of the CT clay/water mixture that holds sand in suspension (Mastbergen 2004, Winterwerp and Van Kesteren 2004, Costello 2007, Van Kesteren 2007).

This initial dilution is increased further by the turbulence at the outlet of the tremie, where the slurry is being discharged at a velocity of about 3 meters per second. This causes the slurry to mix with the water column and further dilute and weaken the slurry.

As shown in Figure 2, the tremie/diffuser addresses the shortcomings of a simple tremie by adding a flow resistance element to the tremie and placing a diffuser at the end of the tremie.

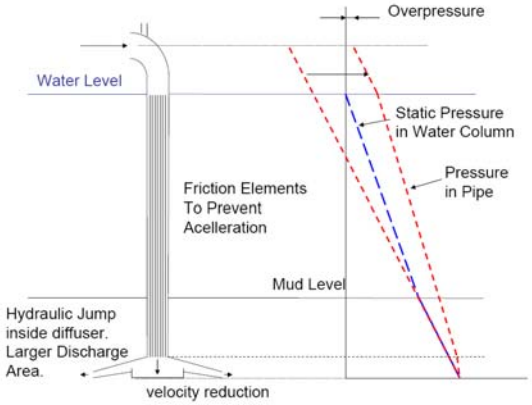

Figure 2. Tremie/Diffuser configuration (After Costello 2007).

Within the vertical tremie pipe, several types of devices have been successfully used to provide flow resistance and counteract the acceleration of the slurry. When the rheological properties of the slurry are known, this flow resistance can be designed to balance the density differential inside and outside of the tremie.

The diffuser decelerates the slurry by dissipating energy through an internal hydraulic jump that transform the super critical flow in the tremie to a subcritical flow near the outlet of the diffuser. The hydraulic jump from supercritical to subcritical flow is the cause of most of the turbulence and mixing outside of a simple tremie. This jump condition can be observed in a kitchen sink. As water from the faucet splashes on the basin, water flows radially in a thin layer until it spreads enough for the flow to slow to subcritical velocity. At that point, the flow noticeably thickens as the subcritical flow regime takes over. The diffuser is designed in a way that the hydraulic jump occurs within the diffuser (Mastbergen et al. 2004). Also, the geometry of the diffuser greatly enlarges the cross sectional area of the opening from which the slurry is discharged, thereby proportionately reducing the velocity while the discharge remains constant. With the tailings mixture properly matched to the tremie/diffuser, the combined effect is a smooth, dispersed, non-segregating discharge with very low shear conditions.

These flow conditions, when combined with Thin Fine Tailings (TFT), MFT, CT or Thickened Tailings (TT) (a mixture of coarse and fine tailings thickened to minimize water content and maximize water and heat recovery), allow the slurry to flow out beneath the overlying water as a separate non-segregating, non-diluting fluid. Depending on rheology, the slurry fluid can flow over large distances subaqueously with minimal slopes. This minimizes the build up of sand at the discharge point that in turn reduces the frequency with which a discharge unit must be relocated. By minimizing segregation of well graded tailings, maximum storage density is achieved, and these tailings can setup with greater strength for easier and sooner reclamation capping.

For TFT and MFT transfers, the same is true. They can be placed using the tremie/diffuser, minimally mixing with the overlying water. To minimize dilution of MFT, at the dredging end of the transfer, a diffuser can be used as a stationary suction intake to gather and dredge MFT sediments.

STATIONARY SUCTION DIFFUSER INTAKE

MFT will flow into a stationary diffuser intake when the MFT level is above the critical level as illustrated in Figure 3. The critical level is related to the undrained shear strength of MFT: a higher strength results in a higher critical level. A higher critical level reduces the amount of MFT that can be dredged. The upper limit depends on the location of the dredge pump. When the pump is placed at diffuser level the upper limit is about 1 kPa. For MFT stronger than 1 kPa, the dredge intake must be pulled through the deposit using a special trailing suction dredge in order to prevent dilution with overlying water.

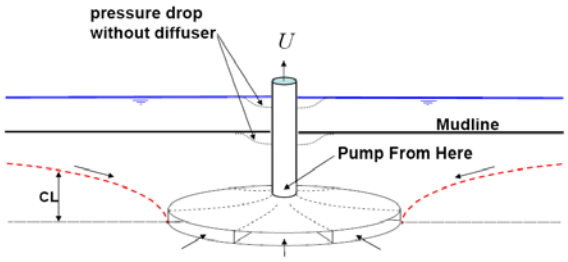

Figure 3. Stationary Suction Diffuser for use Dredging MFT < 1 kPa.

As with the tremie/diffuser discharge, a properly configured diffuser inlet will minimize dilution of the MFT as it flows to the withdrawal point. By enlarging and spreading the area of the intake, the diffuser avoids any high suction condition that otherwise could cause overlying water to be drawn to the inlet. Cavitation is also prevented.

By using the diffuser at both ends of a MFT transfer, the hard-won density of the MFT can remain essentially unchanged as it is transported and placed the new basin. An added benefit is that the higher density slurry transports more solids and less water during all MFT transfers, requiring smaller pipelines and providing more long-term storage in the dredged basin per cubic meter of dredging.

Ideal non-segregating conditions for placing tailings involve dryer tailings and slow discharge

velocity (low shear conditions). This is because the thicker the clay-water mix, the better the slurry can prevent settling of sand particles. However as shear increases, sand that used to be suspended begins to have a settling velocity as it falls through the matrix that used to support it. This relationship has been experimentally shown and compared with theory in Figure 4.

Thicker tailings, gently placed, work best to keep sand integrated with the fines. To the extent that warm water can be recovered at the extraction plant with thickeners for example, energy can be saved, and the water won't have to be pumped to and from the basin. The settling area of each basin could also be smaller when the tremie/diffuser is used.

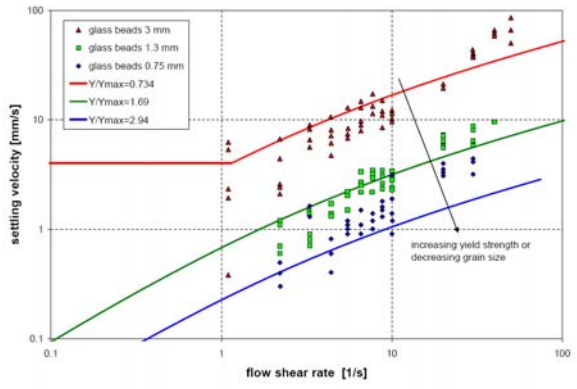

Figure 4. Experimental relationship between yield strength, shear rate and settling velocity (after Van Kesteren 2007).

CASE HISTORIES

Four case histories are presented below. Combined, they illustrate the concepts presented above as they relate to several different applications.

Lake Zevenhuizerplas, The Netherlands

The tremie/diffuser was first designed and used in this reclamation lake after mining the sand and gravel from the deposit (Mastbergen et al. 2004). A dredging contractor was hired to place overburden strippings from a new mine into the mined out lake. The overburden contained a large amount of very fine-grained sediment and organic matter. The contractor discovered that using a standard tremie in this 30 meter deep lake resulted in extensive mixing and turned the lake black from the suspension of the fine clay and organic matter at concentrations as high as 270 mg/l (Mastbergen et al. 2004). The tremie/diffuser was designed by Deltares to minimize this turbidity. A photo of the full size diffuser is shown in Figure 5.

Using the tremie/diffuser avoided turning the lake black and resulted in suspended solids levels rising only to 35 mg/l in the immediate vicinity of the diffuser (Mastbergen 2004). The bathymetry of the lake in the vicinity of the tremie/diffuser before and after the deposition is shown in Figure 6.

Figure 5. Tremie/Diffuser used at Lake Zevenhuizerplas shown upside down (from Mastbergen et al. 2004).

The after-deposition figure shows only one 0.5 meter contour at the diffuser site and no other contours across the 300 meter span of the mapped area.

To the oil sands, Lake Zevenhuizerplas was the project that triggered the research and development of the tremie/diffuser technology and showed that very fine-grained sediment can be placed at great depth without mixing with the overlying water. Dilution was avoided, and the sediment was placed on a very flat slope which translates to less frequent relocation of the discharge apparatus and more uniform layers of more uniformly distributed grain sizes. With more uniform distribution of non-segregated tailings, capping can be achieved sooner and economically, reliably restoring trafficability.

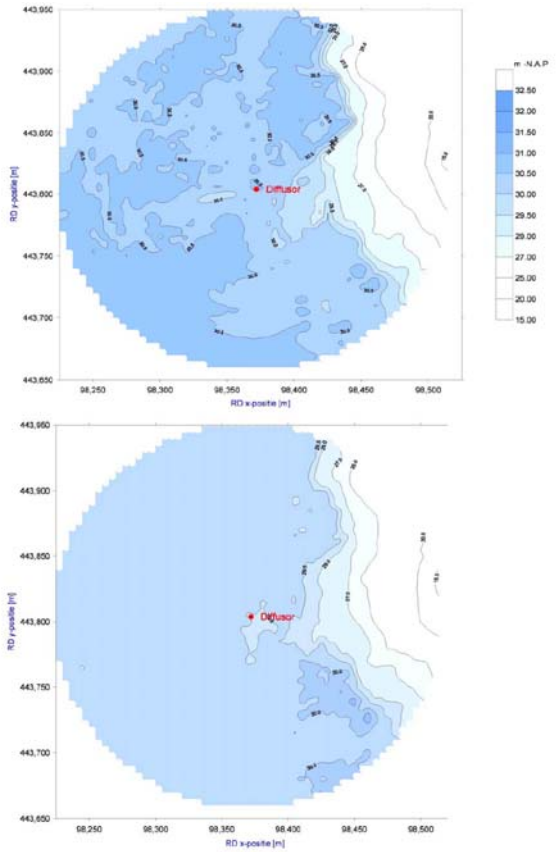

Figure 6. Bathymetry before and after tremie/diffuser placement located in the center (Mastbergen 2004).

SLRIDT Site, Duluth, Minnesota, USA

This site is being remediated from coal tar contamination in very fine-grained sediments in a shallow fresh water estuary. There were two reasons for considering tremie/diffuser technology for this restoration activity. Some of the dredged material would have volatilized during dredging and placement to the extent that ground level concentration of naphthalene would have regularly exceeded standards. To avoid this, it was necessary to find a way to deposit the sediment underwater in a way that it didn't mix with the overlying water. It is mixing that allows the naphthalene to dissolve on its way to volatilization. Secondly, Like Lake Zevenhuizerplas, this project requires the placement of fine-grained organic sediment on the remediated areas to restart and host the restored benthic community. This required development of a placement method that is non-diluting and minimally mixing.

To evaluate the tremie diffuser, a test tank was constructed with a weir at one end and a tremie/diffuser at the other as shown in Figure 7.

The system was sealed at the top to allow collection of air samples, and turbidity and TSS was tested as the sediment was placed through four configurations of the tremie and tremie/diffuser. The initial slurry was 30% solids, with 20% of the sediment mass consisting of clay particles less than one micron.

Figure 7. 1,000 test tank apparatus from SLRIDT Tests.

During the test, there was no dilution of the 3.8 m^3 (1,000 gallons) of sediment placed. After that first test, the slurry was diluted to test the system with lower solids content. Three more tests were run using the same material. In each test, 3.8 m^3 of sediment were pumped into a tank full of water at a rate of 11 m^3/h (50 gpm), displacing 3.8 m^3 of water over the weir. After each test, the remaining water was decanted off and the sediment was pumped back to the holding tank for reuse. During all of these three tests, the solids content remained constant at 18% as shown in Figure 8. That the sediment could be pumped back to the holding tank confirms there was no significant segregation of the sand fraction.

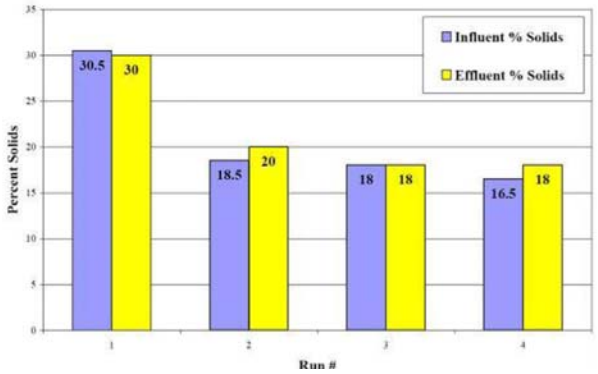

Figure 8. Before and after solids content from pilot-scale tank tests with tremie/diffusers (Costello 2005).

To the oil sands, this confirms that MFT, with its similar or higher solids content can be placed without dilution using the tremie/diffuser. A secondary advantage is that the placement will not adversely affect the quality of the overlying water, and can reduce emissions of volatile compounds contained in the MFT. Finally, because the tremie/diffuser is best located beneath the tailings-water interface, it can potentially be used to place additional MFT beneath a sand cap that has been placed for example in a Base Mine Lake to raise the lake bed, without displacing the cap.

AREVA Tailings Placement, McClean Lake, Saskatchewan, Canada

AREVA Resources Canada Inc. operates a uranium mine and mill at McClean Lake in northern Saskatchewan. Tailings are placed into a mined-out pit lake via a vertical tremie pipe. Currently, a 20% angle of repose is observed in the placed tailings, due to particle size segregation during deposition. The result is a loss of storage in the tailings management facility (TMF). AREVA contacted the authors about the feasibility of using the tremie/diffuser to place its tailings.

The experimental tank built for the SLRIDT Site study was transported to McClean Lake for pilot experiments to determine if sandy tailings with some fines could be placed with less segregation and with an acceptably flat slope. Rheological testing was done on the clay-water mixture and non-segregating operating conditions were identified as requiring at least 35% solids in the delivered slurry. The pilot scale tremie/diffuser from the SLRIDT Site was tuned to those conditions and tests proved successful. By operating outside of specifications at lower solids content, excessive segregation of the tailings was verified during removal of the tailings from the tank as shown in Figure 9.

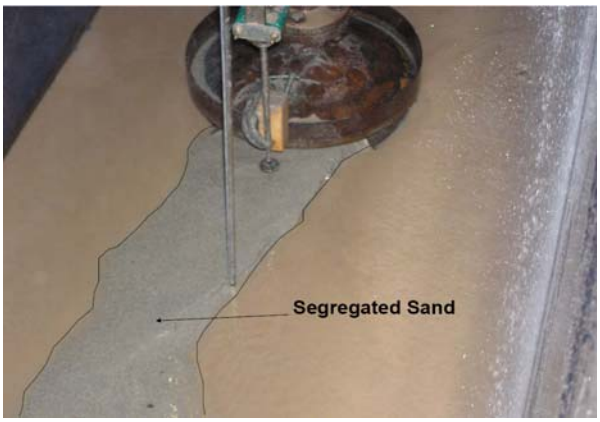

Figure 9. Note the segregation of the gray sand from the fines.

A full scale tremie/diffuser was designed and deployed in autumn 2006 to demonstrate the effectiveness of the diffuser in reducing tailings segregation and tailings stacking during placement. The diffuser was installed on the back side of the deposition barge (Figure 10). Sections of tremie pipe (Φ 150 mm) were added to lower the diffuser to the top of the sediment layer. A total of four orifice plates (Φ 60 mm) were installed during lowering of the diffuser: one at the top of the diffuser, and one at each flanged connection located 1.5 m, 4.5 m, and 7.5 m above the diffuser. The purpose of the orifice plates was to provide enough frictional resistance within the tremie pipe to overcome the tendency of the tailings slurry to accelerate through the vertical section of pipe, thereby ensuring that the pipe runs full, avoiding dilution of the slurry.

The diffuser was operated for seven days. Operating parameters including; slurry density, tailings line flows, depth to settled tailings, and pressure at the top of the tremie pipe were monitored. After four days, operations staff attempted to retrieve the diffuser to tighten a leaking flange connection approximately 7 m below the pond surface. The diffuser was found to be stuck within the tailings layer, several different retrieval attempts were unsuccessful, and pumping through the diffuser was terminated.

Figure 10. Full scale, octagonal tremie/diffuser being deployed at McClean Lake.

Dredge samples of placed tailings were collected at varied distances from the diffuser to assess the properties of tailings material placed by the diffuser. Samples were subjected to grain size determinations and sounding measurements were used to determine the angle of repose of material placed with the diffuser. Depth to tailings measurements were also collected at varied distances from the deposition point.

During the diffuser trial, tailings slurry solids content averaged 29.6% and ranged from 24% to 34%. Flow rates through each of two tailings lines were typically within the range of 30 m^3/h to 35 m^3/h and the combined flow averaged 66 m^3/h. The corresponding average tonnage delivery rate to the tailings management facility (TMF) was approximately 24 tonnes of tailings solids per hour. Moderate line pressures, ranging up to 250 kPa were observed for the tailings line at the deposition barge during operation of the diffuser at the above flow rates. Pressures recorded at the top of the tremie pipe remained relatively low but positive, between 50 kPa and 100 kPa, throughout the test. During previous operation with the open tremie pipe, negative (sub-atmospheric) pressures were typically recorded at the top of the tremie pipe, indicating acceleration of the slurry through the vertical pipe section. Positive pressures recorded during the trial indicate that the orifice plates may be successfully employed to prevent acceleration of the tailings slurry through the length of vertical tremie pipe. In general, no problems with the piping or pumping capacity associated with the tailings delivery system were encountered during operation of the diffuser.

With the operational solids content of the slurries below that of the non-segregating threshold of 35%, segregation still occurred, but to a lesser degree than before. Particle size gradation curves for three tailings samples collected at varied distances from the deposition point in comparison with a curve representing whole tailings collected from the tailings thickener underflow are presented in Figure 11. Tailings close to the diffuser were sandier than those more distant, indicating particle size segregation persisted to some degree during the trial. A comparison of the variations of fines content with distance is also provided in Figure 11 for tailings placed using an open tremie pipe versus those placed with the tremie/diffuser. Depth to tailings measurements indicated an angle of repose corresponding to a 10% grade compared to tailings surface grades from 15% to 20% previously observed resulting from tailings placement through an open tremie pipe. The apparent reduction in the slope of the tailings surface suggests a greater retention in fines near the deposition point and supports the results of the grain size determinations conducted on placed tailings samples.

Data collected following the diffuser trial, albeit limited, indicated improved placement with the diffuser over a simple tremie, with greater retention of fine-grained material near the deposition point. This is likely due to the diffuser's ability to reduce the slurry discharge velocity from greater than 1 m/s to less than 0.04 m/s, and the associated reduction in slurry shear rate, which can reduce segregation. However, it is apparent that even at the design velocity, the slurry, at the attainable density (30% solids), is not viscous enough to hold the coarse-grained particles in suspension during sedimentation. This is consistent with previous scale model and laboratory studies undertaken in the early stages of this project, which suggested that tailings with solids greater than 35% would be required to effectively minimize segregation at the shearing rates produced as a result of pumping the tailings through the diffuser.

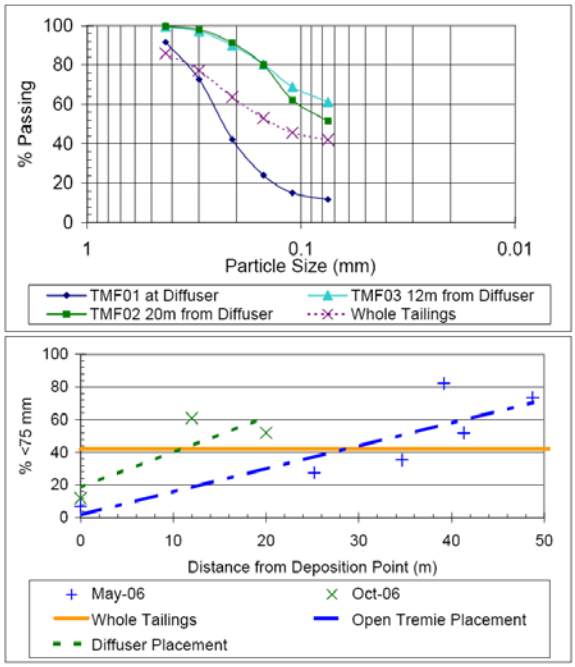

Figure 11. Placed Tailings Particle Size Gradation.

Further full scale testing and permanent installation of a diffuser is scheduled for fall 2008. The rheological properties of the tailings have changed since the initial full scale test. The fines content has increased and the tailings solids content has been increased with a cyclone and tailings thickener. It is expected that the increased tailings density will yield slurry properties that are conducive to non-segregating slurry placement. Configuration and operating parameters will be refined this fall to prevent loss of the diffuser.

To the oil sands, this project illustrates the importance of managing tailings within non-segregating operating conditions and illustrates challenges when applying at a large scale with coarse tailings. Because they are decidedly coarser than oil sand tailings, these tailings make operating in non-segregating conditions all the more difficult. Nevertheless, the method is working and is expected to meet project objectives this year.

Oil Sand Tailings Bench Test

Recently, the authors conducted studies on the deposition of Thickened Tailings from oil sands, that have sand-to-fines ratios ranging from 1.1 to 1.3 (without bitumen removed), and contain no gypsum. The primary purposes of the studies were to determine:

1. The range of tailings properties that can be deposited without resuspension or dilution using a tremie/diffuser,
2. Settling and consolidation properties,
3. Water quality and yield of expressed pore water, and
4. Biogenic gas generation rates.

Flume settling tests were conducted at CANMET on the TT (40-44% solids) with straight tremie and tremie/diffuser configurations for comparison. The 15 m^3/h (250 l/min) tank setup and tremie/diffuser are shown in Figure 12.

Figure 12. Experimental Flume with tremie/diffuser installed.

Column settling tests were conducted to measure sand segregation during settling and produce settled fluid tailings for consolidation tests. Consolidation was achieved on settled fluids using seepage gradients rather than weights. In this way, the entire settling and consolidation process can be experimentally observed in the laboratory. The Seepage Induced Consolidation (SIC) test also measured the conditions under which air can be forced into the sample. The data indicates how gas bubbles, which affect consolidation, migrate through the tailings. The two setups are shown in Figure 13. Finally, rates of gas generation from TT were measured at Barr's biogenerated gas testing facility. These gas generation rates contribute to the consolidation and pore-water yield analysis now being conducted.

Figure 13. Deltares column settling and seepage induced consolidation testing equipment.

While this study is incomplete, preliminary results from the flume settling tests shows that:

1. The use of the tremie alone resulted in segregated TT, whose sand accumulation had to be hand shoveled from the flume after the test.
2. Rheological properties allowed design of a tremie/diffuser that placed TT with minimal segregation or dilution. These successfully placed materials could be pumped from the tank after the test.

Laboratory tests are ongoing. Results will be fed into a one-dimensional consolidation model called DELCON, which can also calculate the release of pore water and gas from the tailings. This data will be used for design input on water yield, consolidation and tailings strength calculations.

SUMMARY

In summary, tremie/diffusers offer many advantages toward achieving the objectives set by the ERCB in its Draft Tailings Directive. It can be used to improve the placement and performance of CT, TT and MFT as follows:

- MFT can be transferred and consolidated more quickly, reducing fluid tailings volume storage during operations, leading to earlier and more certain reclamation in areas with fine tailings.
- Thickened tailings can be produced and placed without the need for additives, thereby maximizing intermediate process water recycle, increasing energy efficiency and reducing fresh water import.
- With successfully thickened tailings, storage and retention time of process-affected wastewater volumes can be reduced.
- With increased efficacy of both CT and TT, long-term storage of fluid tailings in the reclamation landscape can be minimized.
- In combination with soft sediment capping technologies, well-placed, non-segregating CT and TT, and reasonably densified MFT can be capped to create a trafficable landscape at earlier opportunities to facilitate progressive reclamation.

REFERENCES

Costello, M.J., Van Kesteren, W.G.M. and Flynn, W., "A New Environmental Method for Placing Dredged Material in a CDF," Proceedings of Battelle Contaminated Sediment Conference, Savannah, Georgia, USA, 2007.

Costello, M.J. and Van Kesteren, W.G.M., Tremie/Diffuser Tests Report – SLRIDT Site, Duluth, MN, August 8, 2005.

ERCB 2008, Alberta Energy Resources Conservation Board, Tailings Performance Criteria & Requirements for Oil Sands Mining Schemes – Draft, June 2008

Mastbergen, D. R., Van Kesteren, W.G.M. and Loman, G.J.A. (2004), "Controlled Submerged Deposition of Fine Grained Dredged Sediment with Various Diffuser Types", *Proceedings XVIIth World Dredging Congress 2004.*

Tremblay, M.A.J. and Rowson, J., "Tailings Management Best Practice: A Case Study of the McClean Lake JEB Tailings Management Facility," COGEMA Resources Inc., Saskatoon, Saskatchewan, CANADA, 2003.

Van Kesteren, W.G.M., Talmon, A.M., Pennekamp, J.G.S., Costello, M.J. and Flynn, W.F., "Dredged Material Placement Under Non-Segregating Conditions," Proceedings of World Dredging Conference, Orlando, Florida, 2007.

Wells, S., "Advances in CT Deposition at Suncor Energy Oilsands," CONRAD Tailings Seminary, November 8, 2004.

Winterwerp, J.C. and Van Kesteren, W.G.M., "Introduction to the Physics of Cohesive Sediment in the Marine Environment," in Developments in Sedimentology 56, Elsevier, 2004.